Hydrodynamic Modelling and Reduction of Irrigation Releases from the Theewaterskloof Dam to Limit Water Losses

by

Matthys Johannes Saayman

Thesis presented in partial fulfilment of the requirements for the degree of Master of Science in Civil Engineering at Stellenbosch University

Department of Civil Engineering,
Stellenbosch University,
Private Bag X1, Matieland 7602, South Africa.

Supervisor: Prof. G.R. Basson

February 2012

Declaration

By submitting this thesis electronically, I declare that the entirety of the work contained therein is my own, original work, that I am the owner of the copyright thereof (unless to the extent explicitly otherwise stated) and that I have not previously in its entirety or in part submitted it for obtaining any qualification.

Signature: .....
M.J. Saayman

Date: 2012/02/23 .....

Abstract

Hydrodynamic Modelling and Reduction of Irrigation Releases from the Theewaterskloof Dam to Limit Water Losses

M.J. Saayman

Department of Civil Engineering,
Stellenbosch University,
Private Bag X1, Matieland 7602, South Africa.

Thesis: MScEng (Civ)

February 2012

Water is a precious and valuable resource. South Africa is a semi-arid country with an average rainfall of 450 mm, which is well below the global average of 860 mm, and is characterised by large in-season as well as annual variation. As a result, South Africa's water resources are scarce and limited. With an increasing population and the inevitable increase in water cost, the effective management of water resources becomes of the highest priority.

The key to managing the water resources is to utilise the water that is not stored in the catchment through using accurate and reliable forecast data. By implementing a real-time operating system, the unregulated runoff downstream of the storage can be utilised more efficiently.

This thesis looks at the Riviersonderend region, for which the water supply is augmented from the Theewaterskloof Dam. By using measured data and estimations, the Riviersonderend River was simulated by constructing a one-dimensional hydrodynamic model. The ability of the model to represent real-world conditions was demonstrated through a process of model calibration and validation. After validating the hydrodynamic model, a two-week period during the irrigation season was used to determine a reduced dam release hydrograph.

Water that is saved will benefit both the Zonderend Water User Association (ZWUA) and the City of Cape Town. The thesis concludes with an estimation of the possible cost saving for the ZWUA and the City of Cape Town.

Keywords: Real-time, Mike 11, Mike NAM, Sapwat3, calibration, validation,

simulation, optimisation, Theewaterskloof Dam, Riviersonderend River, irrigation, estimation, DHI, hydrograph

Uittreksel

Hidrodinamiese Modellering en Vermindering van Theewaterskloofdam Uitlate vir Besproeiing om Waterverlies te Beperk

("Hydrodynamic Modelling and Optimisation of Irrigation Releases from the Theewaterskloof Dam")

M.J. Saayman

Departement Siviele Ingenieurswese,
Universiteit van Stellenbosch,
Privaatsak X1, Matieland 7602, Suid Afrika.

Tesis: MScIng (Siv)

Februarie 2012

Water is 'n baie waardevolle en kosbare hulpbron. Suid-Afrika is 'n halfdor land met 'n gemiddelde reënval van 450 mm, baie laer as die globale gemiddelde reënval van 860 mm. Verder ervaar Suid-Afrika ook groot binne-seisoen en jaarlikse wisseling in reënval, en die land het dus skaars en beperkte waterbronne. Voortdurende bevolkingsgroei en die onvermydelike verhoging in water koste beteken dat die goeie bestuur van waterbronne 'n groot prioriteit word.

Om agter die kap van die byl te kom met betrekking tot waterbronbestuur moet water benut word wat nie in die opvangsgebied gestoor word nie. Deur 'n intydse hidrodinamiese model te gebruik, kan hierdie water in berekening gebring en gebruik word tesame met akkurate en betroubare voorspellingsdata.

Hierdie verslag ondersoek die Riviersonderendgebied, wat deur die Theewaterskloofdam van water voorsien word. Deur gebruik te maak van gemete data en beramingstegnieke is die Riviersonderendrivier gesimuleer deur 'n eendimensionele hidrodinamiese model saam te stel. Die vermoë van hierdie model om werklike riviertoestande na te boots is deur 'n proses van kalibrasie en stawing gedemonstreer. Nadat die model gestaaf is, is 'n tydperk van twee weke in die besproeiingseisoen gebruik om 'n damuitlaat-hidrograaf saam te stel wat minder water vereis.

Die water wat gespaar sal word, hou 'n voordeel in vir die Zonderend Watergebruikersvereniging (ZWUA), sowel as vir die Stad Kaapstad. Die tesis kom tot 'n slotsom met 'n beraming van die moontlike koste besparing vir die ZWUA en die Stad Kaapstad.

Acknowledgments

I would like to express my sincere gratitude to the following people and organisations ...

For the excellent guidance and technical assistance:

Prof. GR Basson
DHI software
Francois du Plessis
Pieter van Heerden
Wageed Kamish
Felipe Martinez Guerrero
Zonderend Water User Association
WeatherSA
Department of Water Affairs.

The continuous support, prayer and love throughout this project:

Engela Maria 'Elmarie' Saayman (mother)
Frederik Josefus 'Rikus' Saayman
Izak Johannes and Carla Saayman
Mathys Johannes and Jacoba Susanna Elizabeth Crous
Johannes Izak Adolf and Annie Saayman

Elsje Johanna Coetzee

Pieter and Matty Botha, Frans and Annemarie Coetzee, Gerrit and Jo-anni Coetzee, Duncan Gow, Juan and Nita Kidd, Sias and Louis le Roux, Karl Olivier, Herkie and Corinne Sandenbergh, Philip Theron.

Lastly, and by far the most important, I want to thank my Saviour Lord Jesus Christ. Thank you for teaching me Psalm 23 during this adventure. Everything I am and become I owe to You.

Dedications

Hierdie tesis word opgedra aan ...

Frederik Josefus 'Frikkie' Saayman

Contents

List of Figures

List of Tables

Nomenclature

1D	One-dimensional
AOR	Annual operating rule
BOCMA	Breede-Overberg Catchment Management Agency
CK	Time constant
CMA	Catchment management agencies
CQIF	Quantified inter flow coefficient
CQOF	Quantified overland flow coefficient
DHI	Danish Hydraulic Institute
DSS	Decision support system
DWA	Department of Water Affairs
EFR	Environmental flow requirements
EI	Efficiency index
ET_0	Evapotranspiration
FAO	Food and Agriculture Organization
FSL	Full supply level
GUI	Graphical user interface
HEC-RAS	Hydrologic Engineering Centre's River Analysis System
KOBWA	Komati Basin Water Authority
LRA	List of Rateable Areas
MAP	Mean annual precipitation
MAR	Mean annual runoff
m^3/a	Cubic metres per annum
m^3/s	Cubic metres per second
masl	Metres above sea level
MOL	Minimum operating level
NAMC	National Agriculture Marketing Council
OFS-RT	Orange-Fish-Sundays Real Time
QIF	Quantified inter flow
QOF	Quantified overland flow
RAW	Readily available water
REW	Readily evaporative water
RMSE	Root mean square error
RSA	Republic of South Africa

SCE	Shuffled complex evolution
SMS	Short message service
TEW	Total evaporative water
TG	Root zone threshold value
TOF	Threshold for overland flow
WAS	Water administration systems
WMA	Water management area
WUA	Water user association
WRC	Water research commission
US	University of Stellenbosch
ZWUA	Zonderend Water User Association

Chapter 1

Introduction

1.1 Problem Statement

Population growth, irrigation development and other economic activity in South Africa have long surpassed the stage where all the requirements for water can be met from the natural availability thereof (Department of Water Affairs (DWA), 1986). The groundwater resources of the country, although very important for small towns and rural communities, are insufficient to sustain even a significant proportion of the water requirements. Although the country has considerable variation in climate as well as topography, South Africa is classified as semi-arid. The average rainfall for the country is about 450 mm per year (DWA, 2004*a*), which is well below the world average of about 860 mm per year (Easterling *et al.*, 2000), and is characterised by large in-season as well as annual variation. As a result, South Africa's water resources are scarce and limited.

Due to the high variability in river flow within a year and annually, storage needs to be provided to bridge low-flow periods and droughts with adequate degrees of assurance. Agricultural irrigation represents more than 60% of the total water requirements in South Africa (DWA, 2004*b*; World Water Assessment Programme, 2009).

Government funding, especially in the 1970s, made remarkable strides to optimise our precious resources by innovative engineering solutions. In the Western Cape, large projects like the Riviersonderend-Berg River project is a great example of such engineering solutions. The Riviersonderend-Berg River project won the award for most outstanding engineering project of the year in 1980 (DWAF, 1982). The central storage unit of this project, the Theewaterskloof Dam, was constructed in the Riviersonderend drainage region. The amount of water used for irrigation schemes are allocated by DWA, as described in the National Water Act. Every farmer is allocated a certain amount of water for each hectare under irrigation.

The portion of the Riviersonderend catchment included in this study is situ-

ated in the Western Cape and stretches from the Theewaterskloof Dam to the Breede River 116 km eastwards. This catchment consists of 118 water users and covers a total area of 1750.8 km^2 (Midgley *et al.*, 1994). The Theewaterskloof Dam releases augment water used for irrigation in the dry season, from November to April every year.

The Riviersonderend River Irrigation Board had been responsible for the management of agricultural water since 1975 (Ferreira, 2011). Accoriding to Mbedzi (2006) the Department of Water Affairs established the Zonderend Water User Association (ZWUA) in 2006. The main goal of the ZWUA is the effective management of water used for irrigation.

Due to the geometry and hydraulic characteristics of the Riviersonderend region, the management of the region is very challenging. Numerous tributaries flow augment the Riviersonderend River. The flow of these streams are not measured and are dependent on rainfall to generate discharge. Also, the water depth of the river sections varies significantly, causing multiple "Hippo pools" (see explanation on page 9). When possible, the farmers prefer pumping the water for irrigation from these hippo pools. Lastly, irrigation water usage varies significantly every year depending on rainfall and crop market prices. The ZMUA does not have a scheduling system whereby the farmer requests the amount of irrigation water beforehand.

These characteristics make it difficult to determine the behaviour of the river. Currently, the Theewaterskloof Dam release for irrigation is determined by one person. This person phones farmers in the area to determine the state of the river and adjusts the dam release accordingly. Previous attempts have been undertaken to simplify the management of water from the Theewaterskloof Dam (Ferreira, 2011). The latest attempt to optimise the irrigation management system was to insert water measurement devices on all known pumps in the Riviersonderend River in 2005 to determine the water usage of the farmers. Floods in 2007 and 2009 made the task of management more challenging by destroying some of the measuring devices.

Effective management of the dam releases is very difficult using the current system of the ZWUA that is in place. This form of management results in water wastage or possible shortages in the irrigation season. Water shortages in irrigation influence the crop yield, which causes financial losses for the farmers.

With the ever increasing cost of water and other water-related expenditure, the need for efficient management has become a major priority.

Effective management from the Theewaterskloof Dam reduces the expenses for the ZWUA and ultimately for the farmers in the area. Water that is saved by efficient management is still stored in the Theewaterskloof Dam, to be used later in a drought. Also, the water in the Theewaterskloof Dam could be used for drinking water by the ever increasing population of the City of Cape Town.

1.2 Scope of this Study

This study aims to construct a hydrodynamic model of the Riviersonderend River downstream from Theewaterskloof Dam and to improve the dam releases for irrigation. This thesis does not investigate the water quality of the Riviersonderend River.

1.2.1 Literature Review

The thesis starts with the findings of a literature review and also personal observations and discussions, to familiarise the reader with the Riviersonderend area. Various management challenges faced by the ZWUA are described in the study. The study also includes a description of the water management structure defined by the National Water Act (Act No.36 of 1998).

New methods for addressing water resource problems are being developed and implemented using advanced computer facilities for data management and analysis. Among these newly evolved methods are the Decision Support Systems (DSS). This new form of water management is compared to the conventional operation technique commonly used in South Africa. To serve as an example, the Orange-Fish-Sundays real-time operating system is described and illustrated.

A short description of the different software investigated for this thesis is provided in the following section. In the construction of the one-dimensional river model, a variety of software was used. This thesis also includes a in depth study of the software used in the study. This software includes Mike 11, Mike 11 NAM and Sapwat3.

1.2.2 Hydrodynamic Modelling of the Riviersonderend River

The first step in constructing a hydrodynamic model is obtaining data. The data obtained include flow, weather and other data, as mentioned in this section. Due to data limitations or the non-availability of data, estimation techniques were implemented to be used in the simulation.

These estimations were used to determine the discharge that is generated from the unmeasured tributaries. The daily irrigation schedule of the farmers was estimated using Sapwat3. Return flow generated from irrigation was estimated by using the percentage determined in other projects in South Africa. Other losses such as seepage and the evapotranspiration from the riparian zone were not included in the hydrodynamic model.

The chapter ends with a description of the modelling calculations used in the one-dimensional river model. Mike 11 is used to construct the Riviersonderend

River model. The data obtained is included in the river model in different ways and is discussed.

1.2.3 Model Calibration and Validation

To provide a credible basis for the prediction and evaluation of mitigation options, the ability of the model to represent real-world conditions should be demonstrated through a process of model calibration and validation.

After constructing the river model and adding the estimated and obtained data the model is calibrated. The calibration is accomplished by adjusting the river bed roughness as to match the observed and simulated flow. The objective of the calibration is to support the one-dimensional analysis of hydrological conditions in the Riviersonderend River, focussing mainly on low flow water availability. The effect of the augmentation into the Riviersonderend River and irrigation from the river is also quantified.

The next section discuss the calibrated model. The quality of the input data effects the accuracy of river model, these constraints are discussed and compared to more preferable input data.

Once the model had been calibrated, another irrigation period was simulated using the same model set-up to validate the simulated model.

1.2.4 Reduction of Dam Releases for Irrigation

The goal of a real-time operating systems is to optimise the dam outlets to utilise the runoff from tributaries as far as possible, and to ensure that the irrigation requirements are supplied and that the downstream outflows are equal to the requested ecological flow requirements (EFR).

This thesis does not construct a DSS for Riviersonderend catchment, this is mainly due to weather data constraints and the current management system used by the ZWUA, this is discussed in more detail. A historic time period was used to determine the potential reduction of the dam release hydrograph.

Excel was used to determine the dam release hydrograph. The time period used is motivated and the process used to determine the reduced dam release hydrograph is discussed. Initially a dam release hydrograph is calculated without the effect of rainfall and evaporation. By using the calibrated hydrodynamic model, the initial dam release hydrograph is reduced in order to utilise the rainfall downstream from Theewaterskloof Dam.

The estimated water savings were determined by comparing the reduced dam release hydrograph with the actual Theewaterskloof Dam release. Additionally, the cost savings for the ZMUA was determined. The City of Cape Town

is also a beneficiary of water that is saved in Theewaterskloof Dam. The potential cost savings for the City of Cape Town were also determined.

The chapter concludes by discussing the optimization process involved in a real-time DSS. The module (Mike 11, FloodWatch) interaction are also illustrated based on the existing OFS-RT DSS.

Chapter 2

Literature Review

2.1 Introduction

The Riviersonderend catchment is located in the Breede Water Management Area (WMA) in the Western Cape Province of South Africa. This literature review starts off by providing more detail about the Riviersonderend catchment.

The following two sections discuss previous developments in the area influencing the hydraulic behaviour of the Riviersonderend River and provide more information on the farming activity in the area. The Riviersonderend River is mainly utilised by farmers as a source of irrigation water.

Water is managed by the ZWUA and is governed by the greater Breede-Overberg Catchment Management Agency (BOCMA, 2011). The different roles and responsibilities of these management entities, as defined by the National Water Act, are discussed.

The next section introduces the reader to real-time water management systems. Real-time water management systems offer various opportunities to simplify and improve water management. This section also discusses conventional system operation rules in South Africa, and ends by using the example of the Orange-Fish-Sundays real-time (OFS-RT) decision support system in South Africa, which uses similar software to that used in this thesis.

There are numerous software programs that can be used to construct a river model; the river modelling software investigated (HEC-RAS, ISIS Professional, Mike 11) is described, as well as the rainfall-runoff software (ACRU, Mike 11 NAM) and a irrigation requirement planning tool (Sapwat3). This section also includes an investigation of the Mike FloodWatch software, which is used to manage real-time systems.

The software used to simulate the Riviersonderend area is discussed in more detail in the following section. This section includes the algorithms used by

the different software packages used in this thesis and provides more detail on real-time systems.

2.2 Riviersonderend District

The Breede WMA is situated in the south-west corner of South Africa (DWA, 2004*a*); see Figure 2.1. It derives its name from the largest river within its boundaries, namely the Breede River. The WMA is bounded by the Indian Ocean to the south, the Olifants/Doorn WMA in the north-west, the Berg WMA in the west and the Gouritz WMA in the east (see Figure 2.1). It falls entirely within the Western Cape Province.

The topography of the Breede WMA varies considerably from east to west, with subsequent impact on the climate of the region (DWA, 2004*a*). Rainfall is highest in the mountainous regions in the south-west, where the mean annual precipitation is as high as 3 000 mm per annum, whilst the central and north-eastern areas receive as little as 250 mm per annum (DWA, 2004*a*). There is intensive irrigation in the Breede and Riviersonderend River valleys (Breede component of the WMA), as well as in the extreme west of the Western Overberg, notably in the Palmiet River catchment (DWA, 2004*a*).

Figure 2.1: Location of the Breede WMA (DWA, 2004*a*)

Figure 2.2 indicates the different water management areas in the Breede WMA, including the Riviersonderend catchment area (DWA, 2004*a*).

The Riviersonderend catchment lies within the primary drainage region, H, which has a total gross catchment area of 15 530 km^2 and a gross natural mean annual runoff (MAR) of 2 089 million m^3 (Midgley *et al.*, 1994). Most of the rain over the WMA, falls between the months of May and August (DWA, 2004*a*).

Figure 2.2: The different river management areas in the Breede-Overberg catchment district (DWA, 2004*a*)

The Riviersonderend sub-area extends from the source of the Riviersonderend River in the Franschhoek Mountains, upstream of Theewaterskloof Dam, to the confluence with the Breede River (Blackhurst *et al.*, 2002). The Riviersonderend catchment (H60) has an area of 2 253 km^2 and a gross natural MAR of 459 million m^3/s (Midgley *et al.*, 1994).

The northern border of the Riviersonderend River management district runs along the Riviersonderend Mountains, near Genadendal and Greyton. Other important towns in the Riviersonderend district include Riviersonderend and Villiersdorp.

Generally, the Riviersonderend catchment slope and cross-sections are quite

flat. Concerning plant growth, and typical of other rivers in the Western Cape, the Riviersonderend River has abundant water reeds and larger trees on either side of the main channel (Vancoillie, 1985). The Breede River basin study done by the DWA (2004*a*) estimated that an additional system yield of 0.4 million m^3/a could become available through the removal of all alien plants in the Riviersonderend River. The river management agency keeps this abundant plant growth under control by manually clearing the river channel (BOCMA, 2010, 2011).

An interesting and unique characteristic found all along the river is called hippo pools. These hippo pools are deep, long pools up to 3 000 metres in length and over 20 metres deep, providing significant water storage (see Figure 2.3).

Figure 2.3: Satelite image of Riviersonderend hippo pool 10 km downstream from Theewaterskloof Dam

Figure 2.4: Riviersonderend hippo pool 10 km downstream from Theewaterskloof Dam

Hippo pools could also be described as naturally formed dams and, like a dam, these hippo pools (Figure 2.4) lower the river velocity, increasing the lag time of the water. Another similarity to dams is the hippo pools' ability to store water within the main river channel. Farmers from this area prefer pumping water from these hippo pools to use for irrigation (Ferreira, 2011).

The Riviersonderend catchment downstream of Theewaterskloof Dam has experienced high natural discharges during the normal low-flow irrigation season. Figure 2.5 illustrates the magnitude of the increase in volume of the water for the recorded discharge in 2007.

When observing the discharge at Rheenen flow gauge, 101.5 kilometres downstream from Theewaterskloof Dam, it is possible to see how much water is augmented by the tributaries. An example of the magnitude of the amount of water added by the tributaries during the irrigation season of 2007 (November 2007 to April 2008) was the average measured volume of 80 million m^3

Table 2.1: Average monthly flow (million m^3) during the 2007 irrigation season

Month	Dwarstrek	Rheenen
November	10.85	55.67
December	2.92	15.6
January	1.42	8.0
February	2.61	3.37
March	2.43	2.52
April	2.44	2.82
Total	**22.67**	**87.98**

downstream at Rheenen, compared to the upstream 30 million m^3 water measured at Dwarstrek gauging station near Theewaterskloof Dam. The average monthly flow of the 2007 irrigation season is shown in Table 2.1.

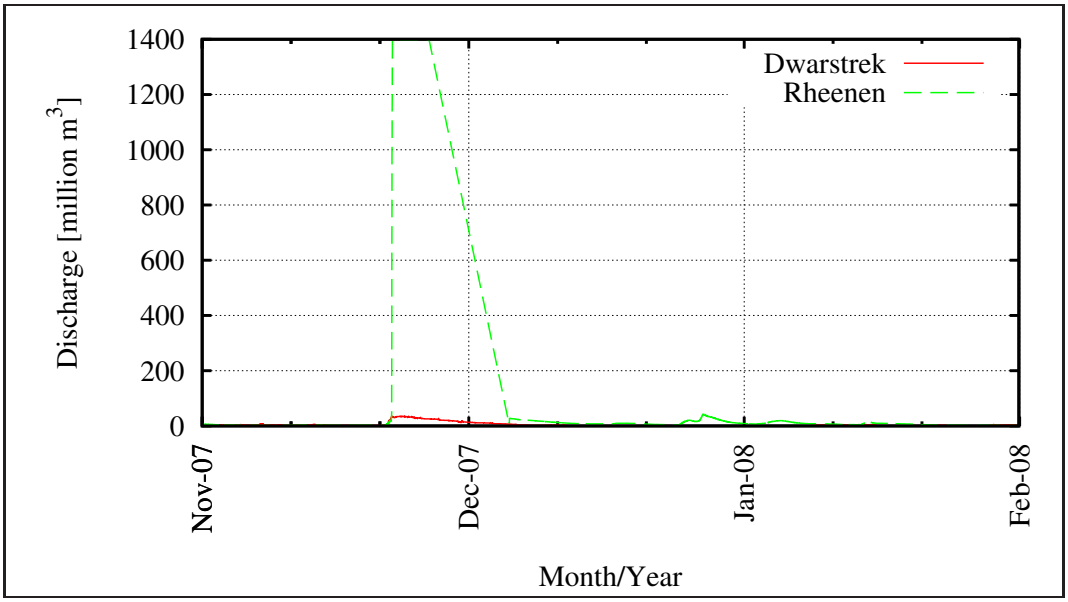

Figure 2.5: Riviersonderend gauging station data for the 2007 flood event

Figure 2.7 shows the Theewaterskloof Dam during a flood event in December 2007. Apart from Theewaterskloof, there are no dams in the main river channel to store excess water. Figure 2.6 shows the Theewaterskloof Dam outlet works releasing water into the Riviersonderend River. The surplus water runs into the Breede River and, ultimately, into the ocean (Vancoillie, 1985). That which is not required for the environmental flow requirement (EFR) in the Riviersonderend and Breede Rivers is lost to the Riviersonderend catchment.

Irrigation water supply project development is a very slow process and is also

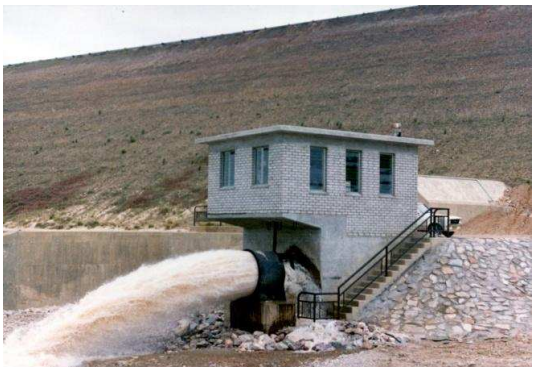

Figure 2.6: Theewaterskloof oulet works

Figure 2.7: Theewaterskloof Dam during flood event

highly capital intensive (DWAF, 1986). An irrigation water supply project undertaken in the Riviersonderend River, called the Riviersonderend-Berg River project, is discussed further in Section 2.3.

2.3 The Riviersonderend-Berg River Project, 1979

The most significant development in the Riviersonderend district is undoubtedly the Riviersonderend-Berg River project.

The storage potential of the Riviersonderend was realised as long ago as in the 1800s, but it was the Irrigation Department that started the first serious investigations into the possibility of a scheme here in 1929 (DWAF, 1982). The mountainous region in the Riviersonderend catchment experiences high rainfall compared to the rest of South Africa (exceeding up to 1 500 mm/year) (DWA, 2004*a*; Van Vuuren, 2011).

The scheme involved linking the two water-rich catchments of the Riviersonderend and Berg Rivers and storing some of the surplus winter runoff in the Riviersonderend catchment in the Theewaterskloof Dam. When the need for water arises, it is delivered by a gravity tunnel to the Berg River Dam and then through a further series of tunnels to where it is needed (DWA, 2005).

The Theewaterskloof Dam is a conventional earth-fill dam. The structure, which was completed in 1979 (DWAF, 1982), is 37,5 m high above the lowest foundation, and has a crest length of 646 metres. The Theewaterskloof Dam has a gross storage capacity of 482 million m^3, and the net storage capacity above the lowest abstraction level is 434 million m^3. When full, the reservoir covers an area of 51 km^2 (DWAF, 1982).

The main purpose of this scheme is to ensure water availability for Cape Town

during the dry summer season and to supply water for the farmers downstream in the Riviersonderend region.

2.4 Farming Activity

Agricultural irrigation represents more than 60% of the total water requirements in South Africa (DWA, 2004*b*; World Water Assessment Programme, 2009). The effective management of agricultural water is therefore of the utmost importance. In the Riviersonderend catchment area downstream of Theewaterskloof Dam there are 118 water users, consisting mainly of farmers (Ferreira, 2011). The farms have 6 097.5 ha under irrigation during the summer irrigation season (Ferreira, 2011).

Appendix A lists the irrigation water users in the Riviersonderend catchment downstream of Theewaterskloof Dam and their allocated annual number of hectare. Each farmer has an amount of 5 700 m^3/ha.

Crops that are farmed in the area during the summer irrigation season include maize, fruit, olives, wine grapes, lucerne and pastures. The most abundant grain type crop in the Riviersonderend region is maize. Various types of fruit are farmed in the area, with apples being the most common.

The water used for irrigation is available from one or more of the following water sources:

- Groundwater,
- On-farm dams,
- Riviersonderend River,
- Natural springs and/or mountain streams.

With the availability of the Riviersonderend River water source, there is minimal usage of the available groundwater in the Riviersonderend catchment. Boreholes are used to supply water for the farm houses and have minimal effect on the water table (boreholes used for irrigation were not included in the simulation done for this thesis). The Riviersonderend catchment does offer a great opportunity to utilise groundwater for future developments.

A study by the DWA (2004*a*) stated that the City of Cape Town was investigating groundwater sites in the Riviersonderend catchment of the Theewaterskloof Dam for possible augmentation of the City's water supply. The Table Mountain Group Aquifer in the Riviersonderend area holds significant potential for development (DWA, 2004*a*).

On-farm dams are common in the Riviersonderend catchment. Typically, the dam will not be in the main tributary channel and is used to store the water

generated by rainfall in one of the smaller sub-catchments within the tributary catchment. This thesis simulates the effect of the on-farm dams by excluding the catchment area of the on-farm dam catchment in the rainfall-runoff calculations (see Section 3.2.4 for more detail). It is assumed that all the water from the on-farm dams is utilised for irrigation during the irrigation season.

The water from natural springs and mountain streams is also stored in on-farm dams, to be used for irrigation.

With increasing electricity costs and the inevitable future increase in agricultural water costs, the farmers' goal becomes clear: use as little water as possible without compromising on crop yield (Hunter, 2006).

A study done by the National Agriculture Marketing Council (NAMC, 2010) examined the cost of electricity for a typical farm in the Northern Cape. Using the same estimation, the electricity cost for one hectare of maize in the study area was just under R2,500 for 2011. The latest cost of water for the ZMUA was R 0.026 per m^3 (Ferreira, 2011). With the volume of water available for every hectare under irrigation, the electricity cost per m^3 was determined using electrical costs obtained from the case study by the NAMC (2010). The electrical cost for pumping agricultural water was calculated to be R 0.44 per m^3.

When comparing the cost of pumping (44 cents/m^3) with the the cost of irrigation water (2.59 cents/m^3), electricity is far more expensive than water. Therefore, it is most likely that the farmers' motive to save water is driven by the desire to consume less electricity.

2.5 National Water Act

The most recent National Water Act No.36 of 1998 of South Africa provides the legal framework for the effective and sustainable management of the country's water resources (RSA, 1998). The Act aims to protect, use, develop, conserve, manage and control water resources as a whole, promoting the integrated management of water resources with the participation of all stakeholders (De la Harpe and Ramsden, 1998).

The Act defines water resources as water bodies such as rivers, streams, wetlands, estuaries and groundwater (De la Harpe and Ramsden, 1998). Furthermore, the Act encompasses the environmental integrity of rivers by assigning an ecological reserve. The reserve is part of the national water resource within each water management area that is under the direct control of the Minister (De la Harpe and Ramsden, 1998). It is water that is 'set aside' to:

- provide for basic human needs, and
- protect water ecosystems.

The ecological reserve for the Riviersonderend River is 65 million m^3/a (DWA, 2004*b*).

2.5.1 Catchment Management Agencies

The Act also includes the establishment of catchment management agencies (CMAs). This represents the second tier of the water resource management framework. A CMA was established in each of the 19 water management areas (De la Harpe *et al.*, 1998; RSA, 1998).

The CMA responsible for catchment H, which includes the Riviersonderend region, is the Breede-Overberg catchment management agency (BOCMA, 2011). BOCMA is responsible for the progressive development and broad implementation of a catchment management strategy (BOCMA, 2011; De la Harpe *et al.*, 1998).

2.5.2 Water User Associations (WUA)

A WUA is a statutory body established by the Minister under the National Water Act. A WUA is a co-operative association of individual water users who wish to undertake water-related activities for their mutual benefit (De la Harpe *et al.*, 1998).

The Zonderend Irrigation Management Board was founded in 1875 (Ferreira, 2011). In 2006, the board was declared an association by the Minister of Water Affairs (Mbedzi, 2006).

The area of operation of the ZWUA includes all properties downstream of Theewaterskloof Dam in respect of which any person is entitled to use water (surface water and groundwater) by virtue of entitlements in terms of Section 22(1) of the Act (Mbedzi, 2006).

The responsibilities and role of a WUA, listed by De la Harpe *et al.* (1998), are as follows:

- Preventing water from any water resources being wasted.
- Protecting water resources.
- Preventing any unlawful water use.
- Removing or arranging to remove any obstruction unlawfully placed in a watercourse.
- Preventing any unlawful act likely to reduce the quality of water in any water resources.
- Exercising general supervision over water resources.
- Regulating the flow of any watercourse by:
  - clearing its channel (see Figure 2.8);

Figure 2.8: Photo of alien plants in Riviersonderend River 10 km downstream from Theewaterskloof Dam

  - reducing the risk of damage to the land in the event of floods; and
  - changing a watercourse back to its previous course where it has been altered through natural causes.
- Investigating and recording:
  - the quantity of water at different levels of flow in a watercourse;
  - the times when; and
  - the places where water may be used by any person entitled to use water from a water resource.
- Constructing, purchasing or otherwise acquiring, control, operation and maintenance of waterworks considered to be necessary for:
  - draining land; and
  - supplying water to land for irrigation or other purposes.
- Supervising and regulating the distribution and use of water from a water resource according to the relevant water use entitlements, by erecting and maintaining devices for:
  - measuring and dividing; or
  - controlling the diversion of the flow of water.

At present, the ZWUA manages the Theewaterskloof Dam releases into the Riviersonderend River by evaluating the river water levels at various locations and adjusting the outlets accordingly. This form of management is dependent

on the experience of the person responsible for regulating the releases. There is, however, a variety of hydrodynamic software that could be utilised to simplify irrigation management.

2.6 Real-Time Management Models

This section briefly describes why real-time management systems are required, how they work, and what information is required to build a good representation of the actual river, and lists the current real-time systems in South Africa. Also, conventional management and the limitations of the conventional water management method are discussed.

2.6.1 Introduction

The operation of water resource systems includes the regulation to reconcile water availability with water requirements (Mwaka, 2011). Factors that influence the operation of water resources are:

- Hydrology - rainfall, evaporation, river flows, reservoir levels, natural river channel water losses, etc.
- Water requirements - e.g. irrigation, municipal, reserve, etc.
- Infrastructure - maintenance schedules, configuration, etc.
- Water resource quality.
- Water pricing/cost.

2.6.2 Conventional System Operation

Most of the water resources in South Africa are operated using conventional operating techniques. This conventional wisdom is based on the principle that water is an annually renewable resource (Mwaka, 2011). The operating decisions are based on the historic behaviour of the river and focussed on the available water resource in dams.

Stochastic modelling is applied to provide tools to relate water availability to the associated risk. The main tool used for water supply management in South Africa is the Annual Operating Rule (AOR). AOR principles, as described by Mwaka (2011), are

- Every year has different water availability and demand characteristics.
- Monthly time scales are sufficient for annual water allocations.

- Annual water availability and demand are determined and allocated in both volume and risk.
- Resources are managed in order to supply water while maintaining tolerable risk for each user.
- In actual or possible drought, restrictions are implemented to sustain supplies for longer.

The conventional system operation method is not ideal. With the increasing cost and value of water, these systems will have to be adapted or changed. Some of the limitations of the conventional management methods include:

- Only water that is stored in a dam can be managed.
- Water quality, EFR and water saving are increasing management challenges, and on smaller time scales (Mwaka, 2011).
- The role of climate change limits the suitability of measured historical data.
- About 40% of the available water in South Africa is not stored in dams (not regulated) (DWA, 2004*b*).

Most of the major dams in South Africa, including the Theewaterskloof Dam, were constructed during the 1970s. Mwaka (2011) shows that, in the past three decades, South Africa stored 6 828 million m^3 of water, with a total of 16 993 million m^3 stored between 1971 and 1980. This is mainly due to the fact that South Africa had limited opportunities for the construction of new dams and also because of the high financial impact on the economy.

2.6.3 Real-time Systems Operation of Water Resources

New methods for addressing water resource problems are being developed and implemented using advanced computer facilities for data management and analysis. Among these newly evolved methods are the real-time DSS.

A real-time DSS involves the sensing of and response to hydrological/hydraulic events nearly simultaneously. The aim is to utilise forecast field hydrology (rainfall, tributary flows, etc.) and translate it into flows and water availability at a required point in future time. Using computer software, a optimised flow is generated, which is related to past water-release decisions to meet contemporary water requirements. Section 2.6.4 investigates the OFS-RT DSS as an example to illustrate how a working DSS functions.

Real-time systems complement and do not replace the conventional operating rules. By monitoring the performance of the AOR, a real-time DSS could be applied to optimise releases by using the minimum amount of water to supply

all water requirements (Mwaka, 2011).

The components of a real-time system include:

- GIS-based framework.
- Hydrological real-time data collection networks, like telemetry, etc.
- Water requirement ordering systems for the water users.
- Rainfall and evaporation data measured hourly or less.
- Hydrological and hydrodynamic models.
- Information dissemination/publishing systems.

2.6.3.1 DSS requirements

At this point it is important to emphasize that the success of a DSS is dependent on the input data in order to manage water resources effectively. For this thesis, the rainfall and evaporation data were measured daily, which accounted for the inaccuracies as discussed in Chapter 3.

The hardware requirements for constructing and running hydrodynamic river modelling software, for example Mike 11, are a computer with Windows 98 or more recent. HEC-RAS and ISIS Professional have similar computer requirements. The person responsible for this computer should be familiar with the software to ensure operating success, and a person from within the WUA would be a suitable candidate.

Weather data can be logged remotely by SMS and forwarded to the computer used for the simulation. Hourly measured weather data is preferred for a more accurate representation of rainfall intensity than that provided daily measured data. Discharge values could be obtained in a similar fashion. Hydro, a department within DWA, has real-time monitoring systems in place in South Africa that are suitable to be used in real-time DSS (Visser, 2010).

The physical adjustment of the dam sluice requires delegated persons to ensure the adjustments are done on time and correctly (Visser, 2010). This could be a challenge, depending on the type of sluice that is currently installed. For example, an automated sluice is able to adjust every four minutes while the conventional, older gate valves take a long time to adjust and are also very labour intensive, resulting in less adjustment and reducing the system efficiency.

2.6.3.2 Real-time DSS Interactions

The simulation-optimisation framework applied in the real-time DSS is illustrated in Figure 2.9. The diagram forms a loop, illustrating how the optimisation recommends sluice adjustment. When a sluice breaks, or is not adjusted

according to schedule, the system adapts to this constraint by continuously adjusting to the real-time conditions of the catchment.

The optimisation criteria (e.g. flood control, hydropower generation, irrigation) are defined as objective functions comprising numerical measures that are used to compare the model output with user-specified targets at each time step of the simulation (e.g. flood level, hydro power demand, irrigation demand). Based on the calculated objective functions, the optimisation algorithm selects new sets of control parameters to be evaluated. The process is repeated a number of times until no further improvement can be made.

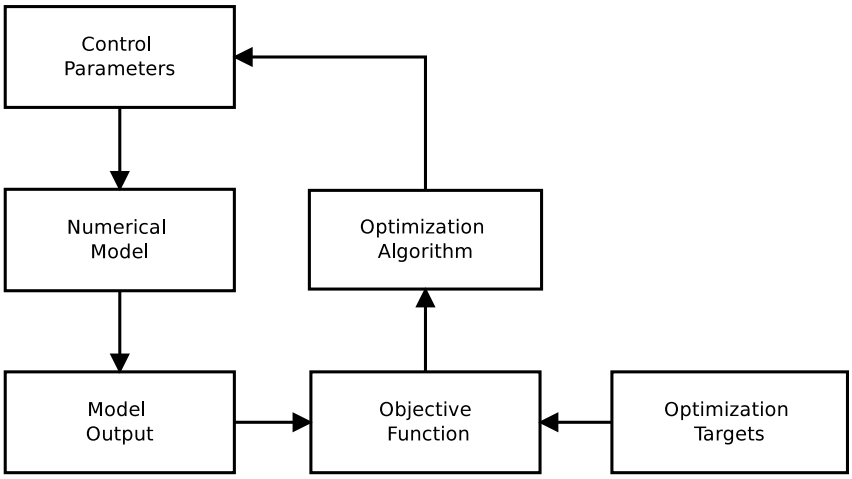

Figure 2.9: Simulation-optimisation framework (Pedersen *et al.*, 2007)

As opposed to conventional technologies, the simulation-optimisation framework is very flexible because it applies to any simulation model and facilitates the definition of any control parameters (both constants and time variables) and objective functions to be optimised. It handles user-defined constraints such as lower and upper search limits of each control parameter efficiently, as well as linear or non-linear equality and inequality constraints. In order to facilitate the optimisation of computationally demanding models, the optimisation framework supports the use of distributed computing solutions.

For this thesis, no optimisation framework was constructed. The dam outlet schedule was however improved by using a similar technique, without utilising computer software like FloodWatch (see Section 2.7.5.1).

2.6.3.3 South African Real-Time Systems

South Africa uses multiple real-time systems, including:

- The Orange-Fish-Sundays Real-Time Decision Support System.
- The Crocodile East Real-Time Decision Support System.

- The Lower Orange River Real-Time Decision Support System.
- The Mhlathuze Real-Time Decision Support System.
- The Letaba Real-Time Decision Support System.
- The Komati Basin Water Authority (KOBWA) Real-Time Decision Support System.

Real-time systems can improve water conservation and minimise losses. Flood forecast and pre-release for flood control and dam safety, climatic change preparedness and capacity building could also be managed by real-time systems.

Real-time operating systems can enable the virtual operation of the unregulated water downstream of the water storage structure by capturing real-time weather/water conditions within the catchment. The water in storage is then only released to supplement the unregulated water in the system.

In order to cope with increasing pressures on water saving, water demand, water quality and dam safety, the DWA implemented the OFS-RT system to calculate the optimal water flow, by running customised DHI Mike 11 software. To serve as an example, the following section describes the OFS-RT operating system.

2.6.4 Application to the Orange-Fish-Sundays Real-Time Model

2.6.4.1 Description of the System

The OFS-RT river system is located in the Eastern Cape of South Africa (Figure 2.10). The area covers the greater part of the Great Fish River catchment, and some of the Sundays River catchment (Pedersen *et al.*, 2007). Water is transferred from Gariep Dam in the Orange River catchment through the Orange-Fish Tunnel to the Great Fish River catchment, where it enters the Grassridge Dam and eventually meets the Elandsdrift Diversion Weir. At this point, the water is released to the downstream part of the Great Fish River or diverted to the Little Fish River. In the Little Fish River, the water passes the De Mistkraal Weir and flows back to the Great Fish River, or through the Skoenmakers Canal to the Darlington Dam. At Darlington Dam, water is released to downstream consumers.

Hundreds of water consumers, mostly agricultural, are dispersed along the rivers in the study area. Over time, the increased irrigation demands have resulted in highly saline return flows in the downstream river reaches (Pedersen *et al.*, 2007). Since saline water has an adverse impact on water quality, a substantial amount of water is constantly diverted through the Orange-Fish

Figure 2.10: Picture showing the Great Fish River and the Sundays River catchments (adapted from Pedersen *et al.* (2007))

Tunnel to dilute the saline water and hence mitigate the problem (Melvil, 2007).

The overall objective of the OFS-RT model is to minimise water losses from the Orange-Fish-Sundays river system and ensure that irrigation demands are met at the right time. Moreover, reservoir water levels downstream of OFS during normal conditions must be kept between a minimum operating level (MOL) and a full supply level (FSL). During normal operating conditions, the reservoir water levels must stay close to MOL in order to facilitate the alleviation of floods and the storage of excess water. During flood events, the reservoirs must contain flood water up to the storage capacity dictated by the

FSL. Should the amount of forecast flood water exceed the storage capacity of the reservoir closest to the origin of the flood, pre-releases must be made in order to release water to downstream reservoirs (Melvil, 2007). This facilitates safe reservoir operation during flood events and helps save excess water for later use.

2.6.4.2 Modelling Approach

The Mike 11 model of the OFS river system includes approximately 850 km of rivers, five dams and diversion weirs and 150 demands scattered along the rivers (Pedersen *et al.*, 2007). Complementing the river model, the spatial and temporal distribution of the salinity of the water is modelled using the advection-dispersion module embedded in Mike 11. The output of the model includes forecast time series of optimal release hydrographs for the dams and diversion weirs.

The optimisation of the numerical model is a time-consuming task because many model evaluations are required to arrive at an optimal solution. In order to reduce the computational effort of the forecast optimisation and ensure that the model state is accurate at the time a forecast is issued, a two-step simulation-optimisation approach is applied (Pedersen *et al.*, 2007).

In the first step, an initial simulation covering a historical period and the forecast period is carried out. This simulation is calibrated by adding tributaries, rainfall, evaporation, return flow, water abstraction and other water losses in order to match the historical flow record. The validity of this initial simulation is validated by applying the same procedure in a different time period. During the historical period, data is used to update the state of the model up to the time of the forecast, based on real-time point observations of river water level, river discharge and salinity. In the forecast period, an initial solution for the optimisation problem is sought based on a concept in which each irrigation demand is lagged and tracked back to the reservoir outlets. The applied procedure accurately narrows the search space of the optimisation carried out in the subsequent step, and thus reduces the need for additional model evaluations (Pedersen *et al.*, 2007).

In order to compute an accurate initial solution, the lagging of the irrigation demands must be accurate (Pedersen *et al.*, 2007). To this end, tabulated relationships are used to relate the travel time of the water released from each reservoir to the point of abstraction. This function is highly dependent on the discharge in the river (see Figure 2.11). The approach ensures that the initial solution is close to the optimal solution, both in terms of the size and the phase of the required demand (Figure 2.12).

In the second step, a mathematical optimisation is made for the forecast period, using the results of the prior simulation to initialise the model state and

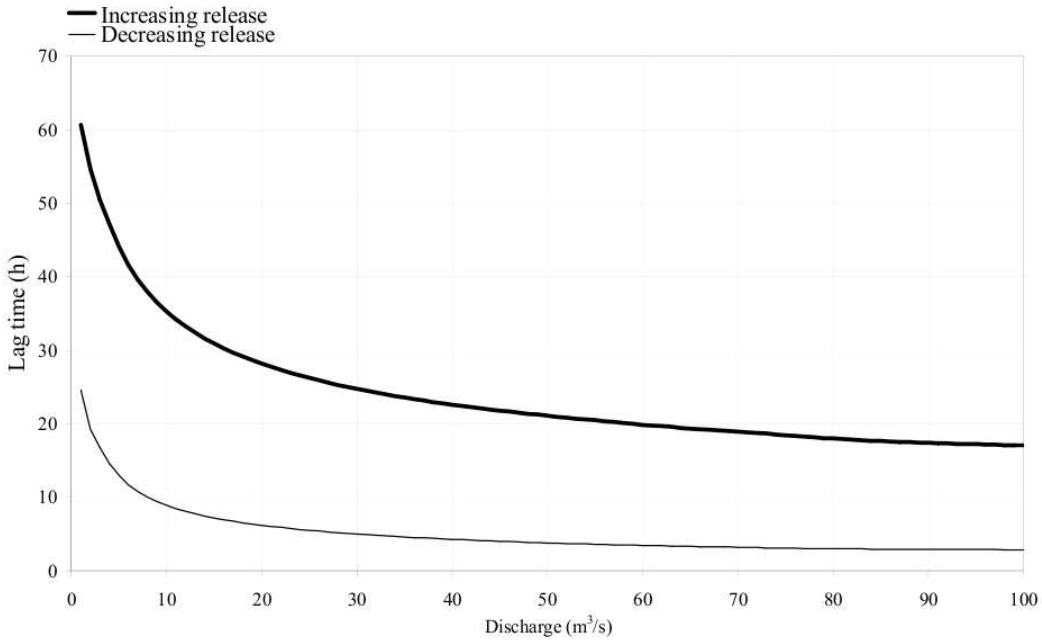

Figure 2.11: Lag-time functions for decreasing and increasing demands approximately 50 km downstream of Darlington Dam (Pedersen *et al.*, 2007)

set the search space (Pedersen *et al.*, 2007). The optimisation algorithm performs a mathematical search and thus computes optimal release hydrographs for the forecast period.

2.6.4.3 Results of the OFS-RT model

As an example of how the framework works, an optimisation run was done for a four-day period during March 2006. During the initial run, the salinity downstream of Grassridge Dam exceeded the maximum allowed concentration. The maximum concentrations achieved from Grassridge Dam to Elandsdrift during the simulation period are shown in Figure 2.13. It is seen that the maximum allowed salinity was exceeded at the downstream end. After the optimisation, the maximum salinity was below the largest salinity allowed.

The calculated release from Grassridge Dam during the initial simulation and the optimised release are compared in Figure 2.14. The optimised release was increased, compared to the release found during the initial simulation. This ensured that the water was diluted to an acceptable salinity level.

A simulation was done for a period during late 2005 and early 2006. The results from this simulation illustrate that the water level in Darlington Dam is kept between the MOL and FSL (Figure 2.15). It also illustrates how the water level is kept close to MOL in order to grant storage capacity in case of sudden flooding.

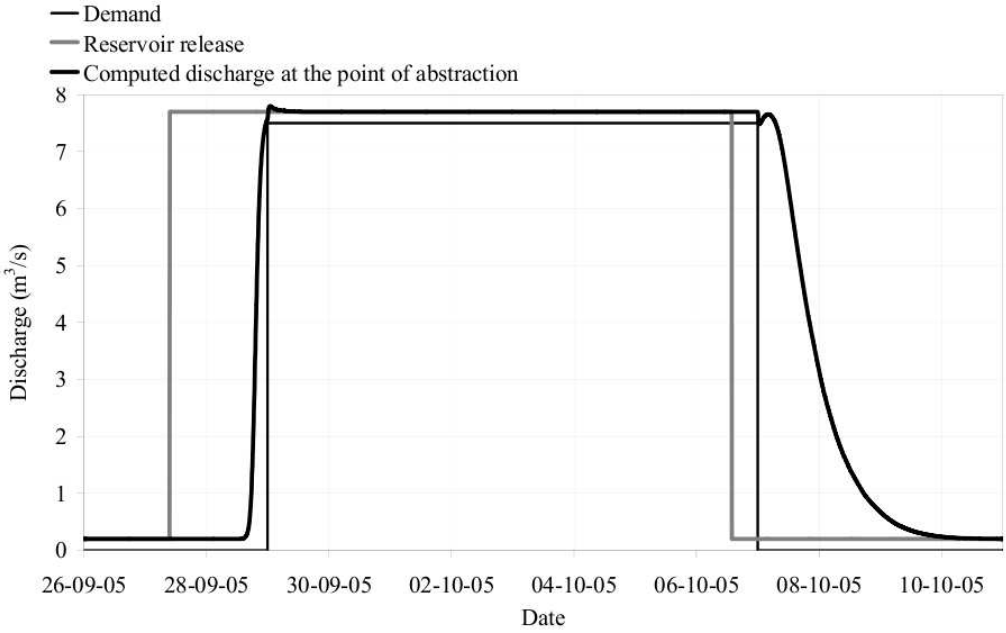

Figure 2.12: Size and phase of a pulse of water released from Darlington Dam as it arrives at the point of abstraction 50 km downstream of the dam (Pedersen *et al.*, 2007)

As a final example, a simulation was done of a one-month period during 2006. During this period, excess water was discharged through the OVIS tunnel (see Figure 2.16). When excess water is conveyed through the tunnel it should be used to fill the downstream reservoirs. In order to avoid unnecessary spilling, the model computes pre-releases from reservoirs downstream of the Orange-Fish Tunnel. The figure also illustrates how releases from Grassridge Dam in excess of the downstream needs are initiated long before FSL is reached. The pre-releases are terminated when the reservoir water level reaches FSL.

Preliminary validation tests indicate that the diversion of water from the Orange River can be reduced by approximately 1.5 m^3/s without violating the objectives described in Section 2.6.4.1. On a yearly basis, this corresponds to a saving of water of the order of 50 million m^3.

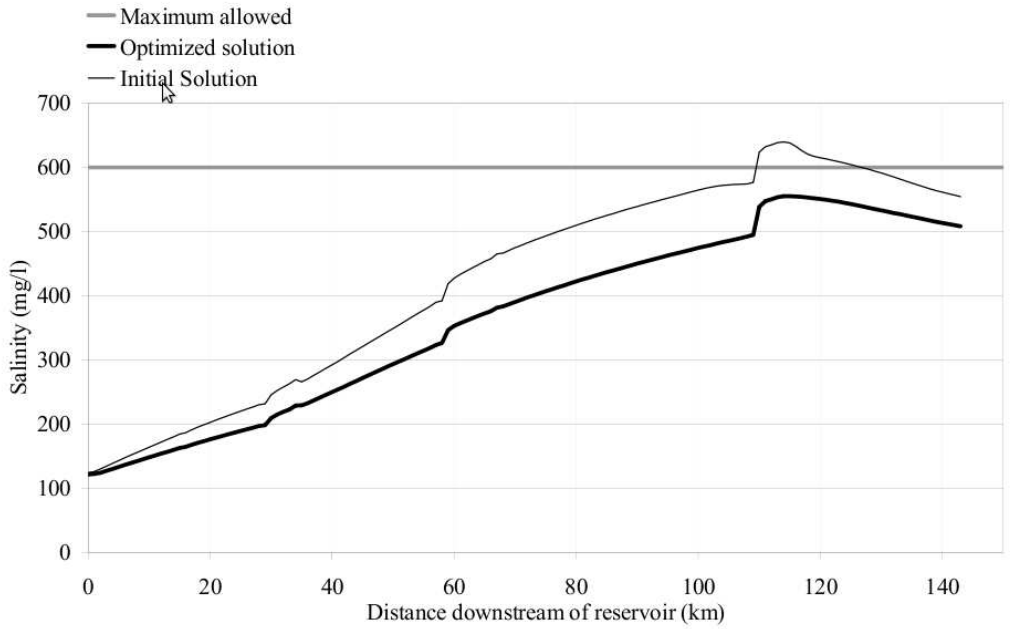

Figure 2.13: Maximum achieved salinity during initial simulation compared to the salinity after optimisation. The maximum allowed salinity is shown (Pedersen *et al.*, 2007)

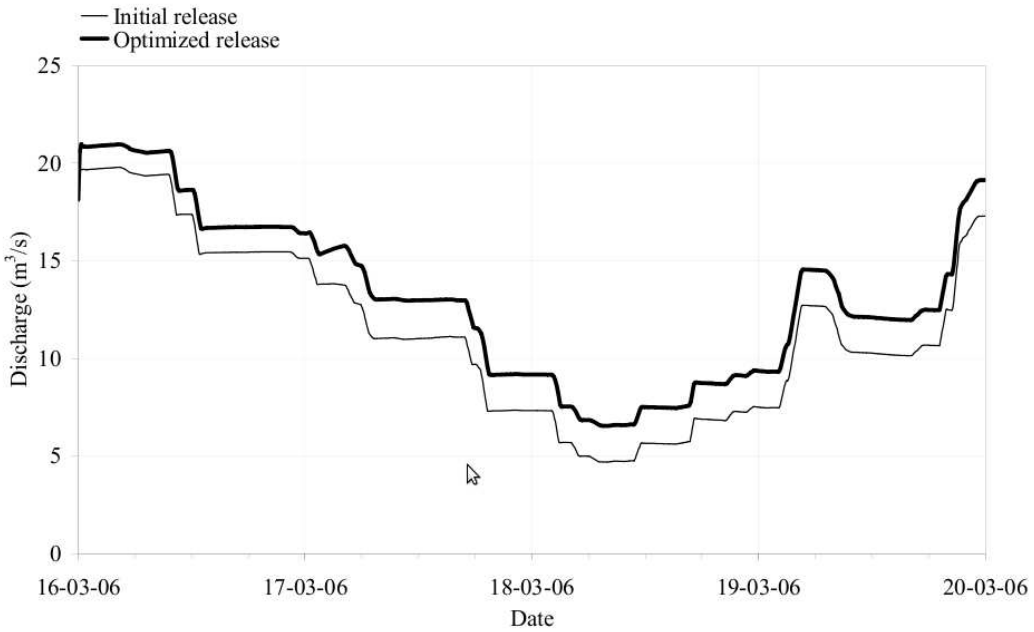

Figure 2.14: Comparison of the initial and optimal reservoir releases for a four-day forecast simulation (Pedersen *et al.*, 2007)

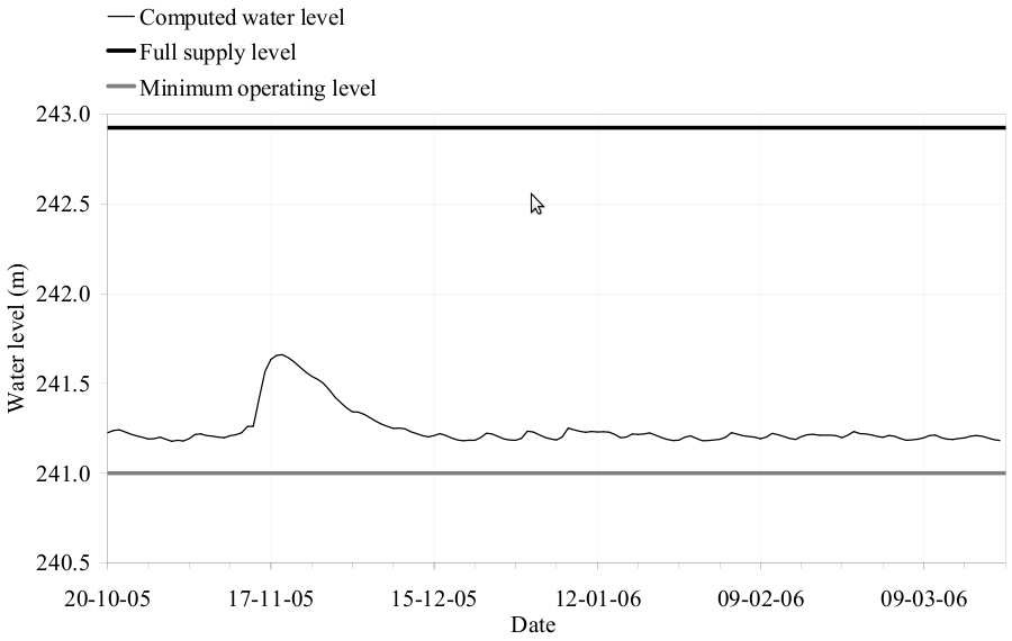

Figure 2.15: Computed water level in Darlington Dam for a six-month period. The water level is maintained close to but above MOL to ensure sufficient storage capacity in the case of sudden flooding (Pedersen *et al.*, 2007)

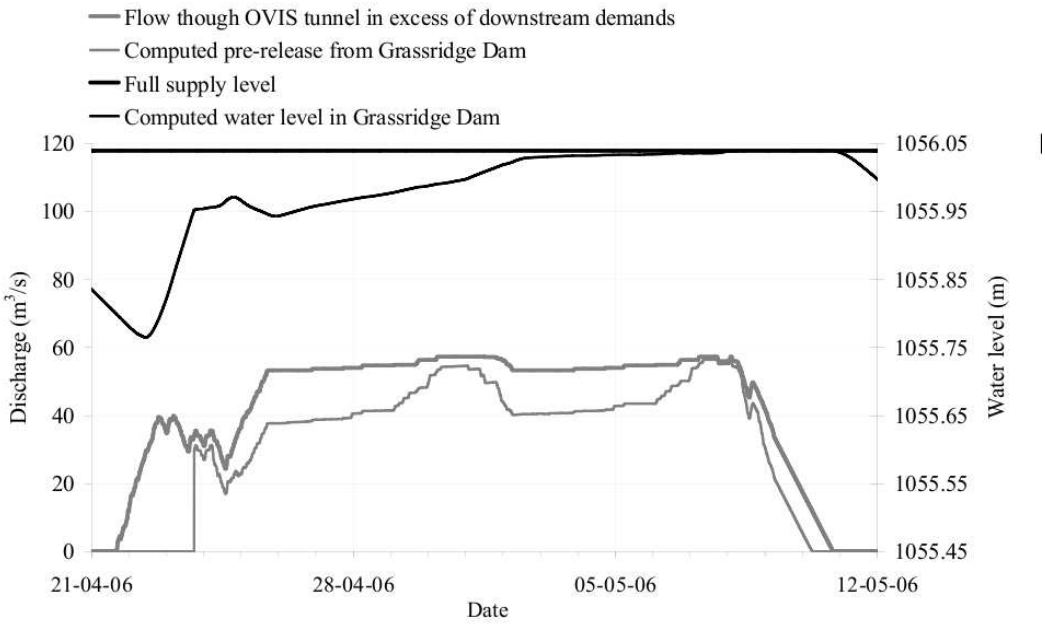

Figure 2.16: The actual discharge through the OVIS tunnel compared with the actual needs. Pre-releases from Grassridge Dam (Pedersen *et al.*, 2007)

2.7 Software Investigated for this Study

2.7.1 River Modelling Software

Numerous hydrological and water resource system models are currently used in South Africa. A short description of the different models considered for this thesis is provided in the following section. The details provided are relatively brief and more detailed information can be obtained from the model developers, most of whom are based in either a university research group or in one of the government departments involved in water resource management.

2.7.1.1 Water Administration Systems (WAS)

WAS is a modelling system that promotes the efficient operational management of water. WAS consists of four main modules that are integrated into a single program that can be used on a single PC, depending on the requirements of the specific irrigation scheme or water office (Pott *et al.*, 2008). The four modules are summarised as follows:

- The Administration module administers the details of all water users of a scheme or water office. Information, including addresses (owners, tenants and postal), scheduled areas, water quota allocations, household and livestock pipes installed, list of rateable areas (LRA), crops planted, planted areas and crop yields, is managed in this module. All information can be printed.

- The Water orders module administers water usage through pressure-regulated sluice gates, water meters and measuring structures. Water orders can be captured using a water order form based on a flow rate and time, or using meter readings based on a start and end reading. Conversion factors can be captured in WAS to convert meter readings automatically if necessary. A range of reports is available for printing, including water allocations and water balances per user, water balance sheets per user and a water usage summary.

- The Water accounts module links to the water orders module and administers all water accounts for a scheme or water management office. The user can choose between two major accounting systems. The first is the current Department of Water Affairs accounting system and the second is a full debit system, from which monthly reports can be printed, including accounts on pre-printed stationery, reconciliation reports, age analysis and audit trail reports.

- The Water release module links to the water orders module and calculates water releases for the main canal or river and all its branches and tributaries, allowing for lag times and any water losses and accruals. A

schematic layout of the total canal network or river system is captured, with details such as the cross-sectional properties, positioning of sluices or pumps, canal or river slope, structures and canal or river capacities. Discharges are converted into the corresponding measuring plate readings where needed. Water distribution sheets and water loss analysis reports can be printed for canal or river systems.

Dr Nico Benadé initially developed WAS to capture water orders that were needed for an open channel simulation model. The model was developed further through Water Research Commission projects done at the Rand Afrikaans University and subsequently by NB Systems. Dr Nico Benadé was responsible for the technology transfer of WAS.

2.7.1.2 ISIS Professional

ISIS Professional is a one-dimensional hydraulic stream flow model based on a finite difference application of the full St Venant's flow equations to a series of cross-sections of the river channel and flood plain and any hydraulic conduits that are built in the flow path. It is aimed at modelling the flow of water in a river channel and can in theory be used in real-time mode, although this has yet to be proven outside of a research environment. The ISIS model is regarded as one of the leading models of its type in the world and originates from the UK as a fully commercial package. The costs associated with the model can be prohibitive and it should only be used where the additional capabilities and ease of use are sufficient to justify the costs over freely available models such as HEC-RAS. The model has been used in South Africa over the past 10 years (Pott *et al.*, 2008).

A range of conservative and non-conservative water quality routines are incorporated in ISIS. The basic requirements for applying the model are regular cross-sections of the river channel and its flood plains, boundary conditions in the form of upstream and tributary inflow series (including water quality), and certain meteorological time series. Friction loss factors and water quality parameters are derived by calibration. This means that reasonable flow and water quality records of in-channel conditions are required. The model is useful to assess short-term downstream water levels and discharges, as well as water quality impacts on upstream operations, or to examine management options related to localised flow and water quality issues. Full backwater effects are simulated. It also comes with powerful graphical interfaces.

2.7.1.3 HEC-RAS

The U.S. Army Corps of Engineers' River Analysis System (HEC-RAS) is software that allows you to perform one-dimensional steady and unsteady flow

river hydraulics calculations (Brunner, 2010). HEC-RAS is an integrated system of software, designed for interactive use in a multi-tasking, multi-user network environment. The system comprise a graphical user interface (GUI), separate hydraulic analysis components, data storage and management capabilities, graphics and reporting facilities.

The HEC-RAS system will ultimately contain three one-dimensional hydraulic analysis components for:

1. steady flow water surface profile computations;
2. unsteady flow simulation; and
3. movable boundary sediment transport computations.

A key element is that all three components will use a common geometric data representation and common geometric and hydraulic computation routines. In addition to the three hydraulic analysis components, the system contains several hydraulic design features that can be invoked once the basic water surface profiles are computed.

This component of the HEC-RAS modelling system is capable of simulating one-dimensional unsteady flow through a full network of open channels. The unsteady flow equation solver was adapted from Dr Robert L. Barkau's UNET model (Brunner, 2010). This unsteady flow component was developed primarily for subcritical flow regime calculations.

The hydraulic calculations for cross-sections, bridges, culverts and other hydraulic structures that were developed for the steady flow component were incorporated into the unsteady flow module. Additionally, the unsteady flow component has the ability to model storage areas and hydraulic connections between storage areas, as well as between stream reaches.

2.7.1.4 Mike 11

This model is also a commercial model originating in Europe and is based on a finite difference application of the full St Venant's flow equations to a series of cross-sections of the river channel and flood plain and any hydraulic conduits that are built in the flow path. A range of conservative and non-conservative water quality routines are also incorporated into this model. The water quality module is a separate module and is not included in the basic module.

The basic requirements for applying the model are regular cross-sections of the river channel and its flood plains, boundary conditions in the form of upstream and tributary inflow series (including water quality), and certain meteorological time series. Friction loss factors and water quality parameters are derived by calibration. This means that reasonable flow and water quality records of in-channel conditions are required.

The model is useful to assess short-term and long-term downstream water levels and discharges, as well as the water quality impacts of upstream operations, or to examine management options related to localised flow and water quality issues. Unsteady uniform flows are simulated under a fully hydrodynamic flow description. It also comes with powerful graphical interfaces.

2.7.2 Algorithms in River Modelling

This thesis utilises the fully hydrodynamic Mike 11 software developed by the Danish Hydraulic Institute (DHI) in Denmark. The reason for choosing this software package was the fully hydrodynamic capabilities, and the availability of the software and software licence at Stellenbosch University. Previous studies have also utilised Mike 11, which provided software support as well as experience with this software within the University.

Although Mike 11 was used, ISIS and HEC-RAS one-dimensional (1D) hydrodynamic simulators work with similar mathematical algorithms. The physical laws which govern the flow of water in a stream are:

- The principle of conservation of mass (Continuity equation).
- The principle of conservation of momentum.

These laws are expressed mathematically in the form of partial differential equations used in the software. The following sections will illustrate the mathematical principles used in the software based on the report done by Sleigh and Goodwill (2000).

2.7.2.1 Deriving the Continuity Equation

The continuity equation is the difference between the sum of the inflows and the sum of the outflows that enter and leave a defined space, which should be equal to the rate of change in the volume of fluid contained within the space (The South African National Roads Agency, 2007).

Consider a short length, Δx, of the channel shown in Figure 2.17.

The following symbols are used in this derivation:

A	*The cross-sectional area of the section.*
h	*Depth of flow at the section.*
z	*Elevation of surface above a datum at the section.*
v	*Mean velocity at the section.*
Q	*Discharge at the section.*
b	*Width of the top of the section.*
x	*Position of the section measured from the upstream end.*
t	*Time.*
g	*Acceleration due to gravity.*
ρ	*Mass density of the fluid.*

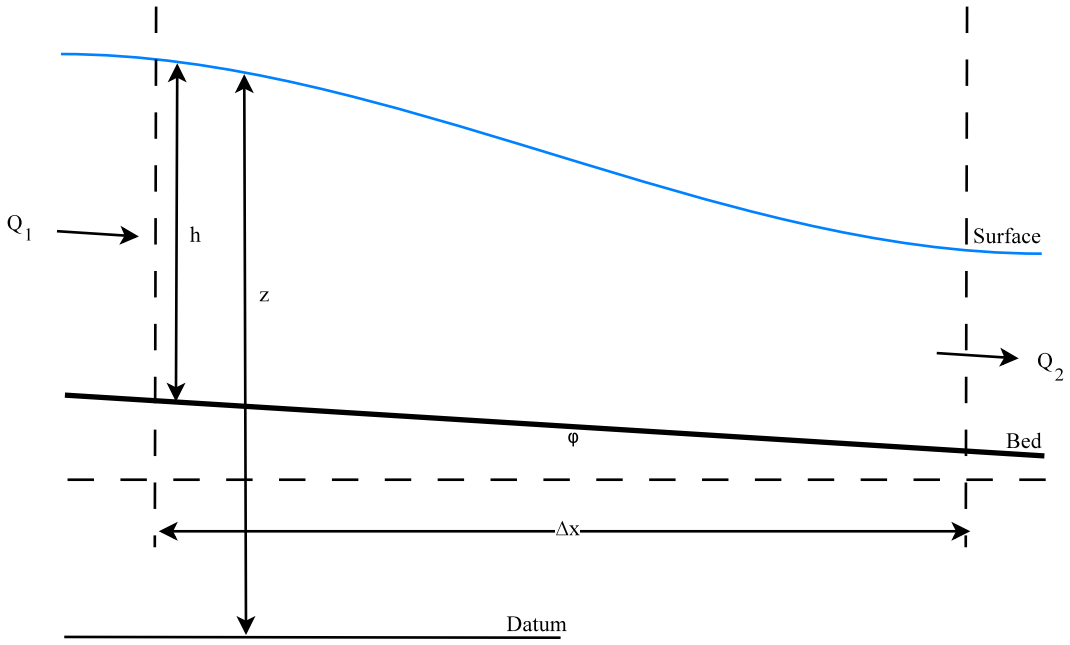

Figure 2.17: Short length of channel

Others symbols are defined in the text at the point where they are introduced.

Assuming that there is no lateral inflow, then

$$Q_2 - Q_1 = \frac{\partial Q}{\partial x}\Delta x \tag{2.7.1}$$

This has a partial derivative since Q is changing with both x and time, t.

Now the volume of water between the sections 1 and 2 is increasing at a rate of

$$b\frac{\partial h}{\partial t}\Delta x \tag{2.7.2}$$

As cross-sectional area $A = bh$, this is equivalent to

$$\frac{\partial A}{\partial t}\Delta x \tag{2.7.3}$$

The terms are equal in magnitude but of opposite sign, so

$$\frac{\partial Q}{\partial x}\Delta x = -b\frac{\partial h}{\partial t}\Delta x \tag{2.7.4}$$

As $\dfrac{\partial Q}{\partial x} = \dfrac{\partial Av}{\partial x}$ then

$$v\frac{\partial A}{\partial x} + A\frac{\partial v}{\partial x} + b\frac{\partial h}{\partial t} = 0 \tag{2.7.5}$$

Equation 2.7.5 is the continuity equation.

2.7.2.2 Deriving the Momentum Equation

By applying Newton's 2^{nd} law to the elemental length of the channel in Figure 2.17, we have the following

$$Force = mass * acceleration$$

$$F = \rho A \Delta x \frac{\partial v}{\partial t} \tag{2.7.6}$$

or

$$F = \rho A \Delta x \left(v \frac{\partial v}{\partial x} + \frac{\partial v}{\partial t} \right) \tag{2.7.7}$$

since v varies with both space (x) and time (t).

Consider the external forces which cause this acceleration:

- change in static pressure changes $(\frac{\partial H}{\partial x})$
- friction of channel walls (F)
- gravity force (ρg)

If ϕ is the bed slope (measured positive as the bed rises from downstream to upstream (see Figure 2.17) then the sum of these three forces are:

$$\frac{\partial H}{\partial x} \Delta x \cos\phi - F \Delta x + \rho g A \Delta x \sin\phi \tag{2.7.8}$$

When working with small slopes, $\phi \cos\phi = 0$ and $\sin\phi = \phi$, using $\phi = i$

$$\frac{\partial H}{\partial x} \Delta - F \Delta x + \rho g A \Delta x i \tag{2.7.9}$$

Now

$$\frac{\partial H}{\partial x} = -\rho g A \frac{\partial h}{\partial x} \tag{2.7.10}$$

and

$$F = \rho g A j \tag{2.7.11}$$

where

j	Energy loss / unit length of channel / unit weight of fluid.

Using Equation 2.7.7

$$\rho A \Delta x \left(v \frac{\partial v}{\partial x} + \frac{\partial v}{\partial t} \right) = -\rho g A \frac{\partial h}{\partial x} \Delta x - \rho g A j + \rho g A \Delta x i \tag{2.7.12}$$

or when rearranged

$$g \frac{\partial h}{\partial x} + v \frac{\partial v}{\partial x} + \frac{\partial v}{\partial t} = g(i - j) \tag{2.7.13}$$

Equation 2.7.13 is the momentum, or dynamic, equation. Using the Chezy expression, j can be written

$$j = \frac{v^2}{C^2 R_m} \tag{2.7.14}$$

where C is the Chezy C-value and R_m is the hydraulic mean radius,

$$R_m = \frac{Area}{WettedPerimeter} = \frac{A}{p} \tag{2.7.15}$$

2.7.3 Rainfall-Runoff Model Software

2.7.3.1 Mike11 NAM

Mike 11 offers the possibility to simulate catchment runoff by using Mike 11 NAM rainfall-runoff software. Mike 11 NAM is a professional engineering software package for rainfall-runoff modelling developed by DHI. This one-dimensional modelling tool, first developed in 1972, has been accepted world-wide, especially for water resource, water quality planning and management applications (DHI, 2009*a*).

Specifically, the Mike 11 software is meant for the simulation of flows, water quality and sediment transport in estuaries, rivers, irrigation systems, channels and other water bodies. Mike11 NAM is a lumped, conceptual rainfall-runoff model simulating overland flow, interflow and baseflow as a function of the water storage in each of four mutually interrelated storages representing the storage capacity of the catchment.

Mike 11 NAM was used in this study to determine the runoff of the tributaries that were not measured. Using Mike 11 for constructing the hydrodynamic model, Mike 11 NAM was chosen due to the already existing relationship between these two software packages (see Section 2.8.2 for a detailed description).

2.7.3.2 ACRU Rainfall-Runoff Model

ACRU is a multi-purpose and multi-level integrated physical-conceptual modelling system that can simulate stream-flow, total evaporation and land cover or management and abstraction impacts on water resources at a daily time step (Mckenzie and Seago, 2007). Input to the menu is controlled by a "menubuilder" program where the user enters parameter or catchment-related values, or uses defaults provided.

The ACRU model uses multi-layer soil water budgeting. Stream-flow is generated as storm-flow and base-flow dependent upon the magnitude of daily rainfall in relation to dynamic soil water budgeting. Components of the soil water budget are integrated with modules in the ACRU system to simulate many other catchment components, including irrigation requirements and system

yield. The model treats groundwater dynamics through a non-linear reservoir and allows riparian zones to be saturated from upland through-flow processes. ACRU requires a degree of calibration. The model is continually being upgraded and has been used extensively throughout Southern Africa.

2.7.4 Irrigation Requirement Planning: Sapwat3

The water pumped from the Riviersonderend River for irrigation was measured monthly and the measurements are used in this thesis. This measured volume of water needed to be distributed daily. In order to distribute this water, a good understanding was necessary of the irrigation requirements of different crops and irrigation system water usage, and this was accomplished using Sapwat3.

Sapwat3 is a crop water-use planning model that can be applied at field or scheme scales. Sapwat was originally developed by Mr Charles Crosby while working for MBB Consulting Engineers, with funding from the Water Research Commission. In 2009, a project (Van Heerden *et al.*, 2009) to further develop Sapwat was initiated with funding from the WRC, and this translated into a new version of the model, referred to as Sapwat3.

Sapwat3 is discussed in more detail in Section 2.8.3.

2.7.5 Real-time System Management

2.7.5.1 Mike FloodWatch

Mike FloodWatch is a decision support system for real-time forecasting that integrates data management, monitoring, forecast modelling tools and dissemination methodologies into a single, user-friendly environment (ESRI ArcMap GIS) (Skotner *et al.*, 2003). Operationally, it can run automatically, manually or as a combination. Moreover, it can be customised using built-in Visual Basic scripting facilities.

The system can be used to manage and examine data imported in real-time from a range of external sources, including point observations (one-dimensional) and grid-based (two-dimensional) data from weather models and radar and satellite imagery. The user can specify quality control procedures for each data stream and link to common commercial database engines (Skotner *et al.*, 2003).

The system includes a scenario management tool that makes it possible to carry out comparative assessments, get immediate answers and respond accordingly (Skotner *et al.*, 2003). The user can identify key information and customise the flow and presentation of this information. User-defined information, such as vital forecast results and observations, can be disseminated either manually,

as part of a scheduled task or on an event-driven basis. Typical dissemination tasks include the following:

- Scheduled uploading of observed and forecast time series and key results to a web server.
- Scheduled notification of flood managers by e-mail or SMS, typically of key forecast results.
- Event-driven notification of flood managers, typically in the early stages of a coming flood.

The Mike FloodWatch system has been installed in numerous countries worldwide, including the OFS-RT system in South Africa (refer to Section 2.6.4). The system is typically used by regional and local river basin authorities to provide real-time forecasts in areas prone to flooding and to issue early, potentially life-saving, warnings to flood response managers and the vulnerable population. Typical applications include:

- Real-time monitoring and decision support.
- Real-time flood forecasting and warning.
- Control of dams, reservoirs and hydraulic structures.
- Dissemination of real-time flood data, flood maps and flood response actions.
- Water resource and environmental monitoring.
- Long-term forecasting.

2.8 Software Used in this Thesis

2.8.1 DHI Water and Environment Model: Mike 11

Mike 11 is a software package for simulating flows, water quality and sediment transport in estuaries, rivers, irrigation channels and other water bodies (DHI, 2011).

Mike 11 is a fully dynamic, one-dimensional modelling tool for the detailed analysis, design, management and operation of both simple and complex river and channel systems (DHI, 2009*a*).

The hydrodynamic (HD) module is the nucleus of the Mike 11 modelling system (DHI, 2009*a*). It forms the basis for most of the modules, including flood forecasting, advection-dispersion, water quality and non-cohesive sediment transport modules. The Mike 11 HD module solves the vertically integrated equations for the conservation of continuity and momentum, i.e. the Saint Venant equations.

2.8.1.1 Saint Venant Equations

Mike 11 applied with the fully dynamic descriptions solves the vertically integrated equations of conservation of volume and momentum (the Saint Venant equations), which are derived on the basis of the following assumptions:

- The water is incompressible and homogeneous.
- The bottom slope is small.
- The wave lengths are large compared to the water depth. This ensures that the flow everywhere can be regarded as having a direction parallel to the bottom.
- The flow is sub-critical.

In the previous section, the derivative of the continuity and momentum equations was illustrated. For a rectangular cross-section with a horizontal bottom and a constant width, the conservation of mass and momentum can be expressed as follows (in the first instance neglecting friction and lateral inflows):

Conservation of mass:

$$\frac{\partial(\rho H b)}{\partial t} = -\frac{\partial(\rho H b \bar{u})}{\partial x} \tag{2.8.1}$$

Conservation of momentum:

$$\frac{\partial(\rho H b \bar{u})}{\partial t} = -\frac{\partial\left(\alpha' \rho H b \bar{u}^2 + \frac{1}{2}\rho g b H^2\right)}{\partial x} \tag{2.8.2}$$

where

ρ	Density.
H	Depth.
b	Width.
$\bar{u}$	Average velocity along the vertical.
α'	Vertical velocity distribution coefficient.

Introducing the bottom slope, I_b, and allowing for the channel width to vary will give rise to two more terms in the momentum equation. These terms describe the projections in the flow direction of the reactions of the bottom and side walls to the hydrostatic pressure.

The momentum equation now becomes:

$$\frac{\partial(\rho H b \bar{u})}{\partial t} = -\frac{\partial\left(\alpha' \rho H b \bar{u}^2 + \frac{1}{2}\rho g b H^2\right)}{\partial x} + \frac{\partial b}{\partial x}\frac{\rho g H^2}{2} - \rho g H b I_b$$

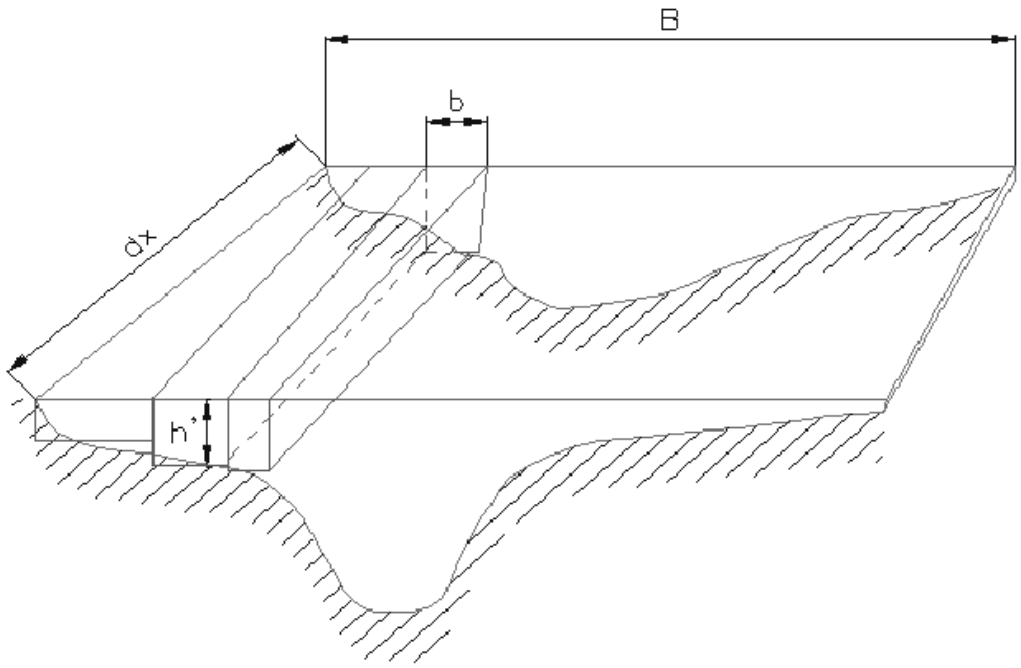

Figure 2.18: Cross-section divided into a series of rectangular channels (DHI, 2009*b*)

$$= -\frac{\partial(\alpha'\rho Hb\bar{u}^2)}{\partial x} - b\frac{\partial\left(\frac{1}{2}\rho g H^2\right)}{\partial x} - \rho g H b I_b \tag{2.8.3}$$

When the water level, h, is introduced into the relationship instead of water depth:

$$\frac{\partial h}{\partial x} = I_b + \frac{\partial H}{\partial x} \tag{2.8.4}$$

and the equations are divided by ρ, the conservation laws of mass and momentum become:

$$\frac{\partial Hb}{\partial t} = \frac{\partial(Hb\bar{u})}{\partial x} \tag{2.8.5}$$

$$\frac{\partial Hb\bar{u}}{\partial t} = \frac{\partial(\alpha' Hb\bar{u}^2)}{\partial x} - Hbg\frac{\partial h}{\partial x} \tag{2.8.6}$$

These equations can be integrated to describe the flow through cross-sections of any shape when divided up into a series of rectangular cross sections, as shown in Figure 2.18.

According to the previous assumptions, $\frac{\partial h}{\partial x}$ is constant across the channel and no exchange of momentum occurs between the sub-channels. If the integrated

cross-sectional area is called A and the integrated discharge Q, and B is the full width of the channel, then:

$$A = \int_0^B H db \tag{2.8.7}$$

$$A = \int_0^B H \bar{u} db = \bar{u} A \tag{2.8.8}$$

Integrating the mass and momentum conservation equations and introducing Equations 2.8.7 and 2.8.8 yields:

$$\frac{\partial Q}{\partial x} + \frac{\partial A}{\partial t} = 0 \tag{2.8.9}$$

$$\frac{\partial Q}{\partial t} + \frac{\partial \left(\alpha \frac{Q^2}{A}\right)}{\partial x} + gA\frac{\partial h}{\partial x} = 0 \tag{2.8.10}$$

Including the hydraulic resistance, e.g. using the Chezy description and the lateral inflow, q, into these equations leads to the basic equations used in Mike 11:

$$\frac{\partial Q}{\partial x} + \frac{\partial A}{\partial t} = q \tag{2.8.11}$$

$$\frac{\partial Q}{\partial t} + \frac{\partial \left(\alpha \frac{Q^2}{A}\right)}{\partial x} + gA\frac{\partial h}{\partial x} + \frac{gQ \mid Q \mid}{C^2 AR} = 0 \tag{2.8.12}$$

Applications related to the Mike 11 HD module include:

- Flood forecasting and reservoir operation.
- Simulation of flood control measures.
- Operation of irrigation and surface drainage systems.
- Design of channel systems.
- Tidal and storm surge studies in rivers and estuaries.

2.8.1.2 The Simulation Editor

Mike 11 comprises a number of different editors in which data can be implemented and edited independently of each other (DHI, 2009*a*). The simulation editor consists of the following supplementary editors:

1. Network editor
2. Cross-section editor
3. Boundary editor
4. Time series editor
5. Parameter editor

As a consequence of the system of separated editor files, no direct linkage exists between the different editors if they are opened individually.

The integration and exchange of information between each of the individual data editors is achieved by using the Mike 11 simulation editor.

The simulation editor serves three purposes:

- It contains simulation and computation control parameters.
- It is used to start the simulation.
- It provides a linkage between the graphical view of the network editor and the other Mike 11 editors, as illustrated in Figure 2.19 below.

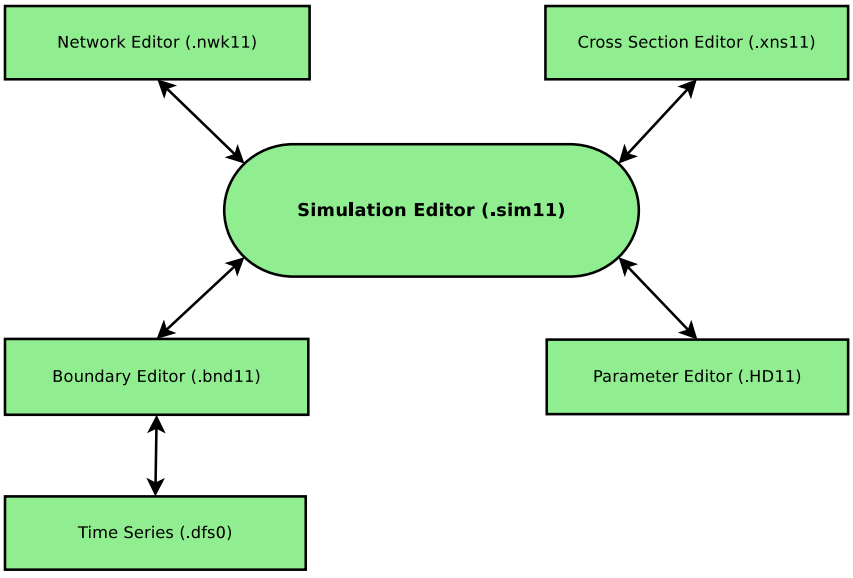

Figure 2.19: Graphical layout of Mike 11 simulation editor and links

Network Editor The network editor is a central unit in the Mike 11 graphical user interface. From the graphical view (the plan plot) of the network editor, it is possible to display information from all other data editors in Mike 11. The network editor consists of two views, a tabular view, where the river network data is presented in tables, and a graphical view, in which graphical editing of the river network can be performed and data from other editors can be accessed for editing, etc.

The two main functions of the network editor are to:

- Firstly, provide editing facilities for data defining the river network.
- Secondly, provide an overview of all data included in the simulation model of the river.

Cross-Section Editor River cross-section data comprises two data sets, the raw and the processed data. Raw data describes the physical shape of a cross-section using (x, z) co-ordinates, typically obtained from a river bed survey. Processed data is calculated from the raw data and contains corresponding values for level, cross-section area, flow width, and hydraulic/resistance radius. The processed data table is applied directly in the computational module.

Each cross-section is uniquely identified by the following three keys:

- River name: String of any length.
- Topo ID: String of any length (topographical identification).
- Chainage: Real number.

Boundary Editor and Time Series Editor Boundary conditions in Mike 11 are defined by the combined use of time series data, prepared in the time series editor, and specifications made for locations of boundary points and boundary types in the boundary editor. That is, the boundary editors make up the time series editor and the boundary editor. Both editors have to be activated in order to specify a Mike 11 boundary condition.

The boundary editor is used to specify boundary conditions for a Mike 11 model. It is used not only to specify common boundary conditions, such as water levels and inflow hydrographs, but also for the specification of lateral flows along river reaches, solute concentrations of the inflow hydrographs, various meteorological data and certain boundary conditions used in connection with structures applied in a Mike 11 model. To be able to insert historic flow data into the river model, the time series editor is used. The time series consists of time and amount of flow measured, and is created in Mike Zero.

Parameter Editor The hydrodynamic parameters editor (HD parameter editor) is used for setting up supplementary data used for the simulation. Most of the parameters in this editor have default values, and in most cases these values are sufficient for obtaining satisfactory simulation results. The HD parameter editor contains 17 different parameters that can be used by the user, and these include:

- Initial river conditions.
- Wind friction on the water surface.
- Bed resistance (This is adjusted in the cross-section editor).
- Bed resistance toolbox: Offers a possibility to make the program calculate the bed resistance as a function of the hydraulic parameters during the computation.
- Wave approximation, which remains fully dynamic.
- Default values in hydraulic calculations (St. Venant equations).
- Quasi steady simulation.
- Heat balance.
- Stratification of flow simulations.
- Additional time series output.
- Map generation.
- Groundwater leakage coefficients.
- Reach lengths, only used in steady state simulations.
- Additional output.
- Flood plain resistance, specified in the cross-section editor.
- User-defined markers.
- Encroachment simulations.

The parameters used in this study include specifying the initial conditions of the river and using the additional output parameter for velocity output.

2.8.2 Mike 11 NAM Model

The NAM hydrological model simulates the rainfall-runoff processes occurring on the catchment scale. NAM forms part of the rainfall-runoff (RR) module of the Mike 11 river modelling system. The rainfall-runoff module can either be applied independently, or used to represent one or more contributing catchments that generate lateral inflows to a river network. In this manner it is possible to treat a single catchment or a large river basin containing numerous catchments and a complex network of rivers and channels within the same modelling framework (DHI, 2009*b*).

A mathematical hydrological model like NAM is a set of linked mathematical statements describing, in a simplified quantitative form, the behaviour of the land phase of the hydrological cycle. NAM represents various components of the rainfall-runoff process by continuously accounting for the water content in four different and mutually interrelated storages. Each storage represents different physical elements of the catchment. NAM can be used either for continuous hydrological modelling over a range of flows, or for simulating single events (DHI, 2009*b*).

2.8.2.1 Data Requirements

The required time series, with a constant or varying time interval between values, are mentioned below, along with the recommended range of frequency. Three to five years of data should be available for calibration and a few additional years for validation of the model. The time series are precipitation (one minute to one day), potential evaporation (one day to one month), and stream-flow data for calibration (one minute to a few hours).

Data requirements for the NAM model consist of:

- Setup parameters - catchment area, topography and soil properties.
- Model parameters - time constants and threshold values for the routing of overland flow, inter-flow and baseflow.
- Meteorological data - precipitation and evaporation.
- Streamflow data for the model calibration.

2.8.2.2 Model Structure

Mike 11 NAM is based on physical structures and equations used together with semi-empirical ones. Being a lumped model, NAM treats each catchment as a single unit. The parameters used are average values for the entire catchment. As a result, some of the model parameters can be evaluated from the physical catchment data, but the final parameter estimation must be performed

by calibration against time series of measured hydrological observations (DHI, 2009*b*).

NAM simulates the rainfall-runoff process by continuously accounting for the water content in four different and mutually interrelated storages that represent different physical elements of the catchment. These storages are:

- Snow storage
- Surface storage
- Lower or root zone storage
- Groundwater storage

In addition, NAM allows the treatment of man-made interventions in the hydrological cycle, such as irrigation and groundwater pumping. In this thesis the man-made interventions are represented by subtracting the on-farm dam catchment from the bigger tributary catchment (see Section 3.2.4). The groundwater is of little effect in the Riviersonderend catchment as the farmers does not irrigate from boreholes because of the availability of the Riviersonderend River. The boreholes in the area are mostly used for on-farm drinking water, which has a negligible effect compared to irrigation usage (Ferreira, 2011).

Based on the meteorological input data, NAM produces catchment runoff as well as information about other elements of the land phase of the hydrological cycle, such as the temporal variation in evapotranspiration, soil moisture content, groundwater recharge, and groundwater levels. The resulting catchment runoff is split conceptually into overland flow, inter-flow and baseflow components.

2.8.2.3 Basic Modelling Components

The modelling components used for this study are discussed in this section. The snow module is not applicable in the Riviersonderend catchment, and the extended groundwater components and irrigation module were not utilised for this thesis.

Surface storage Moisture intercepted on the vegetation as well as water trapped in depressions and in the uppermost, cultivated part of the ground is represented as surface storage. U_{max} denotes the upper limit of the amount of water in the surface storage.

The amount of water, U, in the surface storage is continuously diminished by evaporative consumption as well as by horizontal leakage (interflow). When there is maximum surface storage, some of the excess water, P_N, will enter the

streams as overland flow, whereas the remainder is diverted as infiltration into the lower zone and groundwater storage (DHI, 2009*b*).

Lower Zone or Root Zone Storage The soil moisture in the root zone, a soil layer below the surface from which the vegetation can draw water for transpiration, is represented as lower zone storage. L_{max} denotes the upper limit of the amount of water in this storage (DHI, 2009*b*).

Moisture in the lower zone storage is subject to consumptive loss from transpiration. The moisture content controls the amount of water that enters the groundwater storage as recharge and the interflow and overland flow components.

Evapotranspiration Evapotranspiration demands are first met at the potential rate from the surface storage. If the moisture content U in the surface storage is less than these requirements ($U < E_p$), the remaining fraction is assumed to be withdrawn by root activity from the lower zone storage at an actual rate E_a. E_a is proportional to the potential evapotranspiration and varies linearly with the relative soil moisture content, L/L_{max}, of the lower zone storage.

$$E_a = (E_p - U)\frac{L}{L_{max}} \tag{2.8.13}$$

Overland Flow When the surface storage spills, i.e. when $U > U_{max}$, the excess water P_N gives rise to overland flow as well as to infiltration. QOF denotes the part of P_N that contributes to overland flow. It is assumed to be proportional to P_N and to vary linearly with the relative soil moisture content, L/L_{max}, of the lower zone storage.

$$QOF = \begin{cases} CQOF\dfrac{\frac{L}{L_{max}} - TOF}{1 - TOF}P_N & \text{for } \frac{L}{L_{max}} < TOF \\ 0 & \text{for } \frac{L}{L_{max}} \leq TOF \end{cases} \tag{2.8.14}$$

where

QOF	Quantified overland flow.
$CQOF$	Overland flow runoff coefficient ($0 \leq$ CQOF ≤ 1).
TOF	Threshold value for overland flow ($0 \leq$ TOF ≤ 1).
P_N	Proportion of the excess water that does not run off as overland flow infiltrates into the lower zone storage.

A portion, ΔL, of the water available for infiltration, $(P_N - QOF)$, is assumed to increase the moisture content L in the lower zone storage. The remaining amount of infiltrating moisture, G, is assumed to percolate deeper and recharge the groundwater storage.

Interflow The interflow contribution, QIF, is assumed to be proportional to U and to vary linearly with the relative moisture content of the lower zone storage.

$$QIF = \begin{cases} CKIF \dfrac{\frac{L}{L_{max}} - TIF}{1 - TIF} U & \text{for } \frac{L}{L_{max}} < TIF \\ 0 & \text{for } \frac{L}{L_{max}} \leq TIF \end{cases} \tag{2.8.15}$$

where

QIF	Quantified interflow.
$CKIF$	Time constant for interflow.
TIF	Root zone threshold value for interflow ($0 \leq$ TG ≤ 1).

Interflow and Overland Flow Routing The interflow is routed through two linear reservoirs in series with the same time constant CK_{12}. The overland flow routing is also based on the linear reservoir concept, but with a variable time constant

$$CK = \begin{cases} CK_{12} & \text{for } OF < OF_{min} \\ CK_{12} \left(\dfrac{OF}{OF_{min}} \right)^{-\beta} & \text{for } OF \leq OF_{min} \end{cases} \tag{2.8.16}$$

where

CK	Time constant.
OF	Overland flow (mm/hour).
OF_{min}	Upper limit for linear routing ($= 0.4$ mm/hour).

The constant $\beta = 0.4$ corresponds to using the Manning formula for modelling the overland flow. Equation 2.8.17 ensures in practice that the routing of real surface flow is kinematic, while subsurface flow being interpreted by NAM as overland flow (in catchments with no real surface flow component) is routed as a linear reservoir (DHI, 2009*b*).

Groundwater Recharge The amount of infiltrating water G recharging the groundwater storage depends on the soil moisture content in the root zone

$$G = \begin{cases} (P_N - QOF) \dfrac{\frac{L}{L_{max}} - TG}{1 - TG} U & \text{for } \frac{L}{L_{max}} \leq TG \\ 0 & \text{for } \frac{L}{L_{max}} \leq TG \end{cases} \tag{2.8.17}$$

where

TG	Root zone threshold value for groundwater recharge ($0 \leq$ TG ≤ 1).

Soil Moisture Content The lower zone storage represents the water content within the root zone. After apportioning the net rainfall between overland flow and infiltration to groundwater, the remainder of the net rainfall increases the moisture content L within the lower zone storage by the amount ΔL (DHI, 2009*b*).

$$\Delta L = P_N - QOF - G \tag{2.8.18}$$

Baseflow The baseflow BF from the groundwater storage is calculated as the outflow from a linear reservoir with time constant CK_{BF} (DHI, 2009*b*).

2.8.2.4 Surface and Root Zone Parameters

Maximum Water Content in Surface Storage The maximum water content in the surface storage is defined as U_{max} (mm). This storage is interpreted as including the water content in the interception storage (on vegetation), in surface depression storages, and in the uppermost few centimetres of the ground. Typical values of U_{max} are in the range of 10 to 20 mm (DHI, 2009*b*).

One important characteristic of the model is that the surface storage must be at its maximum capacity, $U \geq U_{max}$, before any excess water, P_N, occurs (DHI, 2009*b*). In dry periods, the amount of net rainfall that must occur before any overland flow occurs can be used to estimate U_{max}.

Maximum Water Content in Root Zone Storage The maximum water content in the lower or root zone storage is defined by L_{max}. L_{max} can be interpreted as the maximum soil moisture content in the root zone available for the vegetative transpiration.

It should be noted that L_{max} represents the average value for an entire catchment, i.e. an average value for the various soil types and root depths of the individual vegetation types. Hence, L_{max} cannot in practice be estimated from field data, but an expected interval can be defined (DHI, 2009*b*).

Overland Flow Runoff Coefficient $CQOF$ determines the extent to which excess rainfall runs off as overland flow, as well as the magnitude of infiltration (DHI, 2009*b*).

$CQOF$ is dimensionless with values between 0 and 1. Physically, in a lumped manner, it reflects the infiltration and also, to some extent, the recharge conditions. Small values of $CQOF$ are expected for a flat catchment having coarse, sandy soils and a large unsaturated zone, whereas large $CQOF$ values are expected for catchments having low, permeable soils such as clay or bare rocks. $CQOF$-values in the range 0.01 to 0.90 have been experienced.

It should be noted that, during periods when the groundwater table is at

the ground surface, the model excludes the infiltration component and hence $CQOF$ becomes redundant (DHI, 2009*b*).

Time Constant for Interflow $CKIF$ [hours]; together with U_{max}, determines the amount of interflow ($(CKIF)^{-1}$ is the quantity of the surface water content U that is drained to interflow every hour). It is the dominant routing parameter of the interflow, because $CK_{12} \ll CKIF$.

Physical interpretation of the interflow is difficult (DHI, 2009*b*). Since interflow is seldom the dominant streamflow component, $CKIF$ is not, in general, a very important parameter. Usually, $CKIF$ values are in the range of 500 to 1 000 hours.

Time Constant for Routing Interflow and Overland Flow The time constant for routing interflow and overland flow, CK_{12} [hours], determines the shape of hydrograph peaks. The value of CK_{12} depends on the size of the catchment and how fast it responds to rainfall. Typical values are in the range of three to 48 hours.

The time constant can be inferred from calibration on peak events. If the simulated peak discharges are too low or arriving too late, decreasing CK_{12} may correct this, and vice versa.

Root Zone Threshold Value for Overland Flow TOF is a threshold value for overland flow in the sense that no overland flow is generated if the relative moisture content of the lower zone storage, L/L_{max}, is less than TOF. Similarly, the root zone threshold values for interflow, TIF, and recharge, TG, act as threshold values for the generation of interflow and recharge respectively (DHI, 2009*b*).

Physically, the three threshold values should reflect the degree of spatial variability in the catchment characteristics, so that a small homogeneous catchment is expected to have larger threshold values than a large heterogeneous catchment (DHI, 2009*b*).

For catchments with alternating dry and wet periods, the threshold values determine the onset of the flow components in the periods when the root zone is being filled up. This can be used in model calibration. It should be noted that the threshold values have no importance in wet periods. The significance of the threshold value varies from catchment to catchment and is usually larger in semi-arid regions (DHI, 2009*b*).

Root Zone Threshold Value for Interflow The root zone threshold value for interflow has the same function for interflow as TOF has for the overland flow. It is usually not a very important parameter, and in most cases it can be given a value equal to zero.

Table 2.2: Effects of changing different NAM parameters on runoff (Supiah and Hashim, 2002)

Parameters	Change	Effects
Root zone storage	Increase	Peak runoff decreased. Runoff volume reduced.
Surface storage	Increase	Peak runoff decreased. Runoff volume reduced.
Overland flow	Increase	Peak runoff decreased. Runoff volume increased.
Root zone threshold	Increase	Peak runoff decreased. Runoff volume reduced.
Time constraint of interflow	Increase	Peak runoff decreased. The triangular shape expands horizontally.
Time constraint of base flow	Increase	Base flow decreased.
Maximum groundwater depth	Increase	Peak runoff decreased. Runoff volume reduced.

2.8.2.5 Initail Conditions

The initial conditions required by the NAM model consist of the initial water content in the surface and root zone storages, together with initial values of overland flow, interflow, and baseflow.

If a simulation commences at the end of a dry period, it is often sufficient to set all initial values to zero, except the water content in the root zone and the baseflow. The water content in the root zone should be about 10 to 30% of the capacity, and the baseflow should be given a value close to the observed discharge (DHI, 2009*b*).

In general it is recommended to disregard the first three to six months of the NAM simulation in order to eliminate the influence of erroneous initial conditions (DHI, 2009*b*). In this thesis, a time period between the years 2000 to 2010 were used with 2005 being simulated first, ensuring minimum influence of erroneous initial conditions.

2.8.2.6 Rainfall-Runoff Output

With the various adjustable parameters it is useful to know the effects of each parameter on the rainfall-runoff editor output. Table 2.2 illustrates the effects of changing different NAM parameters (Supiah and Hashim, 2002). Mike 11 NAM generates a time series file that includes the following:

- Observed discharge.

- Simulated discharge.
- Accumulative observed discharge.
- Accumulative simulated discharge.

In the Riviersonderend River basin, Mike 11 NAM was used to determine the flow of the unmeasured tributaries along the river with a 12 minute time step. This is discussed in more detail in Section 3.3.1.

2.8.2.7 Model Calibration

In the NAM model, the parameters and variables represent average values for the entire catchment. While a range of likely parameter values can be estimated in some cases, it is not possible, in general, to determine the values of the NAM parameters on the basis of the physiographic, climatic and soil physical characteristics of the catchment, since most of the parameters are of an empirical and conceptual nature. Thus, the final parameter estimation must be performed by calibration against time series of hydrological observations (DHI, 2009*b*).

Calibration objectives and evaluation measures . The following objectives are usually considered in the model calibration:

1. A good agreement between the average simulated and observed catchment runoff (i.e. a good water balance).
2. A good overall agreement of the shape of the hydrograph.
3. A good agreement of the peak flows with respect to timing, rate and volume.
4. A good agreement for low flows.

In this respect it is important to note that, in general, trade-offs exist between the different objectives. For instance, one may find a set of parameters that provides a very good simulation of peak flows but a poor simulation of low flows, and vice versa (DHI, 2009*b*).

In the calibration process, the four calibration objectives above should be taken into account. If the objectives are of equal importance, one should seek to balance all the objectives, whereas in the case of priority to a certain objective this objective, should be favoured.

For a general evaluation of the calibrated model, the simulated runoff is compared with discharge measurements (DHI, 2009*b*). Both graphical and numerical performance measures should be applied in the calibration process. The

graphical evaluation includes a comparison of the simulated and observed hydrograph, and a comparison of the simulated and observed accumulated runoff. The numerical performance measures include the overall water balance error (i.e. the difference between the average simulated and observed runoff), and a measure of the overall shape of the hydrograph based on the coefficient of determination.

However, an exact agreement between simulations and observations must not be expected. The goodness-of-fit of the calibrated model is affected by different error sources, including:

1. Errors in meteorological input data.
2. Errors in recorded observations.
3. Errors and simplifications inherent in the model structure.
4. Errors due to the use of non-optimal parameter values.

In model calibration only the non-optimal parameter values should be minimised. In this respect it is important to distinguish between the different error sources, since calibration of the model parameters may compensate for errors in data and model structure. For catchments with a low quantity or quality of data, less accurate calibration results may have to be accepted (DHI, 2009*b*).

Satisfactory calibrations over a full range of flows usually require continuous observations of runoff for a period of three to five years (DHI, 2009*b*). Runoff series of a shorter duration, however, will also be useful for calibration, although they do not ensure efficient calibration of the model.

Automatic Calibration Routine An automatic optimisation routine is available for calibration of the basic NAM model. The automatic calibration routine is based on a multi-objective optimisation strategy in which the four different calibration objectives given above can be optimised simultaneously (DHI, 2009*b*).

Multi-objective calibration measures In automatic calibration, the calibration objectives have to be formulated as numerical goodness-of fit measures that are optimised automatically (DHI, 2009*b*). For the four calibration objectives defined above, the following numerical performance measures are used:

1. Agreement between the average simulated and observed catchment runoff: overall volume error.
2. Overall agreement of the shape of the hydrograph: overall root mean square error (RMSE).

3. Agreement of peak flows: average RMSE of peak flow events.
4. Agreement of low flows: average RMSE of low flow events.

Other equations used in the calibration routine of Mike 11 NAM include:

- The overall volume error equation

$$F_1(\theta) = \left| \frac{1}{N} \sum_{i=1}^{N} (Q_{obs,i} - Q_{sim,i}(\theta)) \right| \tag{2.8.19}$$

- The overall RMSE equation

$$F_2(\theta) = \left[\frac{1}{N} \sum_{i=1}^{N} [Q_{obs,i} - Q_{sim,i}(\theta)]^2 \right]^{\frac{1}{2}} \tag{2.8.20}$$

where

$Q_{obs,i}$	Observed discharge at time i.
$Q_{sim,i}$	Simulated discharge at time i.
θ	The set of model parameters to be calibrated.
N	The number of time steps in the calibration period.

- The average RMSE of peak flow events

$$F_3(\theta) = \frac{1}{M_p} \sum_{j=1}^{M_p} \left[\frac{1}{n_j} \sum_{i=1}^{n_j} [Q_{obs,i} - Q_{sim,i}(\theta)]^2 \right]^{\frac{1}{2}} \tag{2.8.21}$$

where

M_p	Number of peak flow events in the calibration period.
n_j	Number of time steps in event no. j.

Peak flow events are defined as periods when the observed discharge is above a given (user-specified) threshold level.

- The average RMSE of low-flow events

$$F_4(\theta) = \frac{1}{M_l} \sum_{j=1}^{M_l} \left[\frac{1}{n_j} \sum_{i=1}^{n_j} [Q_{obs,i} - Q_{sim,i}(\theta)]^2 \right]^{\frac{1}{2}} \tag{2.8.22}$$

where

M_l	Number of low-flow events in the calibration period.

Low-flow events are defined as periods when the observed discharge is above a given (user-specified) threshold level.

Optimisation algorithm The multi-objective optimisation problem can be formulated as follows:

$$min\left(F_1(\theta), F_2(\theta), F_3(\theta), F_4(\theta)\right), \theta \in \Theta \tag{2.8.23}$$

The optimisation problem is said to be constrained in the sense that θ is restricted to the feasible parameter space Θ (DHI, 2009*b*). The parameter space is defined as a hypercube by specifying lower and upper limits on each parameter. These limits should be chosen according to physical and mathematical constraints in the model and from modelling experiences (DHI, 2009*b*).

The solution for Equation 2.8.23 will not, in general, be a single unique set of parameters, but will consist of the so-called Pareto set of solutions (non-dominated solutions) according to various trade-offs between the different objectives (DHI, 2009*b*). The concept of Pareto optimality implies that the entire parameter space θ can be divided into "good" (Pareto optimal) and "bad" solutions, and none of the "good" solutions can be said to be "better" than any of the other "good" solutions. A member of the Pareto set will be better than any other member with respect to some of the objectives, but because of the trade-off between the different objectives it will not be better with respect to other objectives (DHI, 2009*b*).

In practical applications, the entire Pareto set may be too expensive to calculate, and one is only interested in part of the Pareto optimal solutions (DHI, 2009*b*). To estimate only a single point of the Pareto front, a single-objective optimisation problem is defined that aggregates the different objective functions $F_1(\theta) - F_4(\theta)$.

$$F_{agg}(\theta) = [(F_1(\theta) + A_1)^2 + (F_2(\theta) + A_2)^2 + (F_3(\theta) + A_3)^2 + (F_4(\theta) + A_4)^2]^{\frac{1}{2}} \tag{2.8.24}$$

where

A_i Transformation constants.

A balanced aggregated measure is defined by assigning transformation constants in Equation 2.8.24 such that the different objectives have equal weight in the optimisation. The transformation constants are automatically calculated based on the initially generated population of parameter sets in the optimisation loop (DHI, 2009*b*).

The optimal parameter set is found by minimising Equation 2.8.24 with respect to θ. Optimisation is performed automatically using the shuffled complex evolution (SCE) algorithm. The SCE method is a global search method in the sense that it is designed especially for locating the global optimum of the objective function and not being trapped in local optima (DHI, 2009*b*).

2.8.3 Sapwat3 Irrigation Planning Software

2.8.3.1 Introduction

The Sapwat3 model is used for planning purposes, and is used to estimate the crop water-use requirements of different crops under different irrigation systems and different irrigation management regimes throughout South Africa and neighbouring countries. The research team member responsible for the technology transfer of Sapwat3 was Mr Pieter van Heerden, who is a member of the Picwat consulting team (Pott *et al.*, 2008).

2.8.3.2 Estimating Irrigation Requirements

Sapwat3 was developed to satisfy the need for a user-friendly and credible aid for the estimation of crop irrigation requirements, for the planning of irrigation schemes and for water management by WUAs that can cater for developments in irrigation practice and management (Van Heerden and Crosby, 2002).

On the international front, Sapwat3 links to and is a development of the Food and Agriculture Organization (FAO) planning model Cropwat, which is based on several FAO irrigation and drainage papers (Van Heerden *et al.*, 2009). These papers focus on irrigation management and crop evapotranspiration (Allen *et al.*, 1998).

Sapwat3 is not a crop growth model. It is a planning and management aid that is supported by an extensive South African climate and crop database (Van Heerden *et al.*, 2009; Van Heerden and Crosby, 2005).

The Sapwat3 software takes the user through a process of (Van Heerden and Crosby, 2002):

- Importing weather station data.
- Comparing reference evaporation graphs.
- Selecting crop factors.

Sapwat3 gives a output display that shows the water requirements for that crop, the effective rainfall and the irrigation requirements, and several options are provided, enabling the user to replicate a specific situation.

2.8.3.3 Weather Stations

Sapwat3 uses monthly or daily weather data as the basis for calculating daily Penman-Monteith reference evapotranspiration (ET_0) values for a site, as described by Allen *et al.* (1998). Weather data for use by Sapwat3 comes from five possible sources: CLIMWAT, manual weather stations, automatic weather stations, and the user can build an own weather station or import data from

external sources. Sapwat3 includes the full set of CLIMWAT data, as well as 50 years of daily data for each quaternary drainage region of the country (Van Heerden *et al.*, 2009) and the daily values for some standard and automatic weather stations.

In the Riversonderend catchment, Tygerhoek and Theewaterskloof (H6R001) rainfall stations were available to be imported into Sapwat3. The Theewaterskloof rainfall station, located at the Theewaterkloof Dam, lies in a more rainfall intensive area compared to Tygerhoek rainfall station downstream of Theewaterskloof Dam, refer to Chapter 3.

Tygerhoek rainfall station, owned by Stellenbosch University, is used for for the purpose of research on the surrounding farms. For the purpose of this thesis, the existing weather data from Tygerhoek rainfall station was imported into Sapwat3 to estimate the irrigation requirements.

2.8.3.4 Soil

Broadly speaking, soil is defined as unconsolidated inorganic and organic material on the immediate surface of the earth that acts as a natural medium for the growth of plants and all other soil-living creatures. It is a mix of solid inorganic particles, water, air and organic material. It is an integral part of the landscape and its characteristics, appearance and distribution are determined by climate, parent material, topography, flora, fauna and time (Van Heerden *et al.*, 2009).

Soil can be highly variable in a landscape, with observable differences in depth, texture, structure and slope. The effect of differences in chemical content is sometimes obvious, and changes can sometimes be predicted for specific land-use activities. Not all soils are suitable for irrigation. Irrigation induces changes in the physical, chemical and biological characteristics of a soil; therefore land classification for irrigation should consider the various potential changes and use this as a background for delineating lands on the basis of suitability for irrigation use.

Soil Water A thorough understanding of the soil water balance and the factors that influence it are mathematically described and diagrammatically represented in Figure 2.20 (Allen *et al.*, 1998).

$$\Delta D = I + (P - RO) - E - T + CR - DP \tag{2.8.25}$$

where

ΔD	Change in soil content.
I	Irrigation.
P	Precipitation.
RO	Runoff.
E	Soil surface evaporation.
T	Crop transpiration.
CR	Capillary rise.
DP	Deep percolation.

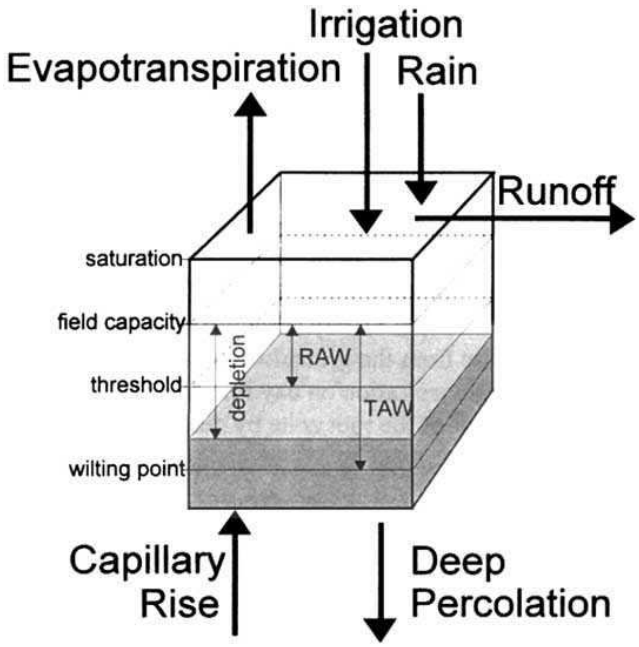

Figure 2.20: A diagrammatic representation of the soil water balance in the root zone of crop

Figure 2.20 illustrate the soil water balance in the root zone of a crop. Water sources for the root zone include rain, irrigation and capillary rise, while the extraction of water is through evapotranspiration (transpiration and soil surface evaporation) and deep percolation. Runoff from soil surface does not add to the soil water content and is usually subtracted from rainfall (Van Heerden *et al.*, 2009). The amount of rainfall, transpiration and soil surface evaporation is linked to the climate of the area, while capillary rise and deep percolation

are mainly influenced by water management of the irrigated and surrounding areas. Figure 2.20 also show diagrammatically the concepts of:

Field capacity	The amount of water that a soil can hold after all free water has been allowed to drain out of the root zone.
Wilting point	The water level in the root zone at which plants will be permanently wilted.
Depletion	The amount of water depleted from the root zone through evapotranspiration.
RAW	Readily available water - the amount of water that is available to a crop without the crop undergoing stress situations.
TAW	Total available water - the total amount of plant available water that a soil can hold in the root zone.

Evaporation from the Soil Surface Where the topsoil is wet following rain or irrigation, the evaporation component ($K_e ET_0$) is at a maximum. As the soil surface becomes drier, soil surface evaporation is reduced until a level of no practically measurable evaporation is reached. Evaporation occurs predominantly from the exposed soil fraction. Hence, evaporation is restricted at any moment by the energy available at the exposed soil fraction; therefore K_e cannot exceed $f_{ew} K_{cmax}$, where f_{ew} is the fraction of soil from which most evaporation occurs, i.e. the fraction of the soil not covered by vegetation and wetted by irrigation or precipitation (Allen *et al.*, 1998).

Evaporation from the soil surface can be assumed to take place in two stages: an energy-limiting stage, and a falling-rate stage. When the soil surface is wet, K_r (dimensionless evaporation reduction coefficient) is 1. When the water content in the upper soil becomes limiting, K_r decreases and becomes zero when the total amount of water that can be evaporated from the topsoil is depleted (Allen *et al.*, 1998).

In the simple evaporation procedure it is assumed that the water content of the evaporation layer of the soil is at field capacity, θ_{FC}, shortly following a major wetting event, and that the soil can dry to a water content level that is halfway between oven dry (no water left) and wilting point, θ_{WP}, The amount of water that can be depleted by evaporation during a complete drying cycle can hence be estimated as (Allen *et al.*, 1998):

$$TEW = 1000(\theta_{FC} - 0.5\ \theta_{WP})Ze \tag{2.8.26}$$

where

TEW	Total evaporable water.
θ_{FC}	Irrigation.
θ_{WP}	Precipitation.
Z_e	Runoff.

Table 2.3: Typical soil water characteristics for different soil types

Soil Type	Soil water characteristics			Evaporation parameters	
	θ_{FC}	θ_{WP}	θ_{FC} - θ_{WP}	Amount of water	
				Stage 1 REW	Stage 1 and 2 TEW (Z_e=0.1 m)
	m^3/m^3	m^3/m^3	m^3/m^3	mm	mm
Sand	0.07-0.17	0.02-0.07	0.05-0.11	2-7	6-12
Loamy sand	0.11-0.19	0.03-0.10	0.06-0.12	4-8	9-14
Sandy loam	0.18-0.28	0.06-0.16	0.11-0.15	6-10	15-20
Loamy sand	0.20-0.30	0.07-0.17	0.13-0.18	8-10	16-22
Silt loam	0.22-0.36	0.09-0.21	0.13-0.19	8-11	18-25
Silt loam	0.28-0.36	0.12-0.22	0.16-0.20	8-11	22-26
Silt clay loam	0.30-0.37	0.17-0.24	0.13-0.18	8-11	22-27
Silty clay	0.30-0.42	0.17-0.29	0.13-0.19	8-12	22-28
Clay	0.32-0.40	0.20-0.24	0.12-0.20	8-12	22-29

When unknown, a value for Z_e, the effective depth of the soil evaporation layer, of 0.1 to 0.15 m is recommended (Allen *et al.*, 1998) and is used in this thesis. Typical values for θ_{FC}, θ_{WP} and TEW are given in Table 2.3 (Allen *et al.*, 1998).

The evaporation reduction coefficient K_r can be calculated with (Allen et al., 1998):

$$K_r = \frac{TEW - D_{e,i-1}}{TEW - REW} \tag{2.8.27}$$

where

K_r	Dimensionless evaporation coefficient dependent on the soil water depletion (cumulative depth of evaporation) from the topsoil layer ($K_r = 1$ when $D_{e,i-1} \leq$ REW).
$D_{e,i-1}$	Cumulative depth of evaporation (depletion) from the soil surface layer at the end of day $i-1$ (the previous day) [mm].
TEW	Total evaporative water. Maximum cumulative depth of evaporation (depletion) from the soil surface layer when $K_r = 0$.
REW	Readily evaporative water: Cumulative depth of evaporation (depletion) at the end of stage 1 [mm] for $D_{e,i-1} >$ REW.

Table 2.3 provides for all the elements required for irrigation water estimates, soil type, field capacity, wilting point, total evaporative water and readily evaporative water, as well as effective depth, evaporation depth and infiltration rate. The parameters used in Sapwat3 are illustrated in Section 3.3.2.

2.8.3.5 Crops

Water influences the growth and development of plants because it is essential for every biological reaction in the plant. It is the most abundant constituent in plants, ranging from about 75 to 90% of a plant's mass by weight. The role of water includes:

1. Involvement in all biological reactions.
2. A structural component in the proteins and nucleic acids in the plant cells.
3. A regulator of plant temperature.

In addition to its in-plant role, water also acts as an environmental regulator of the climate around the plant (Van Heerden *et al.*, 2009).

All annual and deciduous crops have a similar growth and development pattern, i.e. new growth starts at the beginning of the season with new foliage developing and very little ground shading. As the crops develop, foliage develops until the soil surface is mostly or fully overshadowed. Plants then usually go into a reproductive phase during which seed and fruit develop. These ripen towards the end of the season, the foliage starts dying and at the end of the season bare ground is again found.

The problem that faced the irrigation water requirement planner and designer was how to describe this rather complex physiology and phenology in terms that are easily understood and credible. This problem was solved by adopting the four-stage growth cycle approach for describing the growth and development of crops (Allen *et al.*, 1998).

The Four-Stage Crop Cycle Sapwat3 recognises the limitations of the use of A-pan evaporation and uses short grass as reference evaporation, in association with the linked and less empirical four-stage approach for the development of crop factors. The use of short grass reference evaporation reduces the impact of climatic change on crop water use, but has no influence on the length of growth stages. This reference evaporation is in harmony with the growing plant (Van Heerden *et al.*, 2009), so that there is automatic compensation for climatic differences. When full, effective ground cover is reached, the crop factor would be 1.

The four stages of crop development are described as follows:

Initial stage:	Germination and early growth, when the ground surface is barely covered by the crop (ground cover $< 10\%$).
Crop development stage:	From the end of the initial stage to the reaching of effective full ground cover (ground cover 70 to 80%).
Mid-season stage:	From reaching full effective ground cover until the beginning of maturity, as indicated by colour change of leaves and leaf drop.
Late-season stage:	From the end of the mid-season stage to full maturity or harvest.

The basic approach for the estimation of crop water use is still the same as with A-pan and crop factors:

$$ET_{crop} = K_c \cdot ET_0 \tag{2.8.28}$$

where

ET_{crop}	crop evapotranspiration
K_c	crop coefficient
ET_0	reference evaporation

Sapwat3 subdivides South Africa into seven agro-climatic regions to develop default crop factors for each of these regions. Default planting dates for each region and crop are also specified and, where planting date has a noticeable influence on growth stages, individual crop files were developed according to planting month per region. Where noticeable differences between cultivars (e.g. early or late) are found, each is handled as a separate crop (Van Heerden *et al.*, 2009).

The crop factor file was developed according to principles that were derived with the help of crop scientists. Validation of these values takes place continuously and is based on practices in the field and on the experience of irrigation

consultants. The default crop factor files provide for manipulations (Van Heerden *et al.*, 2009).

Sapwat3 uses the Penman-Monteith equation to determine ET_0 and has been published as the standard calculation method in FAO Irrigation and Drainage Report No 56 (Allen *et al.*, 1998).

$$ET_0 = \frac{0.408\Delta(R_n - G) + \gamma\frac{900}{T+273}u_2(e_s - e_a)}{\Delta + \gamma(1 + 0.34u_2)} \tag{2.8.29}$$

where

ET_o	Reference evapotranspiration $[mmday^{-1}]$.
R_n	Net radiation at the crop surface $[MJm^{-2}day^{-1}]$.
G	Soil heat flux density $[MJm^{-2}day^{-1}]$.
T	Mean daily air temperature at 2 m height [°C].
u_2	Wind speed at 2 m height $[ms^{-1}]$.
e_s	Saturation vapour pressure $[kPa]$.
e_a	Actual vapour pressure $[kPa]$.
$e_s - e_a$	Saturation vapour pressure deficit [kPa].
Δ	Slope vapour pressure curve $[kPa°C^{-1}]$.
γ	Psychrometric constant $[kPa°C^{-1}]$.

The calculated reference evapotranspiration, ET_0, provides a standard to which:

1. Evapotranspiration at different periods of the year or in other regions can be compared.

2. Evapotranspiration of other crops can be related.

The equation uses standard weather data records of solar radiation (sunshine), air temperature, humidity and wind speed and is described as being a close, simple representation of the physical and physiological factors governing the evapotranspiration process. By using the FAO Penman-Monteith definition for ET_0, one may calculate crop coefficients by using Equation 2.8.28 (Allen *et al.*, 1998).

When weather data is added to Sapwat3, the program runs sequentially through all the records and does the necessary calculations to determine and store values for use in the calculation of the Penman-Monteith equation. The necessary weather data that is not specified by the user is defined by Sapwat3 using mean weather data (radiation, wind, soil heat flux density, etc.) of the user-specified weather station location.

2.8.3.6 Irrigation Systems

Sapwat3 provides a data table that could be used by the software as a reference table. This gives the user the ability to add, edit or delete data or to adapt values to suit local conditions. Table 2.4 shows the irrigation systems and their efficiencies as included in Sapwat3. In Riviersonderend, the most common irrigation systems are centre pivot and drip (Ferreira, 2011). It is a common tendency for farmers to use a drip irrigation system when possible to improve the the efficiency of fertilizer application. A centre pivot system uses more water than a drip system, Section 3.2.3 explains this in more detail.

Table 2.4: Irrigation systems and efficiencies included in Sapwat3

System	Application efficiency (%)	Distribution uniformity (%)
Centre pivot	80	100
Drip	95	100
Flood: basin	75	100
Flood: border	50	100
Flood: furrow	55	100
Linear	85	100
Micro-spray	90	100
Micro-sprinkler	85	100
Sprinkler: big gun	70	100
Sprinkler: boom	75	100
Sprinkler: dragline	75	100
Sprinkler: hop-along	75	100
Sprinkler: permanent	85	100
Sprinkler: quick-coupling	75	100
Sprinkler: side roll	75	100
Sprinkler: travelling boom	80	100
Sprinkler: travelling gun	75	100
Subsurface	95	100
Sprinkler: perm. (floppy)	85	100

On-farm distribution systems are defined as the distribution from water source, which could be the off-take from a bigger distribution canal or a borehole or a pump out of a river, to field edge. The irrigation system itself is assumed to be that system which distributes water on the field, with the field edge as the assumed boundary.

In the Riviersonderend catchment, the water is pumped from the Riviersonderend River and is delivered to the irrigation field with pipes. A distribution

efficiency of 75% is used in this thesis for Sapwat3 calculations, see Table 2.5 for a list of distribution efficiencies values (Van Heerden *et al.*, 2009).

Table 2.5: Distribution system efficiencies

Distribution system	Farm (%)
Piped supply	100
Lined sump	95
Unlined sump	90
Lined dam, lined canals	90
Lined dam, unlined canals	85
Unlined dam, lined canals	80
Unlined dam, unlined canals	75
Lined canals	95
Unlined canals	85
Dam, river	75

Chapter 3

Hydrodynamic Modelling of the Riviersonderend River

3.1 Introduction

This chapter aims to provide the various methodologies used to construct a hydrodynamic model of the Riviersonderend River. The first section discusses how and where the data was obtained that was required. This data includes flow data, weather data and irrigation data. This section also discuss the method used to determine the tributary catchment area in the Riviersonderend catchment used in Mike 11 NAM. The tributary catchment are determined excluding the on-farm dam catchments and riparian vegetation. The runoff generated by the catchment area, consisting of riparian vegetation, is also used in Mike 11 NAM.

Mike 11 NAM was used to estimate the rainfall-runoff relationships for the Riviersonderend catchment. The process used to calibrate the Mike 11 NAM model using the Baviaanskloof River (tributary) near Genadendal is discussed. Sapwat3 was used to determine the daily irrigation water usage pattern, of the farmers downstream of Theewaterskloof Dam, using the crop water requirements of the most abundant crops in the region, apples and maize. The measured water volume used for irrigation is distributed for according to each farms water usage pattern. Previous studies were investigated to determine the return flow generated by the irrigation. A return flow of 30% for the water irrigated was adopted.

The final section explains how the Mike 11 model was constructed and explains the process applied to construct the hydrodynamic model. This section also discusses how the daily rainfall and evaporation were simulated in the Mike 11 model. The time interval of the meteorological data (daily) is significantly larger than the output time interval used in Mike 11 NAM (twelve minute) and Mike 11 (five minute) which caused inaccuracies.

Copies of all the records (e.g. rainfall, evaporation, water usage, discharge,

cross-sections) used in the construction of the Riviersonderend hydrodynamic model are available digitally on the CD attached to this thesis.

3.2 Obtaining Data

Data collection is an integral aspect of model development. Quality data leads to quality model output, which leads to informed decision making refer to Section 2.6.3.1. Reliable data is the foundation for model development (Stevens and DHI, 2012).

The data that has been collected for this thesis comprises rainfall, evaporation, water discharge and water usage for irrigation and was obtained from the DWA, with the exception of the measured rainfall data at Tygerhoek gauging station. The Tygerhoek rainfall data were obtained from the University of Stellenbosch (US).

Figure 3.1 shows the location of the gauges and weather stations used in this thesis. It is good practice to visit the measuring stations after they have been identified to have an independent assessment of the accuracy of the gauge or weather station. The data used in this thesis were stated to be accurate and reliable by the DWA and the US. A site visit was undertaken to the Riviersonderend catchment, specifically to meet the ZWUA and discuss the challenges they faced in water management (Ferreira, 2011). All the gauging station were in good working order during the time period used (2000 to 2010). The gauging station at Genadendal (H6H005) was damaged in June 2011, and should be investigated before attempting to use the data for future projects.

The gauging stations Rheenen (H6H012), Dwarstrek (H6H009), Genadendal (H6H005) and Genadendal canal (H6H019) were measured continuously with a time step of 12 minutes. Due to the nature of hydrodynamic models, the input weather forecast data should ideally be measured continuously. The rainfall from Theewaterskloof (H6R001) and Tygerhoek was measured daily, and the evaporation at Theewaterskloof (H6E001) was also measured daily. These daily measurements accounted for inaccuracies in the river model. This data will be discussed in more detail the following section.

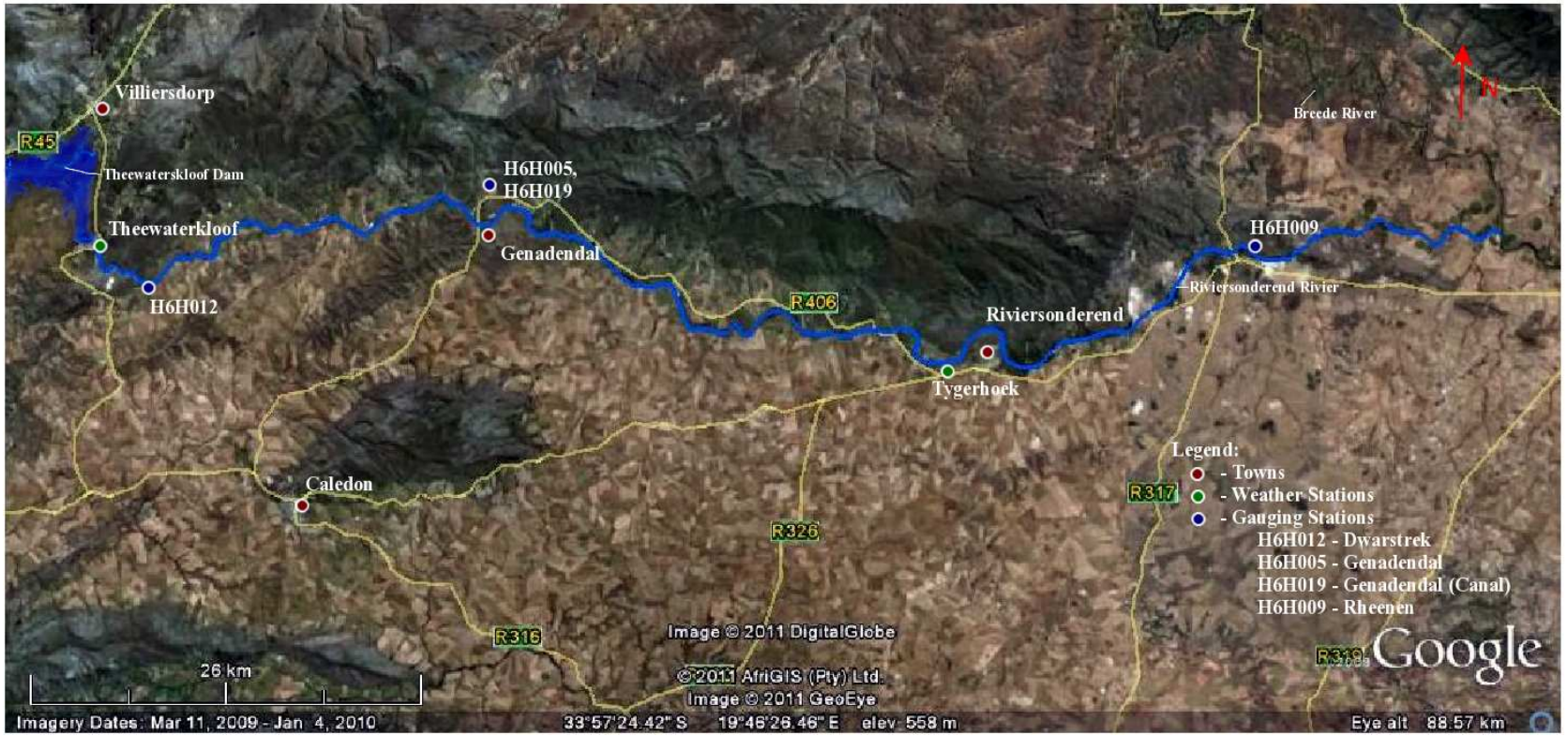

Figure 3.1: Google Earth snapshot of the Riviersonderend River indicating weather stations, flow gauges and water bodies

3.2.1 Flow Data

Flow data were obtained from the DWA (DWA, 2011). There are nine gauging station within the H60 drainage region, namely:

- H6H005 - Baviaanskloof River at Genadendal.
- H6H009 - Riviersonderend at Reenen.
- H6H010 - Waterkloof River at Waggensbooms Kloof.
- H6H012 - Riviersonderend at Dwarstrek.
- H6H015 - Elands River at Twist Niet.
- H6H016 - Left canal from Verdeelkas at Twist Niet.
- H6H017 - Right canal from Verdeelkas at Twist Niet.
- H6H018 - Canal overflow to Elands River at Twist Niet.
- H6H019 - Canal from Baviaanskloof River at Genadendal.

Downstream from Theewaterskloof Dam, two operational stations are available in the Riviersonderend River. Firstly, with the construction of Theewaterskloof Dam a gauging station called Dwarstrek was built about three kilometres from the dam. Figure 3.2 shows a photo of the Dwarstrek gauging station, with a catchment area of 25 km^2, downstream from Theewaterskloof Dam. Secondly, an older gauging station called Rheenen is available 101.5 kilometres from the dam, with a catchment area of 1507 km^2, downstream from Theewaterskloof Dam (see Figure 3.3). Figure 3.4 shows the longitudinal profile of the Riviersonderend River, downstream from Theewaterskloof Dam, with the location of Rheenen and Dwarstrek gauging stations.

Figure 3.2: Dwarstrek (H6H012)

Figure 3.3: Rheenen (H6H009)

The flow of one tributary, the Baviaanskloof River, is measured downstream

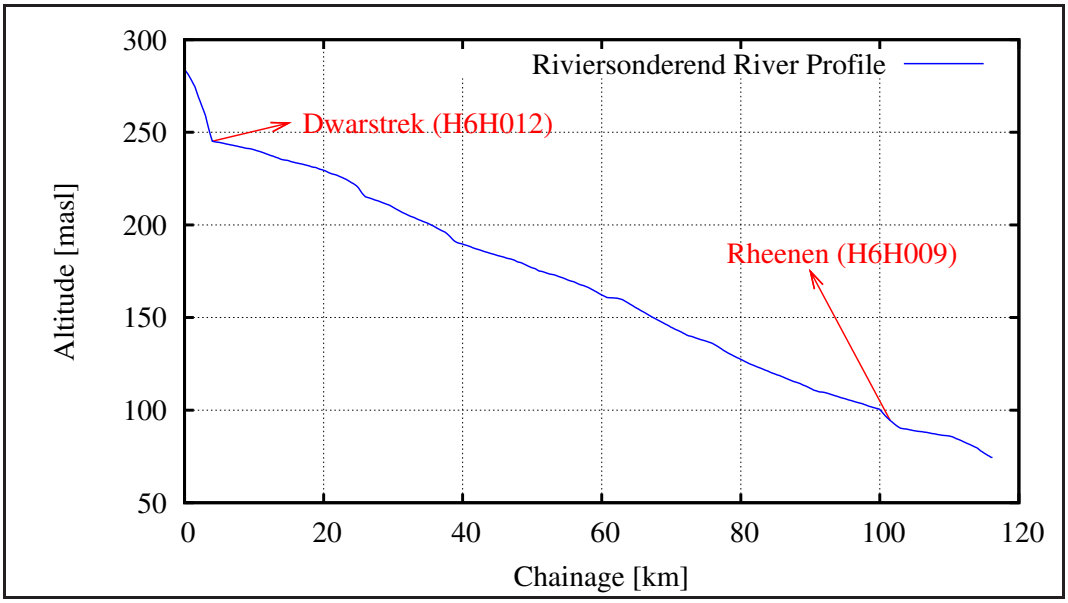

Figure 3.4: Riviersonderend River longitudinal profile downstream from Theewaterskloof Dam

from Theewaterskloof Dam. The Genadendal gauging station (H6H005) has a catchment area of 24 km^2. Additionally, a canal gauging station (H6H019) is operational at the same location. Both these stations are located near Genadendal. See Figure 3.1 for the location of the Genadendal gauging station, including the Baviaanskloof River gauging (H6H005) and canal gauging (H6H019) stations.

The discharge measured at the canal (H6H019) was added to the discharge at the Genadendal gauging station (H6H005) to calculate the discharge from the Baviaanskloof River.

3.2.2 Weather Data

The Riviersonderend mountains have a major effect on the rainfall patterns in this area. Cold fronts coming from the ocean to the south move over the catchment and against the Riviersonderend mountains. The mountains force the cold air upwards, where it condenses and forms rain. The rainfall and evaporation data used in this thesis were obtained from two existing weather stations in the Riviersonderend catchment.

The Riviersonderend region has a natural mean annual precipitation (MAP) of 500.8 mm downstream of Theewaterskloof (WR90, 1994). Two weather stations are located in the Riviersonderend region. Firstly, Theewaterskloof Dam has a weather station measuring rainfall and evaporation, the data for which were obtained from WeatherSA. The second weather station that was used is on the Tygerhoek research farm, which is located close to the town of

Riviersonderend. Daily rainfall data were obtained from Tygerhoek and the Theewaterskloof Dam (see Figure 3.1). The rainfall distribution in the Breede WMA is illustrated in Figure 3.5.

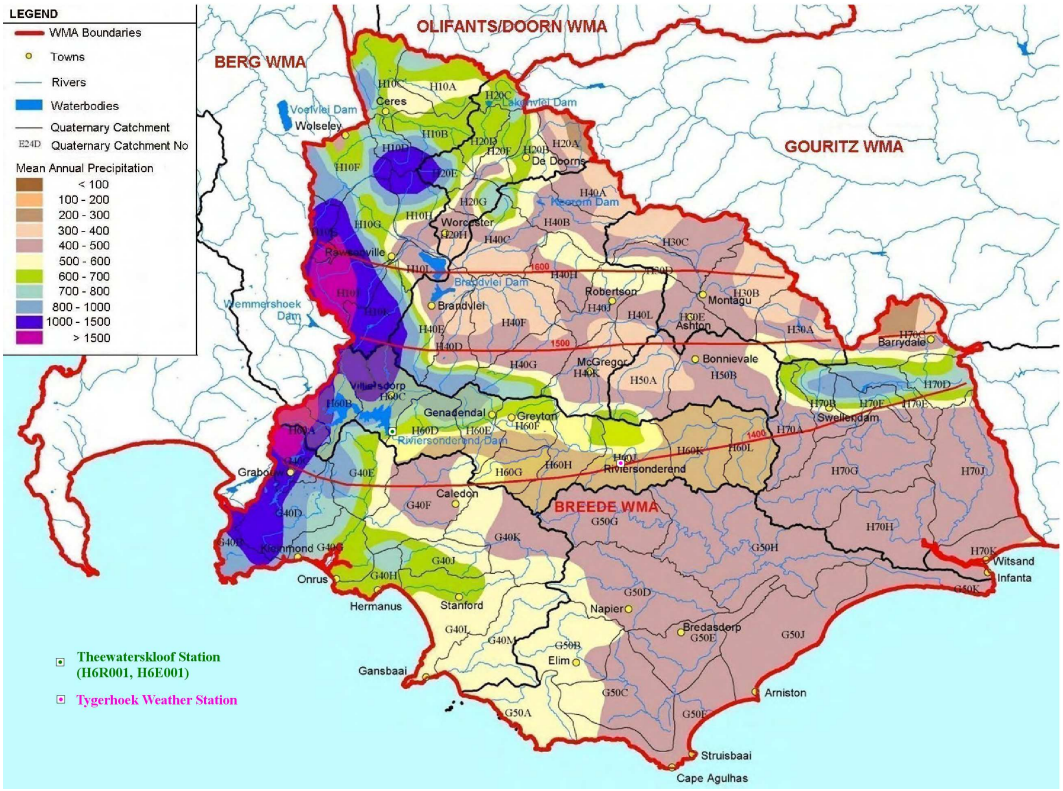

Figure 3.5: Rainfall distribution in the Breede WMA (DWA, 2004*a*)

The evaporation data from the Theewaterskloof weather station, measured in millimetres, was also available as daily measurements. The evaporation was measured using a Symons pan (S-pan); this measured data was multiplied by pan factors to convert the pan measurements to more accurately represent in-field data. See Table 3.1 for the pan factor used in this study.

The weather station rainfall data sets have a correlation coefficient of 0.647 in relation to the daily precipitation from 2000 to 2010 (see Table 3.2 for annual correlation factors). Figure 3.6 shows the monthly rainfall at Theewaterskloof Dam and the Tygerhoek weather station for 2006 to illustrate the correlation between rainfall stations. A correlation greater than 0.8 is generally described as strong, whereas a correlation less than 0.5 is generally described as weak (Du Plessis, 2008).

The possibility of utilising other stations outside of the Riviersonderend catchment (H60) was investigated. The weather stations located in the Breede River Component, north of the Riviersonderend catchment (Figure 2.2), were

Table 3.1: Pan factors specified by WR90 (Du Plessis, 2008)

Month	Lake evaporation	Catchment evaporation
October	0.8	0.81
November	1.00	0.82
December	1.00	0.83
January	1.00	0.84
February	1.00	0.88
March	1.00	0.88
April	1.00	0.88
May	1.00	0.87
June	1.00	0.85
July	0.8	0.83
August	0.8	0.81
September	0.8	0.81

Table 3.2: Daily rainfall correlation coefficient for the Theewaterskloof and Tygerhoek weather stations

Year	Correlation coefficient
2000	0.144
2001	0.282
2002	0.139
2003	0.314
2004	0.825
2005	0.922
2006	0.683
2007	0.910
2008	0.766
2009	0.533
2010	0.754

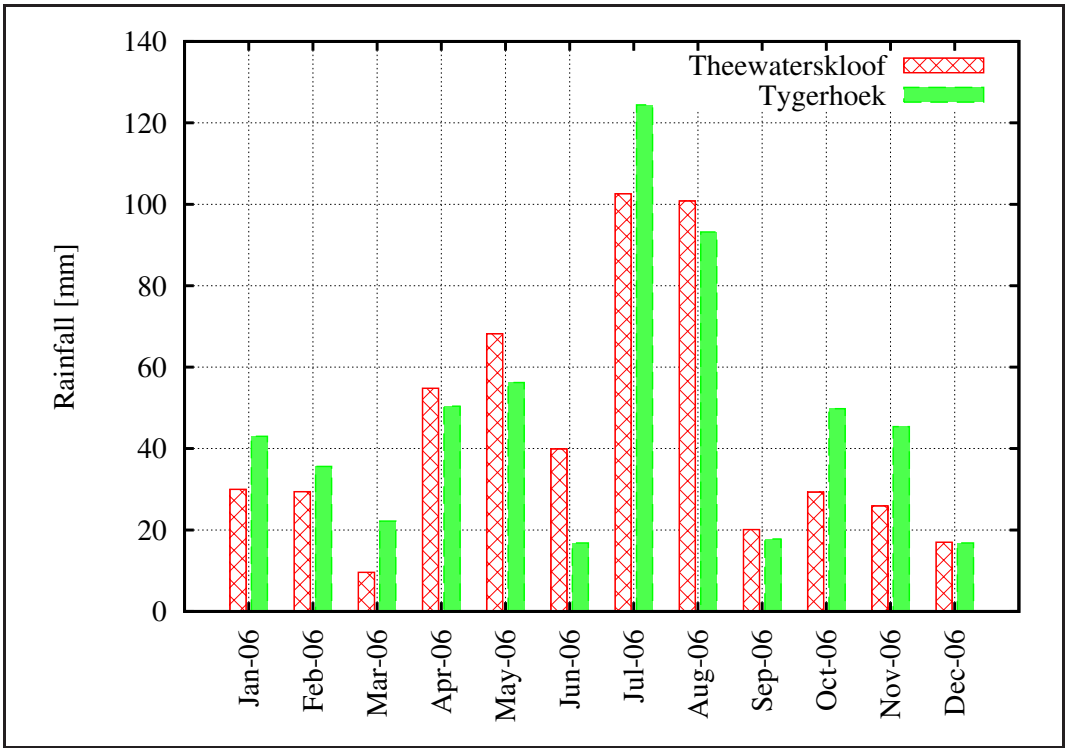

Figure 3.6: Monthly rainfall data of 2006

not used due to the effect the Riviersonderend mountains have on the rainfall distribution (see Figure 3.5).

In the Overberg component of the Breede MWA (Figure 2.2) the weather stations are located close to the coastline. The rainfall increases significantly to the west of the Riviersonderend catchment and does not represent the rainfall distribution downstream from Theewaterskloof Dam.

Theewaterskloof (H6R001) weather station is located in a area that receives a greater MAP than Tygerhoek station (see Figure 3.5). This is used with the rainfall-runoff software where the weighted effect stations' rainfall pattern was distributed amongst each tertiary catchment (ex. H60E). This is discussed in greater detail in Section 3.3.1.

3.2.3 Irrigation Data

In 2006, the ZWUA installed flow measurement devices on the pumps in the Riviersonderend River. Measured irrigation data of the Riviersonderend area was obtained from the ZWUA (Ferreira, 2011).

The water usage was measured using eLectroFlo measurement devices. These devices have no moving parts and are calibrated using the pump power/flow ratio when installed. They operate on the unique relationship that exists be-

tween the power consumption of the motor and the flow rate of the pump (Flo-Check, 2006). A detailed description of the eLectroFlo system is provided by Mehrdad (2010).

As mentioned in Section 2.2, the flood in December 2007 damaged and removed a significant number of eLectroFlo devices. During the course of this study the ZMUA was in the process of replacing the damaged devices (Ferreira, 2011). Therefore, the year 2006 is the most recent period that includes all the available data required to construct the Mike 11 hydrodynamic model.

Although the pump discharge is measured continuously, the results are logged manually. This is a very time-consuming exercise, but it is the most cost-effective way of logging the 161 pumps. The results are logged monthly, with the exception of December and January, which were not logged in most cases (see Figure 3.7 for the measured water usage on Dwarstrek Farm).

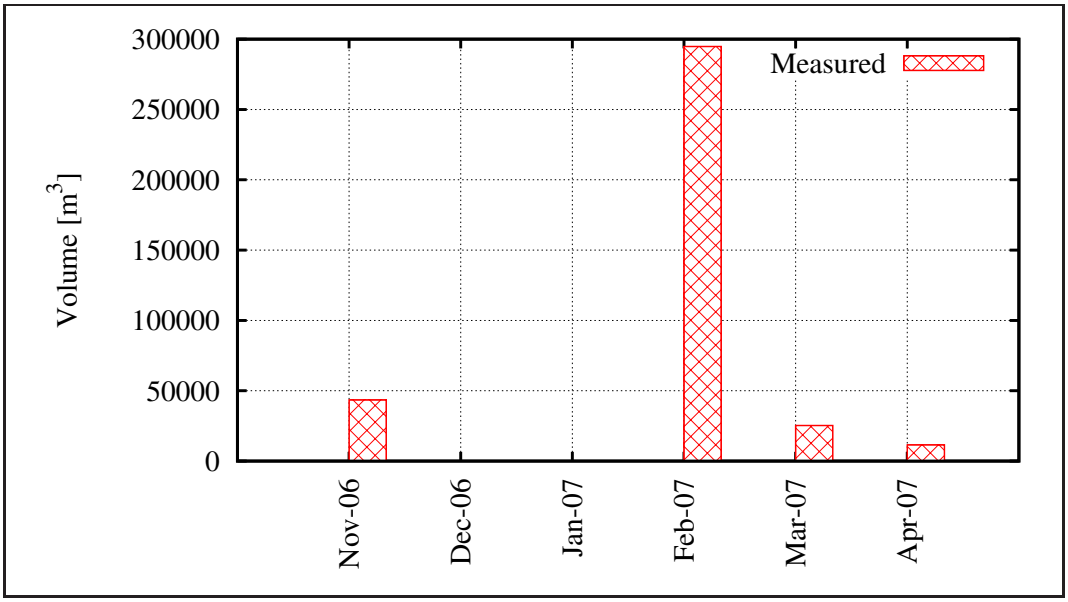

Figure 3.7: The eLectroFlo measurements for Dwarstrek Farm

Sapwat3 (refer to Section 2.8.3) was used to determine the theoretical irrigation requirements of each farm. The measured data (Figure 3.7) was then distributed according to the individual farm irrigation water requirement, determined by Sapwat3, and used in the simulation (see Figure 3.8).

The measured water volume that is pumped for irrigation is allocated according to the irrigation field size (Ha) and irrigation system used (centre pivot or drip). A centre pivot irrigation system uses up to four times more water than drip in order to irrigate the same field, and this was confirmed in Sapwat3 (Van Heerden *et al.*, 2009). For example, when a farm comprising 2 Ha irrigation

field of any crop (1 Ha drip, 1 Ha centre pivot) distributes 10 000 m^3 of water, the centre pivot system will use appropriately 8 000 m^3 and the drip system will use 2 000 m^3 to irrigate the field.

After interviews with farmers in the area, the Sapwat3 water requirements were modified so that January and February required the same amount of water shown in Figure 3.8 (Ferreira, 2011).

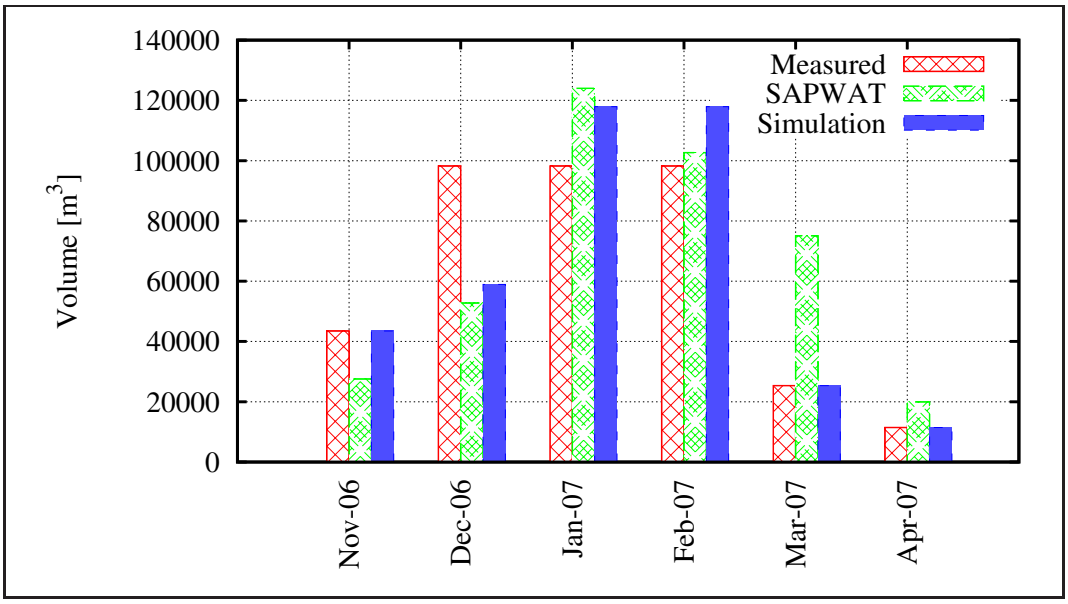

Figure 3.8: Dwarstrek Farm usage for Riviersonderend River simulation (Note: February is split into 3 equal measurements.)

See Appendix B for the monthly water usage of every abstraction point used in the Riviersonderend River simulation in 2006. Sapwat3 was used to determine the daily irrigation schedule of the Riviersonderend farms. The estimation technique for determining the daily irrigation requirements is discussed in Section 3.3.2.

Apart from the farmers that utilise water from the Riviersonderend River other water users such as towns (Riviersonderend), businesses (Nitrophosca) and correctional institutions (Helderstroom Prison) also utilise the river. For these measured non-irrigating water users a constant daily water usage pattern were used in the Mike 11 model.

3.2.4 Augmenting Catchment Areas

A total of 28 tributaries were identified downstream from Theewaterskloof Dam using Google Earth. After the catchments had been investigated, the coordinates of the positions where the tributaries meet the Riviersonderend

River were determined.

Using 1:50 000 maps, each tributary catchment outline downstream from the on-farm dams was determined. On-farm dams are abundant in the Riviersonderend catchment, and this reduces the runoff of the tributaries generated by rainfall. The tributary catchments were reduced by excluding the smaller catchments of the on-farm dam(s) in the rainfall-runoff software calculations. The assumption was made that the on-farm dam stores all the water within its catchment. In total, the on-farm dams upstream of Rheenen (H6H009) towards the Theewaterskloof Dam have a capacity of 16.6 million m^3 and cover a total area of 197 km^2 (DWA, 2003). On-farm dams in the Riviersonderend catchment downstream from the Theewaterskloof Dam covers a total area of 232 km^2.

The total on-farm dam catchment area downstream from Rheenen (H6H009) towards the Riviersonderend/Breede confluence was measured manually using 1:50 000 maps, and a total area of 35 km^2 was calculated.

AutoCAD was used to draw the catchment boundaries and to determine the catchment area. Figure 3.9 shows the Elandskloof River catchment, which flows into the Riviersonderend River 18 km downstream from Theewaterskloof Dam. Figure 3.9 also illustrates how the on-farm dam catchment areas have been excluded from the tributary catchment area.

The catchments were named alphabetically (Catchment A, Catchment B, etc.); (see Figure 3.10). Table 3.3 shows the tributaries, their location and the contributing areas used in the rainfall-runoff simulation. The location of the tributary along the Riviersonderend River is illustrated by providing the distance from Theewaterskloof Dam. Figure 3.10 indicates the position of the tributaries along the river and the catchment area.

A total area of 1 040 km^2 is represented by the tributaries in the Riviersonderend catchment and a total area of 232 km^2 is allocated to the on-farm dams. The area of Riviersonderend catchment, downstream of Theewaterskloof Dam, is 1 750.8 km^2 (Midgley *et al.*, 1994), leaving 478.8 km^2 (see Table 3.4). This remaining area of 478.8 km^2 consists mainly of small tributaries (less than 6 km^2) and the riparian plant zone along the river.

Table 3.3: Augmenting streams on the Riviersonderend River

Catchment	Name	Chainage [m]	Area [km^2]
Catchment A	Teewaterkloof River	500	11
Catchment B	Bergfontein River	5 000	9
Catchment C	Langkloof River	16 500	36
Catchment D	Elandskloof River	18 000	28
Catchment E	Klein-Elandskloof River	20 000	17
Catchment F	Meul River	22 000	23
Catchment G	Baviaanskloof River	31 500	24
Catchment H	Sersants River	31 500	29
Catchment I	Gobos River	37 000	64
Catchment J	Tuinskloof River	39 000	6
Catchment K	Soetmelks River	45 000	29
Catchment L	Kwartel River	47 500	165
Catchment M	Droogas River	50 500	65
Catchment N	Krom River	59 500	20
Catchment O	Slang River	62 500	19
Catchment P	Bok River	66 000	17
Catchment Q	Grootvlei	67 500	19
Catchment R	Maandagsout River	70 000	64
Catchment S	Olifants River	75 000	32
Catchment T	Verdwaalskloof River	80 000	17
Catchment U	Die Poort River	80 500	11
Catchment V	Kleinlaagte River	81 500	9
Catchment W	Jongenskloof River	82 500	18
Catchment X	Meulkloof River	86 000	11
Catchment Y	Bloed River	87 000	16
Catchment Z	Kwassadie River	101 000	160
Catchment AA	Hekswas River	110 000	87
Catchment AB	Freek Botha River	116 000	34
Total			**1 040**

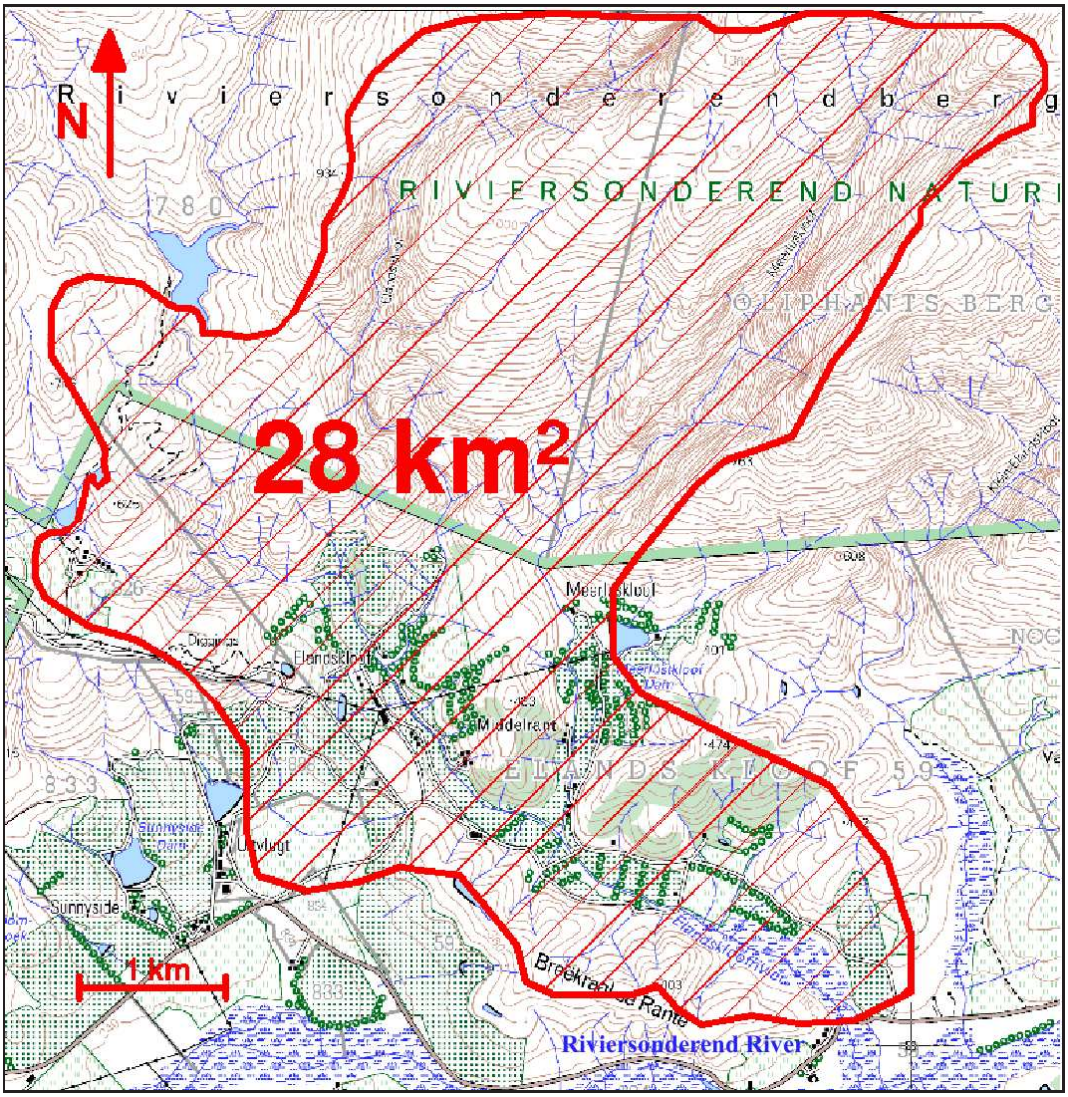

Figure 3.9: Catchment area of a typical Riviersonderend tributary, Elandskloof River

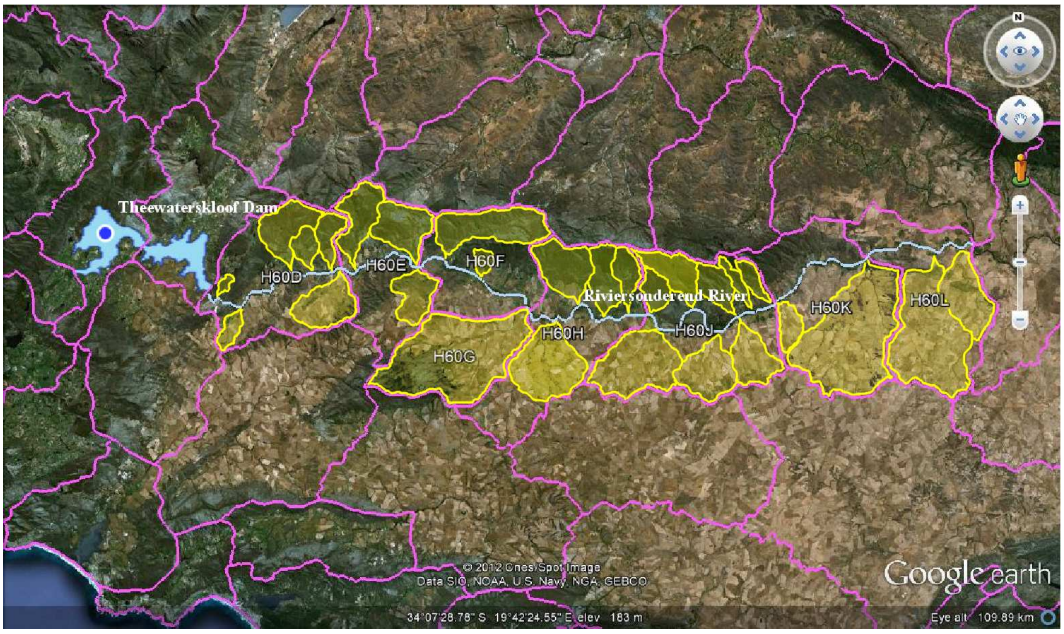

Figure 3.10: Tributary catchments along the Riviersonderend River used in Mike 11 NAM

Table 3.4: Augmenting catchment area in the Riviersonderend catchment, downstream from Theewaterskloof Dam

Augmenting catchments	Total area (km^2)
Tributary catchments	1 040
On-farm dam catchments u/s Rheenen (H6H009)	197
On-farm dam catchments d/s Rheenen (H6H009)	35
Remaining area	478.8
Riviersonderend downstream of Theewaterskloof Dam	1 750.8

3.3 Estimations Used for Modelling

3.3.1 Augmenting Flow Pattern

Mike 11 NAM was used to estimate the flow pattern, generated by rainfall, of the Riviersonderend catchment tributaries (refer to Section 2.8.2) with a 12 minute interval. Mike 11 NAM requires a tributary with measured discharge, rainfall and evaporation data. By adjusting various catchment parameters, the tributary is calibrated to match the observed and simulated flow. These calibrated catchment parameters are used to determine the flow of the remaining 27 tributaries in the Riviersonderend catchment downstream from Theewaterskloof Dam.

Baviaanskloof River, near Genadendal, is the only measured tributary downstream from Theewaterskloof Dam in the Riviersonderend catchment. The measured flow for the Baviaanskloof River was calculated by adding the weir overflow (H6H0005) and the canal abstraction (H6H019) and used as the required 'observed discharge' required by Mike 11 NAM. The time period used to calibrate the Baviaanskloof River is from 2000 to 2010, with a time step of 12 minutes.

Theewaterskloof (H6E001) daily evaporation data was multiplied by the pan factors for catchment evaporation to be used in the rainfall-runoff software (refer to Table 3.1).

The daily rainfall weather data from Theewaterskloof (H6R001) and Tygerhoek were included by assigning a contribution/distribution percentage of 55%/45% respectively for calibration. With Theewaterskloof (H6R001) located in a higher rainfall area than Tygerhoek, Figure 3.5 is used to assign each tertiary catchment its own rainfall station contribution percentage. See Table 3.5 for the contribution/distribution percentages of each tertiary catchment in the Riviersonderend catchment downstream from Theewaterskloof Dam. Figure 3.10 shows the location of the tertiary catchments in the Riviersonderend catchment (Midgley *et al.*, 1994).

As mentioned earlier, the auto calibration function in Mike 11 NAM adjusts various catchment parameters iteratively to match the observed discharge as closely as possible. The calibration objectives for Mike 11 NAM are discussed in Section 2.8.2.7. The parameters that were determined by Mike 11 NAM to best simulate the Baviaanskloof River are shown in Table 3.6. Figure 3.11 shows the output graph generated after 10 000 iterations by Mike 11 NAM over a 10-year time period. The Mike 11 NAM simulated discharge has a time step of 12 minutes, although it is possible to specify a time step as small as one second.

Figure 3.11 shows the calibrated results of Mike 11 NAM. The accumulative discharge of the observed and simulated flow pattern indicates a good water

Table 3.5: Rainfall contribution percentages of Theewaterskloof (H6R001) and Tygerhoek for the Riviersonderend catchment

Tertiary catchment	Theewaterskloof contribution (%)	Tygerhoek contribution (%)
H60D	60	40
H60E	55	45
H60F	30	70
H60G	5	95
H60H	10	90
H60J	40	60
H60K	0	100
H60L	0	100
H60	**25**	**75**

Table 3.6: Parameters used for Mike 11 NAM calculations after calibration

Parameter	Abbreviation	Description / Value
Rainfall stations		Tygerhoek Theewaterskloof
Evaporation station		Theewaterskloof
Surface Root Zone		
Maximum water content in surface storage	U_{max}	0.1 mm
Maximum water content in root zone storage	L_{max}	15.9 mm
Overland flow runoff coefficient	$CQOF$	1
Time constant for routing interflow	$CKIF$	202.9 hours
Root zone threshold value for overland flow.	TOF	0.212
Root zone threshold value for interflow	TIF	0.019
Groundwater		
Root zone threshold value for GW recharge	TG	0.557
Time constant for routing baseflow	CK_{BF}	1 000.987 hours

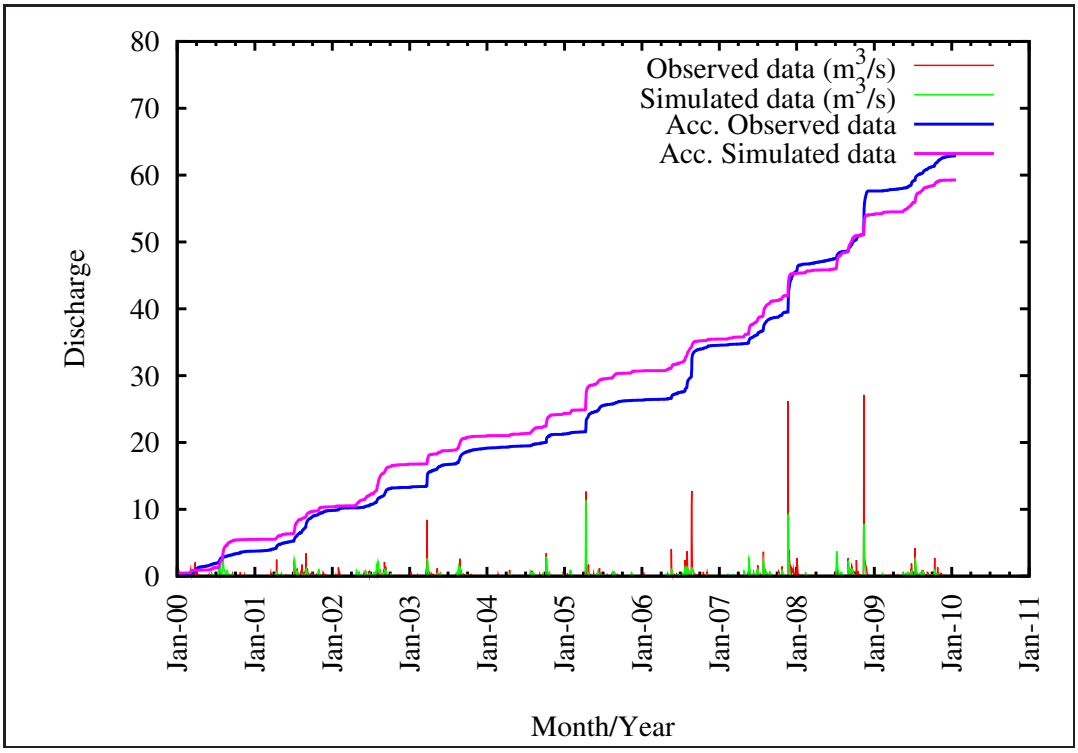

Figure 3.11: Mike 11 NAM output graph for Genadendal tributary

balance, although there are inaccuracies. The irrigation season in 2006-2007 seems to be well calibrated, while the 2005-2006 irrigation season illustrates significant inaccuracy. The measured flow peaks do not match the simulated flow peaks, as shown in Figure 3.11.

The reason for these inaccuracies is the available weather data time intervals. Daily rainfall and evaporation data were used, while Mike 11 NAM attempts to calibrate the catchment parameters against a flow pattern measured every 12 minutes. Mike 11 NAM also produces a time series file with small time intervals (1 hour). The effect of these larger time intervals (daily rainfall and evaporation) tends to smooth and lower the simulated flow pattern.

Although there were inaccuracies in the Mike 11 NAM output, the calibrated catchment parameters were used to estimate the flow patterns of the remaining tributaries.

Appendix D includes the simulated flow patterns for the remaining 27 tributaries used in the Riviersonderend River model for the 2006-2007 irrigation season (November 2006 to April 2007). The time period used for the irrigation season starts a month earlier (October 2006) to establish accurate initial conditions.

The runoff of the remaining area of 478.8 km^2 (see Table 3.4) was included in the rainfall-runoff simulation. The rainfall station contribution percentage is

25% and 75% for Theewaterskloof (H6R001) and Tygerhoek respectively (refer to Table 3.5). Unlike the tributaries, the determined discharge was distributed along the Riviersonderend River.

3.3.2 Daily Irrigation Requirements

With the monthly water usage available, the daily usage pattern had to be estimated using Sapwat3. The daily usage pattern for irrigation varies from year to year, depending on rainfall, soil characteristics, crop type, evapotranspiration of crops and on-farm characteristics. To be able to estimate the daily usage pattern for irrigation there had to be assumptions for and generalisations on the farms.

As determined in Section 2.4 of the literature study, there are multiple crop types in the region. Different crop types have unique water requirements, thereby affecting the water usage pattern of the water user. The specific crops farmed in 2006 were not available. However, as mentioned in Section 2.4, the most abundant crops are maize and apples (Ferreira, 2011). The generalisation was made to use these two crops to determine the irrigation requirements for each farm.

A challenge arose when assigning the actual number of hectares under irrigation. The only data available for area under irrigation was the total hectare allocated to each farm by the DWA. Appendix A lists the water users in the Riviersonderend River basin and the DWA-allocated hectares of each water user.

A farm's actual hectares under irrigation vary each year, depending on agricultural planning and financial restrictions. Google Earth was used to measure the actual area of the orchards on each farm during 2006. Orchards were identified by viewing the satellite images taken during 2006. The rest of the DWA-allocated hectares were assumed to be maize.

Using the two assumptions mentioned above, Sapwat3 was used to determine a daily irrigation schedule to be used for all farms. Using the daily rainfall data from the Tygerhoek research farm, the irrigation schedule for one hectare of apples and one hectare of maize was determined. Sapwat3 uses daily weather data as the basis for calculating daily Penman-Monteith evapotranspiration (ET_0) (see Section 2.8.3.3). The crop evaporation coefficient, k_c, changes with time, depending on the growth stage of the crop.

Apart from the crop water requirement pattern, the irrigation method implemented on-farm also has a big impact on the amount of water used for irrigation. For example, sprinkler irrigation uses much more water than drip irrigation. According to Sapwat3, drip irrigation issues 5 mm of water during every irrigation event, while a centre pivot system delivers 20 mm of water during every irrigation event for the same crop. In other words, a centre pivot

Table 3.7: Sapwat3 parameters for non-grain type crops

Parameter	Description / Value
Weather station	Tygerhoek
Climate	Dry, cold
Water distribution	Dam, river
Distribution efficiency	75%
Quota	5 700 m^3/Ha/a
Field size	1 Ha
Irrigated size	1 Ha
Leeching requirement	5%
Irrigation system	Drip
Irrigation event	5 mm
System efficiency	80%
Soil	Sandy loam
Effective depth	1.2 m
Infiltration	40 mm/day
Crop used	Apples
Plant date	September 2006

system uses four times more water than a drip system when irrigating the same crop with an equal area.

In order to simulate the irrigation system is water efficiency, a weighted factor was used when distributing the water volume used for irrigation. The monthly measured values were distributed amongst the daily irrigation schedules using this weighted factor. For example, a farm with 50% of its area consisting of apples (drip irrigation) and with the remaining 50% being maize (centre pivot) uses approximately 20% of its irrigation water on the apples and 80% on the maize.

Table 3.7 lists all the adjustable parameters used in Sapwat3 for a non-grain crop (apples), while the same parameters are listed in Table 3.8 for grain-type crops (maize). These parameters were used to determine the daily irrigation schedule, which in turn was used in the Riviersonderend simulation. The soil's initial readily available water (RAW) is 85% for maize and apples (Van Heerden *et al.*, 2009).

3.3.3 Irrigation Return Flow

On occation, areas under irrigation generate deep percolated water that drains out beneath the active root zone (Mhlanga *et al.*, 2002). This occurs either with over-irrigation, or when the soil water is displaced downwards by rain falling on already wet soil (Mhlanga *et al.*, 2002; Schulze, 1995). In addition

Table 3.8: Sapwat3 parameters for grain-type crops

Parameter	Description / Value
Weather station	Tygerhoek
Climate	Dry, cold
Water distribution	Dam, river
Distribution efficiency	75%
Quota	5 700 m^3/Ha/a
Field size	1 Ha
Irrigated size	1 Ha
Leeching requirement	5%
Irrigation system	Centre pivot
Irrigation event	20 mm
System efficiency	80%
Soil	Sandy loam
Effective depth	1.2 m
Infiltration	40 mm/day
Crop used	Maize
Plant date	November 2006

to deep percolation water, enhanced surface runoff can also occur on irrigated areas (Schulze, 1995).

To identify the impact of irrigation return flow, it is necessary to assess the physical properties, mixing characteristics and residence times in the river basin (Pearce and Schumann, 2001). A study by the DWA (2004*c*) on the Orange-Fish River provides a detailed description of the preferred methodologies for estimating irrigation return flows.

The method that is most suitable for estimating return flow is the monthly crop water balance (DWA, 2004*c*). A previous study on the Orange-Fish Sundays scheme was used to estimate the return flow percentage for Riviersonderend.

A suggested return flow factor of 31% resulted for the Orange-Fish-Sundays system irrigation scheme (DWA, 2004*c*). This value is justified by another study on the Mbuluzi River Basin in Swaziland that proposed a return flow of 30% (Mhlanga *et al.*, 2002).

Return flow, according to Herold (1990), is the most important calibration parameter. In order to calibrate the Riviersonderend Mike 11 model, a return factor of 30% was adopted. The irrigation requirement for all farms was reduced by 30% to account for the return flow.

3.4 Hydrodynamic Model Setup

3.4.1 Network

The construction of a river model requires familiarity with the area. More importantly, the characteristics of the river being investigated must be simulated as realistically and accurately as possible. Using Google Earth, the river area was investigated by following the main river and inspecting the various tributaries along the river. Figure 3.1 shows the Riviersonderend River and the Theewaterskloof Dam.

The length of the river was determined and subsequently also the distance between each cross-section. Coordinates for the study area were also obtained using Google Earth. Using the coordinates of the study area, a 1:10 000 map was obtained from the Department of Rural Development and Land Reform.

Using the 1:10 000 map, the main river route was identified and indicated as stretching from the Theewaterskloof Dam to the Riviersonderend/Breede River confluence. A total river length of 116.2 km was measured. Cross-sections taken perpendicular to the flow of the channel were selected to be 500 m apart along the river, therefore there were 232 cross-sections in total. The coordinates of each point where the cross-section and main river intersected were determined using the coordinate system of the 1:10 000 map.

3.4.2 Cross-Sections

The geometry of every catchment is unique and should be simulated as such. More specifically, the geometry that is of interest is the shape or profile of the river cross-section and how it changes along the river. These geometric parameters ultimately determine the flood plains and should identify critical hydraulic areas in the river.

No geomorphological channel survey data was available for the Riviersonderend River to be used in the hydrodynamic model. Alternatively, a 1:10 000 map that included 5 m contour lines of the river was used to determine the profile of the cross-sections every 500 m. Each cross-section had a relative elevation of 15 m from the lowest contour of the cross-section upwards. Initially, the upper geometry of the cross-sections was partly constructed using the contour lines (see Figure 3.12).

After these initial calculations, the lowest point of each cross-section was determined using linear interpolation between the contours that cross the main river. The lowest interpolated point of this cross-section is also shown in Figure 3.12. The lowest point is positioned 2 m laterally from the nearest contour line.

The next step in defining the geometry of the river cross-section is by calculating the width of the river flow. Using the 1:10 000 map and Google Earth

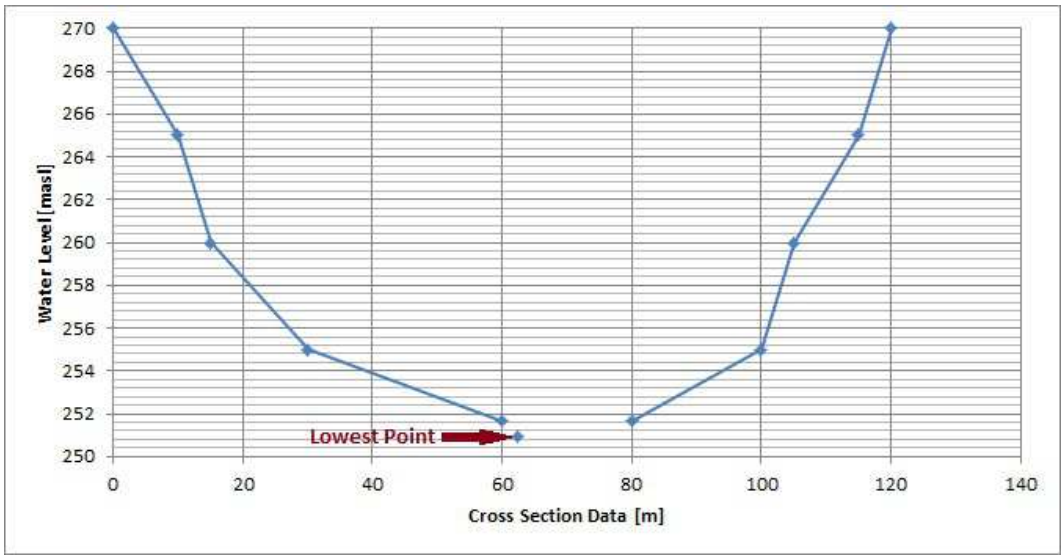

Figure 3.12: Partially constructed cross-section

it is possible to determine the flow width of the river at each cross-section by measuring the river width from the satellite photos. The river width obtained from the 1:10 000 map was compared to the river width measured in Google Earth. The flow width of the river will change with varying discharge.

The width of the river, the upper cross-section profile determined from the contour lines and the lowest point were then connected to construct the final cross-section shape. Additionally, another point was added 0.5 m above the lowest point and 2 m from the opposite river bank to simulate a more realistic river profile for low-flow conditions. See Figure 3.13 for a typical cross-section used in the Riviersonderend Mike 11 river model.

The hippo pools affect the cross-sections of the river, but caused instability in the river model. The solution was to represent the effect of the hippo pools by adjusting the Manning roughness coefficient. A mean Manning coefficient was used that applies to all cross sections in the river.

3.4.3 Boundary Conditions

When doing a one-dimensional hydraulic simulation, it is important to assign boundary conditions. The boundary conditions specified in the Riviersonderend Mike 11 model consist of inflow, outflow, rainfall and evaporation of the water in the river, inflow from tributaries, diffuse non-tributary inflows, water abstractions and return flow.

In the Riviersonderend River, the upstream boundary should be open to allow water inflow. The boundary downstream of the model should also be open. However, it is important to design this bottom boundary to have a

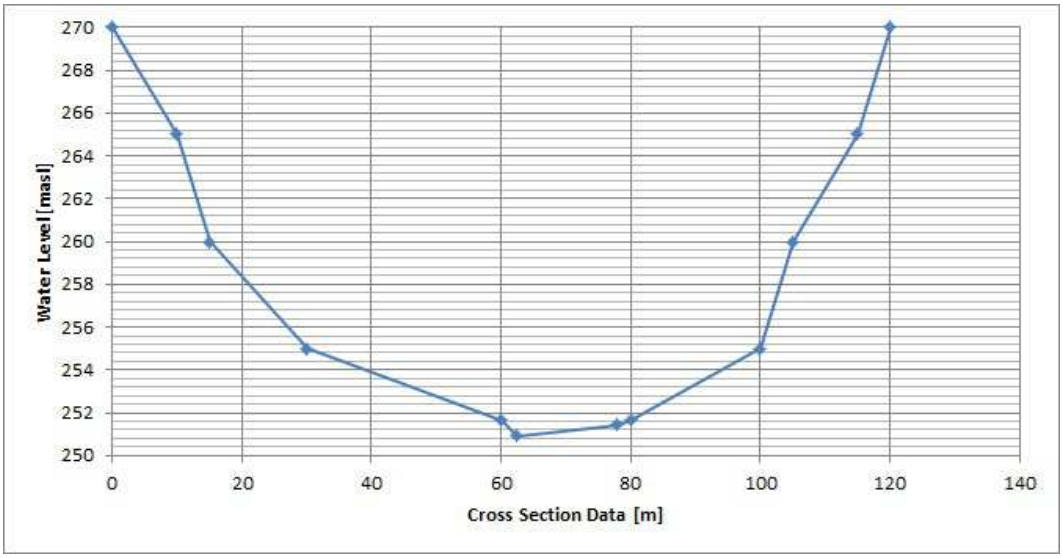

Figure 3.13: Final cross-section used in simulation

flow-depth ratio. This flow-depth water ratio defines the water depth at different discharge intervals. Water reaching the final cross-section responds to the flow-water depth relationship using linear interpolation. Without the flow-water depth relationship, the water will flow freely past the final cross-section, increasing the velocity and decreasing the water depth, resulting in simulation inaccuracies.

Also included in the boundary conditions is the method of simulating evaporation and rainfall on the river water surface. Daily measurements, in millimetre, were available for both rainfall and evaporation. The evaporation measurements were multiplied by lake evaporation pan factors (see Table 3.1). Measurements of the rainfall or evaporation were added/deducted respectively from the river area. For example, the effect of the rainfall is increased during a flood event due to the increase in water surface area of the river.

The inflow from tributaries was determined by using Mike NAM (see Section 2.8.2). The boundary, however, is defined as a point source. This point source is added to the nearest node within 500 m in the river network. Irrigation usage is defined in the same way as the tributaries, but consists of negative values. Mike 11 sees these negative values as outflows from the model, but will only supply the demand if there is water in the river at the point of abstraction. The return flow was simulated by reducing the water abstraction from the river.

3.4.3.1 Flow Conditions

The flow conditions were constructed by creating a time series file. For most of the simulations in the Riviersonderend region, the flow data (breakpoint, or

so-called primary, data) measured at Dwarstrek discharge station was used as the upstream inflow boundary condition.

3.4.3.2 Augmenting Streams

The method used to simulate a tributary was to insert the flow data into the main river at the nearest node. Diffuse non-tributary inflows were simulated using a distributed longitudinal inflow along the river.

3.4.3.3 Evaporation and Rainfall

Evaporation and rainfall are important parts of the model simulation. The most significant characteristic of rainfall and evaporation is the way they vary spatially and temporally over a catchment area (refer to Section 3.2.2). Furthermore, rainfall and evaporation (hot and cold fronts) greatly affect the irrigation required.

The rainfall and net evaporation were simulated as step-accumulated millimetre values on the water surface of the river. The accumulative step method uses the rainfall/evaporation measurement, starting each day at zero and increasing until the daily measurement is reached. See Figure 3.14 for an example of how the accumulative step method is used to simulate rainfall and evaporation. The figure provides an example of how the reality has been approximated to

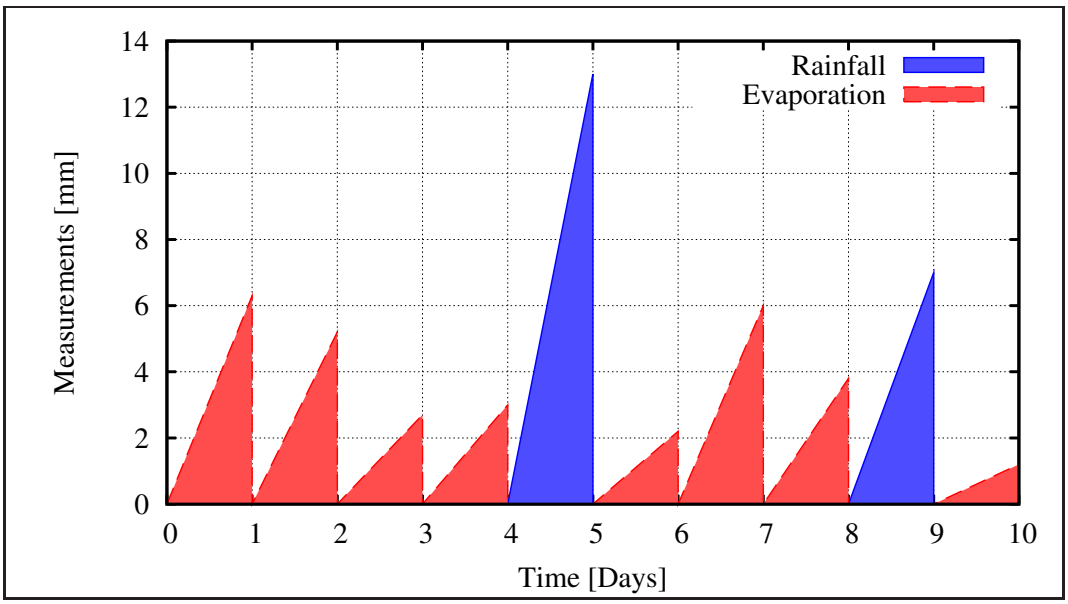

Figure 3.14: Example of accumulative-step method

accommodate the available data (daily) and the software. However, great care must be taken when interpreting model outputs running at small time intervals

(one minute). It is often necessary to lump the output, as shown in Chapter 5.

The rainfall from the two weather stations, Theewaterskloof (H6R001) and Tygerhoek, was allocated along the river. Using the contribution/distribution percentages of H60, shown in Table 3.5, the Theewaterskloof rainfall was used on the first 29 km of the Riviersonderend River downstream from the Theewaterskloof Dam. The Tygerhoek rainfall data was allocated to the remainder of the river length.

3.4.3.4 Irrigation Usage

The measured irrigation data was distributed daily using Sapwat3 (refer to Section 2.8.3) to calibrate the Mike 11 river model. In the hydrodynamic model, the irrigation discharge was withdrawn from the nodes closest to the farms' real location. The unmeasured pumps were also included in the simulation by calculating a theoretical usage pattern using Sapwat3.

3.4.4 Hydraulic Parameters

Manning roughness values were used to assign roughness to the river surface and were determined during the initial calibration of the river model. This is described in detail in Chapter 4. Before the simulation starts the user is required to assign an initial state of river flow. By using the warm-up period of six months, a suitable initial condition was determined at the start of the irrigation season. The initial conditions included the initial water depth and discharge when the simulation started.

Chapter 4

Model Calibration and Validation

4.1 The Role of Model Calibration and Validation

Environmental simulation models are simplified mathematical representations of complex real-world systems. Real-world systems consist of multiple processes and varying events that cannot be accurately depicted by simulated models. However, models can utilise known interrelationships between variables to predict the response of a real-world system.

In this way, models can be useful tools for investigations of how a system would likely respond to changes from its current state. To provide a credible basis for prediction and the evaluation of mitigation options, the ability of the model to represent real-world conditions should be demonstrated through a process of model calibration and validation.

The objective of this work was to support the one-dimensional analysis of river-flow conditions in the Riviersonderend River that focussed on water availability.

4.1.1 Objectives of Model Calibration Activities

Calibration consists of the process of adjusting model parameters to provide a match to observed conditions. The principle study question for this phase of model development addresses the behaviour of water throughout the river. The model should support the analysis of historic flow conditions, natural baseline conditions, and the potential future conditions with and without management interventions. Recent observed conditions are used to calibrate the river model, with the main parameter being roughness.

Calibration tunes the model to represent conditions similar to the flow conditions under study. However, calibration alone is not sufficient to assess the predictive capability of the model, or to determine whether the model devel-

oped via calibration contains a valid representation of flow relationships in the Riviersonderend River. To help determine the adequacy of the calibration and to evaluate the uncertainty associated with the calibration, the model is subjected to validation. In the validation step, the model is simulated with a different set of data independent from that used in the calibration.

4.1.2 Validation Procedure

After the model has been calibrated adequately, the quality of the calibration is evaluated through validation tests using separate input data. This indicates the quality of the calibrated model, and is used to show that the calibration is not only applicable to the time used for the calibration process. Validation also provides a direct measure of the degree of uncertainty that may be expected when the model is applied to conditions outside of the calibration series.

4.2 Riviersonderend Calibration Procedure

This section describes the calibration of the Riviersonderend River model. The hydraulic calibration is performed after configuring the one-dimensional river model. It is an iterative procedure of parameter evaluation and refinement as a result of comparing simulated and observed values of interest.

4.2.1 Calibration and Validation Time Periods

The calibration time period should represent a period in which reliable information is available for both weather data and stream flow gauging. Only daily rainfall and evaporation data were available for the Riviersonderend catchment, which was not the ideal situation.

Three factors influence the time period used for calibration: Firstly, Theewaterskloof Dam is only utilised during the dry summer irrigation season, from November to April of the following year. For the rest of the year the farmers rely on rainfall downstream of the dam for irrigation. Secondly, the water abstracted from the Riviersonderend River was measured from December 2005. Lastly, a flood event in 2007 caused damage to many of the measuring devices, and there was another flood in 2009. Some of these measurement devices have yet to be restored.

Therefore, the irrigation season 2006-2007 was specified for general calibration. This time period contains all the relevant data needed and is consistent with the validation period selected. Model validation was then undertaken for the 2005-2006 irrigation season.

4.2.2 Simulation Time Step

The time used in the simulation is largely dependent on the data available in the area. As mentioned in Chapter 3.2.1, the Riviersonderend catchment has three river discharge stations that measure continually and log every 12 minutes. The rainfall data from Tygerhoek and the Theewaterskloof (H6R001) weather station were measured daily (see Section 3.2.2).

Theewaterskloof (H6E001) weather station was used to provide the daily evaporation for the Riviersonderend catchment. The model was run with a one-minute time step.

Rainfall and evaporation were disaggregated using accumulative steps, described in more detail in Section 3.4.3.3. The negative effect of simulating every minute with daily rainfall data is the poor representation rainfall intensity. In addition, the use of daily rainfall data can introduce another sort of error into the simulation, as sub-periods of the most intense precipitation are assumed to occur simultaneously on all land areas covered by a given rainfall station, whereas storms typically move across the catchment, resulting in progressive offsets in the exact timing of maximum precipitation and leading to inaccuracies in the simulation of flow peaks.

4.2.3 Calibration Locations

The river gauge at Rheenen was available for the calibration and validation time periods. Dwarstrek was used to drive the simulation of releases from the Theewaterskloof Dam, and so cannot be used as a primary calibration site.

4.2.4 Calibration Performance Evaluation

The reliability of the Riviersonderend River hydrodynamic model was evaluated on the basis of the efficiency index (EI), as described by Nash and Sutcliffe (1970). There are several related studies available for model performance evaluation, such as those by Aitken (1973) and Fleming (1975).

The procedure of Nash and Sutcliffe (1970) has been widely used for the detection of systematic errors with respect to long-term simulation (Supiah and Hashim, 2002). The EI was developed to evaluate the percentage of accuracy or goodness of the simulated values with respect to their observed values. The EI as described by Nash and Sutcliffe (1970) is as follows :

$$EI = \frac{\sum_{i=1}^{n}(q_0 - q)^2 - \sum_{i=1}^{n}(q_0 - q_s)^2}{\sum_{i=1}^{n}(q_0 - q)^2} \tag{4.2.1}$$

where

q_o	Observed flow at time i (12-minute time step).
q	Mean value of observed flow $= \frac{1}{n}\sum q_o$.
q_s	Simulated flow at time i (one-minute time step).
n	Number of data points.

The EI equal to 1 indicates the best (perfect) performance of the model.

The root mean square error (RMSE) method used by Fleming (1975) was another method applied to evaluate the reliability of Mike 11 during this study. This method can be regarded as a measure of absolute error between the computed and observed flows. RMSE values tend to be zero for perfect agreement between observed and simulated values. RMSE is defined as follows:

$$RMSE = \sqrt{\frac{1}{n}\sum_{i=1}^{n}(q_0 - q_s)^2} \tag{4.2.2}$$

During the calibration of the Riviersonderend River Mike 11 model, both the *EI* and *RMSE* were determined.

4.3 Model Calibration

The irrigation season used for the model calibration was from November 2006 to April 2007. The simulated discharge was compared to the measured discharge in Rheenen with the aim for them to be as close to one another as possible.

The calibration of the model focussed of the lower flows (less than 2.5 m^3/s), being more relevant to the model's intended use.

What follows is a summary of the input data used in the construction of the hydrodynamic Riviersonderend model using Mike 11. The input data are are as follows:

- **Dam Release:** The hydrograph measured at Dwarstrek (H6H012) gauging station, with a 12-minute time step, was used as the Theewaterskloof Dam releases (see Section 3.2.1). The model is also able to function with zero inflow.
- **Rain:** Daily rainfall measurements from two weather stations, Theewaterskloof (H6R001) and Tygerhoek, were used to simulate the effect of rainfall on the river water surface. Theewaterskloof (H6R001) rainfall data were used on the first 29 km of Riviersonderend River downstream from Theewaterskloof Dam, while Tygerhoek rainfall measurements were used on the remaining river length (see Section 3.2.2).

- **Evaporation:** Theewaterskloof (H6E001) weather station was used to simulate the effect of daily evaporation on the river water surface using lake evaporation pan factors (see Section 3.2.2).
- **Augmenting Runoff:** Mike 11 NAM was used to estimate the rainfall-runoff relationship of the tributaries along the Riviersonderend River by calibrating against the measured discharge from the Baviaanskloof River tributary near Genadendal (see Section 3.3.1). The estimated discharge, with a 12-minute time step, from the remaining 27 tributaries was simulated using point inflows along the river. The estimated hydrograph of the small tributary catchments, including the riparian zone were distributed over river length (116,2 km).
- **Irrigation Usage:** Measured irrigation usage was distributed daily using Sapwat3. The water pumped from the Riviersonderend River was simulated by inserting abstraction points on the river model. GPS coordinates were provided for all the abstraction points being monitored by ElectroFlow measurement devices (see Section 3.3.2).
- **Return Flow:** The return flow was simulated by reducing the daily irrigation abstractions by 30% (see Section 3.3.3).

Evaporation from the plants along the river was not included in the simulation. The plants in the main channel are cleared by the ZWUA and their numbers vary from year to year.

4.4 Calibrated Model

Figure 4.2 shows the calibrated Mike 11 hydrodynamic model of the Riviersonderend River. By using the calibration performance evaluation equations (see Section 4.2.4), the EI and RMSE were determined to be 1.9 and 0.2 respectively.

The calibration of the model was done by adjusting the roughness of the river bed, with low flows given first priority. By increasing the roughness, the lag time of the river hydrograph was increased. Using the cross-section editor in Mike 11, the roughness could be changed to adjust the lag time of the river. River bed roughness is represented by using Manning (n) values. The river bed roughness does not change along the length of the river in order to improve model stability (Melvil, 2007).

The lower part of the river cross-section has a different Manning value than the upper river bank. A Manning value of 0.08 was used for the floodplain, while a Manning value of 0.1 was used in the main channel of the river. Typically, the main channel of the river is less rough than the upper floodplain. The “hippo pools” within the main river channel are expected to have the same effect as

increasing the roughness of the lower part of the river.

Riviersonderend River has abundant reeds and alien vegetation, which increase river bed roughness (see Figure 4.1). The higher flood plains are smoother consisting of agriculture or grassland.

Figure 4.1: Photograph of the abundant plants in the main channel of the Riviersonderend River

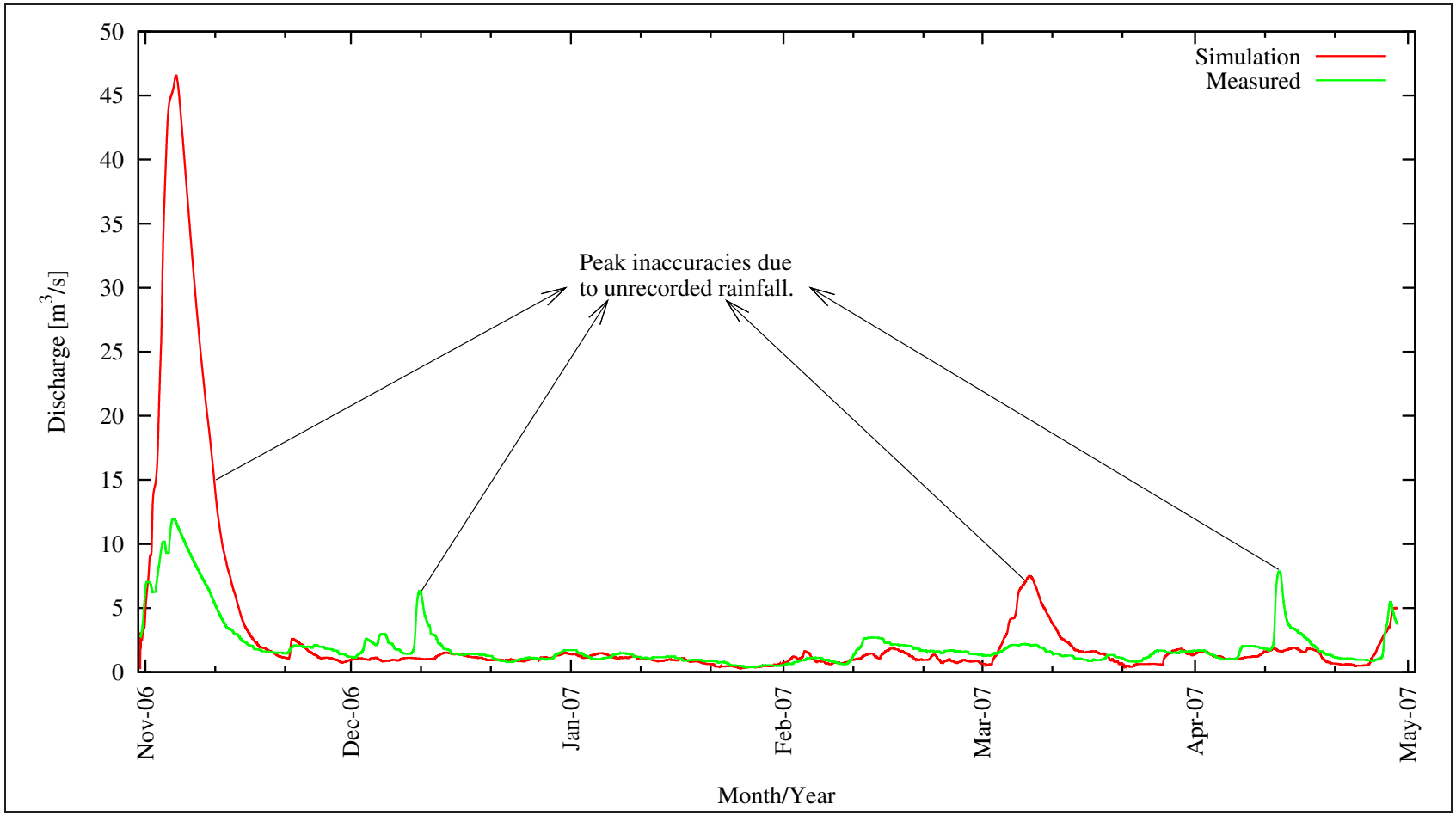

Figure 4.2: Calibrated hydrograph of Riviersonderend Mike 11 model

4.5 Quantifying Input Data

This section illustrates the effect that irrigation and augmentation have on the calibrated hydrograph shown in Figure 4.2. The quantification of the input data was done at Rheenen gauging station (101.5 km downstream from Theewaterskloof Dam) for the 2006/2007 irrigation season.

4.5.1 Augmentation

Augmentation in the Riviersonderend model consists of the 28 tributaries (see Table 3.3) and the remaining small (less than 6 km^2) catchments, including the riparian zone along the river (see Table 3.4).

The volume that was added into the Riviersonderend River by the 28 tributaries is illustrated in Figure 4.3. An additional 1.83 million m^3 of water was added to the river model originating from the remainder of the Riviersonderend catchment (478.8 km^2) consisting mainly of the alluvial and riparian zone, was distributed along the length of the river model (see Table 3.4 on page 76). Figure 4.3 also indicates the position of the tributaries along the river.

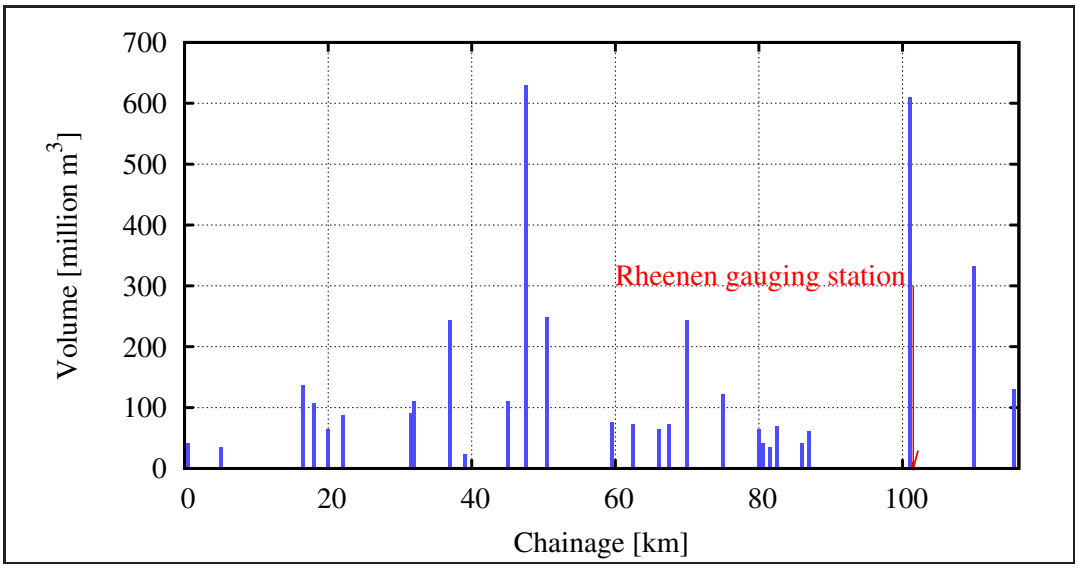

Figure 4.3: Volume of water from tributaries along the Riviersonderend River during the 2006-2007 irrigation season

Figure 4.4 shows the calibrated model output with and without augmentation. The augmentation affects the flow peaks of the simulated hydrograph significantly. These augmentation hydrographs, determined by Mike 11 NAM, were calibrated against the only measured tributary downstream from Theewaterskloof Dam (Baviaanskloof River) (see Section 3.3.1).

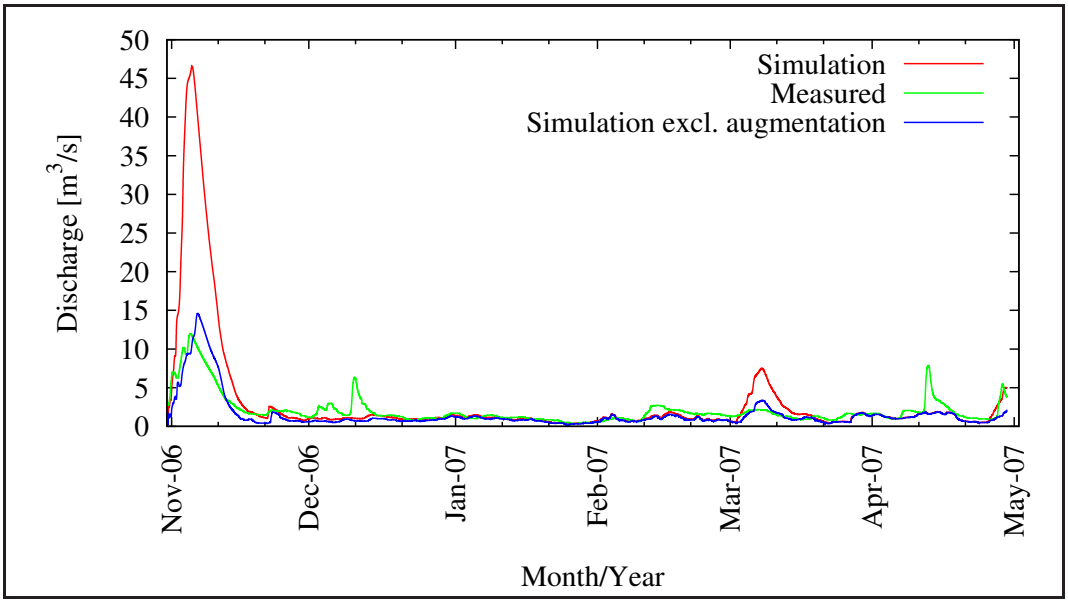

Figure 4.4: The effect of augmentation during the 2006/2007 irrigation season

The inaccuracies in the flow peaks of Figure 4.2 are due to the representation of the Riviersonderend catchment by the Baviaanskloof River.

Firstly, the Baviaanskloof River catchment receives more precipitation compared to the majority of the Riviersonderend catchment (see Figure 3.5). Secondly, the catchment is located in the mountains, making it very steep compared to the majority of the Riviersonderend catchment downstream from Theewaterskloof Dam.

Ideally, more catchment should have been used in the Mike 11 NAM calibration. Baviaanskloof River is not an ideal representation of the Riviersonderend catchment, but the only measured tributary available.

4.5.2 Irrigation

The location of the abstraction point on the Riviersonderend River is shown in Figure 4.5. Figure 4.5 shows the volume of water abstracted from the Riviersonderend River during the 2006-2007 irrigation season.

Figure 4.6 shows the final simulation with and without the effect of irrigation. By excluding the effect of irrigation the return flow is also excluded (see Section 4.3). Irrigation affects the flow conditions of the river model measured at Rheenen, and this could be seen especially when inspecting the low-flow conditions (see Figure 4.7).

In the Riviersonderend catchment, irrigation is the highest consumer of water and largely defines the low-flow conditions measured at Rheenen (H6H009). By using Sapwat3 to estimate the daily irrigation requirements, various as-

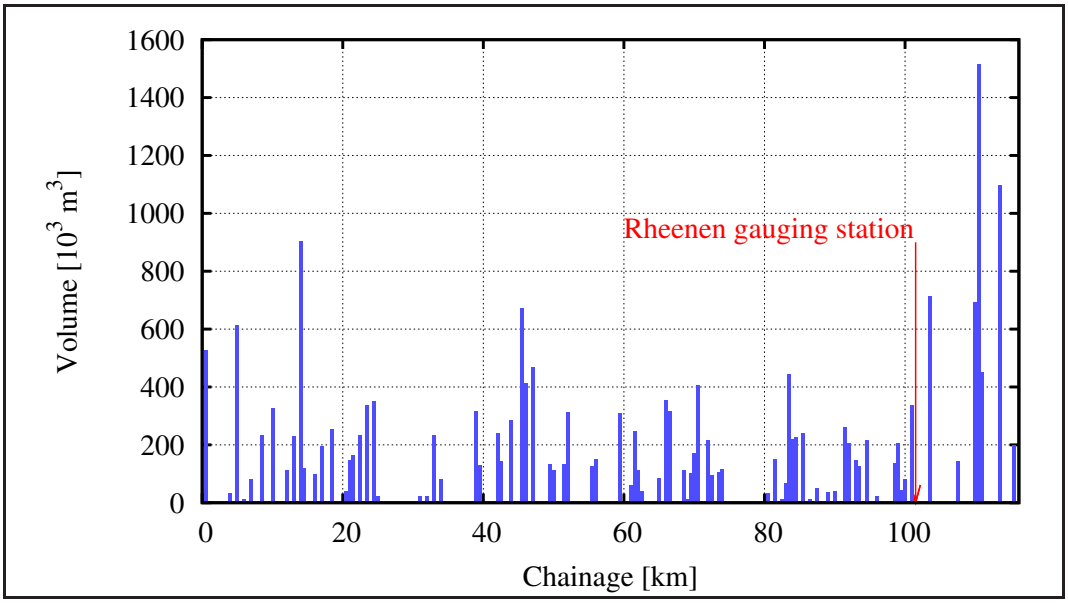

Figure 4.5: Location of abstraction points along the Riviersonderend River used in the hydrodynamic model for the 2006/2007 irrigation season

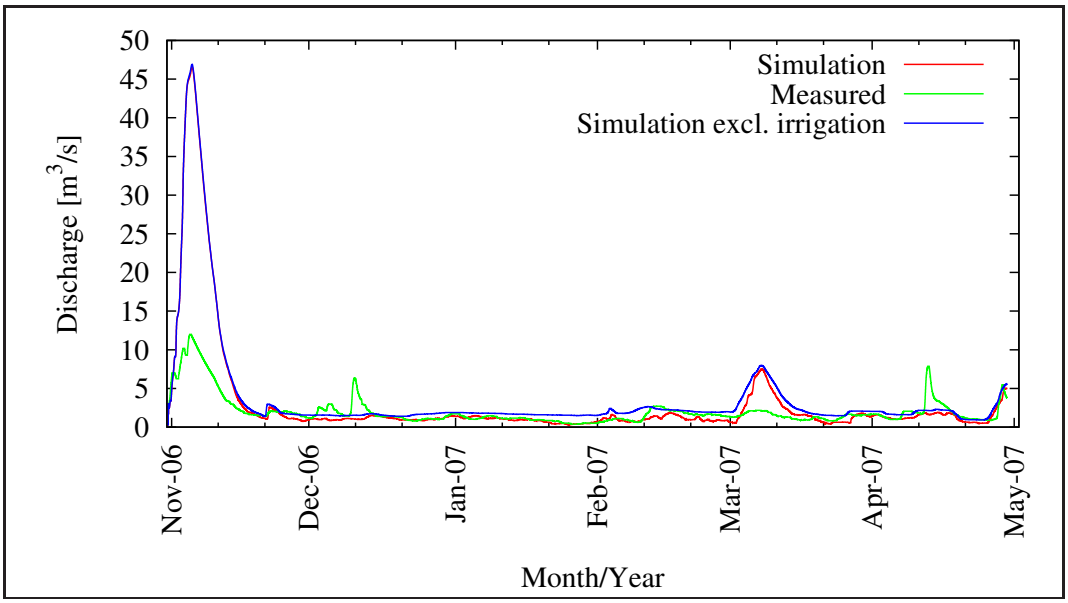

Figure 4.6: The effect of irrigation during the 2006/2007 irrigation season

sumptions (see Section 3.3.2) limited the accuracy of the estimated irrigation schedule.

The measured water usage was logged monthly and distributed daily using Sapwat3. This distribution could be improved with more accurate on-farm information (irrigation method, crop type, plant dates). This information was

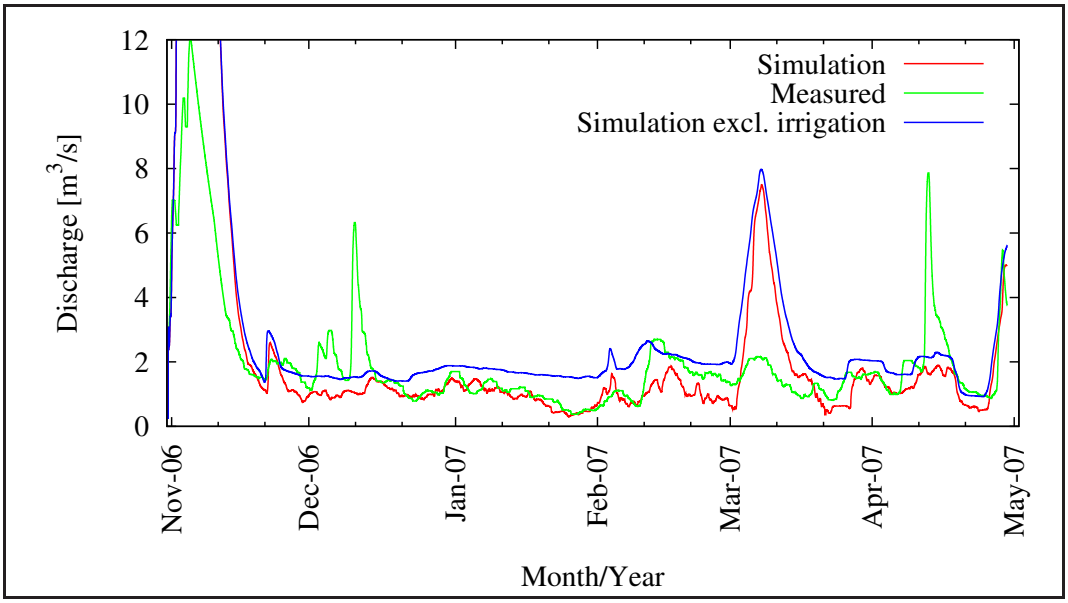

Figure 4.7: The effect of irrigation on low-flows during the 2006/2007 irrigation season

not available to be used in the model. The irrigation requirement time step (daily) is large compared to the simulation time step of one minute, resulting in a smoother hydrograph with lower peaks.

4.6 Discussion of Results

4.6.1 Low-flow Conditions

This section discusses the low-flow conditions (less than 2.5 m^3/s) of the river model, which was the main focus of the calibration. The final calibrated model, with a one-minute time step, was evaluated by using the calibration performance evaluation equations (see Section 4.2.4). The EI and RMSE were determined to be 1.4 and 0.06 respectively.

In order to compare the simulated data with the measured data more clearly, Figure 4.8 was drawn to illustrate the accumulative flow pattern for discharge less than 2.5 m^3/s. The time interval for the accumulative discharge is 12 minutes.

The two lines in Figure 4.8 run parallel to one another and change direction together, which is good for a calibrated model.

Figure 4.9 shows the average daily flows below 2.5 m^3/s of the observed and simulated hydrographs.

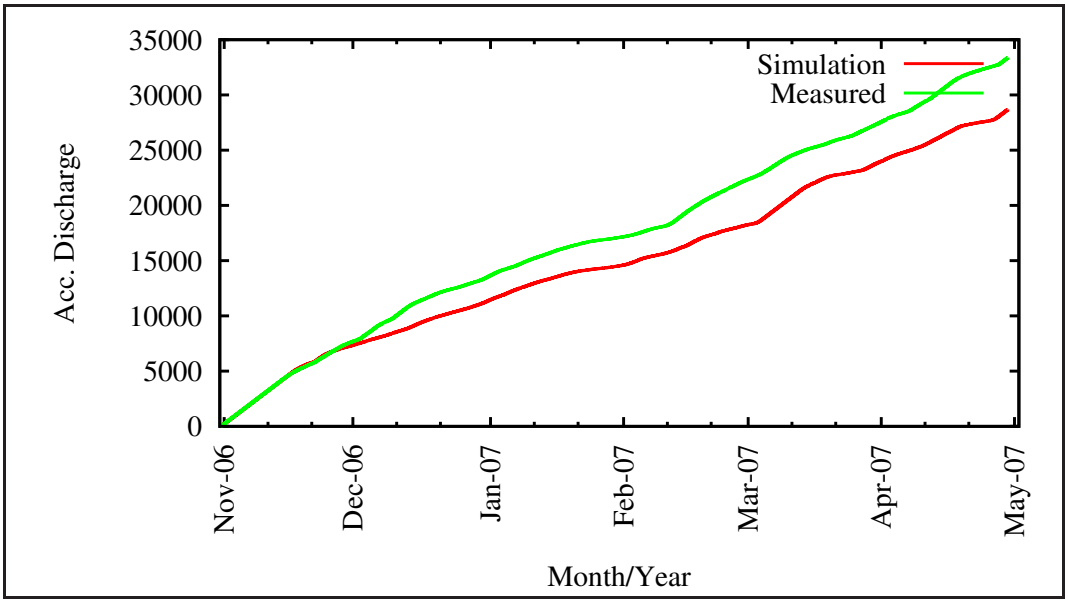

Figure 4.8: Accumulated discharge less than 2.5 m^3/s of the calibration model

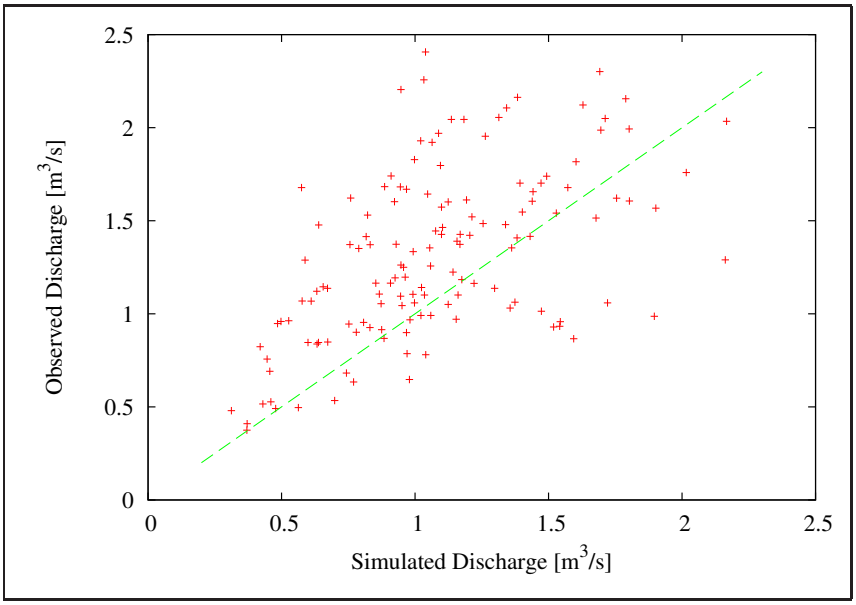

Figure 4.9: Scatter plot of the daily average flows below 2.5 m^3/s

4.6.2 Calibration Constraints

In order to achieve an ideal model calibration, the measured and simulated discharge should be the same. When inspecting Figure 4.2 it can be seen that the simulation follows the same pattern as the measured discharge. The differences, especially the flow peaks, occur due to various data limitations. These limitations include that:

- The model simulation was run with one-minute intervals while the available rainfall and evaporation data were measured daily.
- Only two rainfall stations are located in the Riviersonderend River basin, therefore the rainfall intensity and distribution are not accurate.
- All the estimated discharge of the augmenting streams was based on one NAM module calibration on the measured tributary at Genadendal.
- The water usage for irrigation was logged monthly. The daily schedule and irrigation time had to be estimated using Sapwat3.

4.7 Model Validation

4.7.1 2005/2006 Irrigation Season

In order to prove the validity of the model, another irrigation season was simulated with the model set-up remaining unchanged. This additional simulation was again compared to the measured flow data at Rheenen.

The following input data was required for this simulation:

- Measured flow data at Dwarstrek and Rheenen gauging stations;
- Rainfall and evaporation;
- Measured irrigation usage.

The only irrigation season with all the required input data was from December 2005 to April 2006. The derived flow pattern of the augmenting streams is illustrated in Appendix D, and the irrigation usage data is included in Appendix C. The 2005/2006 irrigation season was simulated with all the model parameters unchanged. Figure 4.10 illustrates the result of the simulation compared to the measured data at Rheenen.

From inspecting Figure 4.10 it is apparent that the two hydrographs are close to one another. By using the calibration performance evaluation equations (see Section 4.2.4), the EI and RMSE were determined to be -0.08 and 0.62 respectively for discharge below 2.5 m^3/s. These two attributes are a measure of the reliability of the river model.

Similar to the calibrated model of 2006, the peak discharge is poorly represented due to the similar limitations mentioned in Section 4.6.2.

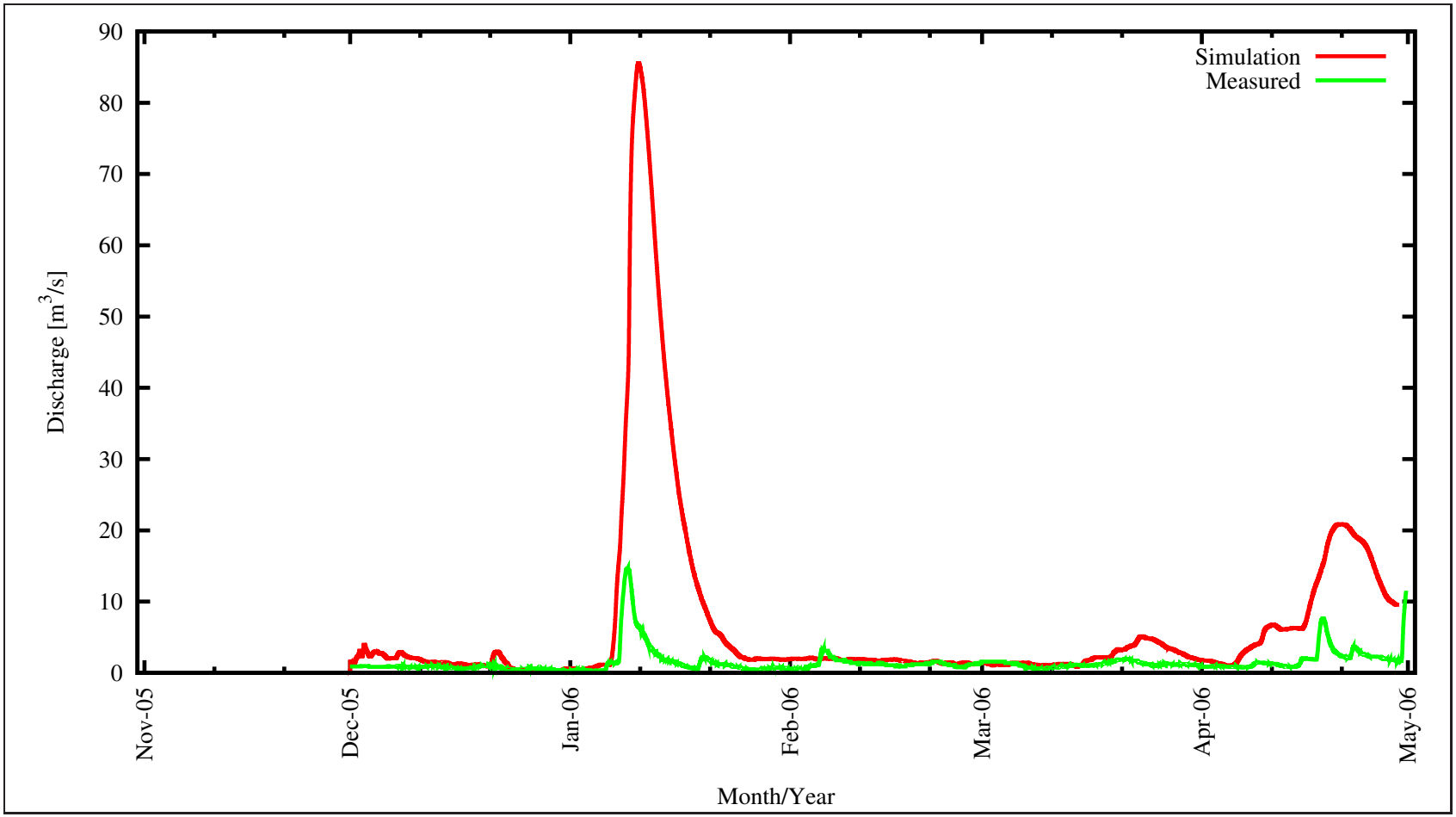

Figure 4.10: Validation of the Riviersonderend River model (2005/2006 irrigation season)

4.7.2 Validating River Bed Roughness

A historic flood event in the dry summer season is used to validate the river bed roughness of the river model. During November 2009 a flood event occurred that is suitable to be used.

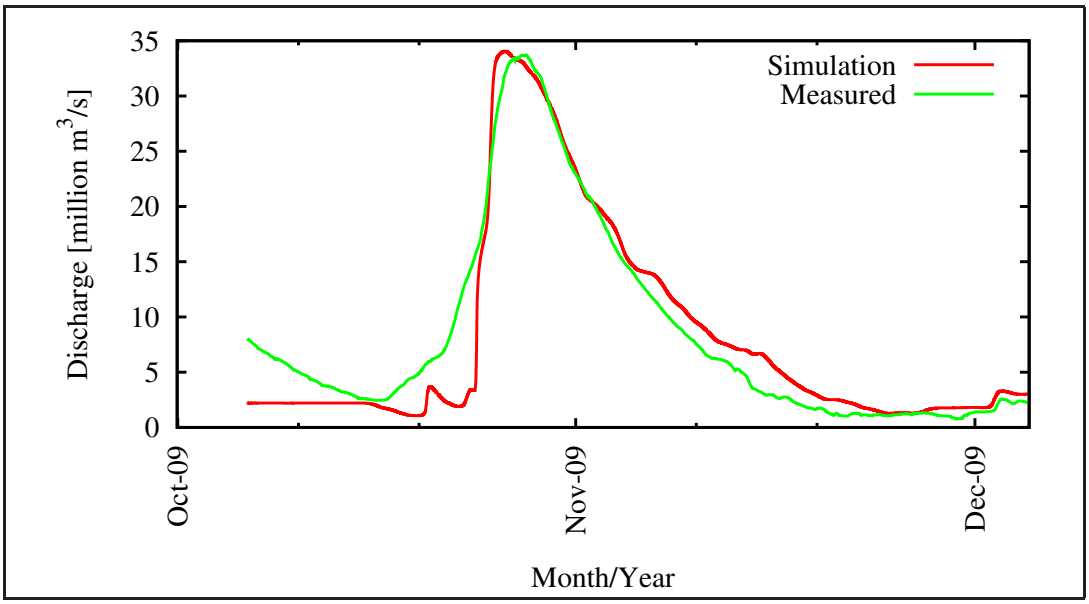

Figure 4.11: Validation of the river bed roughness

The validation results of the river bed roughness are illustrated graphically in Figure 4.11. Notice how not only the major peak, but also the smaller minor peak, is aligned. By using the calibration performance evaluation equations (see Section 4.2.4), the EI and RMSE were determined to be 0.91 and 2.72 respectively.

4.8 Summary and Discussion

After the available input data was added, the model was calibrated by adjusting the river bed roughness (see Figure 4.2). With the parameters of the calibrated model unchanged, another irrigation season was simulated in order to validate the river model. Using the 2005 irrigation usage, weather data and calibrated augmenting streams, as well as the same return flow percentage, the model was run again (refer to Figure 4.10 for the results).

As mentioned in Section 4.4, the low flows were given priority and adequate results were achieved. The Riviersonderend River simulation is an acceptable representation of the real Riviersonderend River for low flows. The variation in

the flow peaks was discussed in Section 4.5.1. The ideal information required versus the information available is shown below:

- Real-time rainfall data from multiple stations spread over the catchment vs. daily rainfall from the Theewaterskloof and Tygerhoek stations.
- Real-time evaporation data from multiple stations spread over the catchment vs. daily evaporation from the Theewaterskloof Dam weather station, but this is not as crucial as the rainfall data.
- Multiple real-time measured augmenting streams vs. estimating stream discharge based on one measured augmenting stream.
- Instantaneous irrigation usage vs. monthly water usage logged manually.

These limitations in the input data, especially the rainfall data, are the cause in the inaccuracies of the simulated river model (see Section 4.5.1).

Chapter 5

Reduction of Dam Releases for Irrigation

5.1 Introduction

The goal of real-time operating systems is to optimise the dam outlets to utilise the runoff from tributaries as far as possible, and to ensure that the irrigation requirements are supplied and that the downstream outflows are equal to the requested ecological flow requirements (EFR).

The amount of time that a hydrograph takes to reach a specific point downstream in a river is known as the lag time. Having an accurate estimation of the lag time is important to ensure that the water users have enough water to meet their requirements. The technique used to determine the lag time of the Riviersonderend River is described in this chapter.

The next section uses Excel to determine the dam release hydrograph. The time period used is motivated and the process used to determine the reduced dam release hydrograph is discussed. Initially, a dam release hydrograph is calculated without the effect of rainfall and evaporation. By using the calibrated hydrodynamic model, the initial dam release hydrograph is reduced in order to utilise the rainfall downstream from Theewaterskloof Dam.

The estimated water savings were determined by comparing the reduced dam release hydrograph with the actual Theewaterskloof Dam release. Additionally, the cost savings for the ZMUA were determined. The City of Cape Town is also a beneficiary when water is saved in the Theewaterskloof Dam. The potential cost savings for the City of Cape Town are also determined.

The chapter concludes by discussing the optimisation process involved in a real-time DSS. The module interactions are also illustrated, with various recommendations based on the existing OFS-RT DSS.

5.2 Riviersonderend River Lag Time Calculation for Low Flows

The amount of time that a hydrograph takes to reach a specific point downstream in a river is known as the lag time. Having an accurate estimation of the lag time is important to ensure that the water users have enough water to meet their requirement schedule. A previous study by Vancoillie (1985) determined the lag time from the Theewaterskloof Dam to the Rheenen gauging station to be 6.48 days calculated for a flood event of 30 million m^3/s.

Lag time is determined by the discharge. The lag time determined by Vancoillie (1985) is not suitable to be used for low flows.

In order to get a more accurate estimation for the low flows, another technique was used to determine the Riviersonderend River lag time. Instead of calculating the lag time from the dam to the measurement station, the Riviersonderend River Mike 11 model was used to determine the lag time between the water user abstraction points. This was accomplished by calculating the relationship between lag time and discharge.

The effect of the discharge on the lag time is determined by simulating a series of discharge increments in the river model. These increments are simulated individually. Using MikeView, the average velocity is determined between every water user abstraction point, illustrated in Figure 4.5, for each discharge individually. The discharges used are shown in Table 5.1.

Table 5.1: Discharge increment used to determine lag time

Discharge Increment (m^3/s)
0.001
0.01
0.1
0.2
0.3
0.4
0.5
1.0
1.5
2.0
2.5
3.0

See Figure 5.1 for the relationship between velocity and discharge.

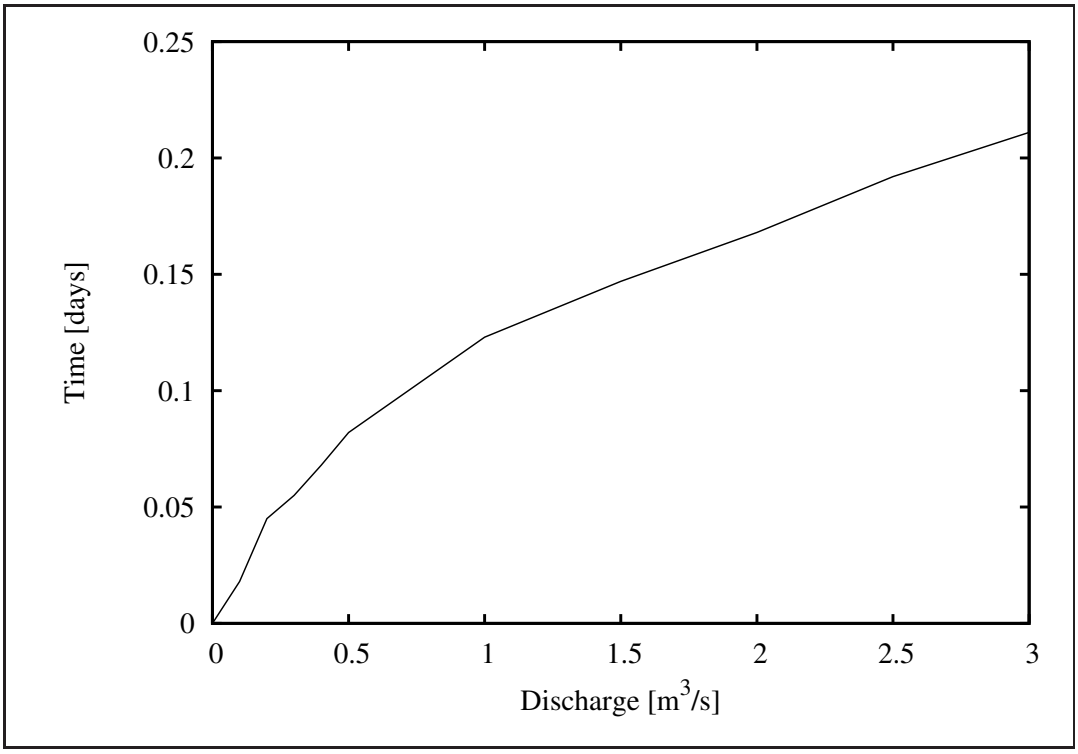

Figure 5.1: Discharge-velocity relationship at the most downstream reach between abstraction points of the Riviersonderend River

The average velocity, between the water user abstraction points, was used to determine the average lag time using equation 5.2.1.

$$T_{lag} = \frac{(D/v_{avg})}{24 \cdot 60 \cdot 60} \tag{5.2.1}$$

where

T_{lag}	Lag time (days).
v_{avg}	Average velocity (m/s).
D	Distance between abstraction points in river (m).

Finally, an equation was determined that best represents the relationship between discharge and lag time for each reach between the abstraction points. Equation 5.2.2 shows the determined lag time equation for the most downstream reach of the Riviersonderend River (115500 - 116000 m).

$$T_{lag} = 1.1893 \cdot Q^{(-0.882)} \tag{5.2.2}$$

See Figure 5.2 for the relationship between the discharge and the lag time, including a trend line for the most downstream reach of the Riviersonderend River.

The technique used to construct the time-discharge graph, as in Figure 5.2, was repeated for each river segment. Appendix E contains all the calculated graphs, showing the discharge-time relationship, trend line and equation used for calculations of the river segments. These time-discharge graphs in Appendix E were used to calculate the lag time, depending on the particular discharge.

This discharge-lag time relationship was used in Excel to determine the dam release hydrograph by lagging the water requirement upstream. This is discussed in the following section.

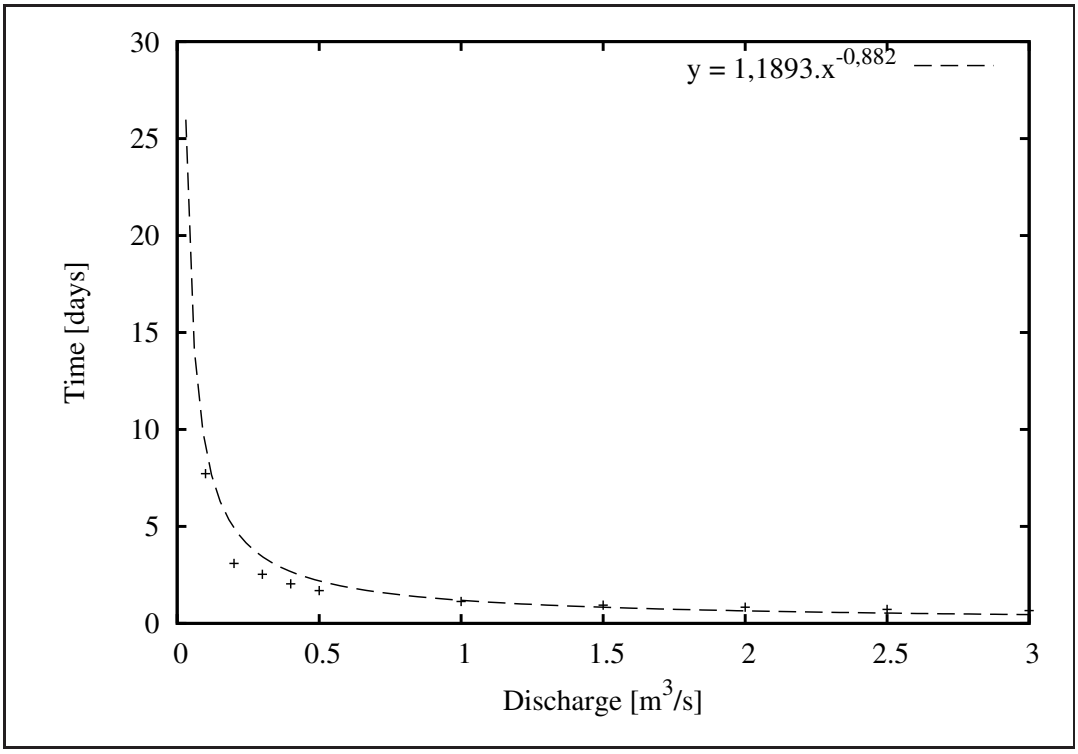

Figure 5.2: Discharge-time relationship and trend line at the most downstream reach of the Riviersonderend River

5.3 Reduction in Theewaterskloof Dam Release

This section describes the methodology used to reduce the Theewaterskloof Dam release hydrograph for irrigation using Excel and the Mike 11 calibrated model constructed for the Riviersonderend River. The time period used for this improvement was the first two weeks in February 2007 (see Section 5.3.1).

By excluding the weather data, the initial dam release hydrograph was constructed using Excel. Starting with the EFR, the lag-time equations (Section 5.2) were used to lag the irrigation requirements for the first two weeks in February upstream towards Theewaterskloof Dam.

This initial dam release hydrograph was then simulated using the calibrated Mike 11 model constructed in Chapter 4. The added effect of rainfall, evaporation and runoff from tributaries and the riparian zone in the Mike 11 model was integrated by adjusting the dam release hydrograph. This is explained in more detail in Section 5.3.3

5.3.1 Time Period

Historical data was used to demonstrate the effect of using a hydrodynamic model to reduce dam releases for irrigation. A water request system should be implemented, with hourly measured weather data, to simulated more recent events.

The time period used for the calculations of the reduction of the dam releases was the first two weeks of February 2007. The weather data and measured irrigation usage were included in the calibrated hydrodynamic Mike 11 model.

The time series used during the 2006/2007 irrigation season was motivated by the following:

- February is the most important irrigation month, during which water is crucial for the crop growth cycle (Ferreira, 2011).
- A rain event occurred during this time period, providing an opportunity to illustrate the effect of including rainfall in the dam release schedule.
- The weather data (rainfall, evaporation) and irrigation usage data were available during this time period.

The dam release hydrograph was constructed to supply the water user demands and the EFR of the Riviersonderend River for the first two weeks of February 2007 alone. The calculated hydrograph therefore does not include the water usage prior to February 2007.

5.3.2 Calculating the Initial Dam Release Hydrograph

The initial dam outlet hydrograph was determined while excluding the effect of rainfall and evaporation. The process used to calculated the initial dam release hydrograph is described in the following steps:

1. Starting with the EFR at the end of the river (116 000 m downstream from Theewaterskloof Dam), the average discharge at 116 000 m was calculated using Excel. An EFR of 0.5 m^3/s was used in the optimisation process at the downstream end of the Riviersonderend River (DWA, 2004*a*).

2. Using Equation 5.2.2 for chainage 115 500 - 116 000 m (see Section 5.2) the average lag-time is determined between the water abstraction points.

3. The hydrograph at 116 000 m is then lagged upstream to 115 500 m by deducting the calculated average lag time.

4. Once the hydrograph is lagged upstream, the discharge is added to the existing water requirement at 115 500 m, creating a new hydrograph at 115 500 m.

5. Steps 1 to 4 were then repeated using the average discharge of the newly calculated hydrograph and the discharge-lag time equation for the relevant reach between the water abstraction points.

This process was repeated in Excel until the dam release hydrograph at Theewaterskloof Dam was constructed (see Figure 5.3).

The deviation from the EFR in the outflow (Figure 5.3) is caused by:

- Using the average discharge of the calculated hydrograph to determine the lag time.

- The effect of time on a hydrograph in a hydrodynamic model (see Section 5.3.2.1), which could not be represented in Excel.

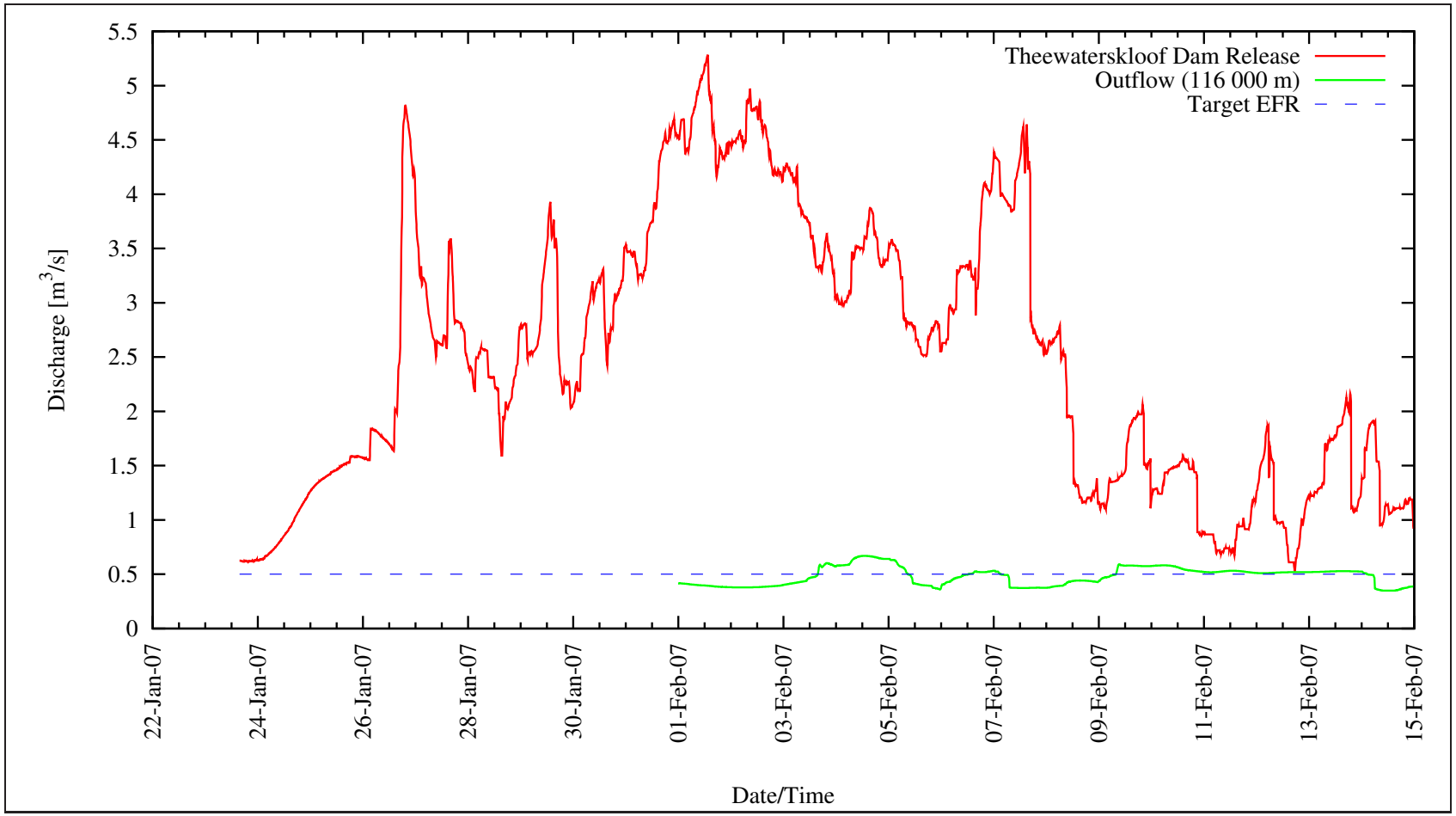

Figure 5.3: Graph showing the dam release hydrograph and the simulated downstream result excluding rainfall (target outflow EFR of 0.5 m^3/s)

5.3.2.1 The Effect of Time on a Hydrograph

The calculation process to determine the Theewaterskloof Dam release hydrograph (using Excel) does not take into account the way a hydrograph changes with time. In reality, the hydrograph flattens and the duration of the peak discharge decreases as it moves along the river due to the attenuation effects of in-channel storage. See Figure 5.4 for an example of the way a hydrograph deforms with time in the Riviersonderend River.

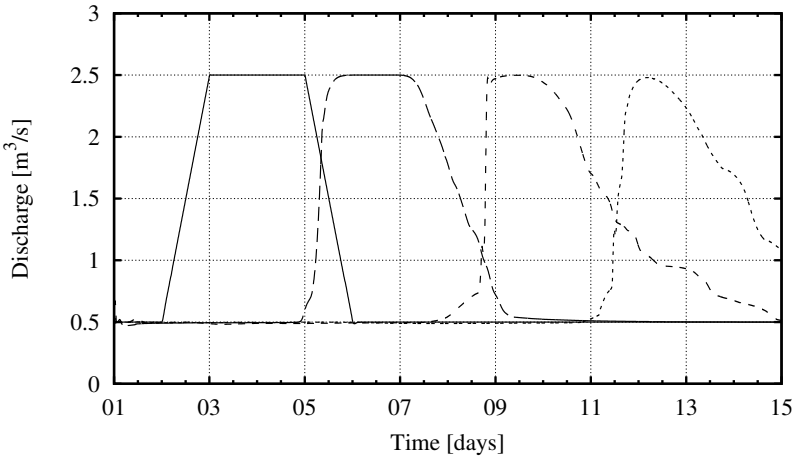

Figure 5.4: Graph indicating how a hydrograph changes with time in the Riviersonderend River

Assuming that the hydrograph does not change its shape when it is lagged affects the accuracy of the optimisation model. Ideally, the discharge and duration should be adjusted, with the volume remaining unchanged, to achieve a more accurate dam outlet hydrograph.

The process, however, does ensure that all the water requirements are met, while maintaining ecological integrity.

5.3.3 Dam Release Hydrograph by Using Hydrodynamic Model

Another dam release hydrograph was calculated by including the measured weather data (rainfall and evaporation) for the same time series. The effect of the rainfall, evaporation, tributary and riparian zone runoff was incorporated by using the Mike 11 hydrodynamic model.

The initial dam release hydrograph (see Figure 5.3) was used as the calibrated hydrodynamic model inflow. Excel was used to calculate the adjustments of the dam releases to reduce the hydrograph. The calculated reduced dam release hydrograph is shown in Figure 5.5.

The hydrograph at the final cross-section of the river model should ideally consist of the EFR alone. The difference between the simulated hydrograph and the EFR is inverted and lagged upstream. The process used to lag the hydrographs in Excel were the same as described in Section 5.3.2.

The outflow (at 116 000 m) was greater than the EFR, which was to be expected after the rainfall and evaporation data were added using the hydrodynamic model. The water from the tributaries forms part of the rainfall and has a significant effect on the outflow of the river model.

The river discharge did fall below the EFR twice (see Figure 5.5). This was caused by the the assumptions mentioned in Section 5.3.2.

The majority of the reduction in the dam release hydrograph was at the peak of the hydrograph. The volume of the reduction in the hydrograph was determined to calculate the amount of water that could be saved after rainfall was included in the calculation process. A total of 412 892 m^3 of water was reduced when the effect of rainfall downstream from Theewaterskloof Dam was utilised for the first two weeks in February 2007. Using the same reduction percentage, it would have been possible to save 2 661 375 m^3 in the 2006-2007 irrigation season.

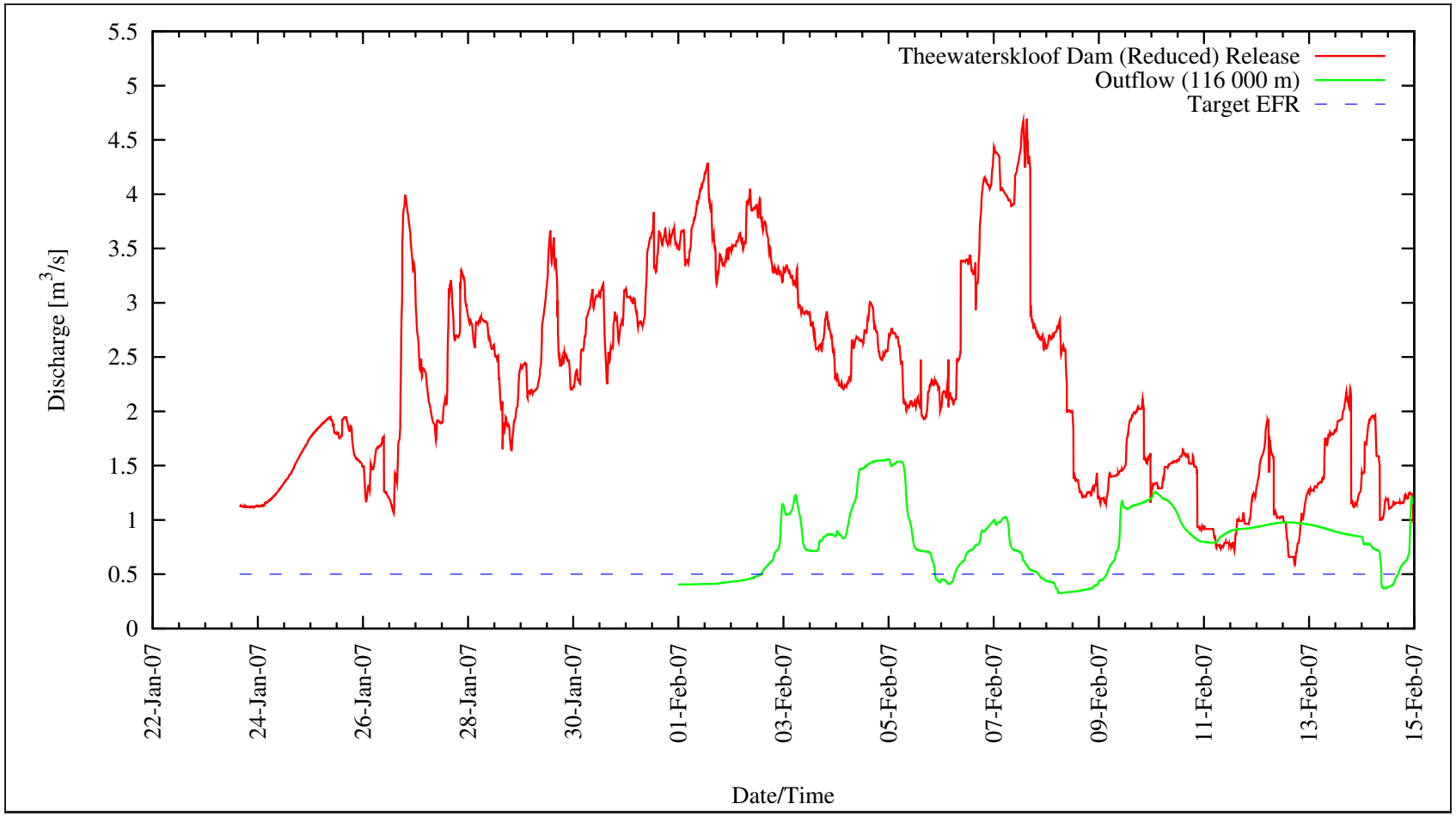

Figure 5.5: Graph showing the reduced dam release hydrograph and the simulated downstream outflow (target outflow IFR of 0.5 m^3/s)

5.4 Estimating Savings

The reduced dam release hydrograph was compared to the actual release discharge from Theewaterkloof Dam (see Figure 5.6).

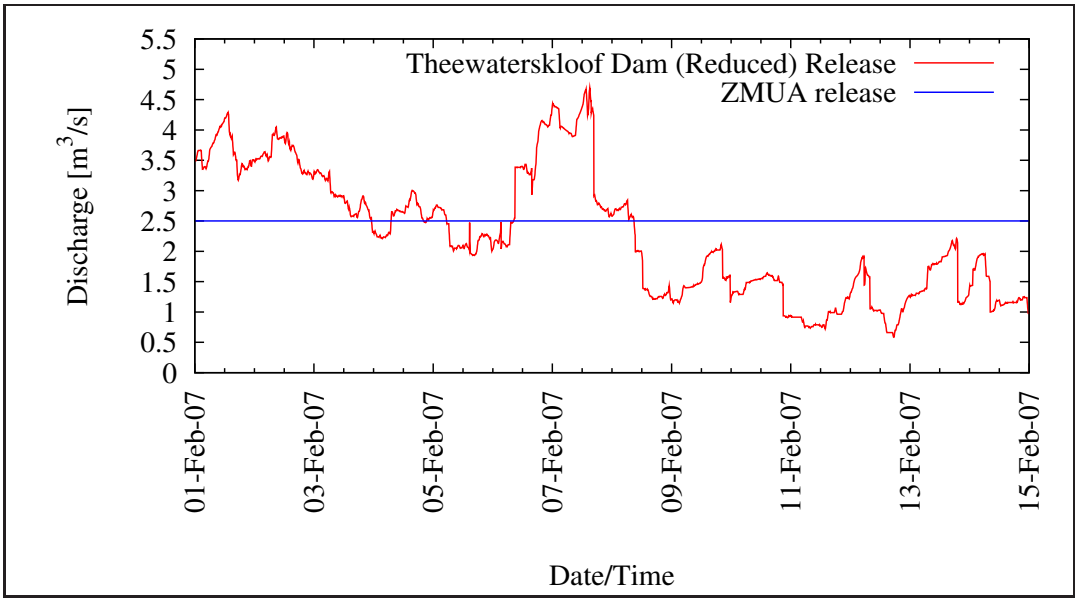

Figure 5.6: Estimating the possible water savings using the reduced dam release hydrograph and actual ZMUA dam releases

During the first two weeks in February 2007, the ZMUA released a constant discharge of 2.5 m^3/s (Ferreira, 2011). This constant release from the Theewaterskloof Dam (2.5 m^3/s) is common practice during the irrigation season to ensure the availability of water for the farmers downstream (Ferreira, 2011).

The possible water savings for the ZMUA for the first two weeks in February 2007 were calculated. By calculating the difference between the reduced hydrograph and the constant 2.5 m^3 released by the ZWUA, a total volume of 280 000 m^3 could have been saved without compromising on water availability. The price of water for irrigation in the Riviersonderend area was R 0.0259 per m^3 (Ferreira, 2011). With a total volume of 280 000 m^3 saved, the cost saving is calculated to be R 7,250 for the first two weeks in February 2007. Using the same reduction percentage, a total estimated cost saving of R 78,337 could have been achieved in the 2006-2007 irrigation season.

Table 5.2 shows the water usage for the past 10 years and the possible savings. On average, the ZWUA could save up to R 69,793 every irrigation season by utilising the rainfall downstream from Theewaterskloof. Although this is a low cost saving, the actual benefit could be more water available for the City of Cape Town.

With its increasing water demand, the City of Cape Town is looking for sustainable engineering solutions. The most cost-effective method to increase water availability is to optimise existing water systems like the Theewaterskloof Dam. This water saving will delay the implementation of any new projects, thereby buying valuable time. Another solution would be to undertake new projects to increase water availability, such as the Berg River Dam (DWA, 2008).

In order to put this into perspective: undertaking new projects will cost the City of Cape Town between R 5/m^3 and R 8/m^3. When applying this cost (R 5/m^3) to the volume of water that could possibly be saved in the optimisation of Theewaterskloof Dam, a saving of R 13,4 million could be achieved during an irrigation season (see Table 5.3).

Table 5.2: Possible savings for the ZWUA

Irrigation season	Water used (m^3)	Water savings (m^3)	Cost savings
2000-2001	32 905 620	3 045 349	R 78,875
2001-2002	24 773 040	2 292 695	R 59,381
2002-2003	29 100 780	2 693 219	R 69,754
2003-2004	30 477 060	2 820 591	R 73,053
2004-2005	21 059 280	1 948 994	R 50,479
2005-2006	32 113 980	2 972 085	R 76,977
2006-2007	31 022 820	2 871 100	R 74,361
2007-2008	24 699 780	2 285 915	R 59,205
2008-2009	33 744 420	3 122 979	R 80,885
2009-2010	31 270 590	2 894 031	R 74,955
Average			R 69,793

Table 5.3: Possible savings for the City of Cape Town

Irrigation season	Water used (m^3)	Water savings (m^3)	Cost savings
2000-2001	32 905 620	3 045 349	R 15,226,747
2001-2002	24 773 040	2 292 695	R 11,463,477
2002-2003	29 100 780	2 693 219	R 13,466,095
2003-2004	30 477 060	2 820 591	R 14,102,955
2004-2005	21 059 280	1 948 994	R 9,744,971
2005-2006	32 113 980	2 972 085	R 14,860,423
2006-2007	31 022 820	2 871 100	R 14,355,500
2007-2008	24 699 780	2 285 915	R 11,429,576
2008-2009	33 744 420	3 122 979	R 15,614,893
2009-2010	31 270 590	2 894 031	R 14,470,153
Average			R 13,473,479

5.5 Required Information for Constructing a DSS

This section describes the data and infrastructure necessary to determine a optimal dam release schedule for Theewaterskloof Dam. The information in this section is based on the OFS-RT DSS.

The following data is required to operate a real-time DSS:

- Accurate weather forecast data. Hourly measured data could be acquired from WeatherSA, but weather stations are needed within the Riviersonderend catchment to have a better representation of the rainfall and evaporation.
- Water request system. In this thesis, the measured irrigation usage was distributed using Sapwat3. Irrigation usage, however, varies significantly on a annual basis. Similar to the OFS-RT system, the farmers should request irrigation water weekly.

For this thesis, a real-time DSS was not constructed due to the abovementioned constraints. The process recommended to optimise the Theewaterskloof Dam release hydrograph was based on the OFS-RT system. A schematic drawing of the data flow and module interaction for a simulation loop is illustrated in Figure 5.7.

The optimisation simulation draws its data from the FloodWatch database (see Section 2.7.5.1). Optimisation of the system can only be accomplished by adjusting the Theewaterskloof Dam release hydrograph. The optimisation simulation uses the AutoCal Module of FloodWatch to adjust the dam releases, using the initial results as basis.

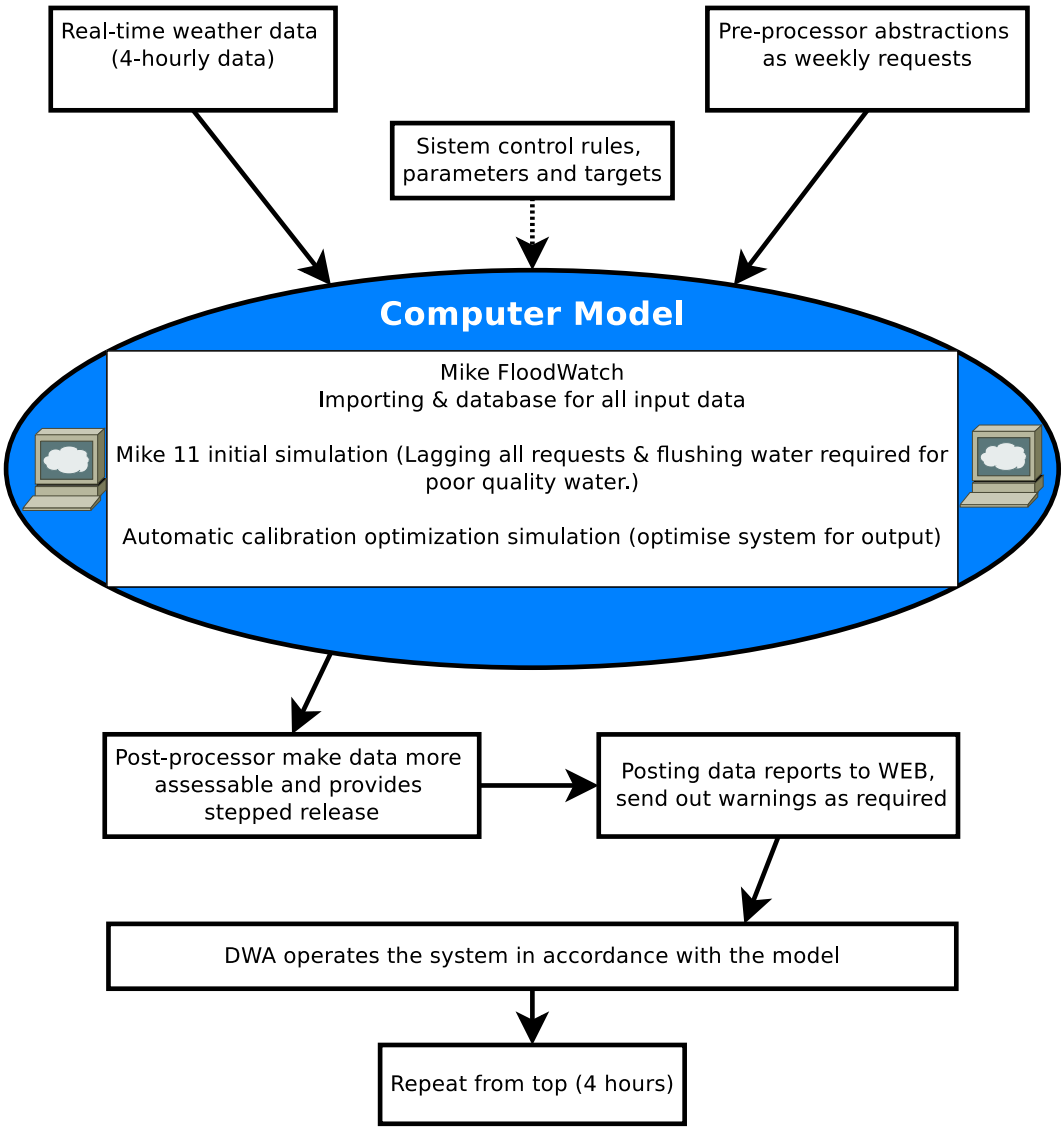

Figure 5.7: Schematic drawing of the model interaction based on OFS-RT DSS

Chapter 6

Conclusions and Recommendations

6.1 Conclusions

The Theewaterskloof Dam is the sole storage unit for irrigation water in the Riviersonderend River. Using the available data, a one-dimensional hydrodynamic simulation model was used to simulate the flow of the Riviersonderend River from the Theewaterskloof Dam, over a distance of 116.2 km. The model included weather data, irrigation usage, return flow, estimated inflow augmenting streams and the rest of the catchment flow generated by rainfall-runoff simulation.

To provide a credible basis for the prediction and evaluation of mitigation options, the ability of the model to represent real-world conditions was demonstrated through a process of model calibration and validation. The model was calibrated against the measured flow at the Rheenen gauging station. Following the model calibration process for the 2006-2007 irrigation season, the model was validated by simulating the 2005-2006 irrigation season with the model setup remaining unchanged.

The simulated results are acceptable, considering the limited data available. Various differences that occurred in the model, especially the flow peaks, were due to limited rainfall data. The ideal information required to calibrate the model versus the information available is shown below:

- Real-time rainfall data from multiple stations spread over catchment vs. daily rainfall from the Theewaterskloof and Tygerhoek stations.
- Real-time evaporation data from multiple stations spread over catchment vs. daily evaporation from the Theewaterskloof station.
- Multiple real-time measured augmenting streams vs. estimating stream discharge based on one measured augmenting stream.

- Instantaneous irrigation usage vs. monthly water usage logged manually.
- Actual crop type and hectares under irrigation.

These limitations in the input data are the most likely cause of the inaccuracies of the simulated river model peaks. However, the low-flow data was well calibrated with these data constraints.

The calibrated hydrodynamic model was used to reduce the dam release hydrograph for a two-week period. The hydrograph was constructed to supply all irrigation requirements while maintaining the target EFR. Two hydrographs were constructed: the first excluding weather data and the second including weather data. The rainfall includes the amount of water (millimetres) on the surface of the river and the flow of the tributaries. After comparing the reduced hydrograph with the actual historic dam release, the volume of water saved was determined.

The cost implications were determined for the water saved in the Theewaterskloof Dam, based on a crude example. Although the saving for the ZWUA was low for the case illustrated, the actual benefit could be the increase in water yield that was available for the City of Cape Town. The potential volume of water and cost savings was determined for the ZWUA and the City of Cape Town based on the incremental cost of additional water resource augmenting projects.

6.2 Recommendations

The core of any real-time system is the quality and availability of the input data, and the accuracy of the weather forecast. To construct a model with greater accuracy and to ensure the success rate of the hydrodynamic model, it is recommended that automatic rainfall stations (Figure 6.1) are installed in the river catchment to measure rainfall at intervals of less than one hour. The cost for a Davis Vantage Vue wireless weather station was R 5,299 during the course of this study.

Figure 6.1: Picture of a wireless weather station suitable to be used for hourly rainfall data

Before a real-time system can be implemented for the Riviersonderend River, the farmers need to have a water-use forecast system. The ZWUA would have to implement a weekly water request system for two weeks at a time. In other words, the farmers would be requested to apply in advance, and every seven days, for water for a two-week period.

It is necessary to have a weather and runoff forecasting system for the model to be able to function in real time.

The hydrodynamic Riviersonderend River model should be tested more thoroughly by implementing the proposed dam release schedule. The simulated data should be re-calibrated and compared to the actual discharge and water level on multiple sections along the river to ensure model accuracy.

The hydrodynamic Riviersonderend River model could only be calibrated against the flow gauging station at Rheenen, 101.5 km downstream from the Theewaterskloof Dam. To improve the reliability of the model, it should be calibrated against multiple points along the river. The final recommendation is to construct more flow gauging stations in the Riviersonderend River. This does not have to entail constructing more broad-crested weir-type gauging stations, such as those at Rheenen and Dwarstrek. An alternative to broad-crested weir-type gauging stations is the commonly used velocity-area method (Herschy, 1993), which could be installed along stable sections of the river, i.e. rated sections.

List of References

Aitken, A.P. (1973). Assessing Systematic Errors In Rainfall-runoff Models. *Journal of Hydrology*, , no. 20, pp. 121–136.

Allen, R.G., Pereira, L.S., Raes, D., Smith, M. and Ab, W. (1998). Crop evapotranspiration - Guidelines for computing crop water requirements - FAO Irrigation and drainage No 56. *Irrigation and Drainage*, pp. 1–15.

Blackhurst, R., Beuster, H., Sprinks, A. and Rossouw, J.N. (2002). Breede Water Management Area: Water Resources Situation Assessment - Main Report P 18000/00/0101.

BOCMA (2010). Status Quo and Situation Assessment of Riviersonderend. In: *Annual BOCMA Meeting*, March, p. 3.

BOCMA (2011). Breede-Overberg Catchment Management Agency Website.

Brunner, G. (2010). HEC-RAS, River Analysis System Hydraulic Reference Manual.

De la Harpe, J., Ferriera, J. and Potter, A. (1998). An Overview of the Water Management Institutions of South Africa.

De la Harpe, J. and Ramsden, P. (1998). A Guide to the National Water Act of South Africa.

DHI (2009*a*). Mike 11 - A modelling system for Rivers and Channels - User Guide.

DHI (2009*b*). Mike 11 Reference Manual.

DHI (2011). STIAS, Stellenbosch, South Africa. In: *Overview of Mike Software*, pp. 1–8.

Du Plessis, J.A. (2008). *Hidrologie 424 Benuttingshidrologie*. Stellenbosch University, Civil Engineering Department, Room 408, Stellenbosch, 7600.

DWA (2003). Breede River Basin Study - Report: P H 00/00/2402.

DWA (2004*a*). Breede Water Management Area Internal Strategic Perspective, Report no: P WMA 18/000/00/0304.
Available at: `http://www.dwaf.gov.za/documents/`

DWA (2004*b*). National Water Resource Strategy.

DWA (2004*c*). The Orange-Fish Sundays System: Estimating Irrigation Return Flows.

DWA (2005). Western Cape Reconciliation Strategy. In: *Cape Town, South Africa*, August, pp. 20–22.

DWA (2008). Berg River Dam : Designed with Rivers in mind. *The Water Wheel*, , no. July/August, pp. 33–37.

DWA (2011). Hydrological Services - Surface Water (Data, Dams, Floods and Flows). Available at: `http://www.dwaf.gov.za/hydrology/`

DWAF (1982). Riviersonderend-Berg Rivier Project Overview.
Available at: `http://www.dwaf.gov.za/documents/`

DWAF (1986). Water for Irrigation. In: DWAF (ed.), *Management of the Water Resources of the Republic of South Africa.*, 1st edn, chap. 2, pp. 2.16–2.18. Departmeny of Water Affairs, Pretoria. ISBN 0 621 11004 3.

Easterling, D., Meehl, G. and Parmesan, C. (2000). Climate extremes: observations, modelling, and impacts. *Science*, vol. 289, no. 5487, pp. 33–37.

Ferreira, C. (2011 August). Riviersonderend Irrigation Management Association.

Fleming, G. (1975). *Computer Simulation Techniques In Hydrology*. 1st edn. Elsevier, New York.

Flo-Check (2006). eLectroFlo Water ans Energy Meter.

Herold, C.E. (1990). Calibration Procedures for the Monthly Time Step Hydro-Salinity Model.

Herschy, R. (1993 January). The velocity-area method. *Flow Measurement and Instrumentation*, vol. 4, no. 1, pp. 7–10. ISSN 09555986.

Hunter (2006). *IrrigatIon HydraulIcs*. 1st edn. Hunter Industries Incorporated, California. ISBN ED-002-B.
Available at: `www.HunterIndustries.com`

Mbedzi, S.S. (2006). Transformation of the Zonderend River Irrigation Board, Magisterial District of Caledon, Western Cape Province, into the Zonderend River Water User Association, Water Management Area Number 18, Western Cape Province.

Mckenzie, R. and Seago, C. (2007). Current Analytical Methods and Technical Capacity of the four Orange Basin States.

Mehrdad, M. (2010). A Unique Approach to Energy Savings Through Power Quality - An Introduction to ElectroFlow.

Melvil, J.A. (2007). *Real-Time Model Development for the Full River System*. MscEng, Stellenbosch University.

Mhlanga, B.F.N., Ndlovu, L.S. and Senzanje, A. (2002). *Impacts Of Irrigation Return Flows On The Receiving Waters: A case of Sugarcane irrigated fields at the Royal Swaziland Sugar Corporation (RSSC) in the Mbuluzi River Basin (Swaziland).* Ph.D. thesis, University of Zimbabwe.

Midgley, C.D., Pitman, W.V. and Middleton, B.J. (1994). Surface Water Resources of South Africa 1990. User's Guide, Report 298/1/94; Appendices, Reports 298/2.1-2.6/94; Books of Maps, Reports 298/3.1-3.6/94.

Mwaka, B. (2011). Overview of Real-Time Water Resources System Operation. In: DWA (ed.), *Real-Time Systems (DSS)*, June. DWA, Stellenbosch.

NAMC (2010). The Effect of Electricity Costs on Irrigation Farming. *BFAP*, , no. April, pp. 1–6.

Nash, J. and Sutcliffe, J. (1970). River Flow Forecasting Through Conseptual Models, Part 1: A Discussion on Principals. *Journal of Hydrology*, vol. 10, pp. 282–290.

Pearce, M.W. and Schumann, E.H. (2001). The impact of irrigation return flow on aspects of the water quality of the Upper Gamtoos Estuary , South Africa. *Water Research Commission (WRC)*, vol. 27, no. 3, pp. 367–372.

Pedersen, C.B., Madsen, H., Skotner, C. and G. Cox (2007). Real-Time Optimization of Dam Releases Using Multiple Objectives. Application to the Orange-Fish-Sundays River Basin, South Africa.

Pott, A., Benade, N., Van Heerden, P., Annandale, J. and Steyn, M. (2008). Technology Transfer and Integrated Implementation of Water Management Models in Commercial Farming.

RSA (1998). National Water Act No 36 of 1998.

Schulze, R.E. (1995). *Hydrology and Agrohydrology.* Pietermaritzburg, South Africa.

Skotner, C., Klinting, A. and Ammentorp, H.C. (2003). Mike Flood Watch: Managing Real-Time Forecasting.

Sleigh, P. and Goodwill, I. (2000). The St Venant Equations.

Stevens and DHI (2012). Hydrological and Hydraulic Modeling Overview. Available at: `www.stevenswater.com`

Supiah, S. and Hashim, N. (2002). Rainfall Runoff Simulation Using Mike 11 NAM. *SA Journal of Civil Engineering*, vol. 15, no. 2, p. 13.

The South African National Roads Agency (2007). *Drainage Manual.* 5th edn. ISBN 1-86844-328-0.

Van Heerden, P.S. and Crosby, C.T. (2002). Sapwat User Manual.

Van Heerden, P.S. and Crosby, C.T. (2005). The Upgrading and Updating if the Sapwat pragram and website in 2003/04.

Van Heerden, P.S., Crosby, C.T., Theron, E., Schulze, R.E. and Tewolde, M.H. (2009). Integrating and Updating of Sapwat and Planwat to Create a Powerful and User-Friendly Irrigation Planning Tool. WRC report no. TT 391/08.

Van Vuuren, L. (2011). Water History - Blood, sweat and tears at Riviersonderend. *The Water Wheel*, vol. June, no. 312, pp. 22–25.

Vancoillie, C.A.J. (1985 November). *Skedulering Van Theewaterskloofdamloslatings Na Riviervloei-Ontledings Deur Middel Van Liniere Programmering.* Master of Science in Civil Engineering, Stellenbosch University.

Visser, A.J.C. (2010). *Real-time management of river systems by using a hydrodynamic model with optimisation.* Ph.D. thesis.

World Water Assessment Programme (2009). The United Nations World Water Development Report 3: Water in a Changing World.

Appendices

Appendix A

Allocated Areas under irrigation

This Appendix include all the water users in the Riviersonderend catchment downstream from Theewaterskloof. The data was obtained from the ZWUA, the total area allocated by the DWA for these water users is 6097.5 ha.

Table A.1 lists all the measured water users in the Zonderend sub district A.

Table A.2 lists all the measured water users in the Zonderend sub district B.

Table A.3 lists all the measured water users in the Zonderend sub district C.

Finally, table A.4 lists the water users that were not measured by FlowCheck.

Farms - Flo-Check	ZWUA	Allocated Area [Ha]
Theewaterskloof	TWK Plase	120.00
Dwarstrek	WP Frost	68.90
Mariasdal	Wicus Leeuwner Boerdery	52.00
Elandsberg	Helpmekaar Trust	80.00
Phisantekraal	G le Roux (Edms) Bpk	80.00
Phisantekraal	Porseleinberg Boerdery	100.00
Ongegund	P van Niekerk	72.20
Spes Bona	NJ van Niekerk	90.00
Uitkyk	RRF Philip	98.00
Spinlea	DL Hobson	66.00
Middelplaas	Middelplaas Trust	90.00
Klein Ezeljacht	Jurie Fourie Trust	52.00
Champagne	P Reuvers Plase	65.00
Oakdene	Oakdene	61.00
Bakenskloof	Rustenmeyer Bk	50.30
Helderstroom Tronk	Helderstroon Gevangenis	87.50
SS Dam Vlot	Japie Groenewald Trust	239.00
Meerlustkloof	Agrisouth Orchards	120.00
Amanzi	Amanzi Trust	30.00
Meulrivier	Monteith Trust	120.00
Jagersbos	J Sedgwick	67.50
TOTAL		**1809.40**

Table A.1: Sub District A measured water user.

Farms - Flo-Check	ZWUA	Allocated Area [Ha]
Ouplaas	Ouplaas Trust	120.00
Nuweplaas	JB Walker Plase	120.00
Oerwerzicht	Oerwerzicht Trust	120.00
Kleine Eike	Kleine Eike Boerdery	130.00
Zandvlakte	Die Zandvlakte Trust	23.00
Elsenkloof	PR Malherbe	42.00
The Oaks	Bartley Farms	120.00
Riverside	De Kock Sandfontein	80.00
Punt Boerdery	Richshaw Trade Invest	44.50
Soetmelksvlei	JG Muller	40.00
B Sender	B Sender	43.00
Soetmelksvlei	GF Muller	40.00
Ganskraal	Dr Beyers	153.50
Esperance	Bolton Sugar and Citrus	10.00
Noordhoek	Japie Groenewald	60.00
Nethercourt	Johan du Toit Trust	30.00
Nethercourt	Stephen du Toit Trust	30.00
Schuitsberg	Joens Trust	80.00
Vrede	Nico Human Trust	120.00
Vredelust Trust	Vredelust Trust	25.50
Klein Plasie	ML Swart	39.50
Langverwacht	Langverwacht Trust	20.00
Neetlingskroon	Blydskap Trust	100.00
Concordia	Concordia Trust	50.00
Mandaryn	Suiderland Plase	120.00
De Pan	AL du Preez	8.00
Middelpunt	Middelpunt Trust	40.00
Vader Erbe	Theron Familie Trust	60.00
Brakdam	Johbil (Edms) Bpk	22.00
Tygerhoek	Tygerhoek Proefplaas	111.50
TOTAL		**2002.50**

Table A.2: Sub District B measured water users.

Farms - Flo-Check	ZWUA	Allocated Area [Ha]
Riviersonderend		non-farm
Appelskraal	Appelskraal Plase	50.00
Kleinlaagte/Loch Lotus	D Cloete	115.50
Rustenburg	Lorraine Trust	24.00
Grootvlakte	BG Viljoen	70.00
Ongegund	Ongegund Trust	32.00
Tevrede	Gerhard Solms Trust	40.00
Van der Wattskraal	Heldersig Trust	10.00
Haelkraal	Haelkraal Trust	120.00
Stormsvlei Hotel	MJ Spies	22.00
Doornkloof	Noekies Trust	55.50
Rheenen	G de Wet Trust	81.50
Rheenen	Mooiuitsig Boerdery (Edms) Bpk	40.60
Bromberg	GJ Groenewald	13.50
Sangasdrift	Sangasdrift Trust	70.00
Avontuur	Pont Boere	40.00
Avontuur	Avontuur Farm Trust	48.00
Klipfontein	AHF van Zyl	206.50
Geminag	Rossouw Broers	10.00
Kwasarie (Rheenen)	N and M 2000 Trust	20.00
Vaandrightsdrift	AHF Bekker	41.50
Vaandrightsdrift	Vaandrigsdrift Trust	120.00
Pleasant View	Oosthuizen Trust	120.00
Klipfontein	P Urschel	20.00
Merweda/Robyn	Robos Trust	101.00
Riviera	JG Crous	50.00
Jubileeskraal	JC Badenhorst	42.50
TOTAL		**1564.10**

Table A.3: Sub District C measured water users.

Farms	Allocated Area [Ha]
Astralita	10.50
Ambolati	10.00
Aloe Ravine	2.00
Bloemenkraal Landgoed	19.50
Cloud Nine	50.50
Danie du Toit Trust	15.00
Wessel du Toit Trust	15.00
Departement Landbou	100.00
M Donkin	10.00
Enrico Beyers	50.00
Express Model Trading	60.00
Maandagsourtivier Trust	3.00
Fletchers Trust	10.00
Gemeenskap van Genadendal	34.50
DC Human (Haelkraal)	10.00
Hansie Human Familie Trust	10.00
Iphuphaletu Farming	10.00
JP O ' Connell Trust	10.00
Lincorso Trust	79.00
TWK Munisipaliteit	11.00
SW Viljoen Familie Trust/VanderWattskraal	22.50
Nooitgedagt Trust	30.00
E van As Streicher	10.00
Trade Avail CC	22.00
Van Dyk Trust	50.00
Andrew Starke Farms	17.00
Pikkie Viljoen Trust	9.00
Wijnberg Farm Trust	30.00
Webber Family Trust	11.00
TOTAL	**721.50**

Table A.4: Unmeasured water users.

Appendix B

Irrigation Usage Graphs for 2006-2007

This Appendix is a compilation of the irrigation water requirement graphs of 118 farmers, which water usage were measured in the Riviersonderend catchment downstream from Theewaterskloof. Each graph shows the measured data, the irrigation water requirement estimated by Sapwat3 and the distribution used in the Mike 11 simulation. The remaining 43 farmers water usage were not measured and Sapwat3 was used to estimate the irrigation requirement.

All the data, including measured, Sapwat3 and the irrigation water requirements used in this thesis are available digitally on a CD attached to this thesis.

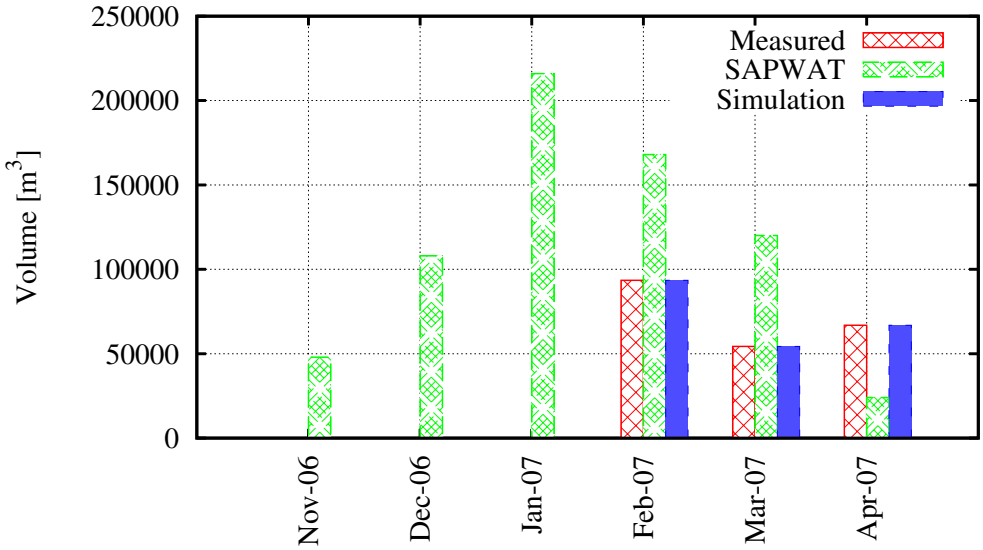

Figure B.1: Theewaterskloof measured, estimated and simulated water usage.

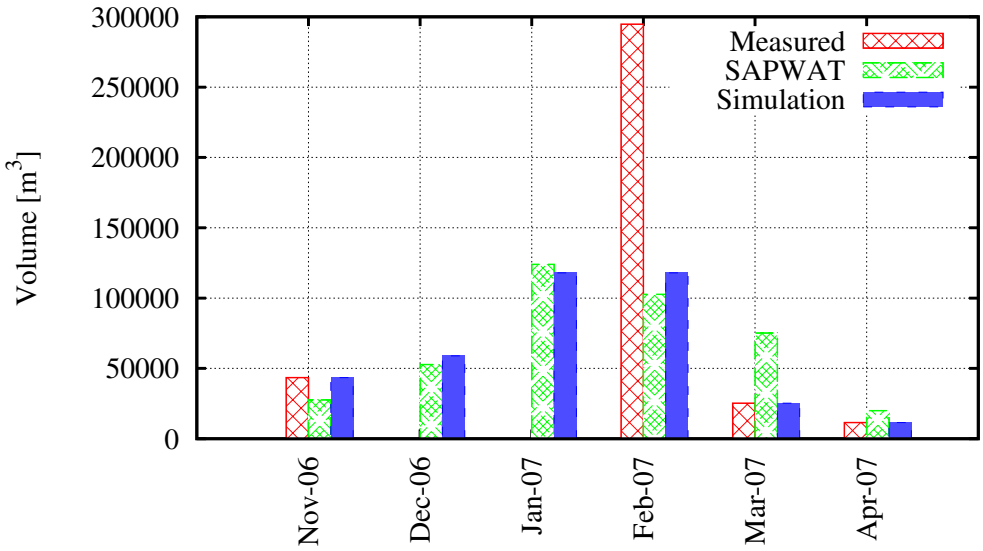

Figure B.2: Dwarstrek measured, estimated and simulated water usage.

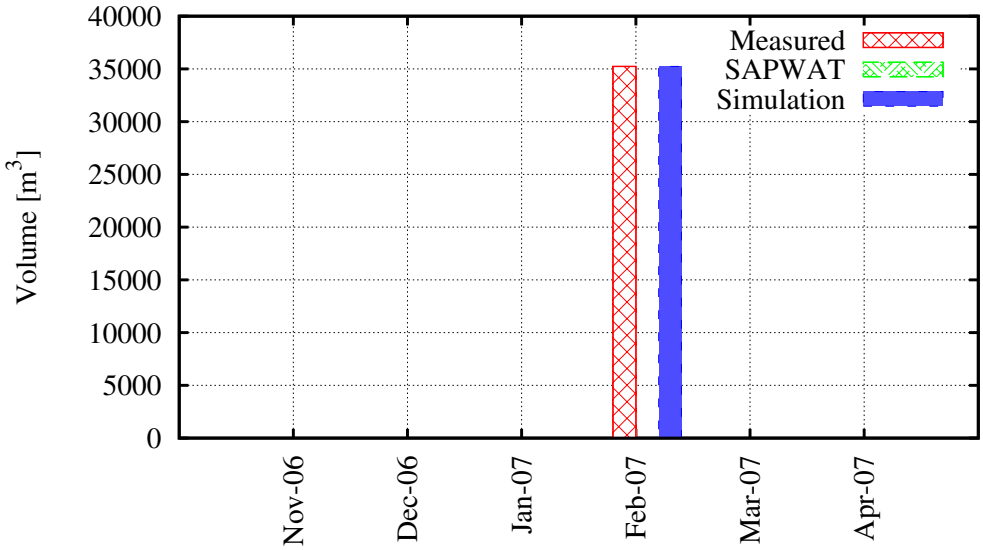

Figure B.3: Ruensveld Wes measured, estimated and simulated water usage.

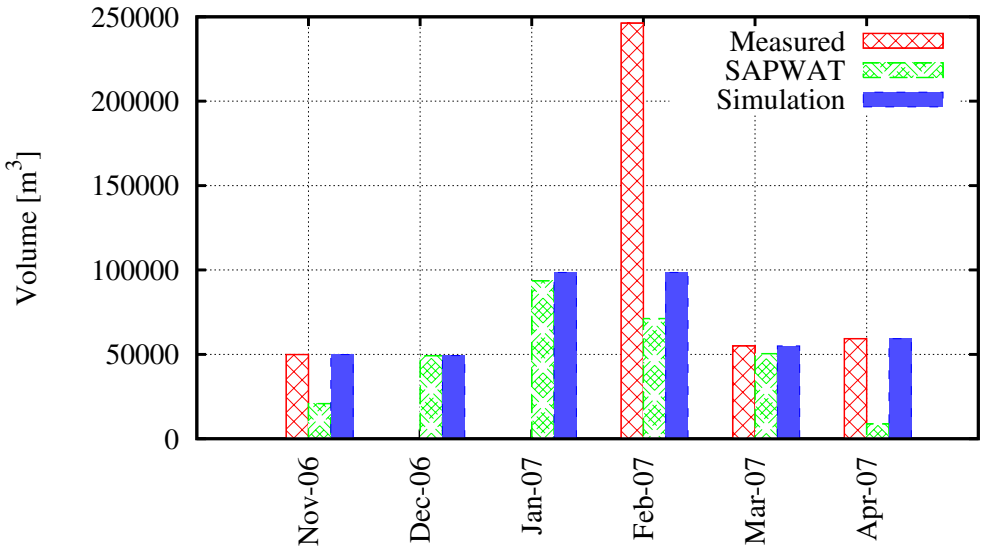

Figure B.4: Maraisdal measured, estimated and simulated water usage.

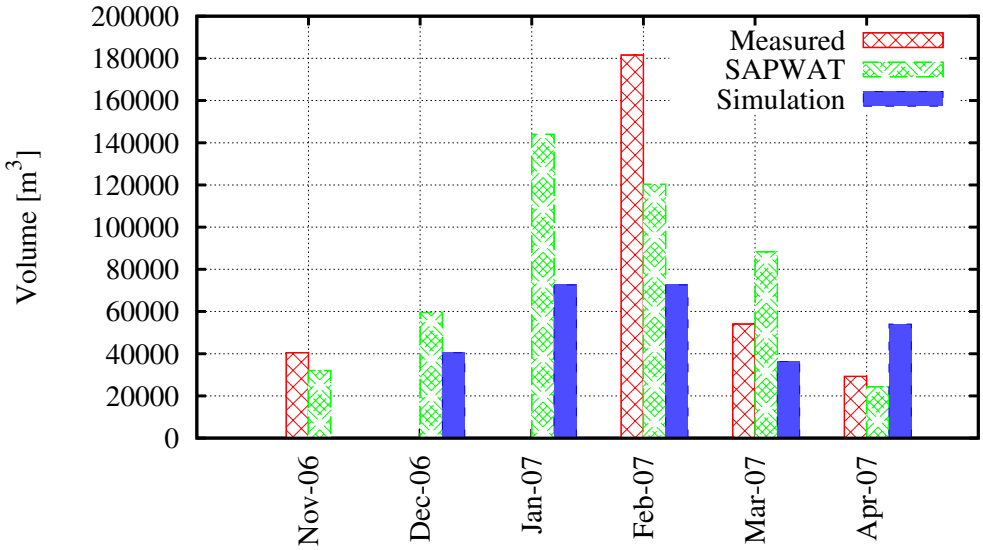

Figure B.5: Elandsberg measured, estimated and simulated water usage.

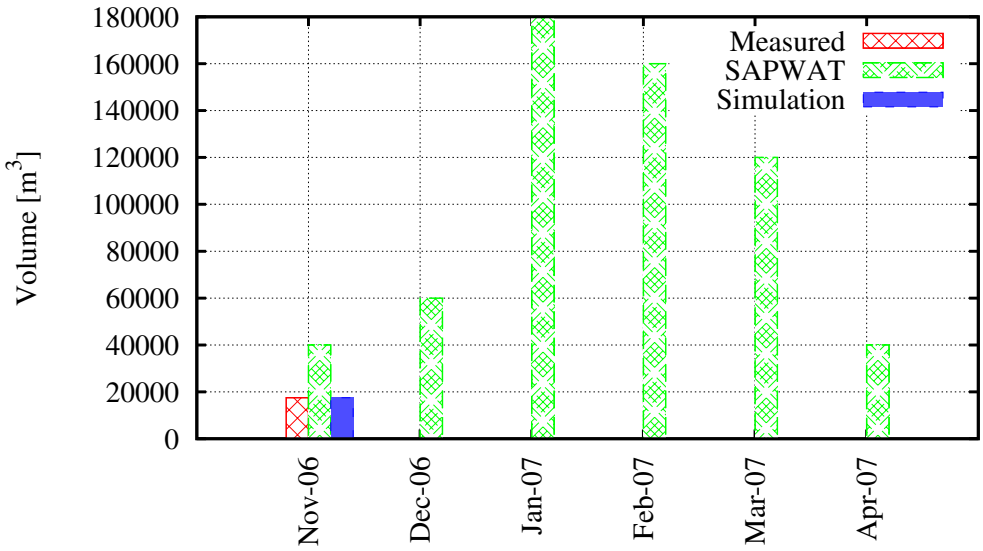

Figure B.6: Phisantekraal 2 measured, estimated and simulated water usage.

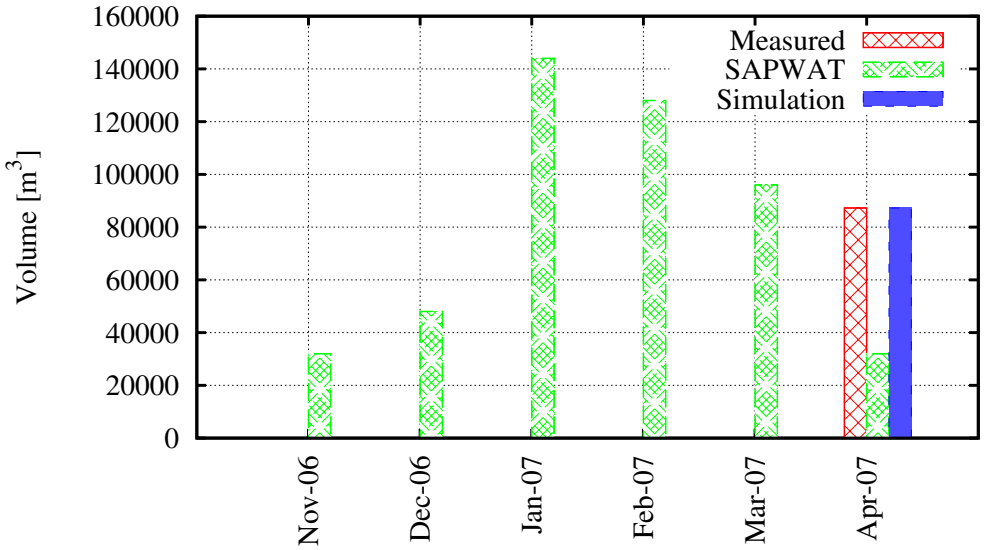

Figure B.7: Phisantekraal 1 measured, estimated and simulated water usage.

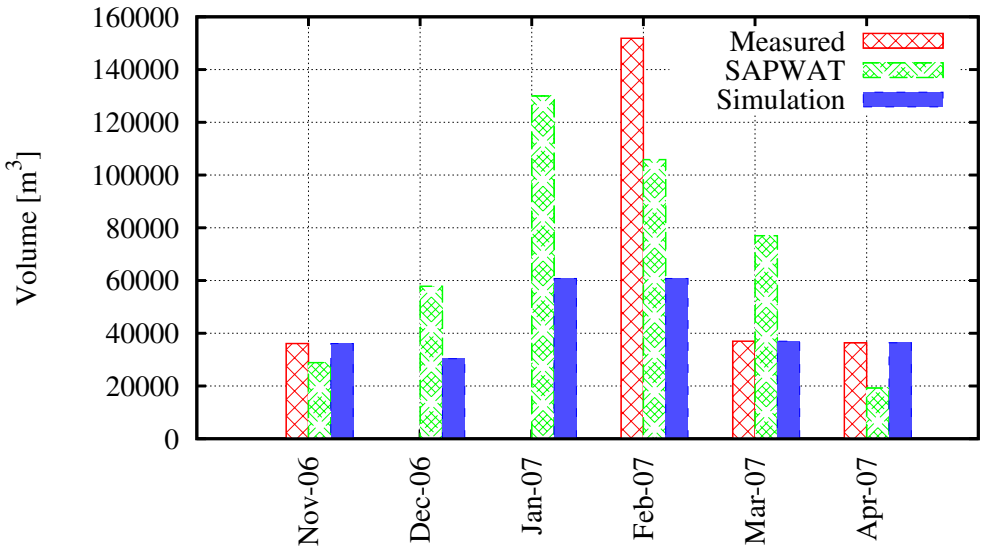

Figure B.8: Ongegund 2 measured, estimated and simulated water usage.

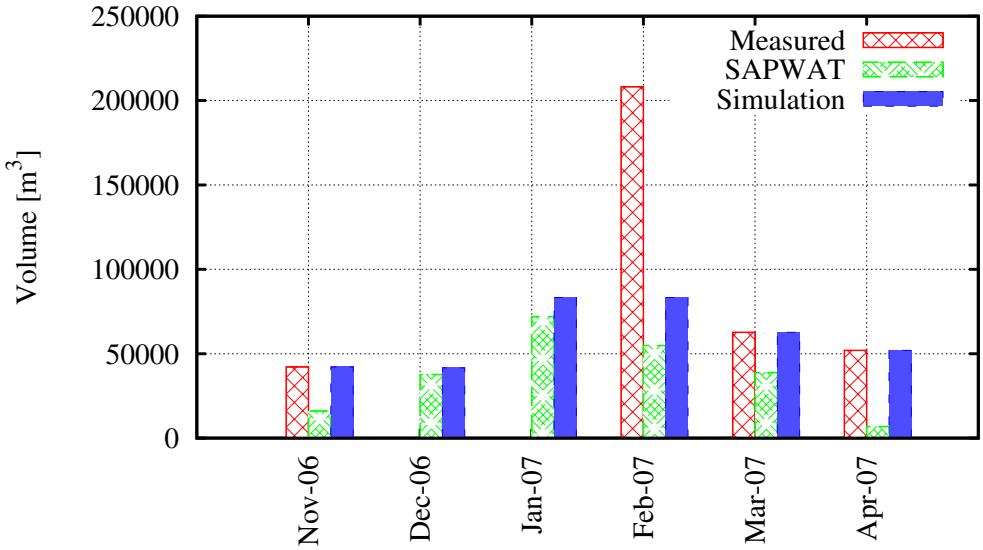

Figure B.9: Spes Bona 1 measured, estimated and simulated water usage.

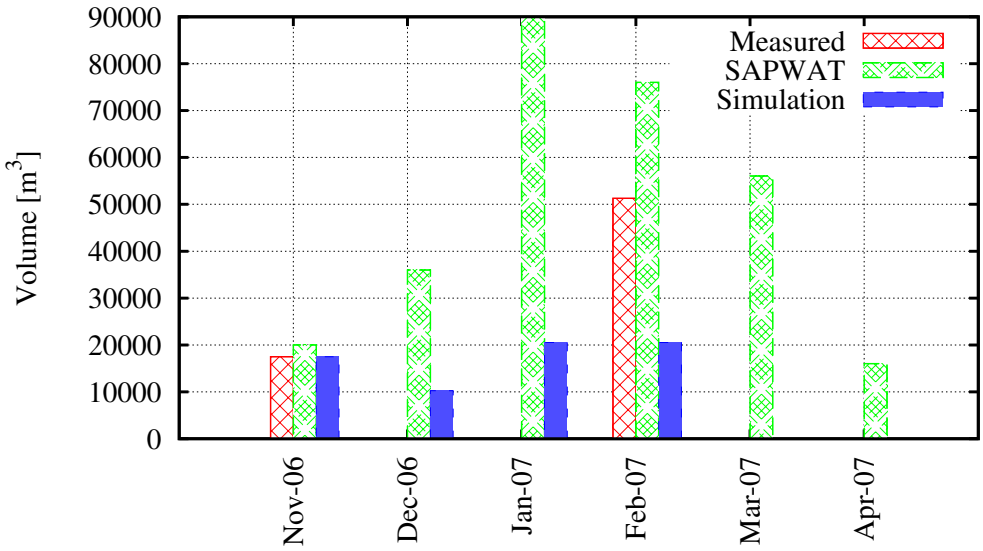

Figure B.10: Spes Bona 2 measured, estimated and simulated water usage.

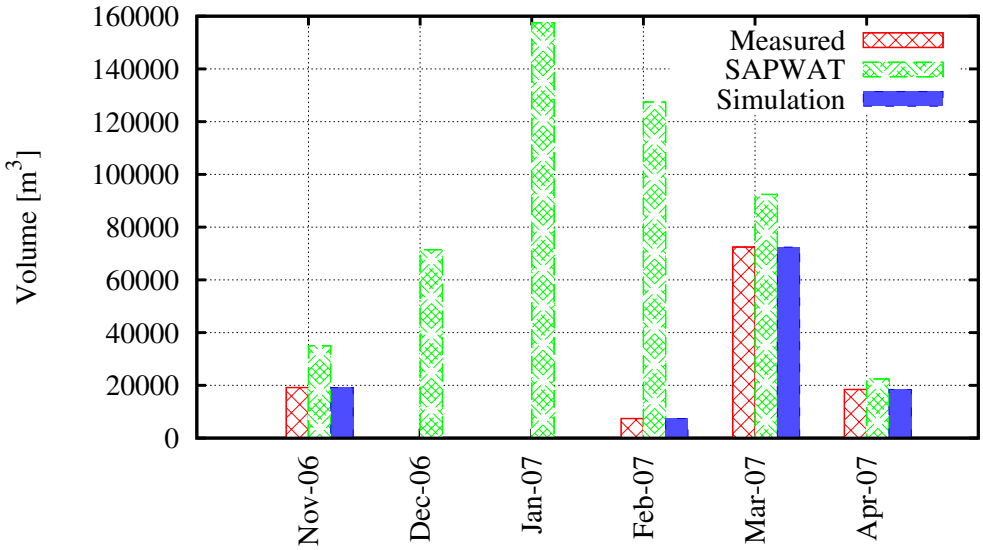

Figure B.11: Helderstroom measured, estimated and simulated water usage.

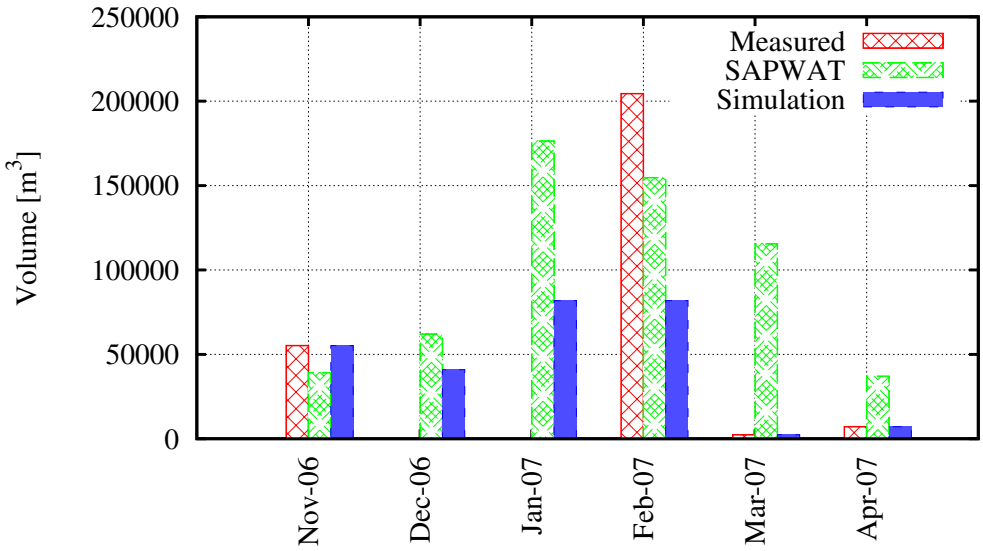

Figure B.12: Uitkyk measured, estimated and simulated water usage.

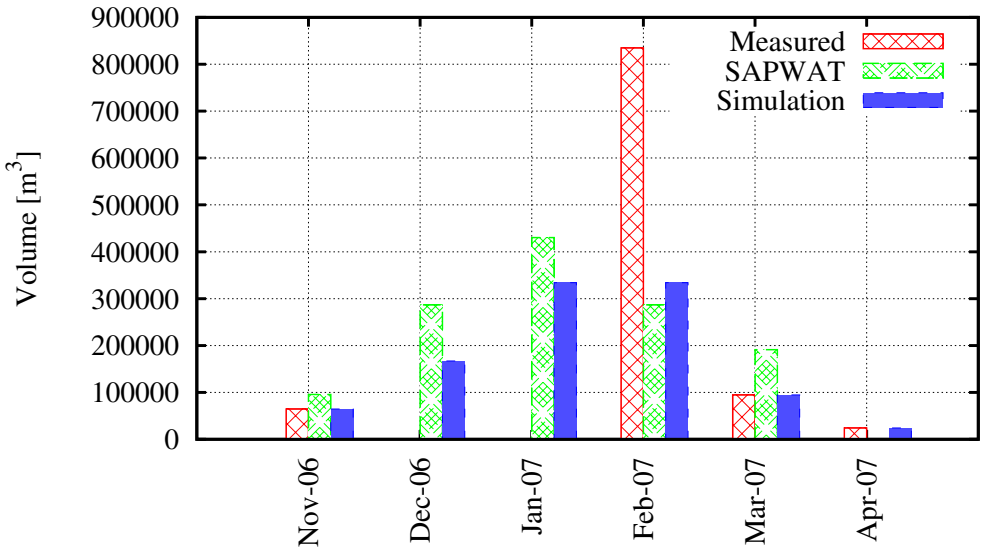

Figure B.13: Sunnyside measured, estimated and simulated water usage.

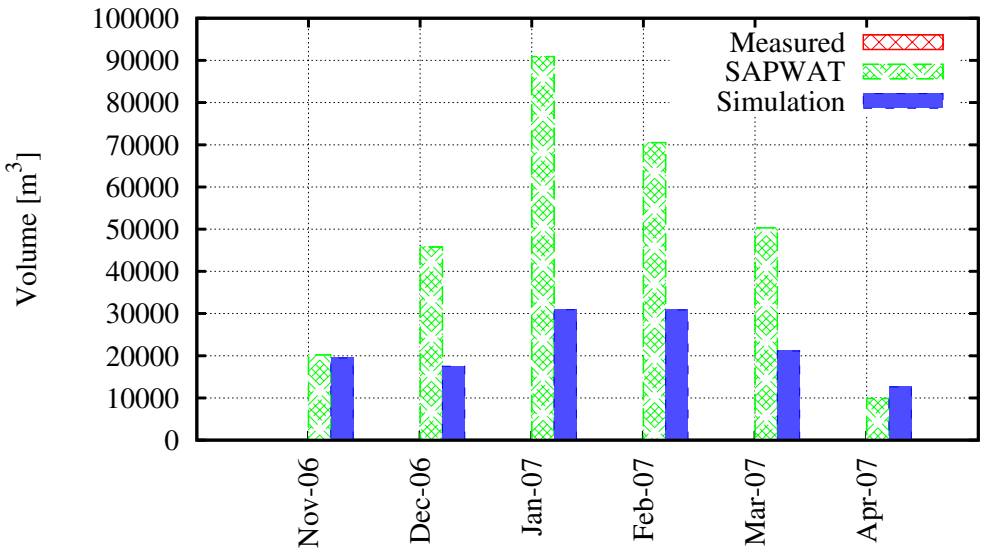

Figure B.14: Elandskloof/Cloud 9 measured, estimated and simulated water usage.

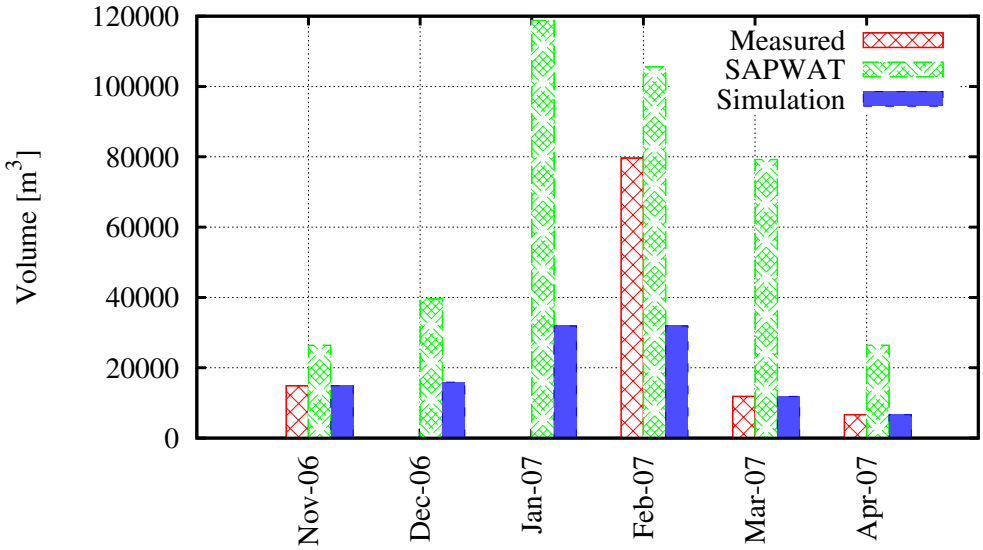

Figure B.15: Spinlea measured, estimated and simulated water usage.

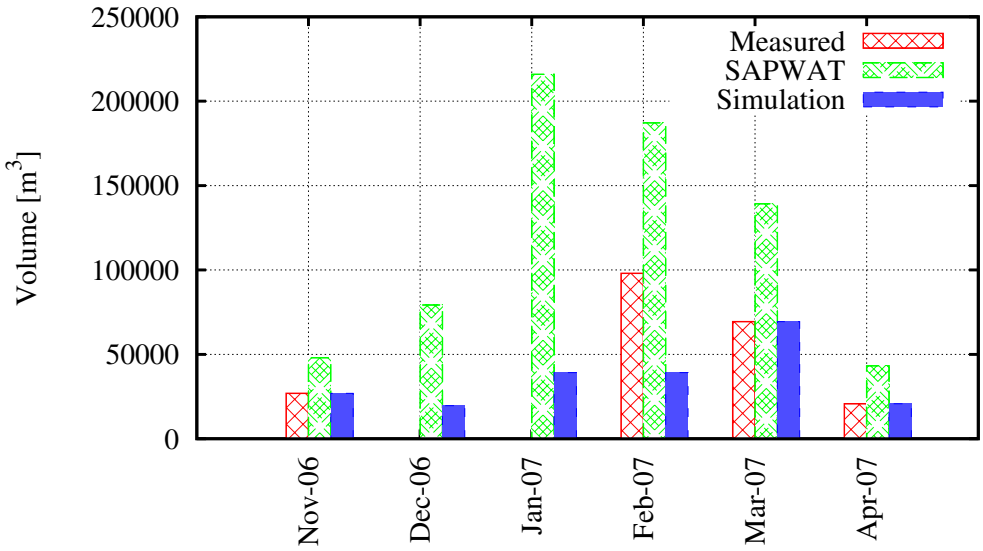

Figure B.16: Meerlustkloof measured, estimated and simulated water usage.

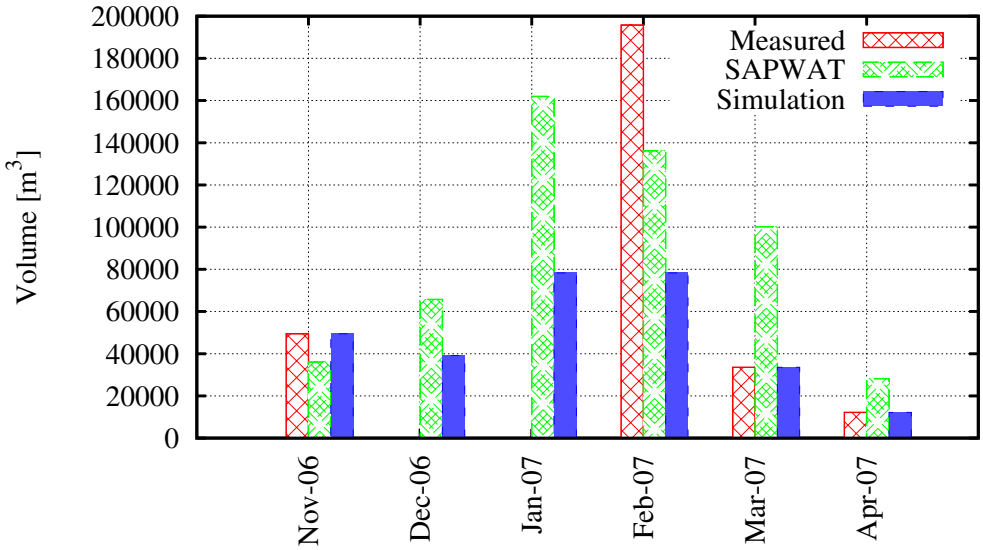

Figure B.17: Middelplaas measured, estimated and simulated water usage.

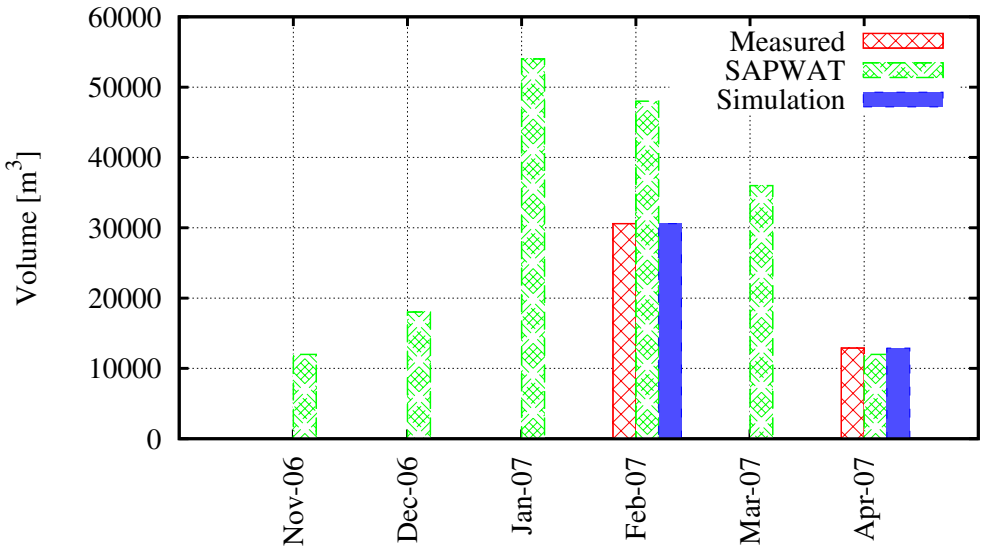

Figure B.18: Amanzi measured, estimated and simulated water usage.

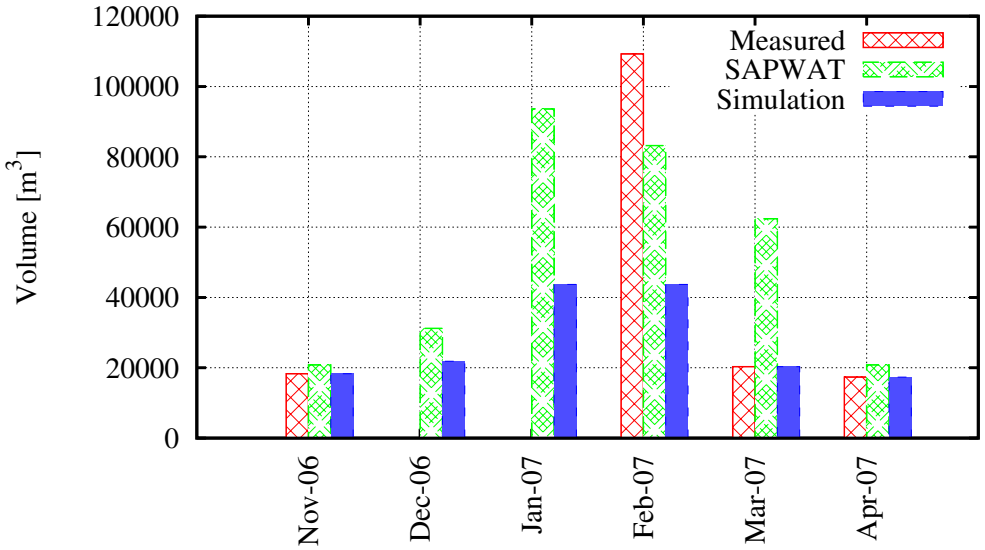

Figure B.19: Klein Ezeljacht measured, estimated and simulated water usage.

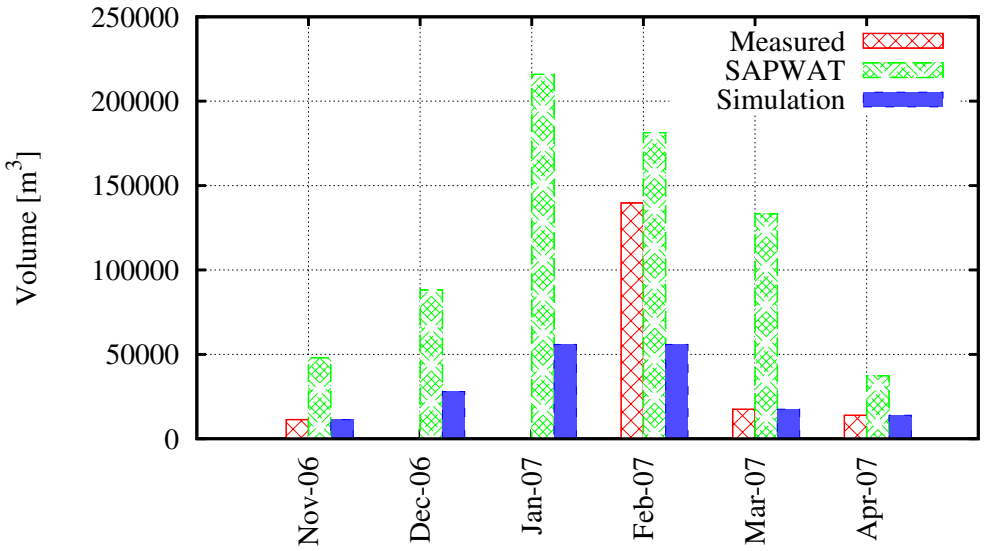

Figure B.20: Meulrivier measured, estimated and simulated water usage.

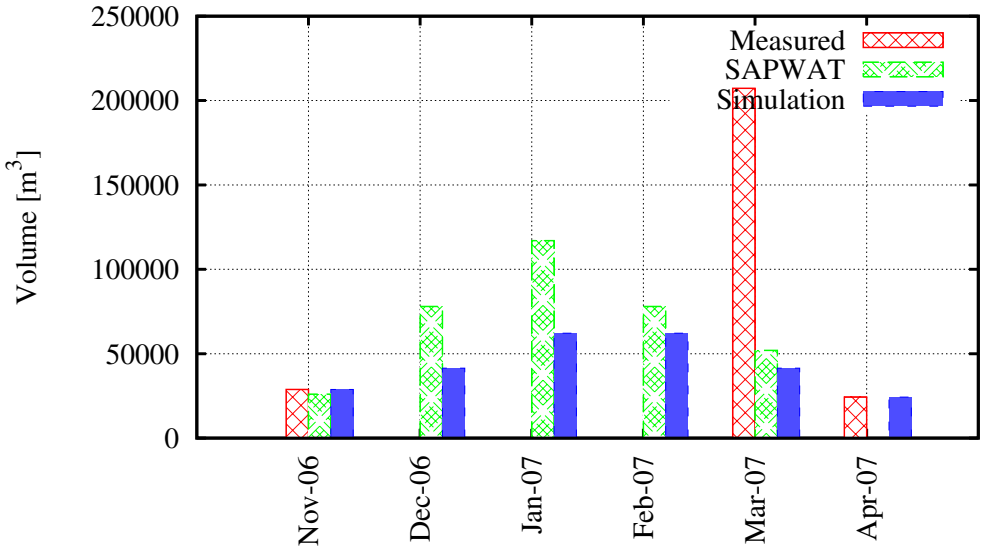

Figure B.21: Champagne measured, estimated and simulated water usage.

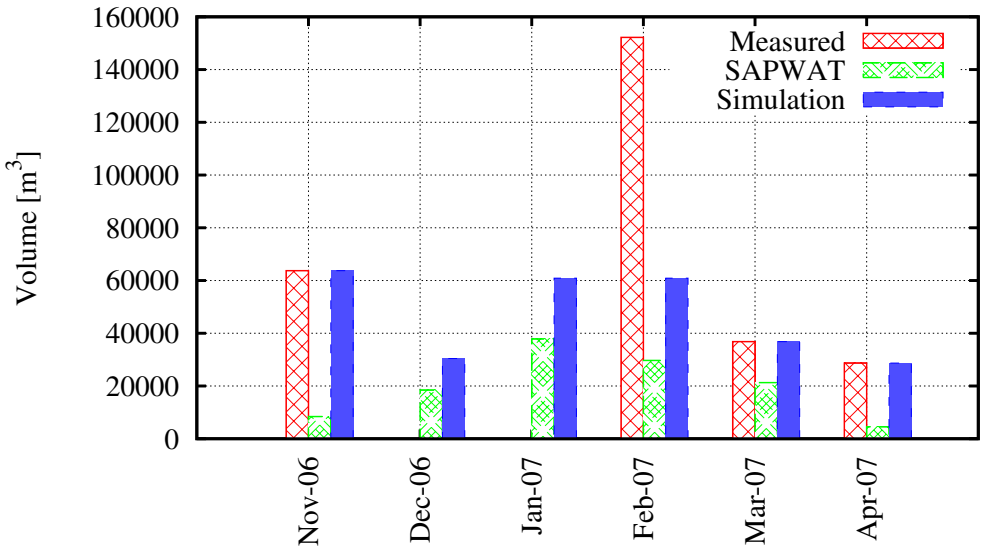

Figure B.22: Oakdene measured, estimated and simulated water usage.

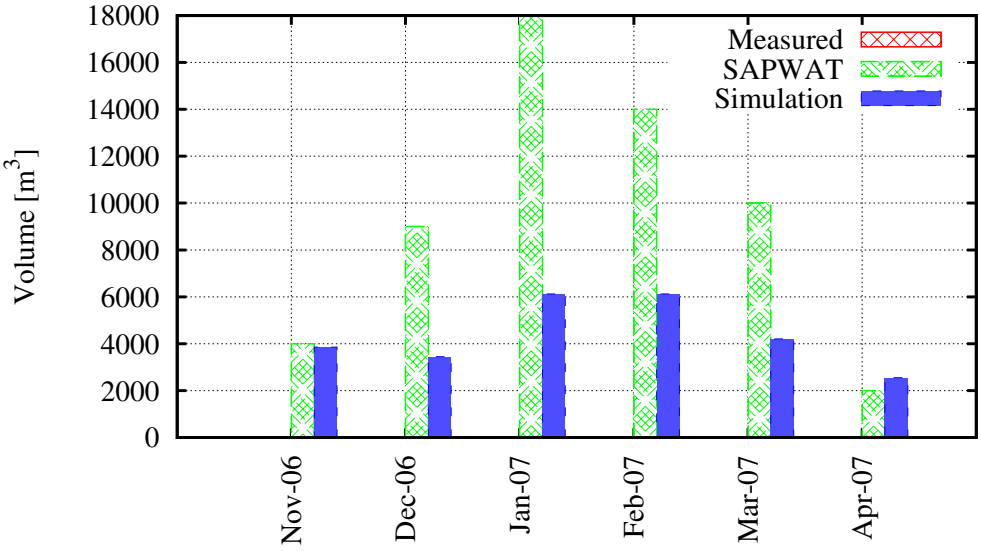

Figure B.23: Oakdene (M. Donkin) measured, estimated and simulated water usage.

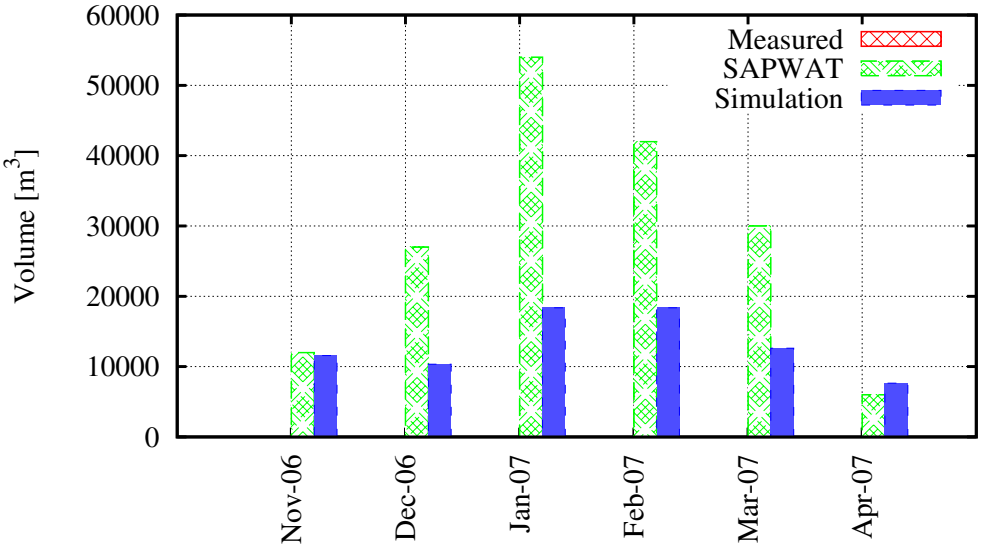

Figure B.24: Oakdene (Nooitgedagt Trust) measured, estimated and simulated water usage.

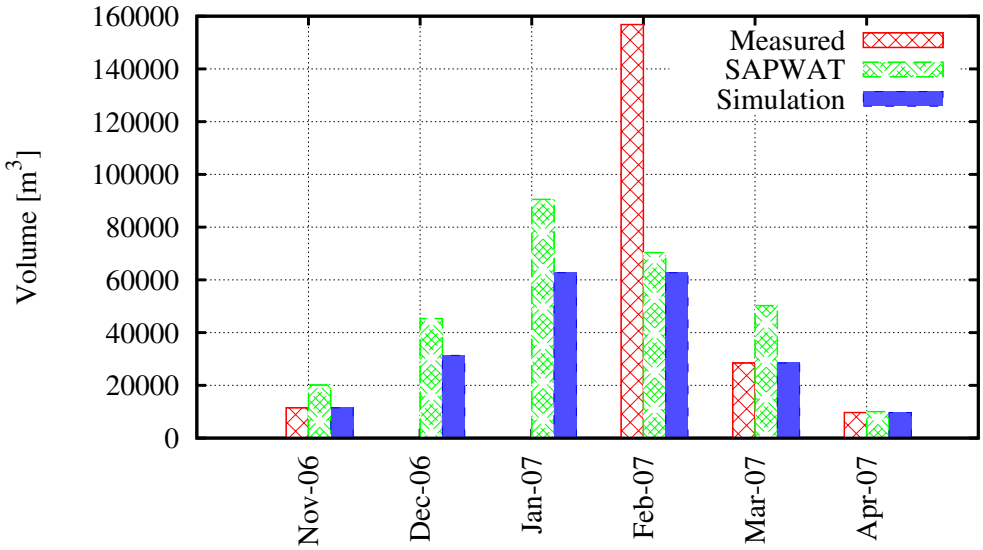

Figure B.25: Bakenskloof measured, estimated and simulated water usage.

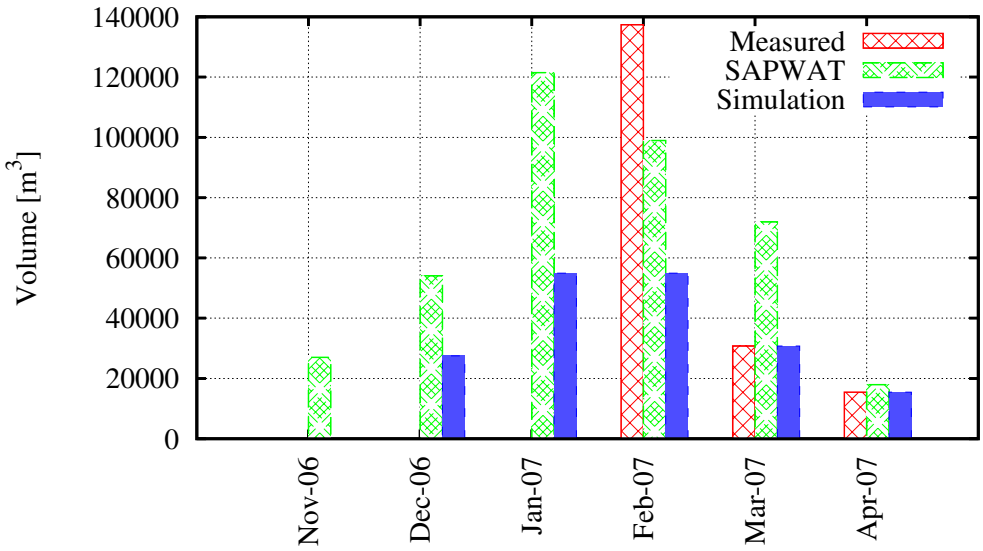

Figure B.26: Jagersbos measured, estimated and simulated water usage.

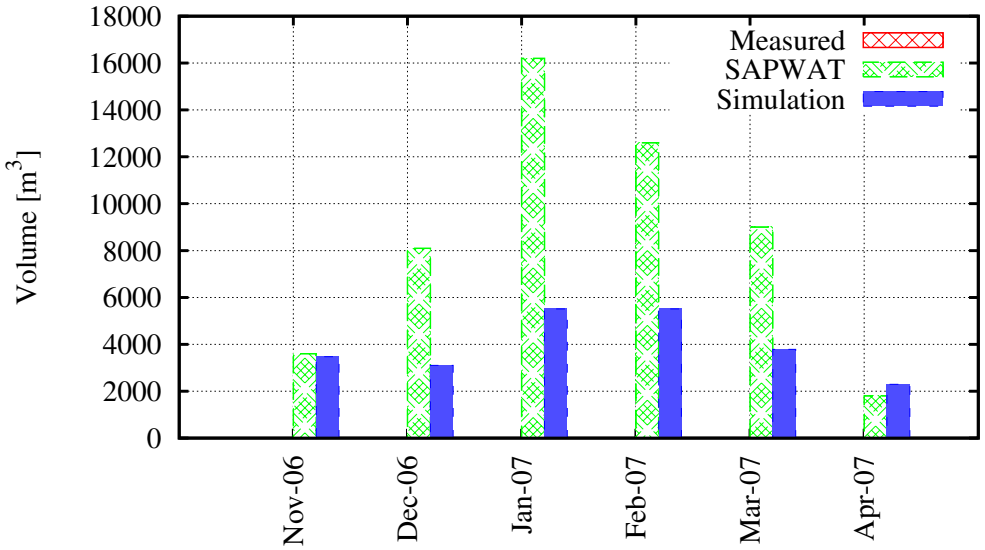

Figure B.27: Pikkie Viljoen measured, estimated and simulated water usage.

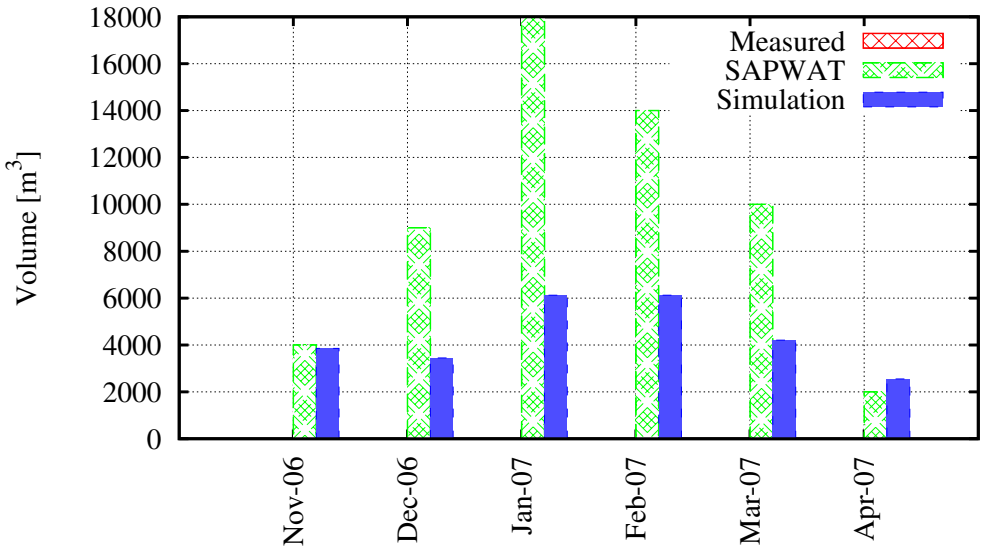

Figure B.28: M. Bothma measured, estimated and simulated water usage.

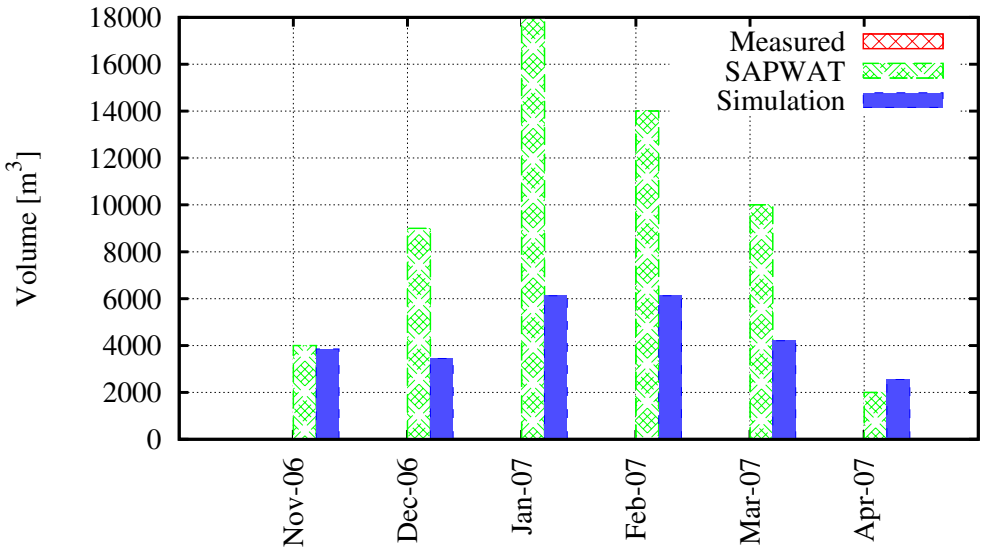

Figure B.29: Ambolati measured, estimated and simulated water usage.

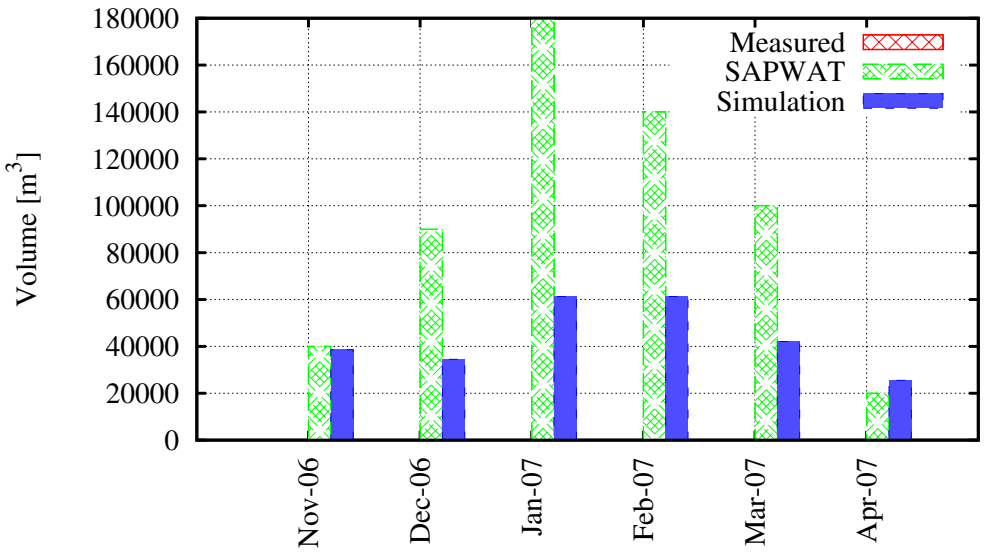

Figure B.30: Department of Agriculture measured, estimated and simulated water usage.

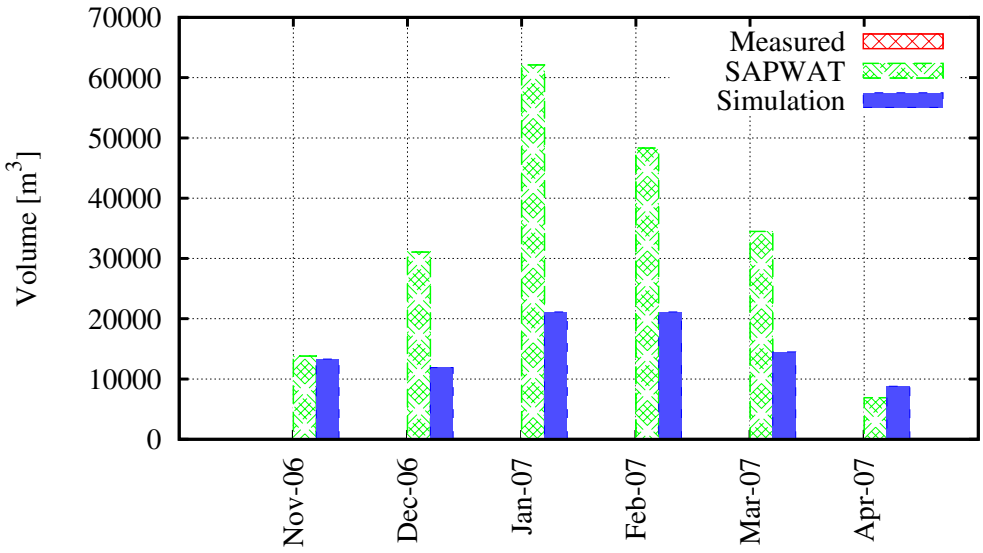

Figure B.31: Genadendal Community measured, estimated and simulated water usage.

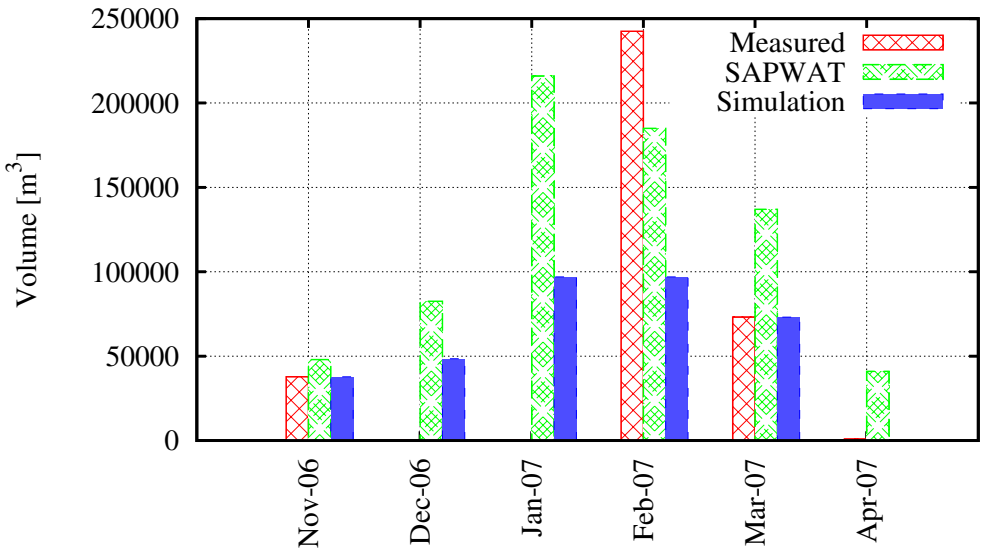

Figure B.32: Ouplaas measured, estimated and simulated water usage.

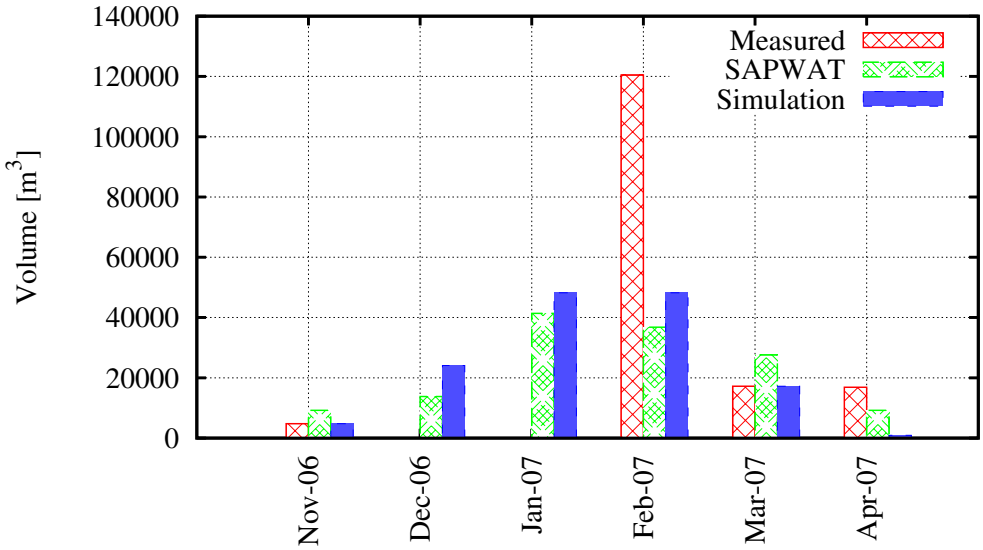

Figure B.33: Zandvlakte measured, estimated and simulated water usage.

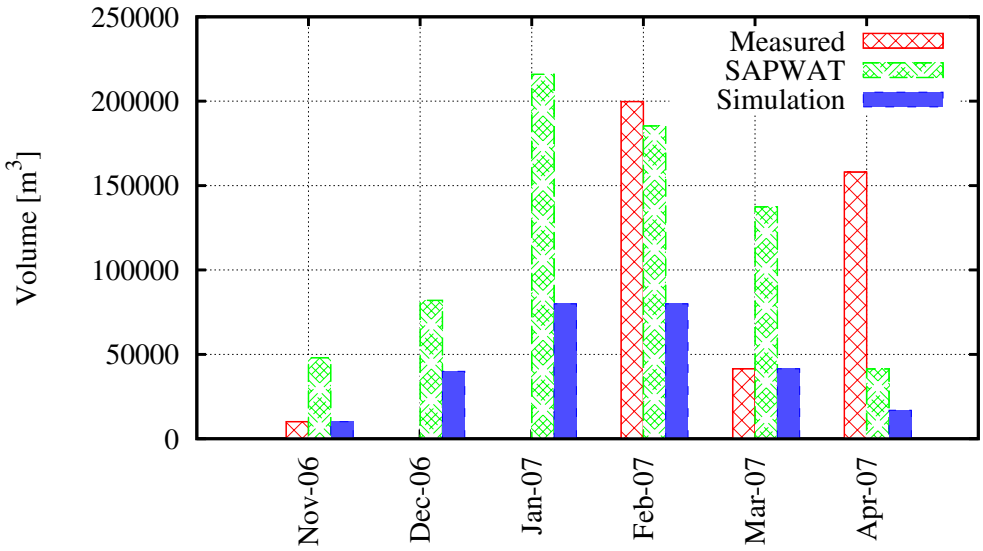

Figure B.34: Nuweplaas measured, estimated and simulated water usage.

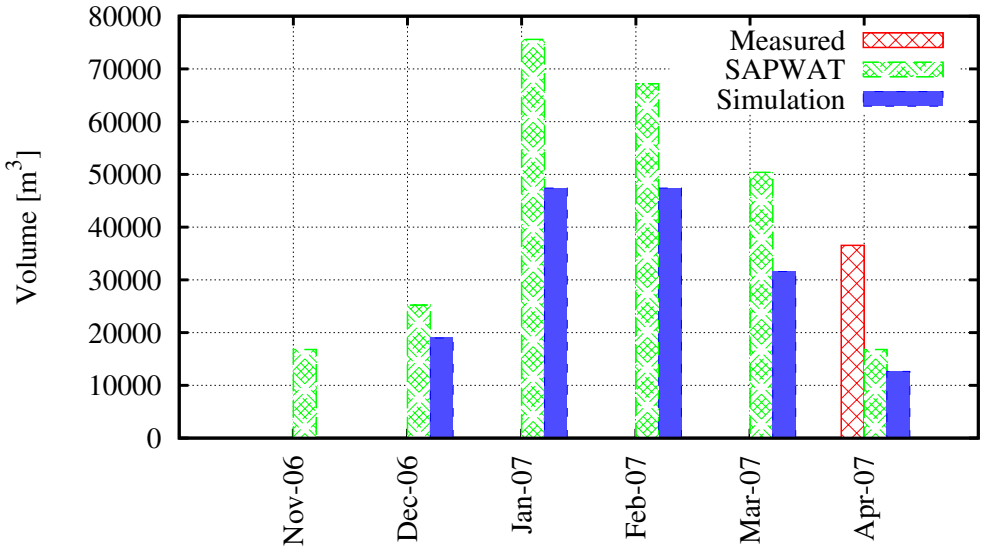

Figure B.35: Elsenkloof measured, estimated and simulated water usage.

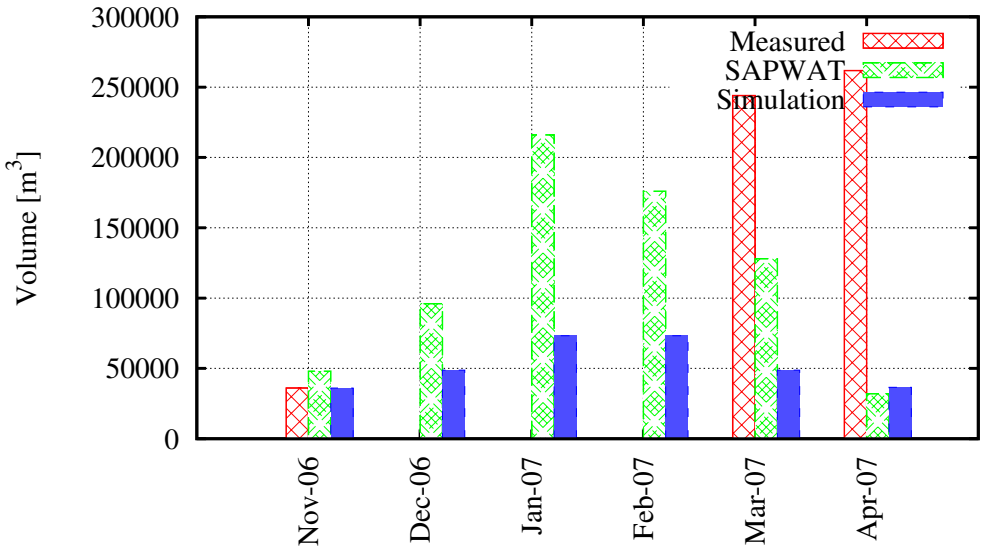

Figure B.36: Oewerzicht measured, estimated and simulated water usage.

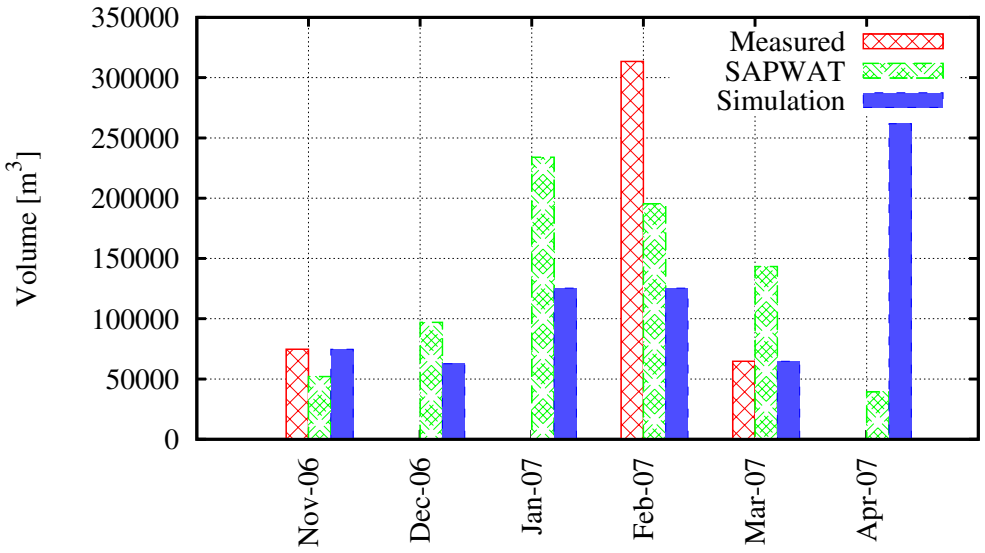

Figure B.37: Klein Eike measured, estimated and simulated water usage.

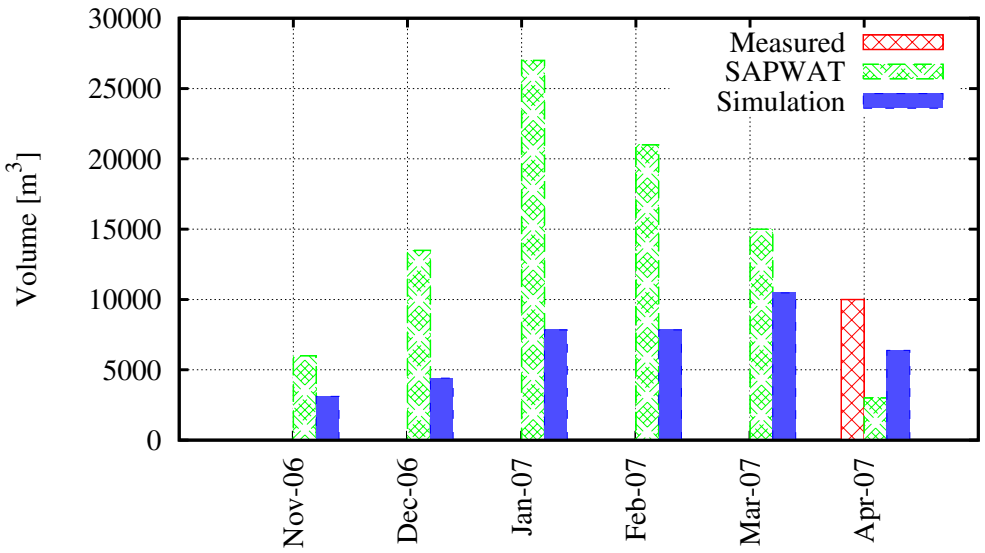

Figure B.38: Danie du Toit Trust measured, estimated and simulated water usage.

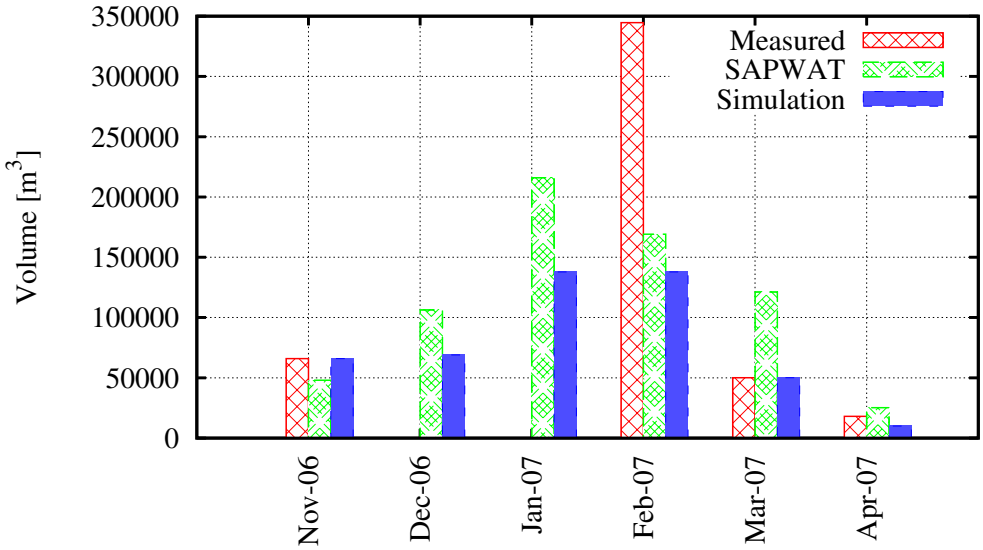

Figure B.39: The Oaks measured, estimated and simulated water usage.

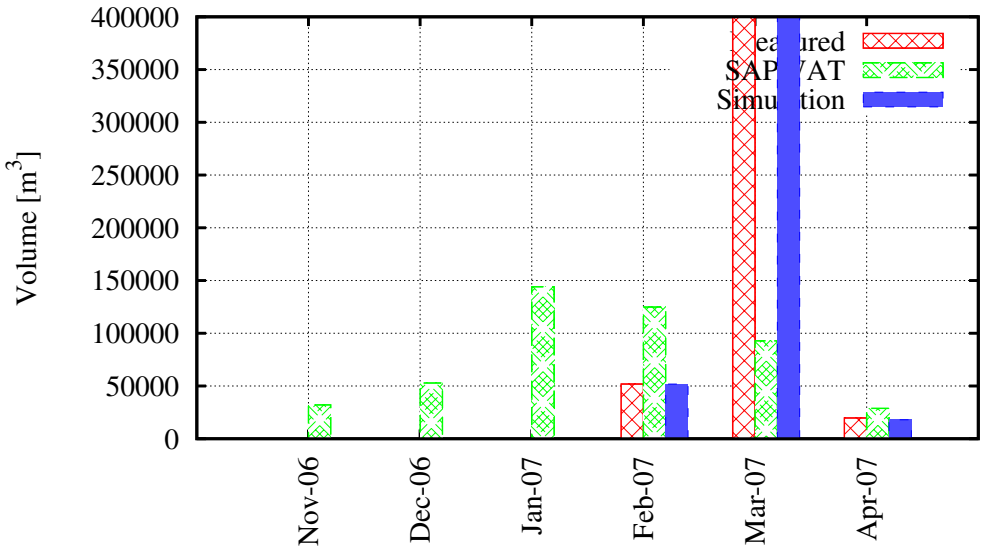

Figure B.40: Riverside measured, estimated and simulated water usage.

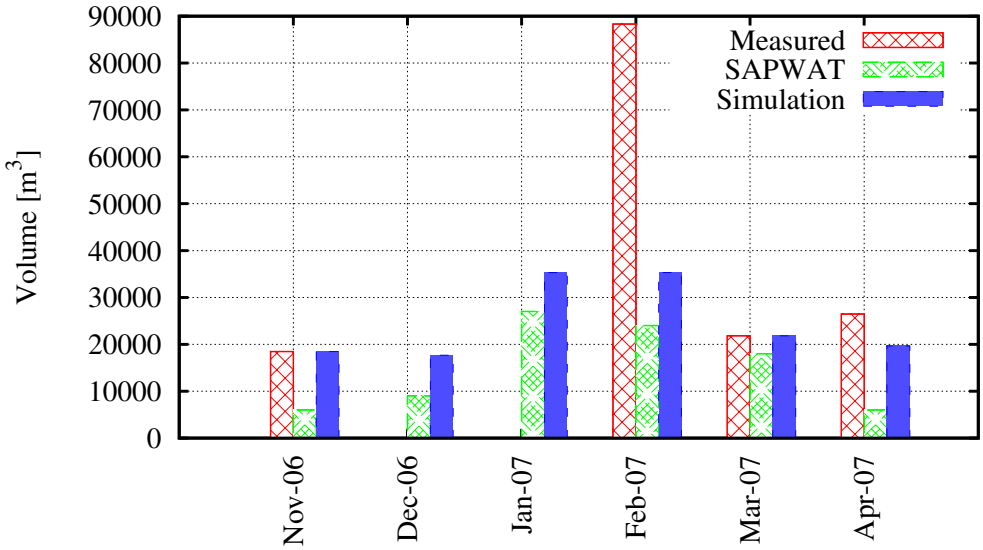

Figure B.41: Nethercourt 1 measured, estimated and simulated water usage.

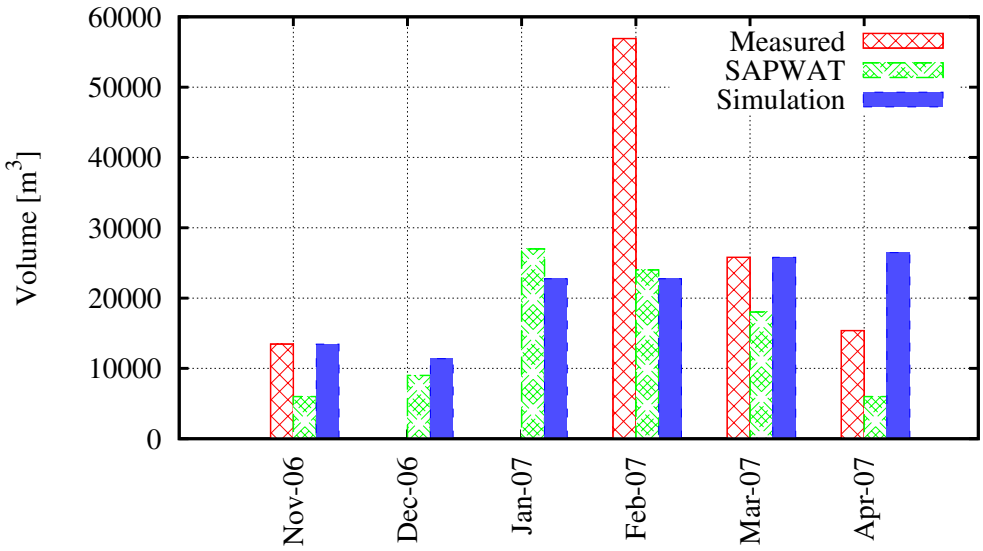

Figure B.42: Nethercourt 2 measured, estimated and simulated water usage.

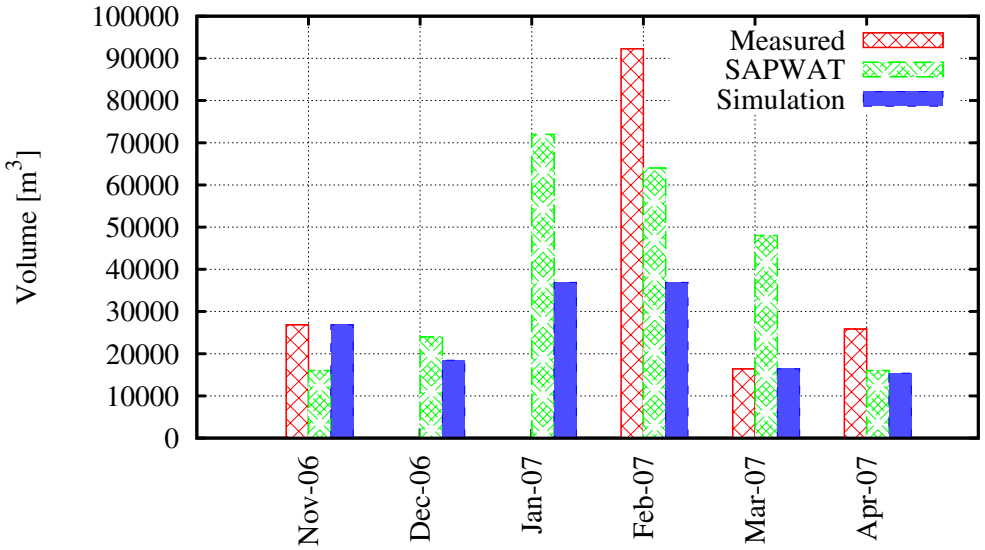

Figure B.43: Soetmelksvlei measured, estimated and simulated water usage.

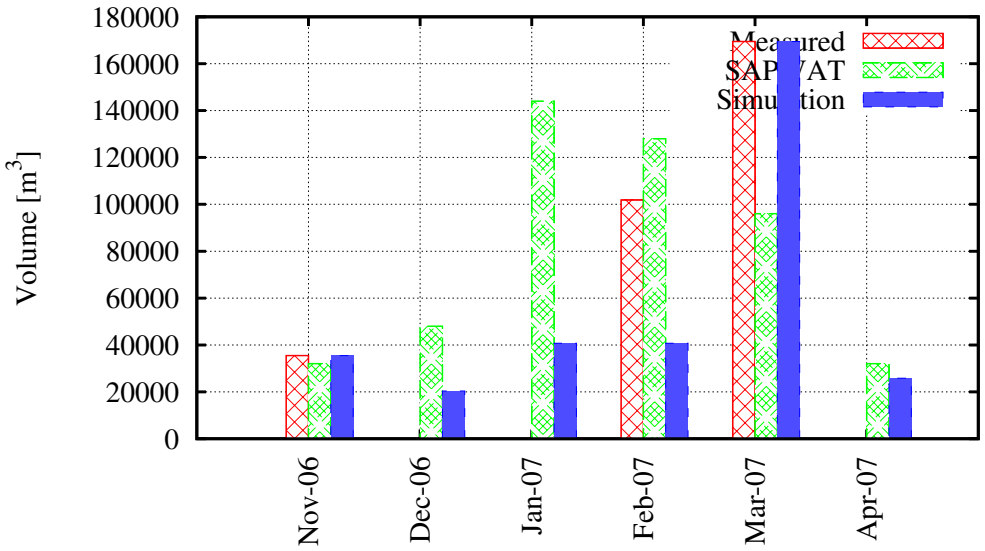

Figure B.44: Schuitsberg measured, estimated and simulated water usage.

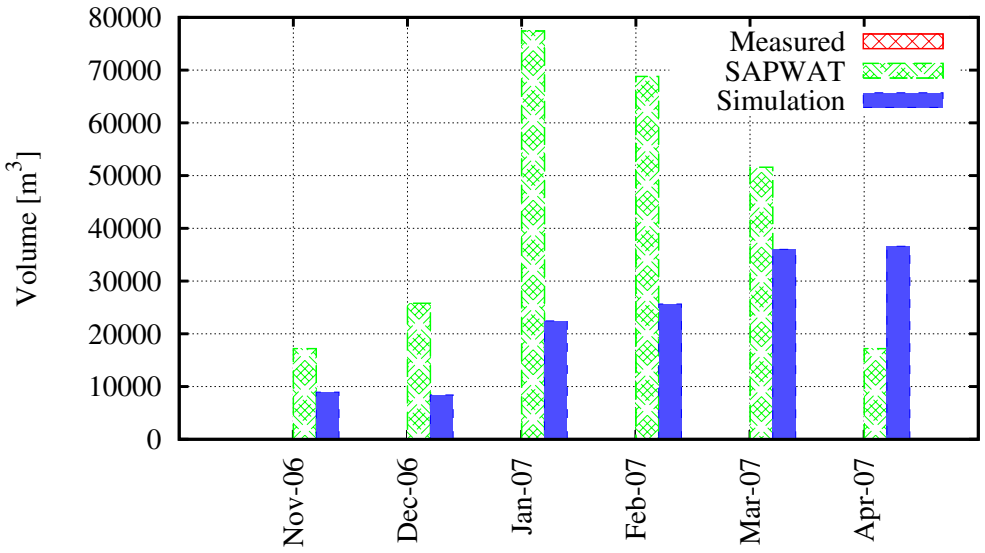

Figure B.45: Soetmelksvlei (B. Sender) measured, estimated and simulated water usage.

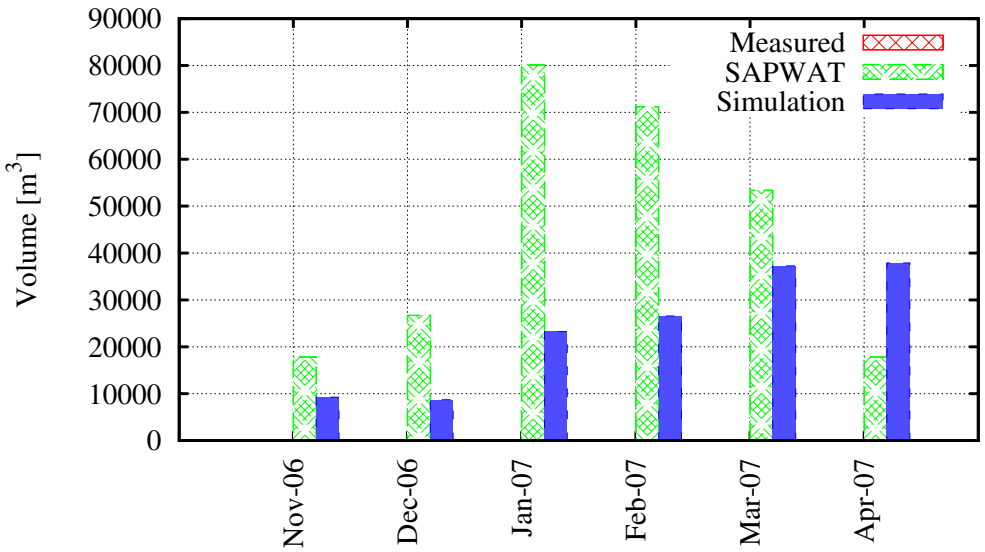

Figure B.46: Punt Boerdery measured, estimated and simulated water usage.

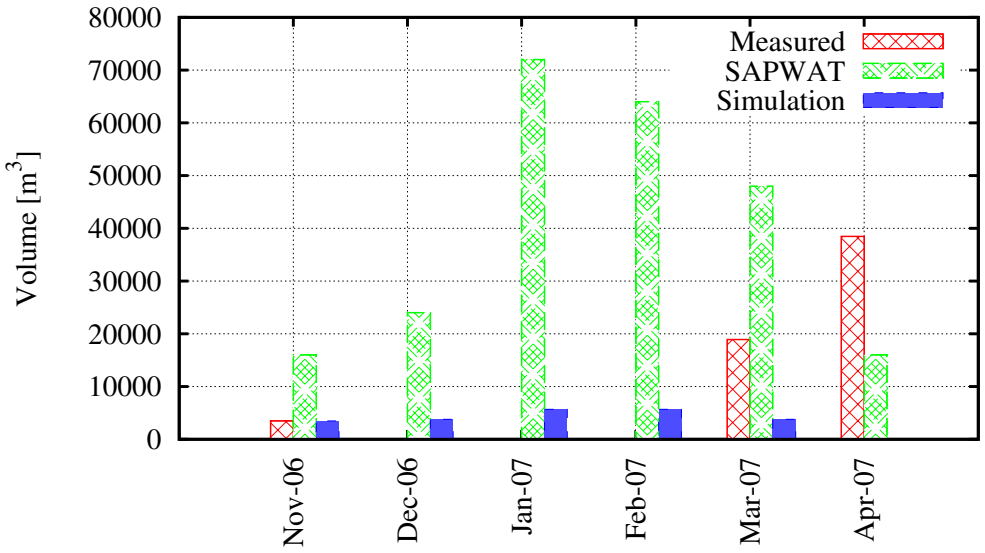

Figure B.47: Soetmelksvlei (Koert se kraal) measured, estimated and simulated water usage.

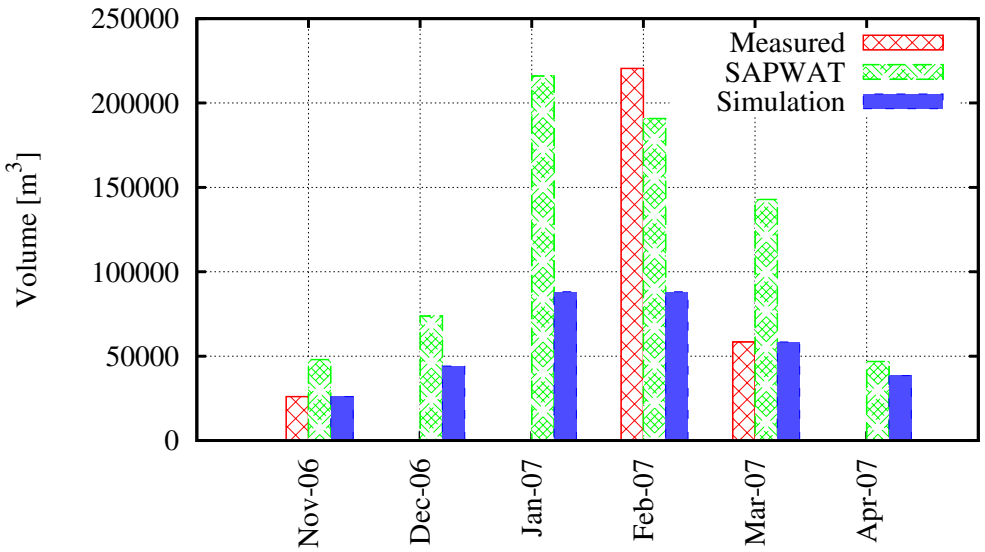

Figure B.48: Vrede measured, estimated and simulated water usage.

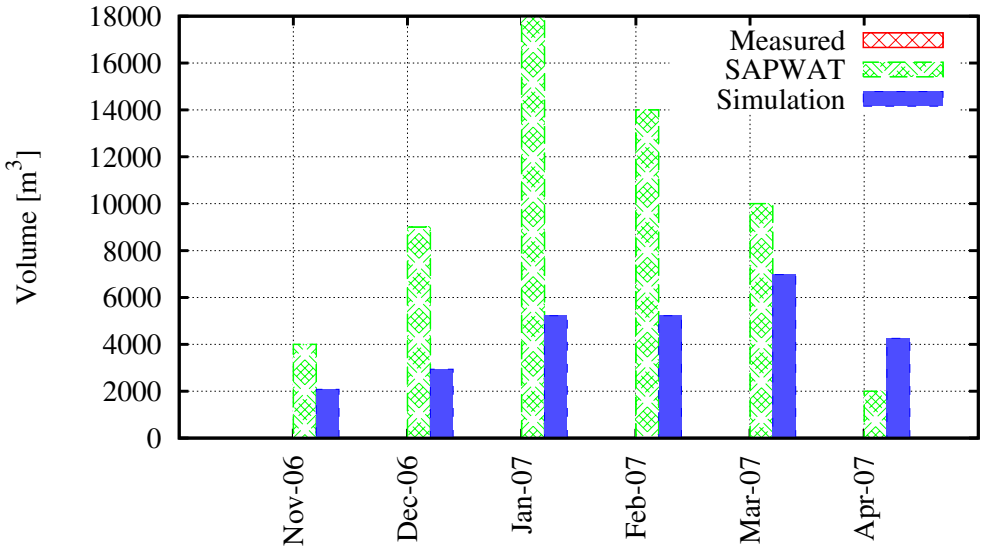

Figure B.49: H. Human Trust measured, estimated and simulated water usage.

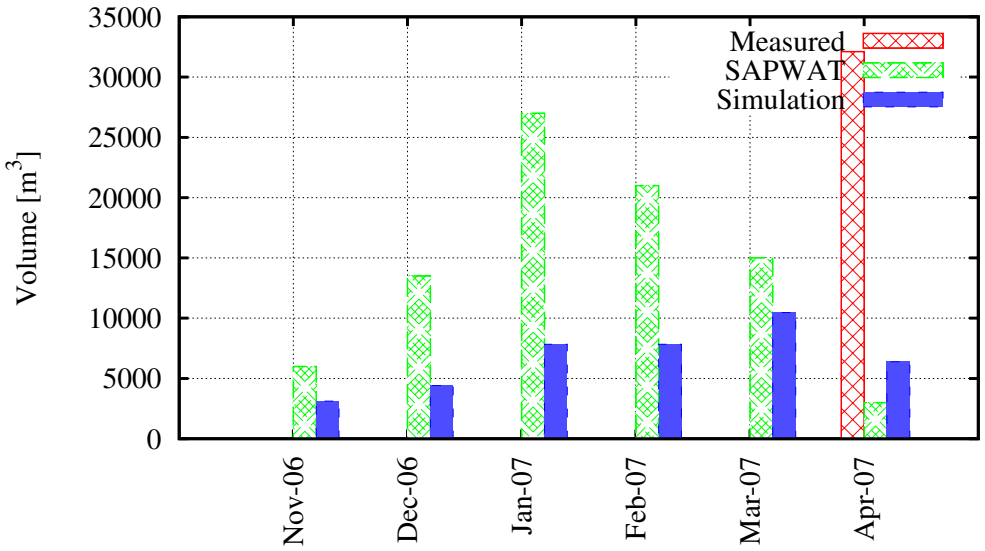

Figure B.50: S. du Toit Trust measured, estimated and simulated water usage.

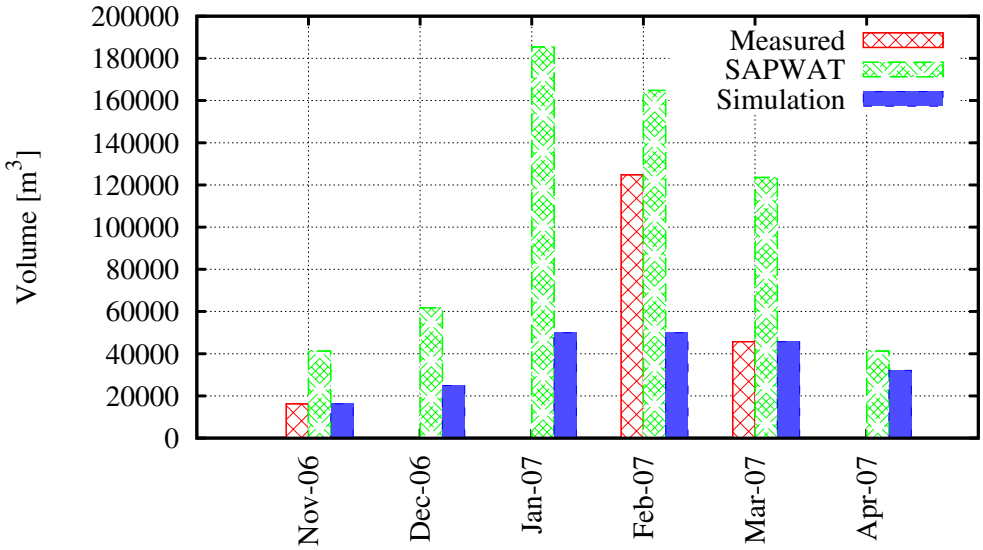

Figure B.51: Ganskraal measured, estimated and simulated water usage.

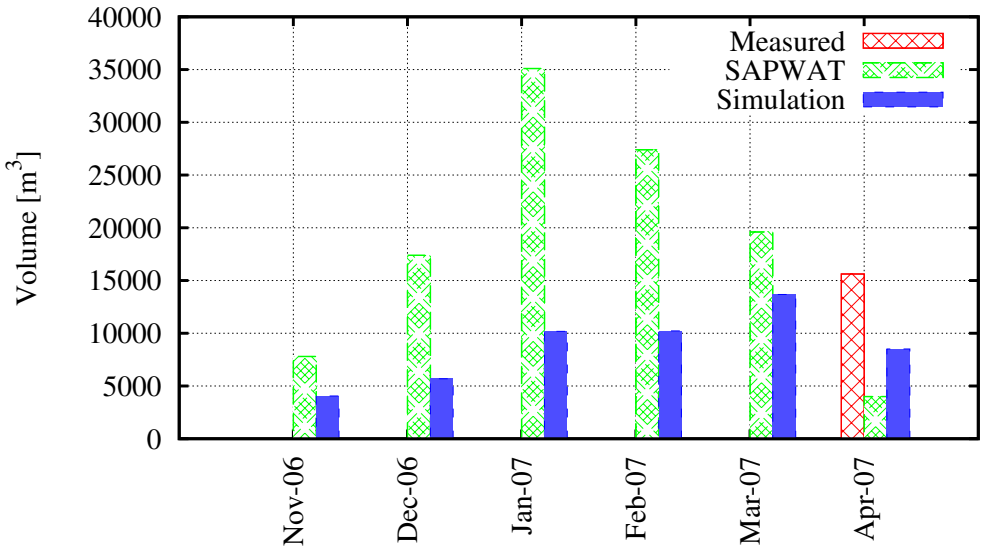

Figure B.52: Bloemenkraal measured, estimated and simulated water usage.

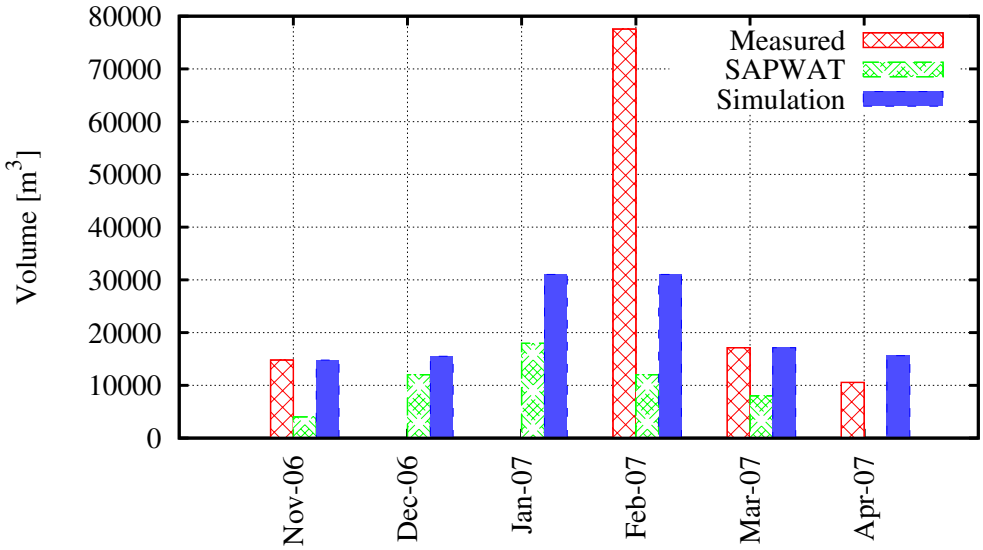

Figure B.53: Ganskraal measured, estimated and simulated water usage.

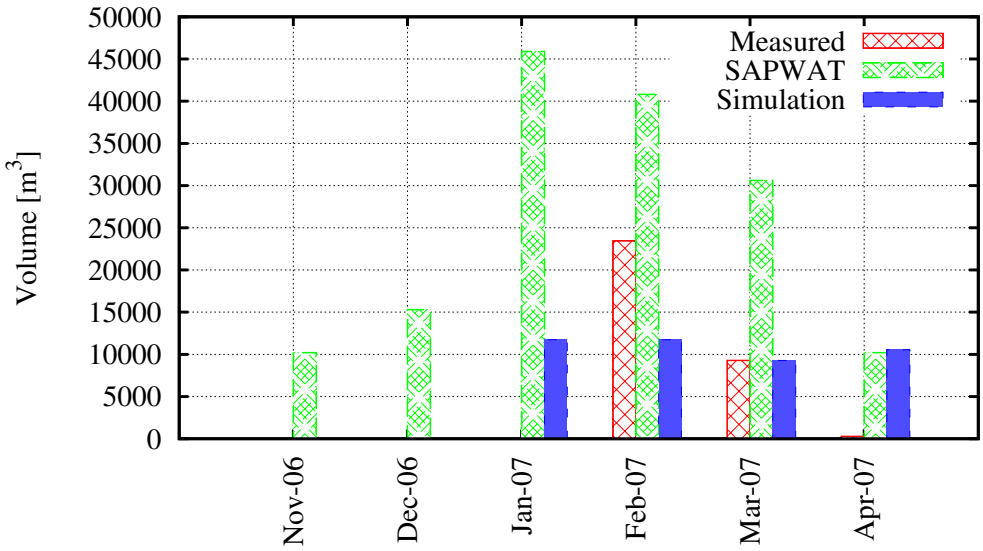

Figure B.54: Vredelust measured, estimated and simulated water usage.

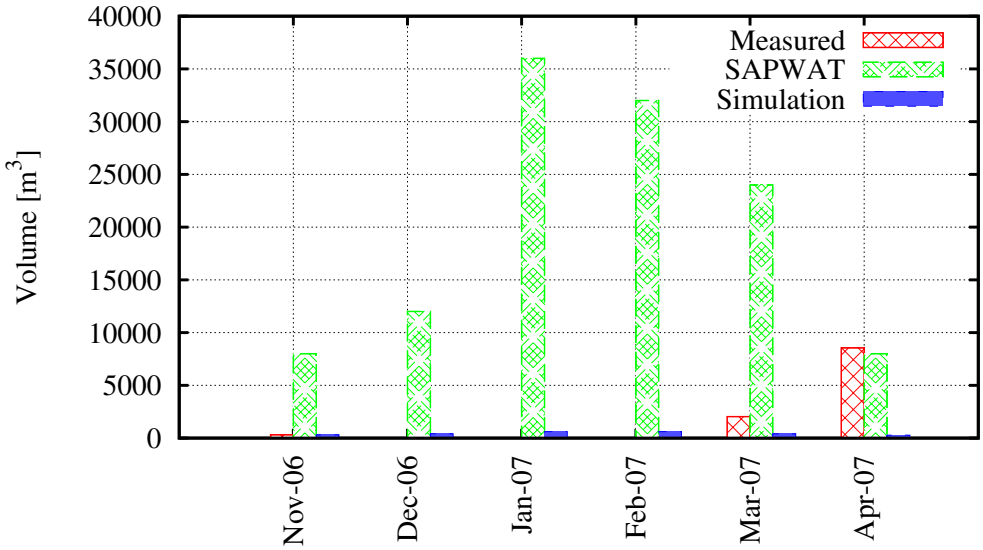

Figure B.55: Langverwaght measured, estimated and simulated water usage.

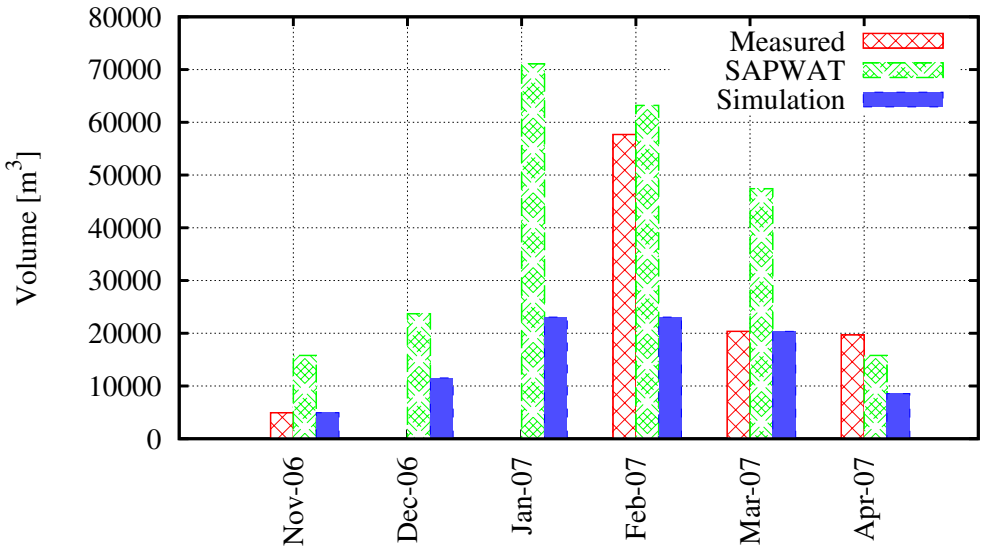

Figure B.56: Kleinplasie measured, estimated and simulated water usage.

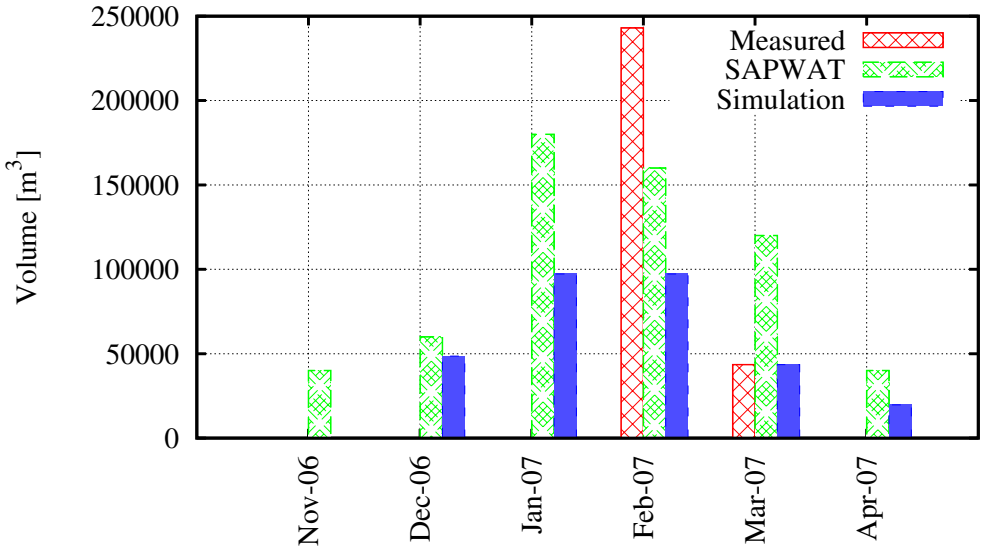

Figure B.57: Neethlingskroon measured, estimated and simulated water usage.

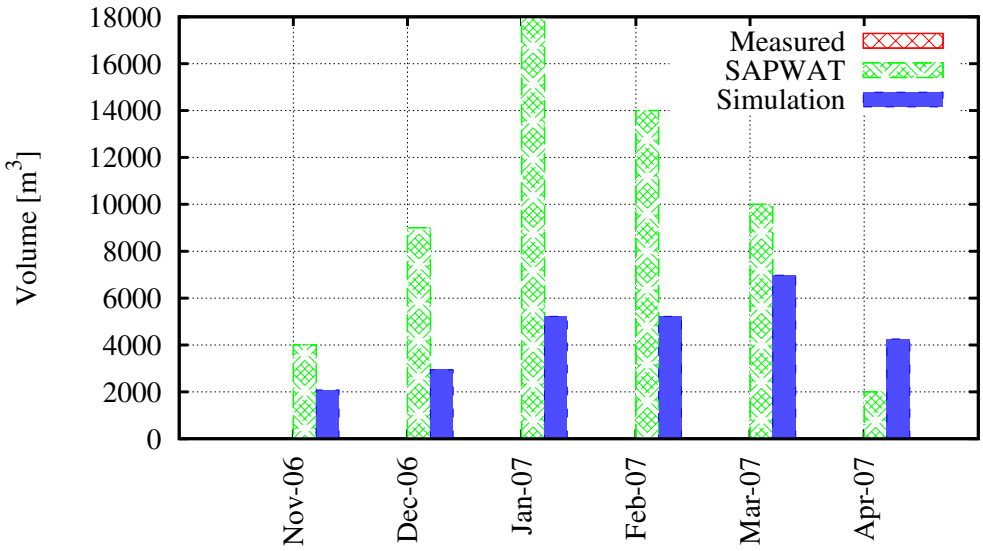

Figure B.58: Bokrivier Farms measured, estimated and simulated water usage.

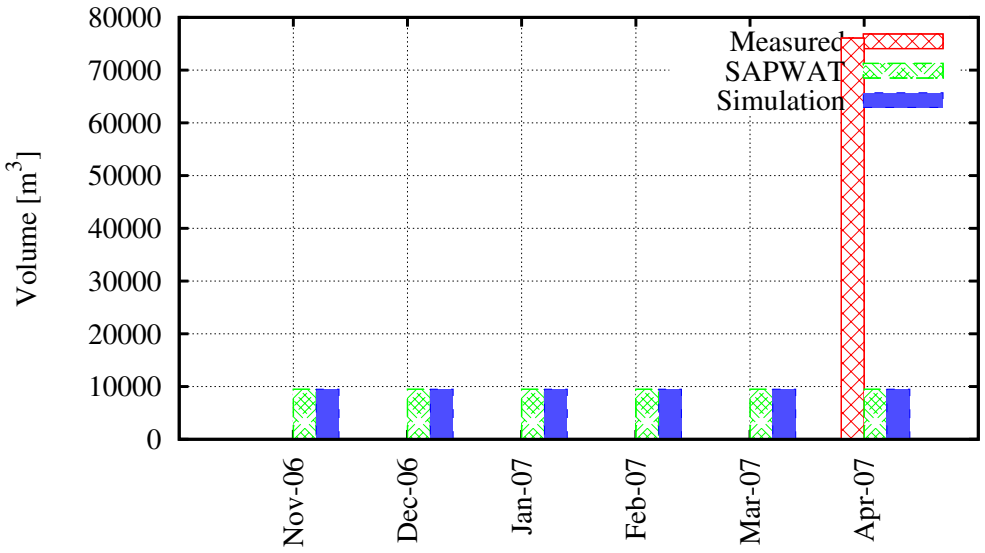

Figure B.59: Bokrivier Landgoed measured, estimated and simulated water usage.

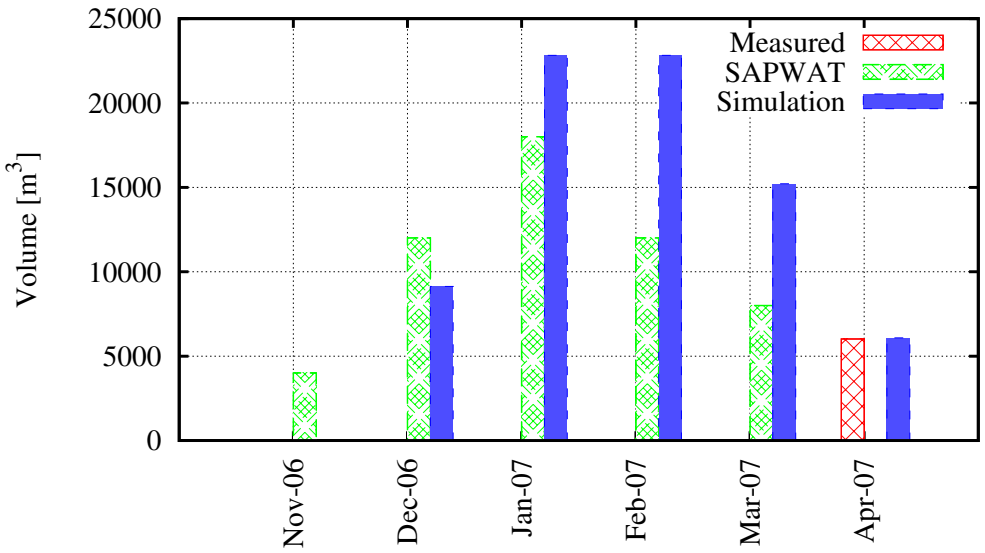

Figure B.60: Esperance measured, estimated and simulated water usage.

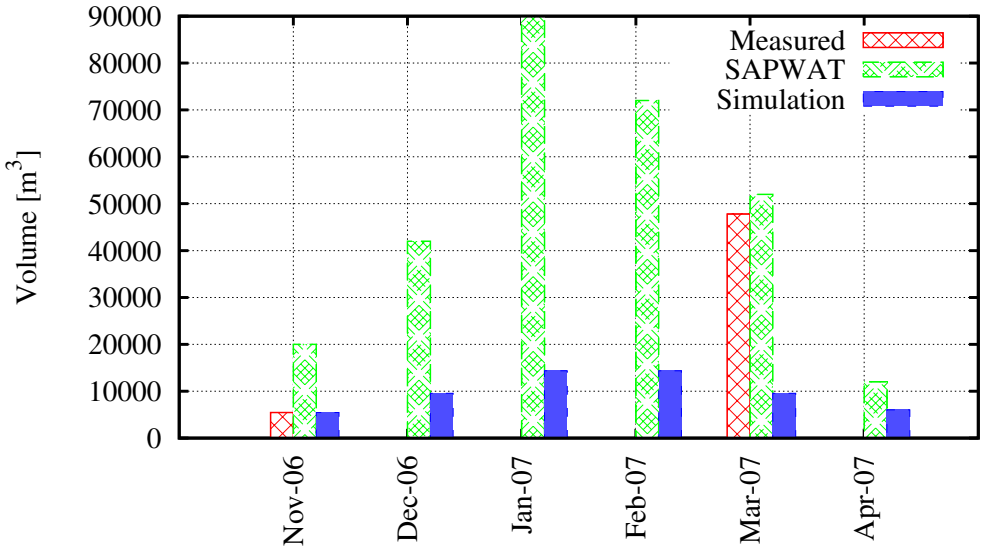

Figure B.61: Concordia measured, estimated and simulated water usage.

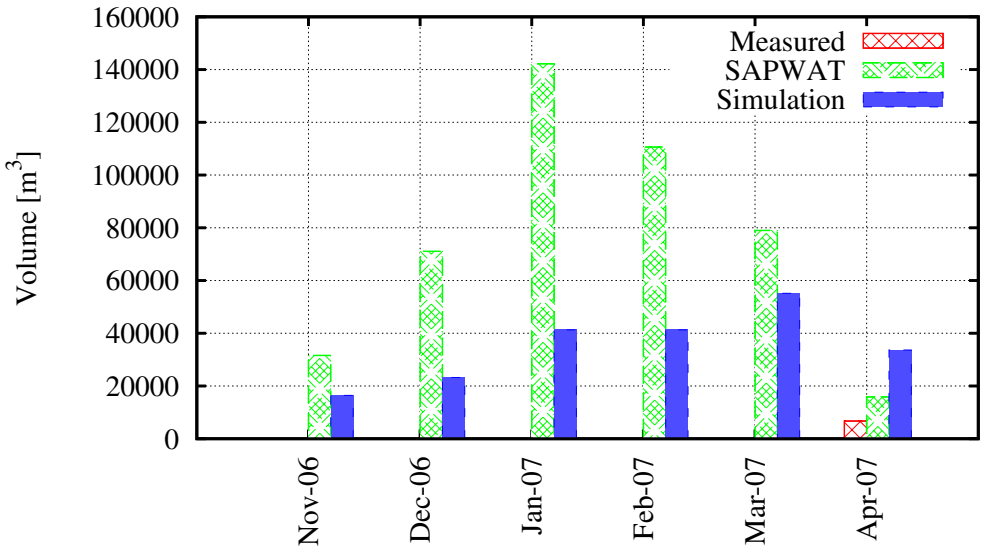

Figure B.62: Lincorso measured, estimated and simulated water usage.

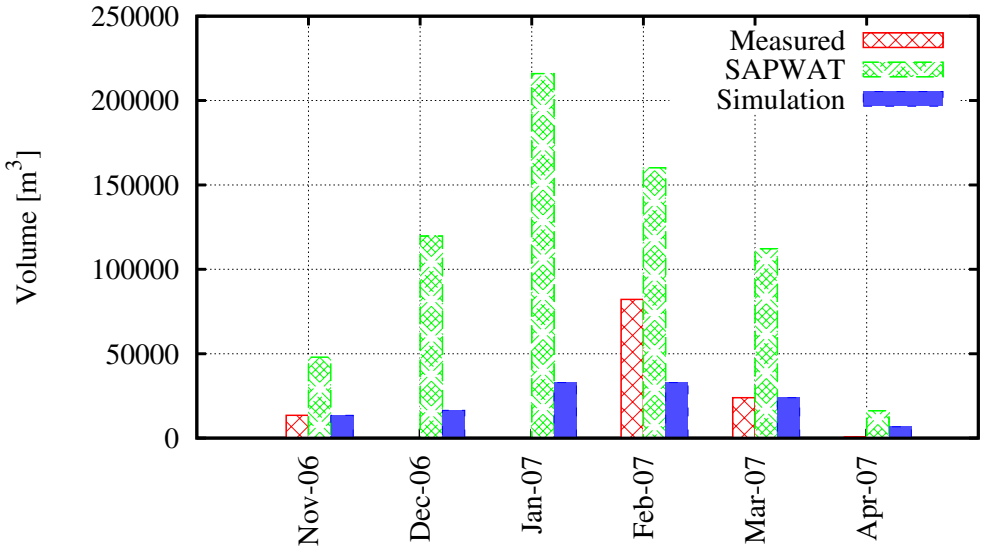

Figure B.63: Mandaryn measured, estimated and simulated water usage.

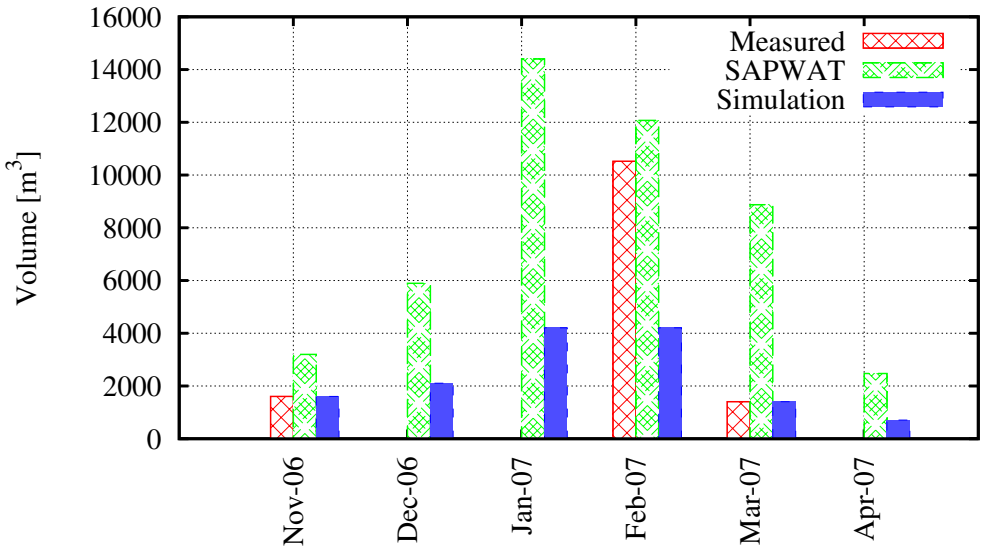

Figure B.64: De Pan measured, estimated and simulated water usage.

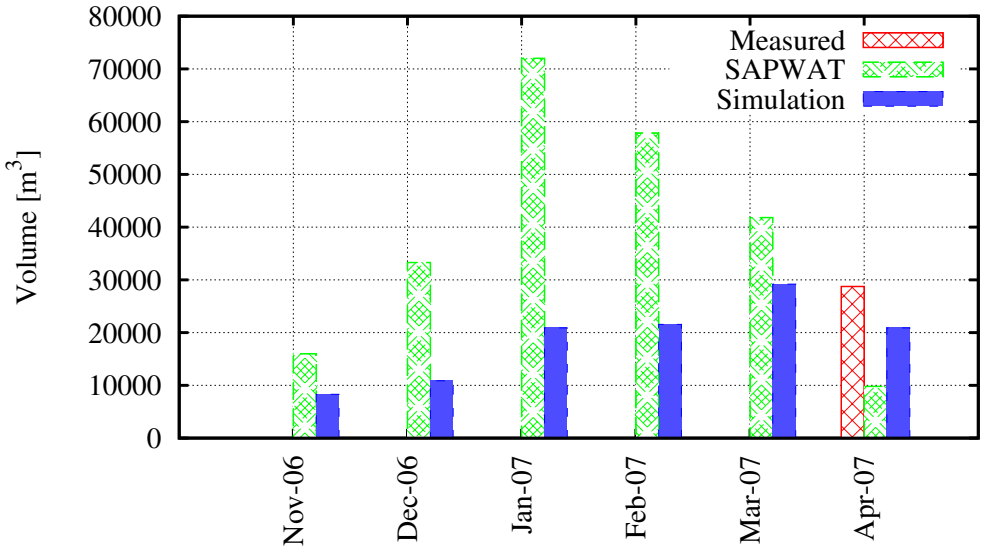

Figure B.65: Middelpunt measured, estimated and simulated water usage.

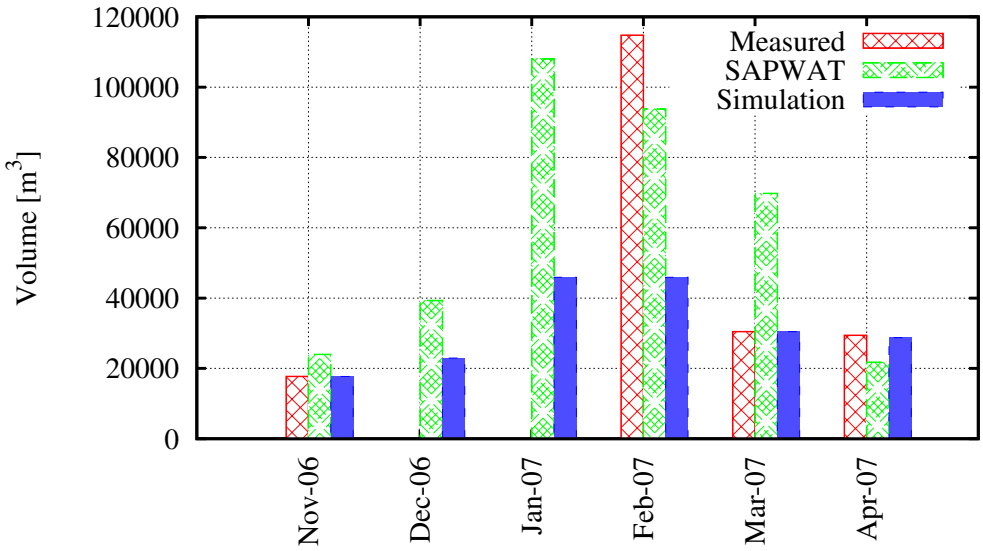

Figure B.66: Vater Erbe measured, estimated and simulated water usage.

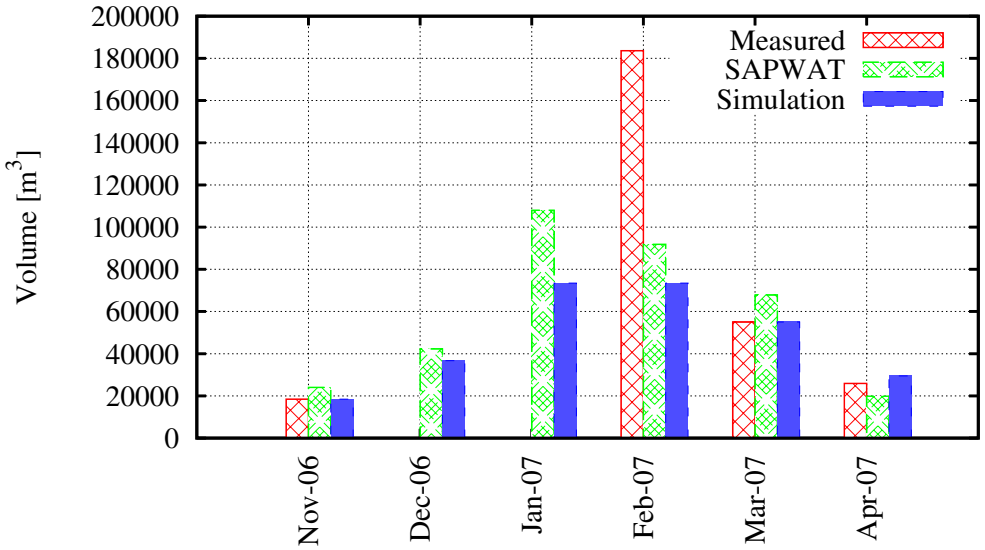

Figure B.67: Noordhoek measured, estimated and simulated water usage.

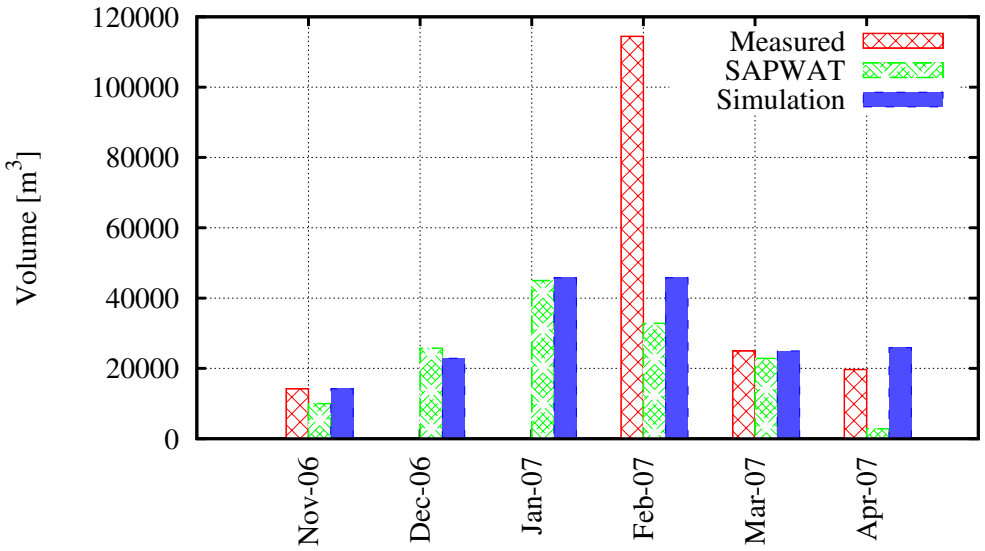

Figure B.68: Brakdam measured, estimated and simulated water usage.

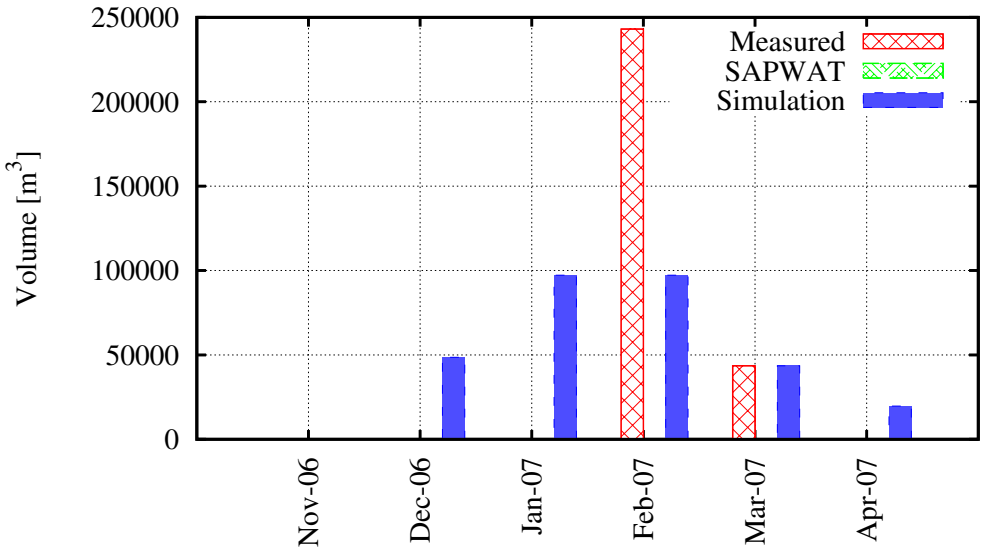

Figure B.69: Noordhoek (J. Groenewald) measured, estimated and simulated water usage.

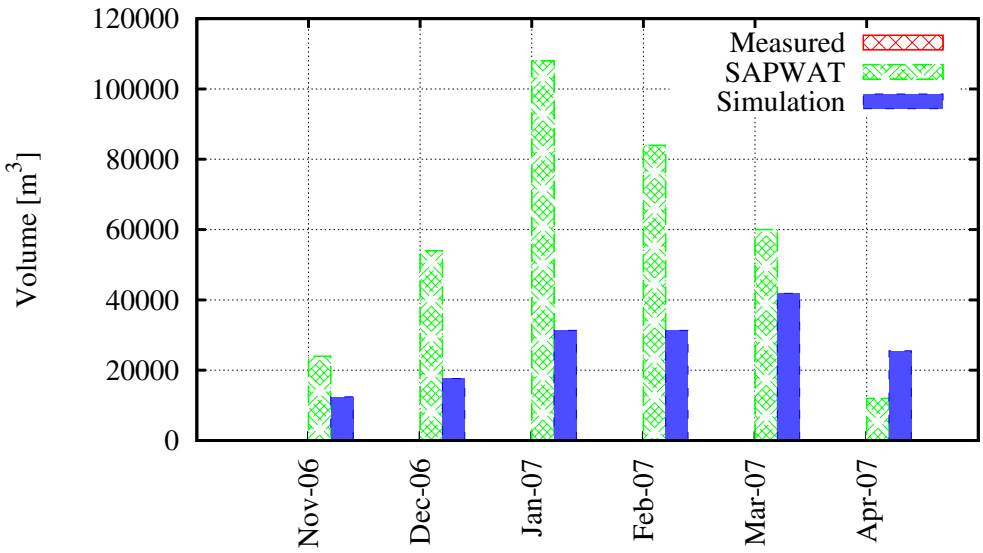

Figure B.70: Blydskap measured, estimated and simulated water usage.

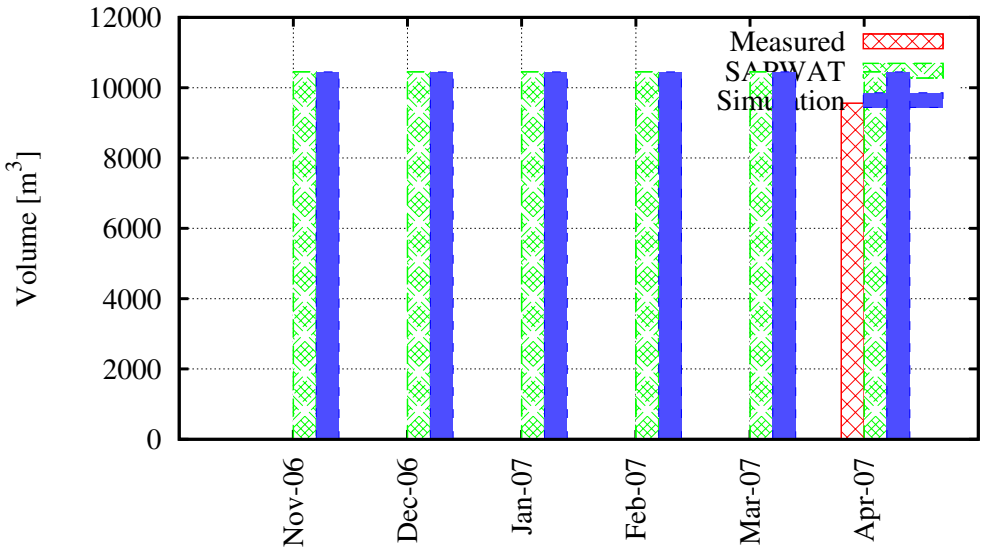

Figure B.71: TWK municipality measured, estimated and simulated water usage.

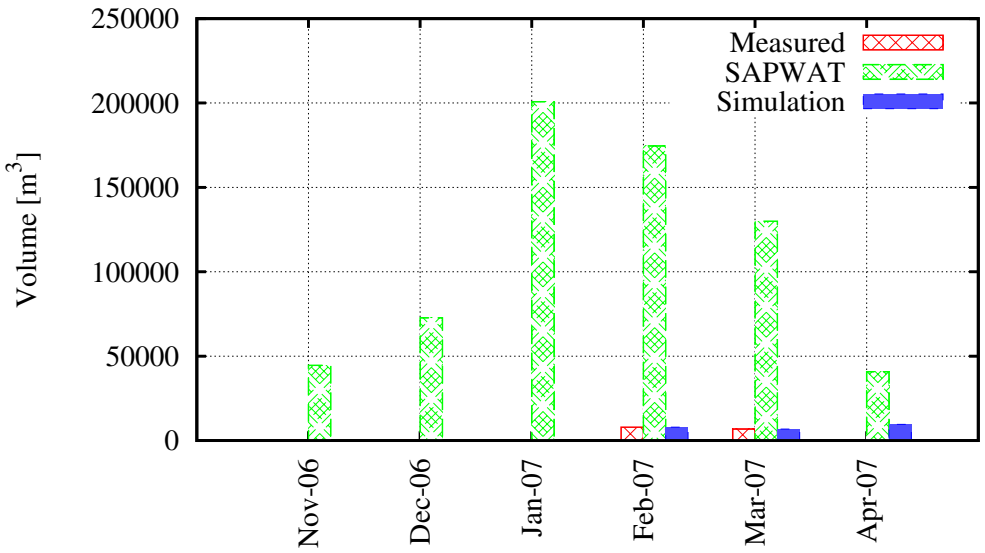

Figure B.72: Tygerhoek measured, estimated and simulated water usage.

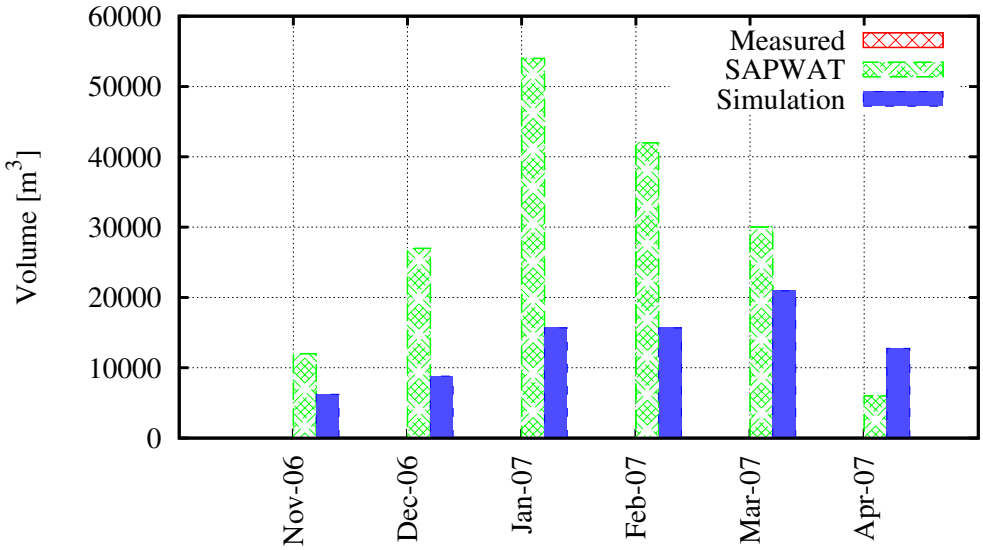

Figure B.73: Wijnberg measured, estimated and simulated water usage.

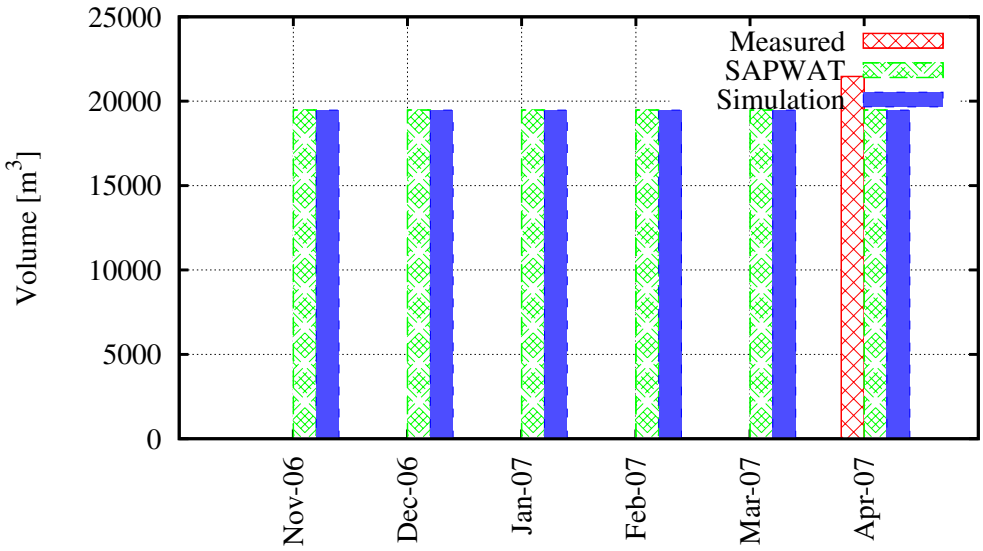

Figure B.74: Nitrophosca measured, estimated and simulated water usage.

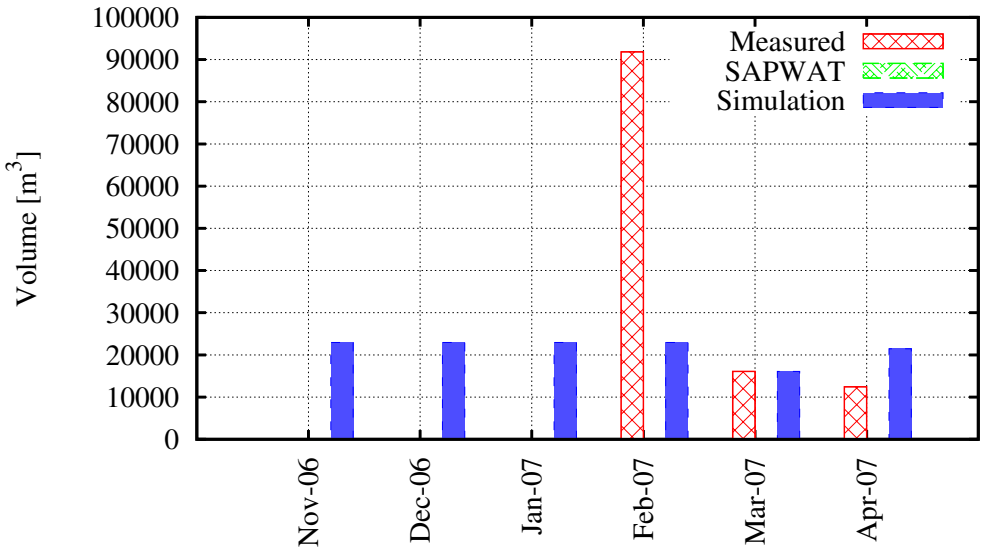

Figure B.75: Riviersonderend municipality measured, estimated and simulated water usage.

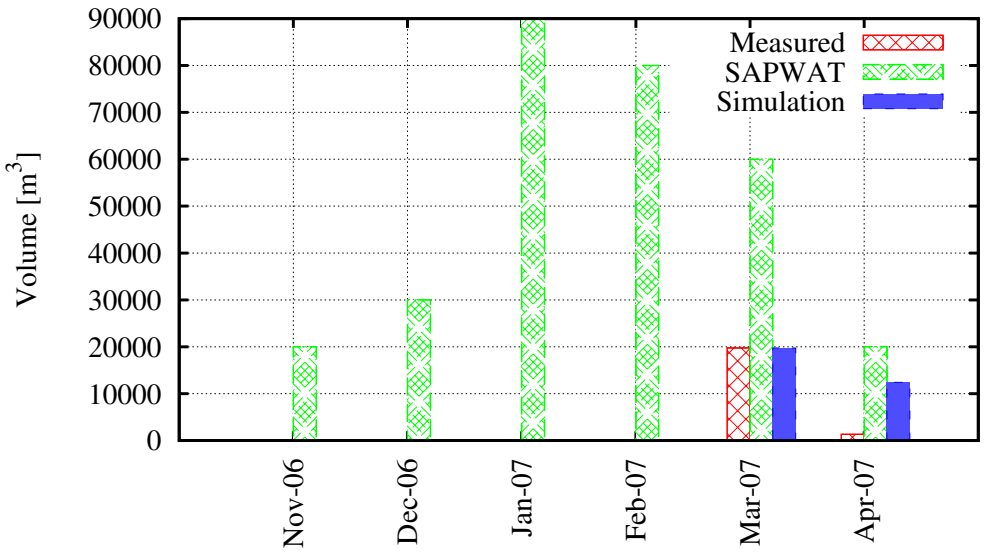

Figure B.76: Appelskraal measured, estimated and simulated water usage.

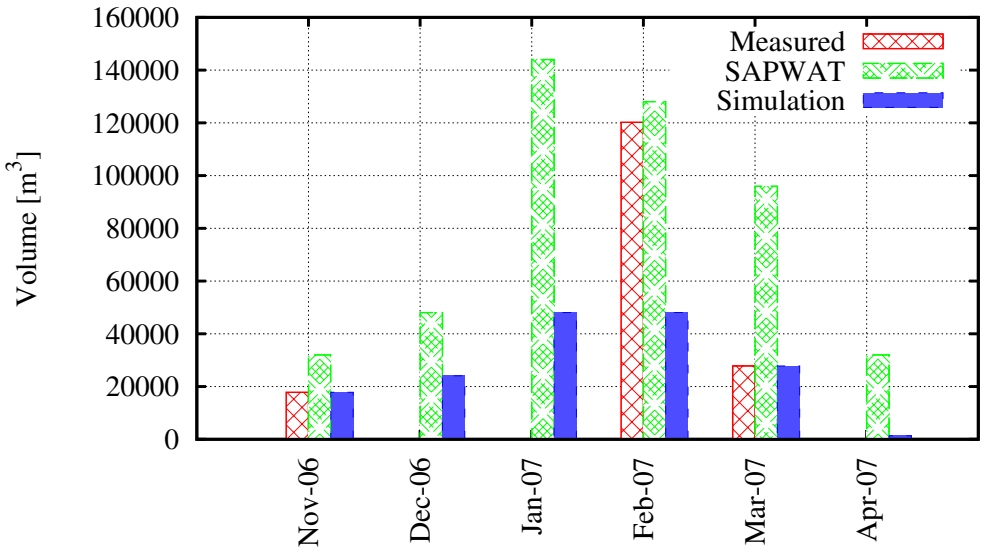

Figure B.77: Kleinlaagte measured, estimated and simulated water usage.

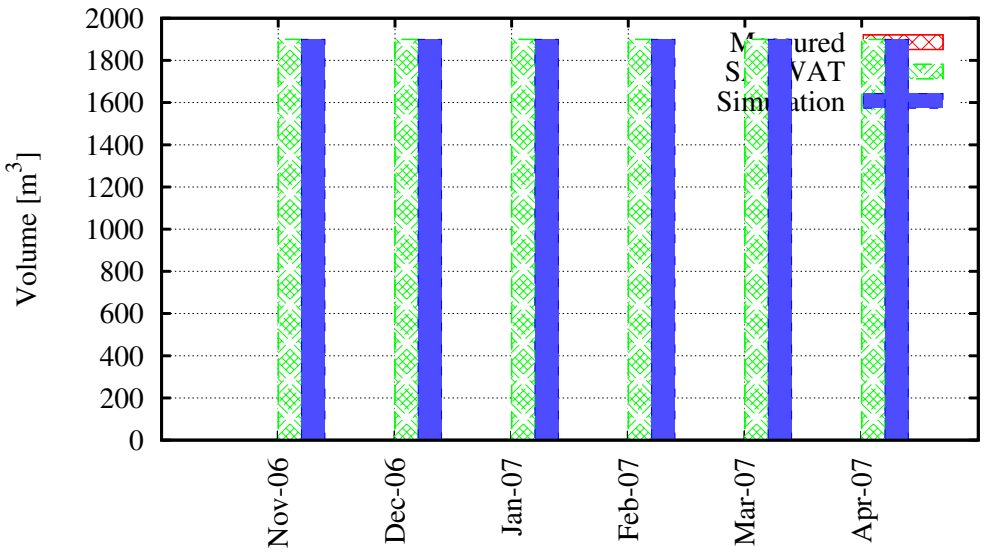

Figure B.78: Aloe Ravine Resort measured, estimated and simulated water usage.

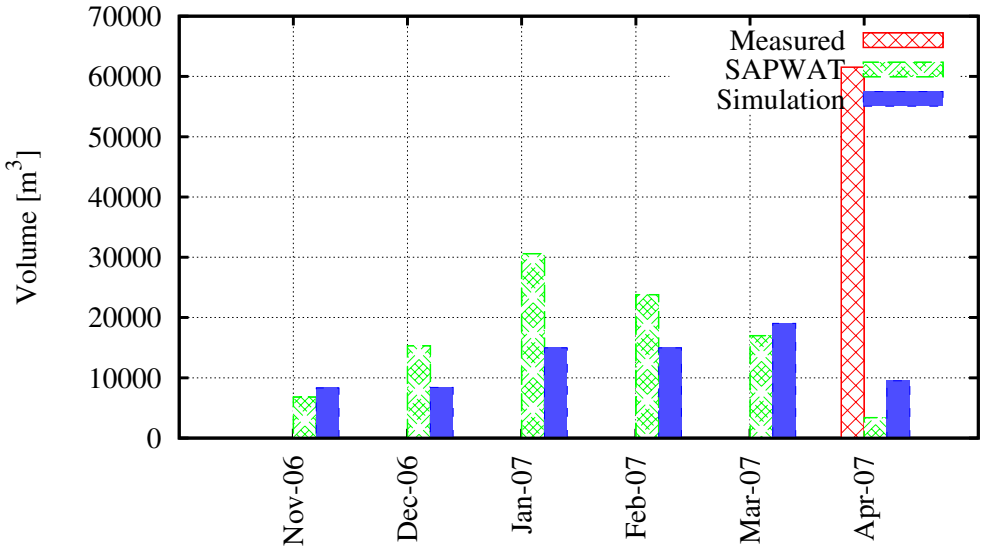

Figure B.79: A. Starke Trust measured, estimated and simulated water usage.

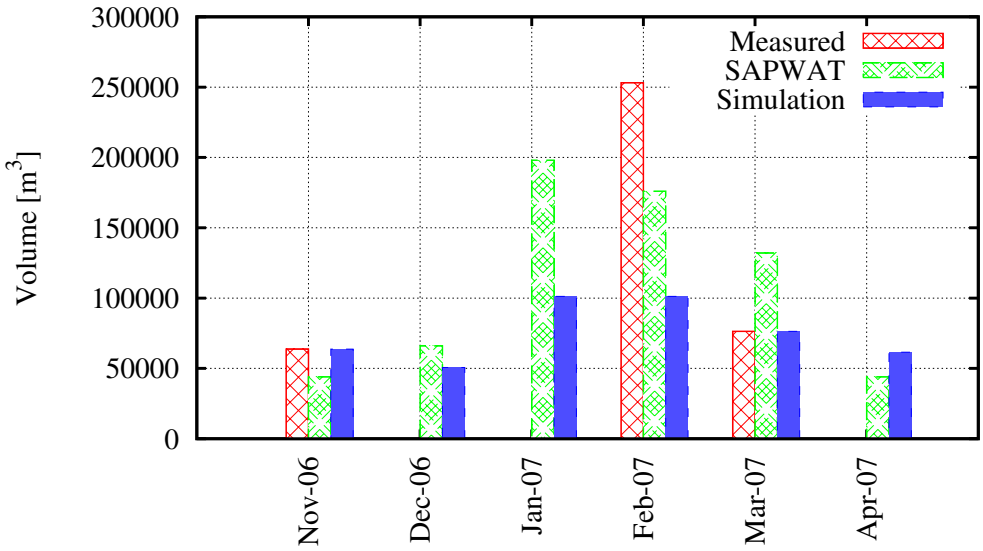

Figure B.80: Haelkraal measured, estimated and simulated water usage.

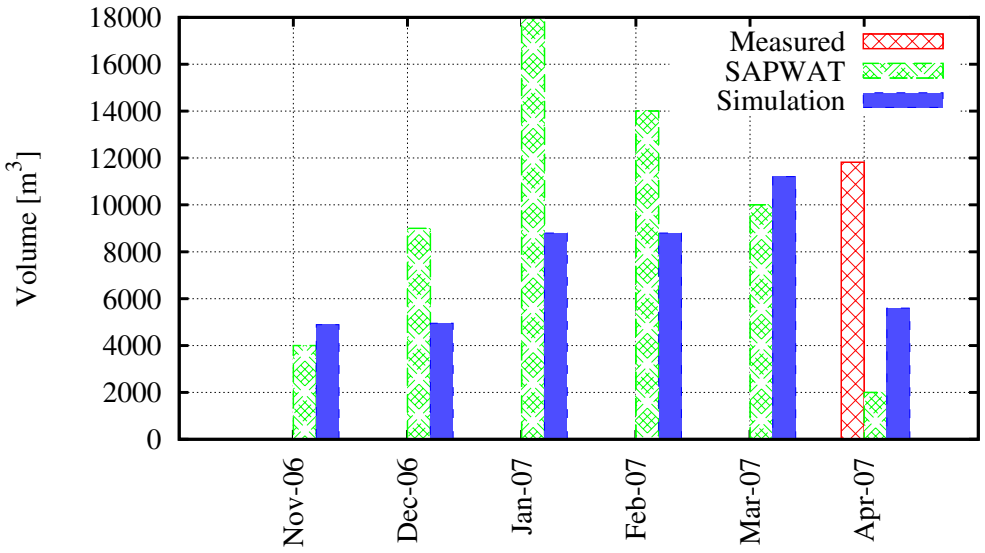

Figure B.81: Haelkraal (D. Human) measured, estimated and simulated water usage.

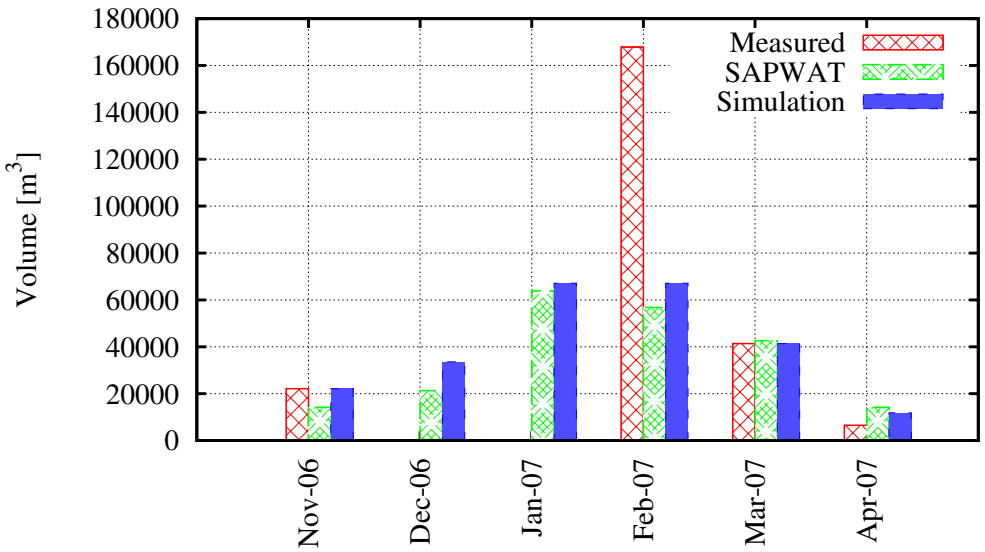

Figure B.82: Loch Lotus measured, estimated and simulated water usage.

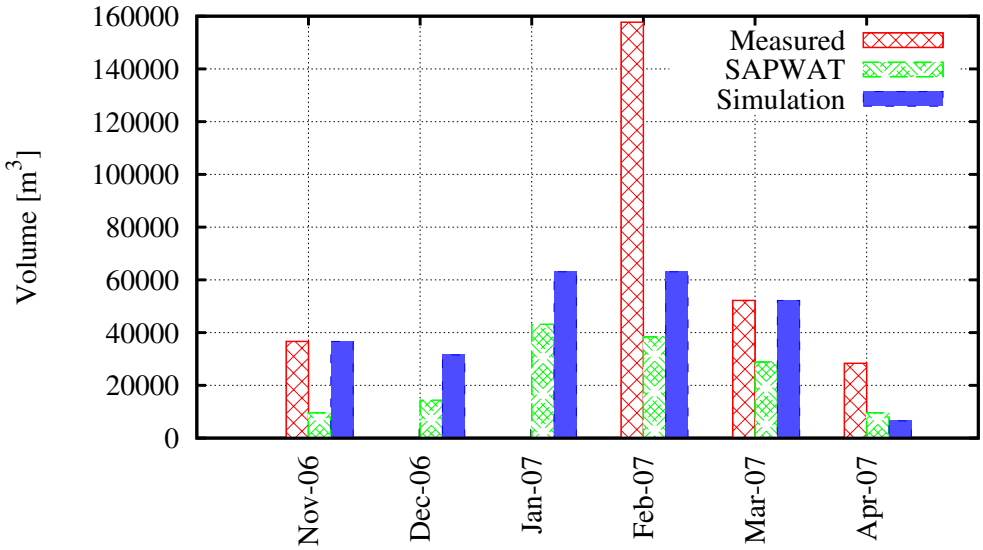

Figure B.83: Rustenburg measured, estimated and simulated water usage.

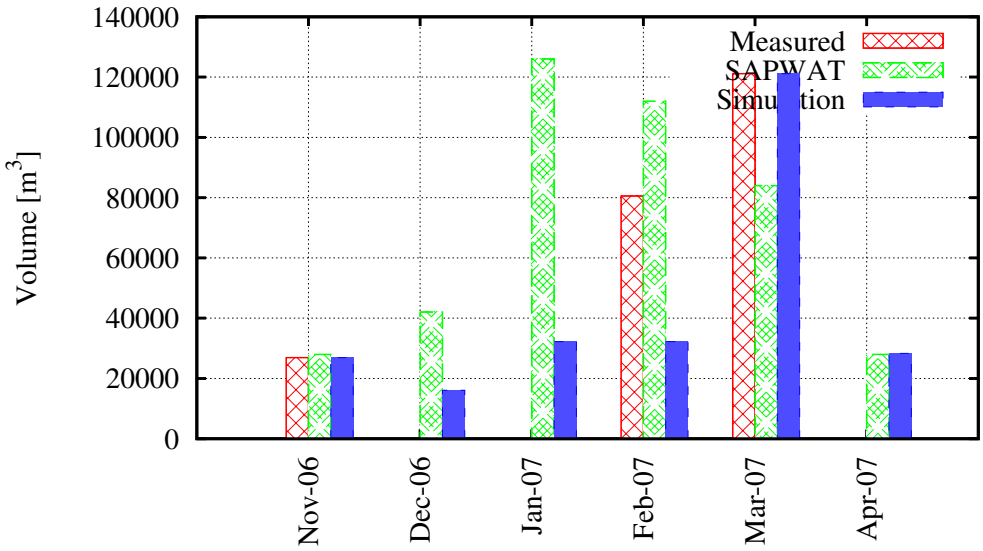

Figure B.84: Grootvlakte measured, estimated and simulated water usage.

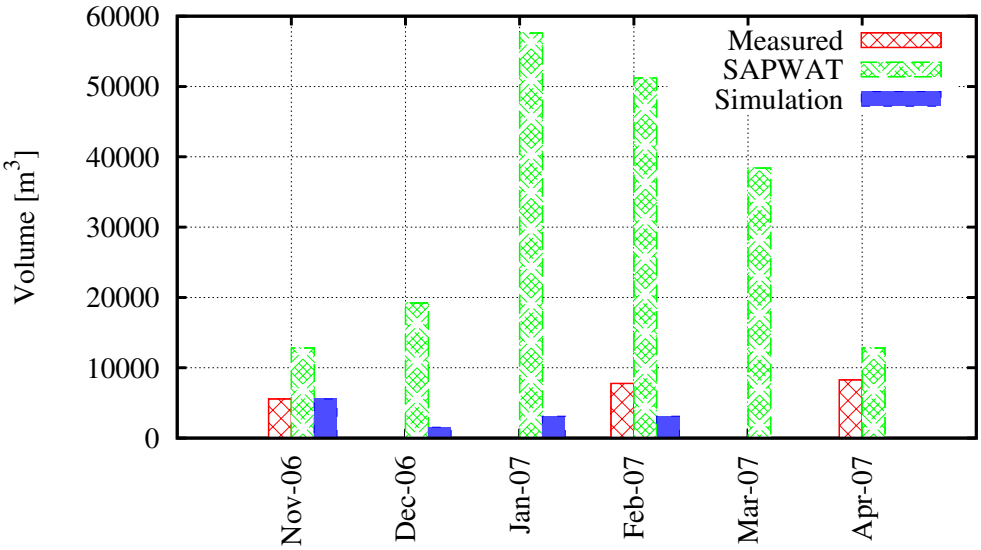

Figure B.85: Ongegund measured, estimated and simulated water usage.

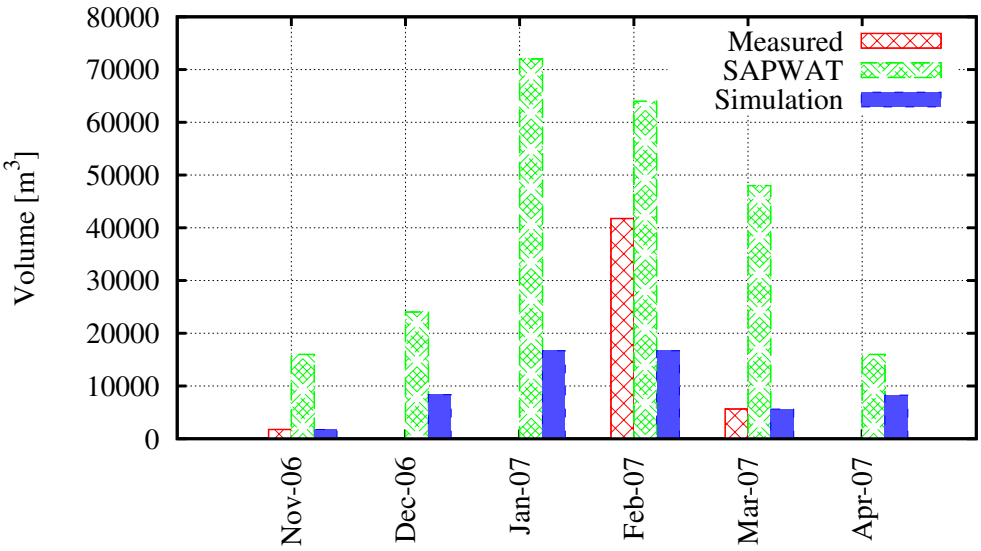

Figure B.86: Tevrede measured, estimated and simulated water usage.

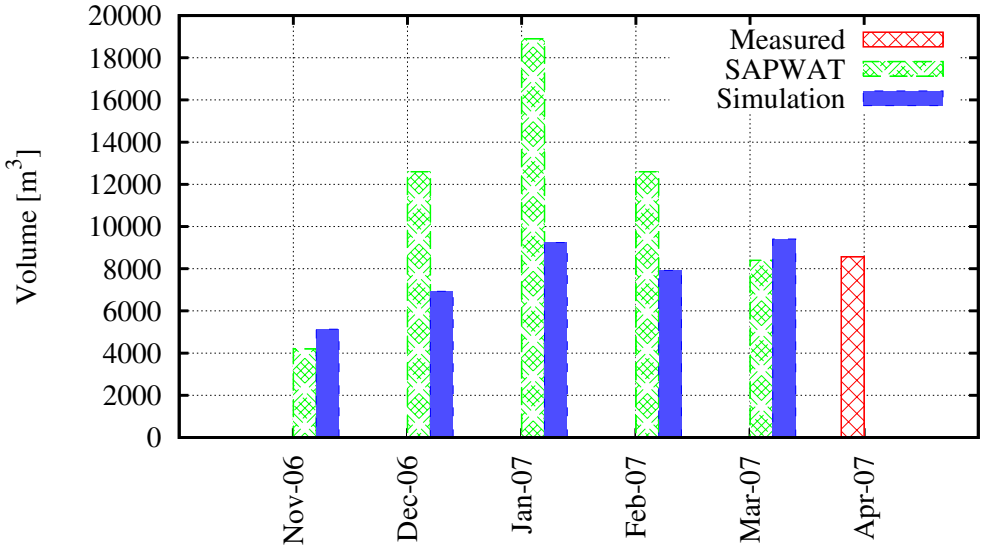

Figure B.87: Van der Watts Kraal 1 measured, estimated and simulated water usage.

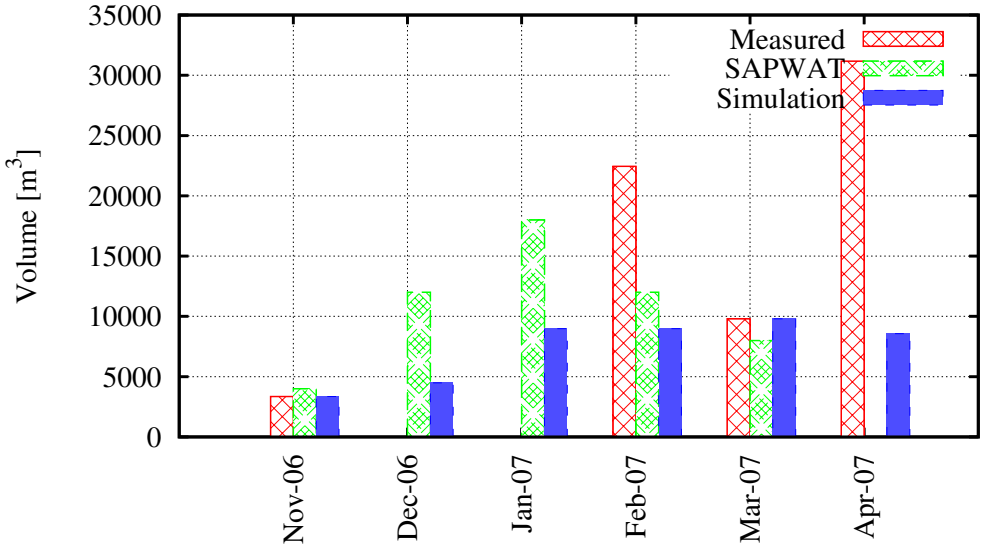

Figure B.88: Van der Watts Kraal 2 measured, estimated and simulated water usage.

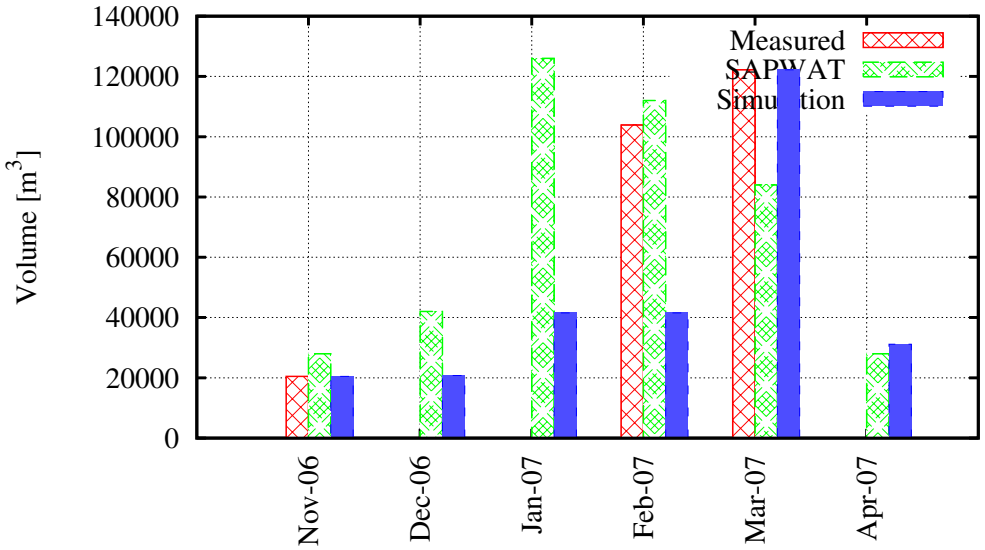

Figure B.89: Sangasdrift measured, estimated and simulated water usage.

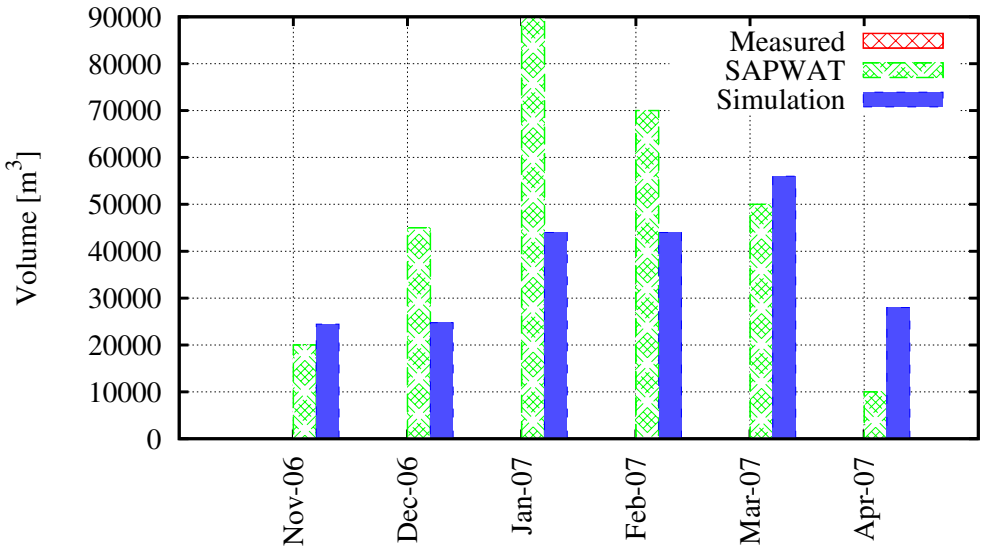

Figure B.90: Van Dyk Trust measured, estimated and simulated water usage.

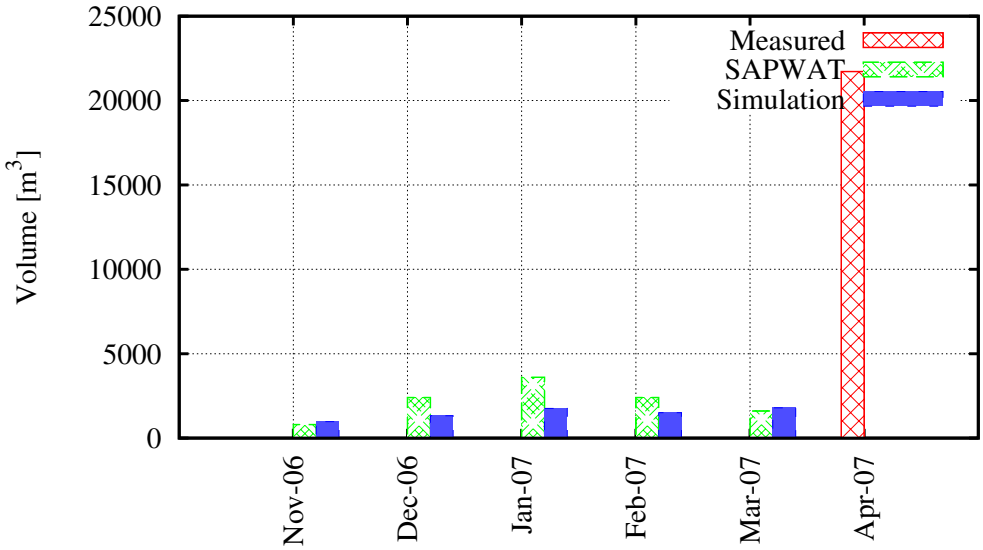

Figure B.91: S.W. Viljoen measured, estimated and simulated water usage.

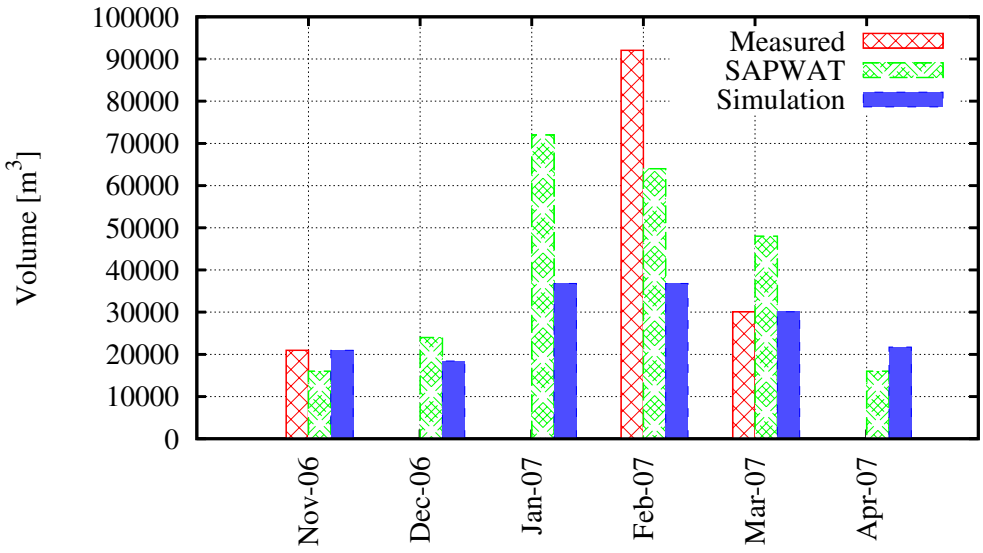

Figure B.92: Avontuur measured, estimated and simulated water usage.

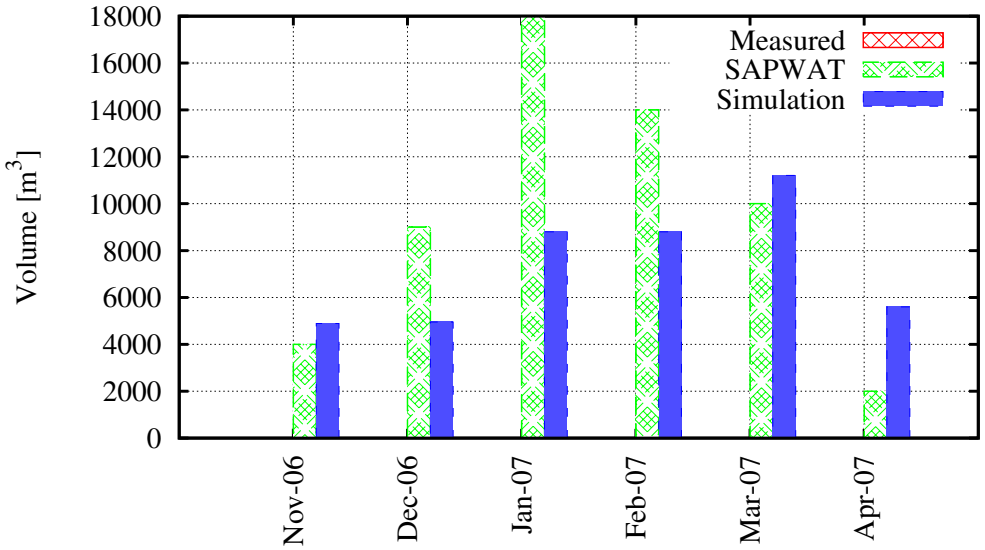

Figure B.93: Fletchers Trust measured, estimated and simulated water usage.

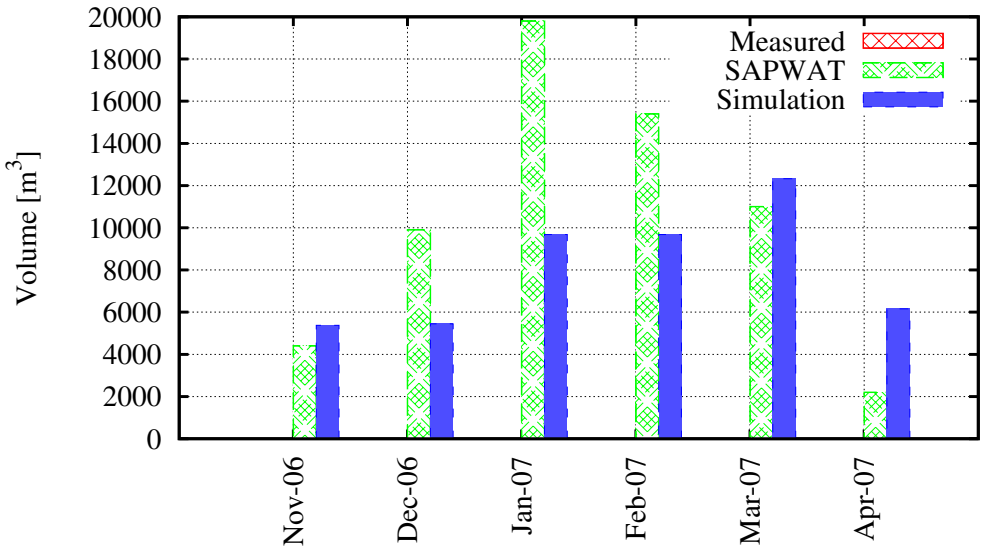

Figure B.94: D.B. Froneman measured, estimated and simulated water usage.

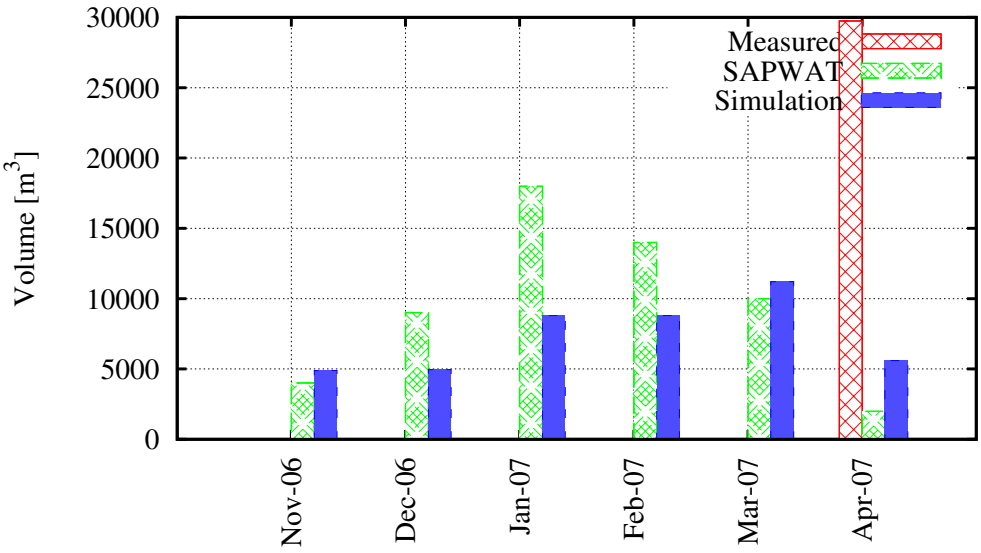

Figure B.95: J.P. O'Connel Trust measured, estimated and simulated water usage.

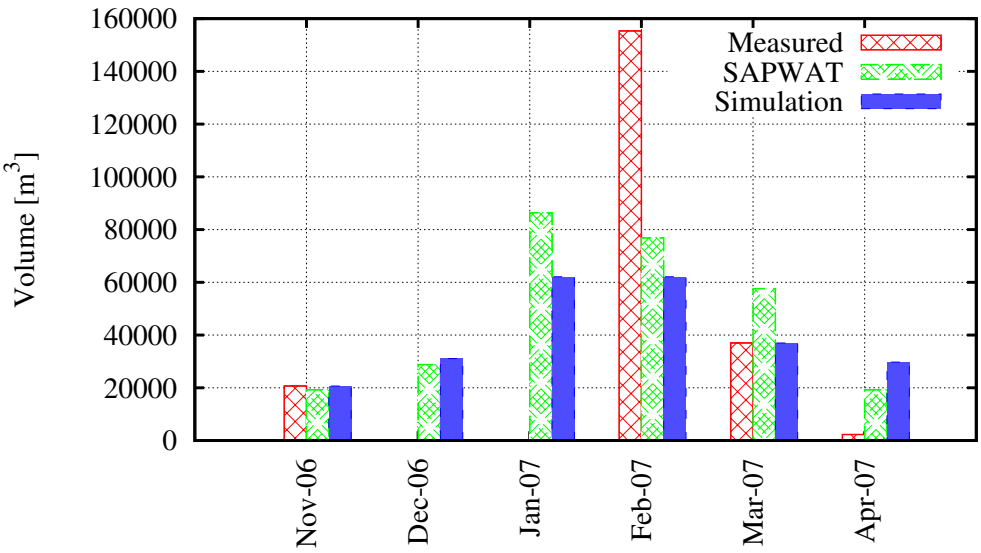

Figure B.96: Avontuur measured, estimated and simulated water usage.

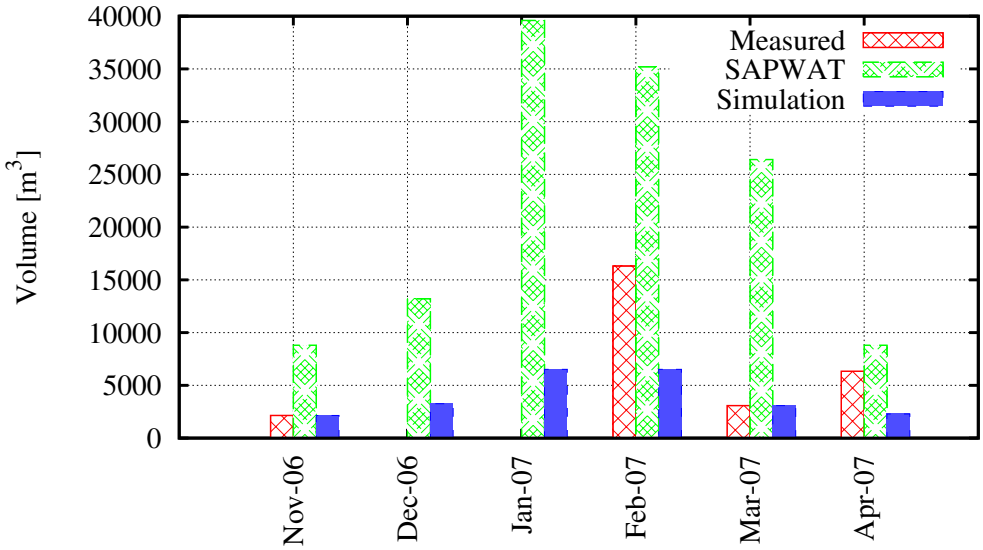

Figure B.97: Stormvlei Hotel measured, estimated and simulated water usage.

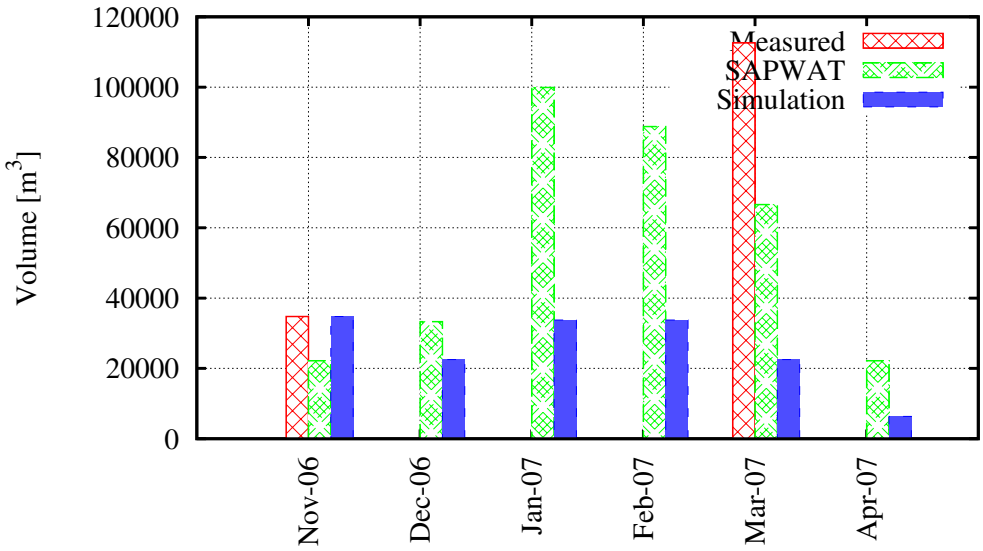

Figure B.98: Doornkloof measured, estimated and simulated water usage.

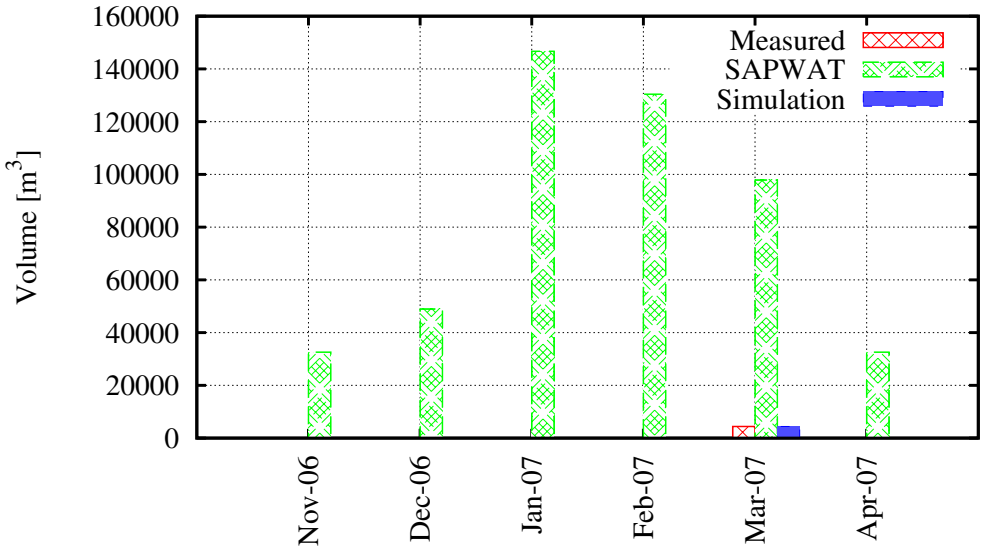

Figure B.99: Rheenen measured, estimated and simulated water usage.

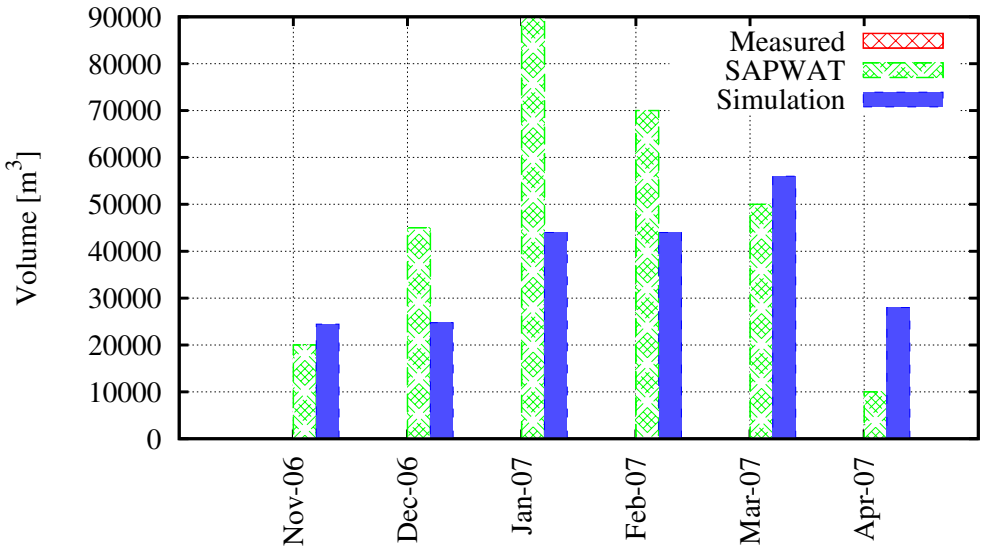

Figure B.100: Enrico Beyers measured, estimated and simulated water usage.

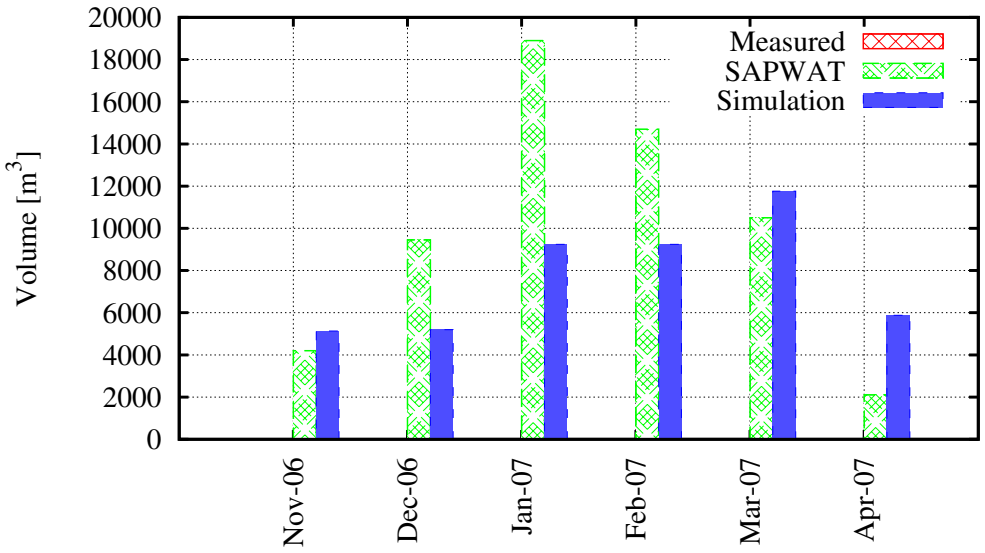

Figure B.101: Astralita measured, estimated and simulated water usage.

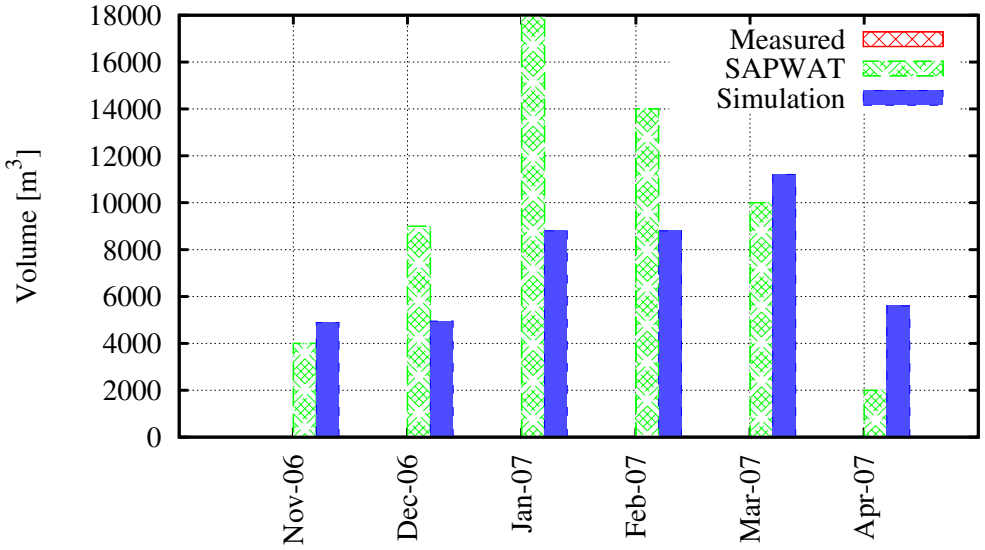

Figure B.102: E. van As/Streicher measured, estimated and simulated water usage.

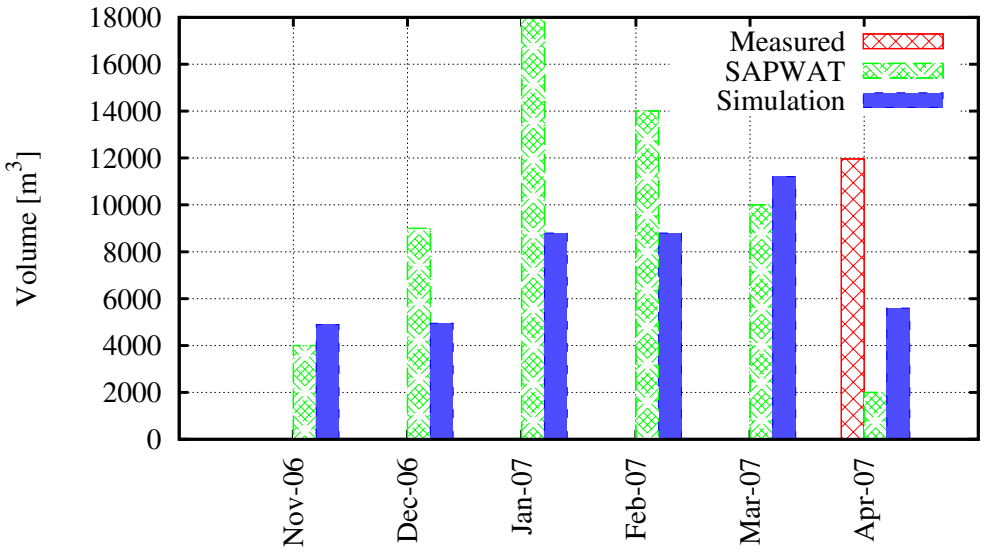

Figure B.103: S.W. Viljoen Trust measured, estimated and simulated water usage.

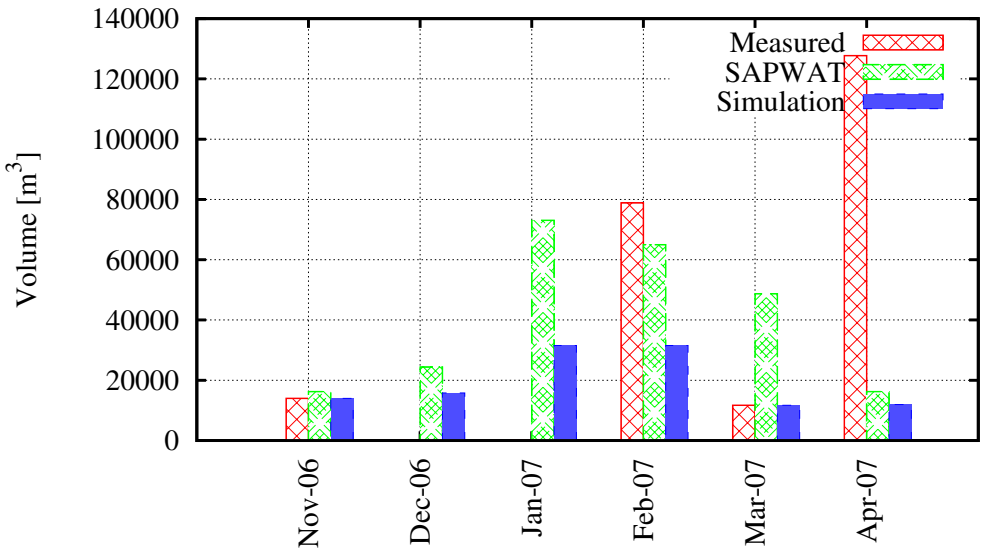

Figure B.104: Rheenen measured, estimated and simulated water usage.

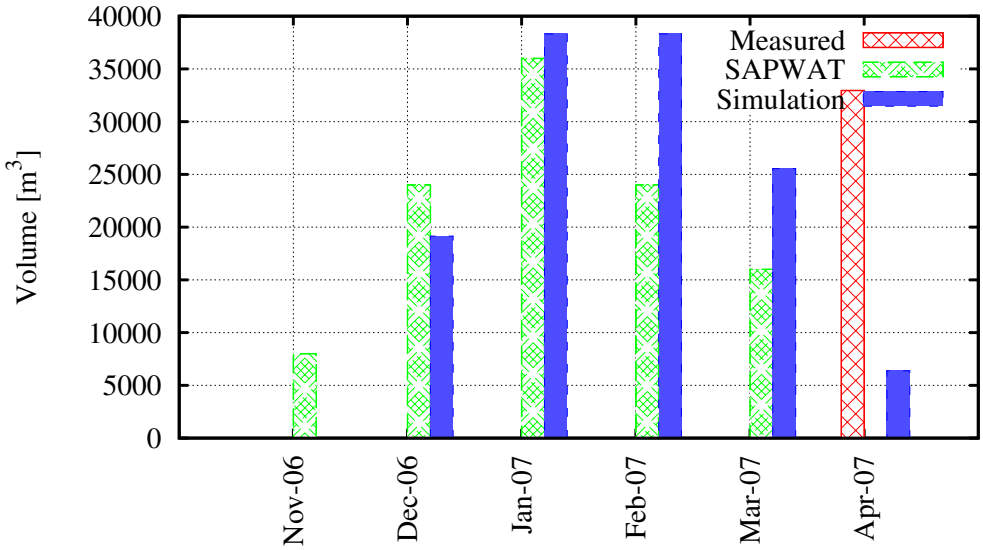

Figure B.105: Kwasarie measured, estimated and simulated water usage.

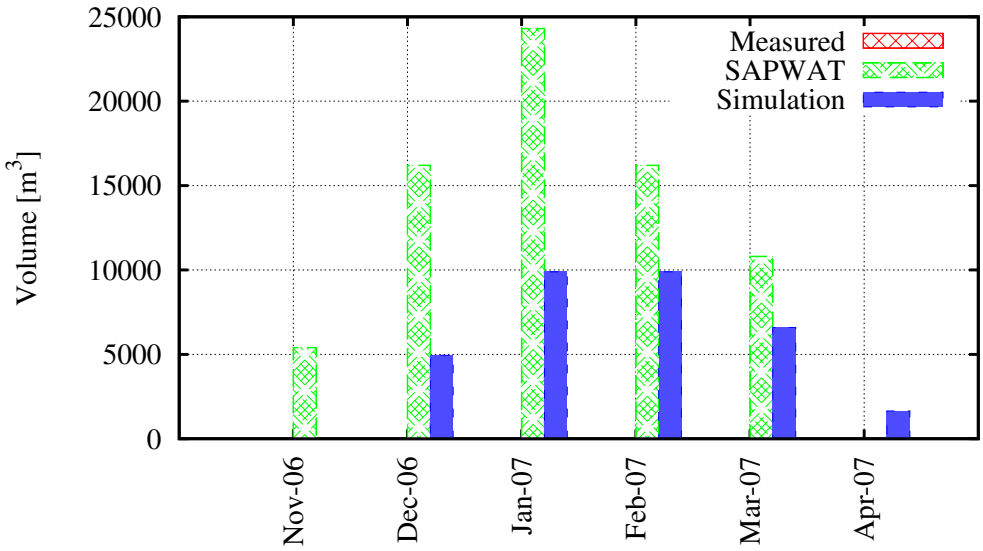

Figure B.106: Bromberg measured, estimated and simulated water usage.

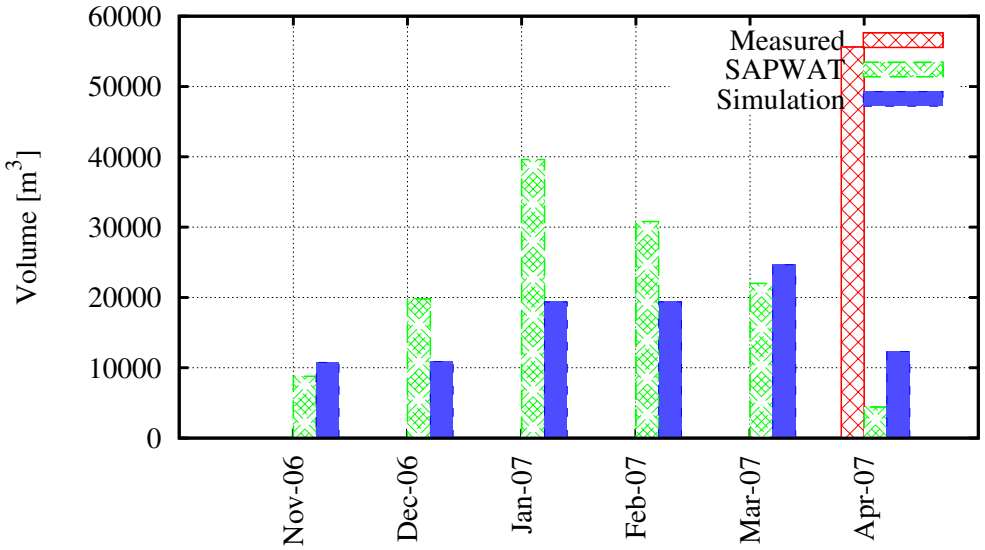

Figure B.107: Tradervail measured, estimated and simulated water usage.

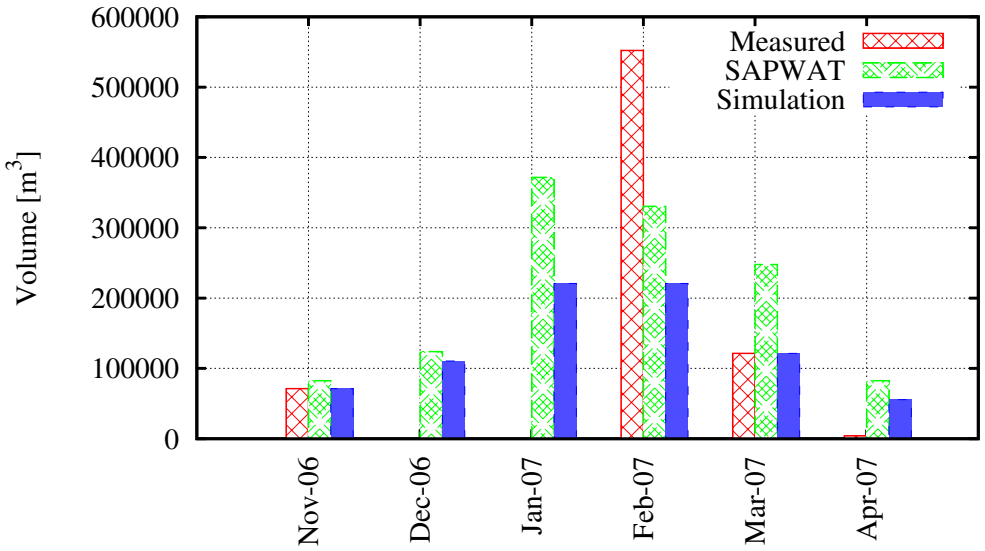

Figure B.108: Klipfontein 1 measured, estimated and simulated water usage.

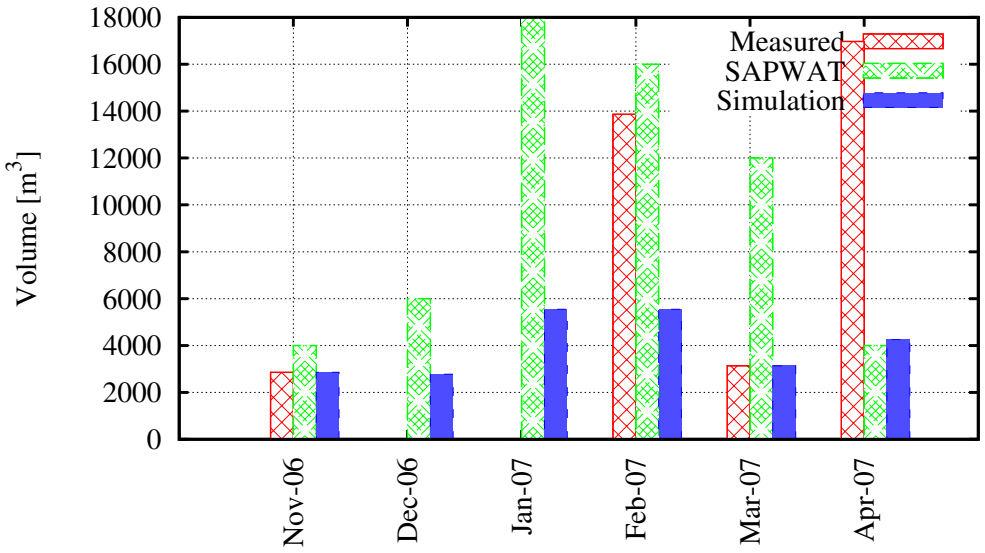

Figure B.109: Geminag measured, estimated and simulated water usage.

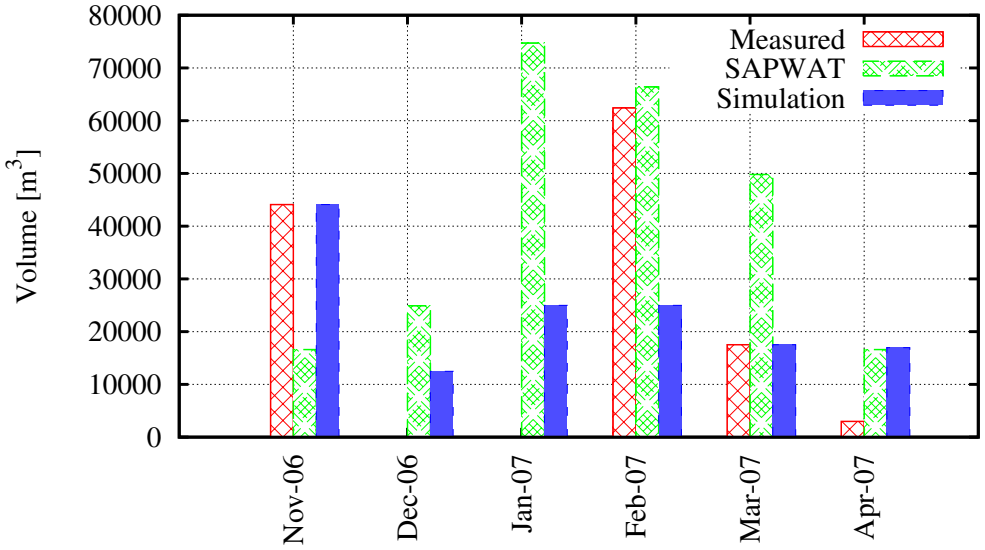

Figure B.110: Vaandrightsdrift 1 measured, estimated and simulated water usage.

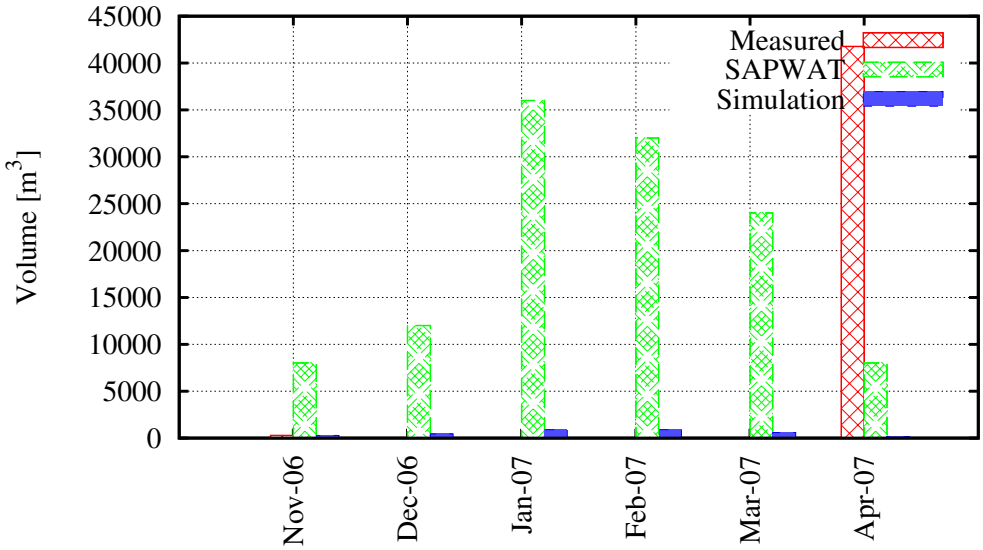

Figure B.111: Klipfontein 2 measured, estimated and simulated water usage.

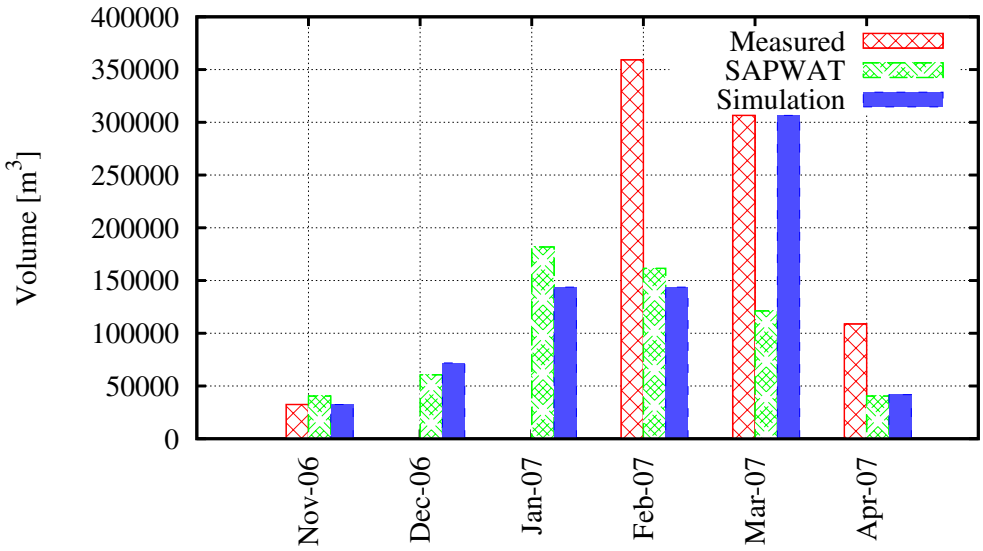

Figure B.112: Merweda measured, estimated and simulated water usage.

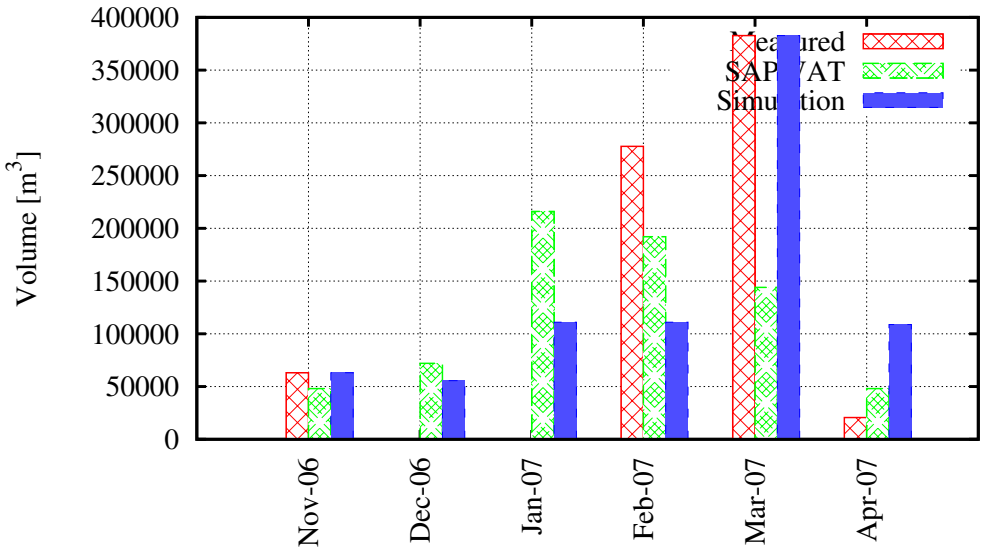

Figure B.113: Vaandrightsdrift 2 measured, estimated and simulated water usage.

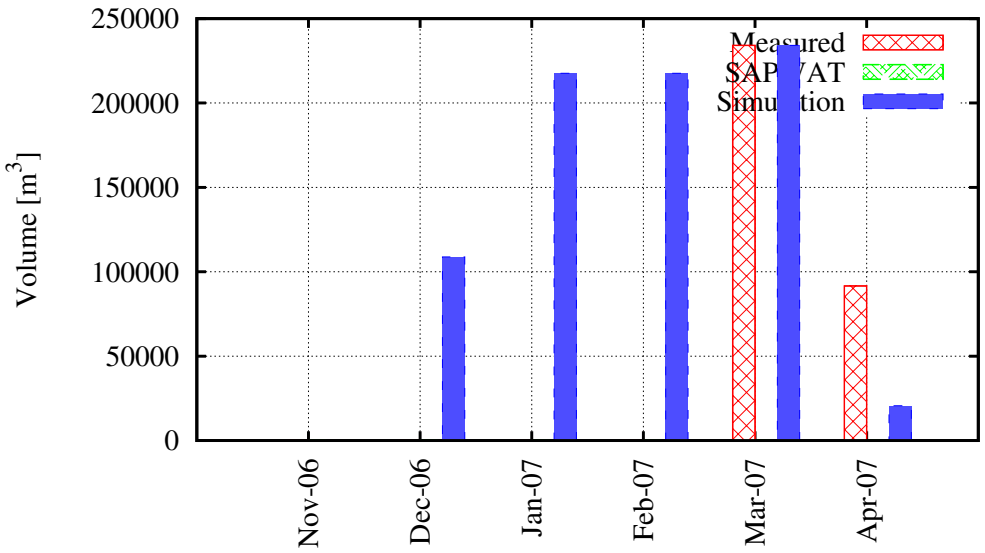

Figure B.114: Robyn measured, estimated and simulated water usage.

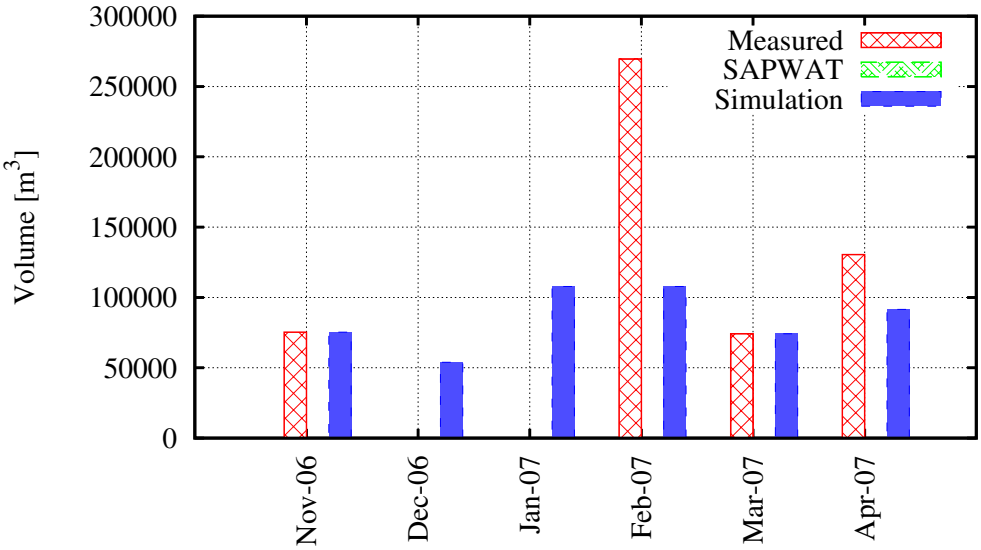

Figure B.115: Ruensveld Oos measured, estimated and simulated water usage.

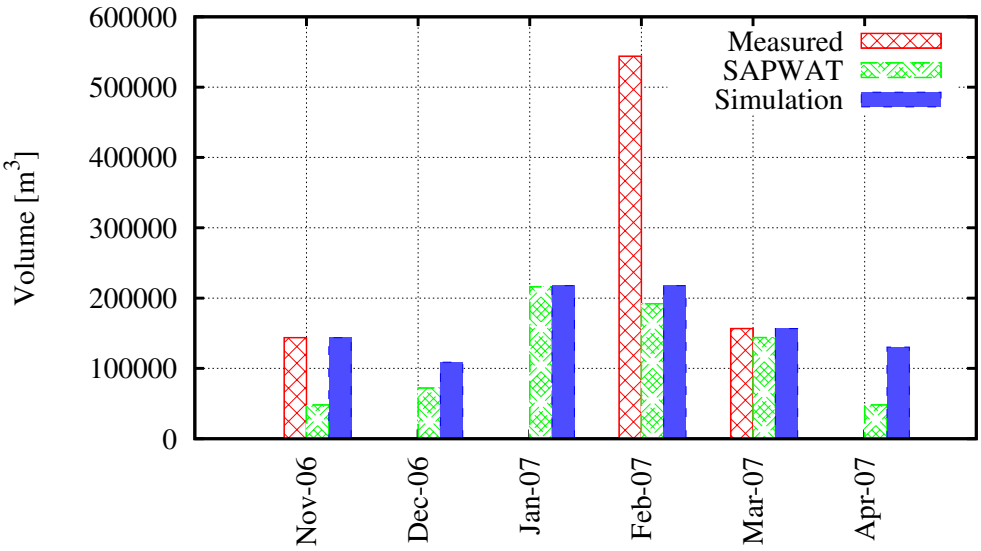

Figure B.116: Pleasant View measured, estimated and simulated water usage.

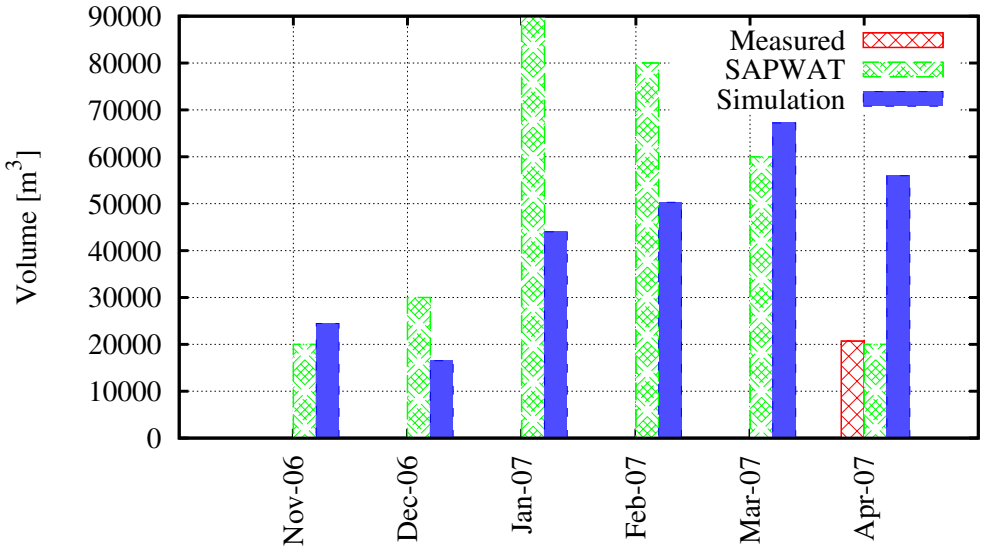

Figure B.117: Riviera measured, estimated and simulated water usage.

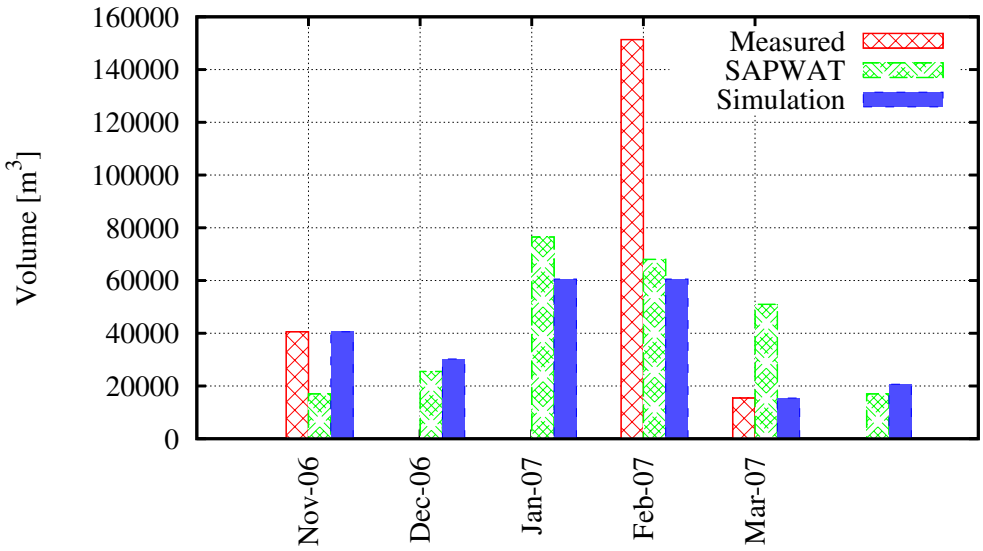

Figure B.118: Jubileeskraal measured, estimated and simulated water usage.

Appendix C

Irrigation Usage Graphs for 2005-2006

This Appendix is a compilation of the irrigation water requirement graphs of 118 farmers, which water usage were measured in the Riviersonderend catchment downstream from Theewaterskloof. Each graph shows the measured data, the irrigation water requirement estimated by Sapwat3 and the distribution used in the Mike 11 simulation. The remaining 43 farmers water usage were not measured and Sapwat3 was used to estimate the irrigation requirement.

All the data, including measured, Sapwat3 and the irrigation water requirements used in this thesis are available digitally on a CD attached to this thesis.

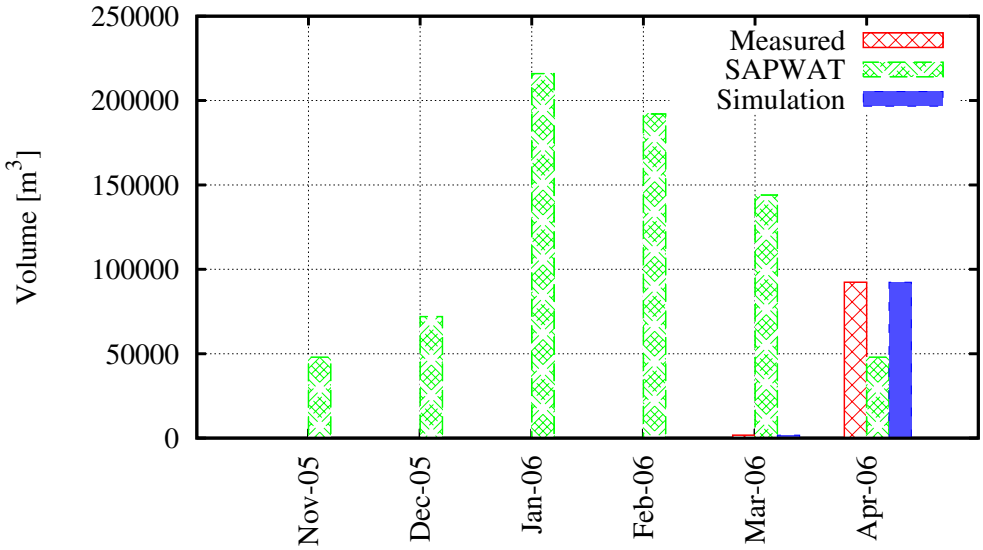

Figure C.1: Theewaterskloof measured, estimated and simulated water usage.

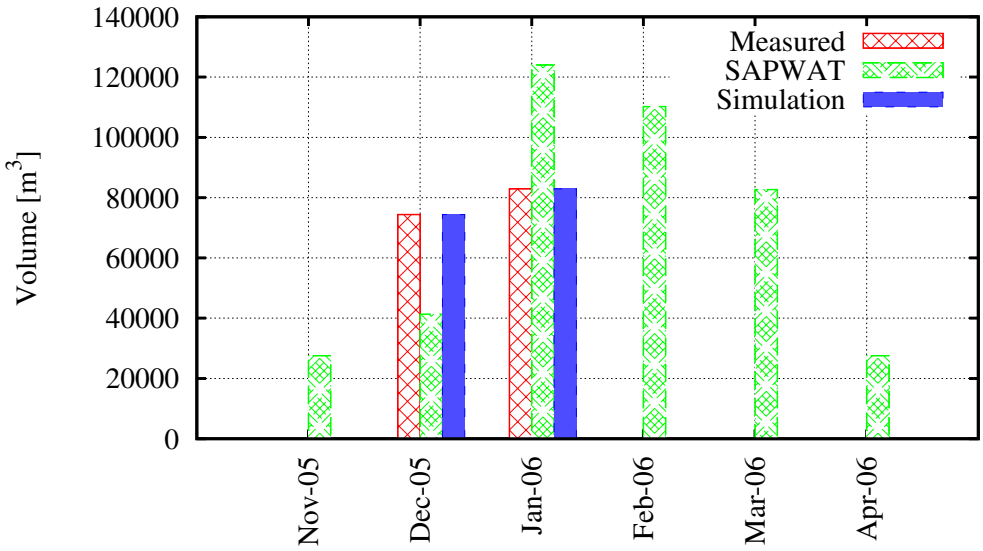

Figure C.2: Dwarstrek measured, estimated and simulated water usage.

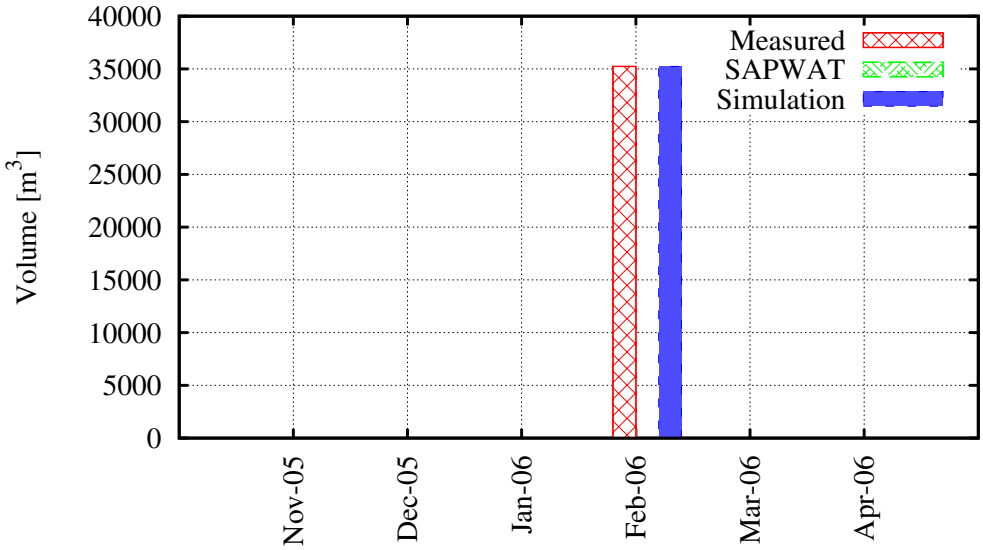

Figure C.3: Ruensveld Wes measured, estimated and simulated water usage.

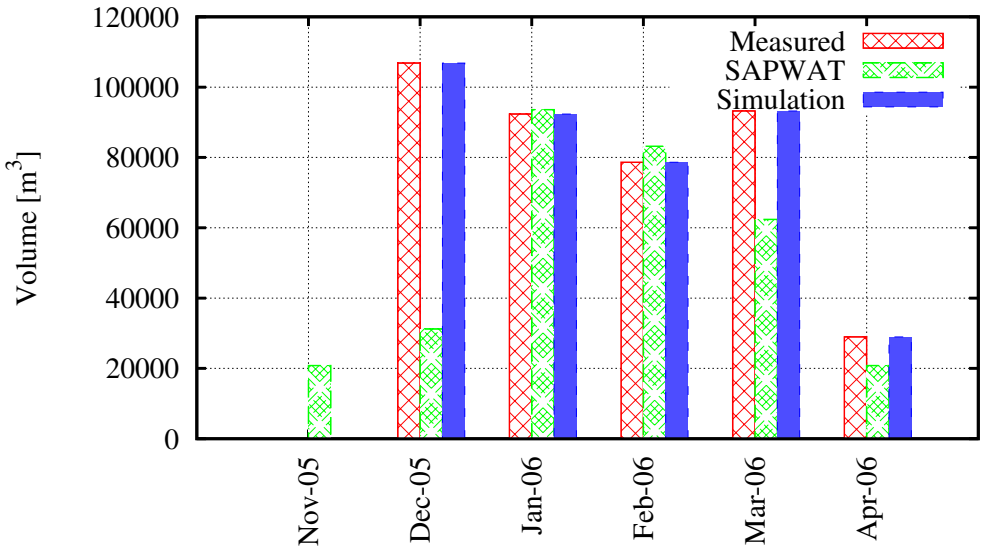

Figure C.4: Maraisdal measured, estimated and simulated water usage.

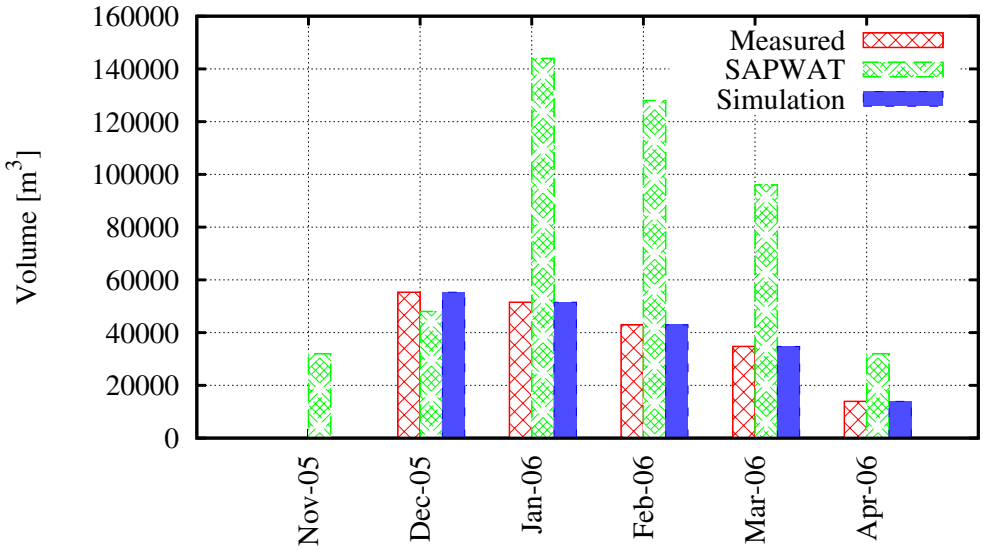

Figure C.5: Elandsberg measured, estimated and simulated water usage.

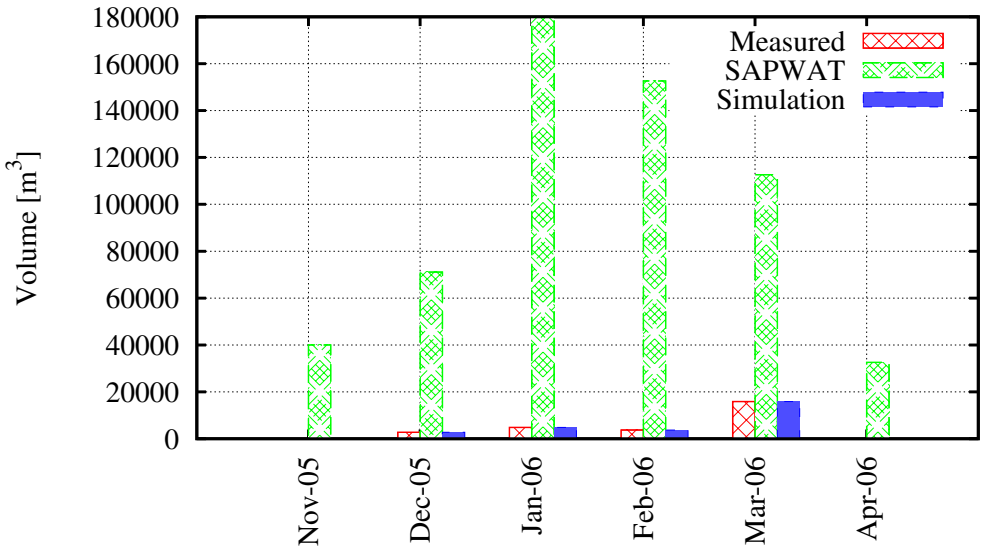

Figure C.6: Phisantekraal 2 measured, estimated and simulated water usage.

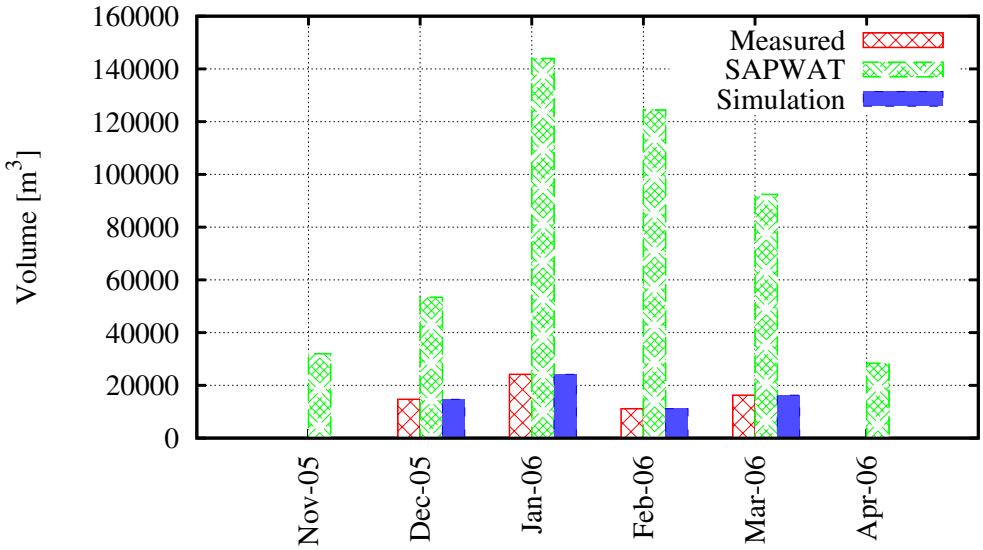

Figure C.7: Phisantekraal 1 measured, estimated and simulated water usage.

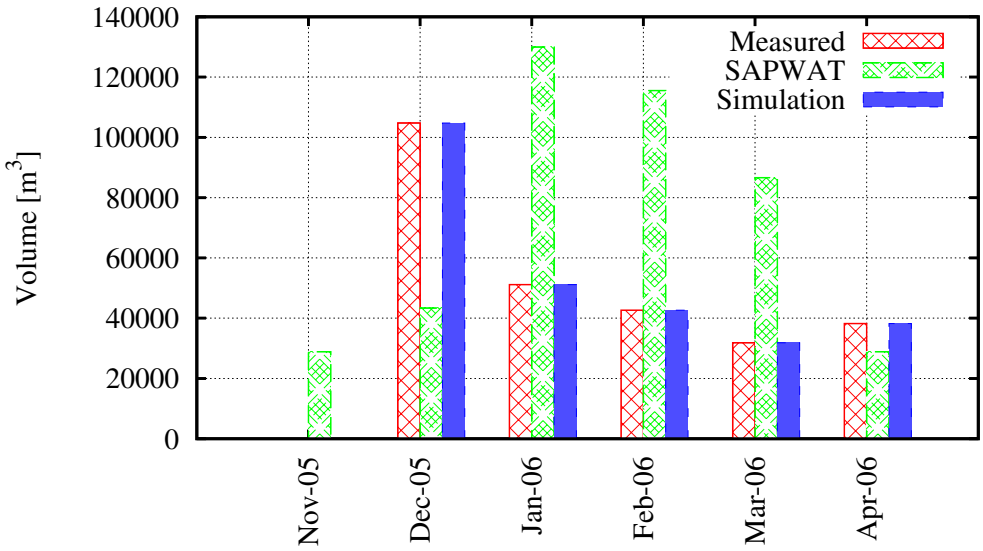

Figure C.8: Ongegund 2 measured, estimated and simulated water usage.

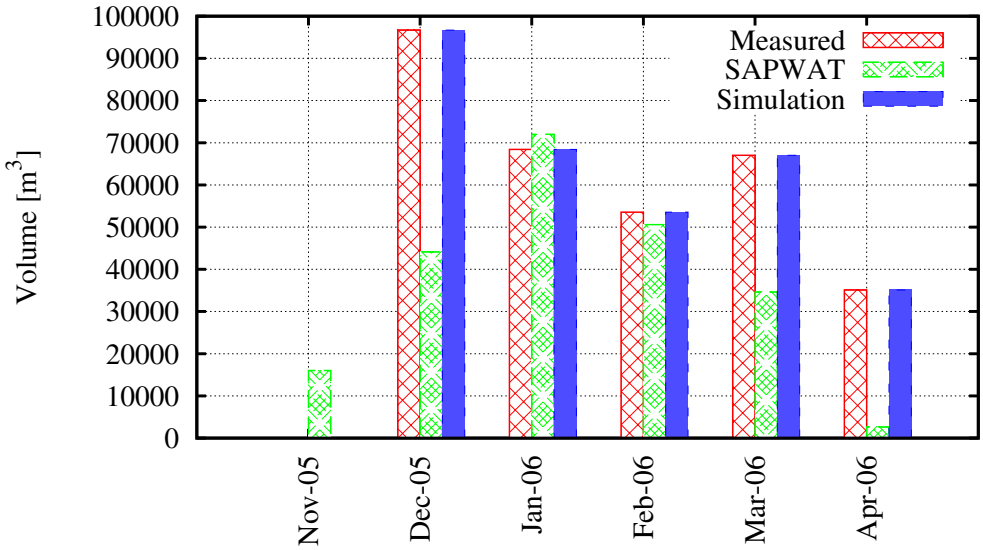

Figure C.9: Spes Bona 1 measured, estimated and simulated water usage.

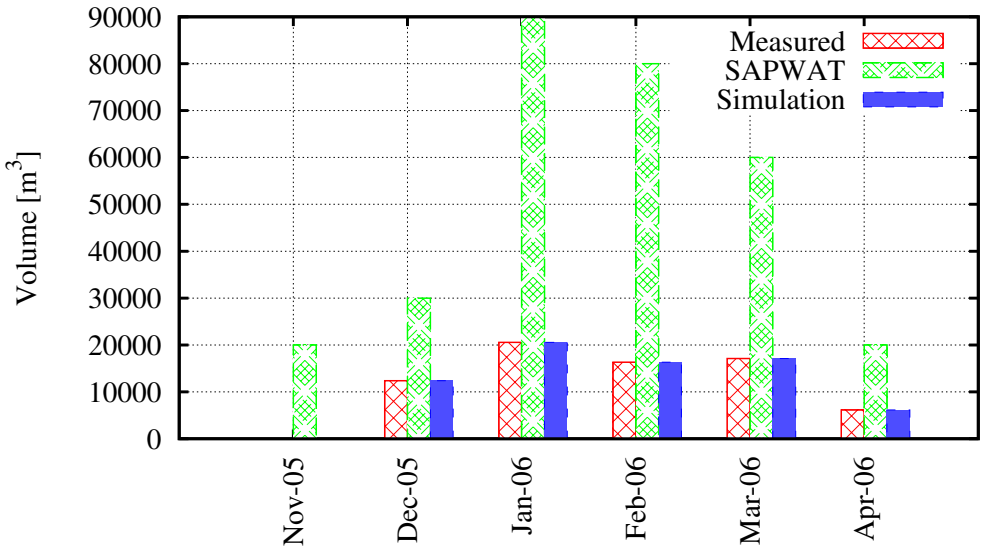

Figure C.10: Spes Bona 2 measured, estimated and simulated water usage.

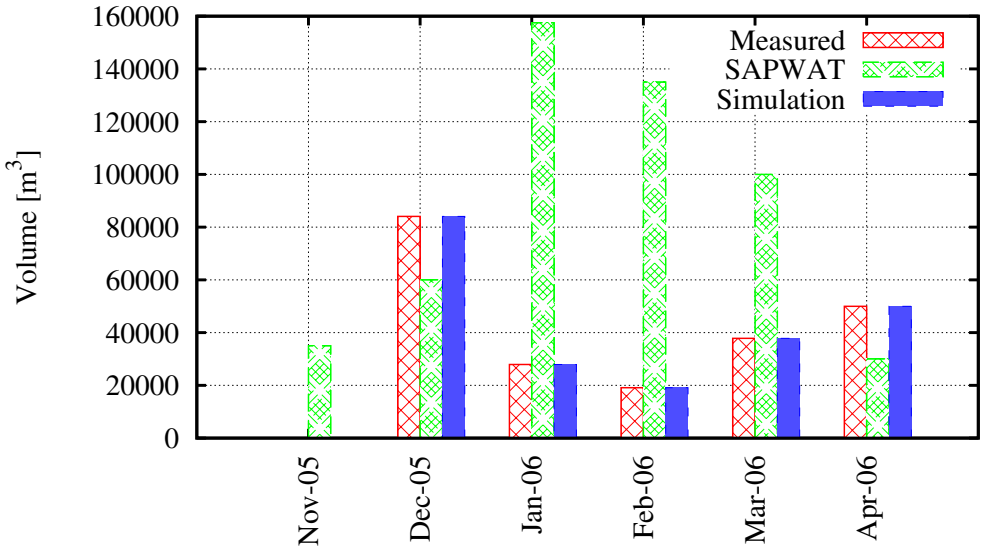

Figure C.11: Helderstroom measured, estimated and simulated water usage.

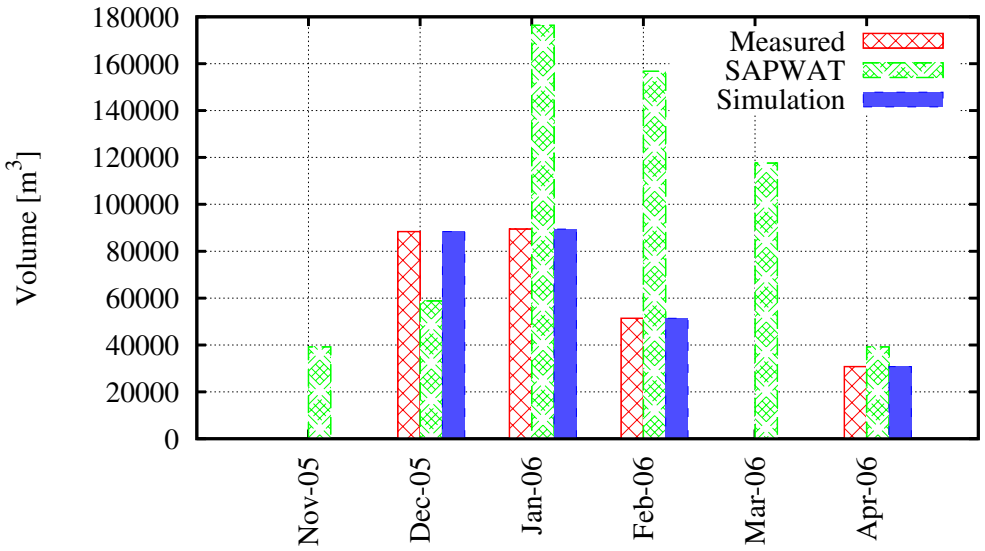

Figure C.12: Uitkyk measured, estimated and simulated water usage.

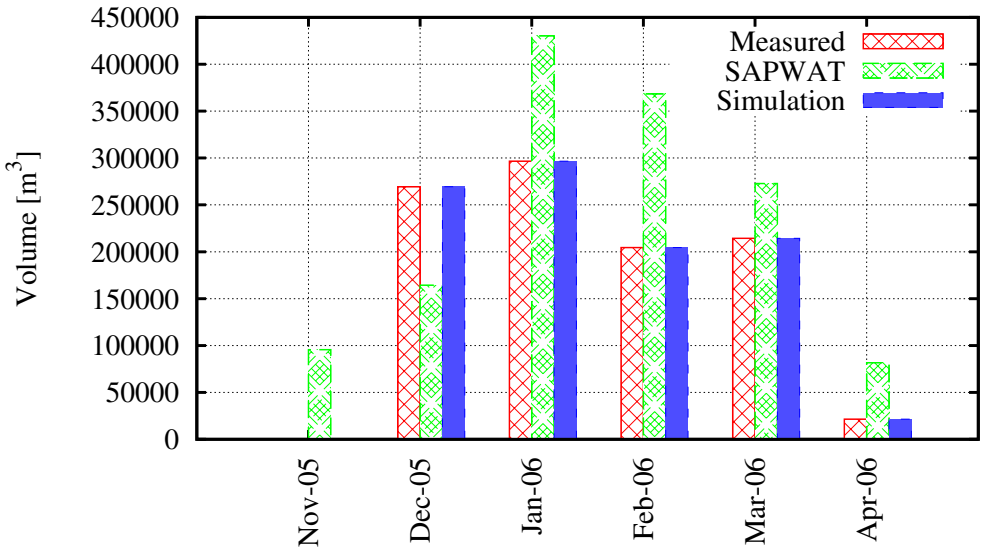

Figure C.13: Sunnyside measured, estimated and simulated water usage.

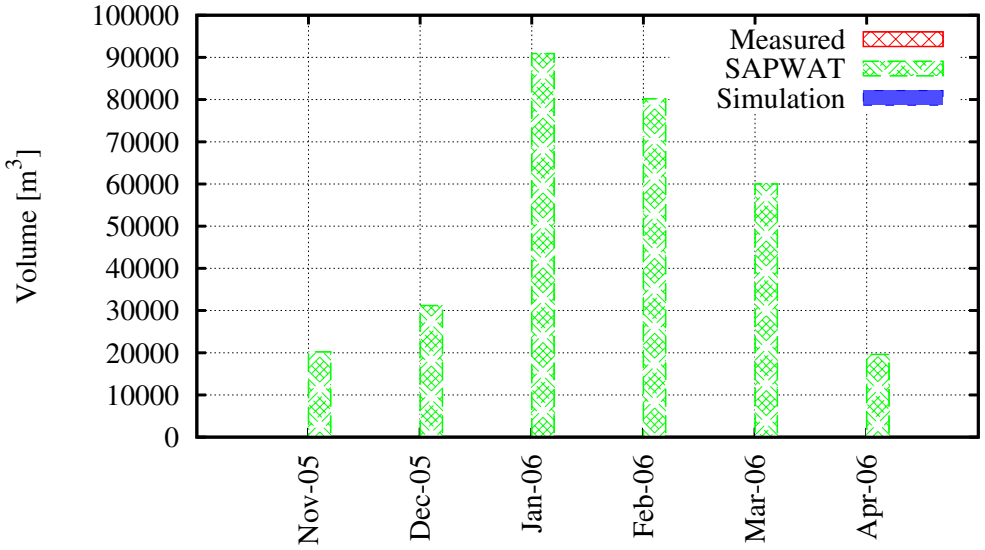

Figure C.14: Elandskloof/Cloud 9 measured, estimated and simulated water usage.

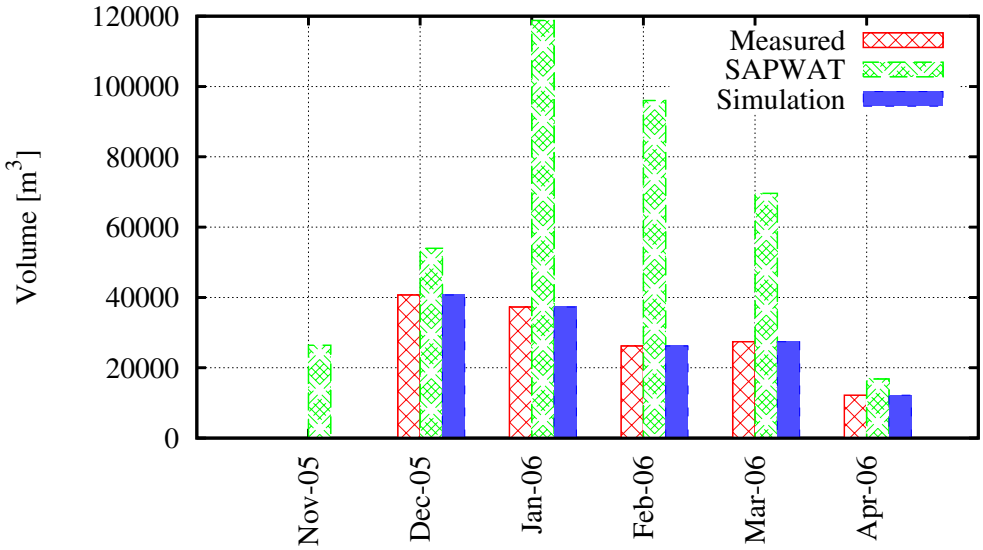

Figure C.15: Spinlea measured, estimated and simulated water usage.

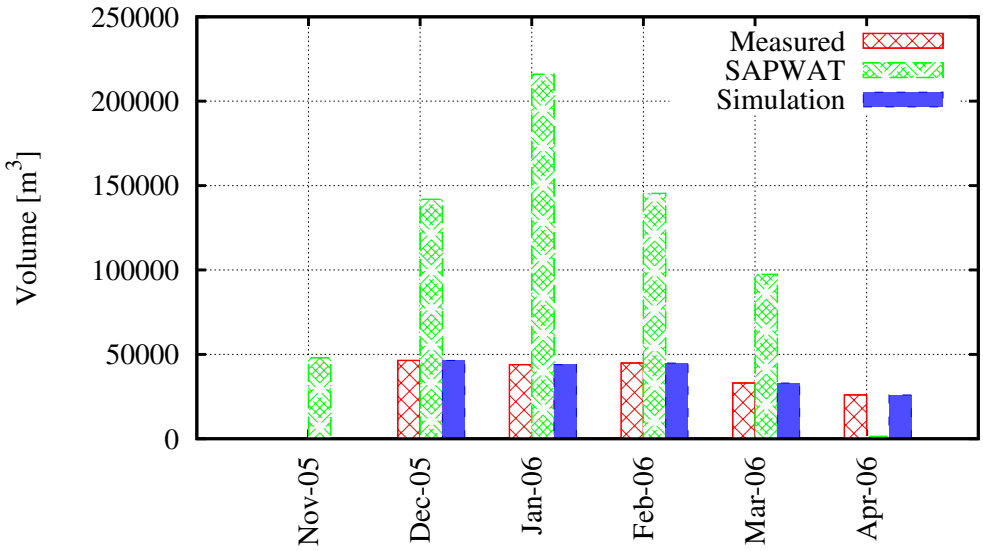

Figure C.16: Meerlustkloof measured, estimated and simulated water usage.

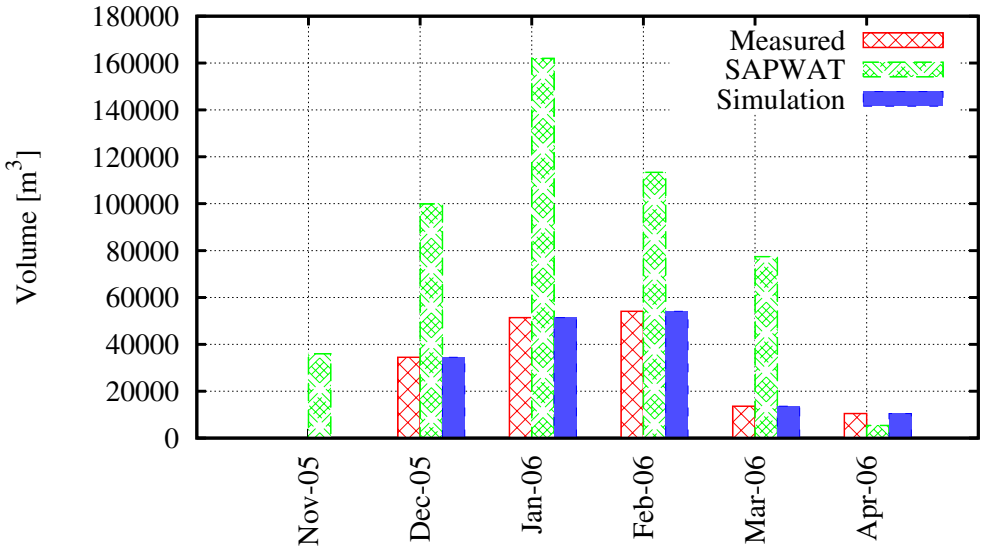

Figure C.17: Middelplaas measured, estimated and simulated water usage.

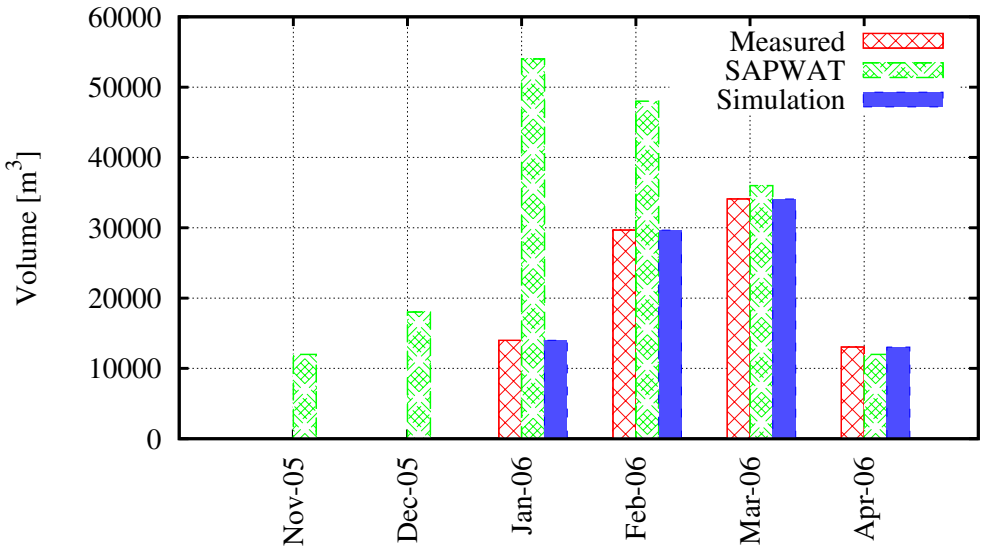

Figure C.18: Amanzi measured, estimated and simulated water usage.

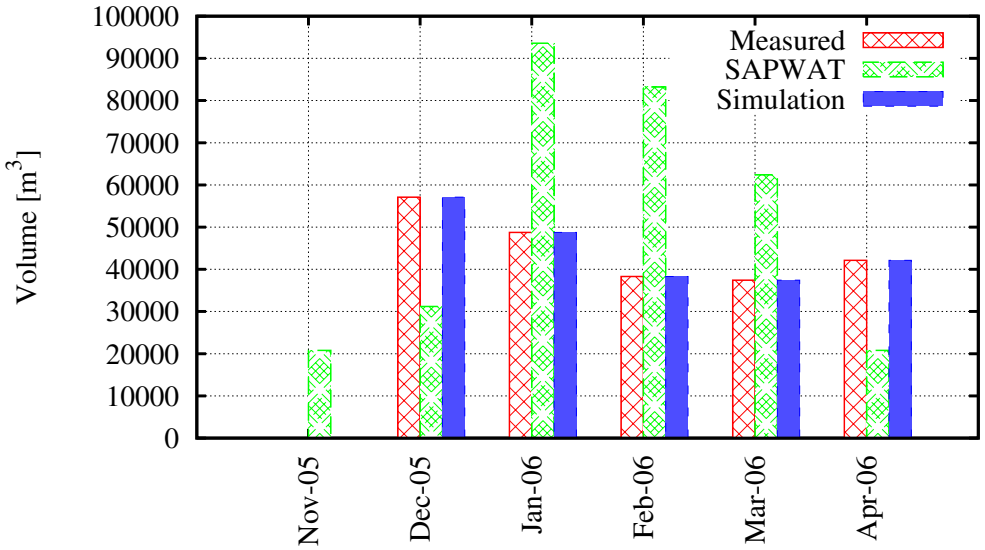

Figure C.19: Klein Ezeljacht measured, estimated and simulated water usage.

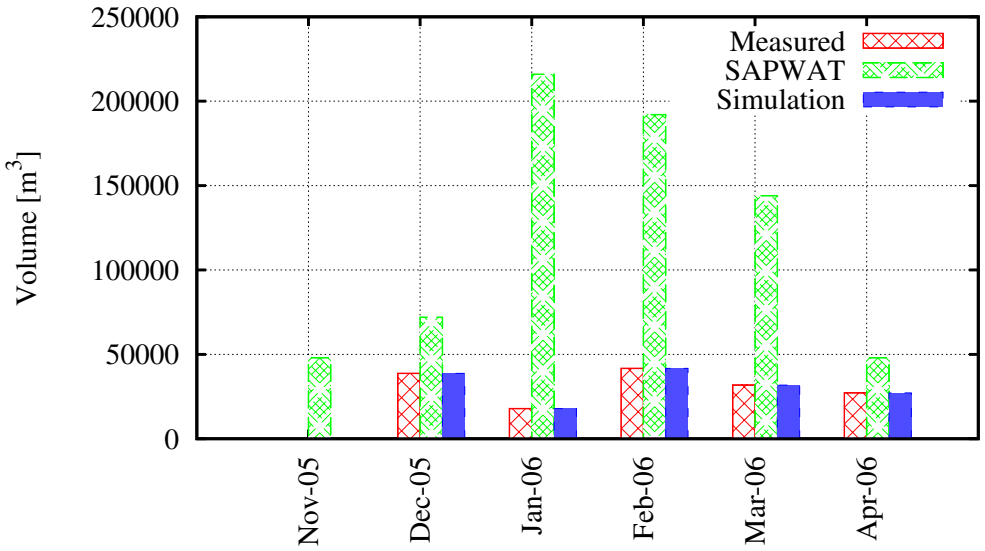

Figure C.20: Meulrivier measured, estimated and simulated water usage.

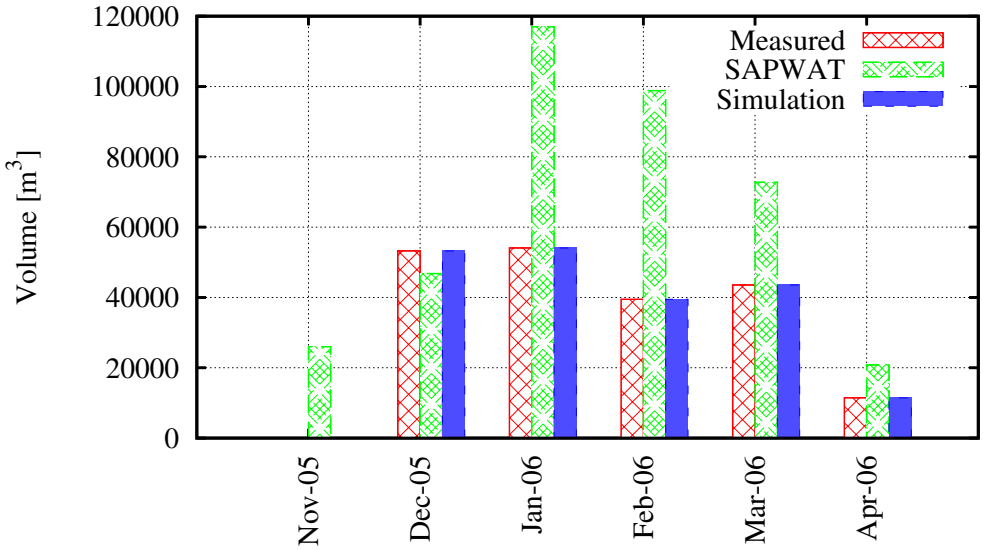

Figure C.21: Champagne measured, estimated and simulated water usage.

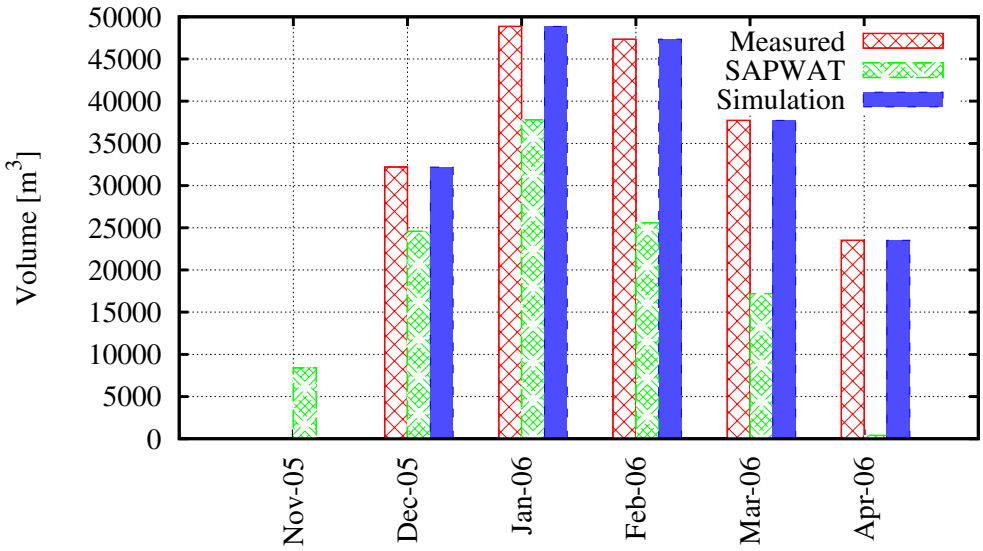

Figure C.22: Oakdene measured, estimated and simulated water usage.

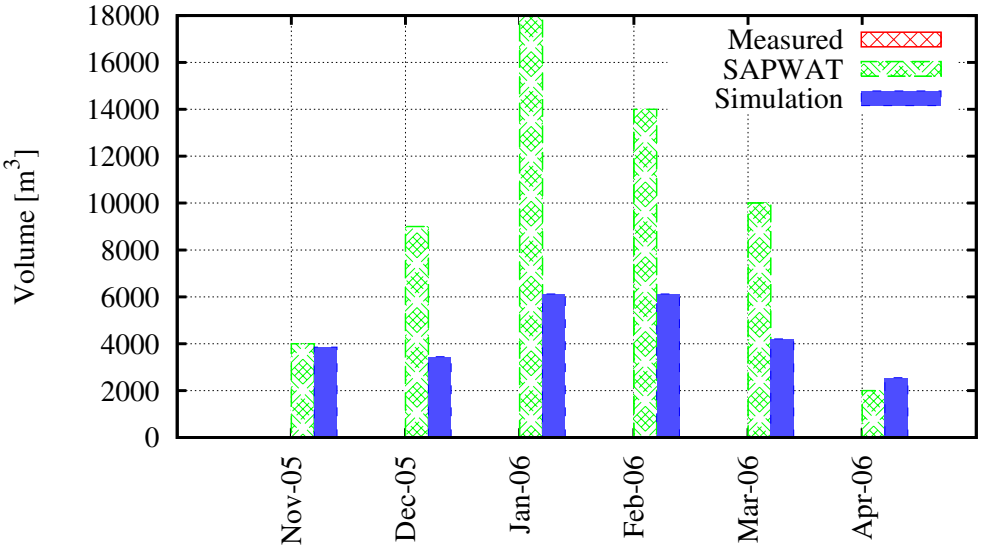

Figure C.23: Oakdene (M. Donkin) measured, estimated and simulated water usage.

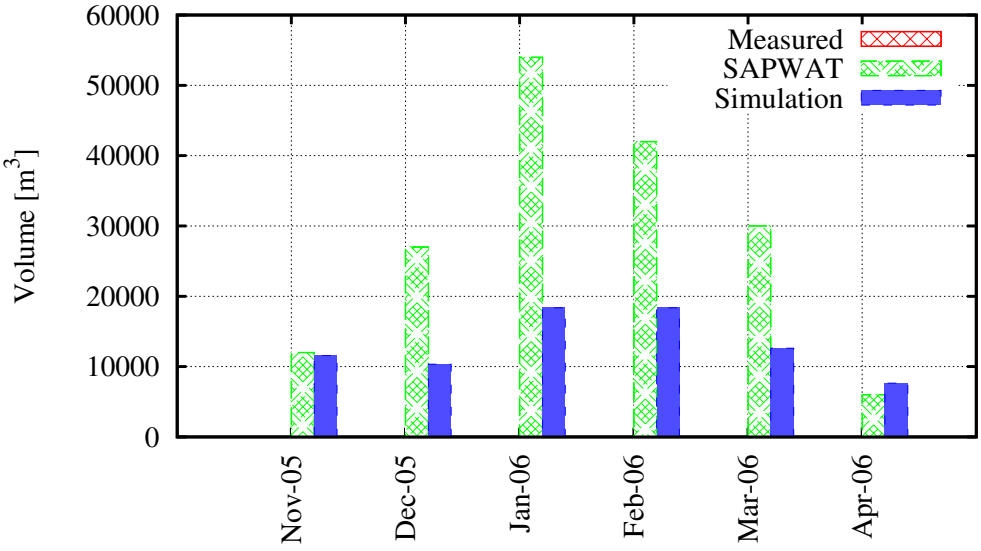

Figure C.24: Oakdene (Nooitgedagt Trust) measured, estimated and simulated water usage.

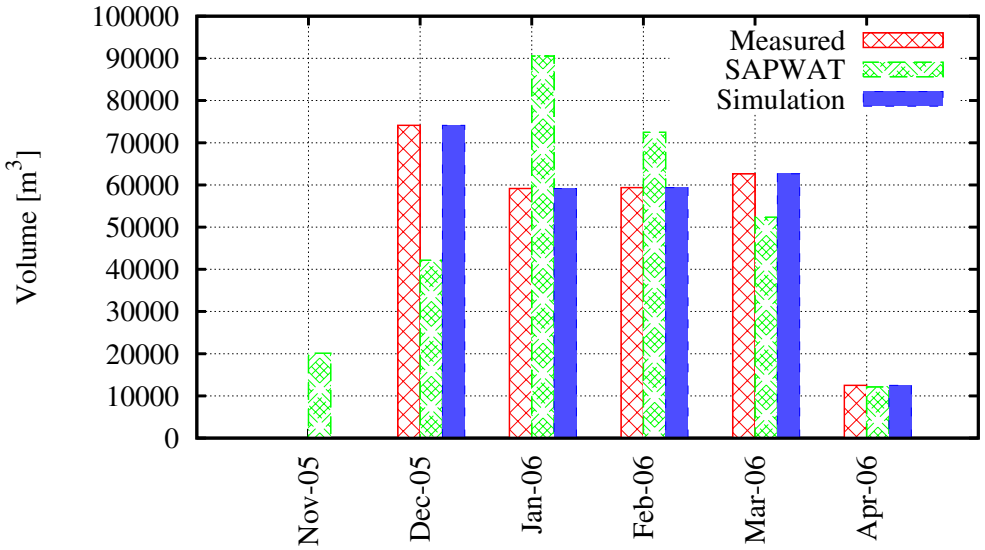

Figure C.25: Bakenskloof measured, estimated and simulated water usage.

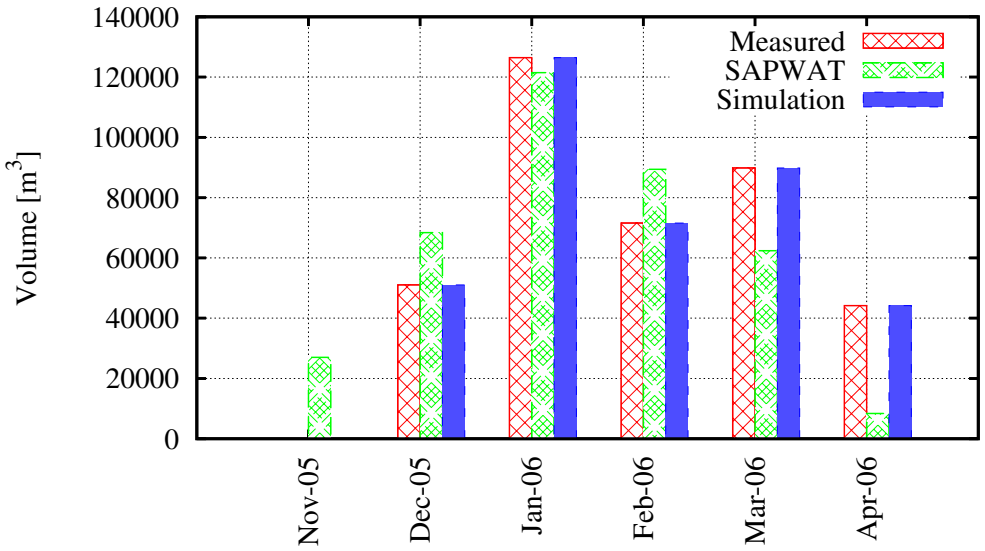

Figure C.26: Jagersbos measured, estimated and simulated water usage.

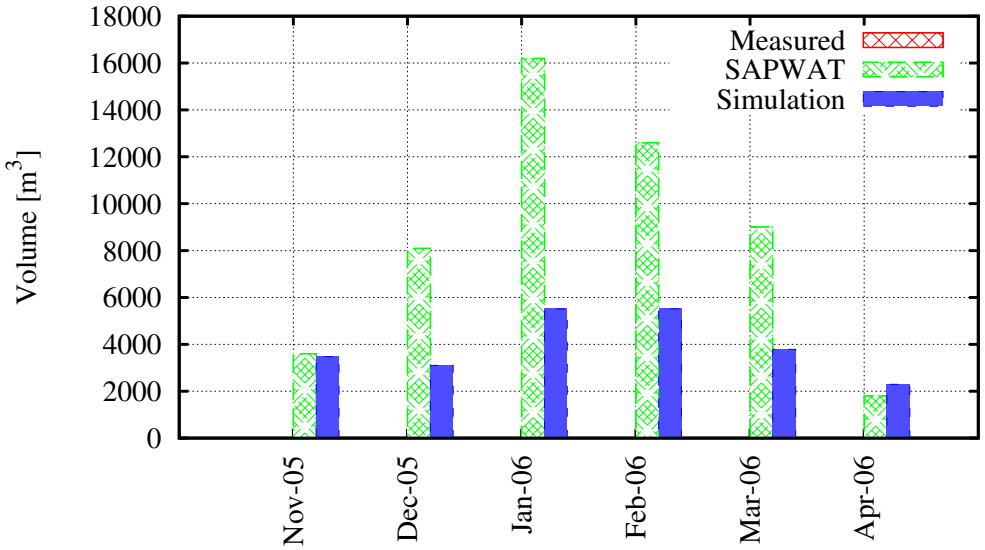

Figure C.27: Pikkie Viljoen measured, estimated and simulated water usage.

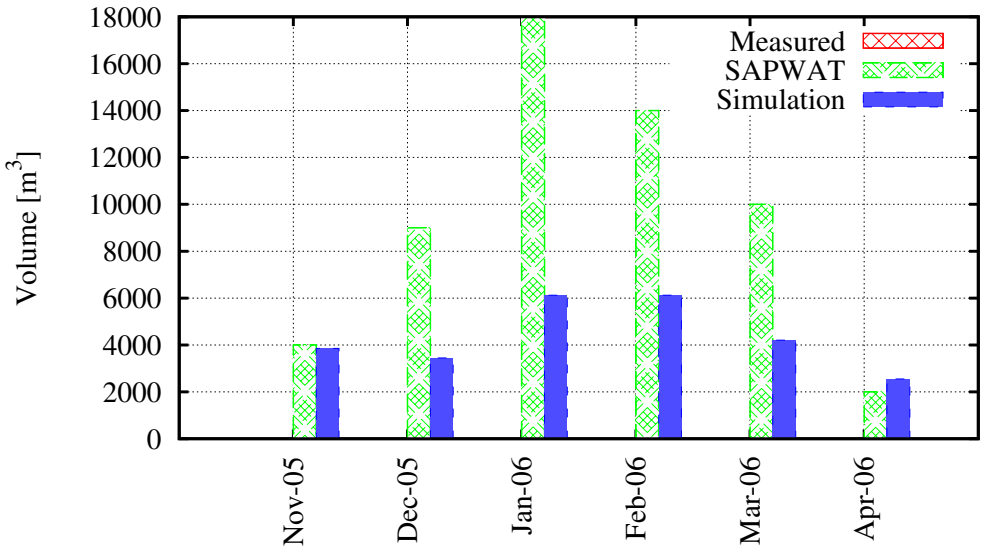

Figure C.28: M. Bothma measured, estimated and simulated water usage.

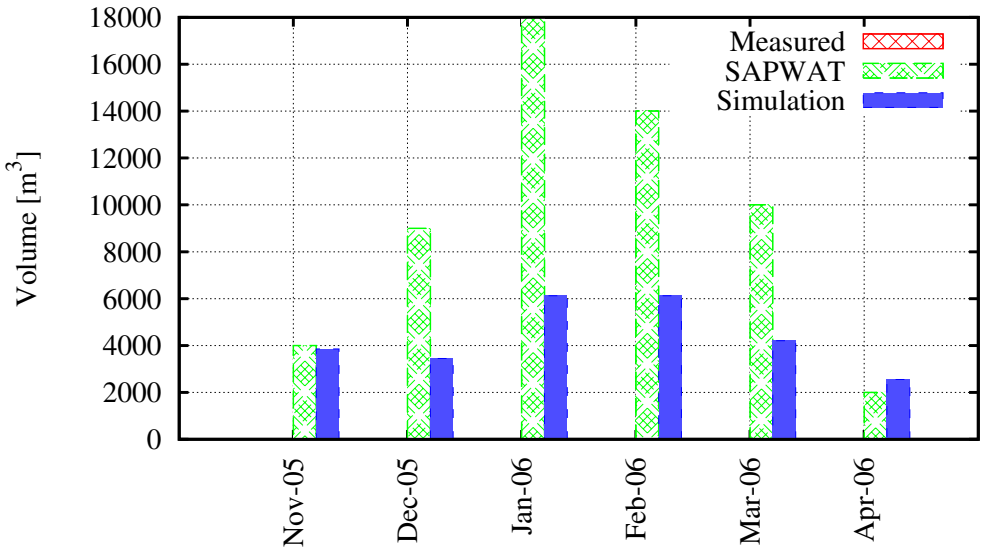

Figure C.29: Ambolati measured, estimated and simulated water usage.

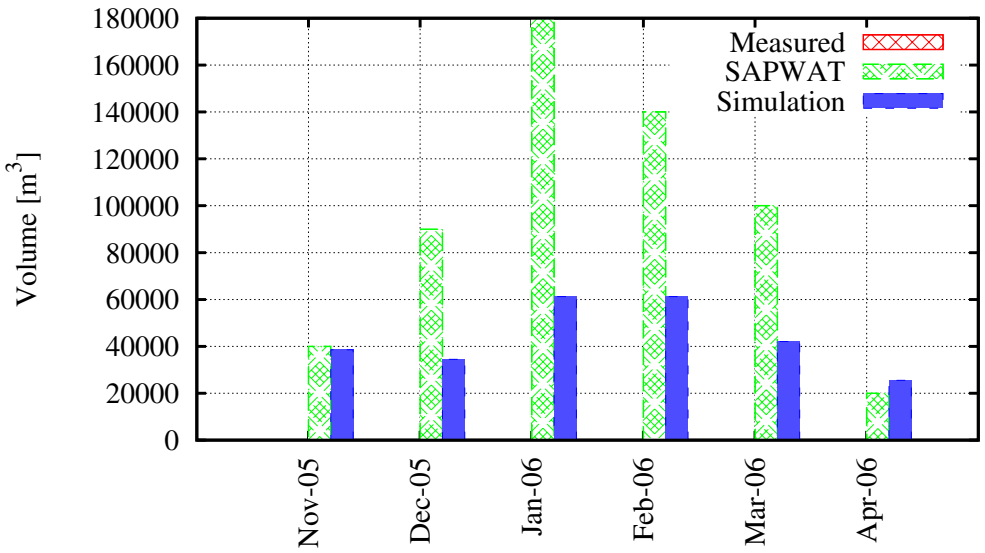

Figure C.30: Department of Agriculture measured, estimated and simulated water usage.

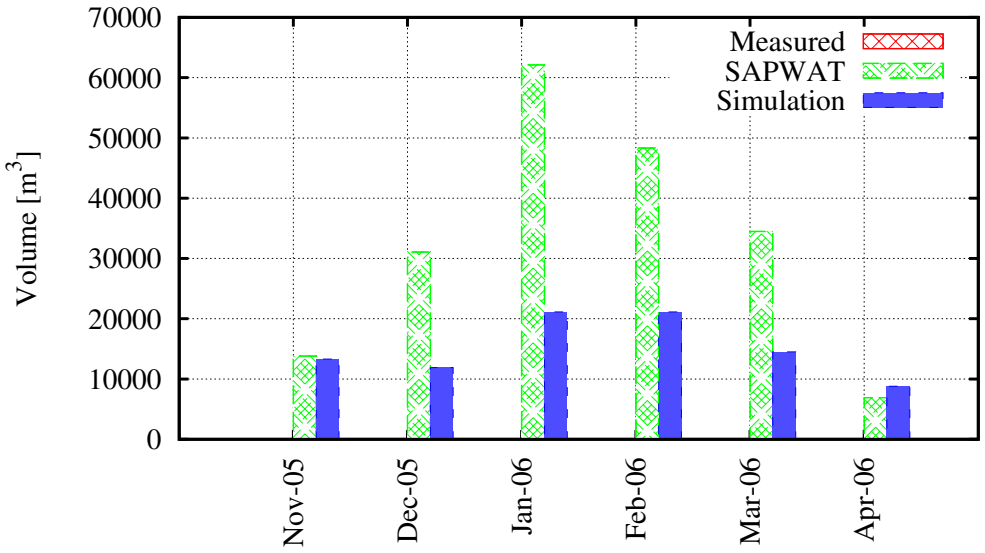

Figure C.31: Genadendal Community measured, estimated and simulated water usage.

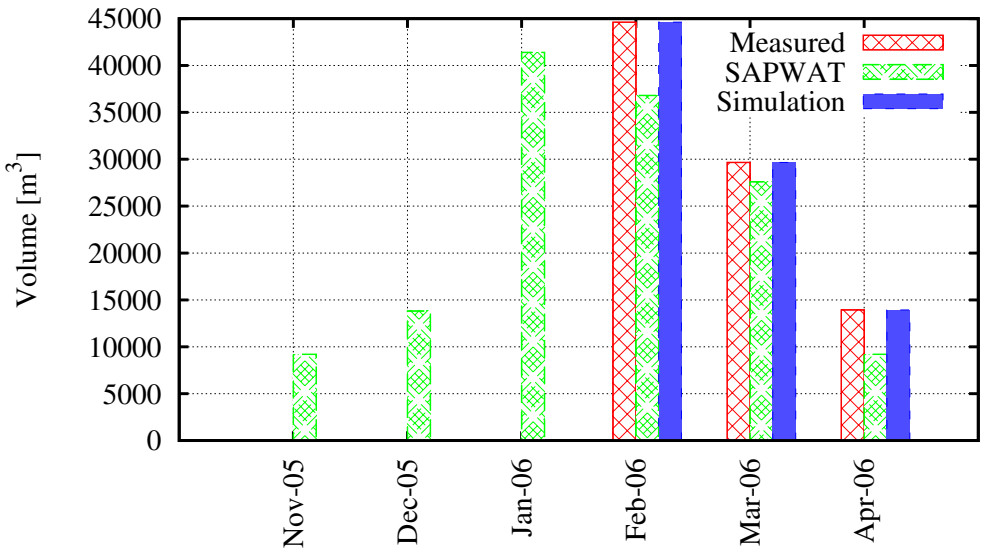

Figure C.32: Ouplaas measured, estimated and simulated water usage.

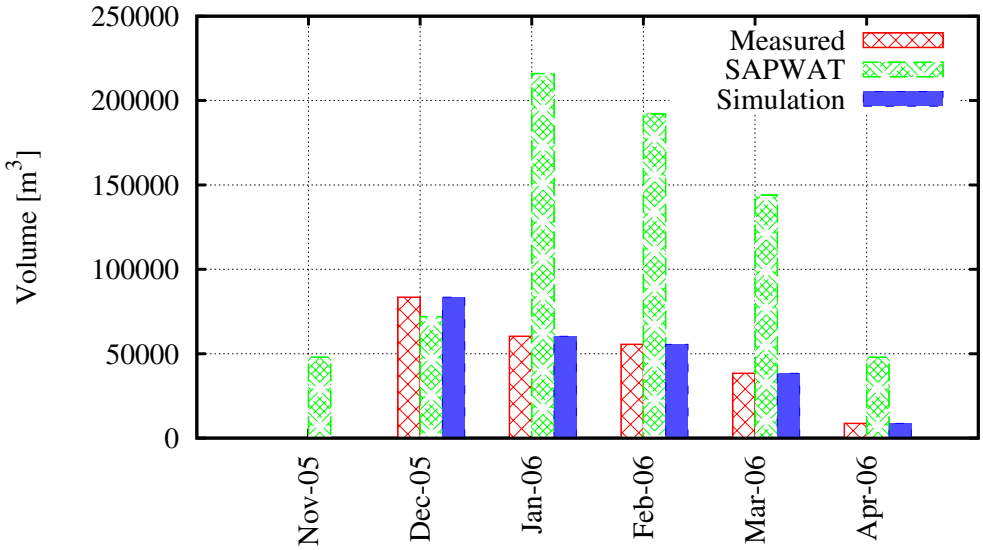

Figure C.33: Zandvlakte measured, estimated and simulated water usage.

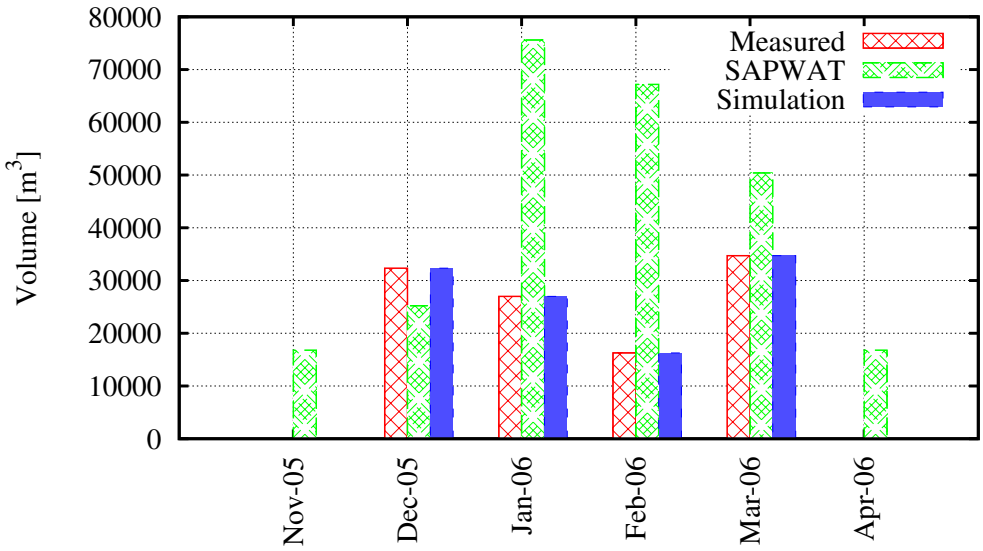

Figure C.34: Nuweplaas measured, estimated and simulated water usage.

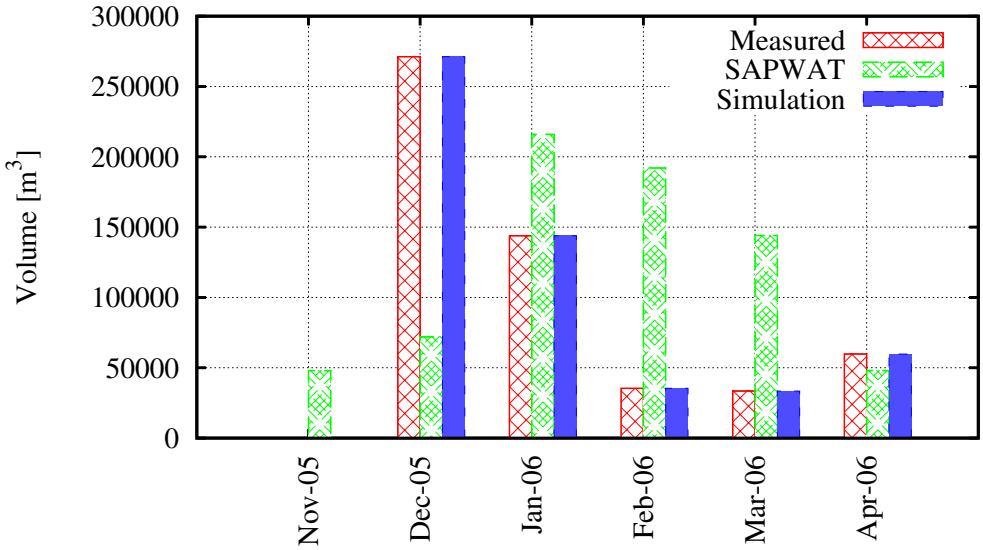

Figure C.35: Elsenkloof measured, estimated and simulated water usage.

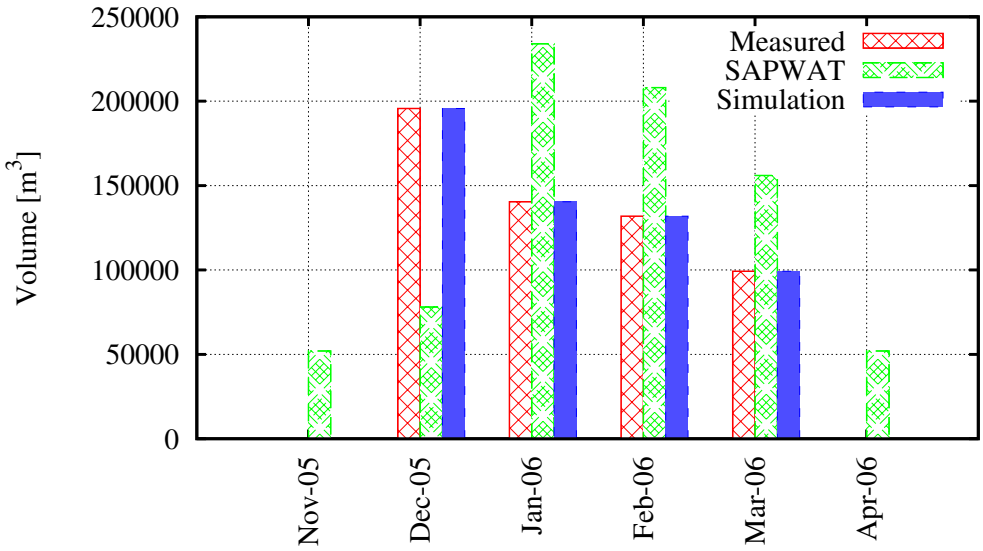

Figure C.36: Oewerzicht measured, estimated and simulated water usage.

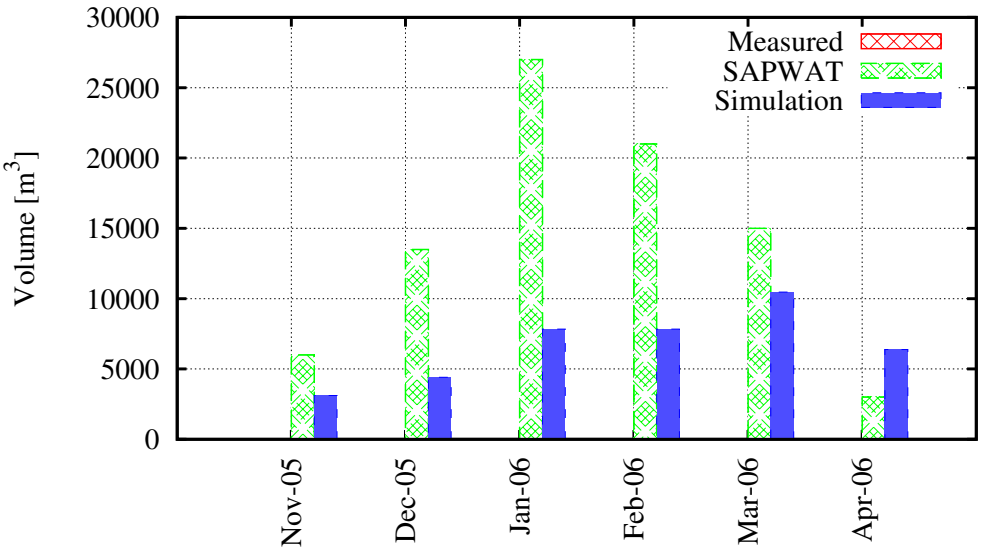

Figure C.37: Klein Eike measured, estimated and simulated water usage.

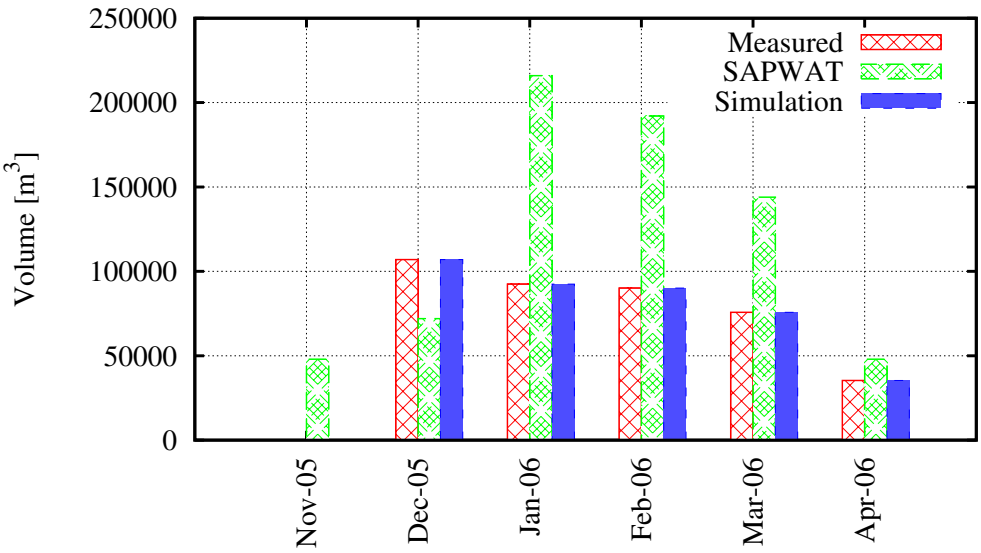

Figure C.38: Danie du Toit Trust measured, estimated and simulated water usage.

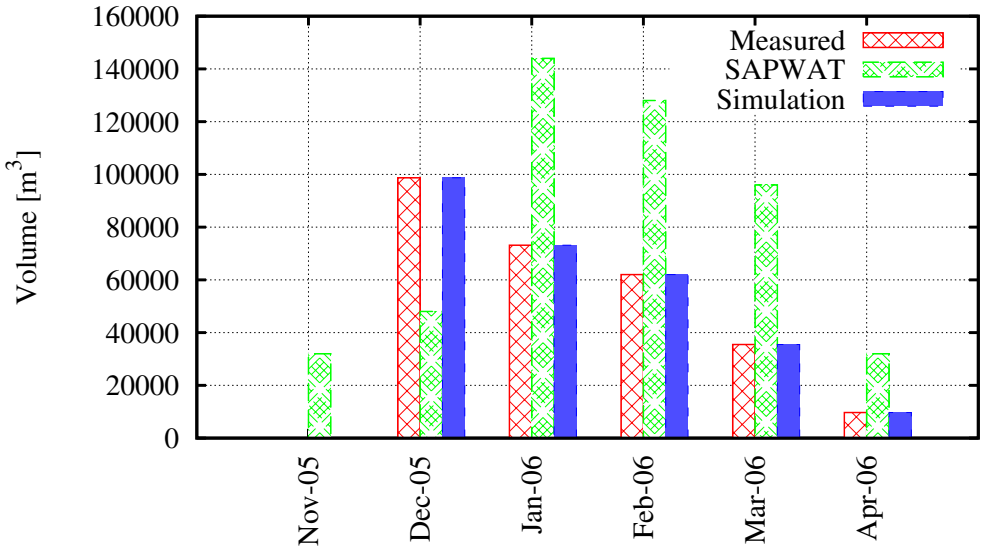

Figure C.39: The Oaks measured, estimated and simulated water usage.

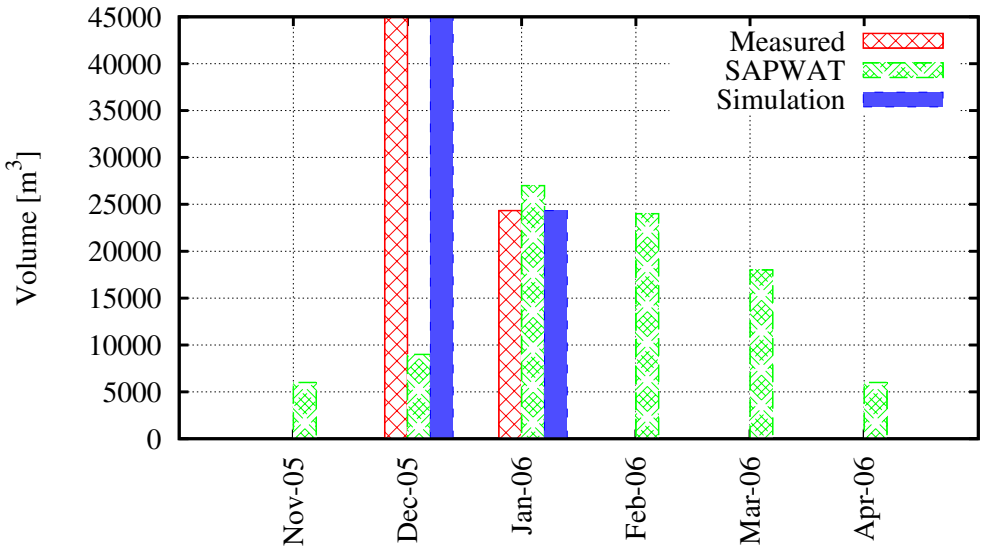

Figure C.40: Riverside measured, estimated and simulated water usage.

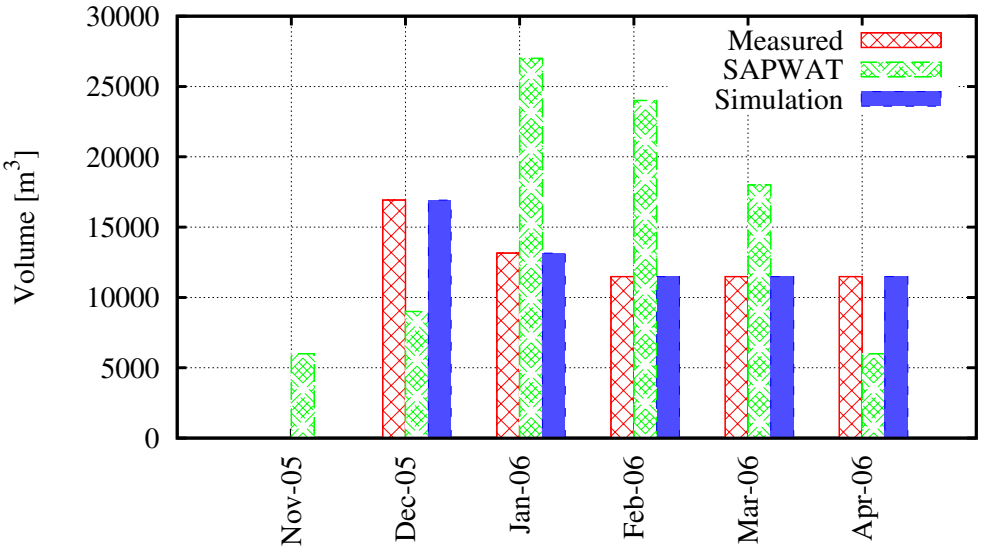

Figure C.41: Nethercourt 1 measured, estimated and simulated water usage.

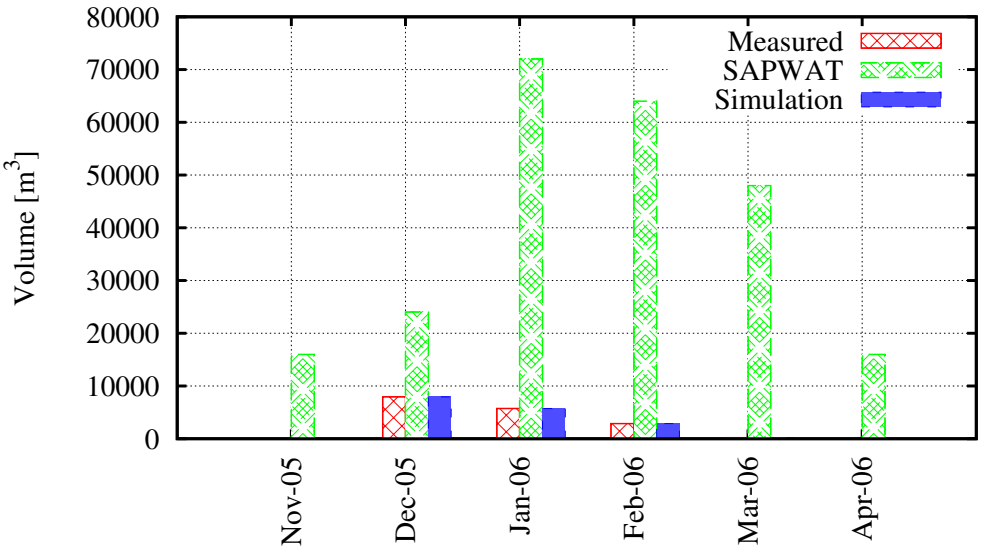

Figure C.42: Nethercourt 2 measured, estimated and simulated water usage.

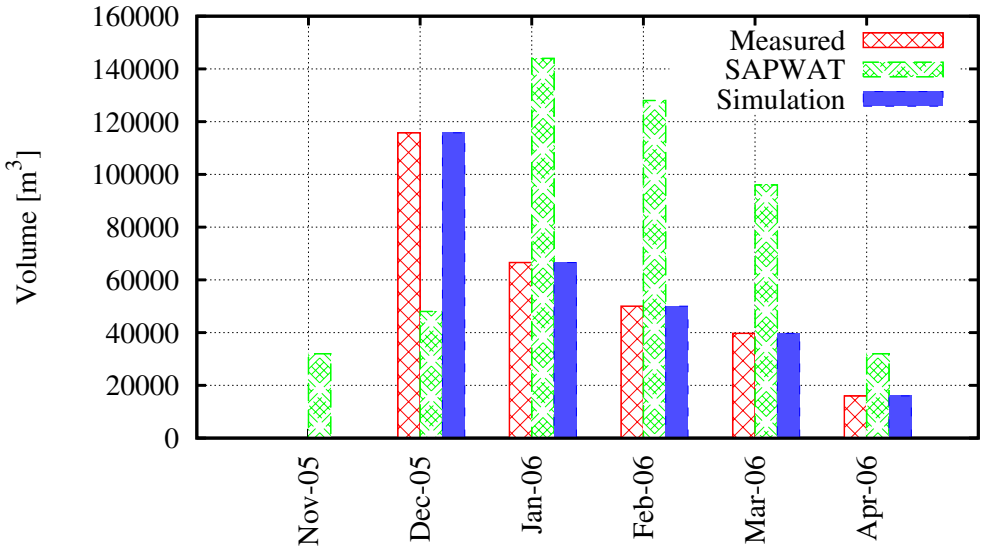

Figure C.43: Soetmelksvlei measured, estimated and simulated water usage.

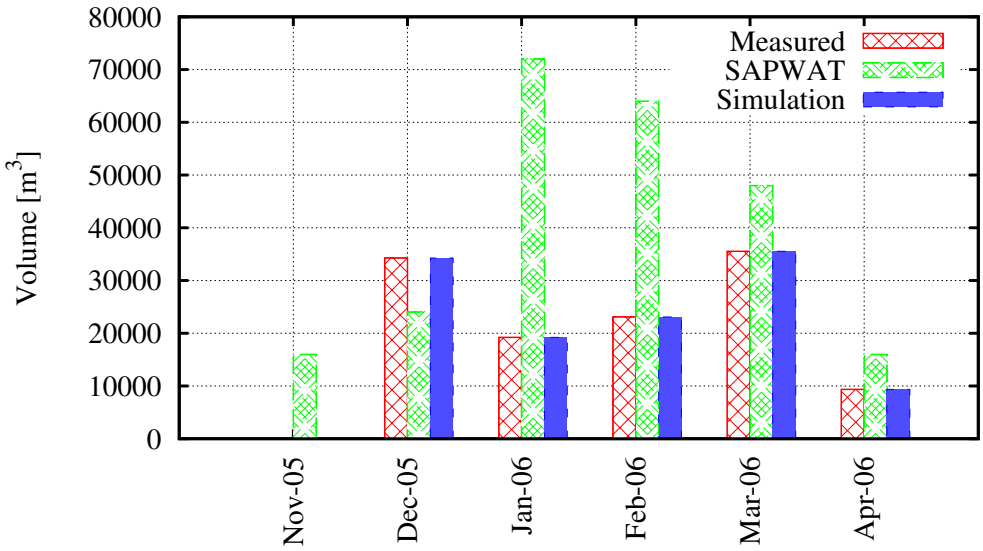

Figure C.44: Schuitsberg measured, estimated and simulated water usage.

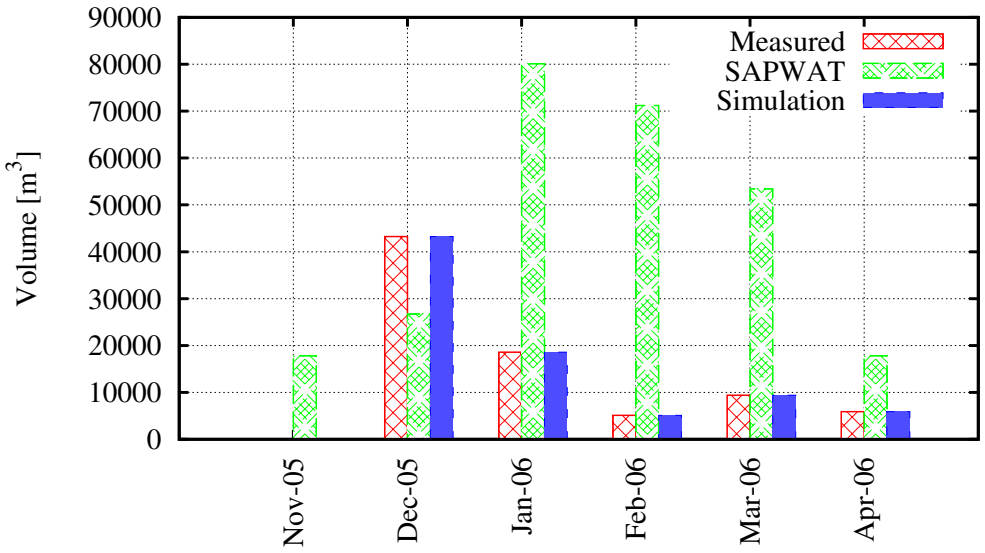

Figure C.45: Soetmelksvlei (B. Sender) measured, estimated and simulated water usage.

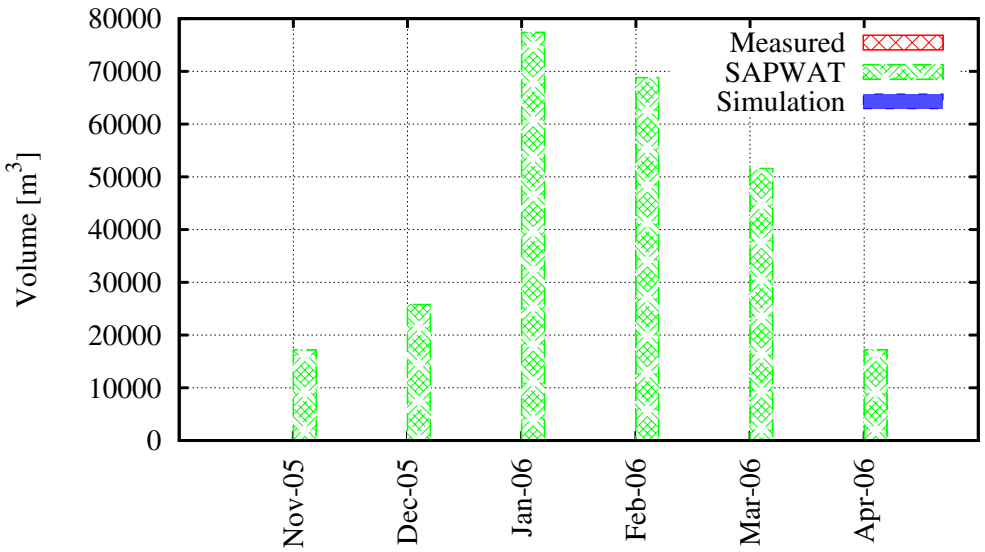

Figure C.46: Punt Boerdery measured, estimated and simulated water usage.

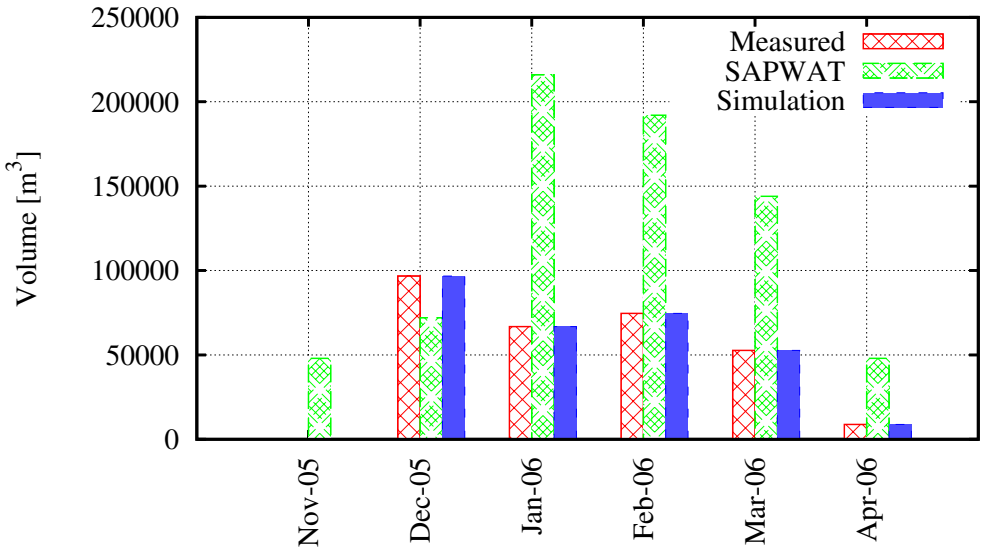

Figure C.47: Soetmelksvlei (Koert se kraal) measured, estimated and simulated water usage.

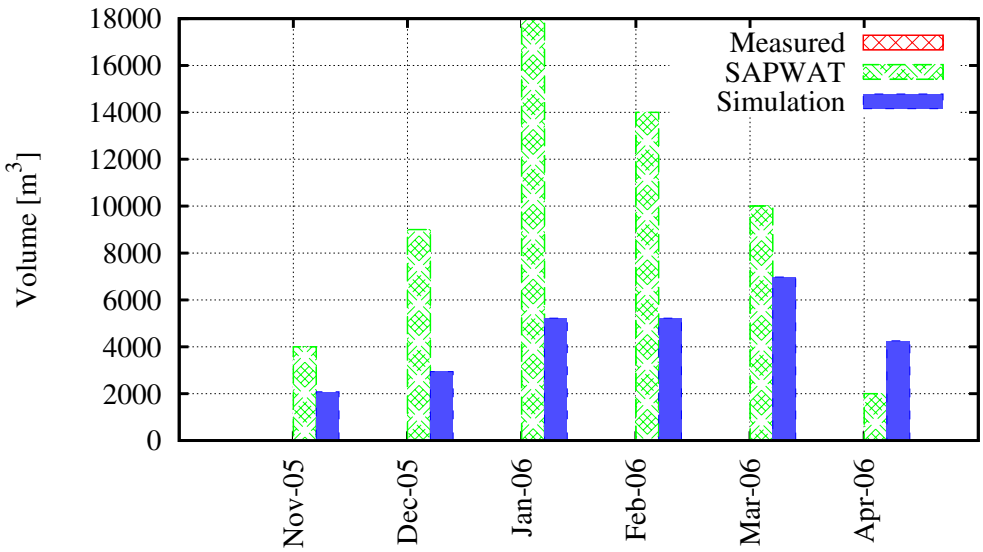

Figure C.48: Vrede measured, estimated and simulated water usage.

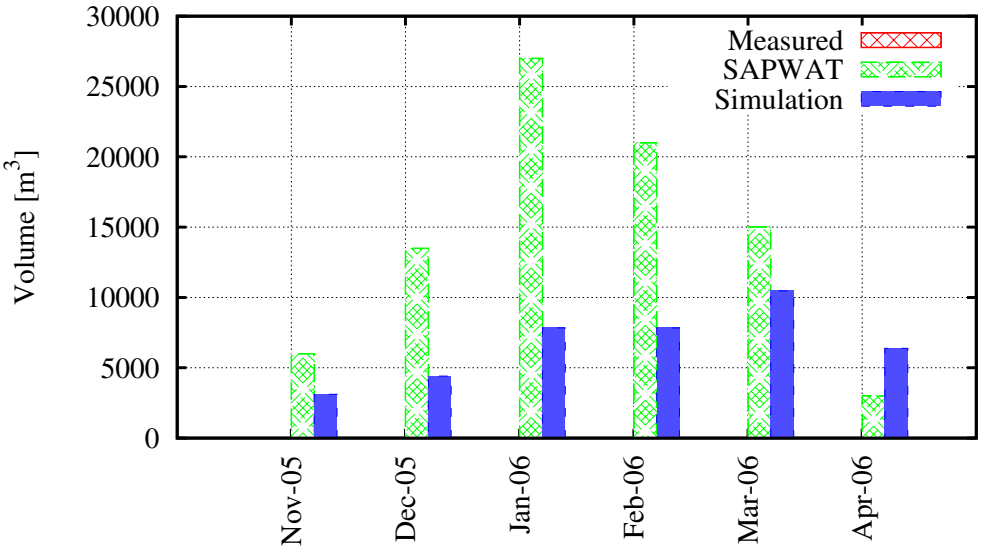

Figure C.49: H. Human Trust measured, estimated and simulated water usage.

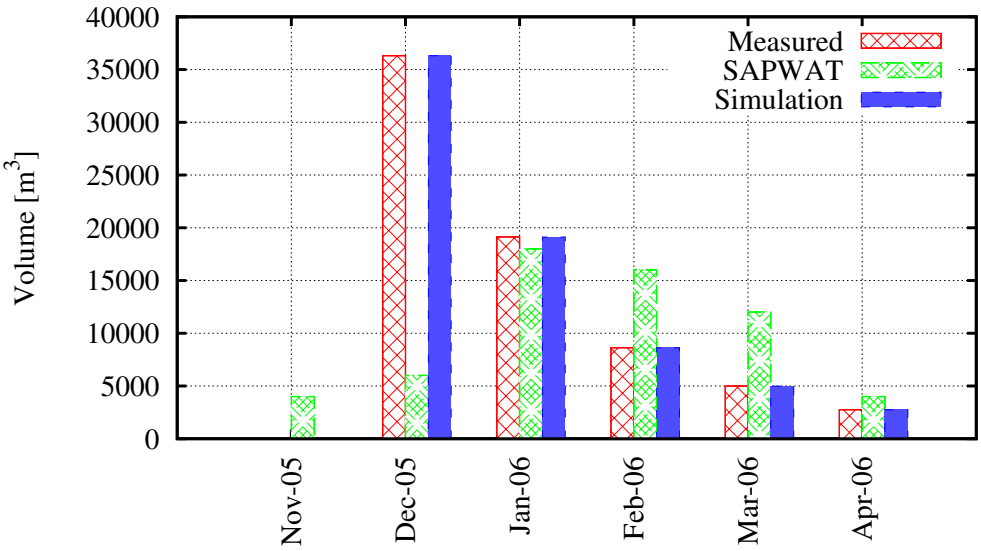

Figure C.50: S. du Toit Trust measured, estimated and simulated water usage.

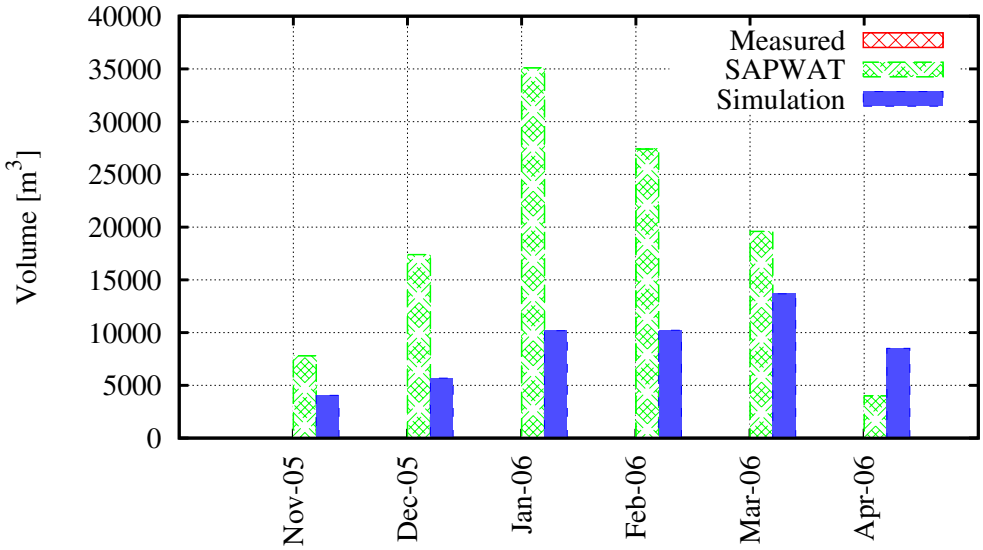

Figure C.51: Ganskraal measured, estimated and simulated water usage.

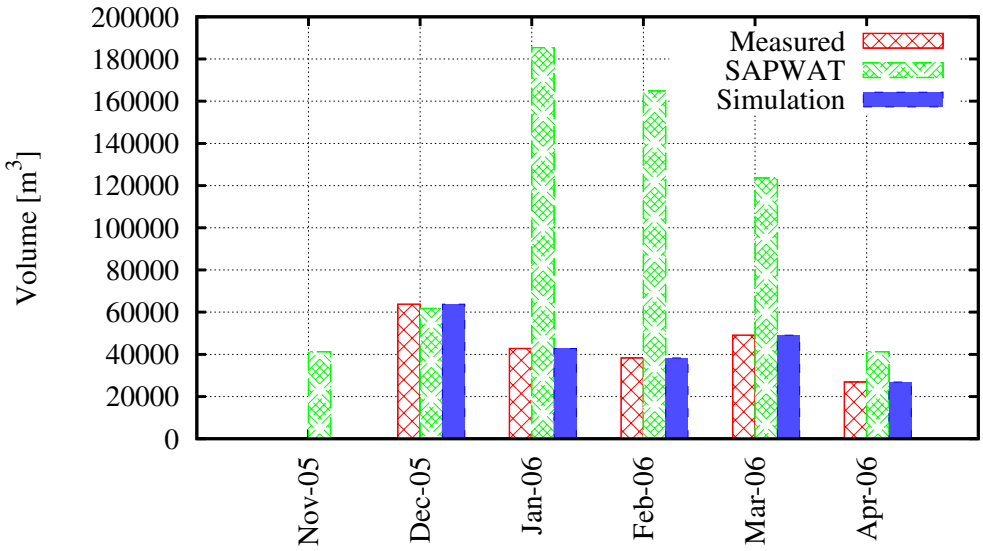

Figure C.52: Bloemenkraal measured, estimated and simulated water usage.

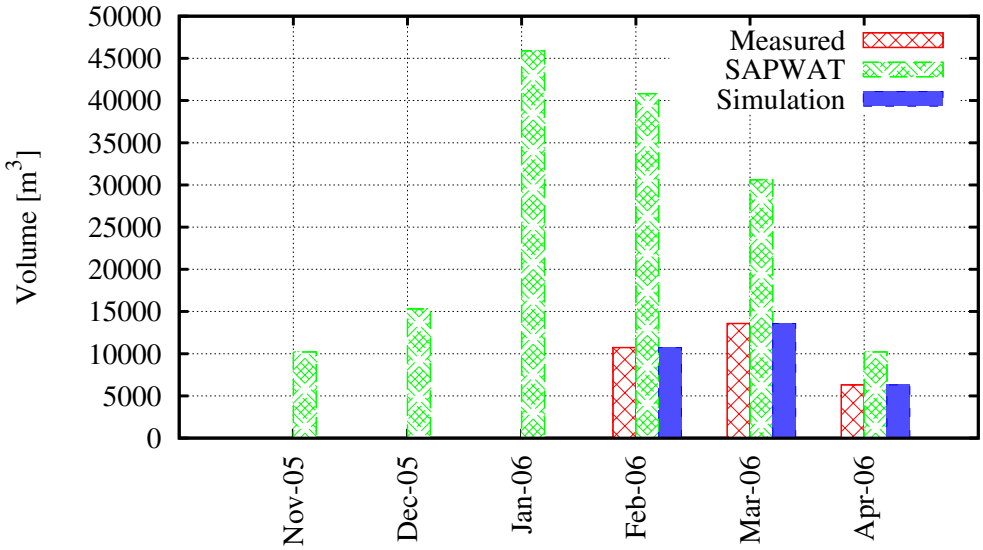

Figure C.53: Ganskraal measured, estimated and simulated water usage.

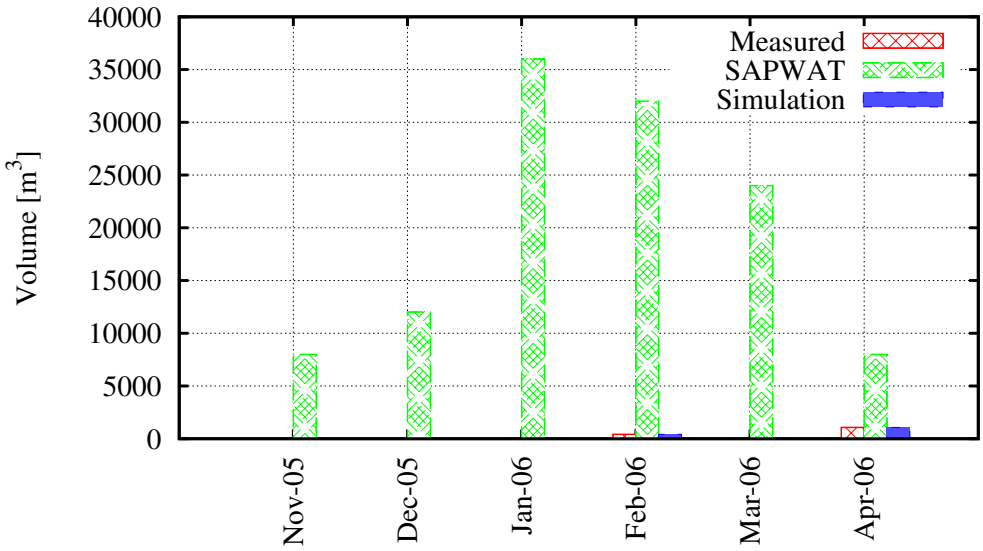

Figure C.54: Vredelust measured, estimated and simulated water usage.

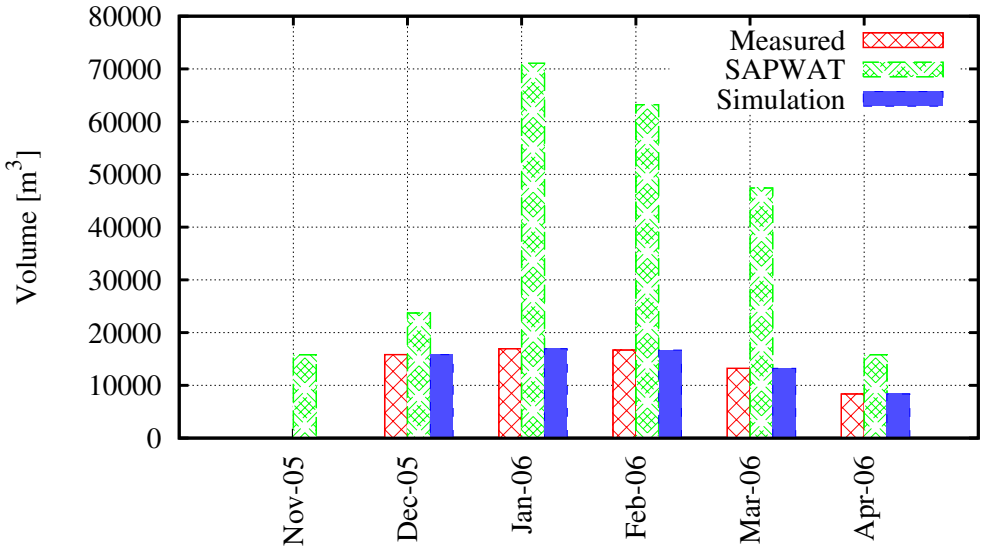

Figure C.55: Langverwaght measured, estimated and simulated water usage.

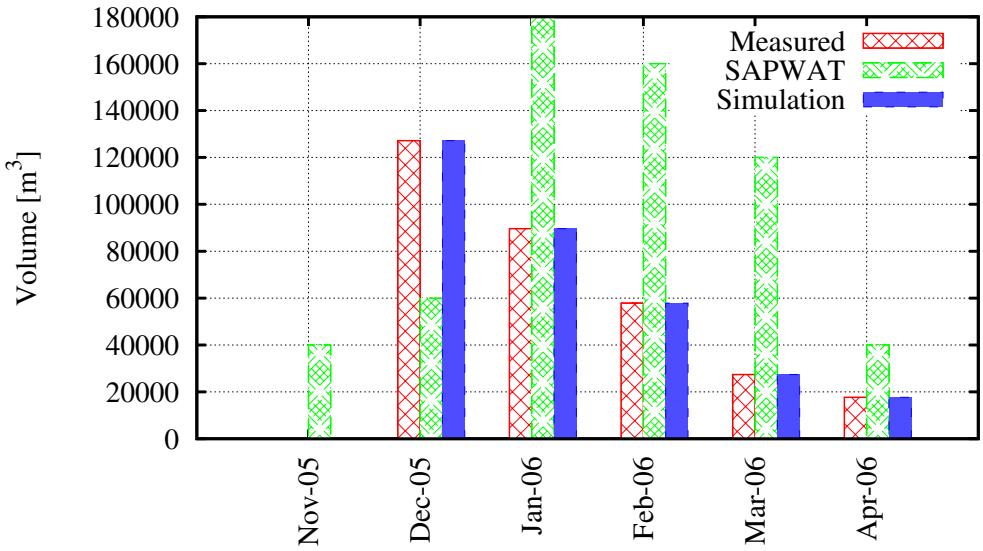

Figure C.56: Kleinplasie measured, estimated and simulated water usage.

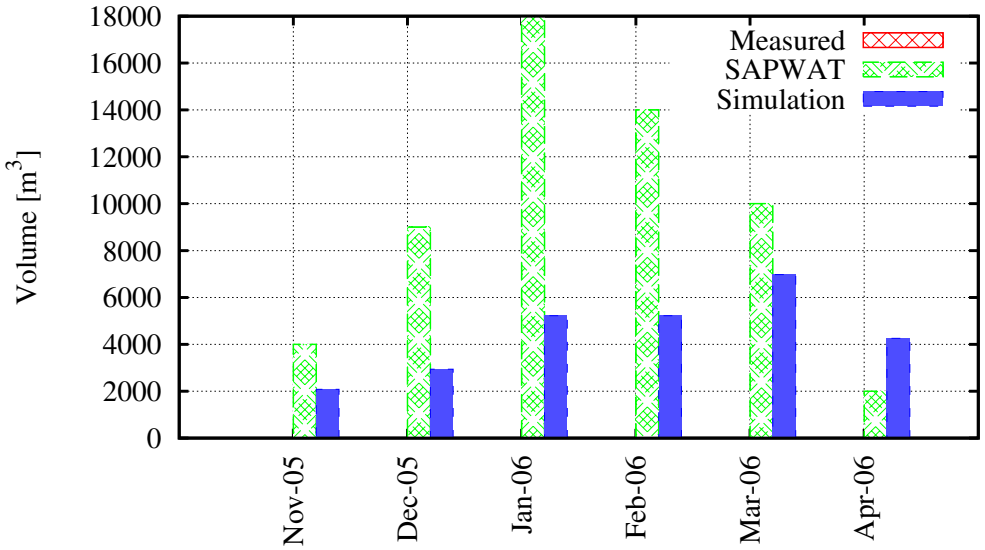

Figure C.57: Neethlingskroon measured, estimated and simulated water usage.

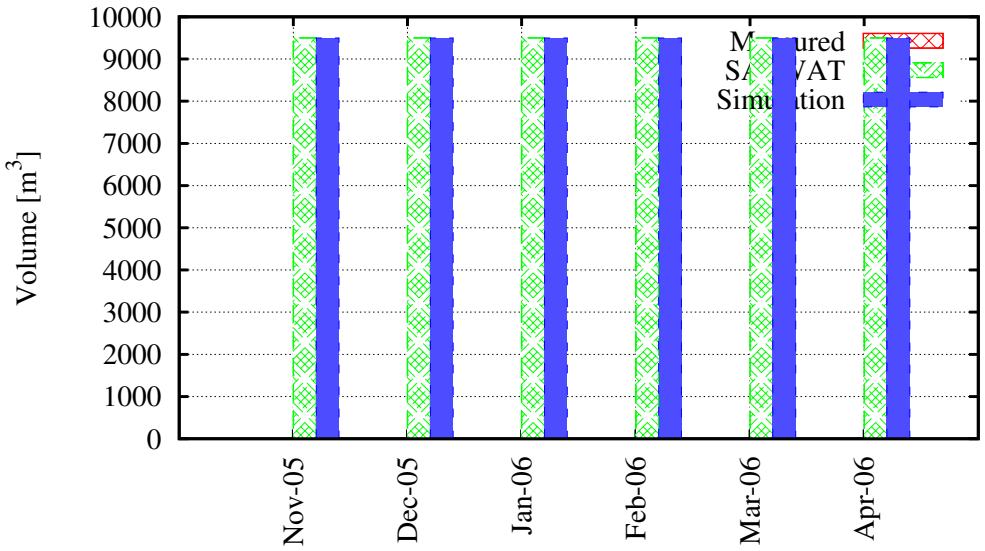

Figure C.58: Bokrivier Farms measured, estimated and simulated water usage.

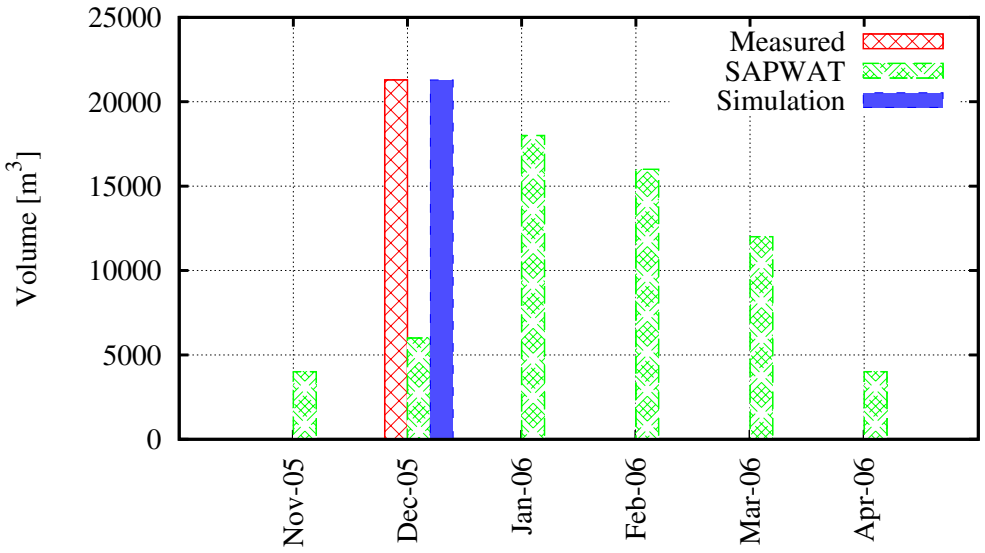

Figure C.59: Bokrivier Landgoed measured, estimated and simulated water usage.

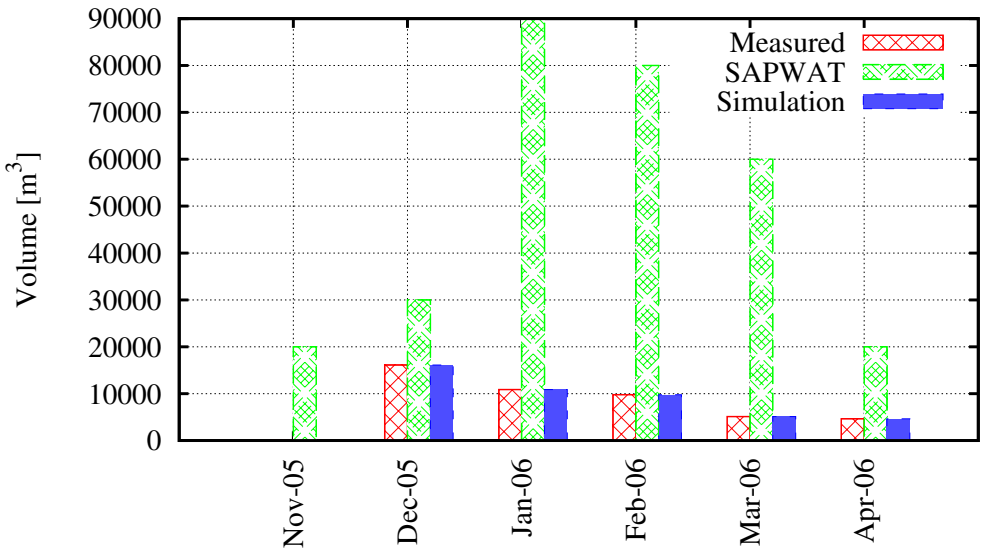

Figure C.60: Esperance measured, estimated and simulated water usage.

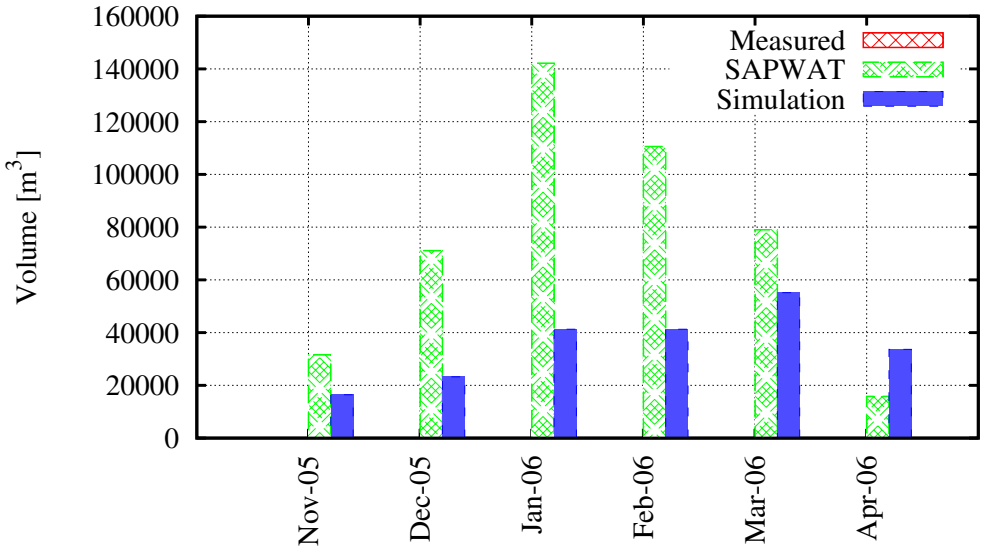

Figure C.61: Concordia measured, estimated and simulated water usage.

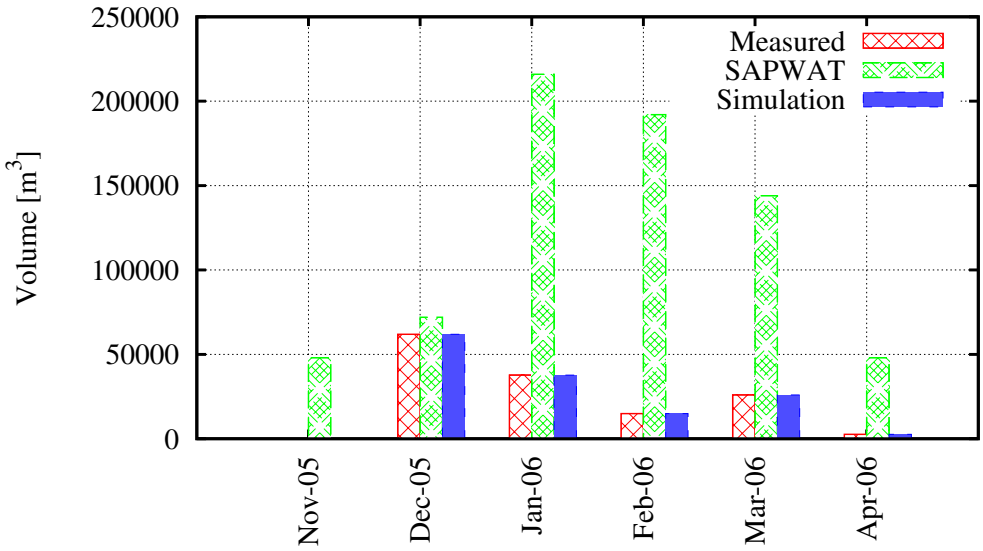

Figure C.62: Lincorso measured, estimated and simulated water usage.

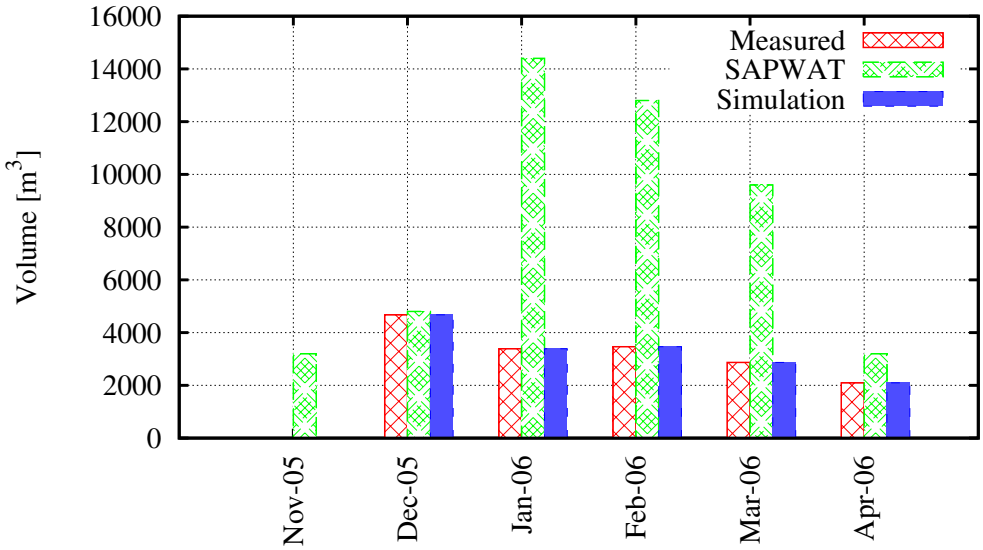

Figure C.63: Mandaryn measured, estimated and simulated water usage.

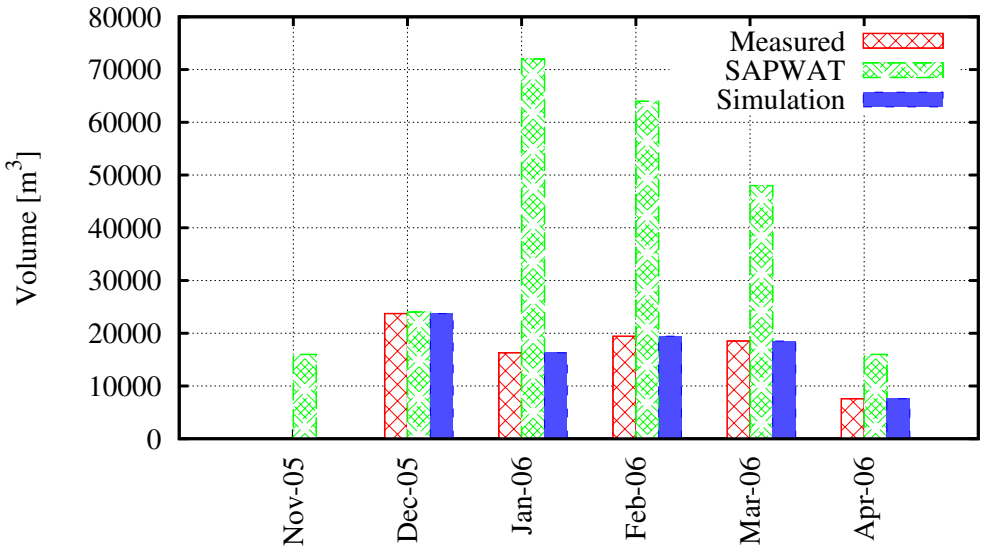

Figure C.64: De Pan measured, estimated and simulated water usage.

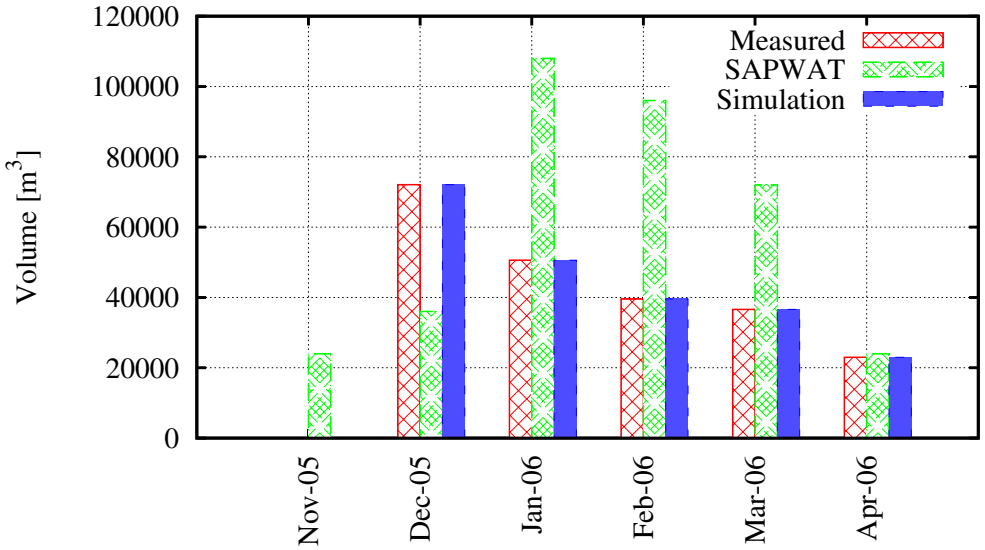

Figure C.65: Middelpunt measured, estimated and simulated water usage.

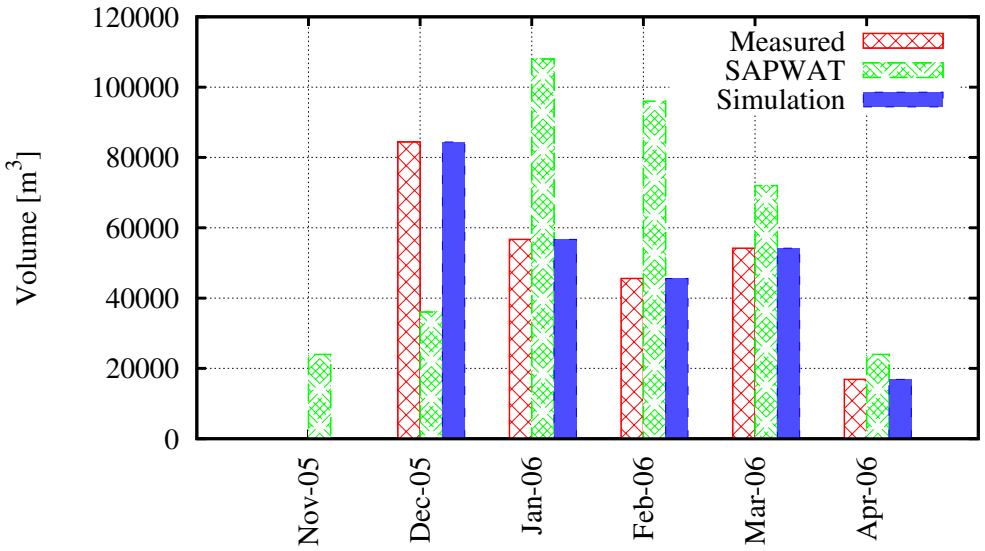

Figure C.66: Vater Erbe measured, estimated and simulated water usage.

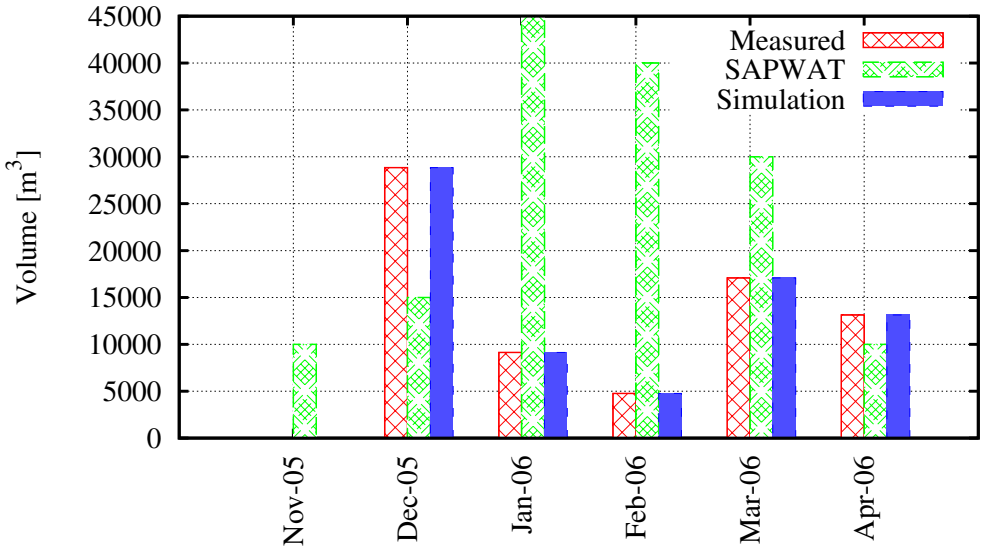

Figure C.67: Noordhoek measured, estimated and simulated water usage.

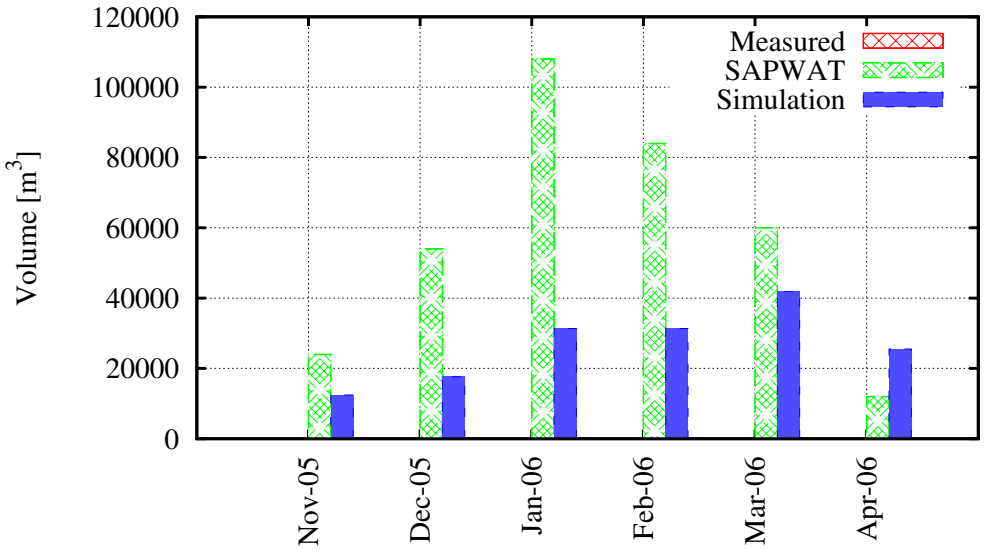

Figure C.68: Brakdam measured, estimated and simulated water usage.

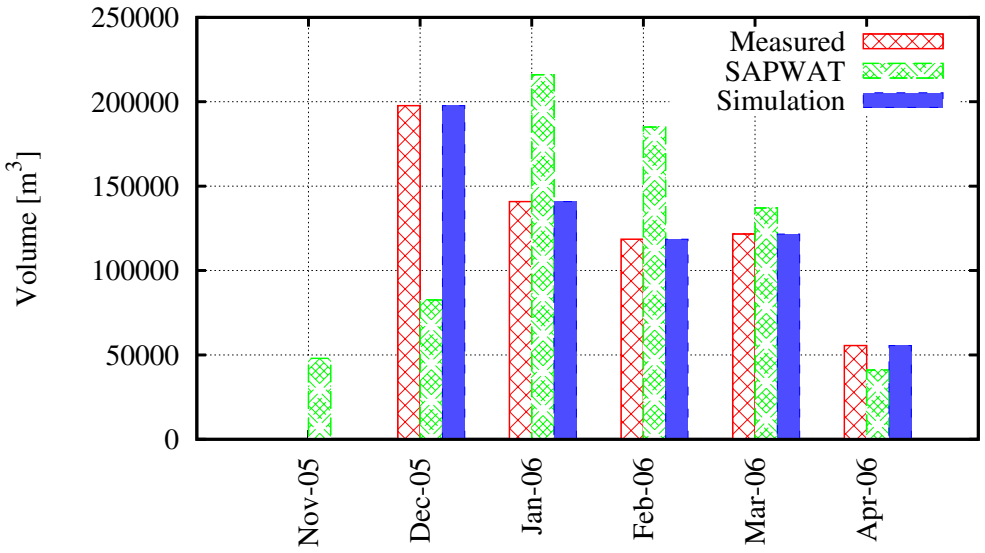

Figure C.69: Noordhoek (J. Groenewald) measured, estimated and simulated water usage.

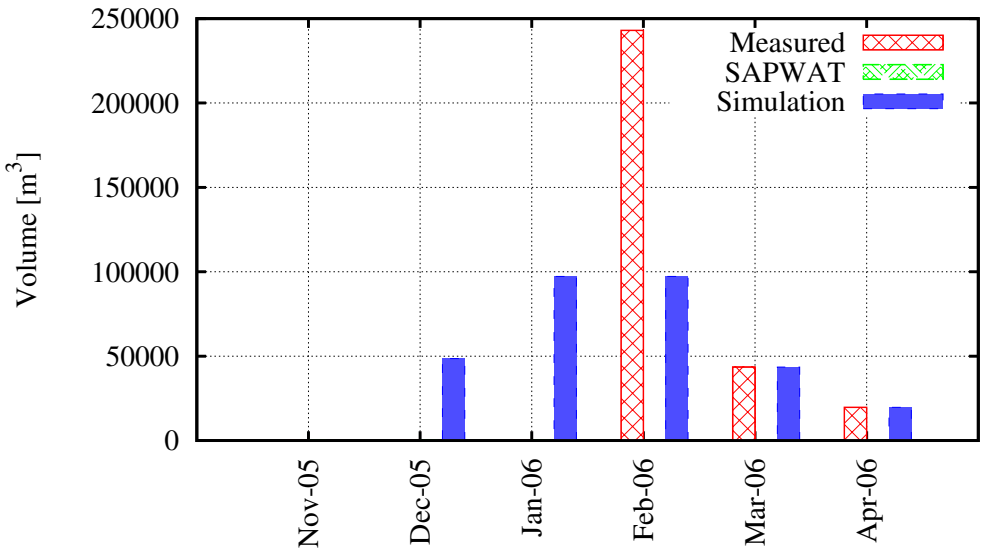

Figure C.70: Blydskap measured, estimated and simulated water usage.

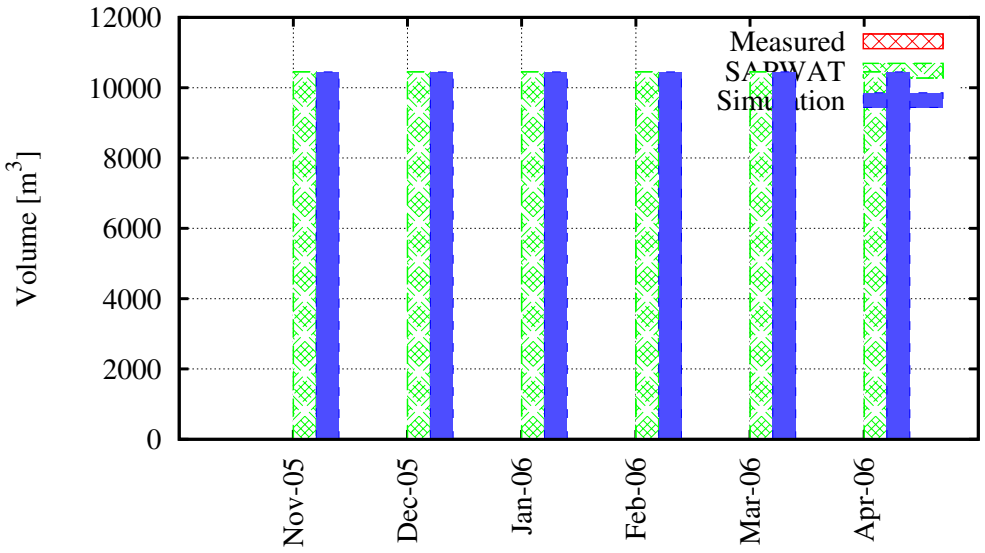

Figure C.71: TWK municipality measured, estimated and simulated water usage.

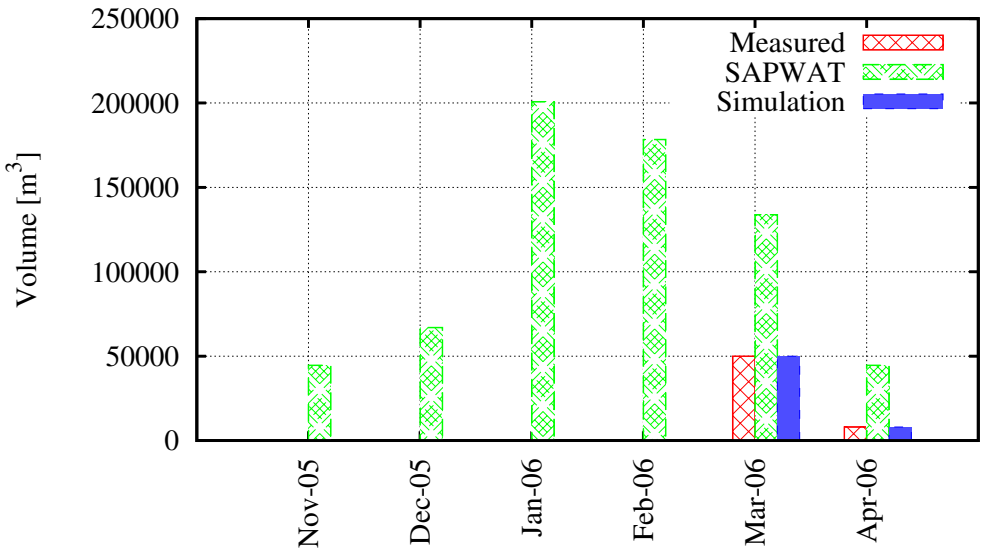

Figure C.72: Tygerhoek measured, estimated and simulated water usage.

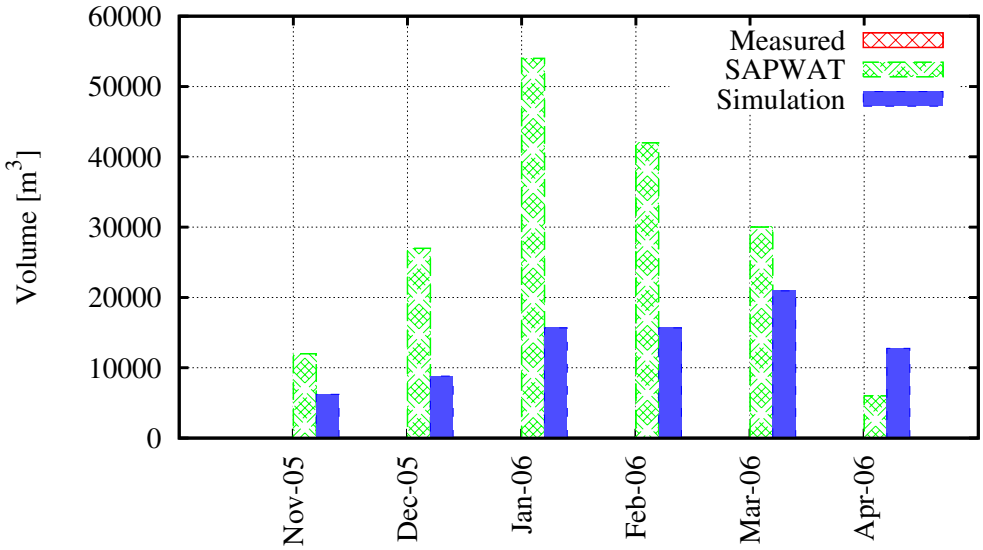

Figure C.73: Wijnberg measured, estimated and simulated water usage.

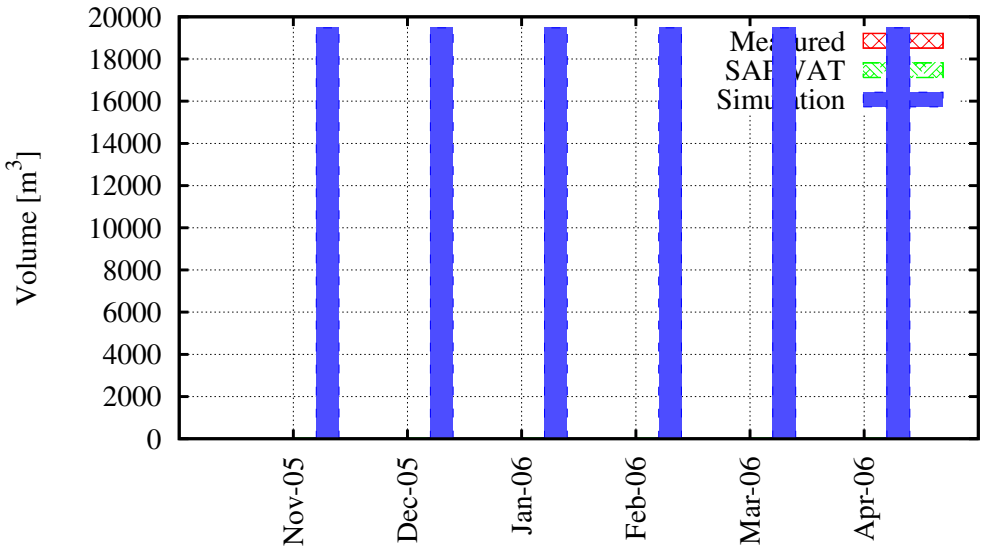

Figure C.74: Nitrophosca measured, estimated and simulated water usage.

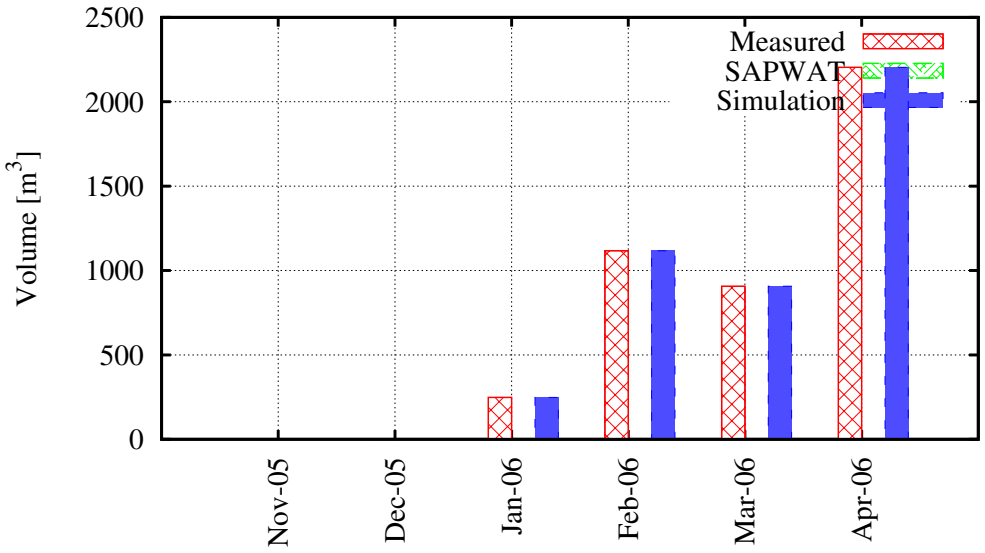

Figure C.75: Riviersonderend municipality measured, estimated and simulated water usage.

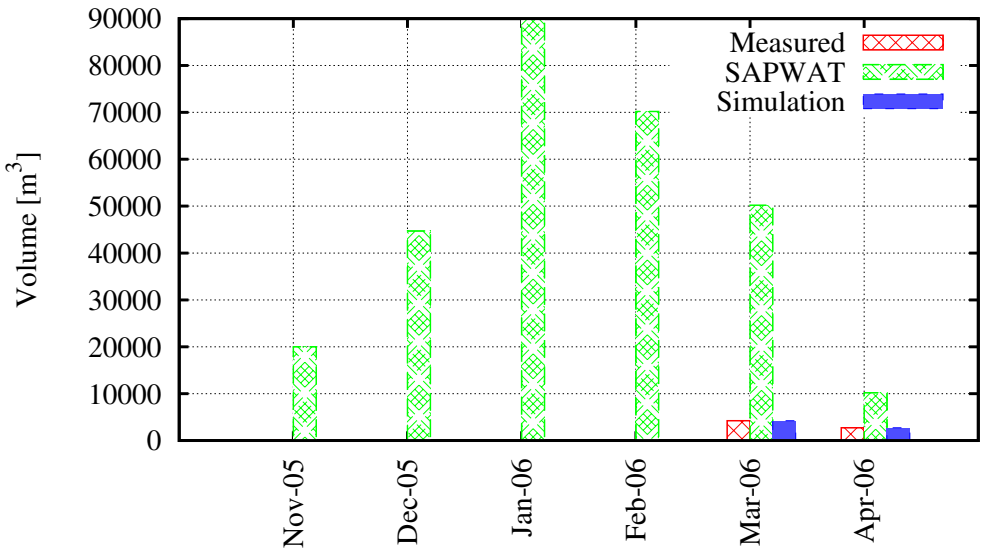

Figure C.76: Appelskraal measured, estimated and simulated water usage.

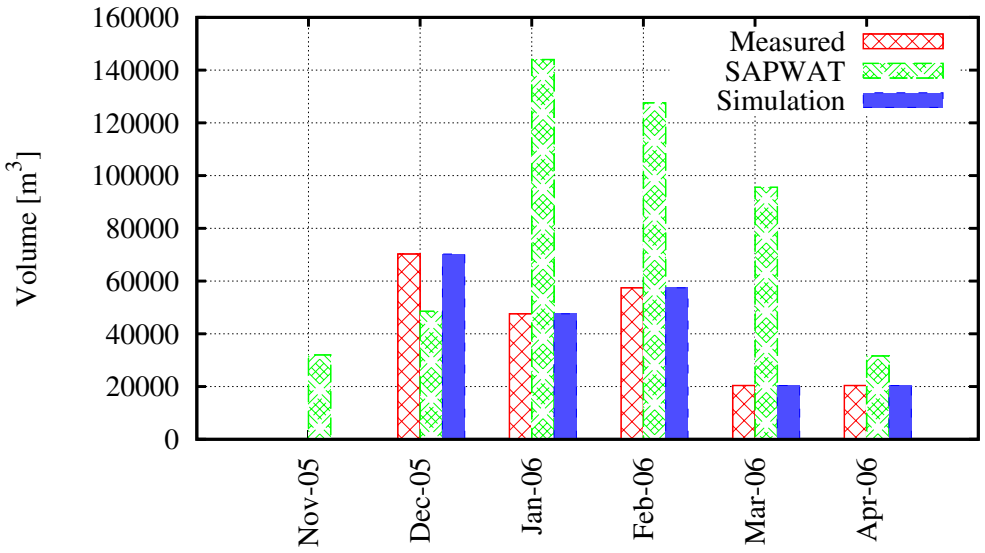

Figure C.77: Kleinlaagte measured, estimated and simulated water usage.

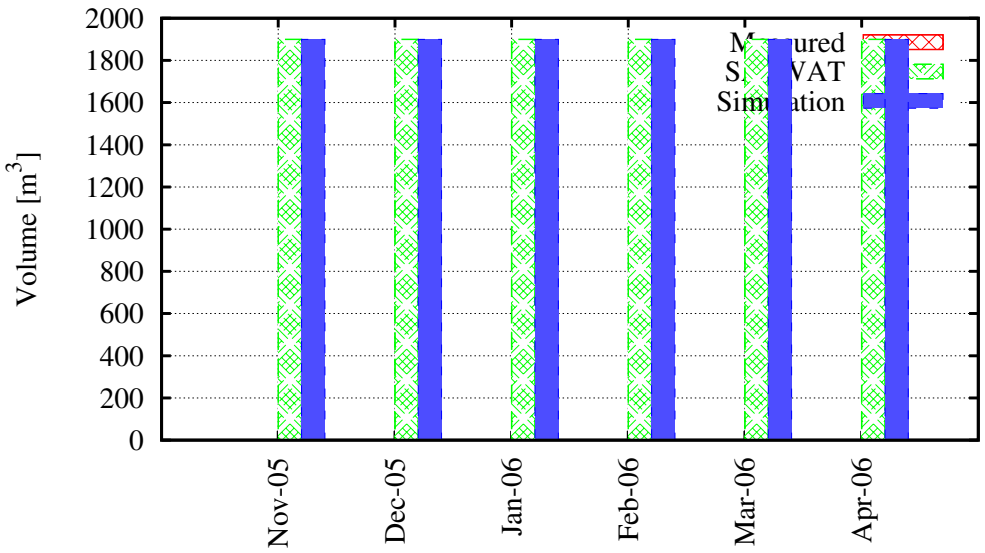

Figure C.78: Aloe Ravine Resort measured, estimated and simulated water usage.

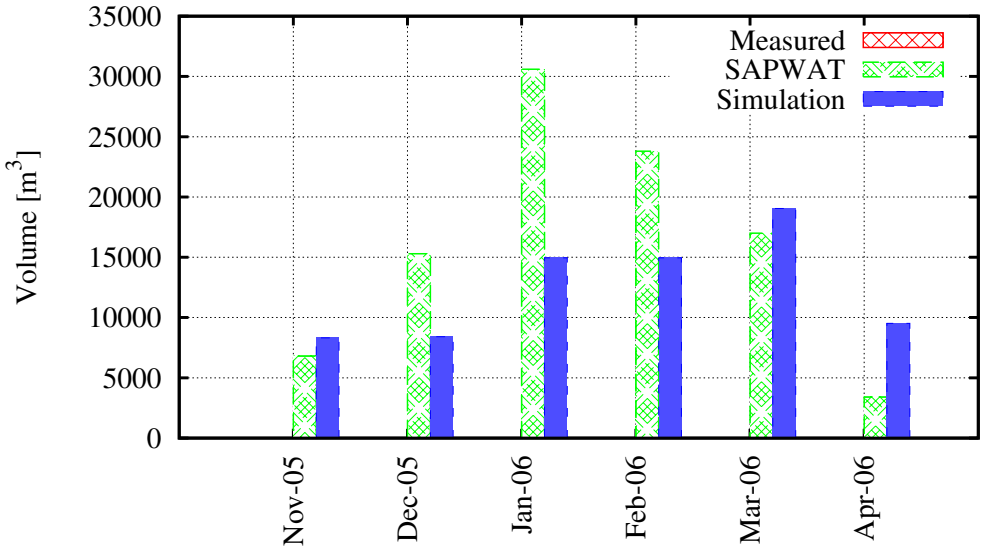

Figure C.79: A. Starke Trust measured, estimated and simulated water usage.

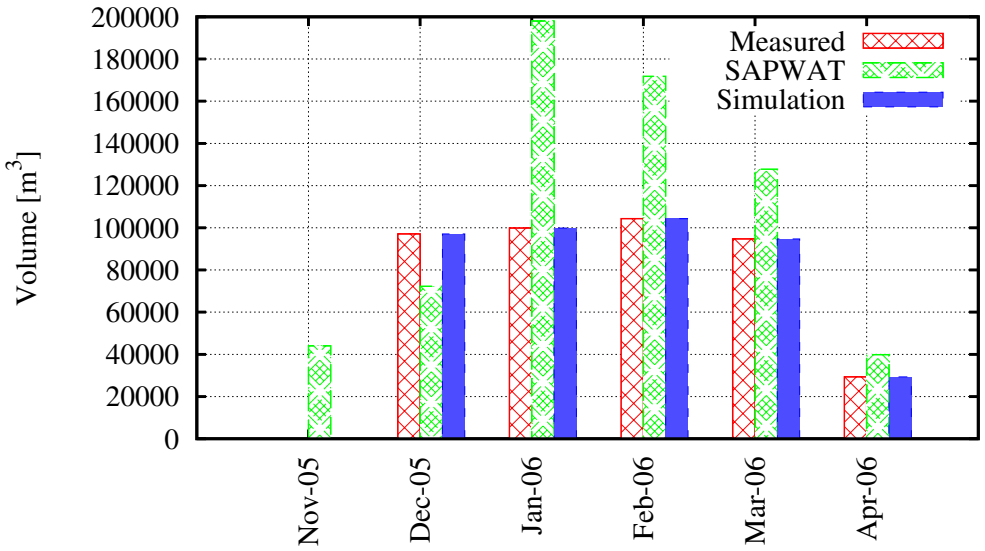

Figure C.80: Haelkraal measured, estimated and simulated water usage.

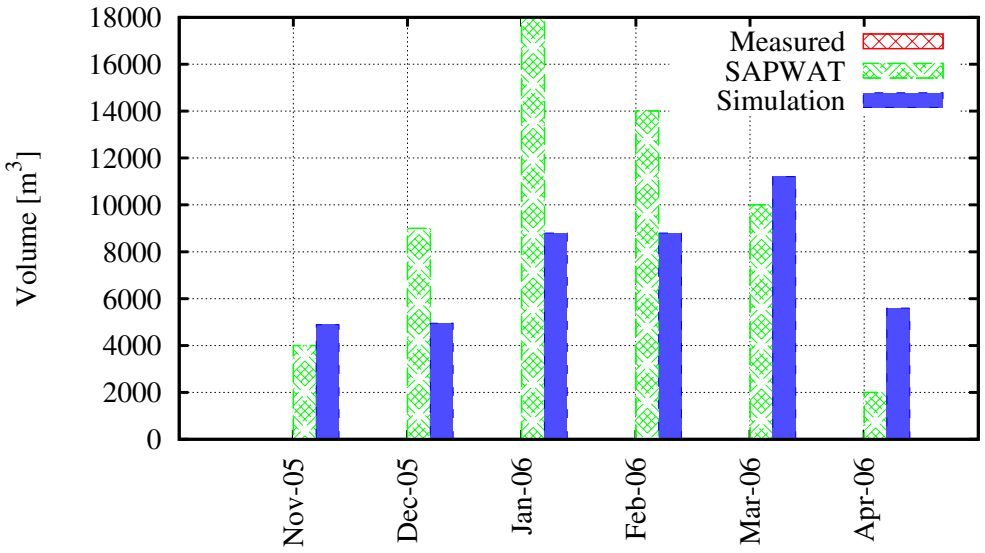

Figure C.81: Haelkraal (D. Human) measured, estimated and simulated water usage.

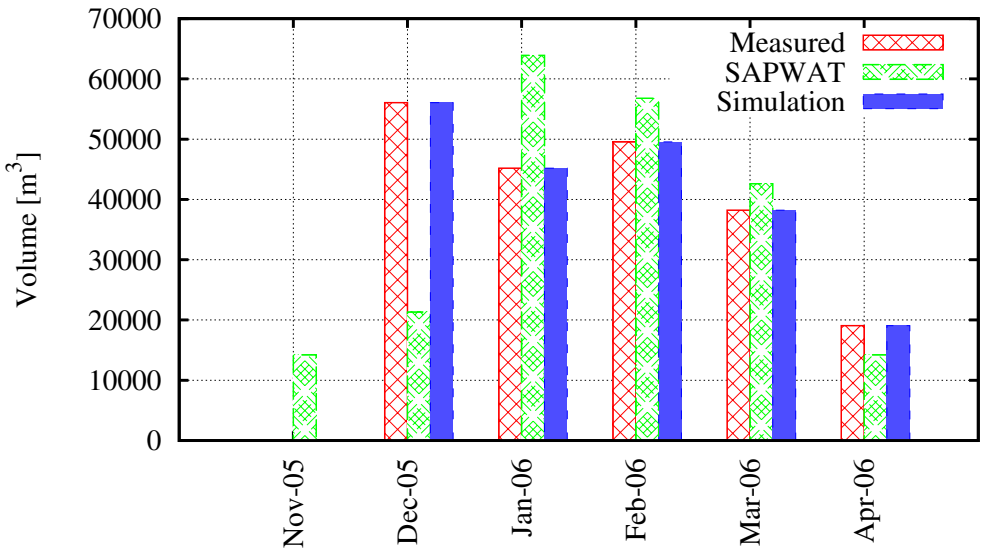

Figure C.82: Loch Lotus measured, estimated and simulated water usage.

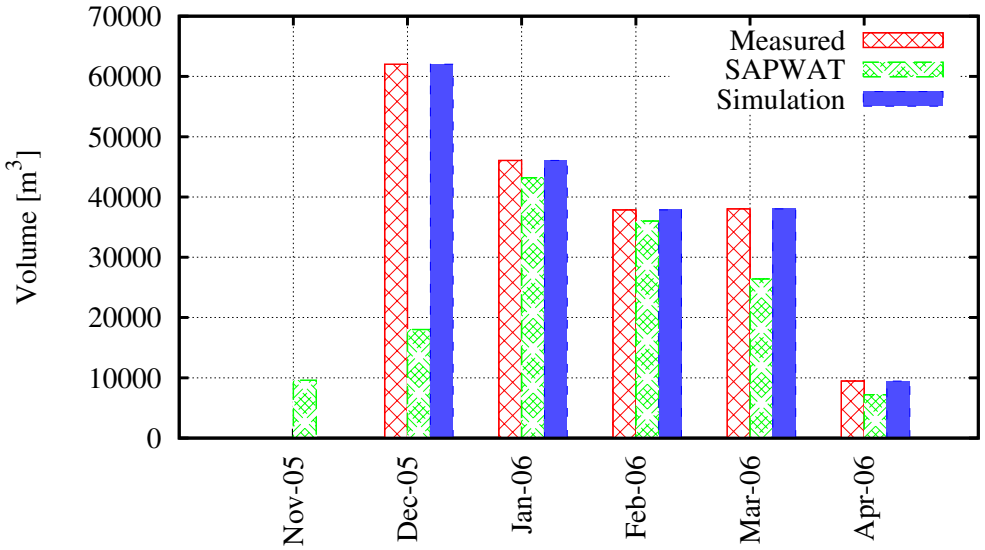

Figure C.83: Rustenburg measured, estimated and simulated water usage.

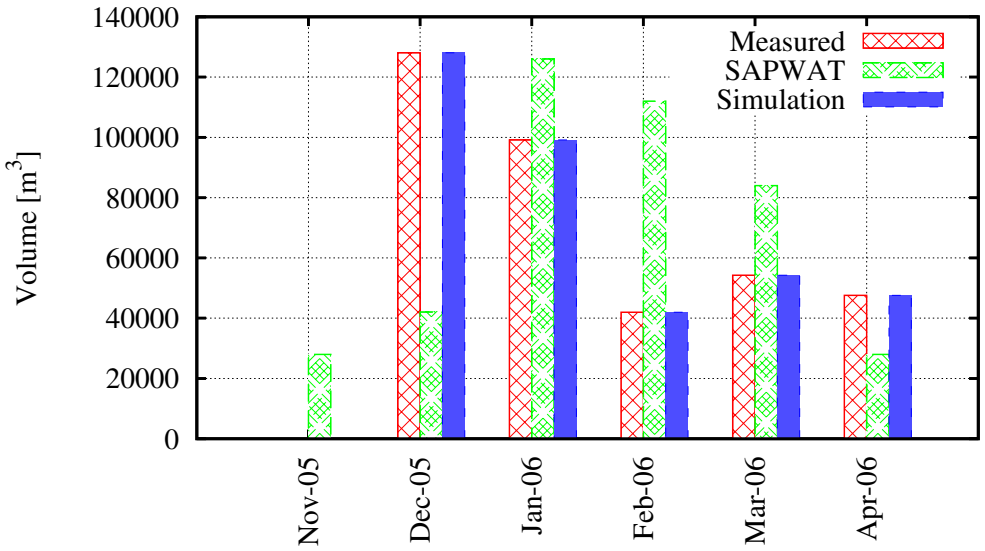

Figure C.84: Grootvlakte measured, estimated and simulated water usage.

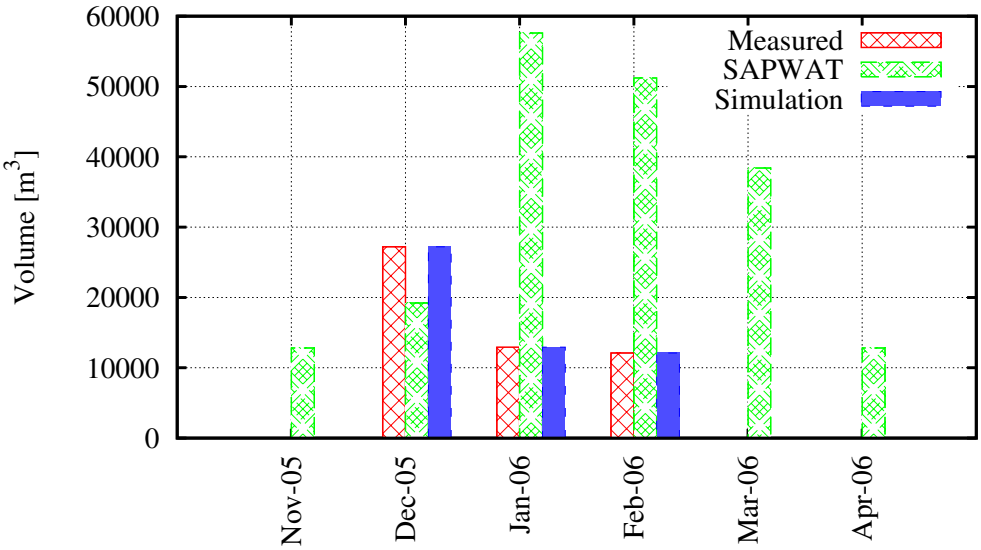

Figure C.85: Ongegund measured, estimated and simulated water usage.

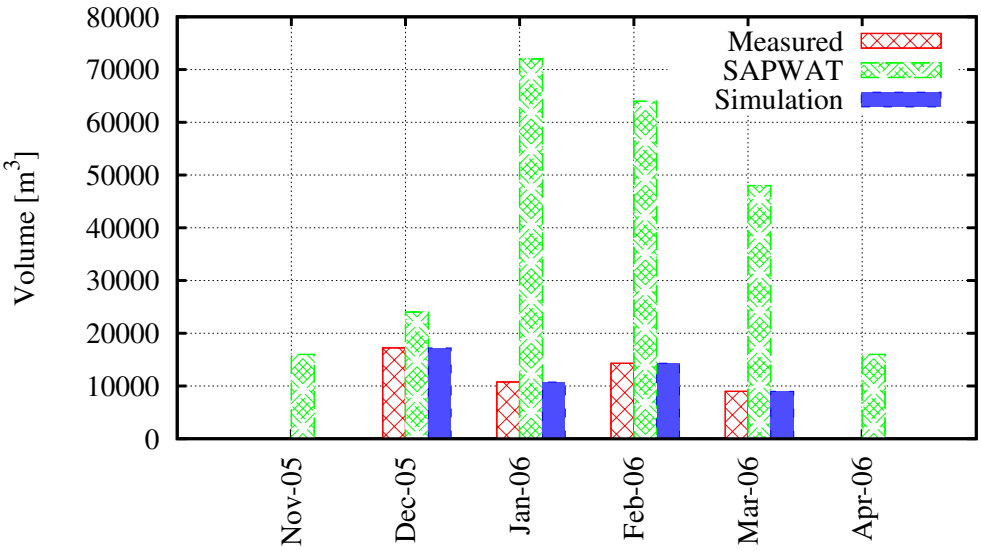

Figure C.86: Tevrede measured, estimated and simulated water usage.

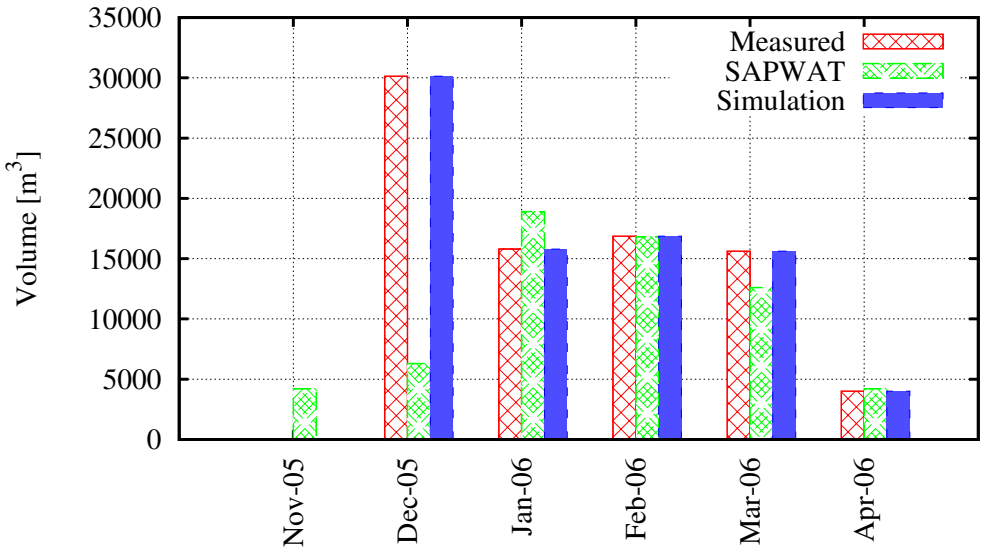

Figure C.87: Van der Watts Kraal 1 measured, estimated and simulated water usage.

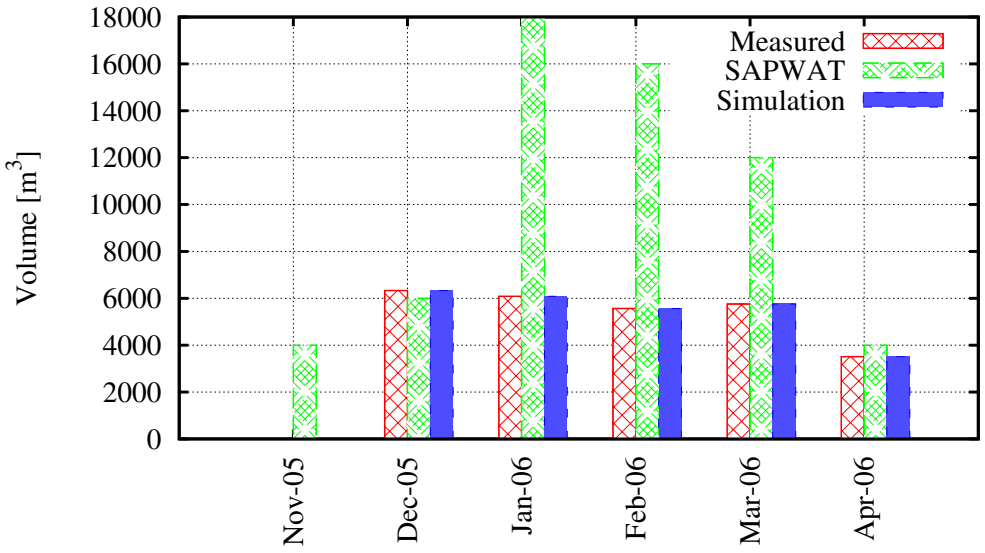

Figure C.88: Van der Watts Kraal 2 measured, estimated and simulated water usage.

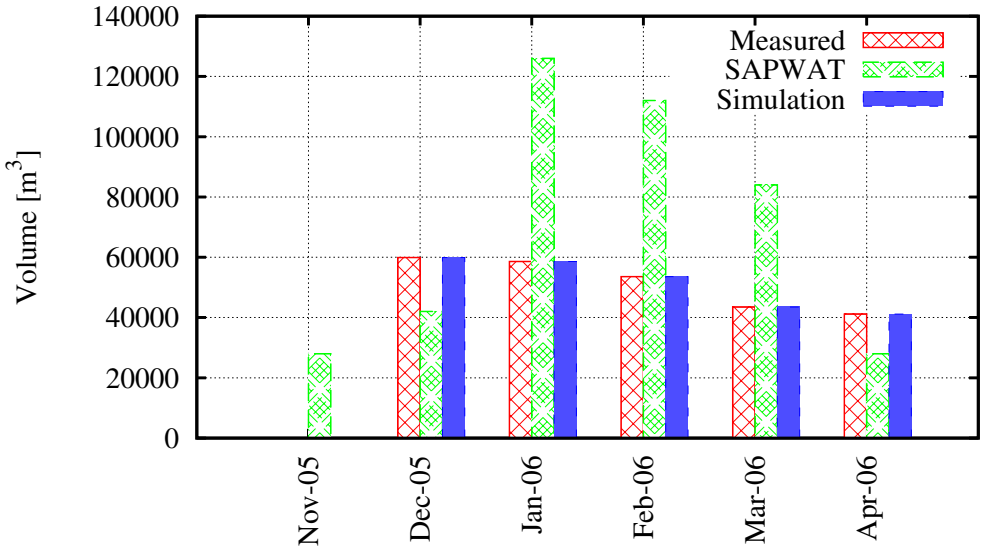

Figure C.89: Sangasdrift measured, estimated and simulated water usage.

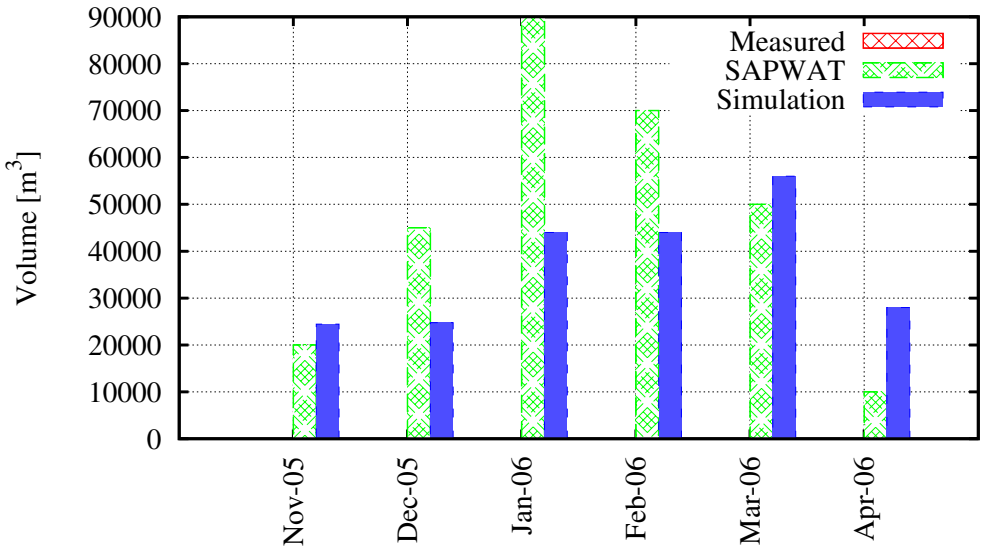

Figure C.90: Van Dyk Trust measured, estimated and simulated water usage.

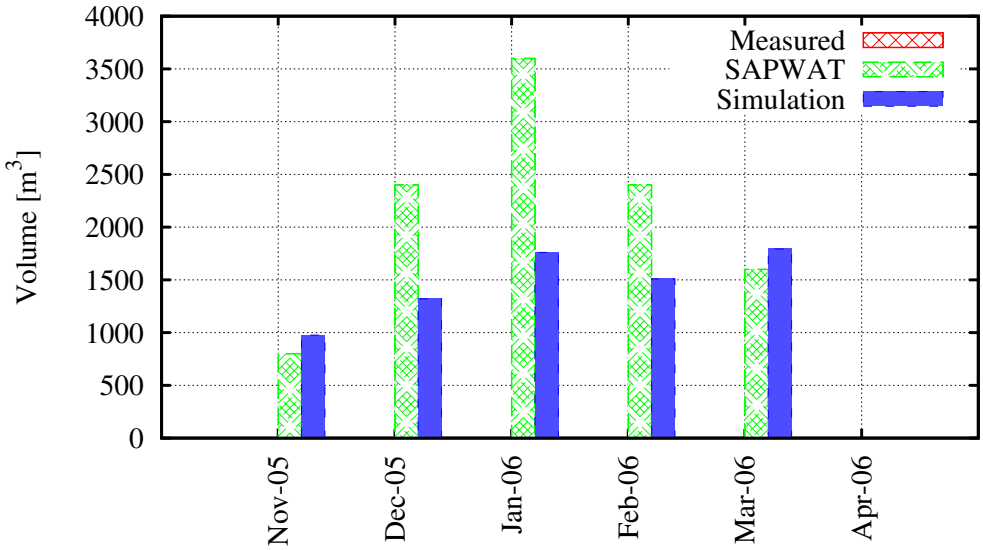

Figure C.91: S.W. Viljoen measured, estimated and simulated water usage.

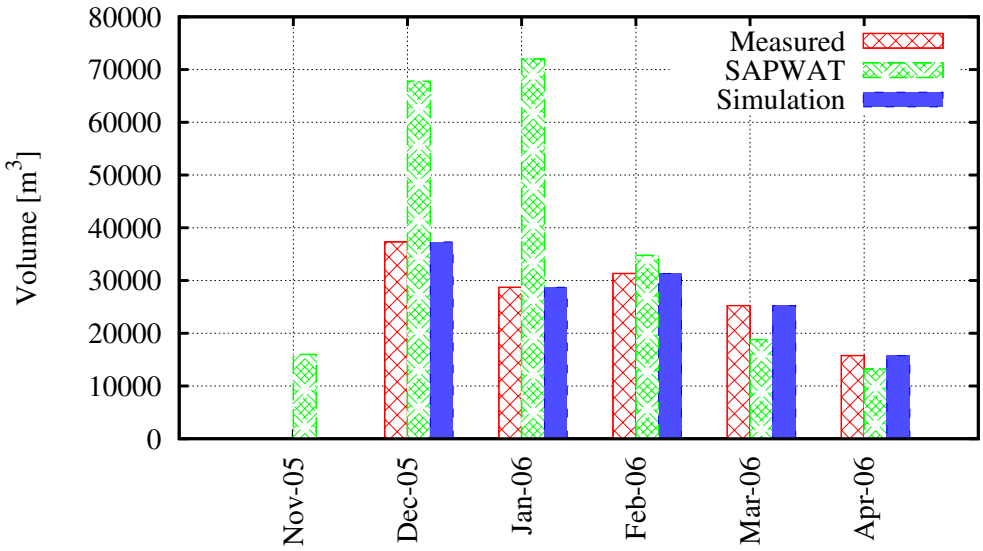

Figure C.92: Avontuur measured, estimated and simulated water usage.

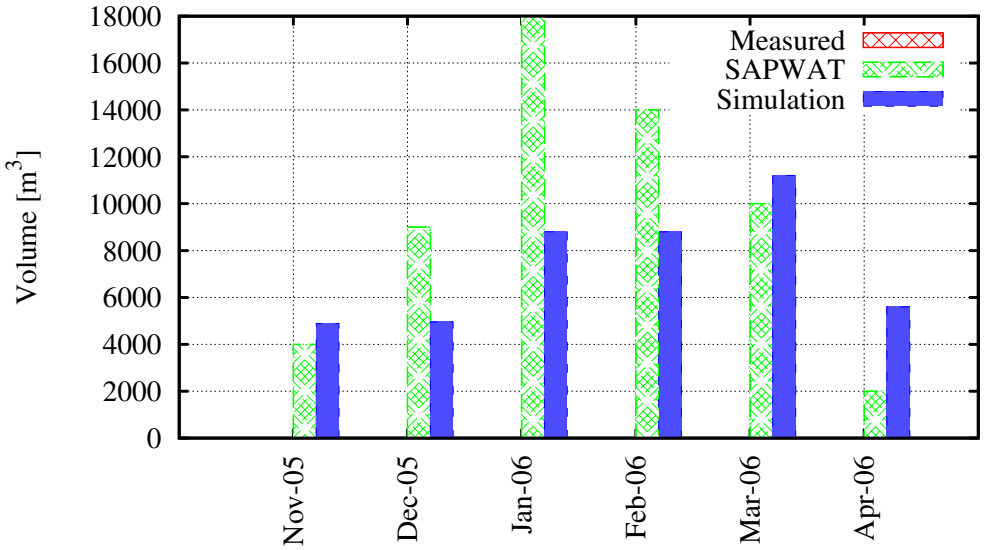

Figure C.93: Fletchers Trust measured, estimated and simulated water usage.

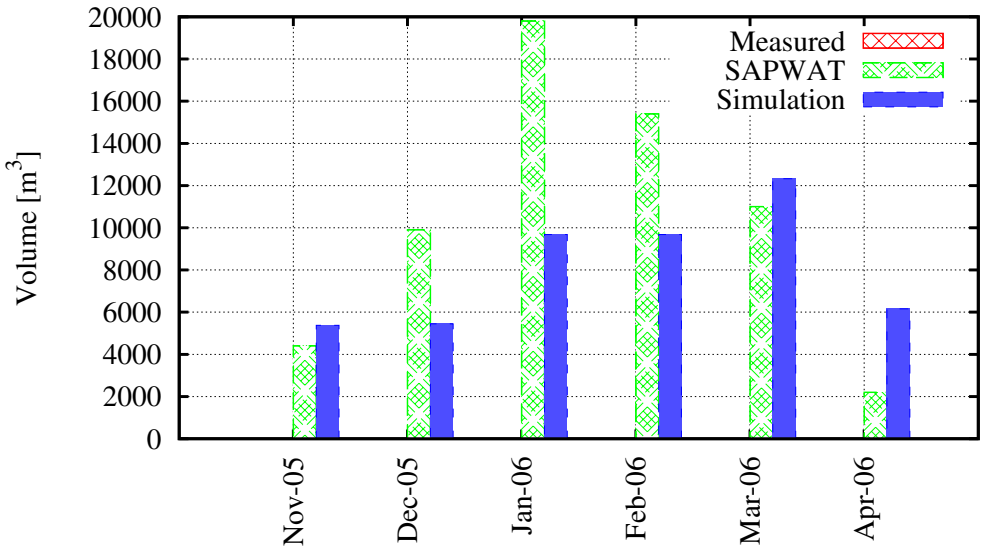

Figure C.94: D.B. Froneman measured, estimated and simulated water usage.

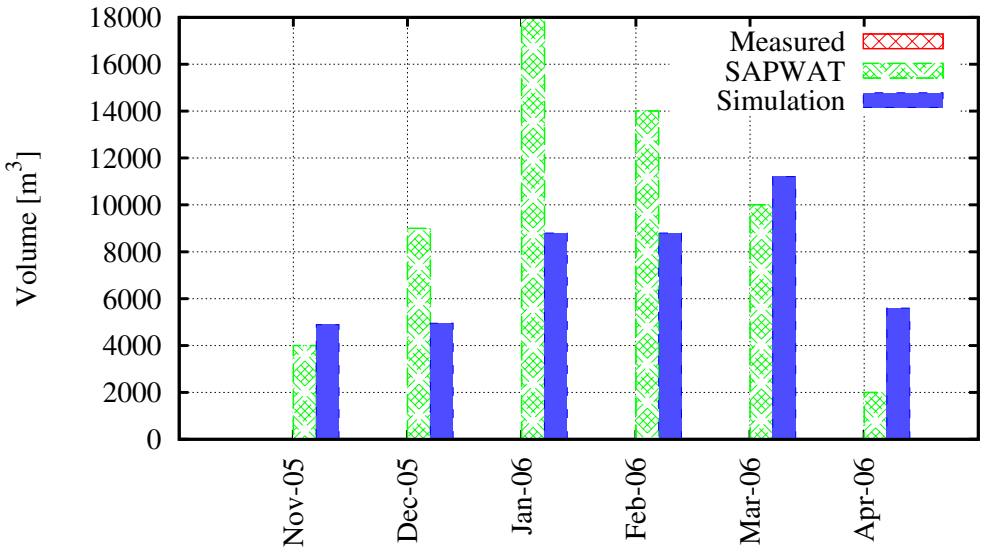

Figure C.95: J.P. O'Connel Trust measured, estimated and simulated water usage.

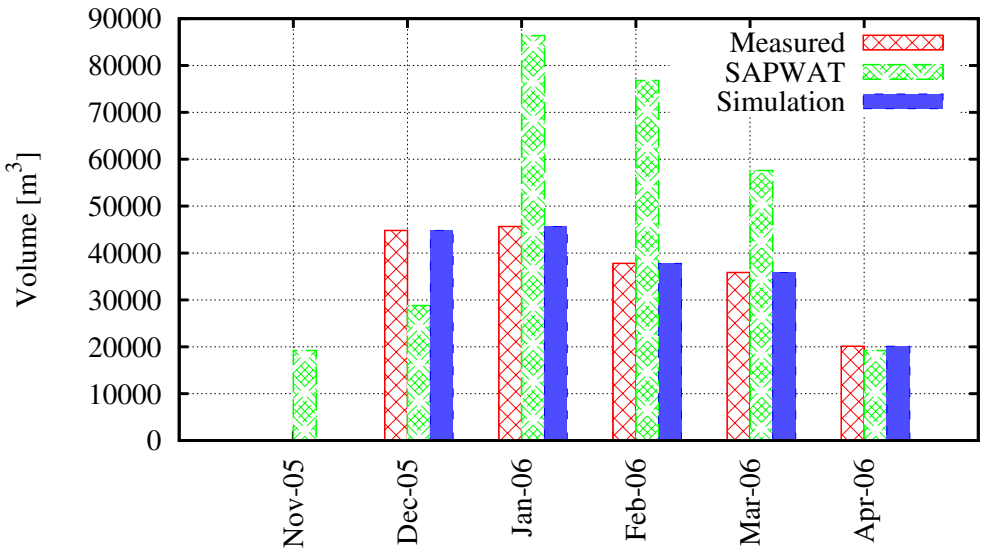

Figure C.96: Avontuur measured, estimated and simulated water usage.

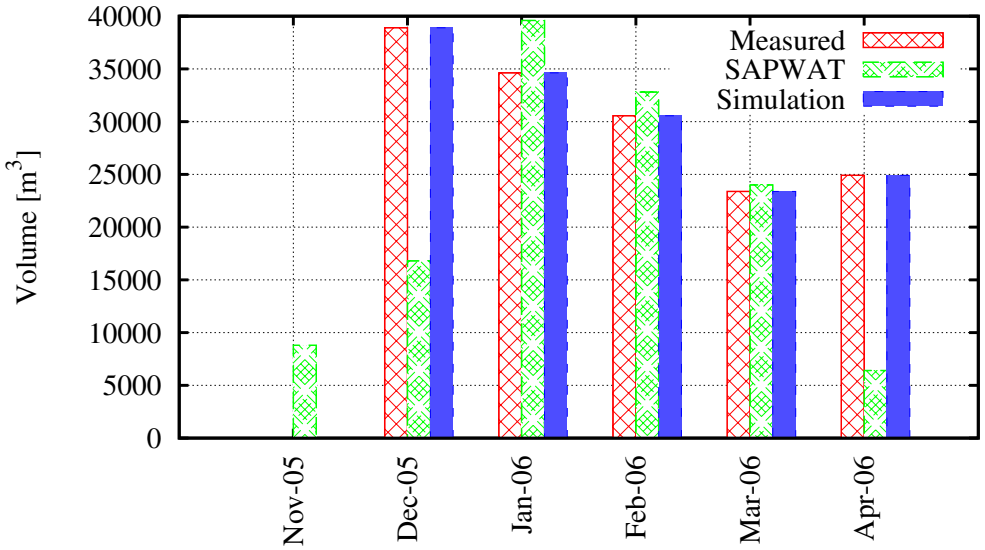

Figure C.97: Stormvlei Hotel measured, estimated and simulated water usage.

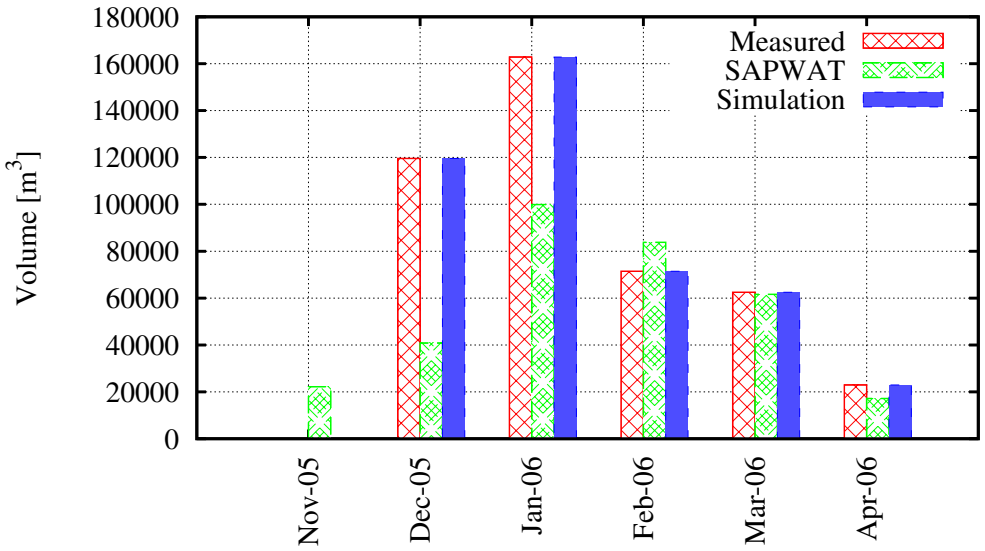

Figure C.98: Doornkloof measured, estimated and simulated water usage.

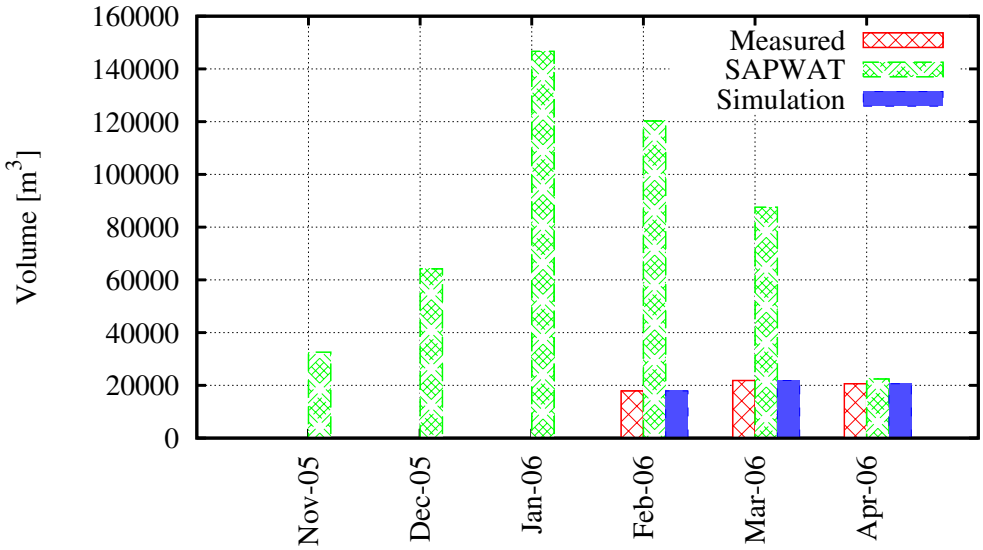

Figure C.99: Rheenen measured, estimated and simulated water usage.

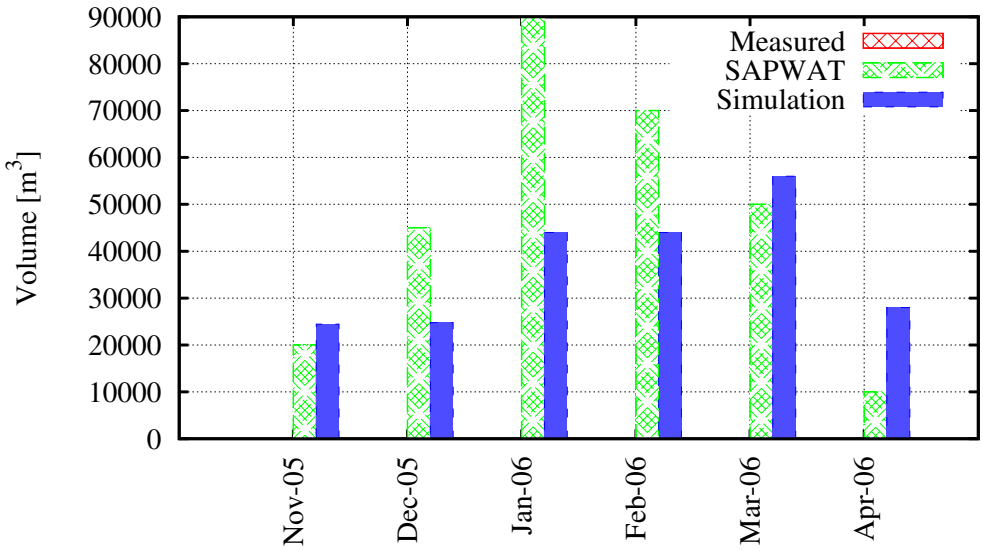

Figure C.100: Enrico Beyers measured, estimated and simulated water usage.

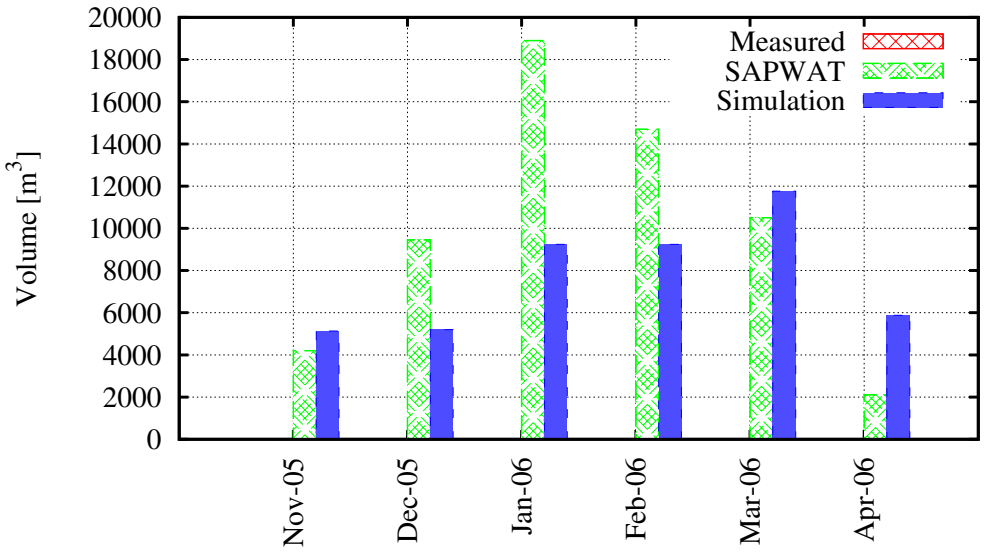

Figure C.101: Astralita measured, estimated and simulated water usage.

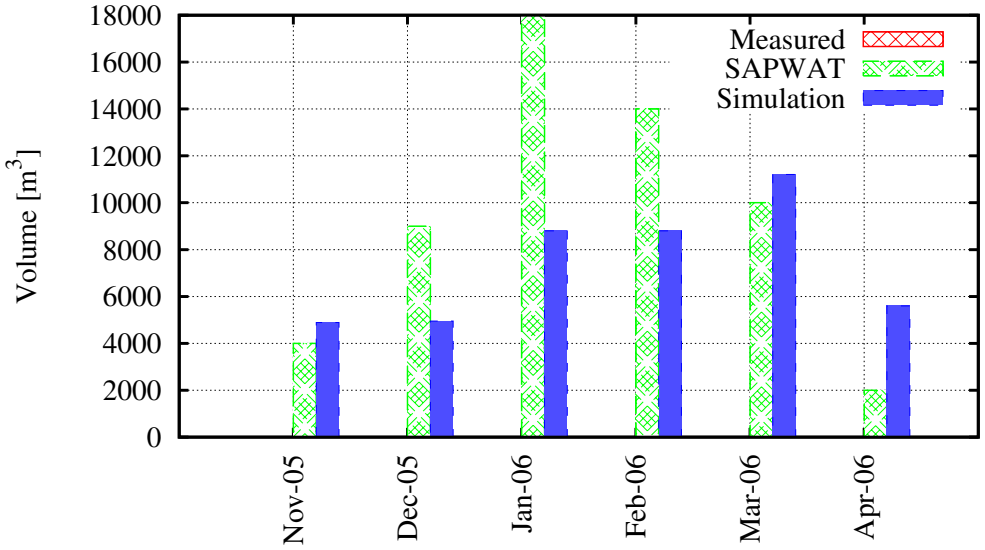

Figure C.102: E. van As/Streicher measured, estimated and simulated water usage.

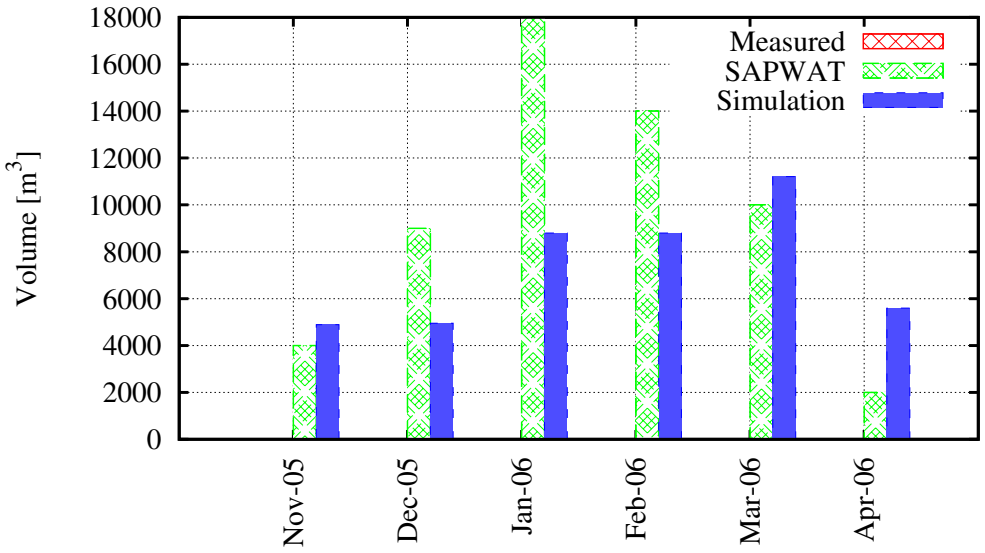

Figure C.103: S.W. Viljoen Trust measured, estimated and simulated water usage.

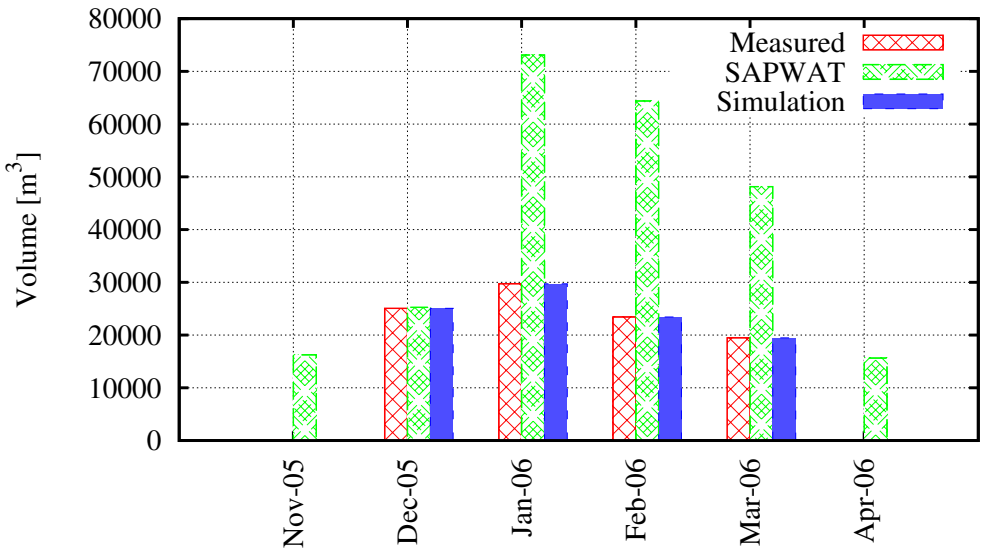

Figure C.104: Rheenen measured, estimated and simulated water usage.

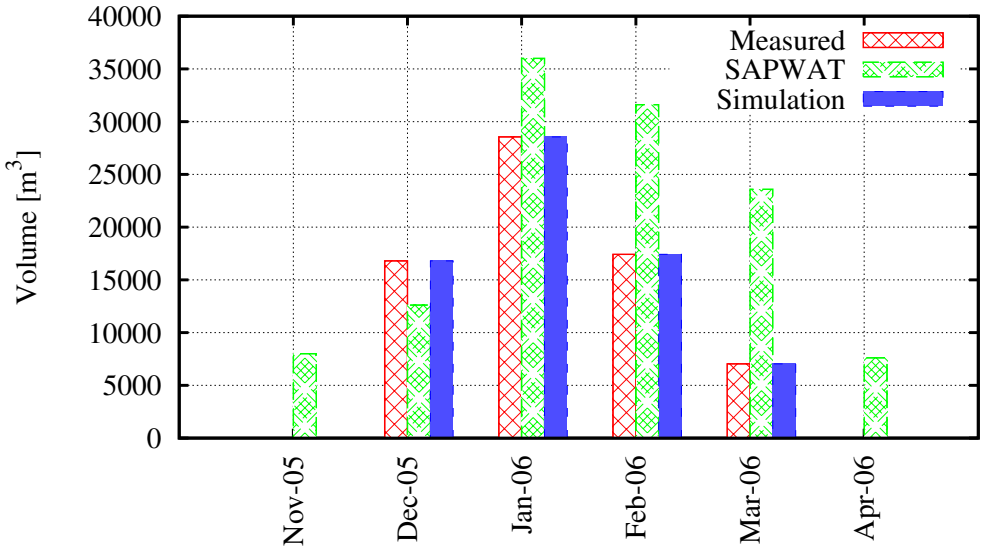

Figure C.105: Kwasarie measured, estimated and simulated water usage.

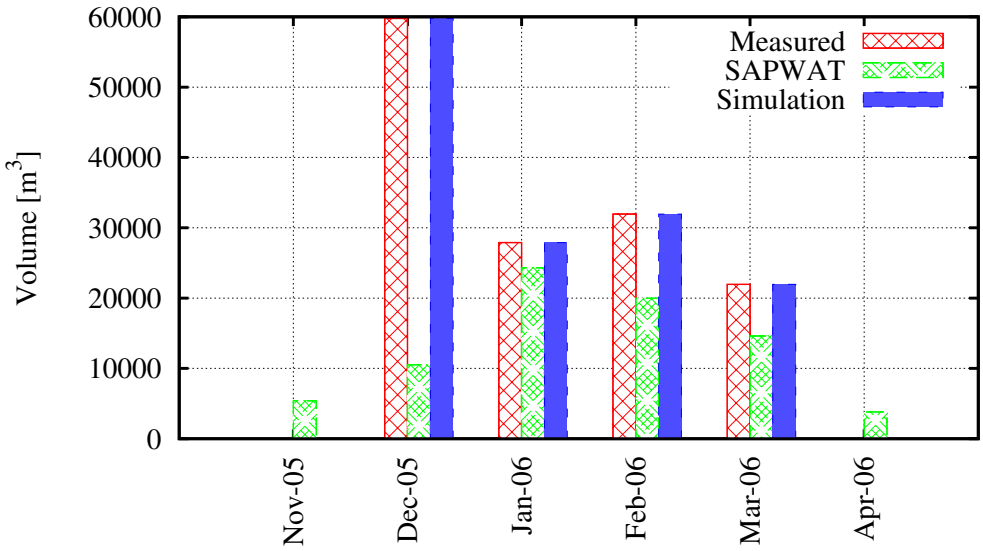

Figure C.106: Bromberg measured, estimated and simulated water usage.

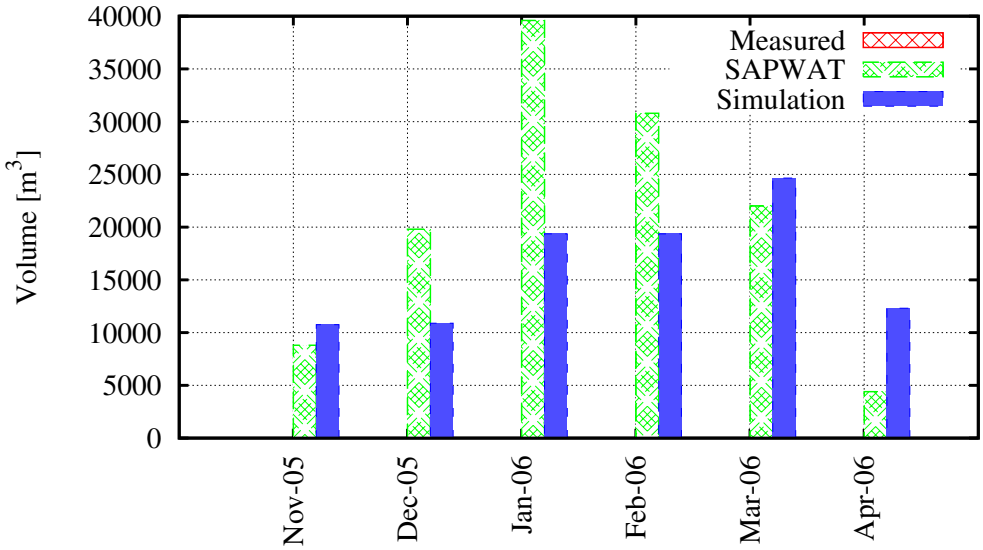

Figure C.107: Tradervail measured, estimated and simulated water usage.

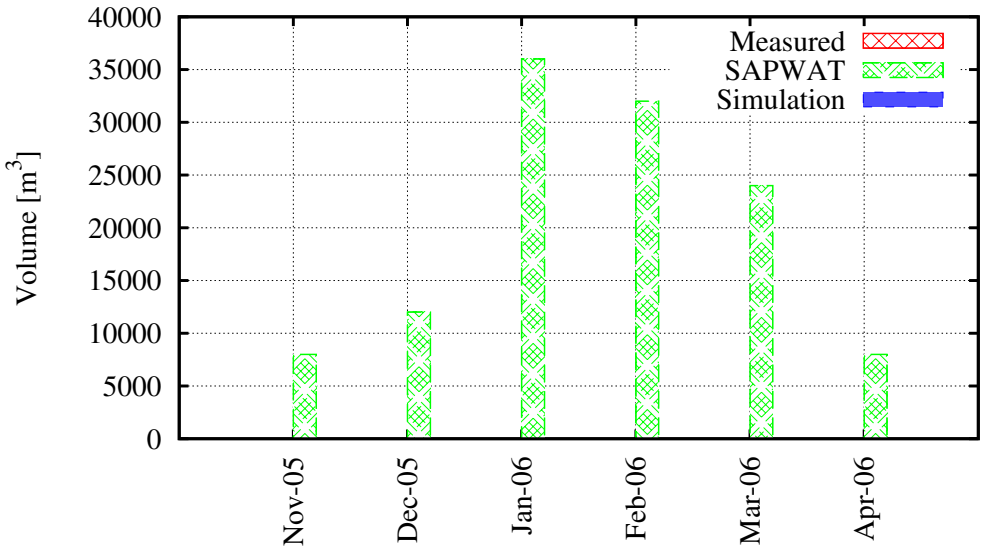

Figure C.108: Klipfontein 1 measured, estimated and simulated water usage.

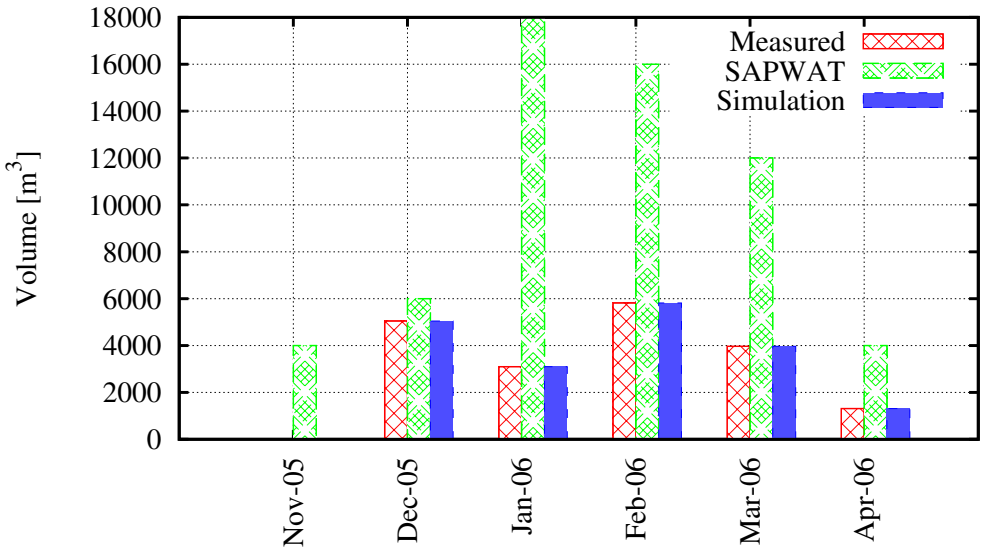

Figure C.109: Geminag measured, estimated and simulated water usage.

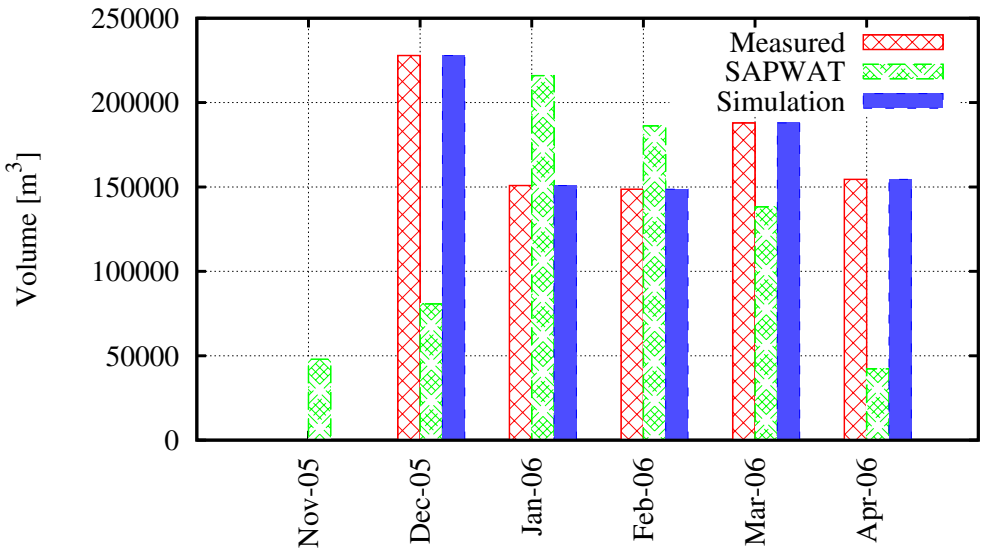

Figure C.110: Vaandrightsdrift 1 measured, estimated and simulated water usage.

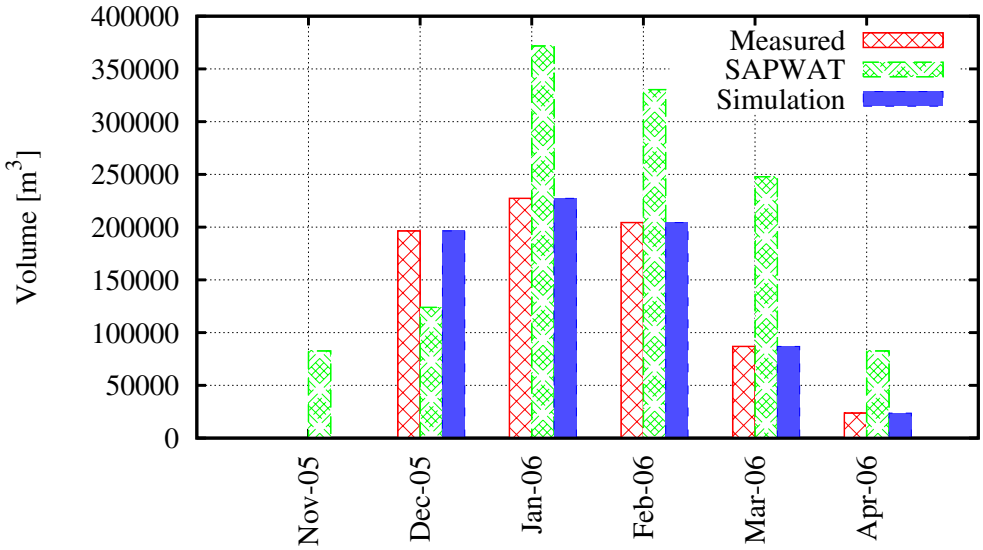

Figure C.111: Klipfontein 2 measured, estimated and simulated water usage.

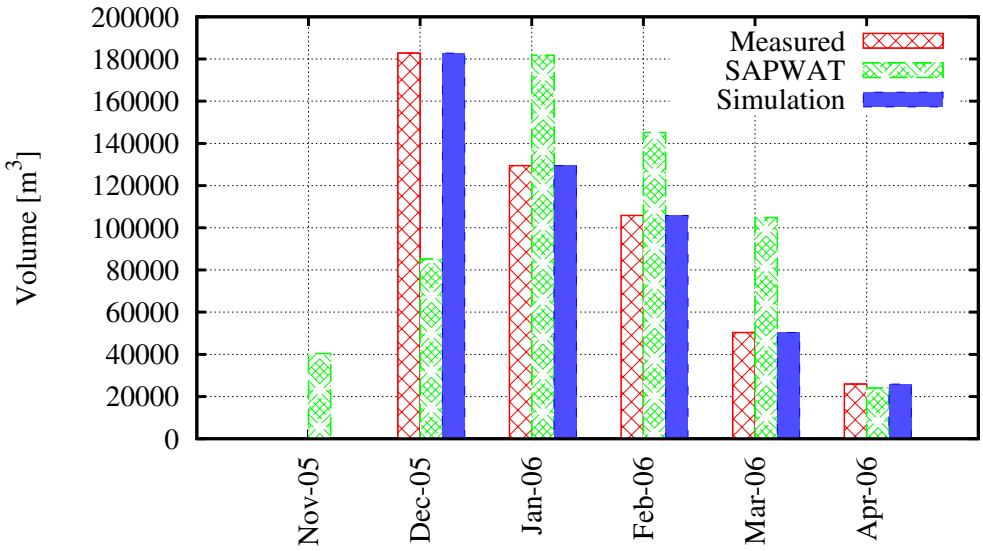

Figure C.112: Merweda measured, estimated and simulated water usage.

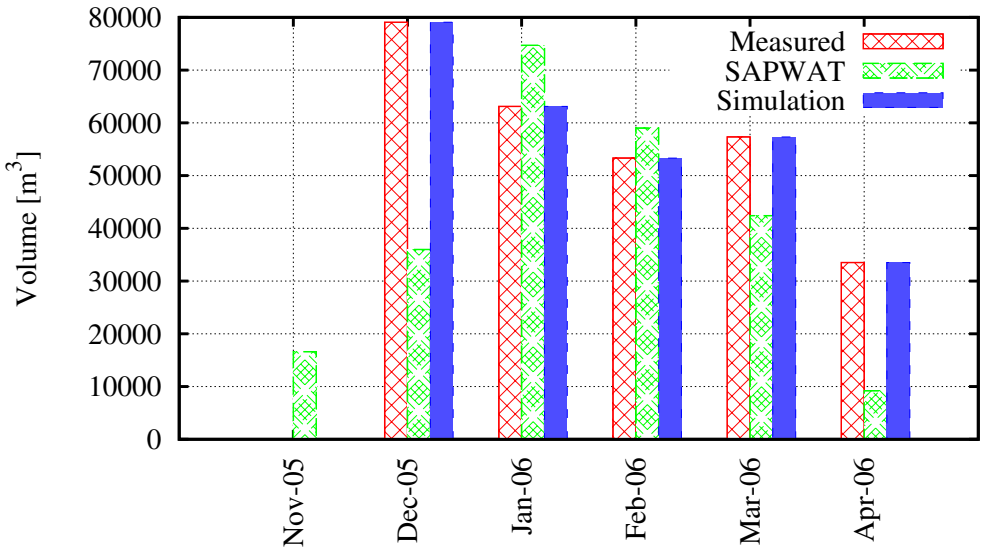

Figure C.113: Vaandrightsdrift 2 measured, estimated and simulated water usage.

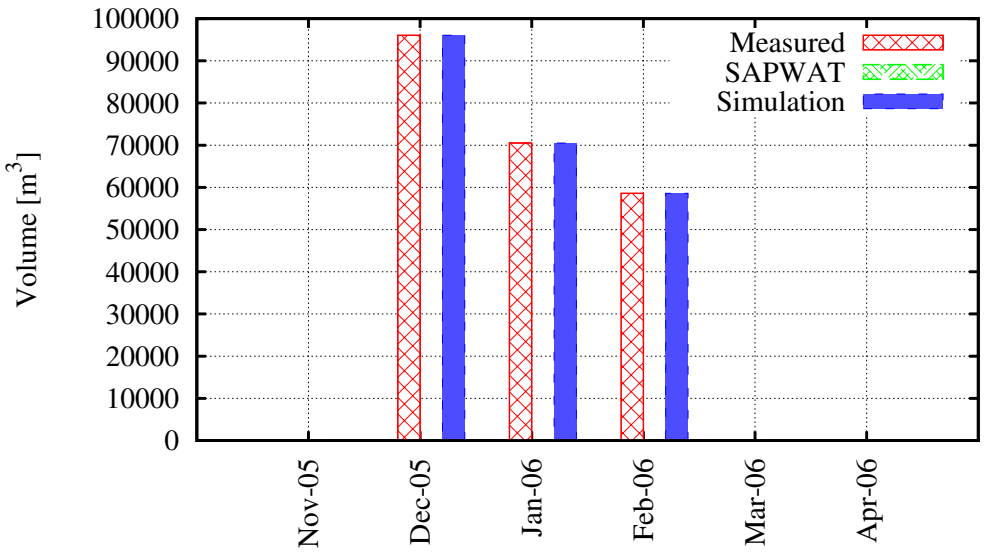

Figure C.114: Robyn measured, estimated and simulated water usage.

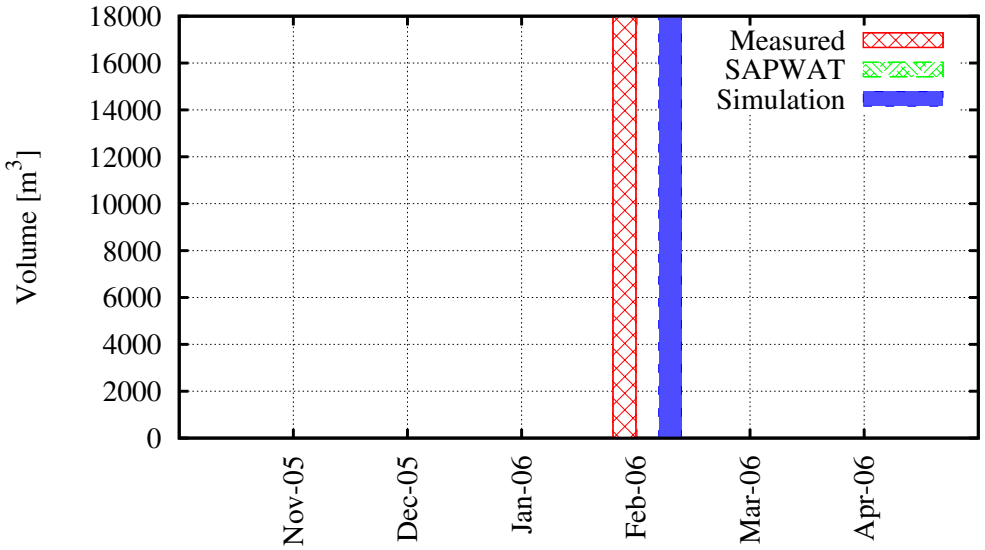

Figure C.115: Ruensveld Oos measured, estimated and simulated water usage.

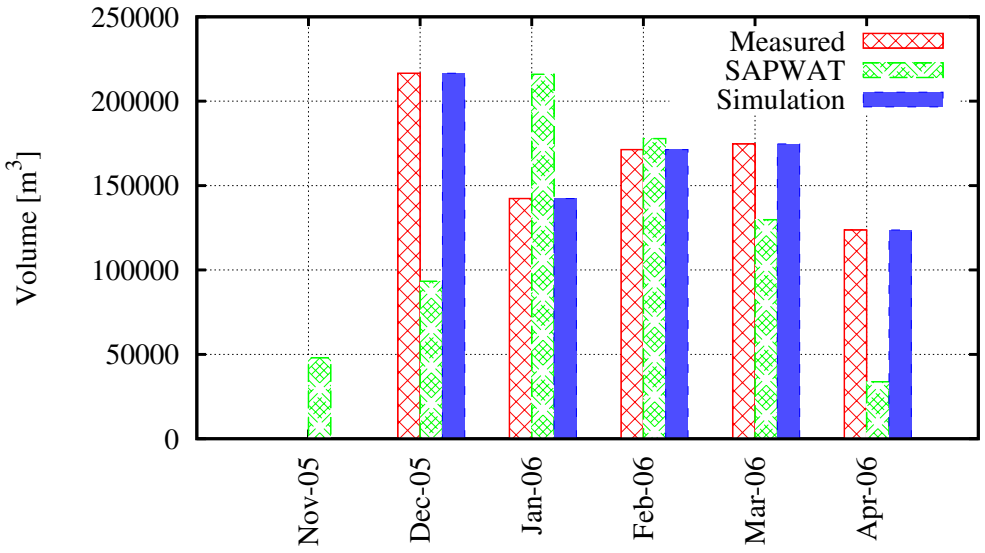

Figure C.116: Pleasant View measured, estimated and simulated water usage.

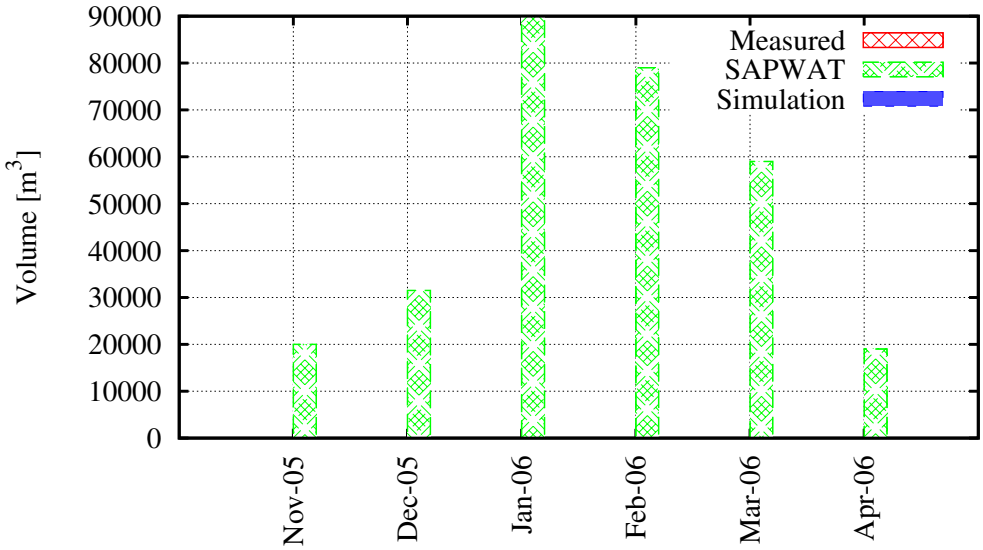

Figure C.117: Riviera measured, estimated and simulated water usage.

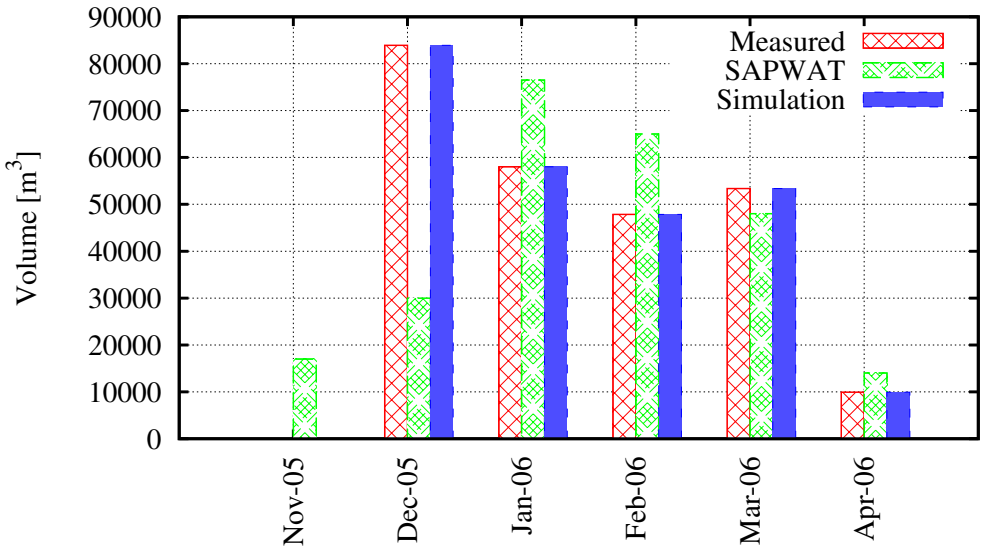

Figure C.118: Jubileeskraal measured, estimated and simulated water usage.

Appendix D

Mike 11 NAM Tributary Flow Simulation Results

D.1 2006-2007 Irrigation Season

The results are illustrated for the 27 tributaries along the Riviersonderend River, see figure D.1-D.19.

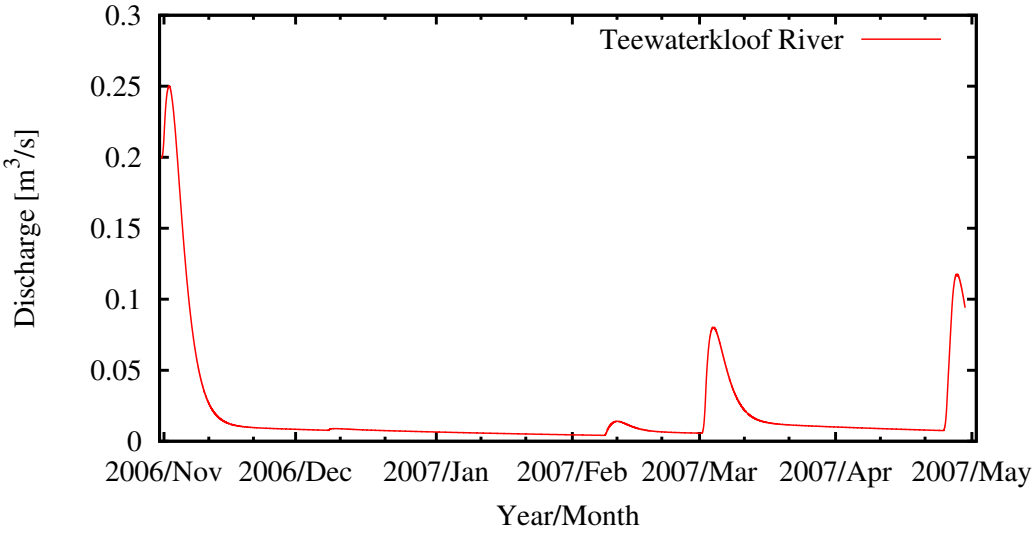

Figure D.1: Catchment A hydrograph for 2006.

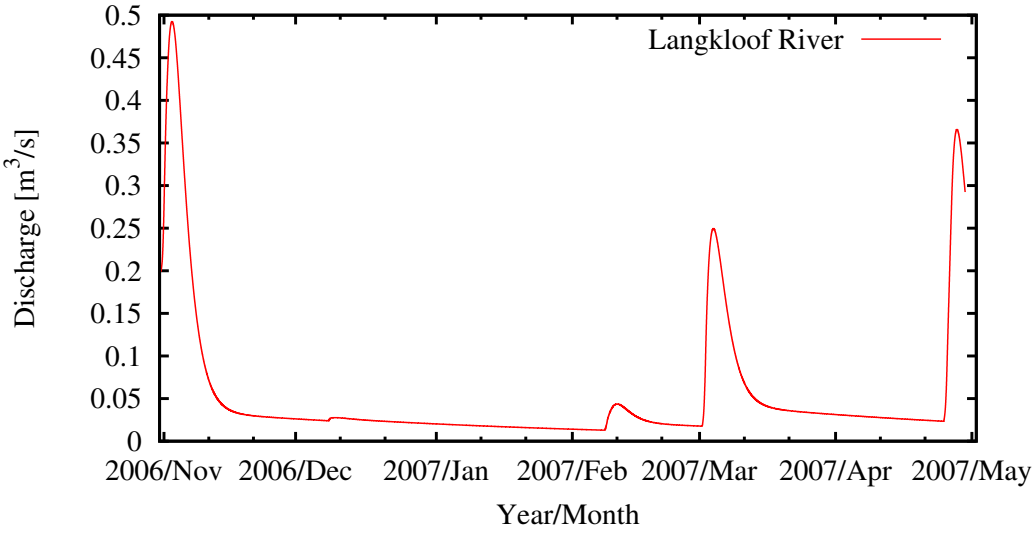

Figure D.2: Catchment B hydrograph for 2006.

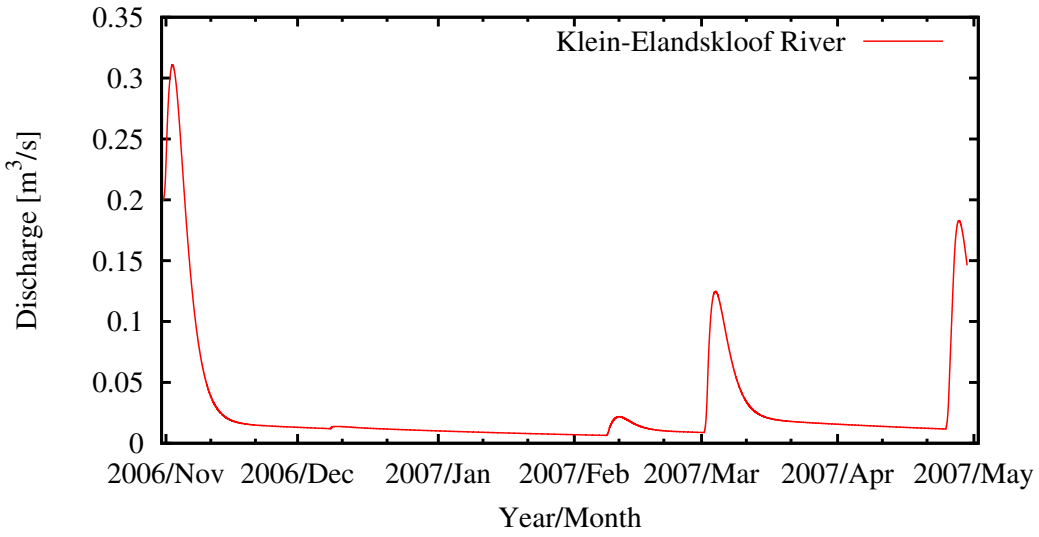

Figure D.3: Catchment C hydrograph for 2006.

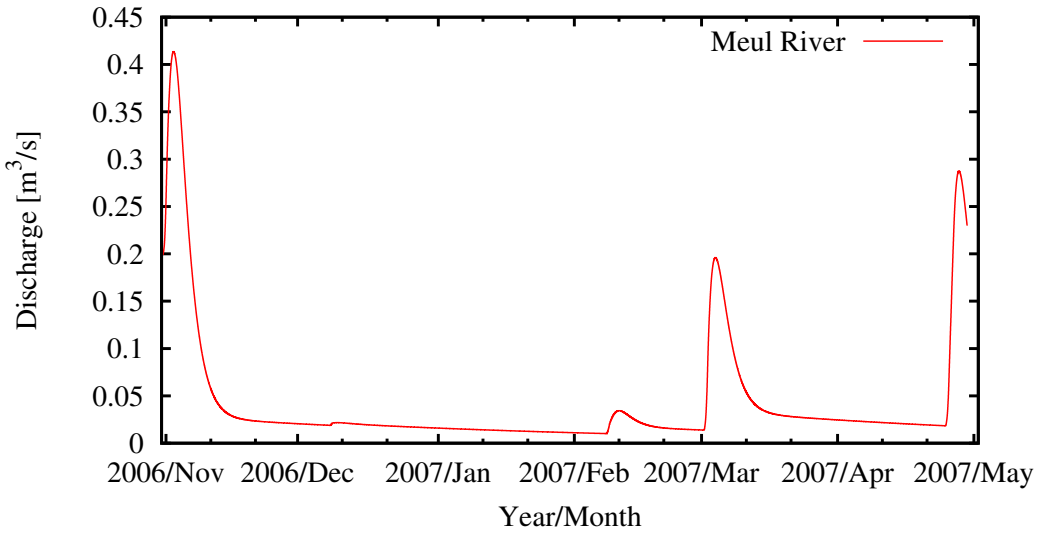

Figure D.4: Catchment D hydrograph for 2006.

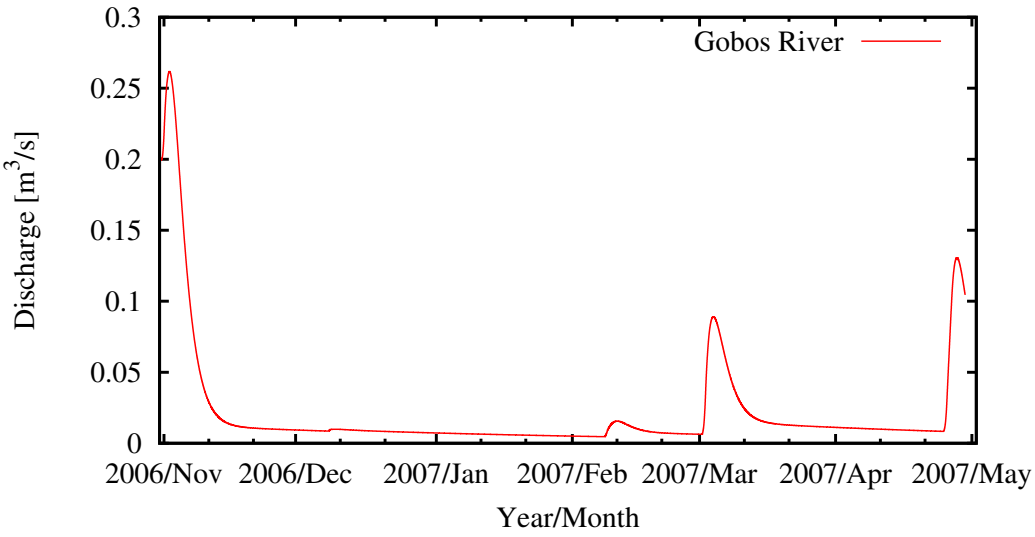

Figure D.5: Catchment E hydrograph for 2006.

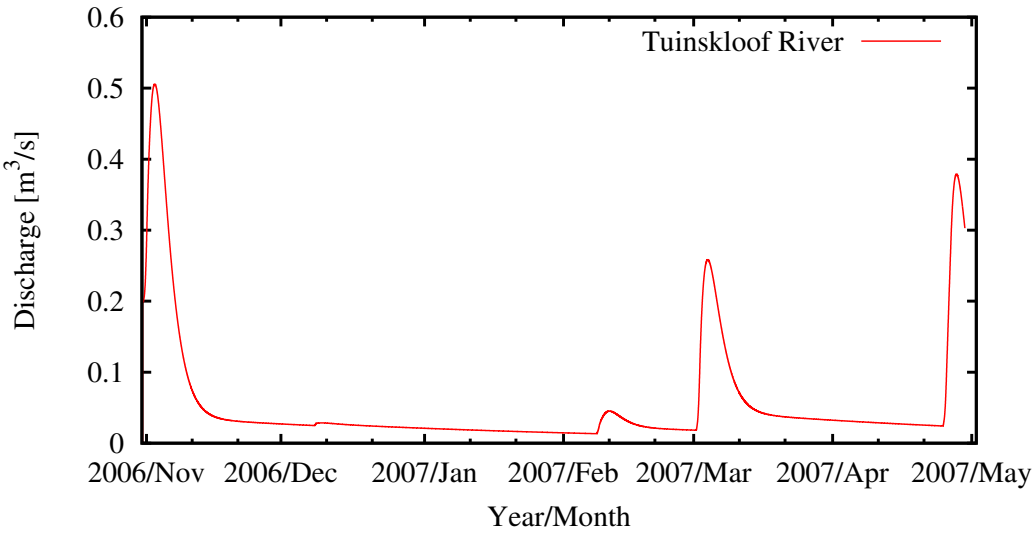

Figure D.6: Catchment F hydrograph for 2006.

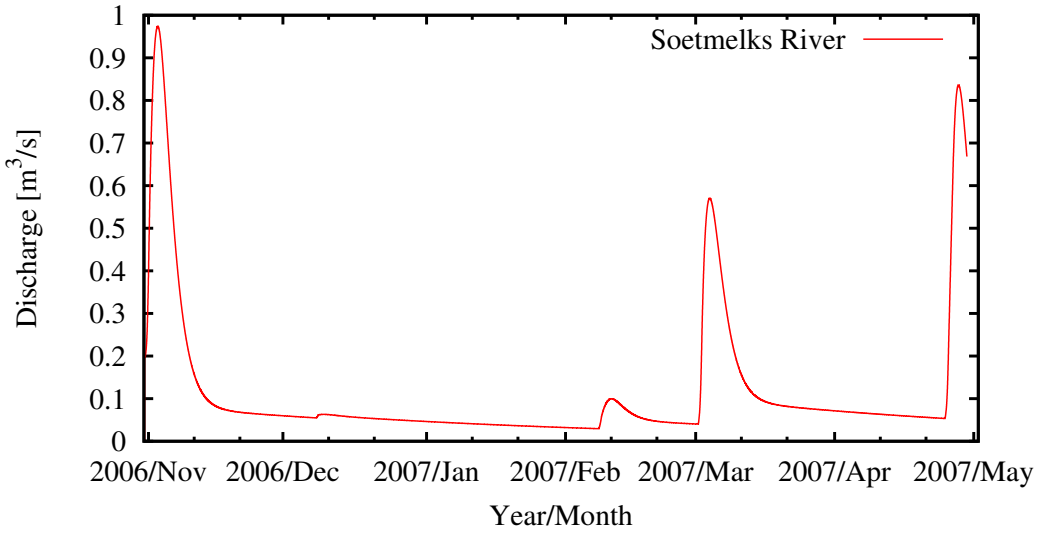

Figure D.7: Catchment G hydrograph for 2006.

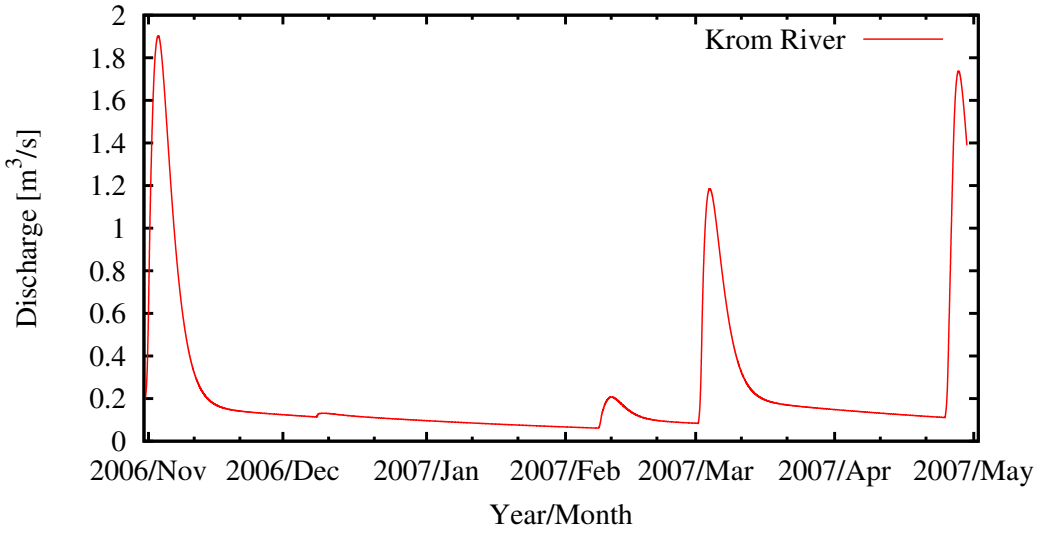

Figure D.8: Catchment H hydrograph for 2006.

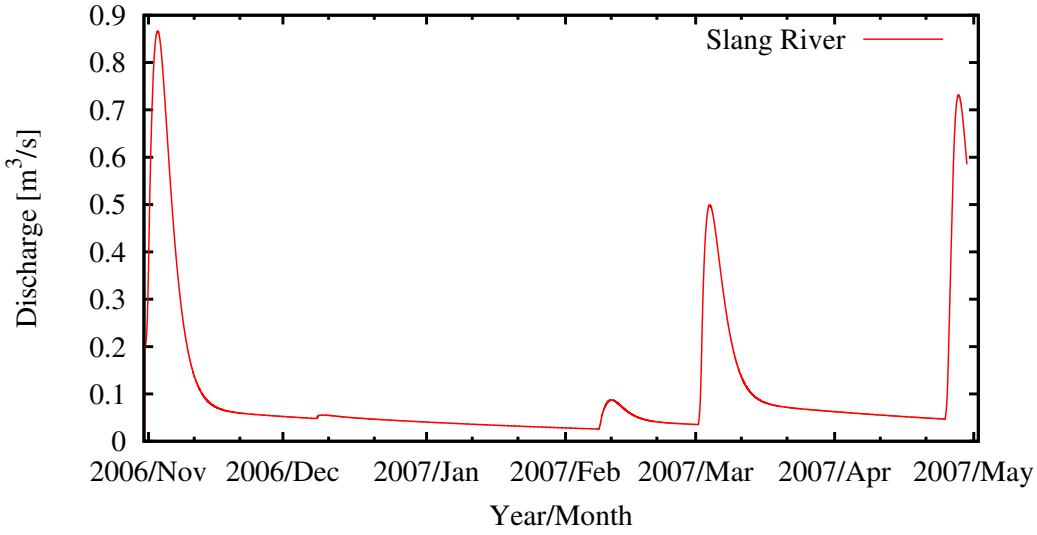

Figure D.9: Catchment I hydrograph for 2006.

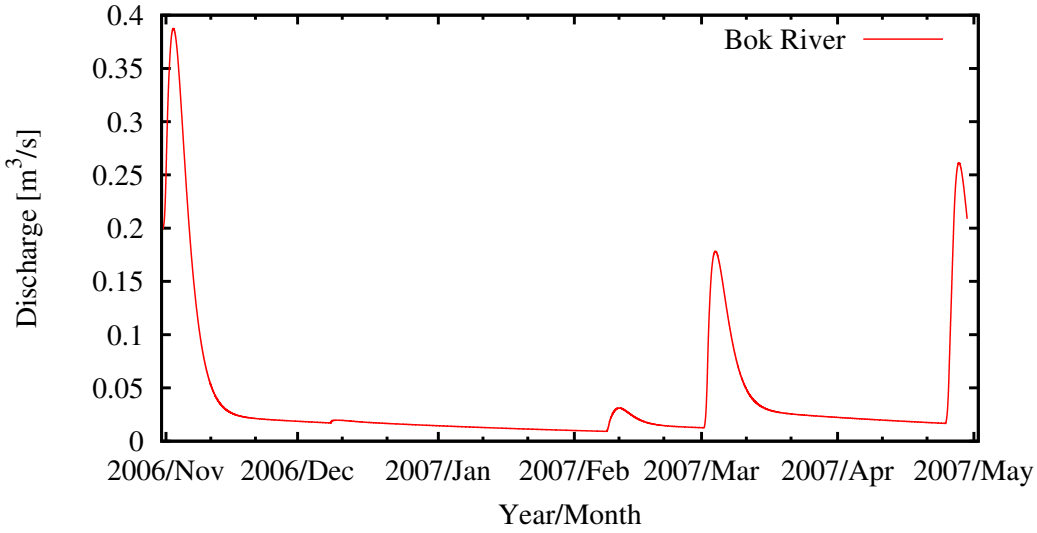

Figure D.10: Catchment J hydrograph for 2006.

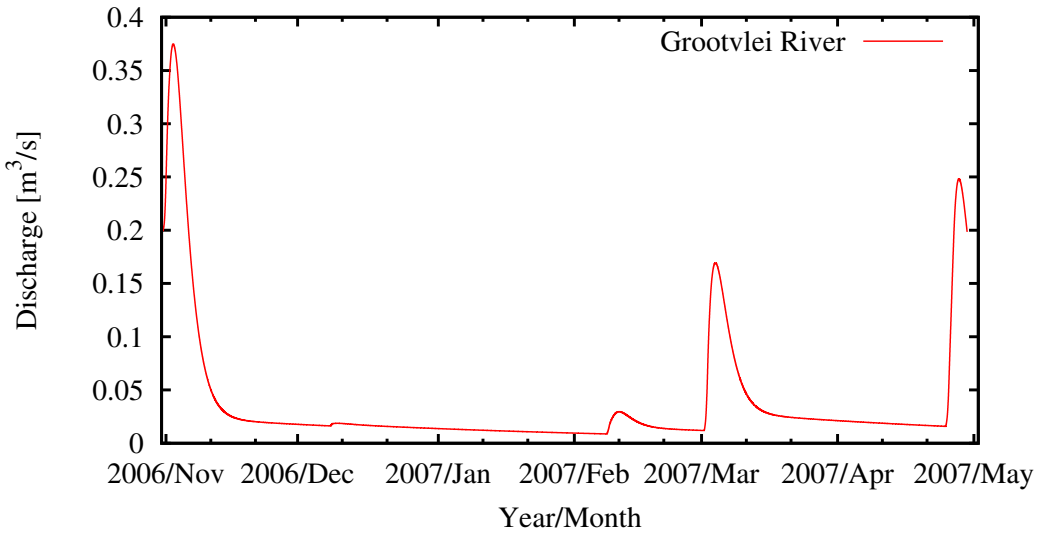

Figure D.11: Catchment K hydrograph for 2006.

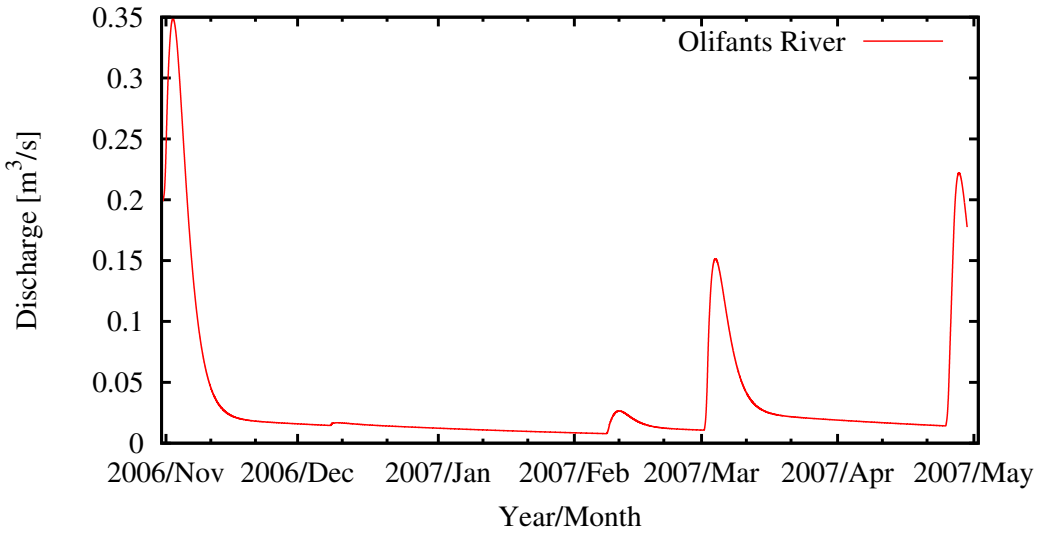

Figure D.12: Catchment L hydrograph for 2006.

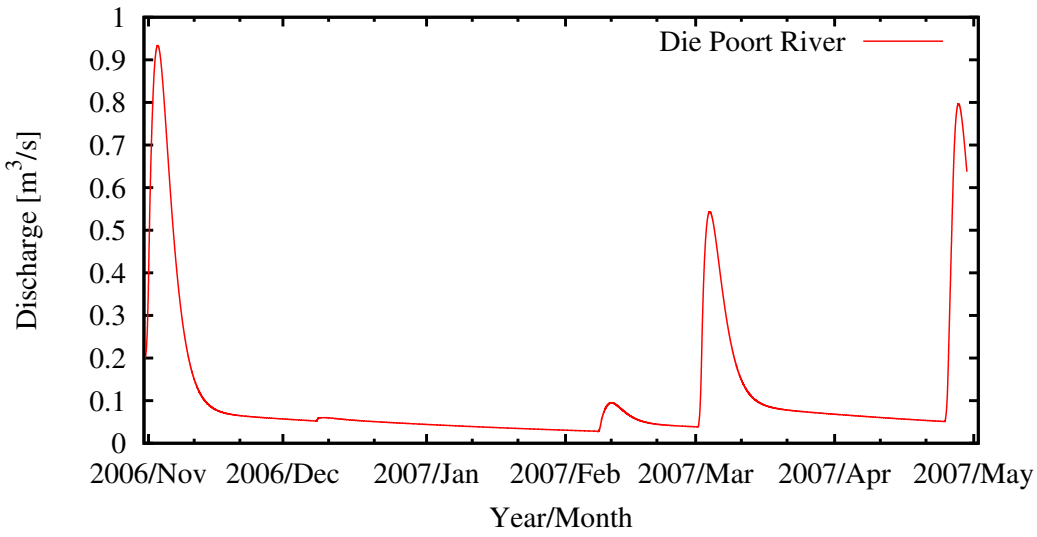

Figure D.13: Catchment M hydrograph for 2006.

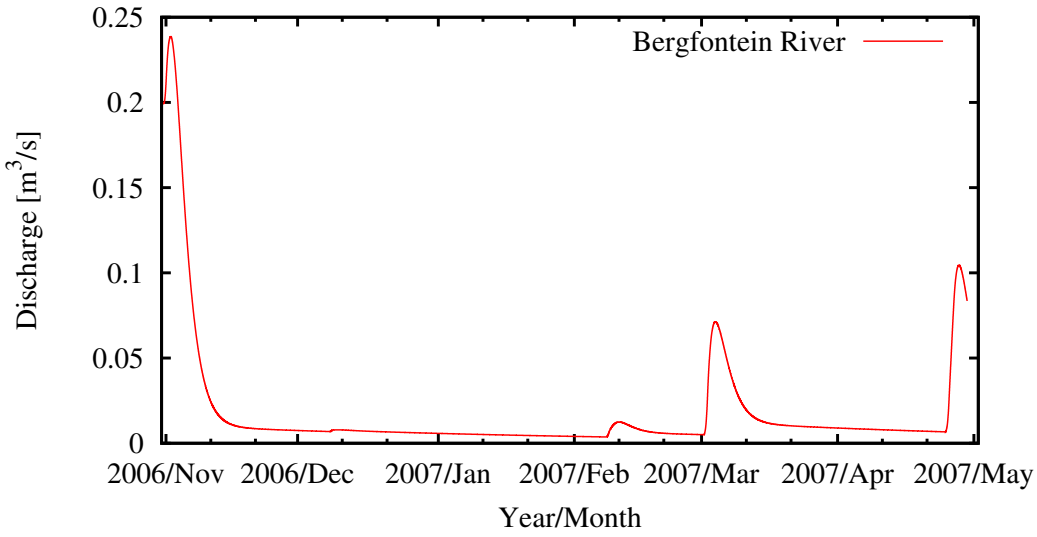

Figure D.14: Catchment N hydrograph for 2006.

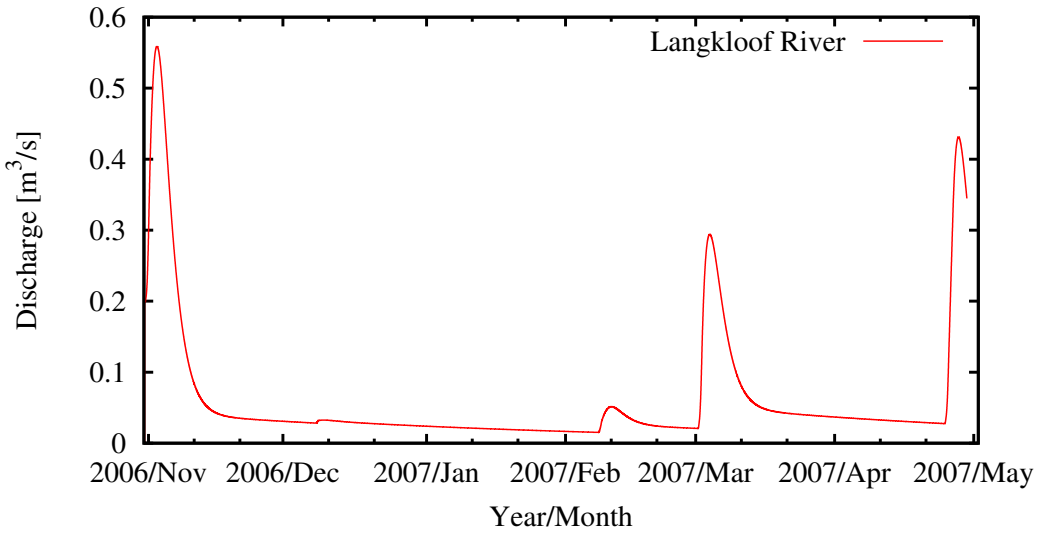

Figure D.15: Catchment O hydrograph for 2006.

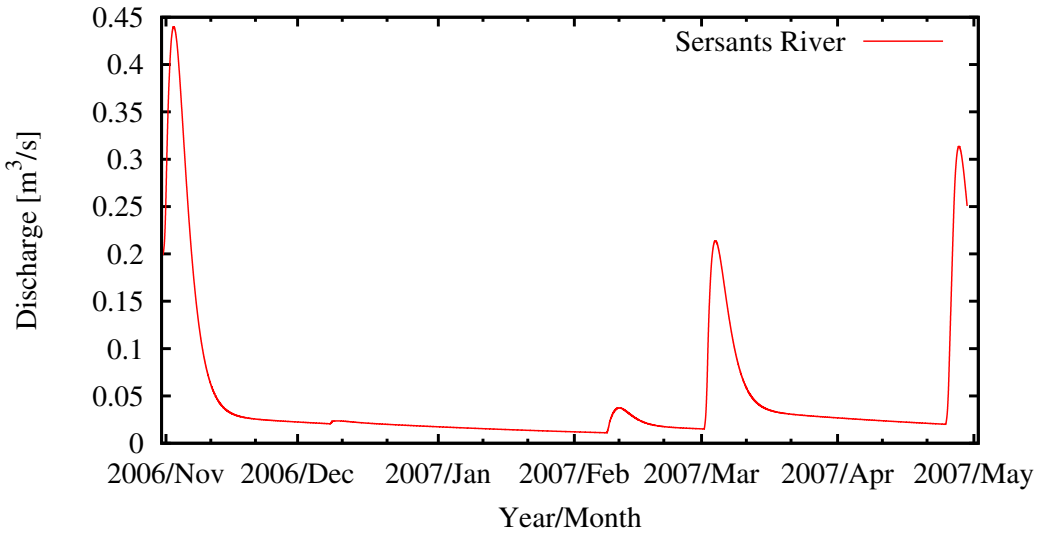

Figure D.16: Catchment P hydrograph for 2006.

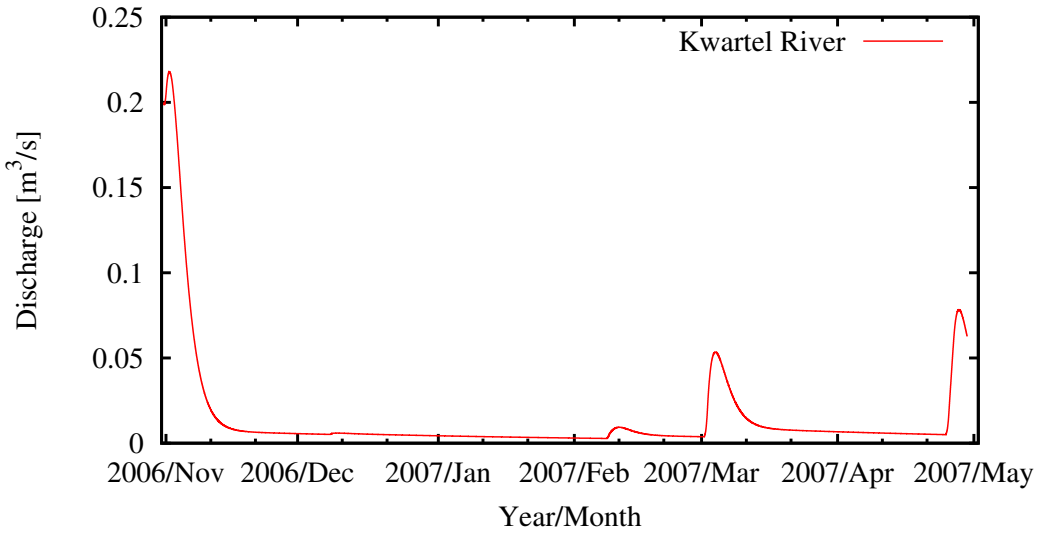

Figure D.17: Catchment Q hydrograph for 2006.

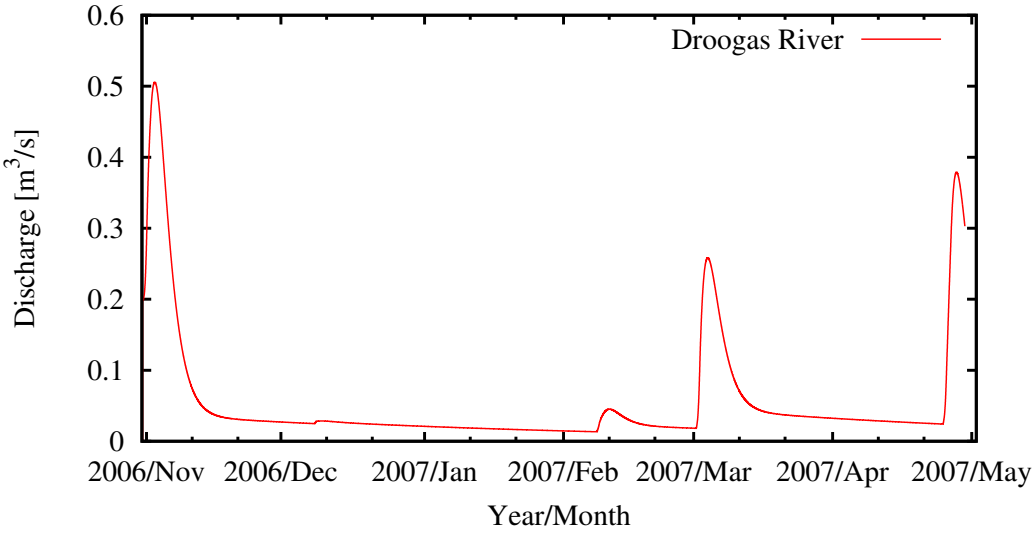

Figure D.18: Catchment R hydrograph for 2006.

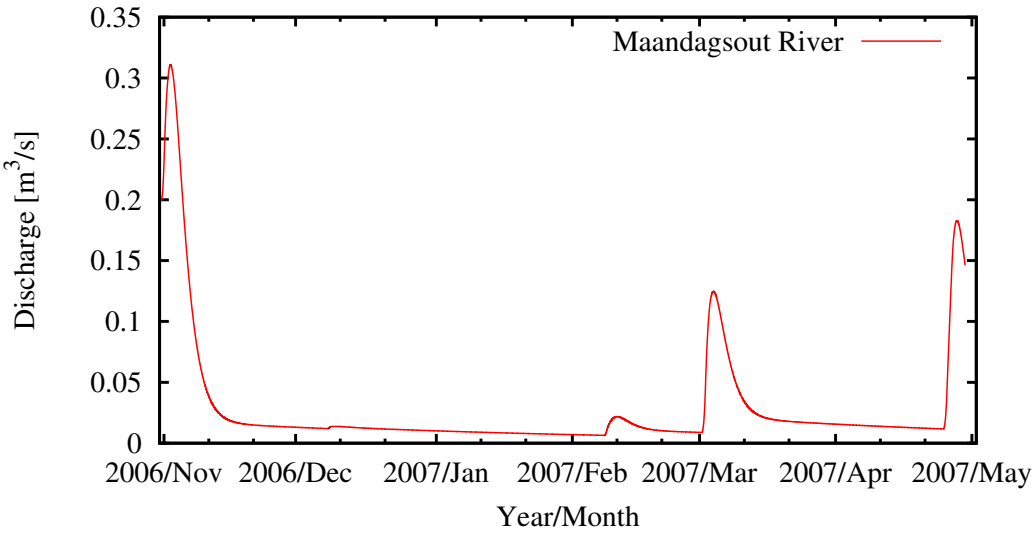

Figure D.19: Catchment S hydrograph for 2006.

D.2 2005-2006 Irrigation Season

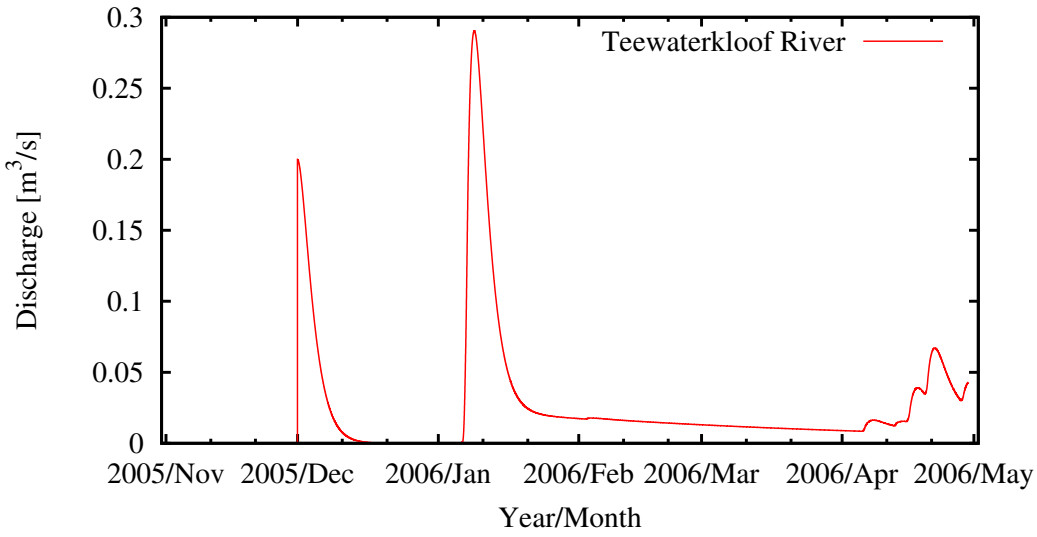

Figure D.20: Catchment A hydrograph for 2005.

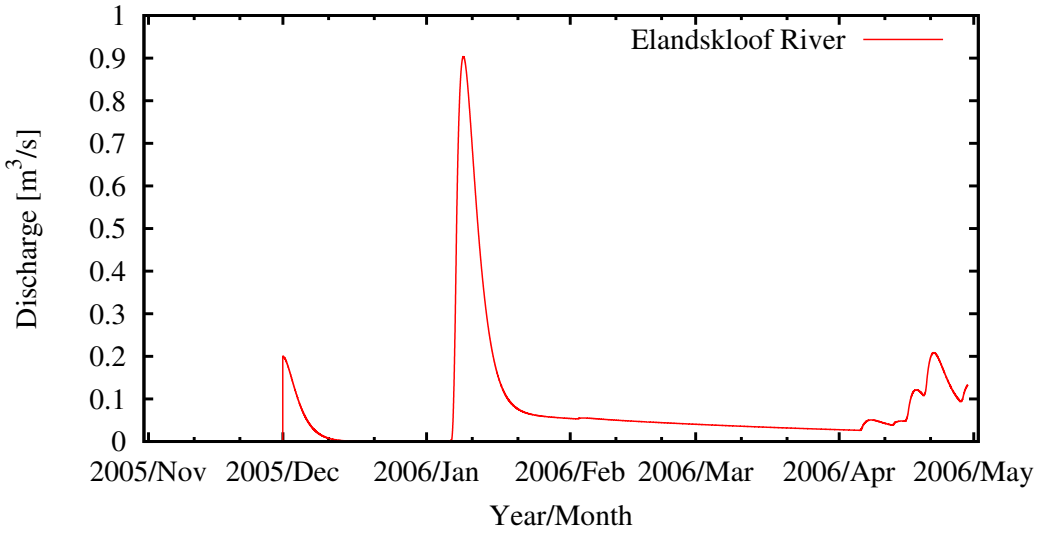

Figure D.21: Catchment B hydrograph for 2005.

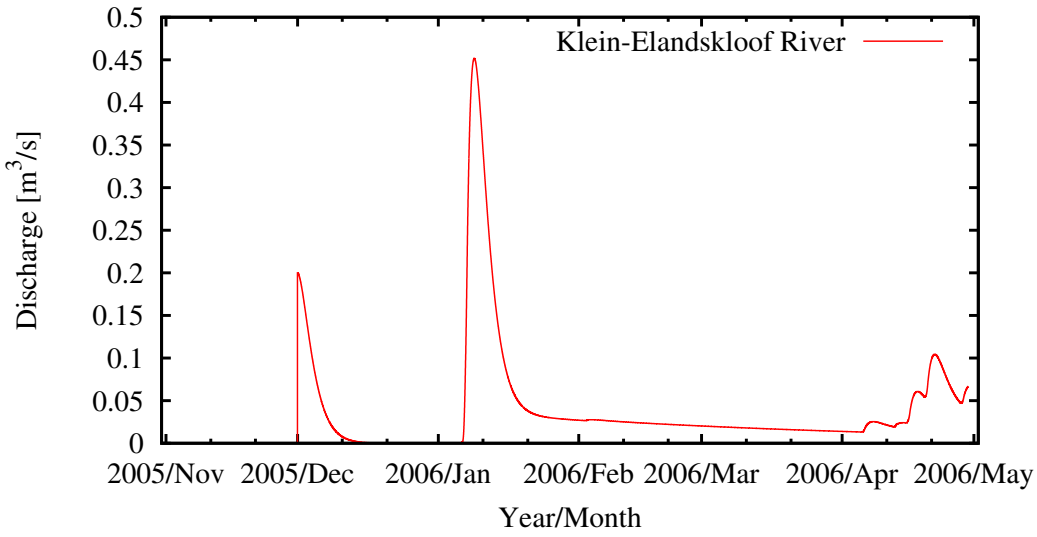

Figure D.22: Catchment C hydrograph for 2005.

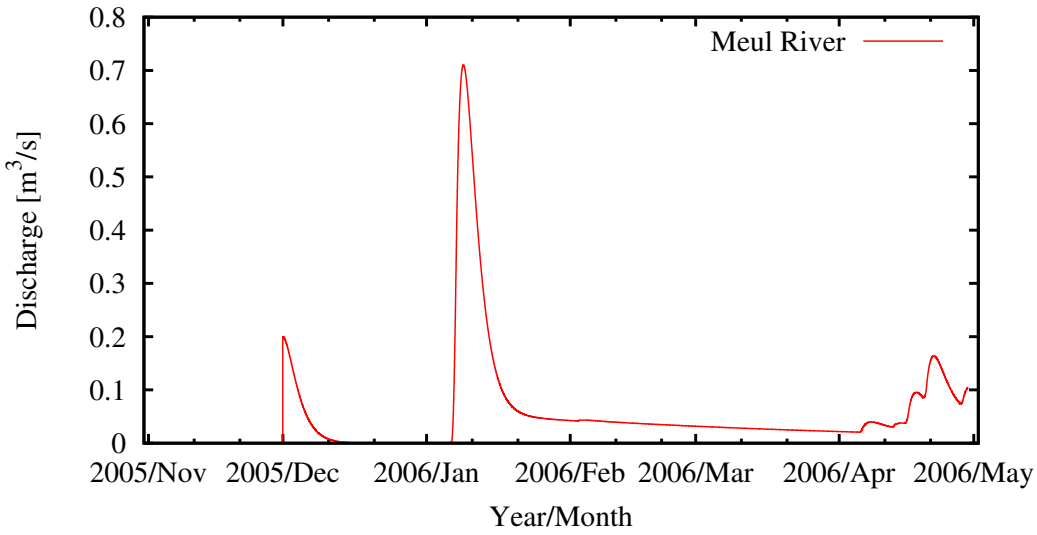

Figure D.23: Catchment D hydrograph for 2005.

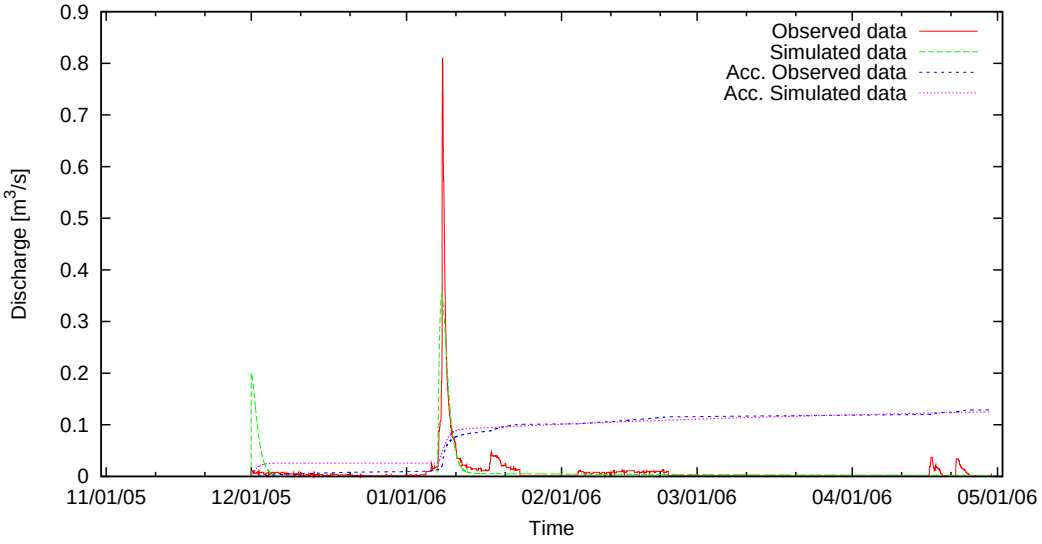

Figure D.24: Genadendal Catchment hydrograph for 2005 used as the basis to estimate tributary flow.

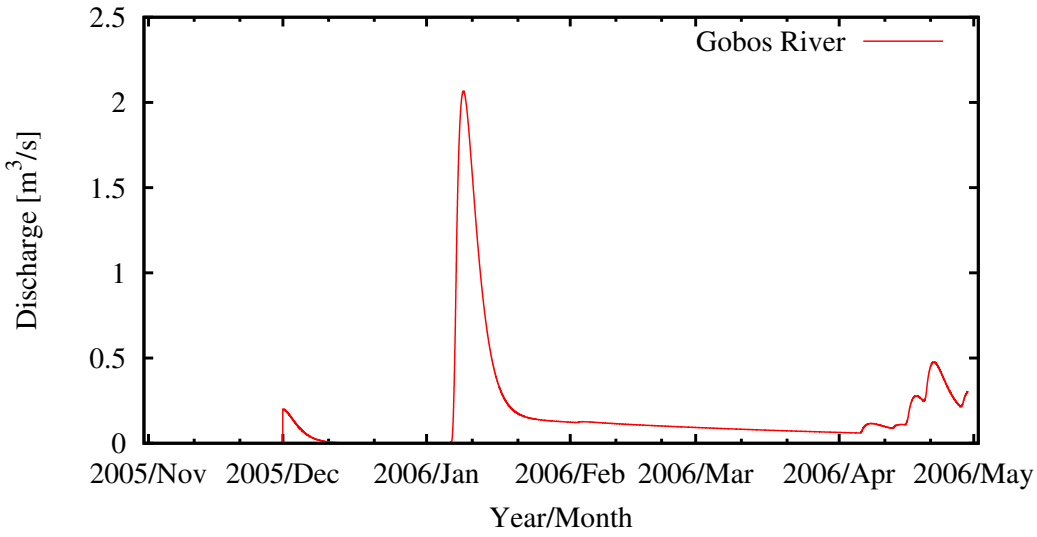

Figure D.25: Catchment E hydrograph for 2005.

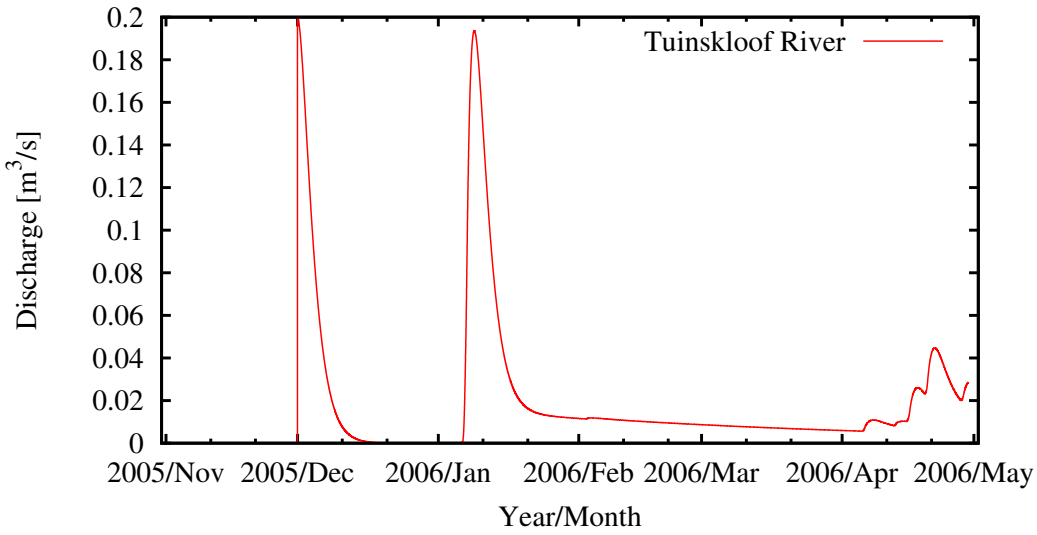

Figure D.26: Catchment F hydrograph for 2005.

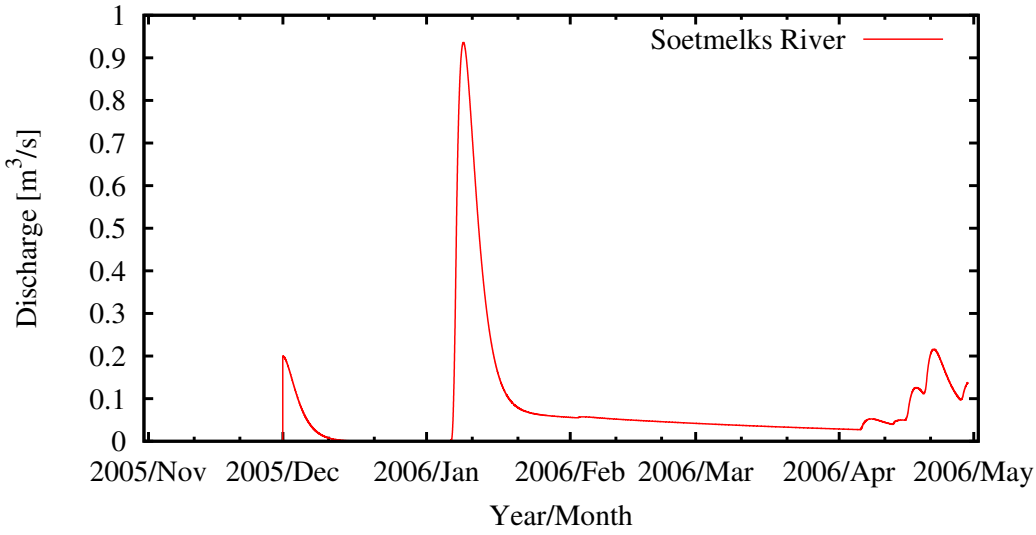

Figure D.27: Catchment G hydrograph for 2005.

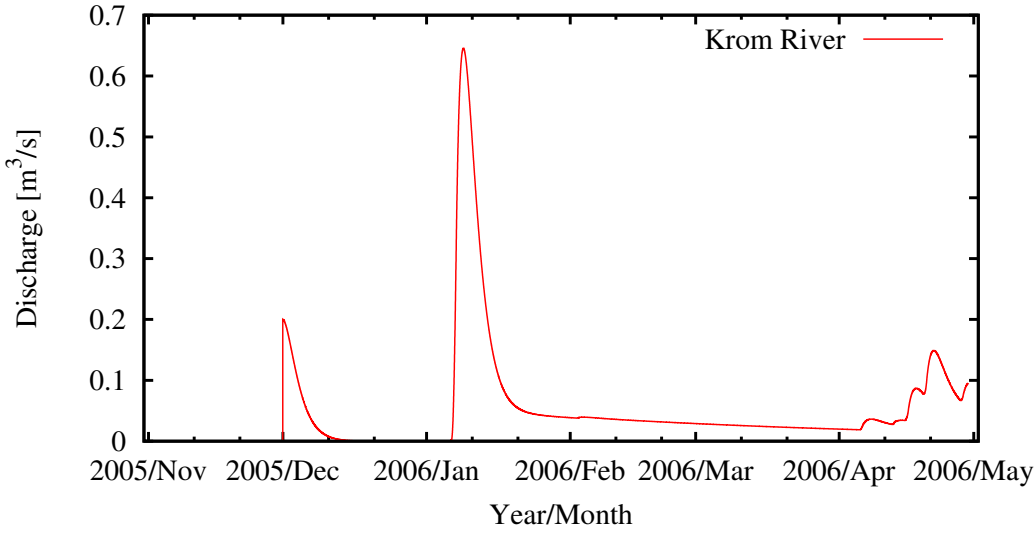

Figure D.28: Catchment H hydrograph for 2005.

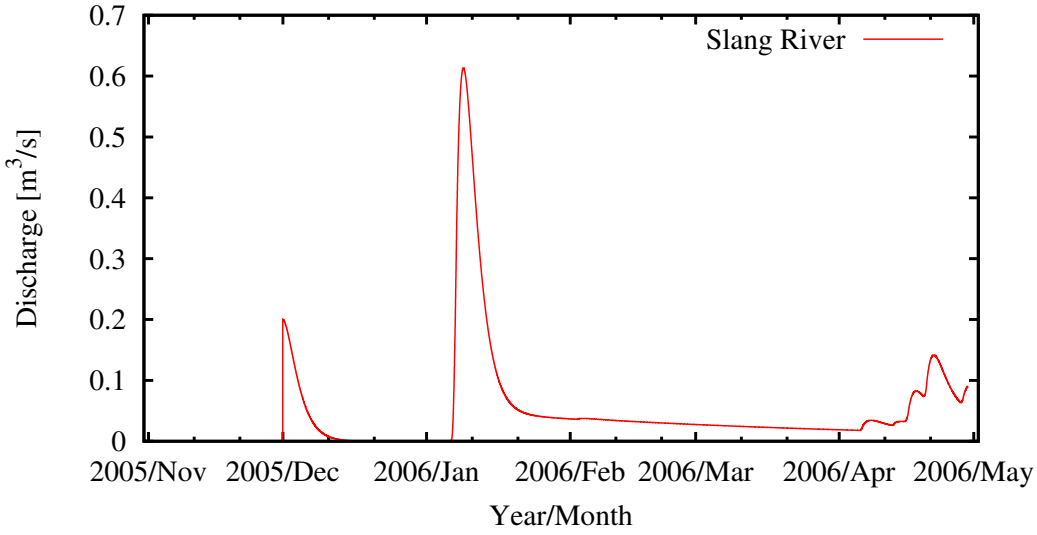

Figure D.29: Catchment I hydrograph for 2005.

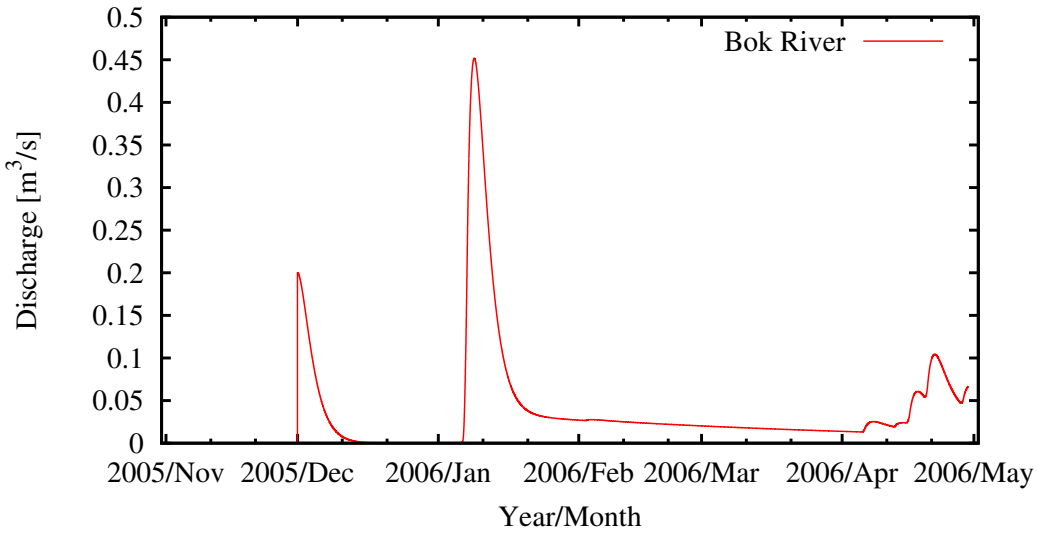

Figure D.30: Catchment J hydrograph for 2005.

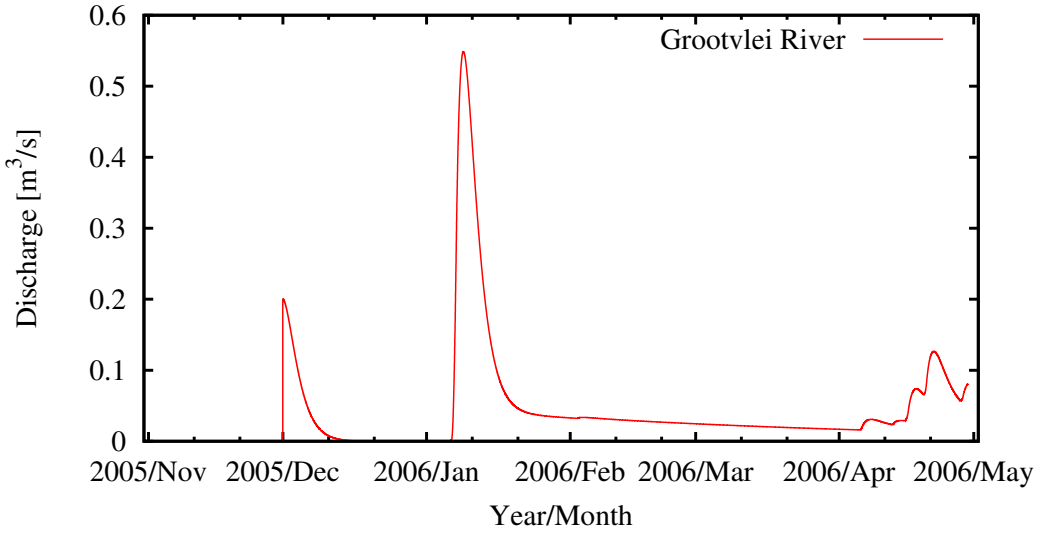

Figure D.31: Catchment K hydrograph for 2005.

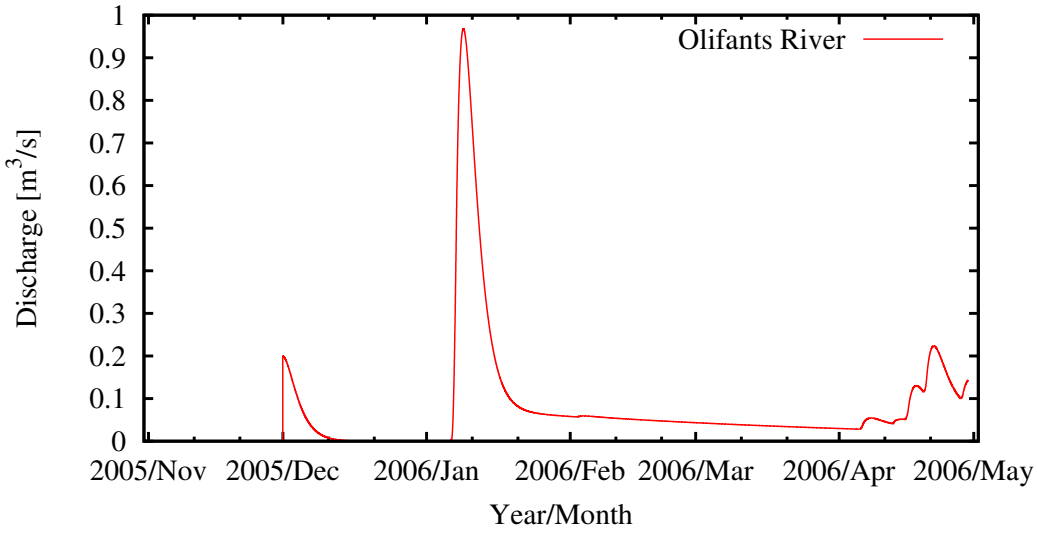

Figure D.32: Catchment L hydrograph for 2005.

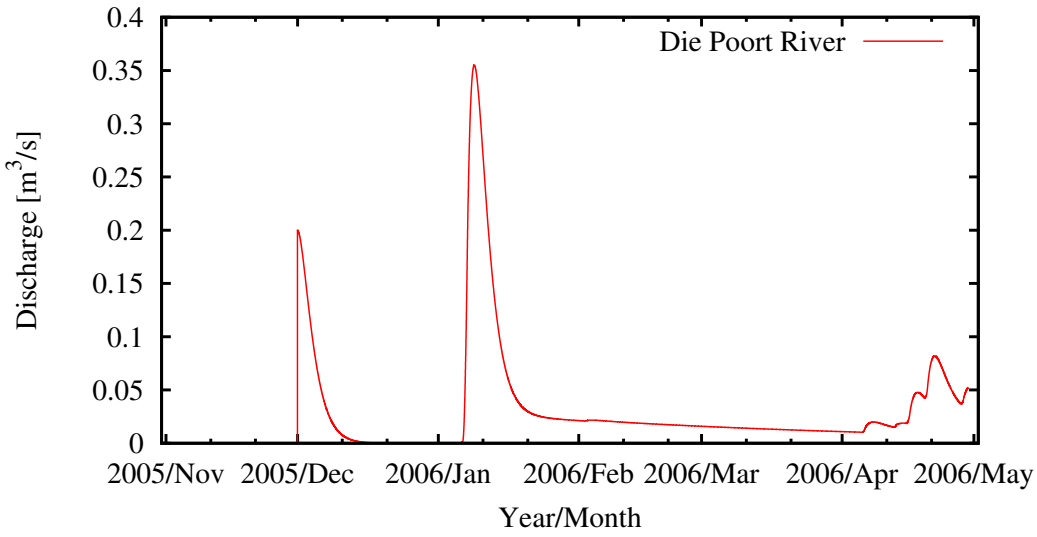

Figure D.33: Catchment M hydrograph for 2005.

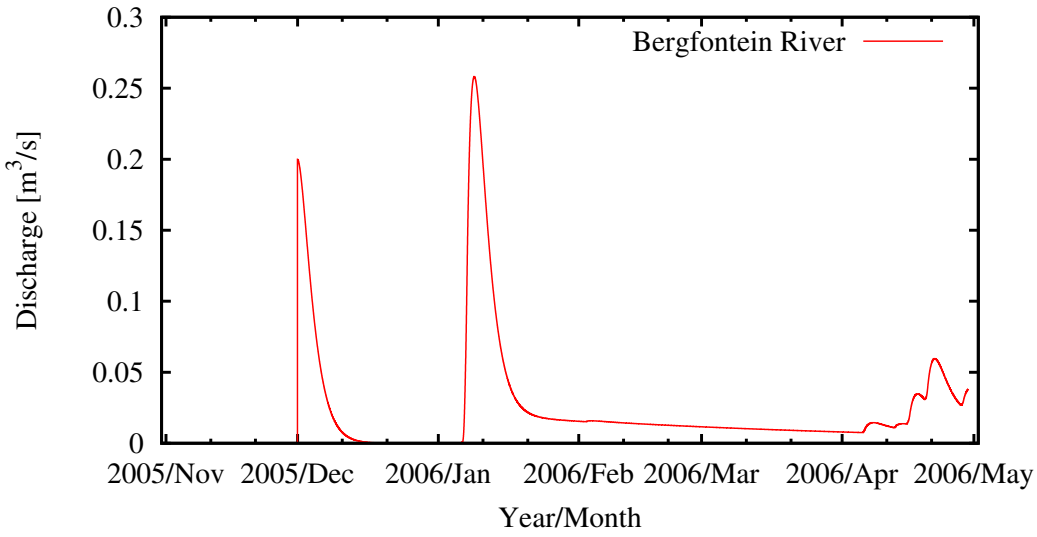

Figure D.34: Catchment N hydrograph for 2005.

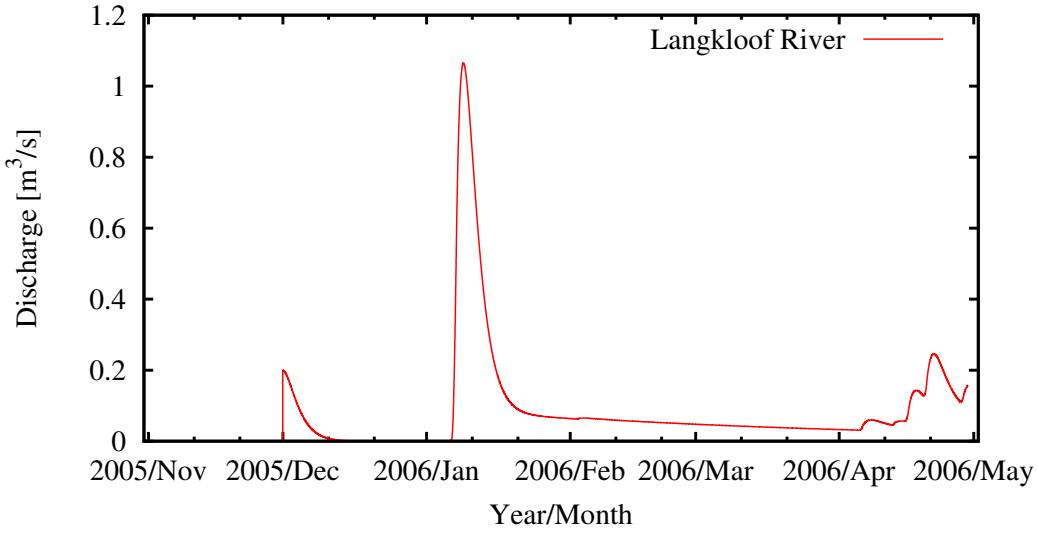

Figure D.35: Catchment O hydrograph for 2005.

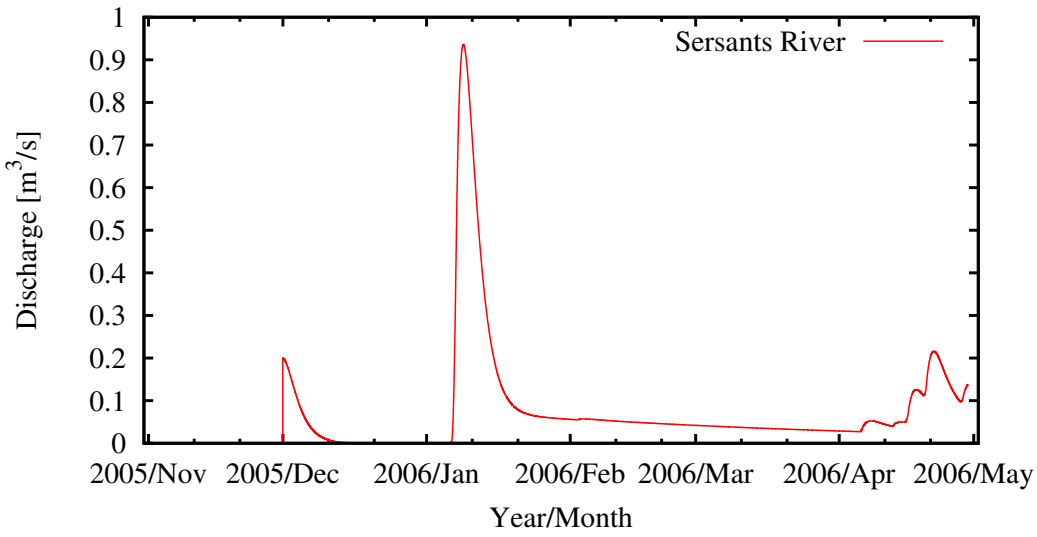

Figure D.36: Catchment P hydrograph for 2005.

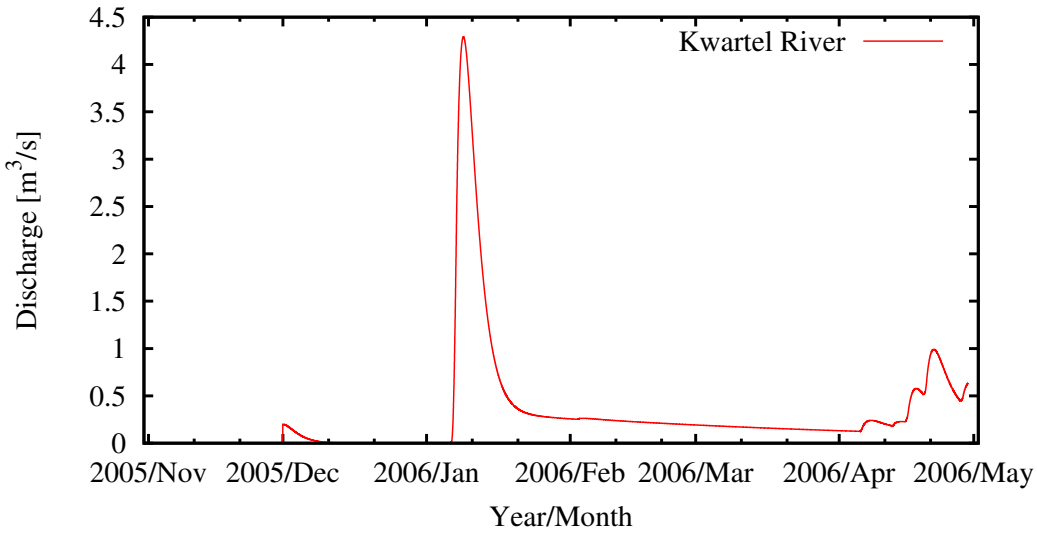

Figure D.37: Catchment Q hydrograph for 2005.

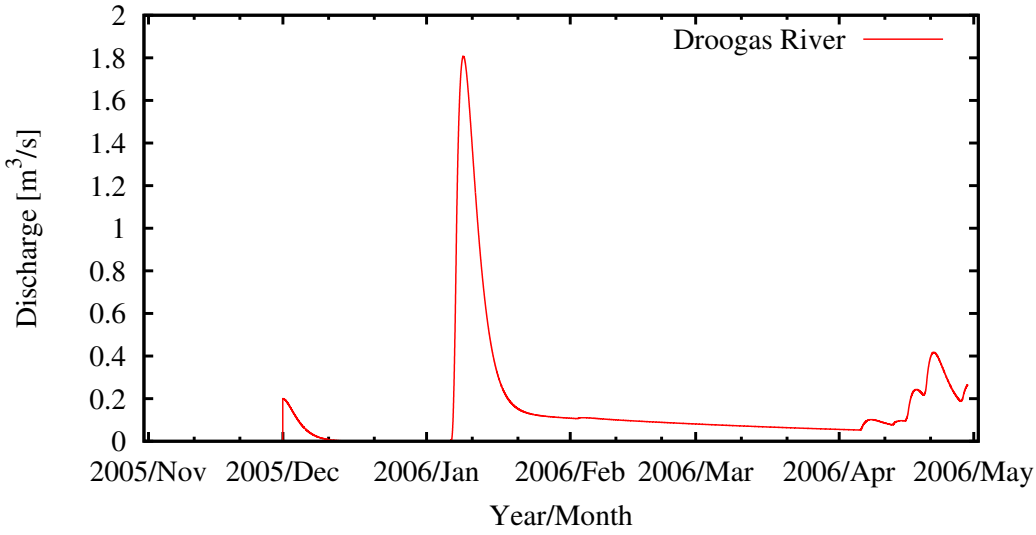

Figure D.38: Catchment R hydrograph for 2005.

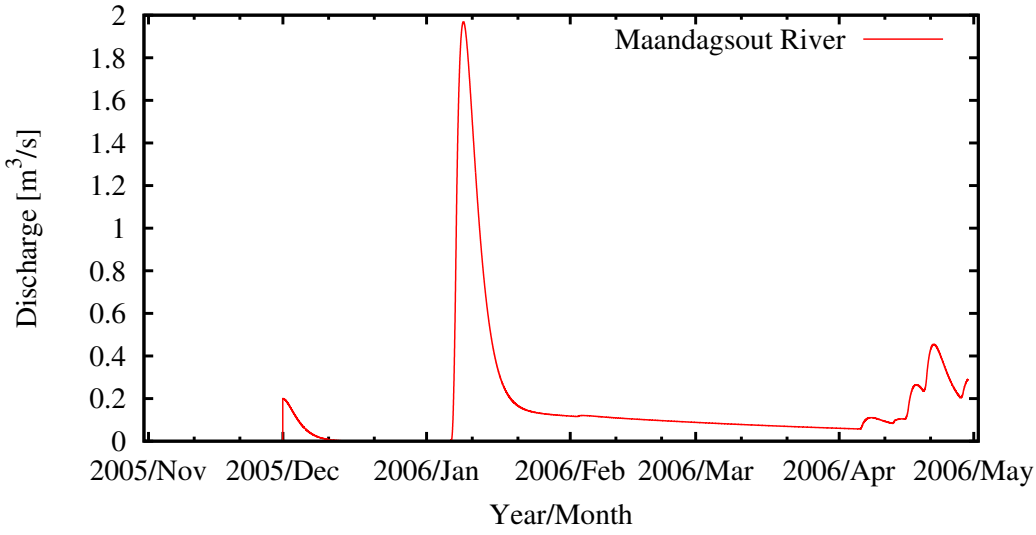

Figure D.39: Catchment S hydrograph for 2005.

Appendix E

Discharge-Time Relationship Graphs

In order to to construct an reduced dam release hydrograph for Theewaterskloof Dam, the relationship between the discharge and lag-time were determined between every abstraction point. This appendix illustrate this relation by plotting the data derived from the hydrodynamic river model and adding a trend line. The trend line equation is also shown.

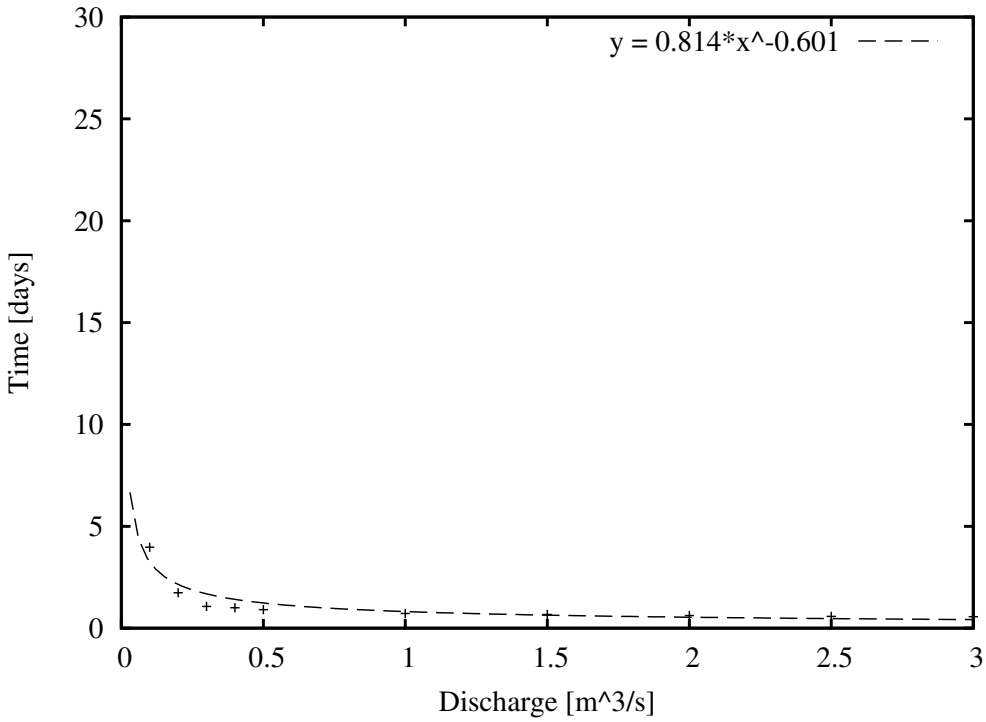

Figure E.1: Discharge-Time relationship between chainage 0-500m.

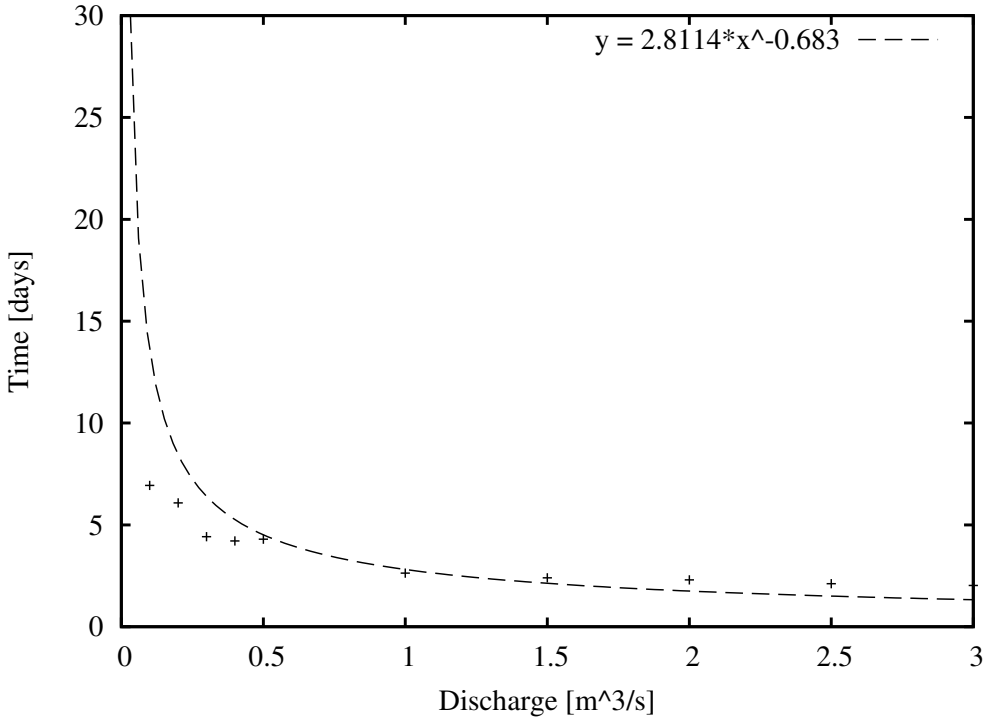

Figure E.2: Discharge-Time relationship between chainage 500-4000m.

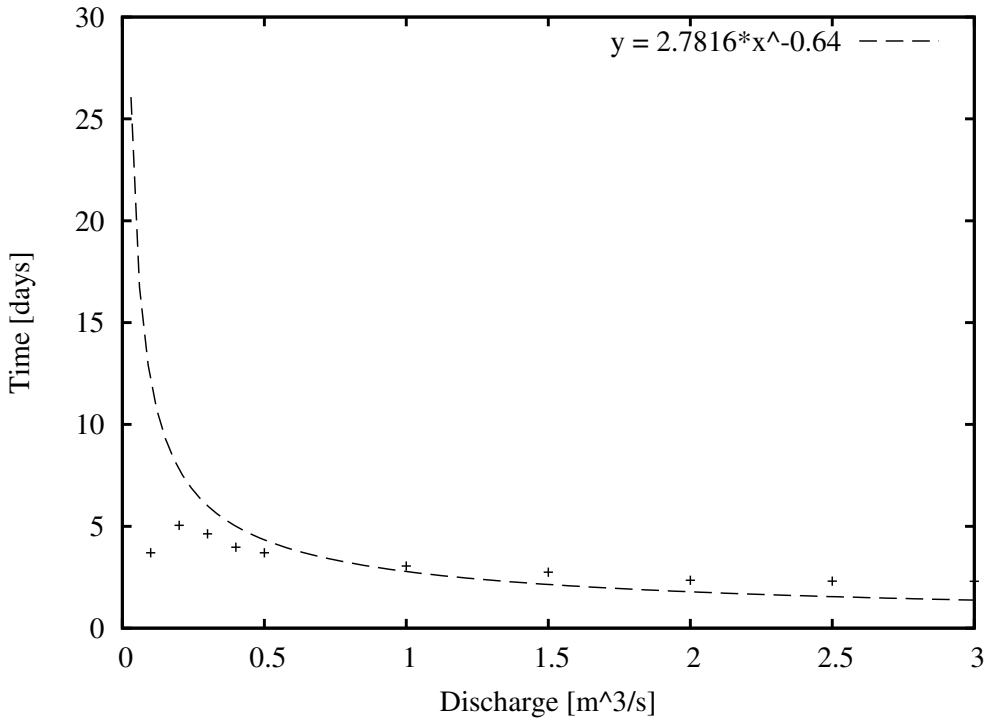

Figure E.3: Discharge-Time relationship between chainage 4000-5000m.

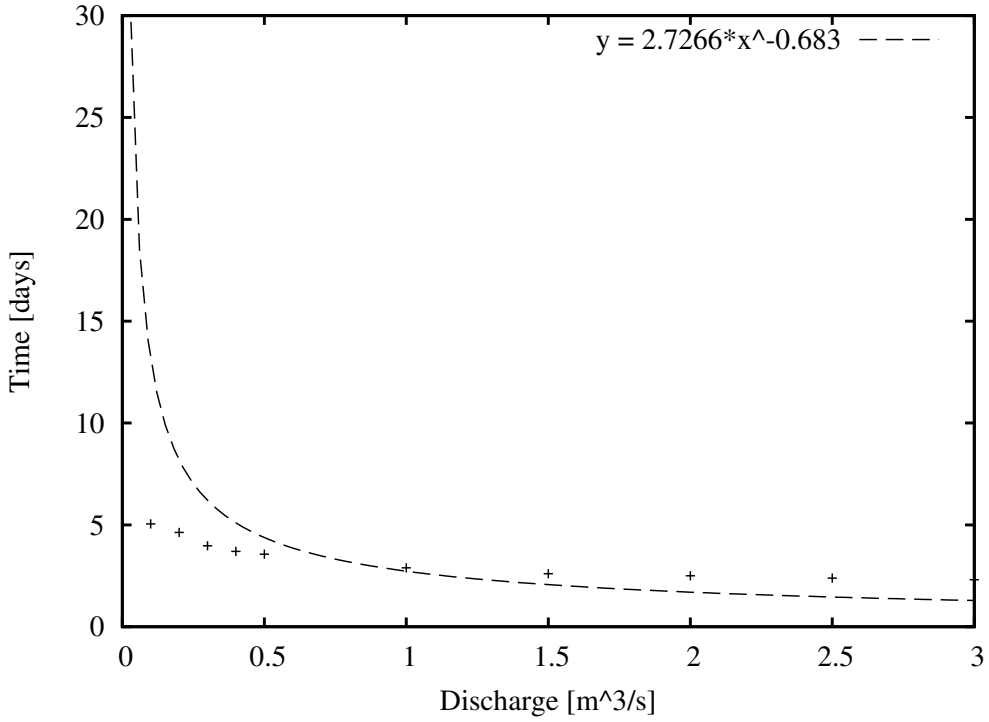

Figure E.4: Discharge-Time relationship between chainage 5000-6000m.

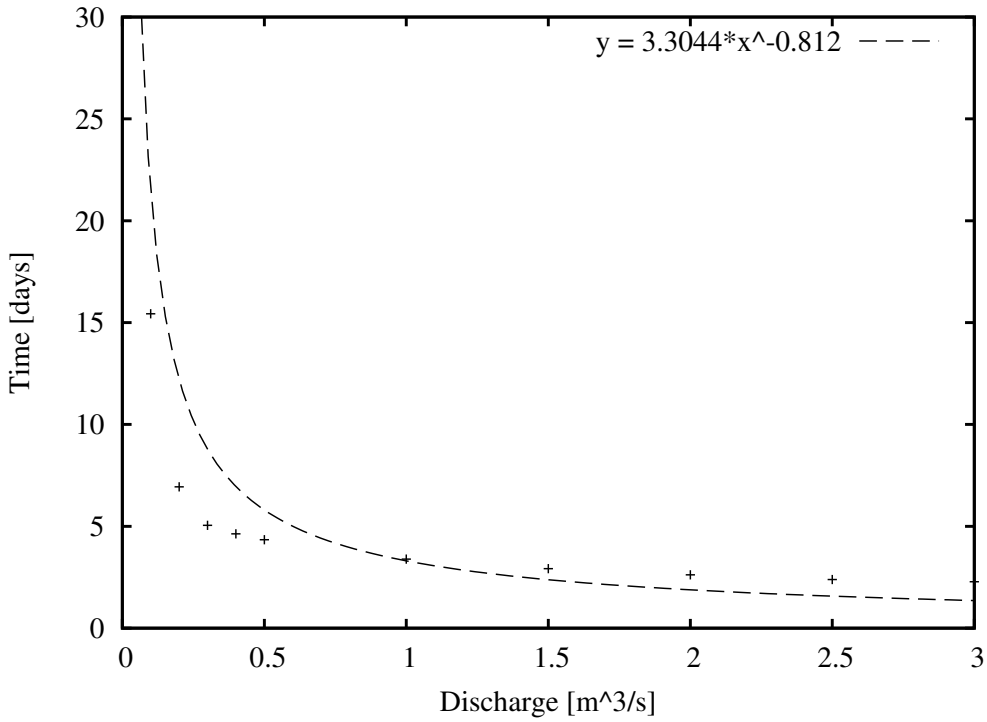

Figure E.5: Discharge-Time relationship between chainage 6000-7000m.

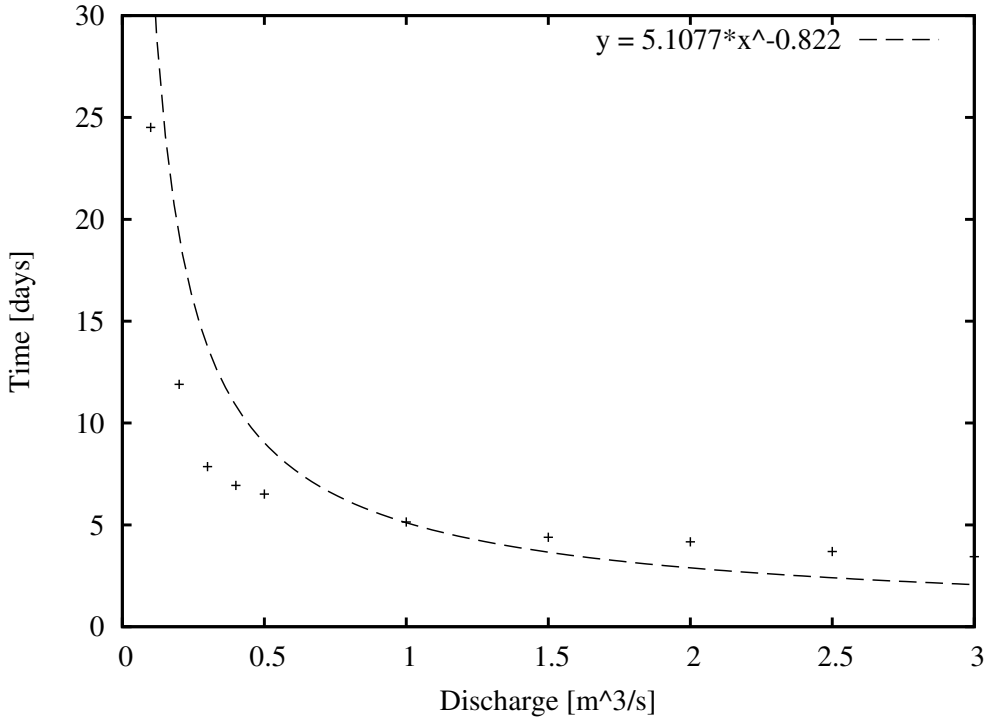

Figure E.6: Discharge-Time relationship between chainage 7000-8500m.

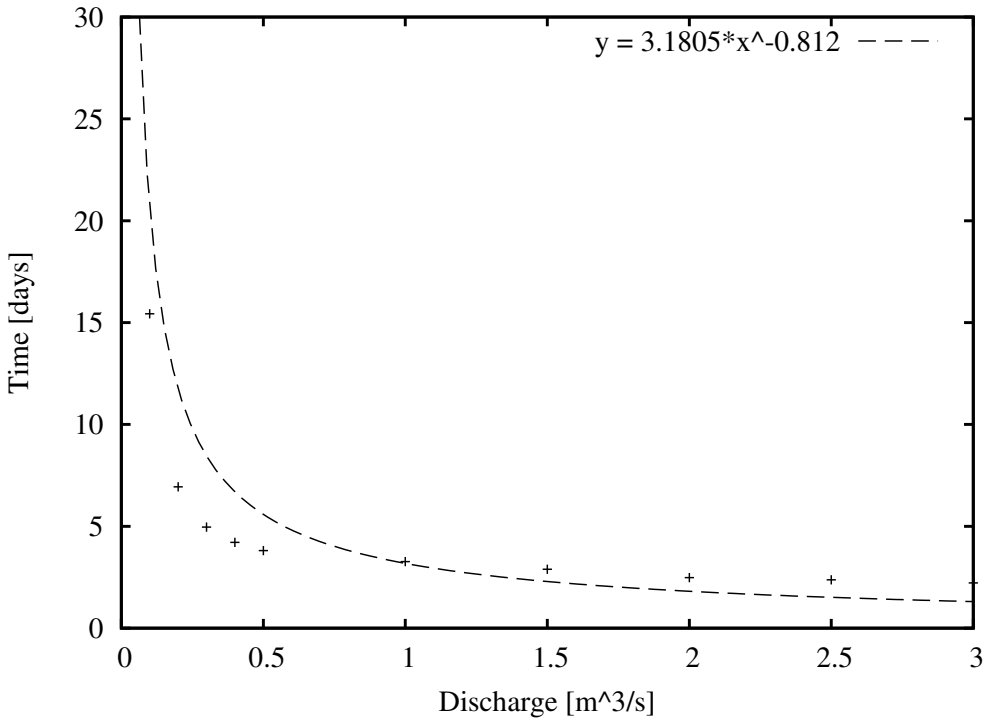

Figure E.7: Discharge-Time relationship between chainage 8500-10000m.

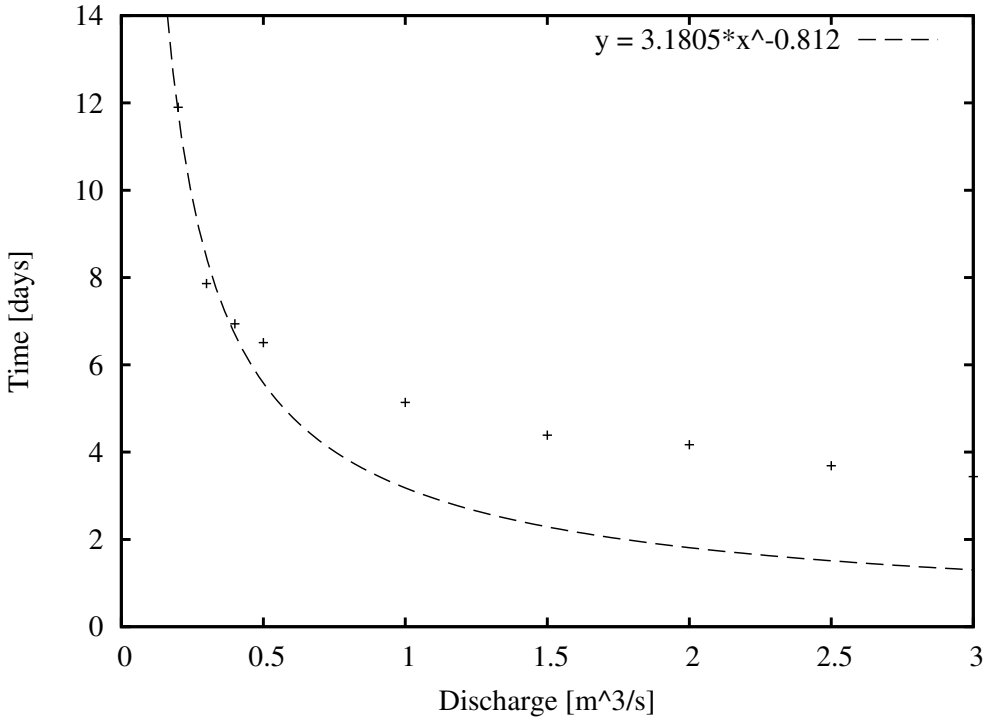

Figure E.8: Discharge-Time relationship between chainage 10000-11000m.

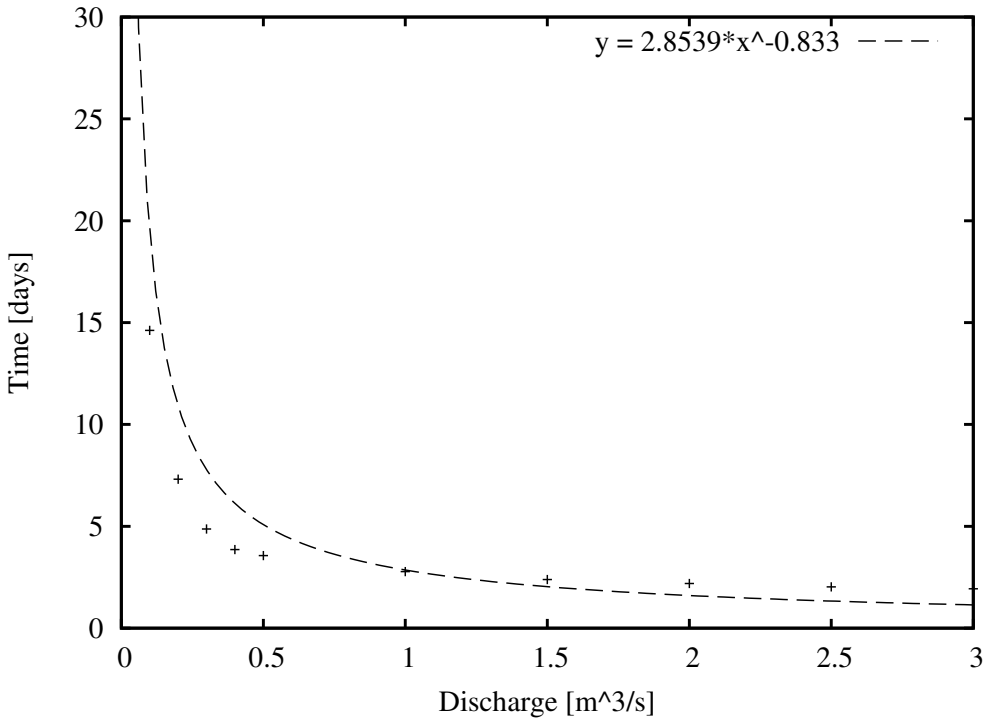

Figure E.9: Discharge-Time relationship between chainage 11000-12000m.

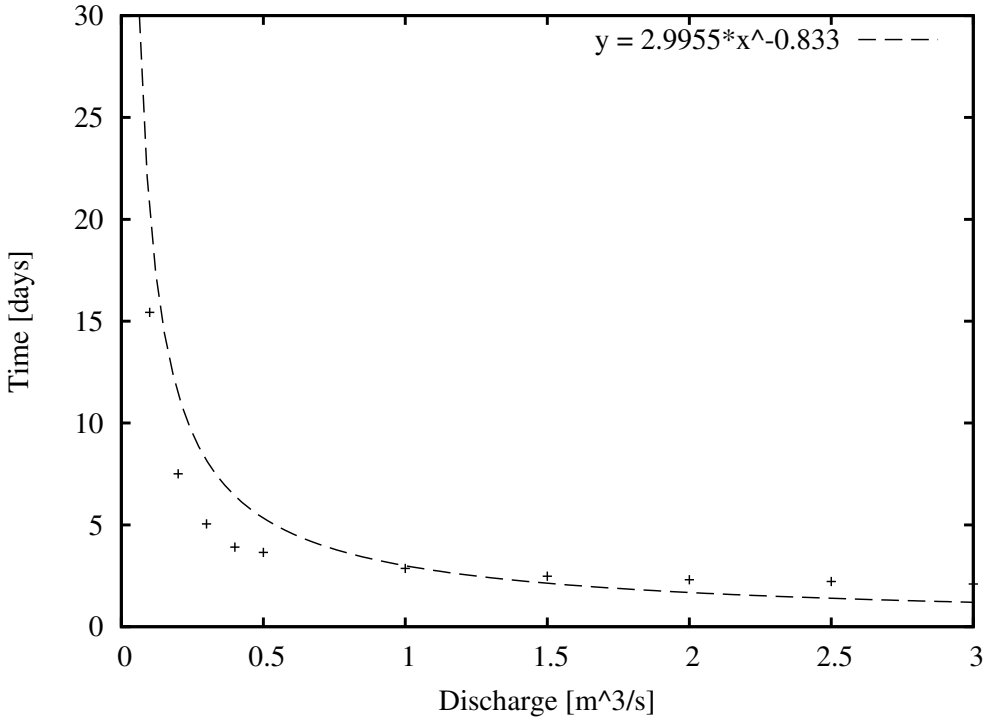

Figure E.10: Discharge-Time relationship between chainage 12000-13000m.

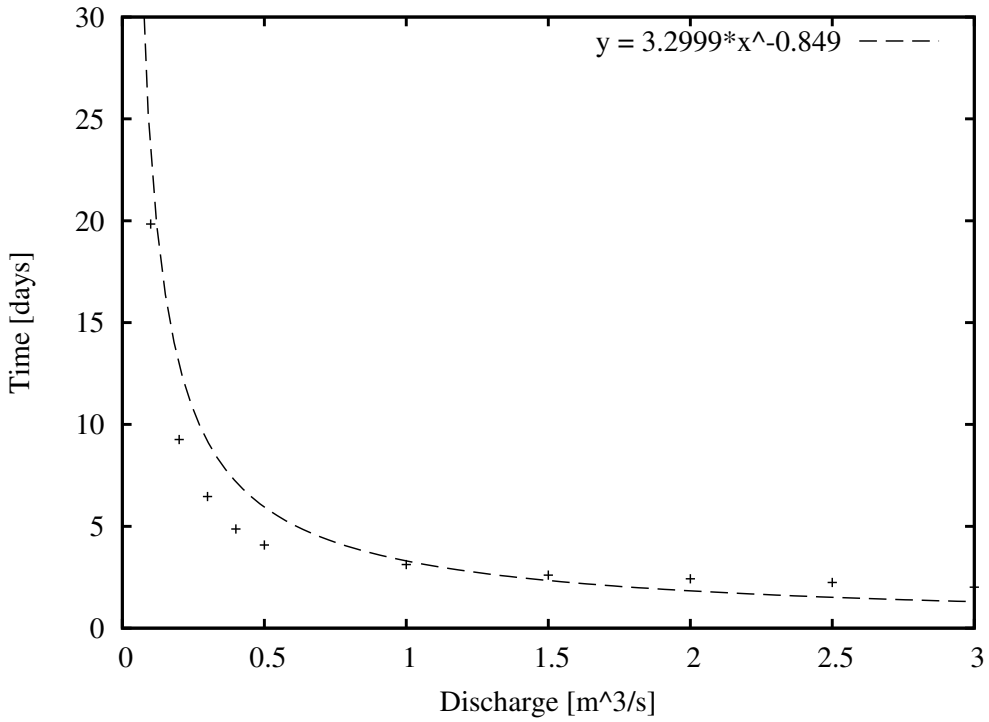

Figure E.11: Discharge-Time relationship between chainage 13000-14000.

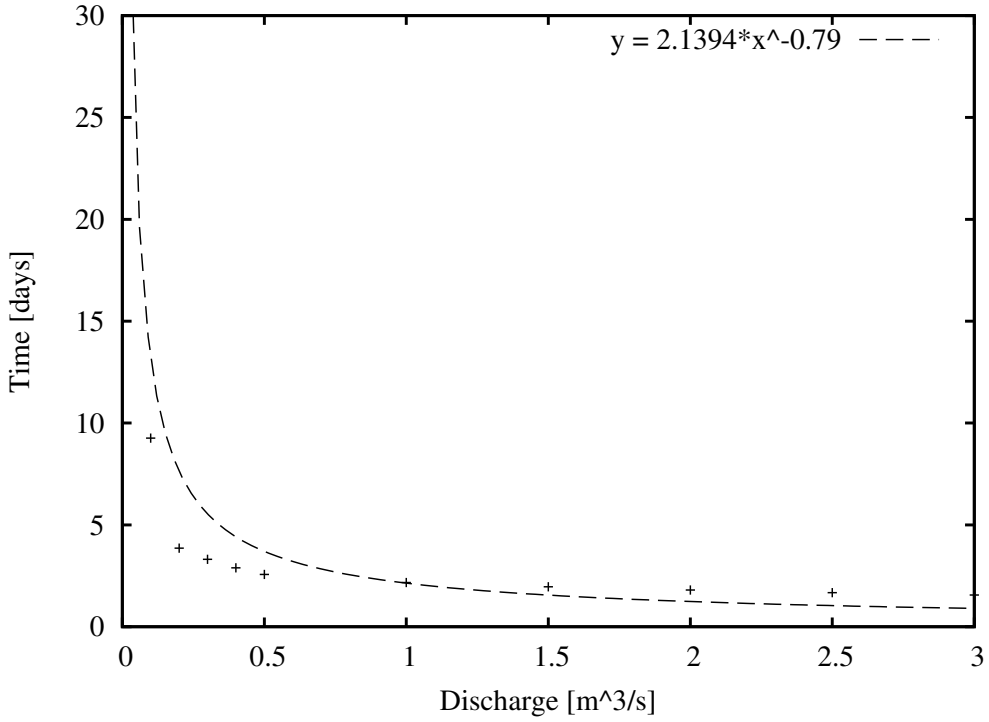

Figure E.12: Discharge-Time relationship between chainage 14000-14500m.

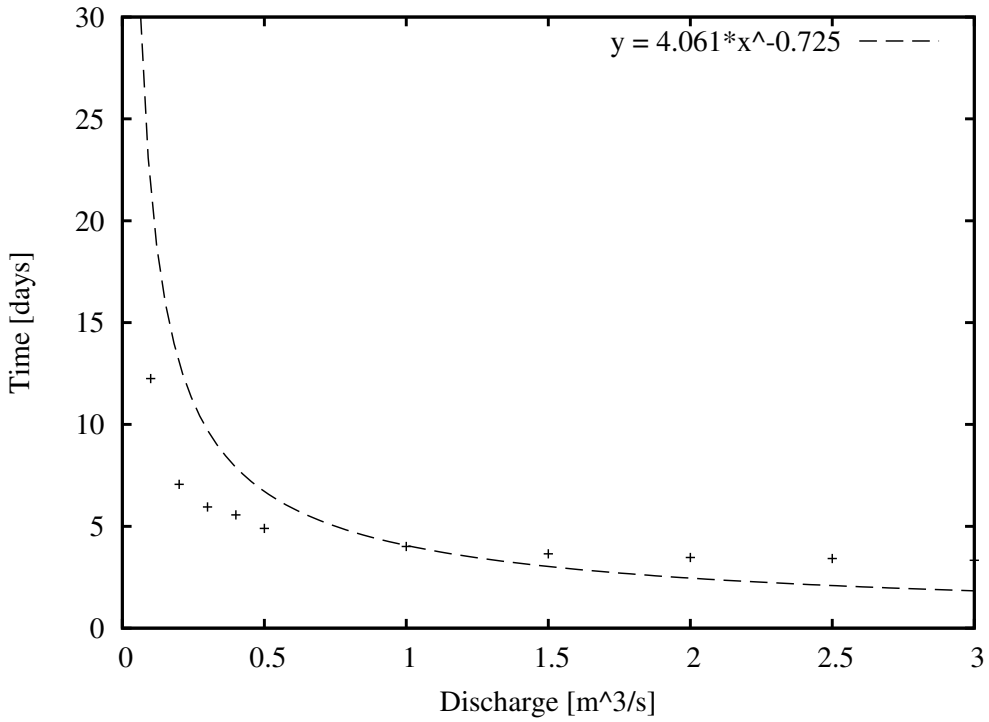

Figure E.13: Discharge-Time relationship between chainage 14500-16000m.

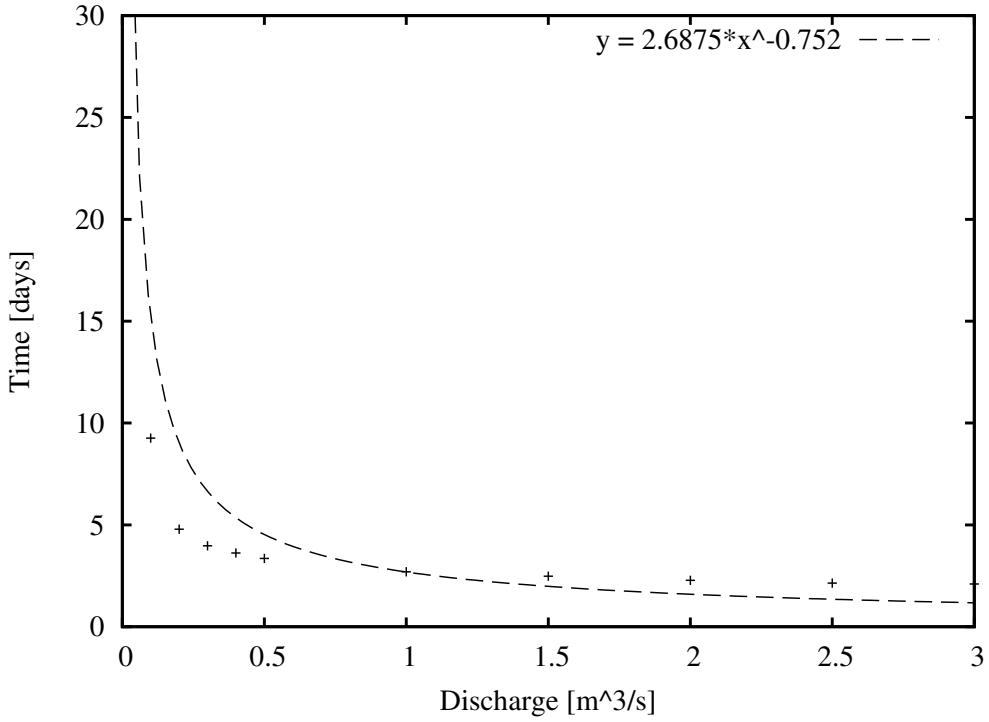

Figure E.14: Discharge-Time relationship between chainage 16000-17000m.

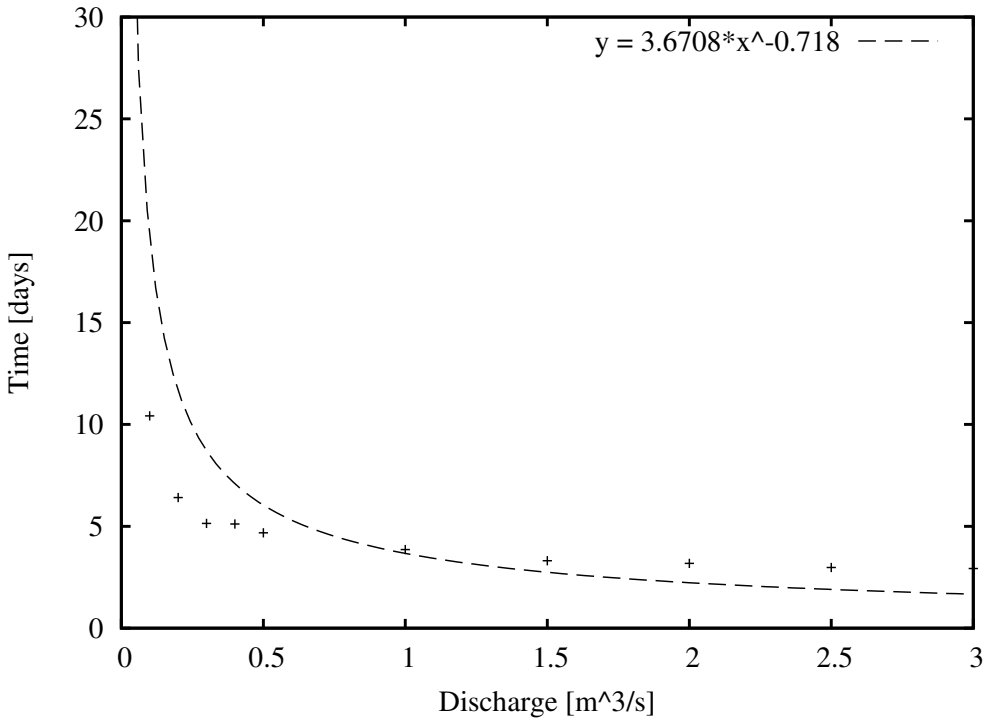

Figure E.15: Discharge-Time relationship between chainage 17000-18500m.

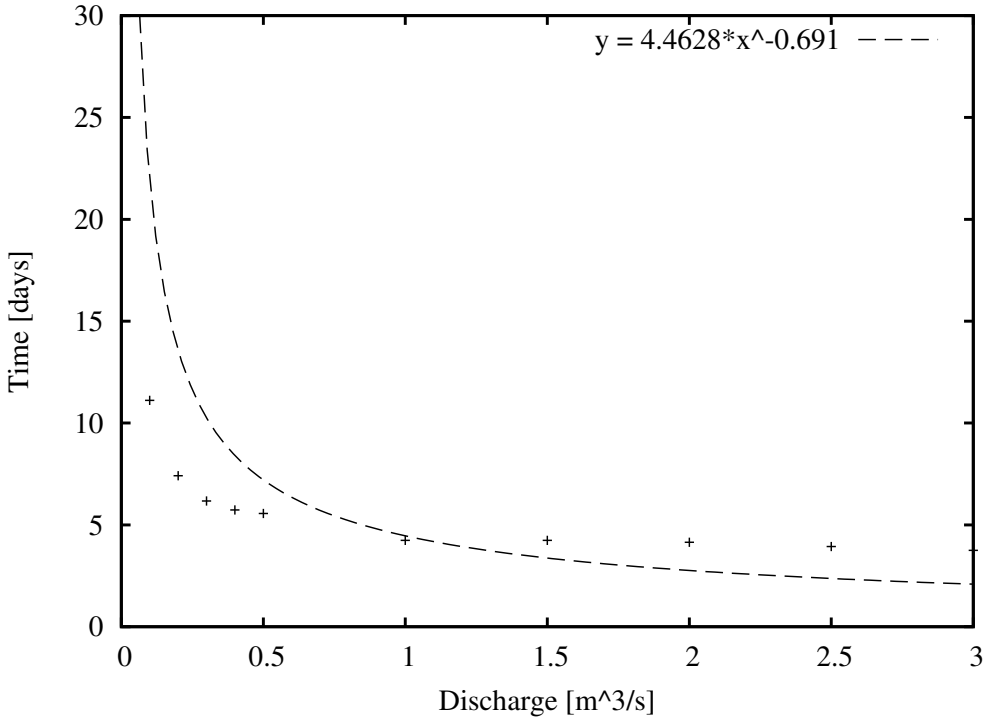

Figure E.16: Discharge-Time relationship between chainage 18500-20500m.

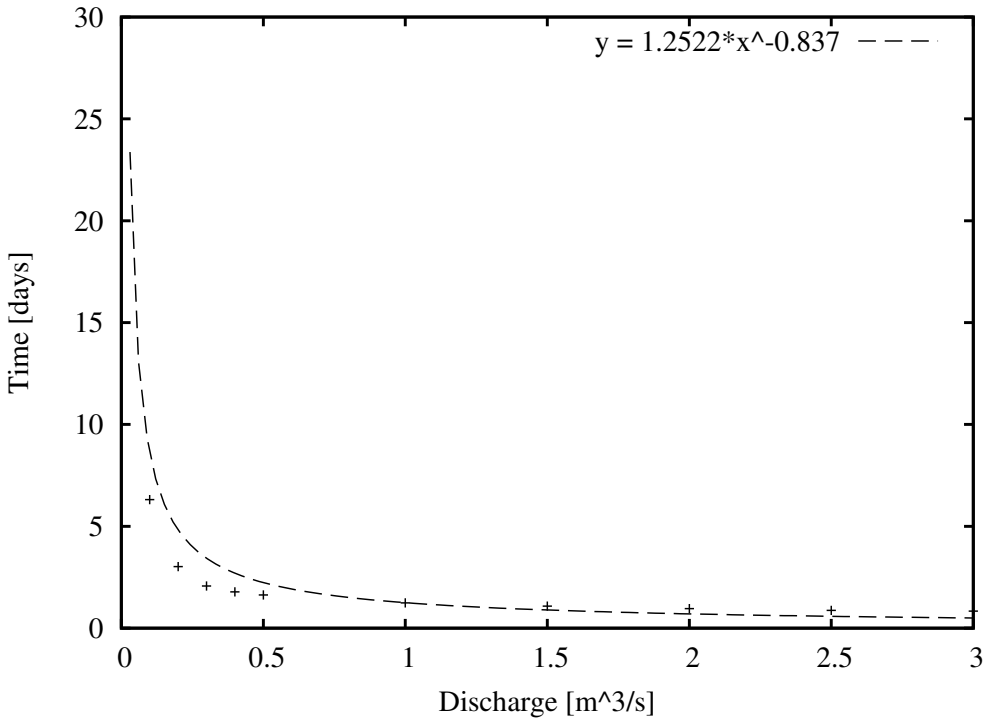

Figure E.17: Discharge-Time relationship between chainage 20500-21000m.

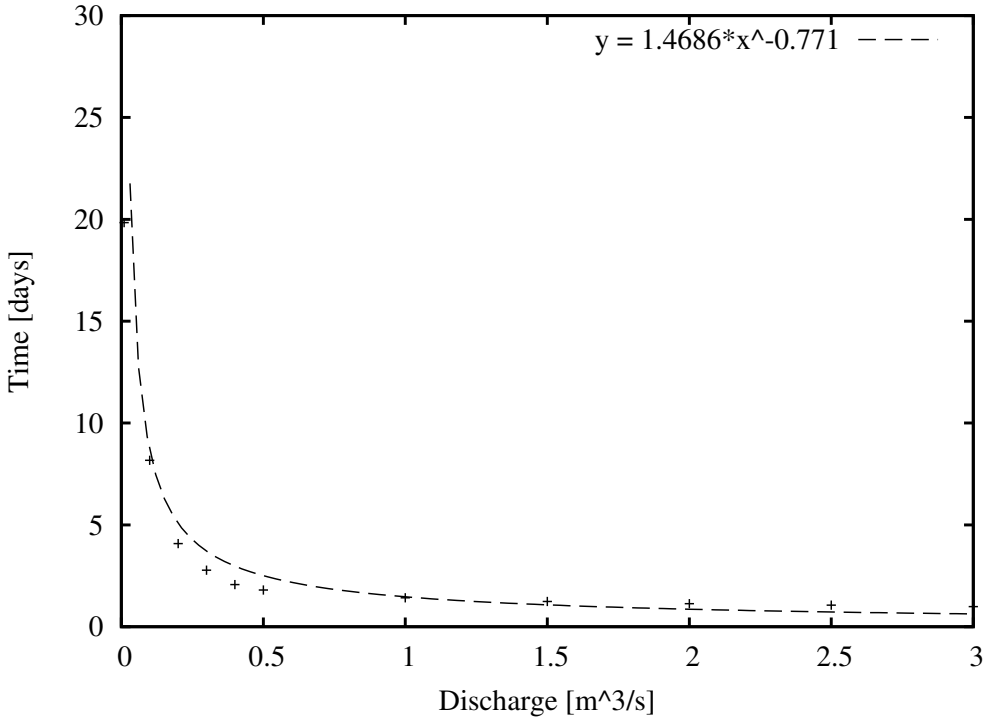

Figure E.18: Discharge-Time relationship between chainage 21000-21500m.

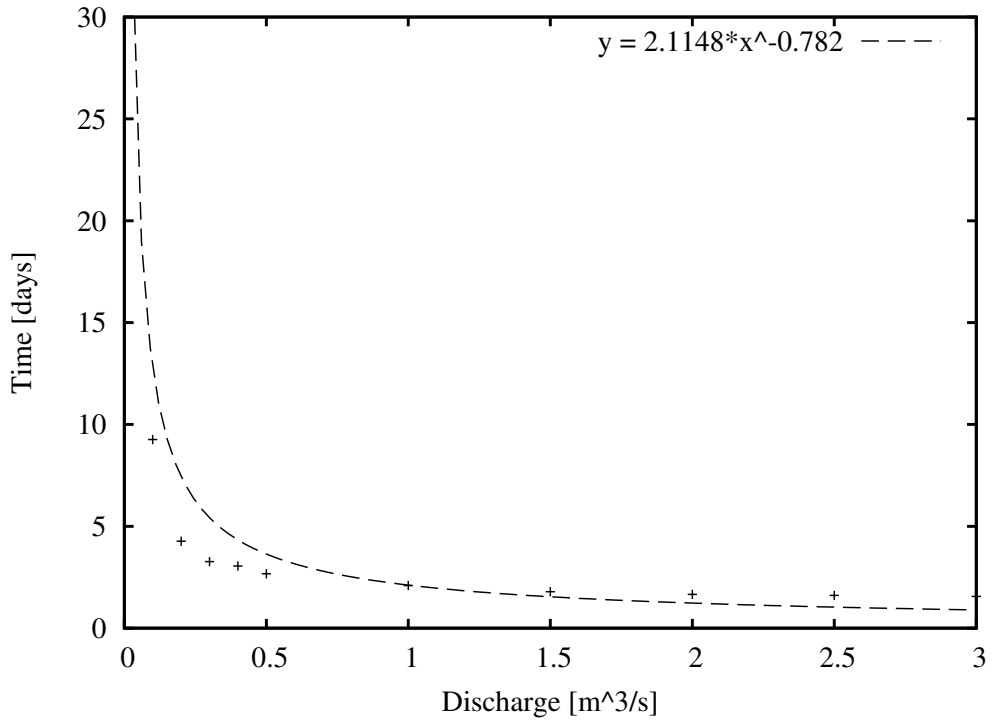

Figure E.19: Discharge-Time relationship between chainage 21500-22500m.

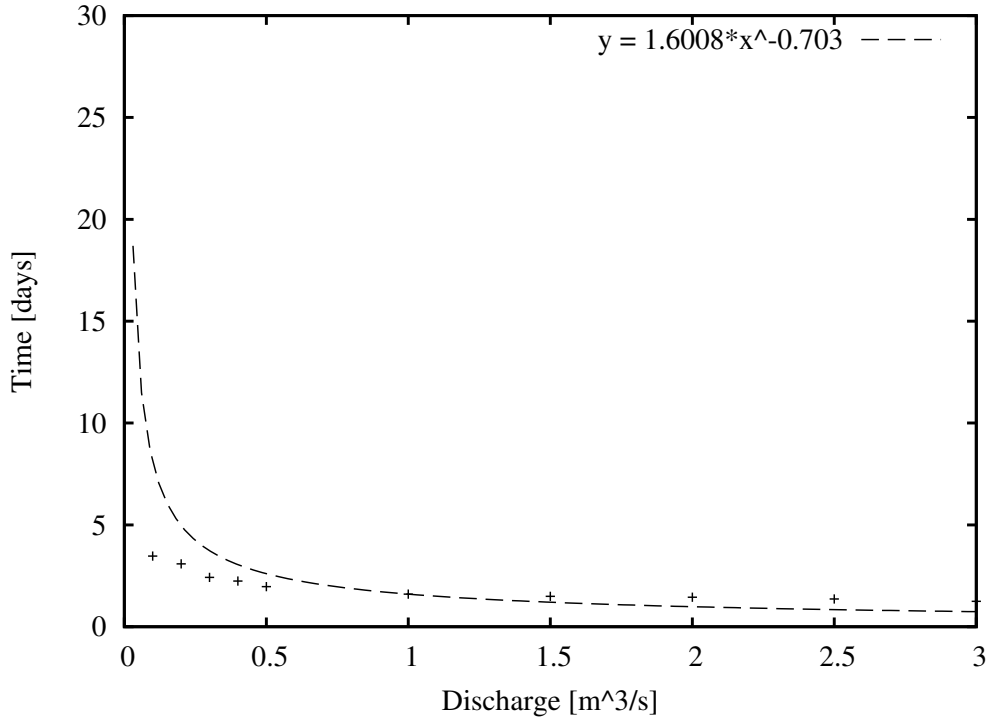

Figure E.20: Discharge-Time relationship between chainage 22500-23500m.

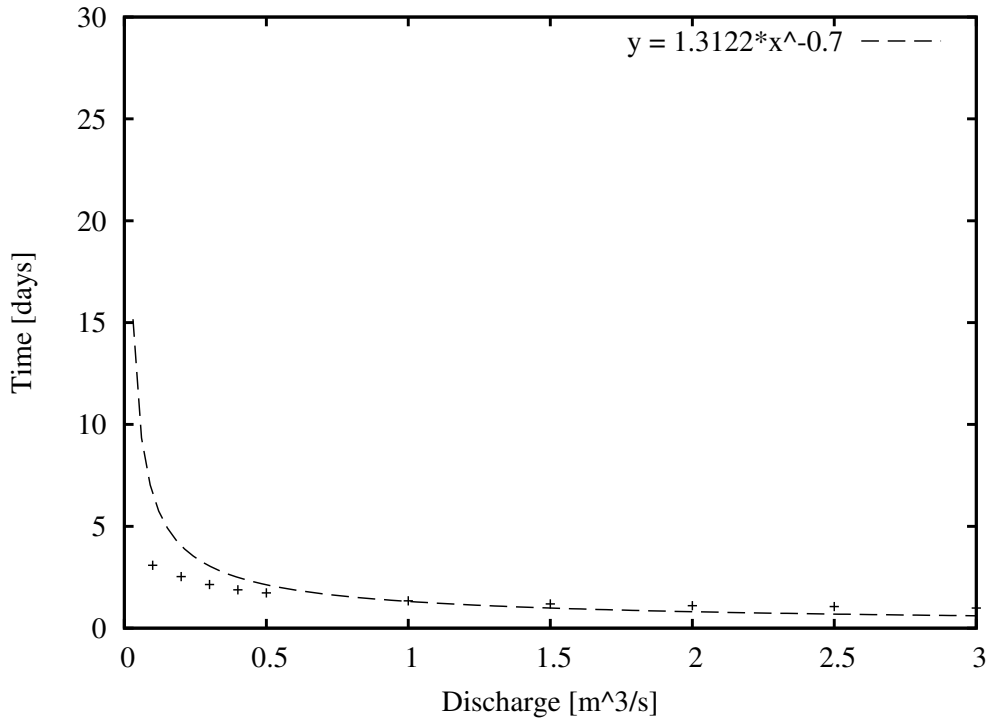

Figure E.21: Discharge-Time relationship between chainage 23500-24500m.

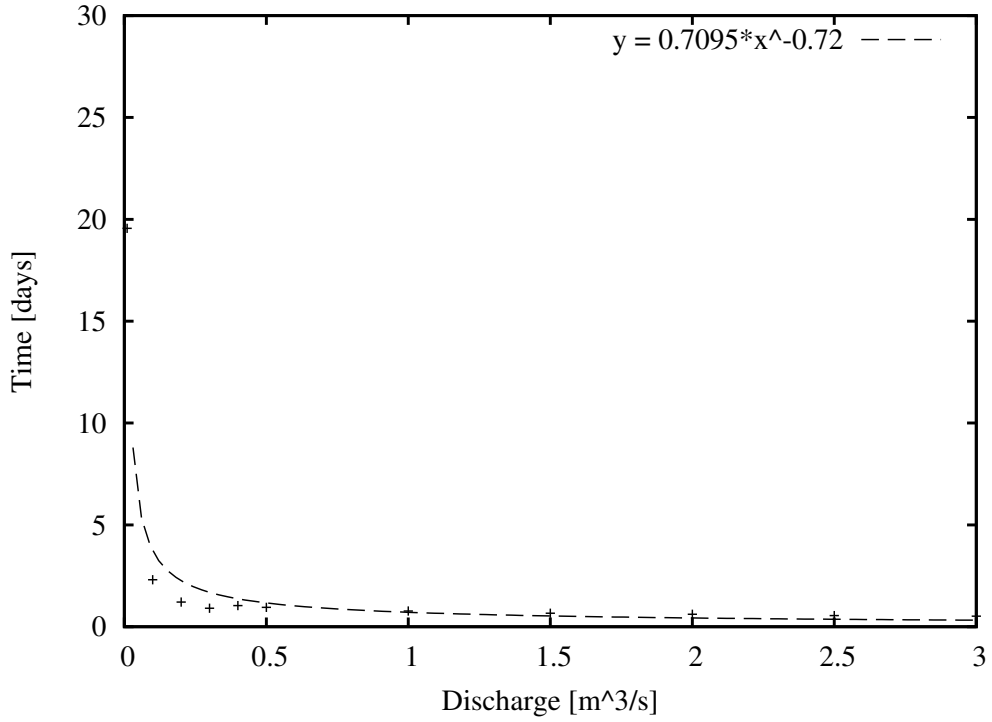

Figure E.22: Discharge-Time relationship between chainage 24500-25000m.

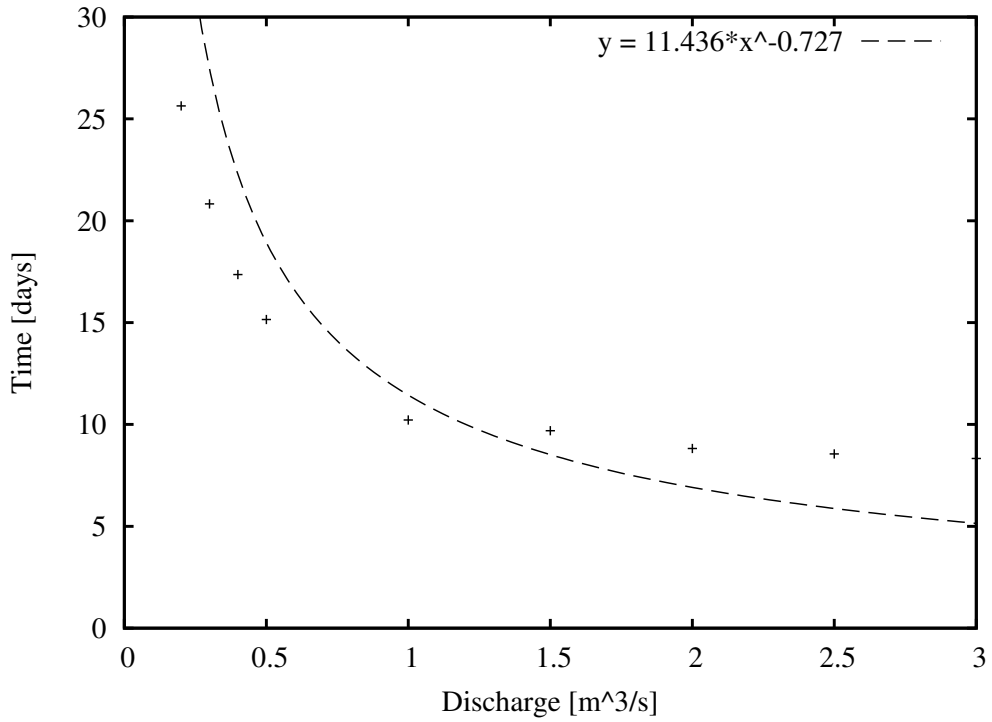

Figure E.23: Discharge-Time relationship between chainage 25000-31000m.

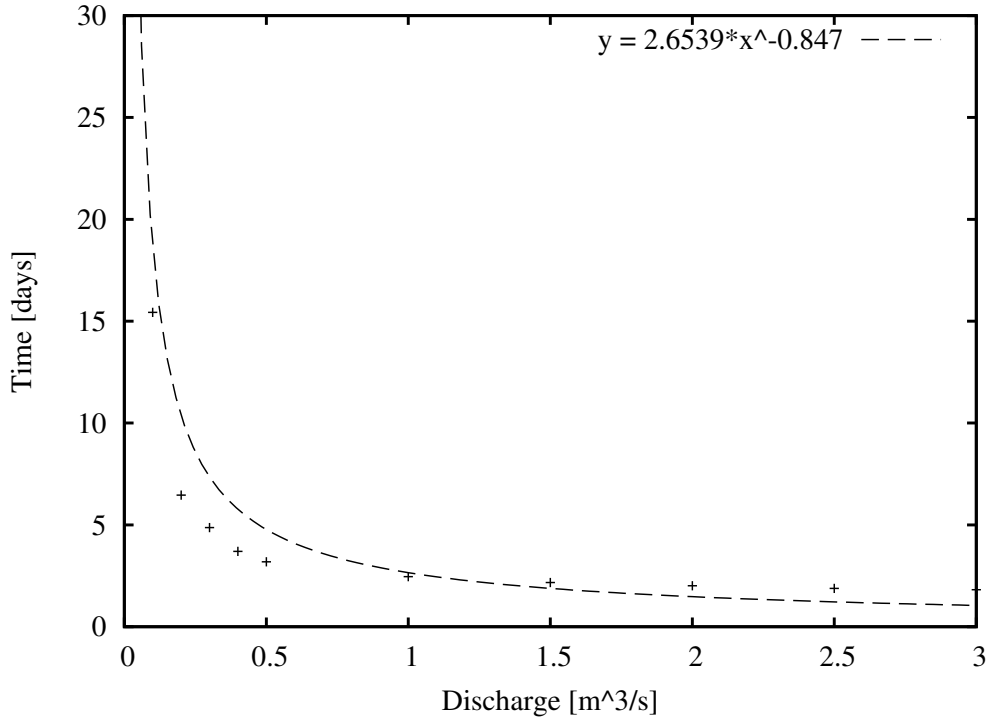

Figure E.24: Discharge-Time relationship between chainage 31000-32000m.

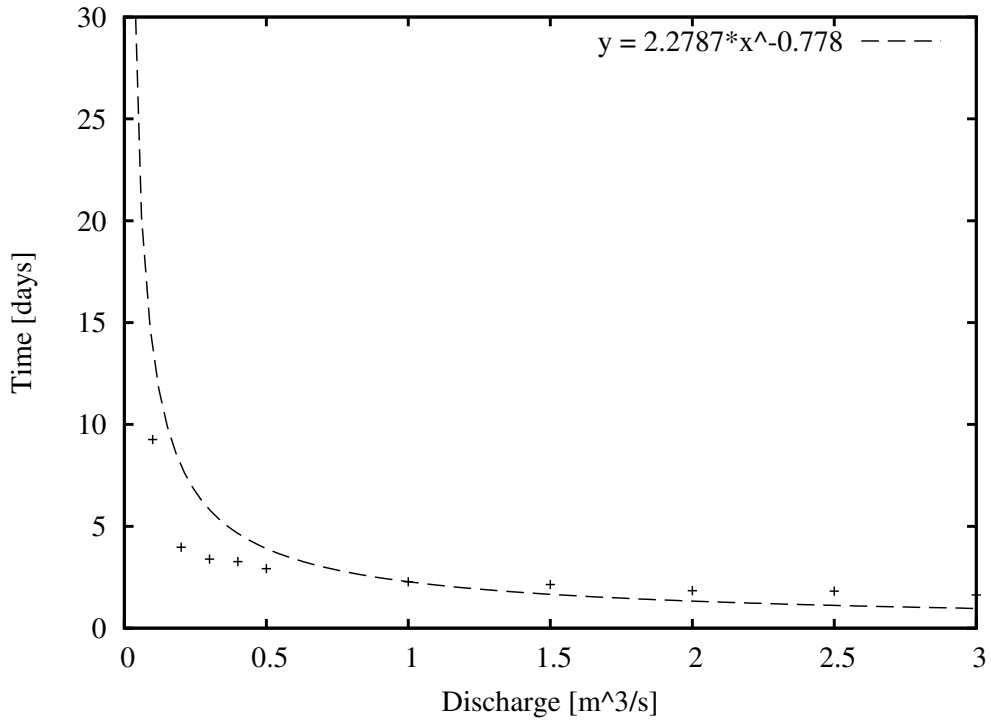

Figure E.25: Discharge-Time relationship between chainage 32000-33000m.

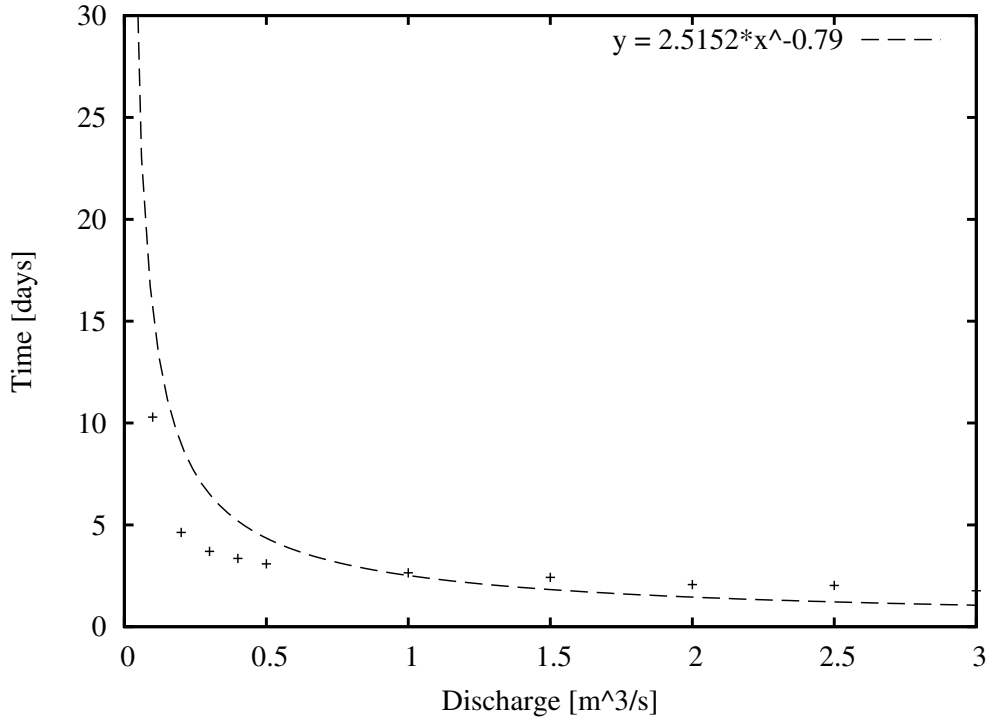

Figure E.26: Discharge-Time relationship between chainage 33000-34000m.

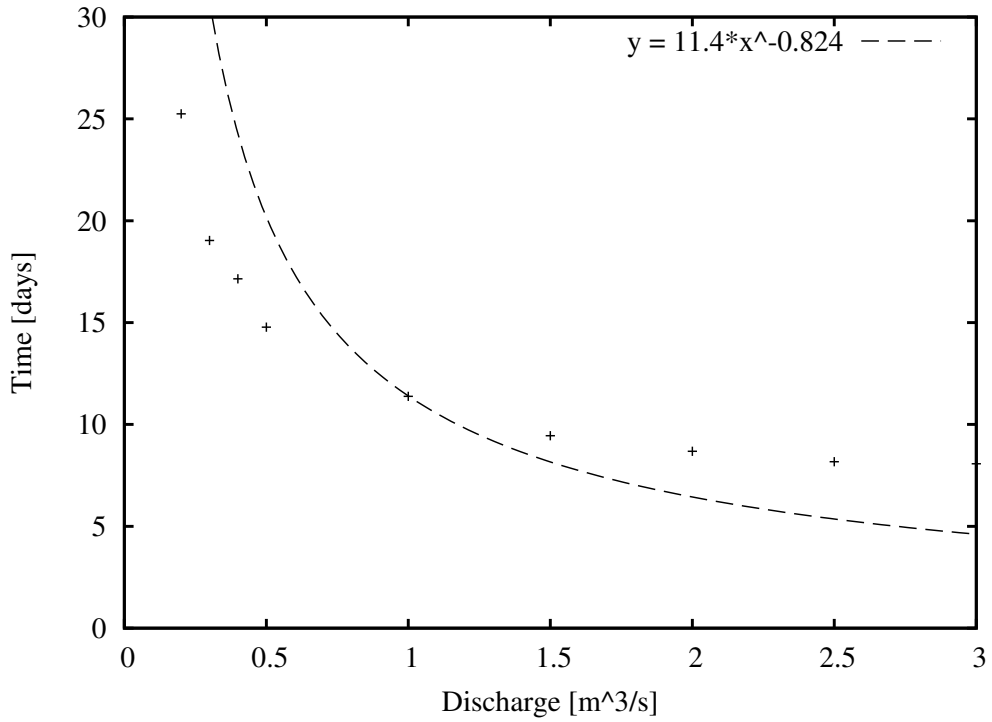

Figure E.27: Discharge-Time relationship between chainage 34000-39000m.

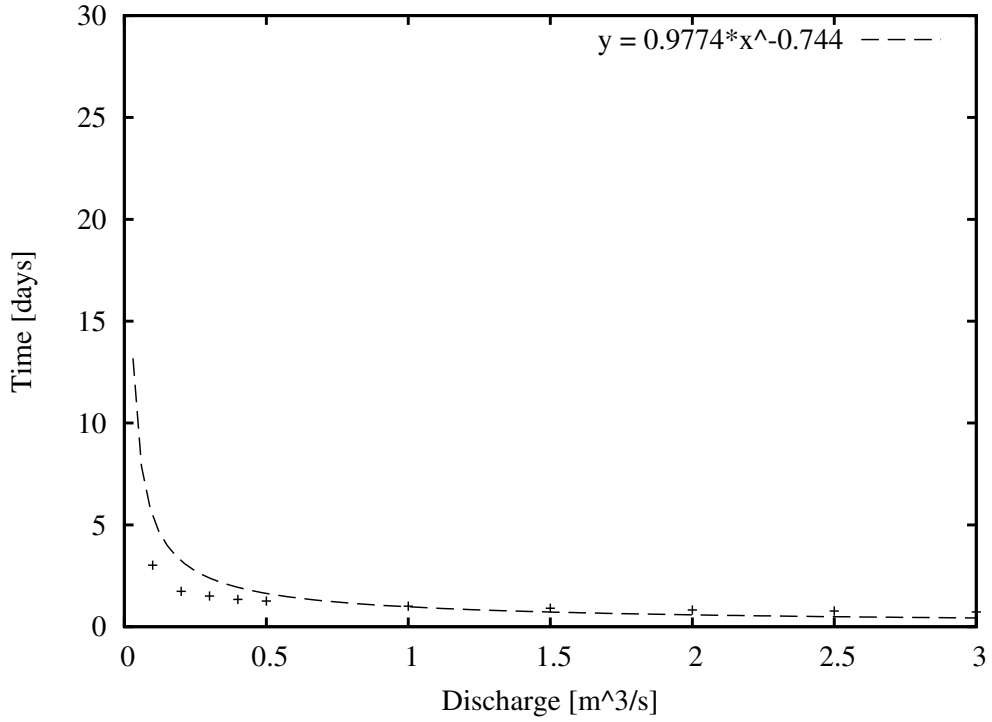

Figure E.28: Discharge-Time relationship between chainage 39000-39500m.

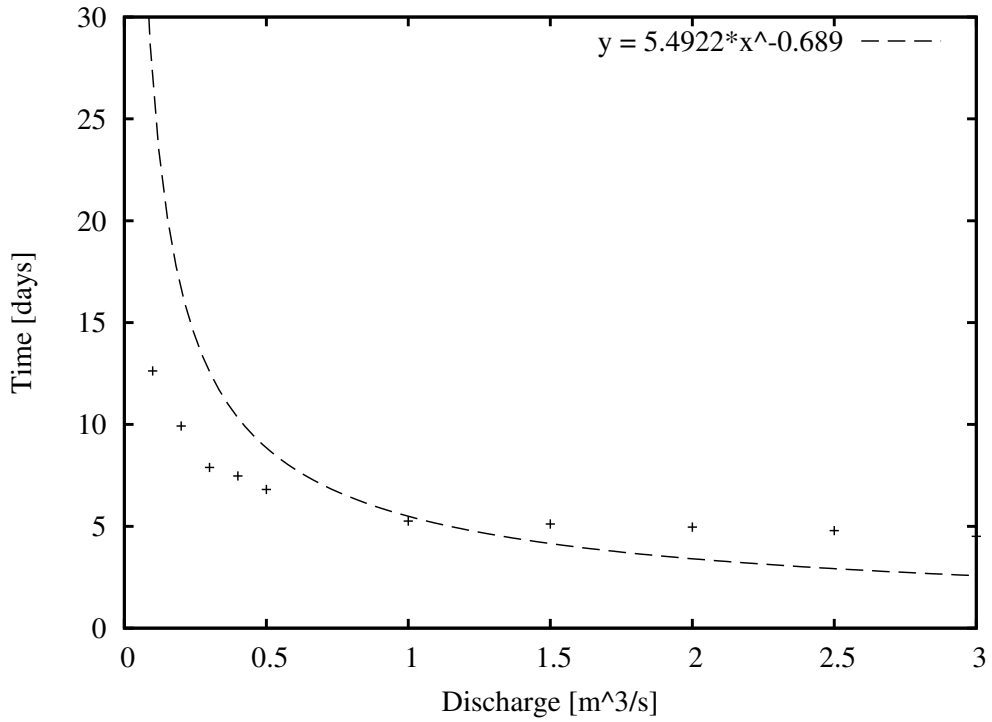

Figure E.29: Discharge-Time relationship between chainage 39500-42000m.

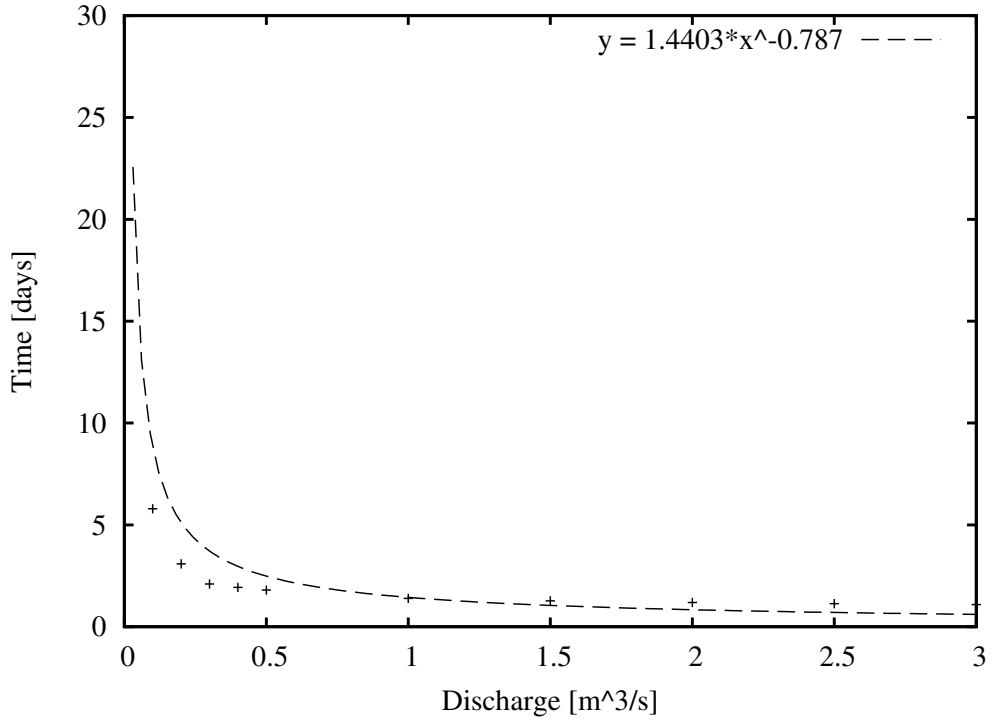

Figure E.30: Discharge-Time relationship between chainage 42000-42500m.

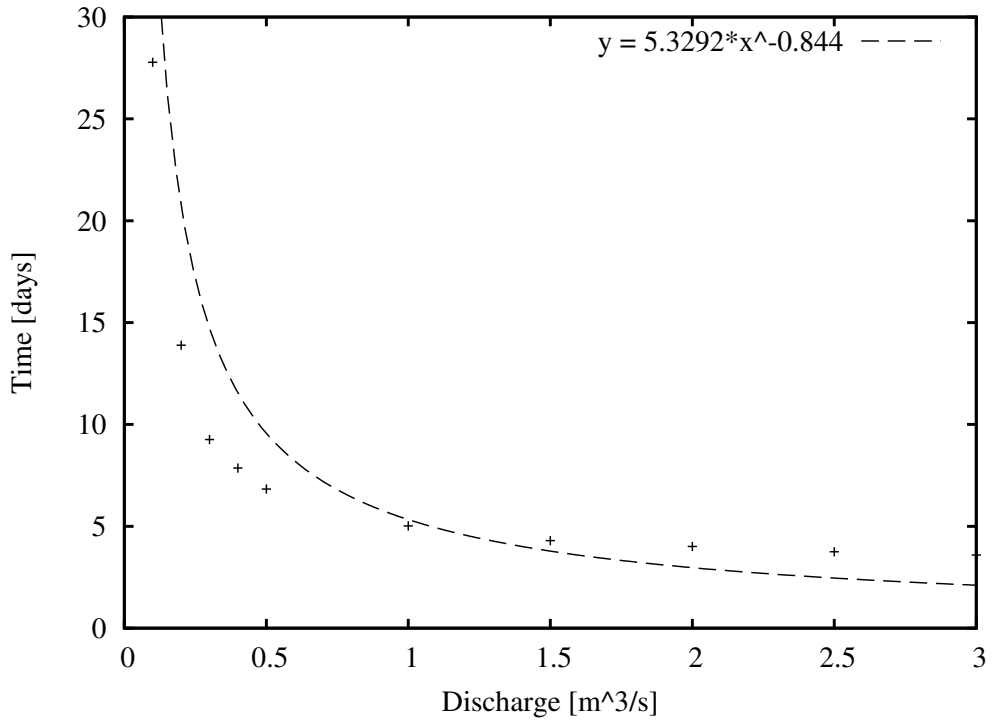

Figure E.31: Discharge-Time relationship between chainage 42500-44000m.

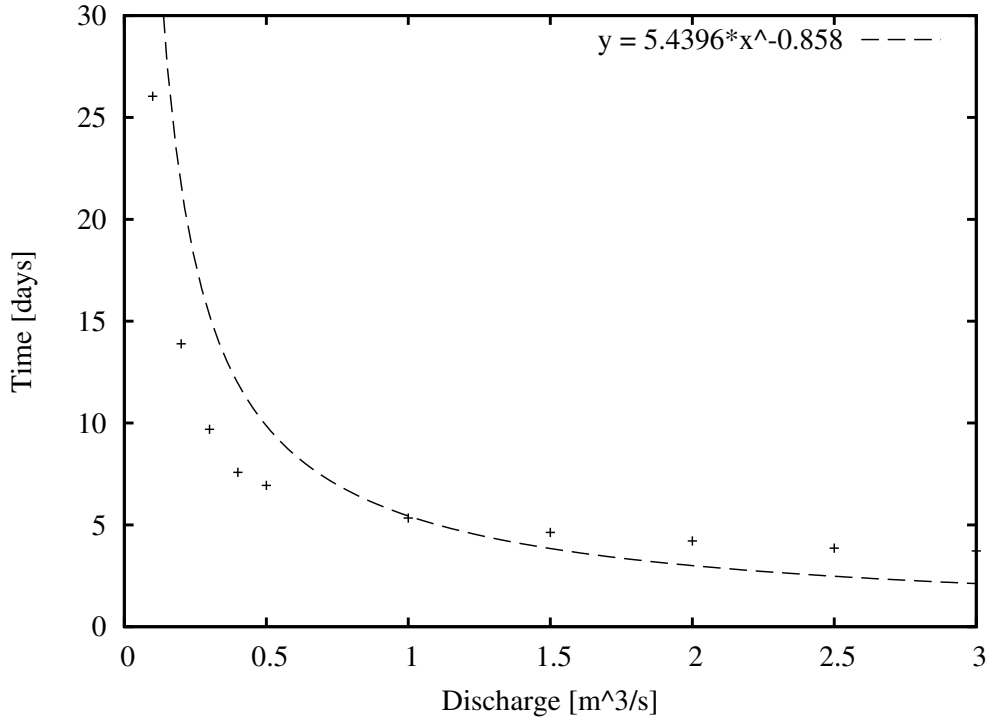

Figure E.32: Discharge-Time relationship between chainage 44000-45500m.

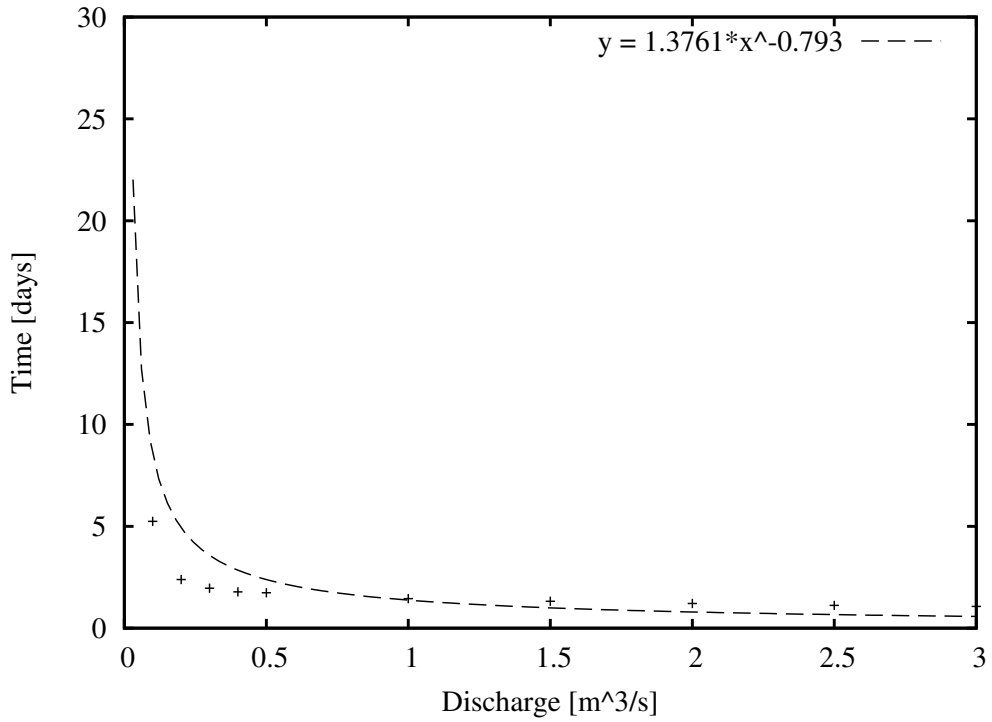

Figure E.33: Discharge-Time relationship between chainage 45500-46000m.

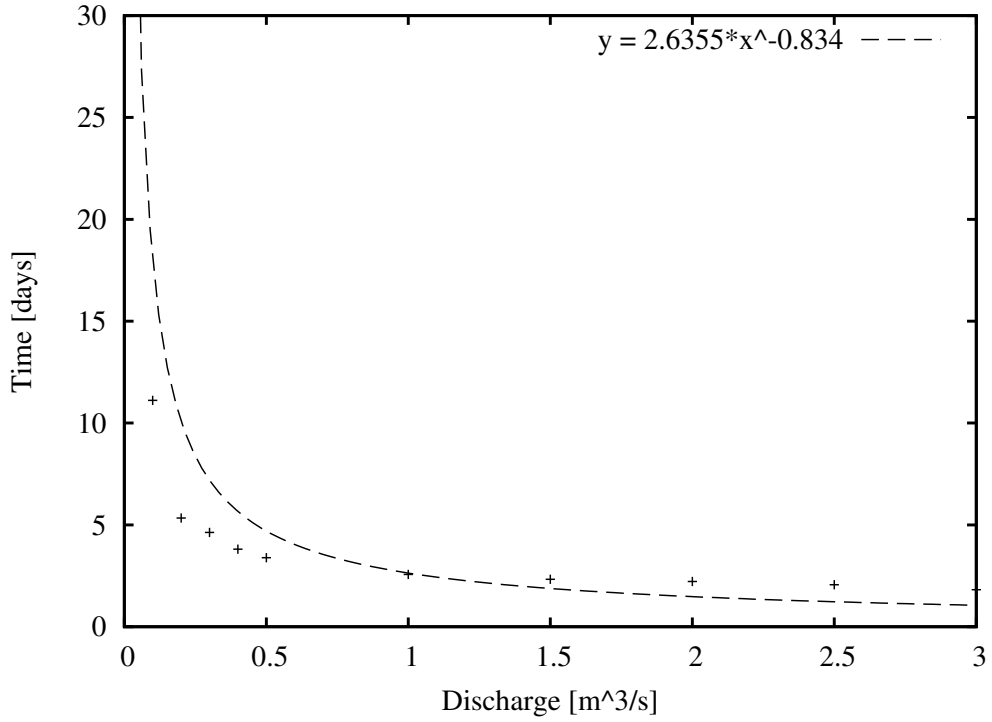

Figure E.34: Discharge-Time relationship between chainage 46000-47000m.

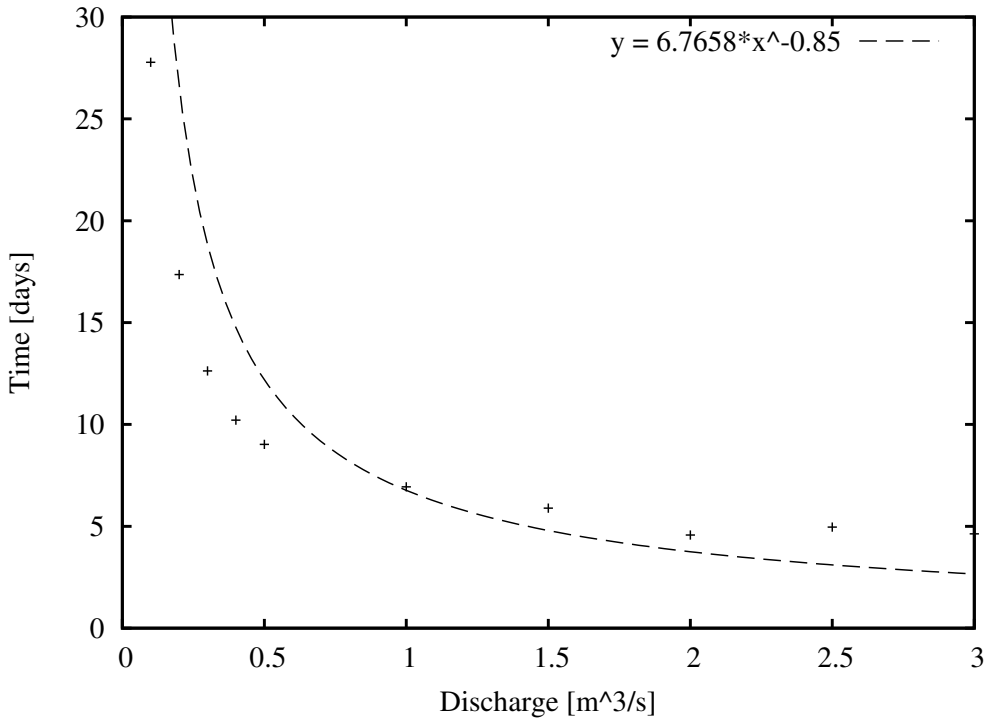

Figure E.35: Discharge-Time relationship between chainage 47000-49500m.

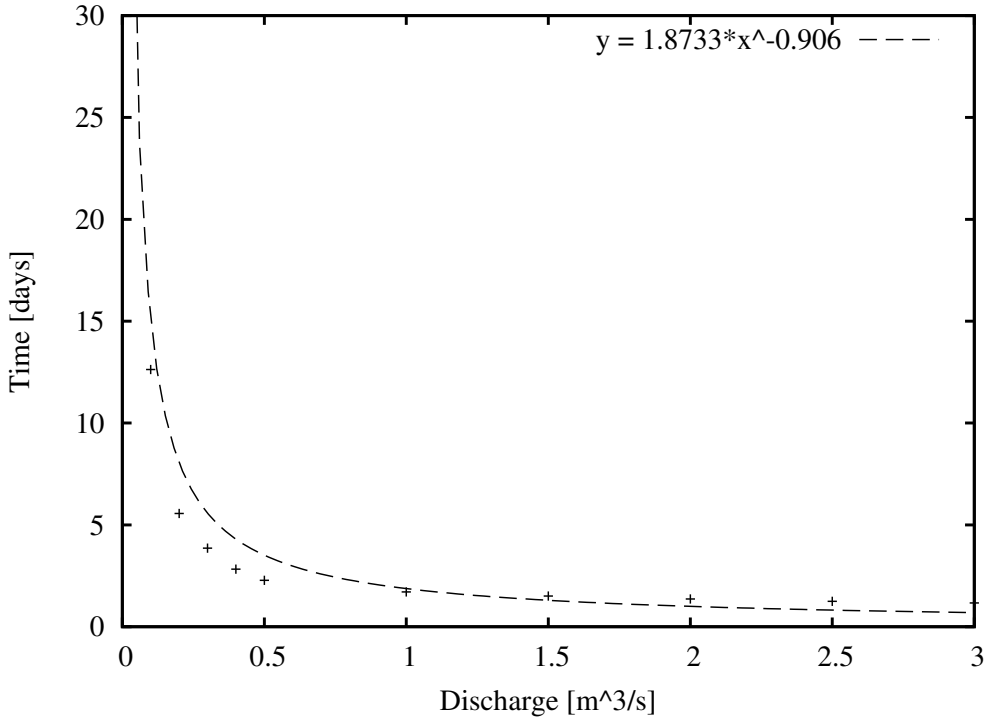

Figure E.36: Discharge-Time relationship between chainage 49500-50000m.

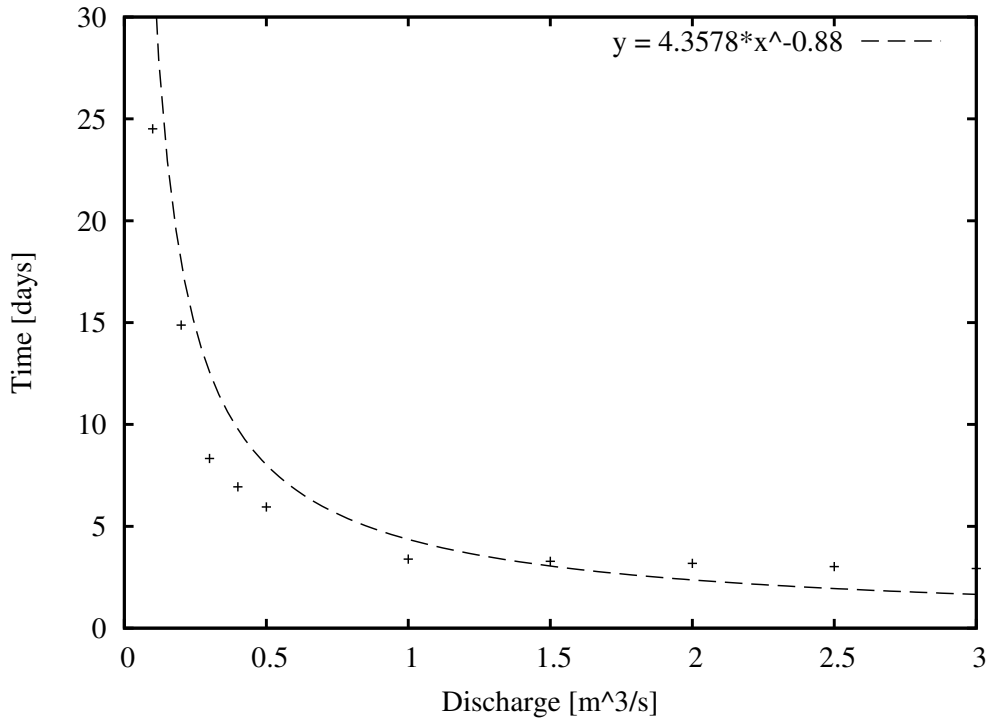

Figure E.37: Discharge-Time relationship between chainage 50000-51500m.

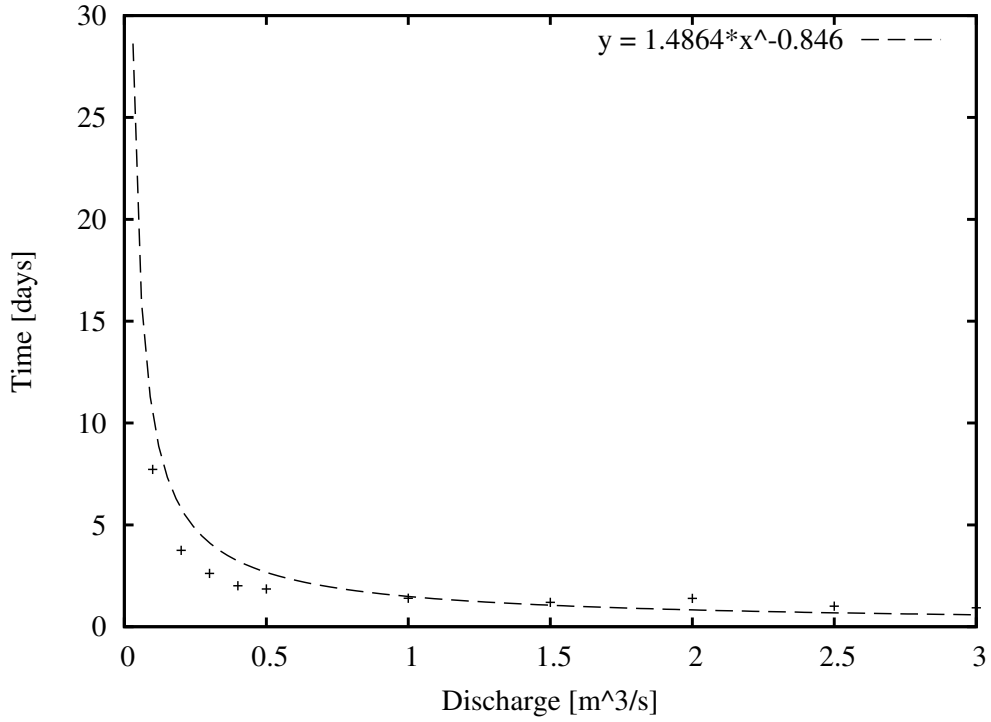

Figure E.38: Discharge-Time relationship between chainage 51500-52000m.

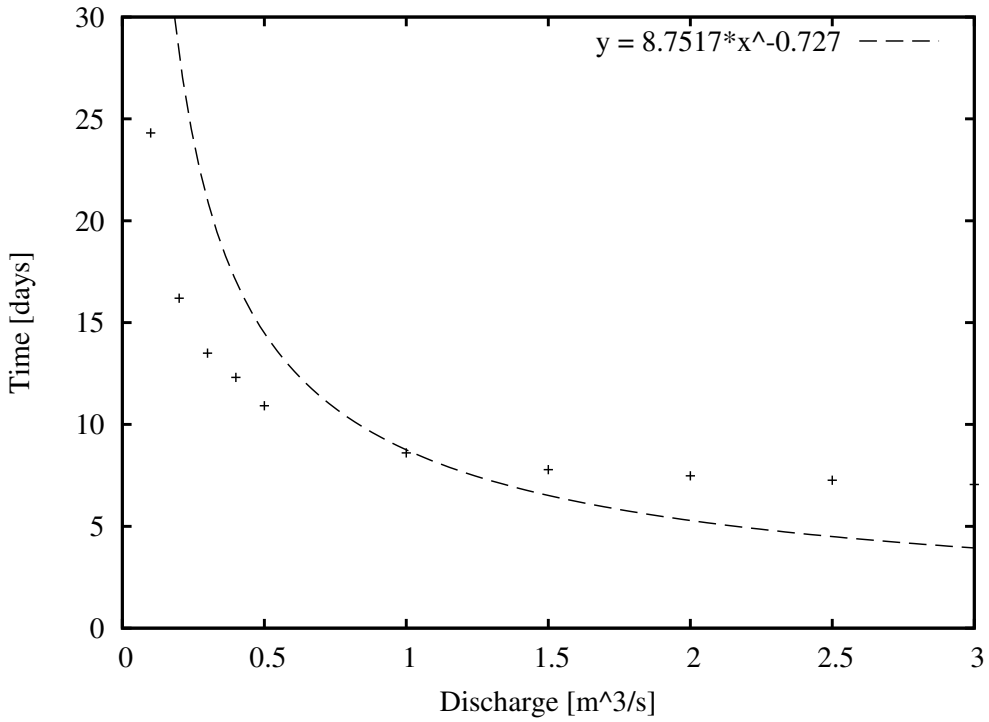

Figure E.39: Discharge-Time relationship between chainage 52000-55500.

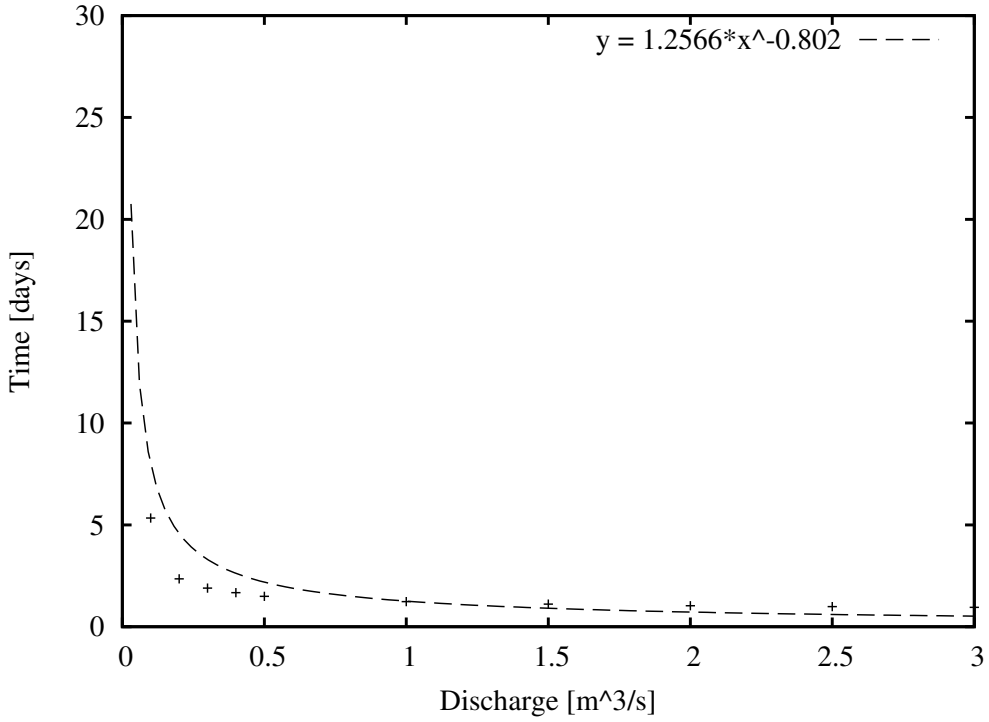

Figure E.40: Discharge-Time relationship between chainage 55500-56000m.

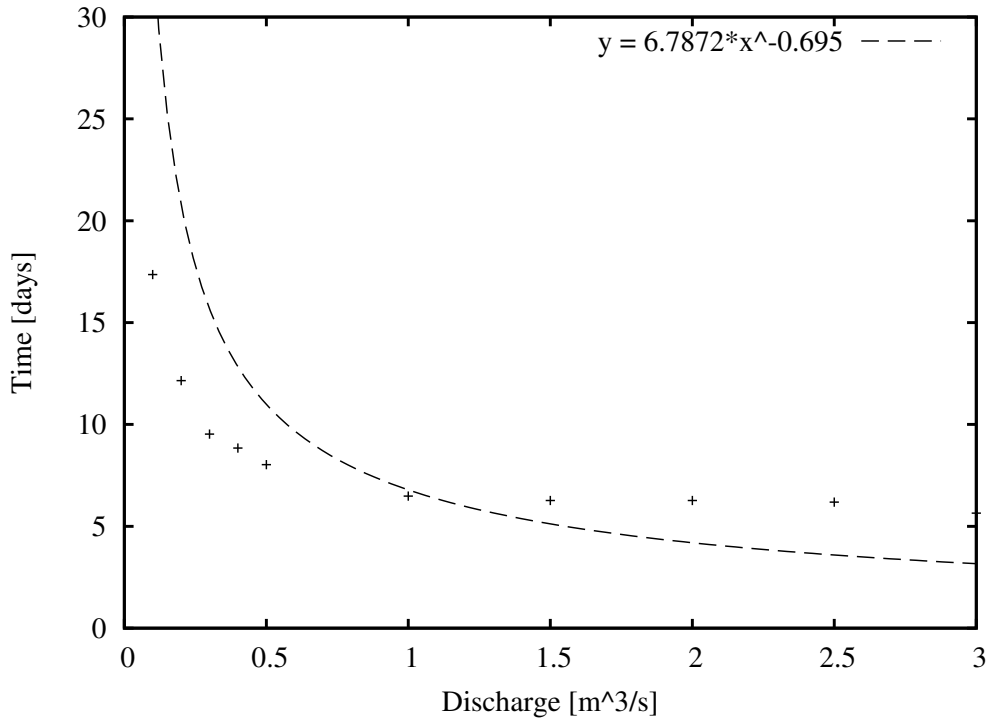

Figure E.41: Discharge-Time relationship between chainage 56000-59500m.

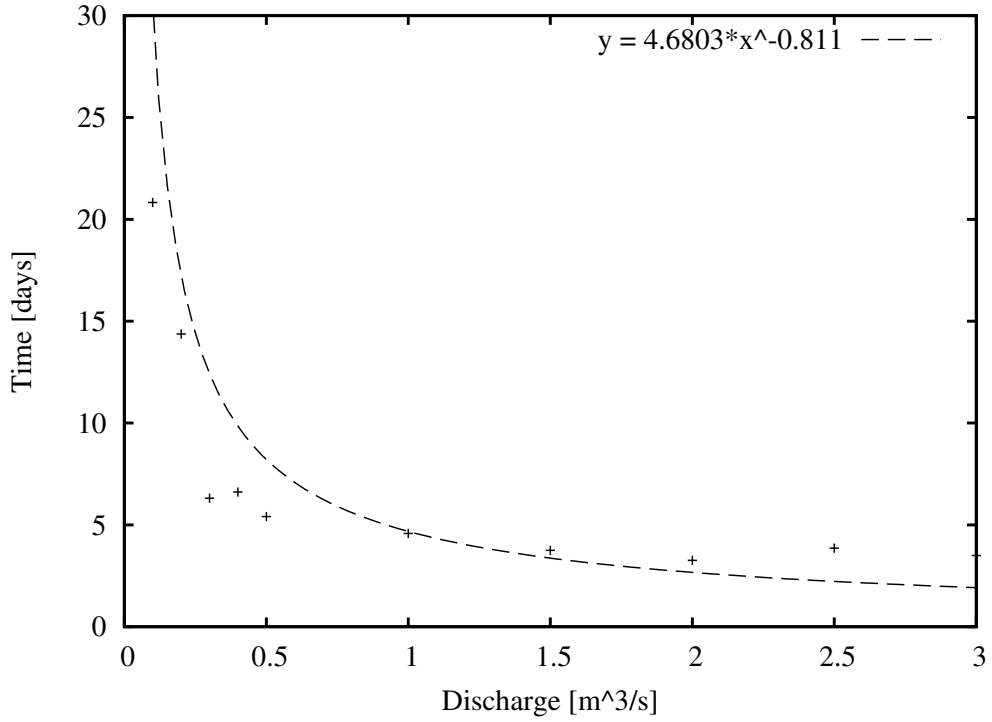

Figure E.42: Discharge-Time relationship between chainage 59500-61000m.

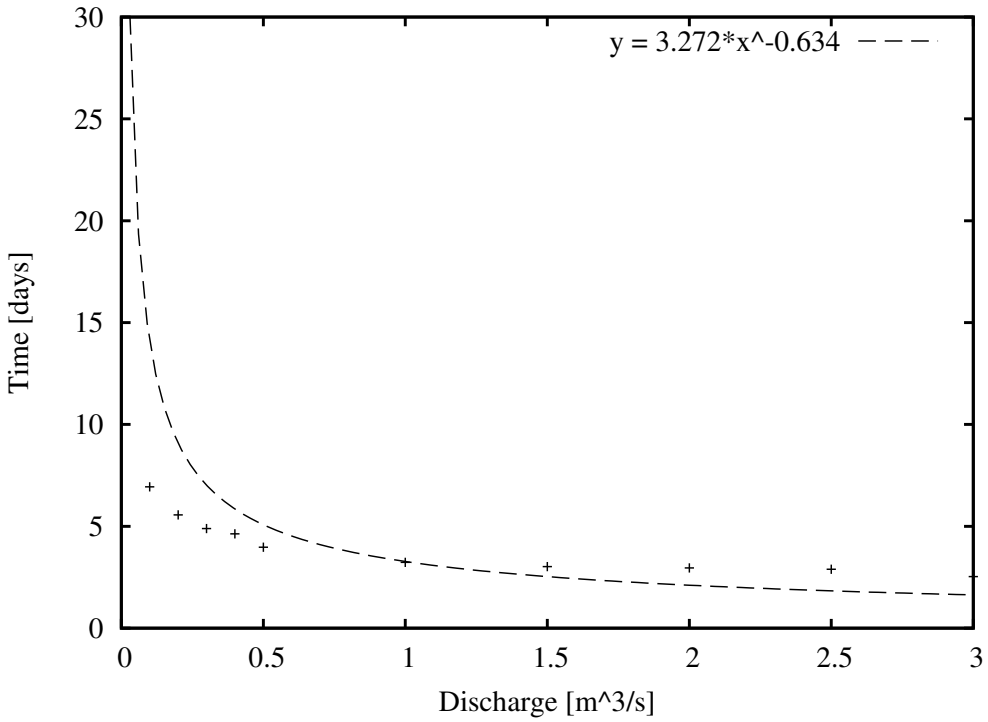

Figure E.43: Discharge-Time relationship between chainage 61000-61500m.

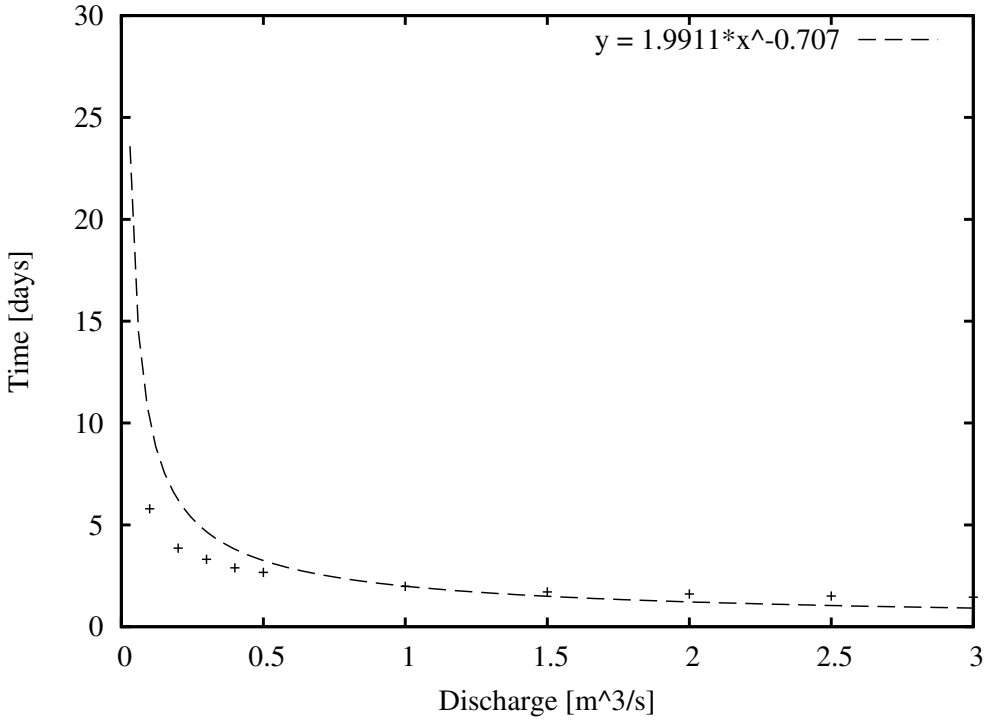

Figure E.44: Discharge-Time relationship between chainage 61500-62000m.

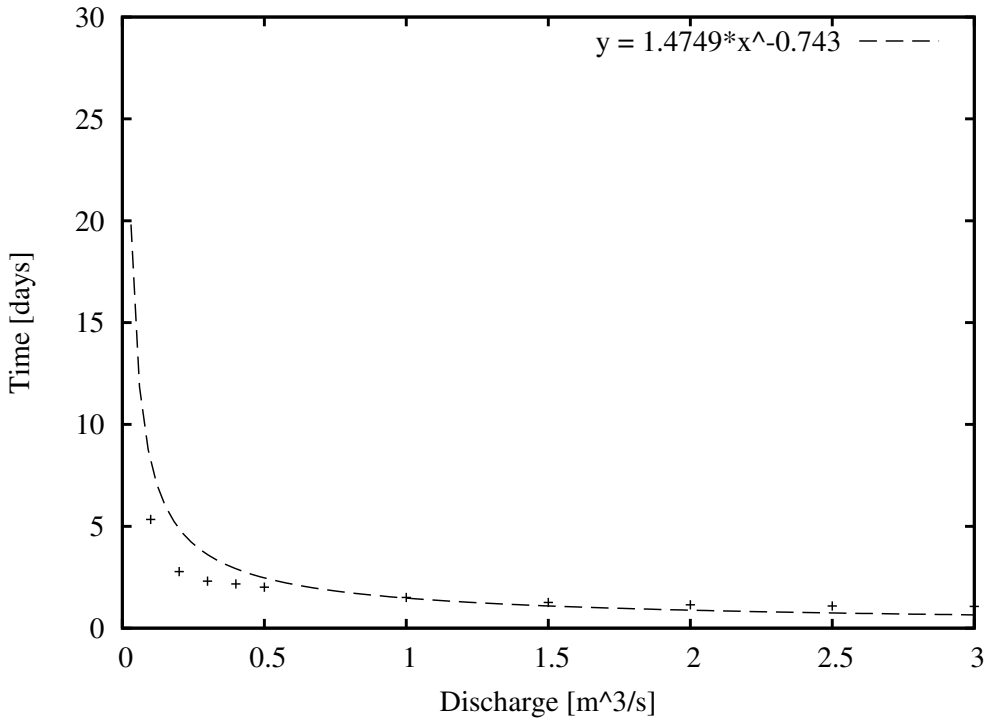

Figure E.45: Discharge-Time relationship between chainage 62000-62500m.

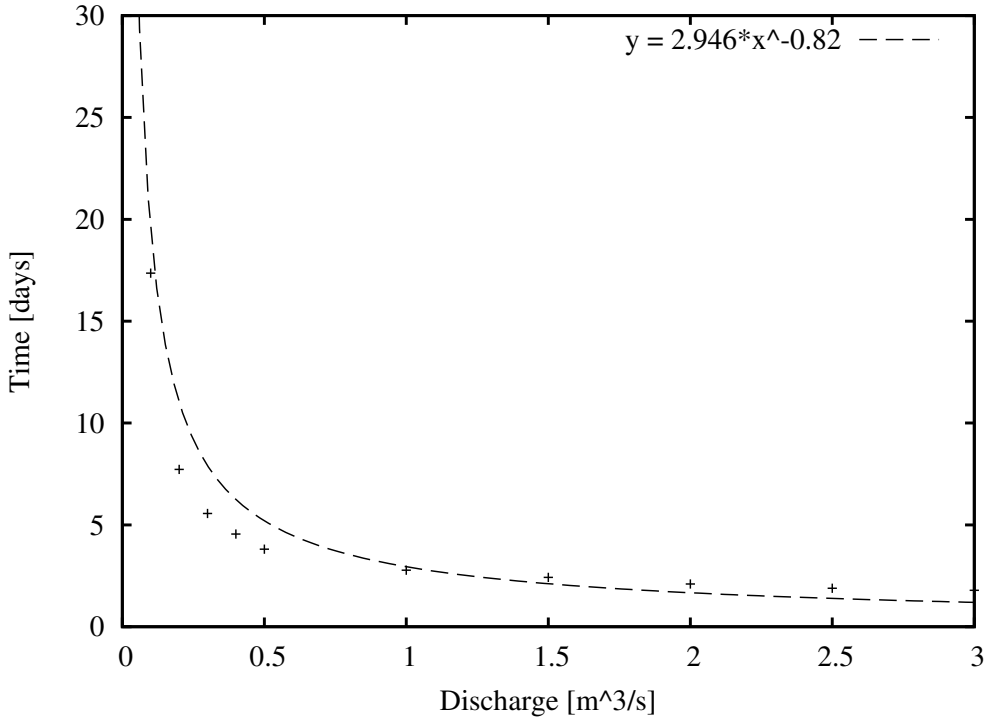

Figure E.46: Discharge-Time relationship between chainage 62500-63500m.

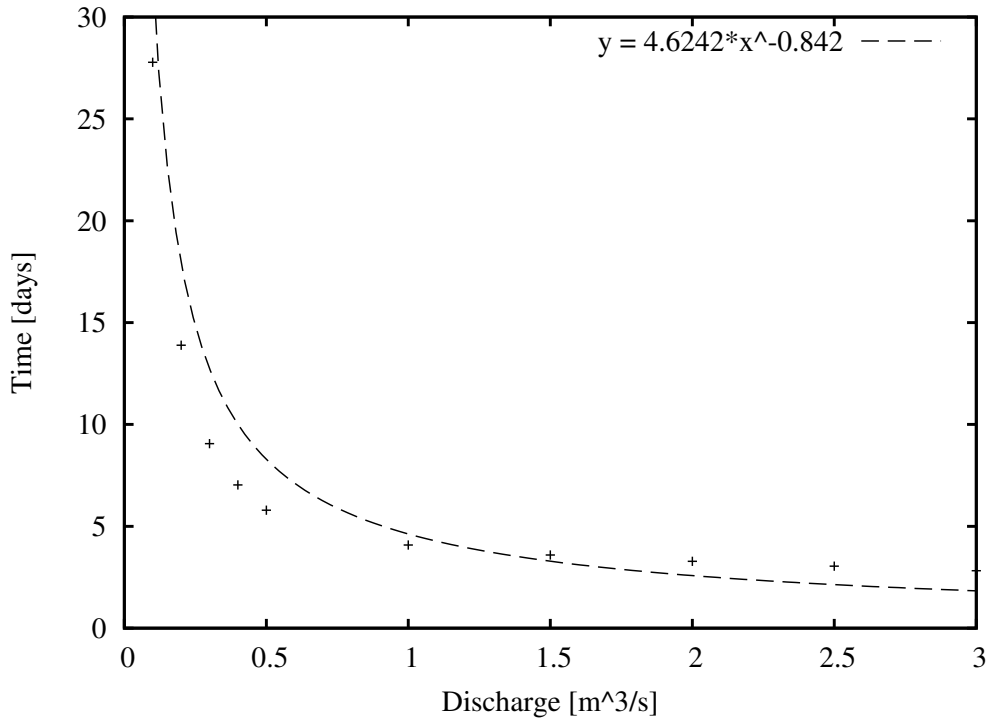

Figure E.47: Discharge-Time relationship between chainage 63500-65000m.

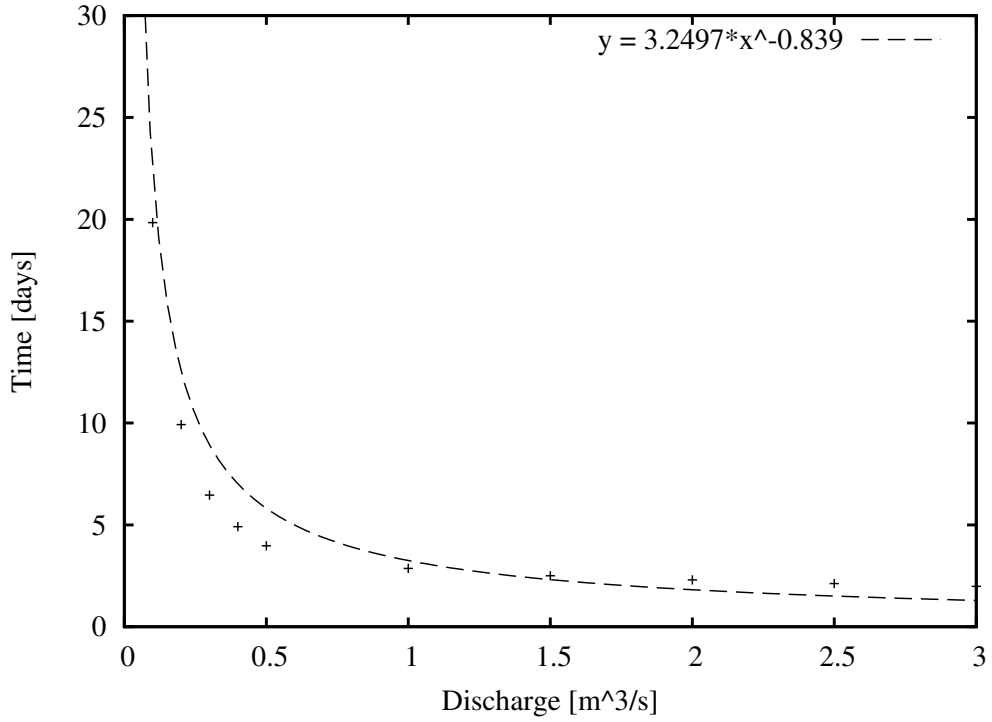

Figure E.48: Discharge-Time relationship between chainage 65000-66000m.

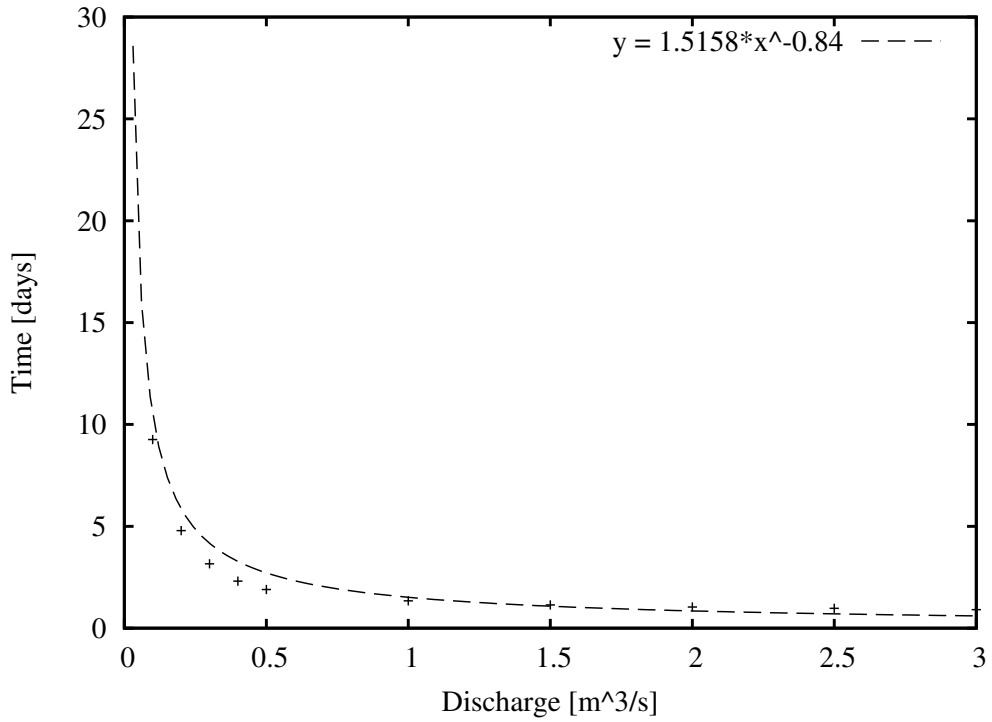

Figure E.49: Discharge-Time relationship between chainage 66000-66500m.

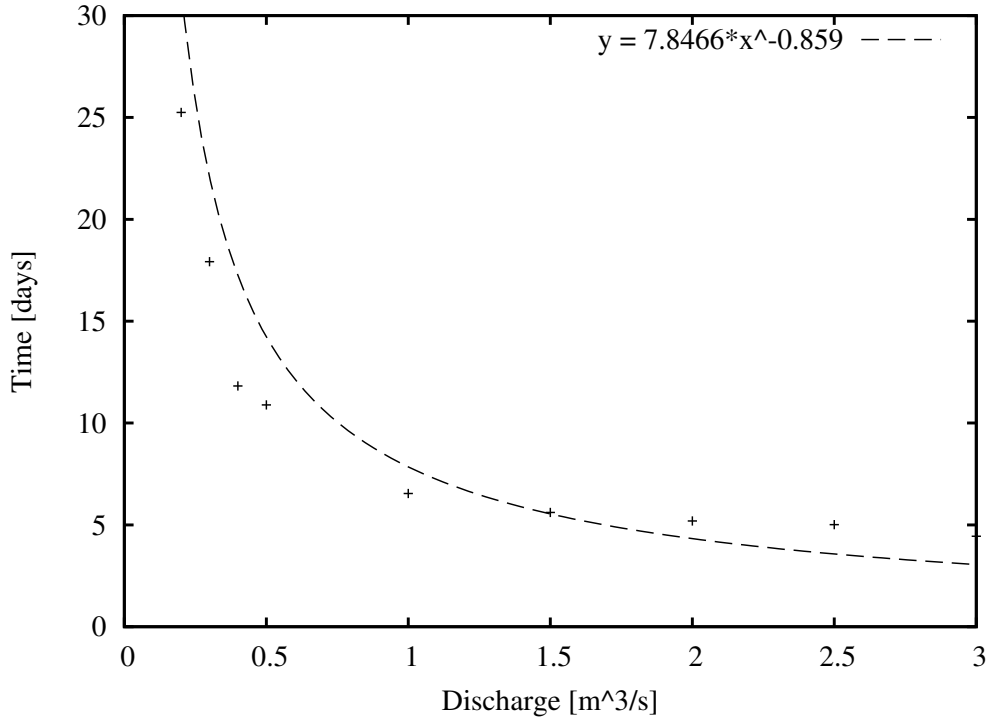

Figure E.50: Discharge-Time relationship between chainage 66500-68500m.

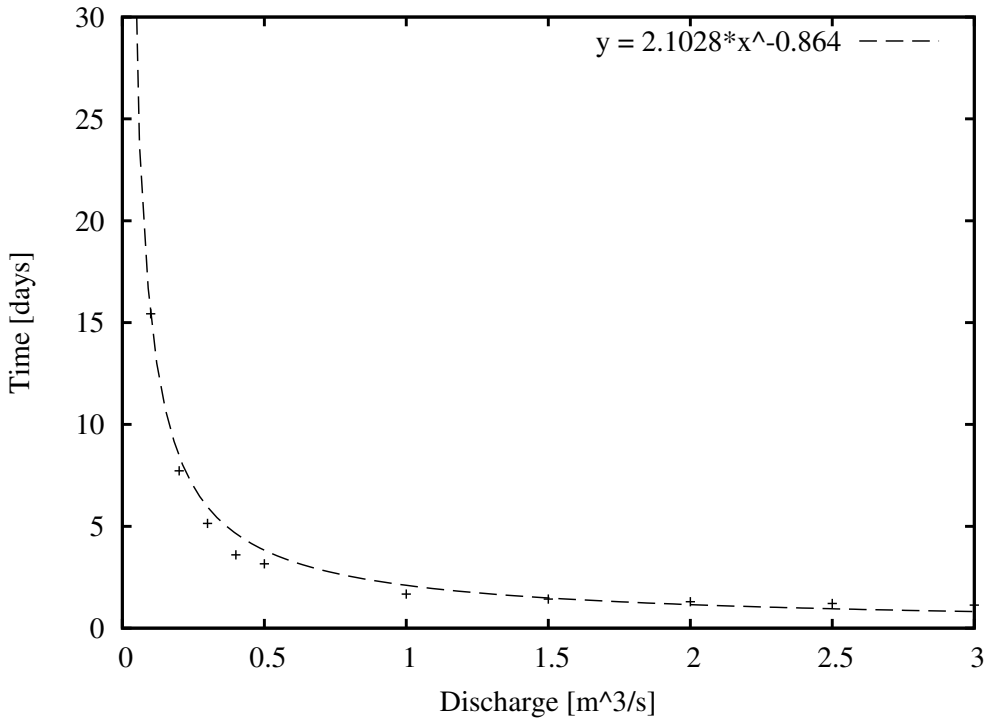

Figure E.51: Discharge-Time relationship between chainage 68500-69000m.

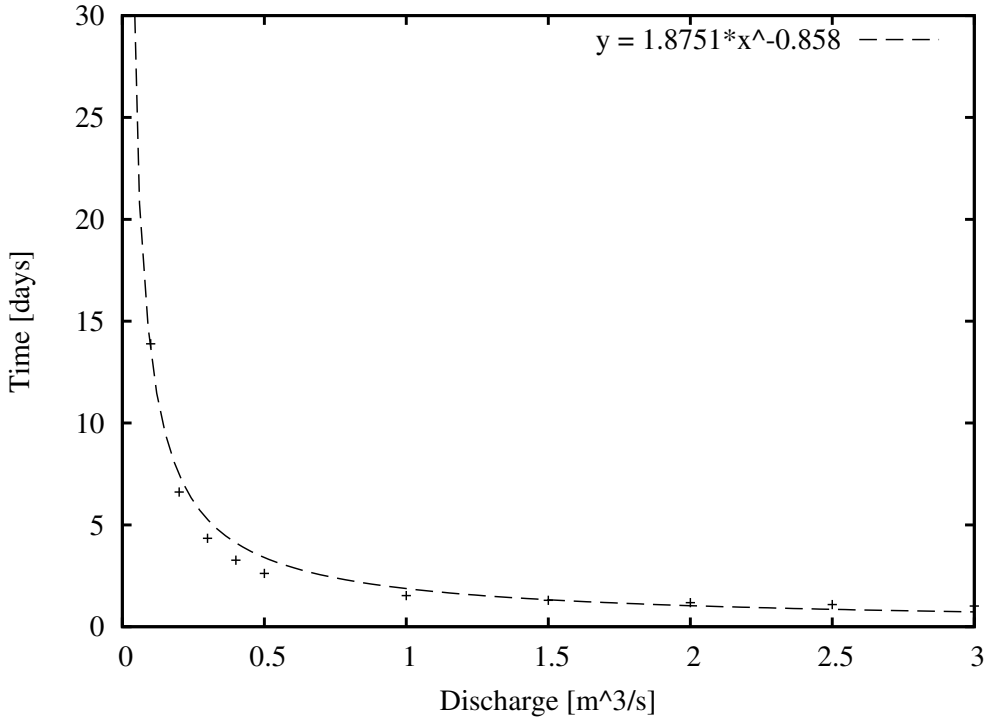

Figure E.52: Discharge-Time relationship between chainage 69000-69500m.

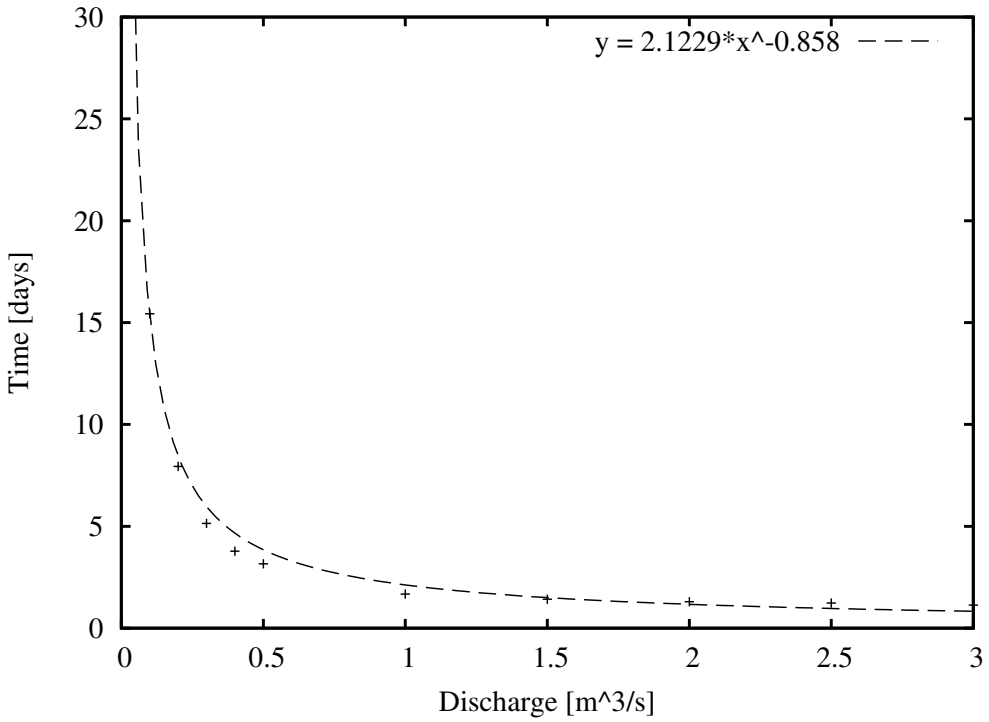

Figure E.53: Discharge-Time relationship between chainage 69500-70000m.

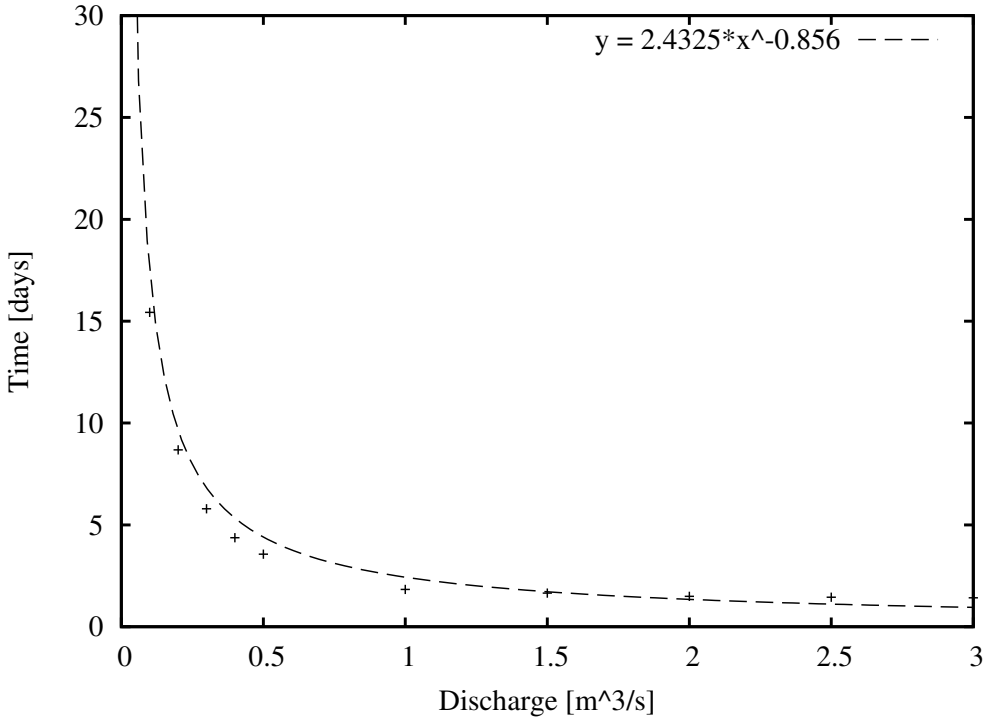

Figure E.54: Discharge-Time relationship between chainage 70000-70500m.

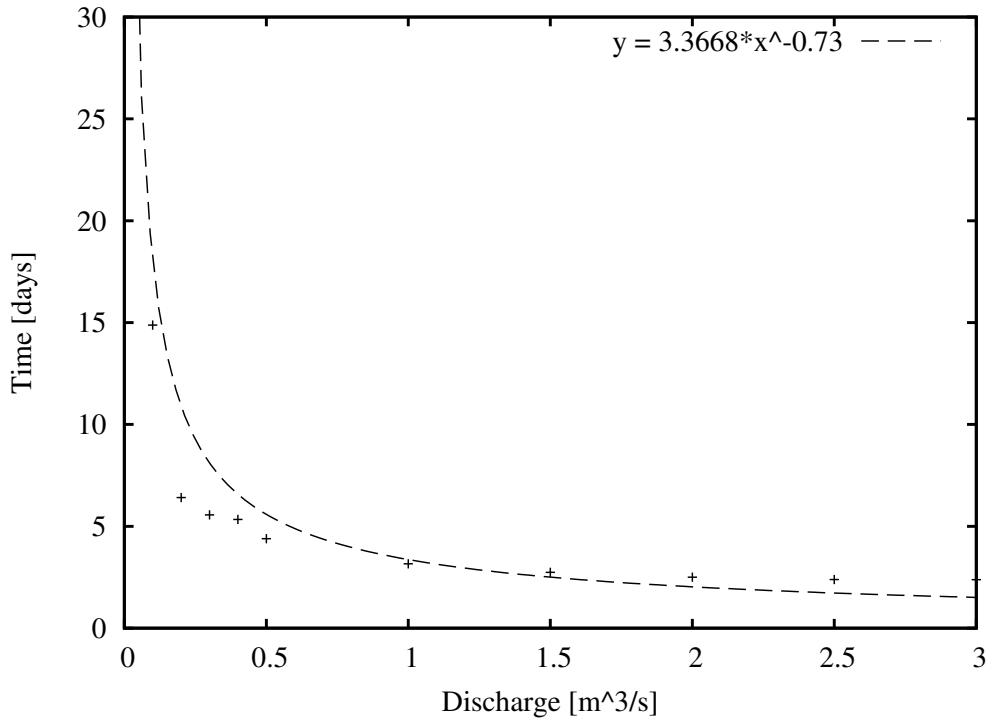

Figure E.55: Discharge-Time relationship between chainage 70500-72000m.

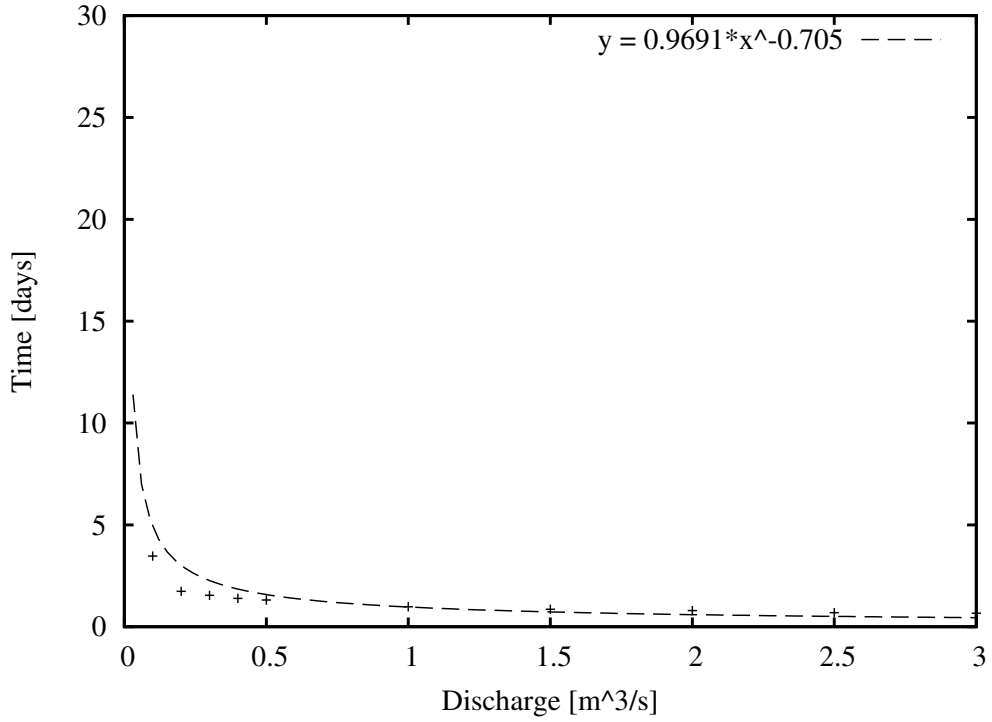

Figure E.56: Discharge-Time relationship between chainage 72000-72500m.

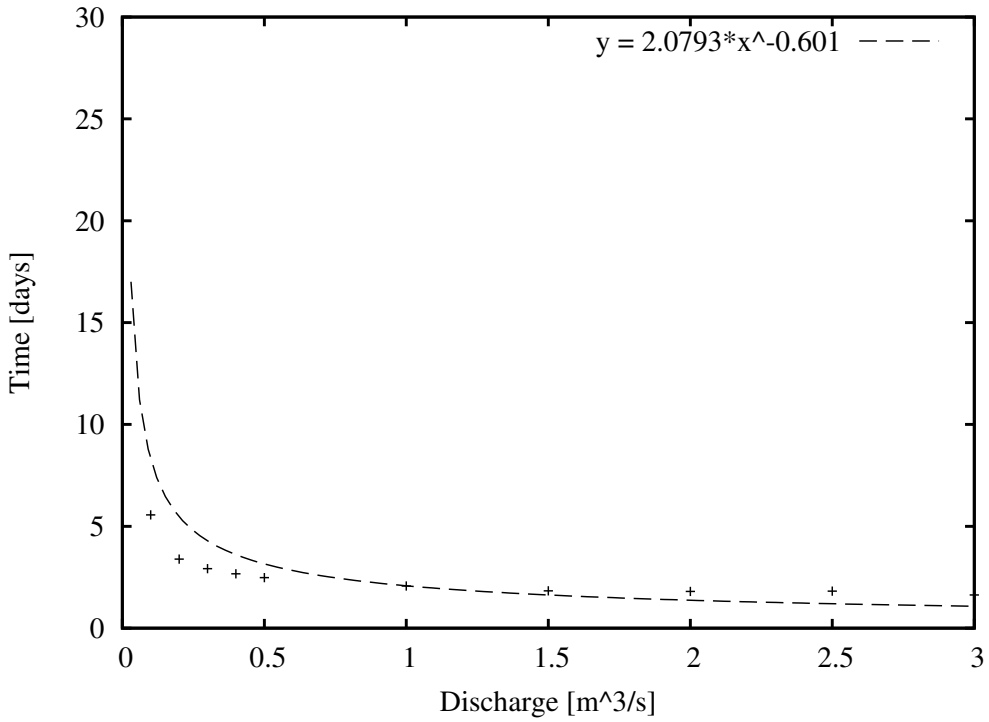

Figure E.57: Discharge-Time relationship between chainage 72500-73500m.

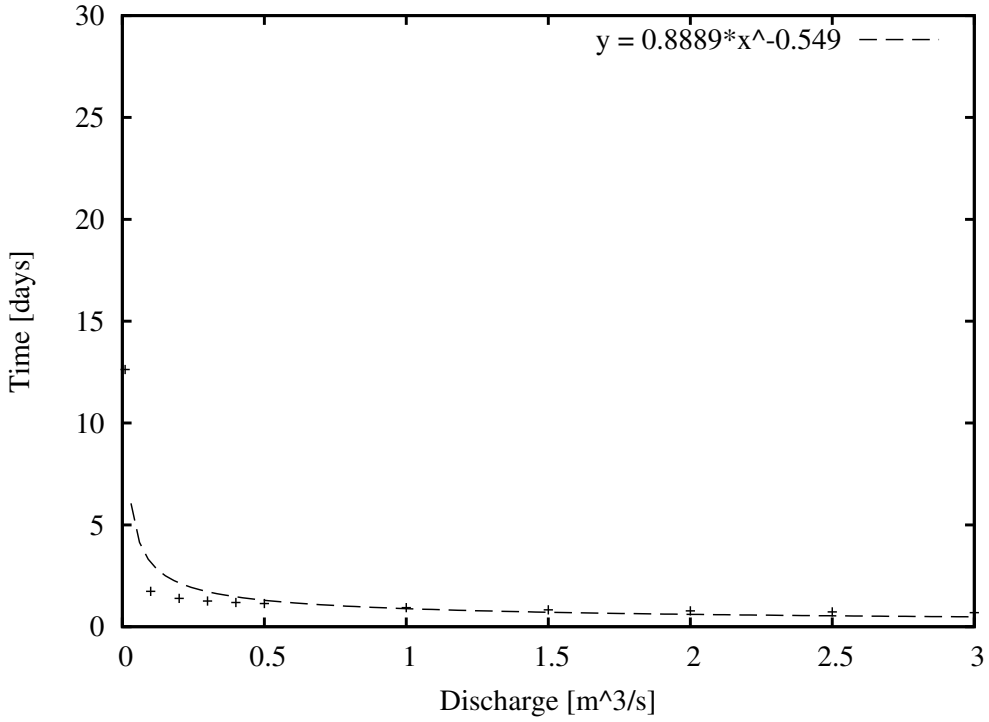

Figure E.58: Discharge-Time relationship between chainage 73500-74000.

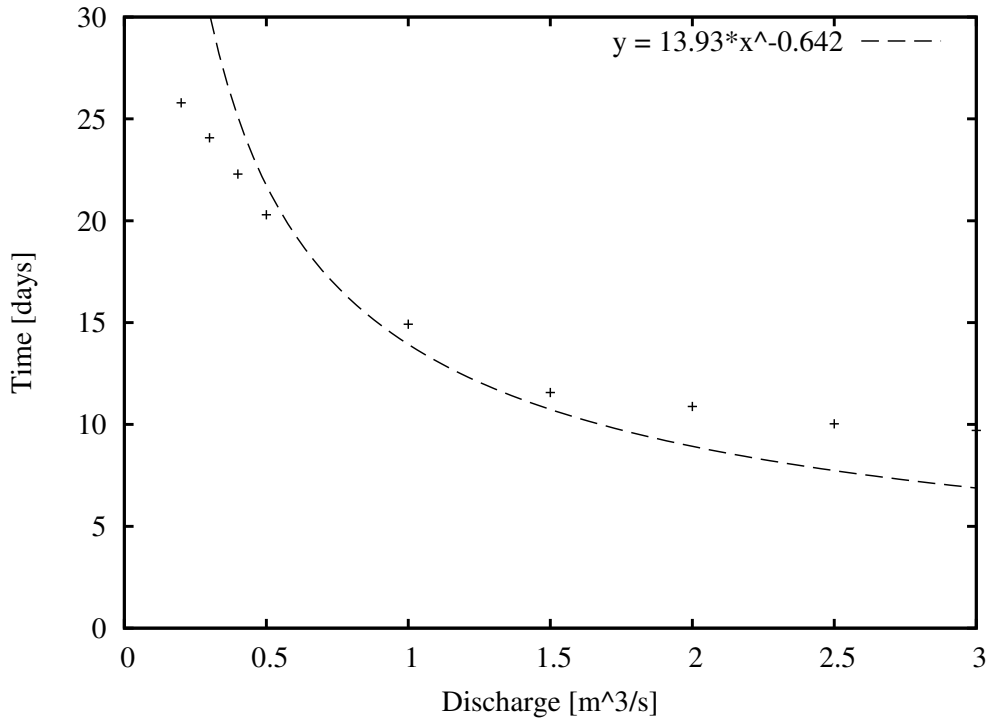

Figure E.59: Discharge-Time relationship between chainage 74000-80500.

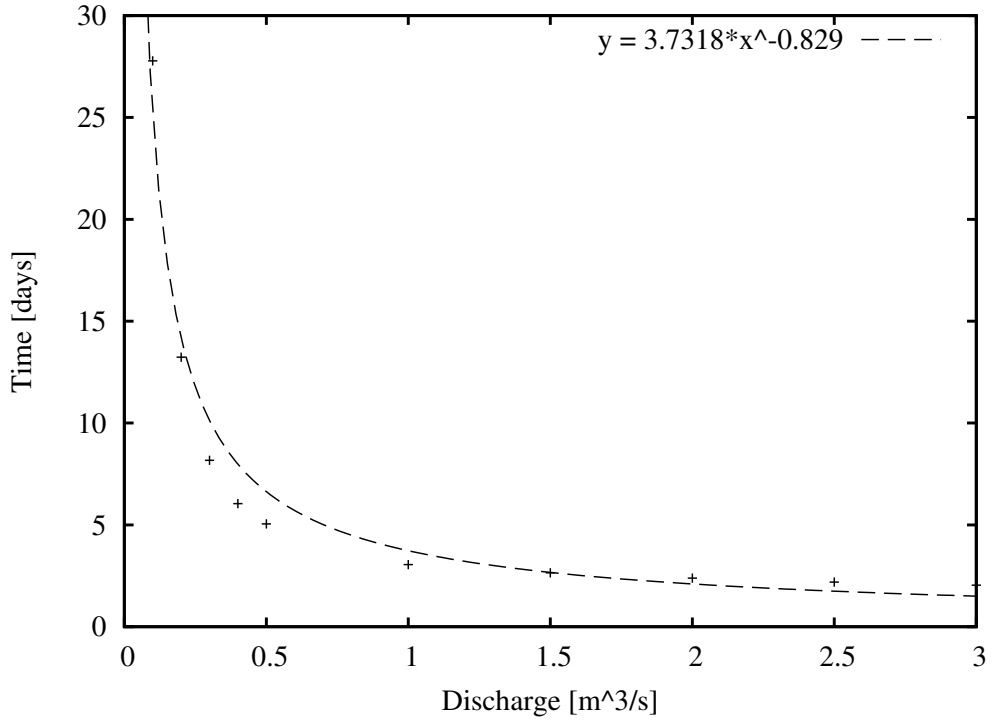

Figure E.60: Discharge-Time relationship between chainage 80500-81500m.

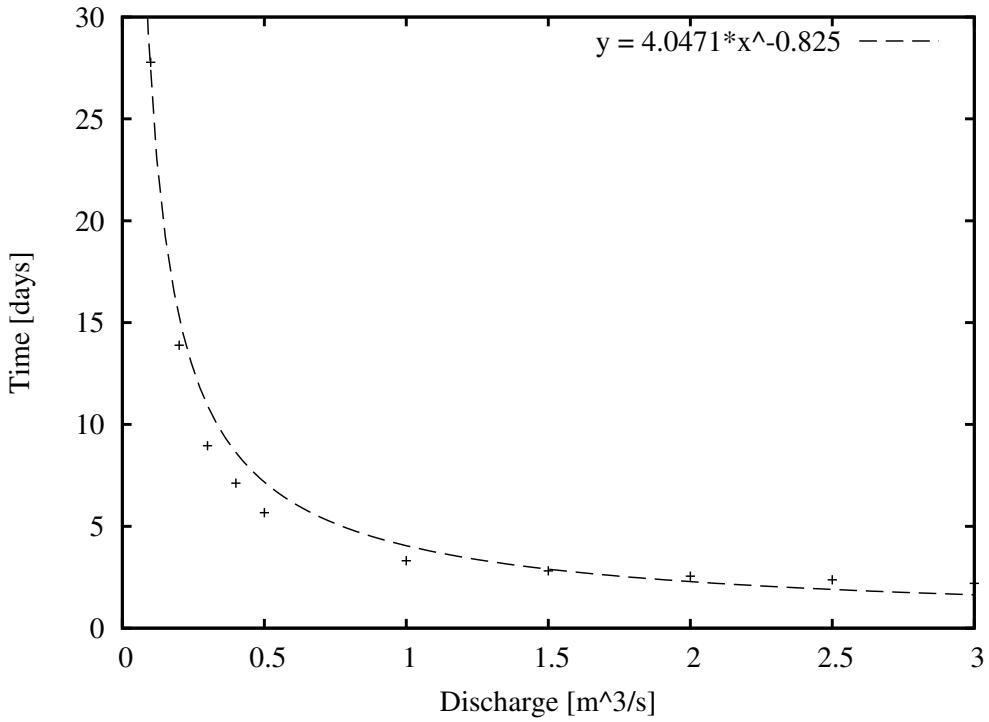

Figure E.61: Discharge-Time relationship between chainage 81500-82500m.

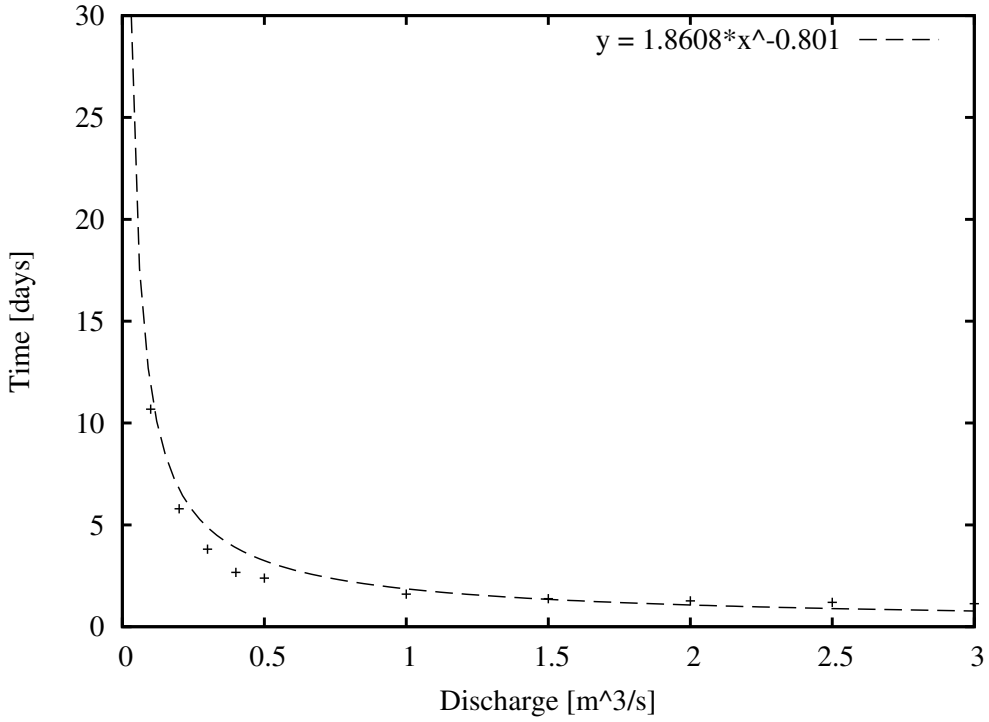

Figure E.62: Discharge-Time relationship between chainage 82500-83000m.

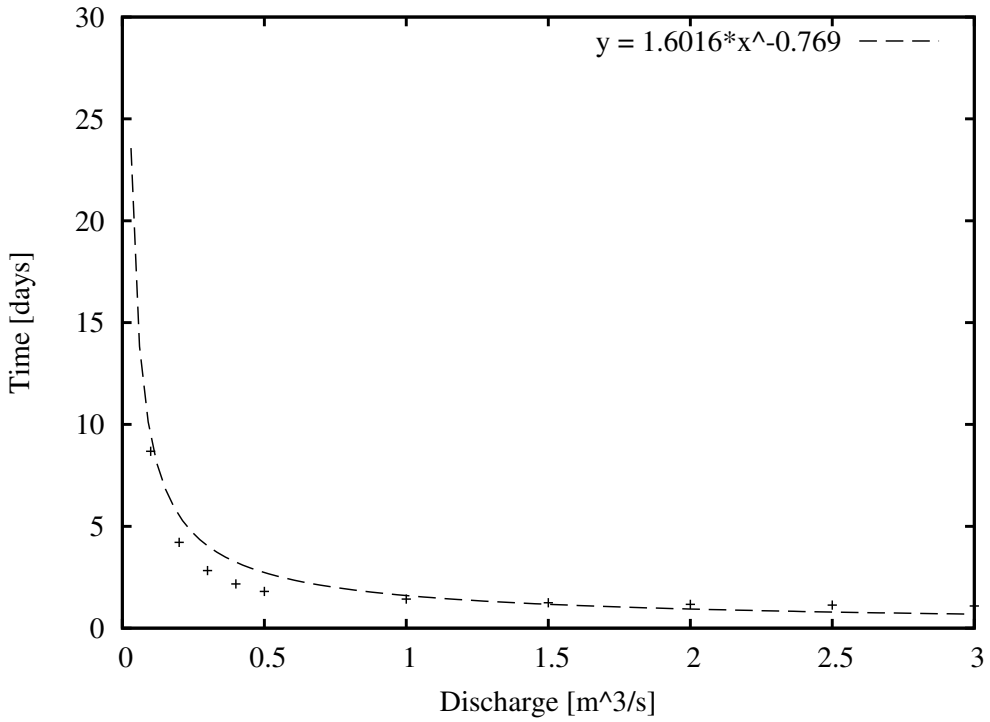

Figure E.63: Discharge-Time relationship between chainage 83000-83500m.

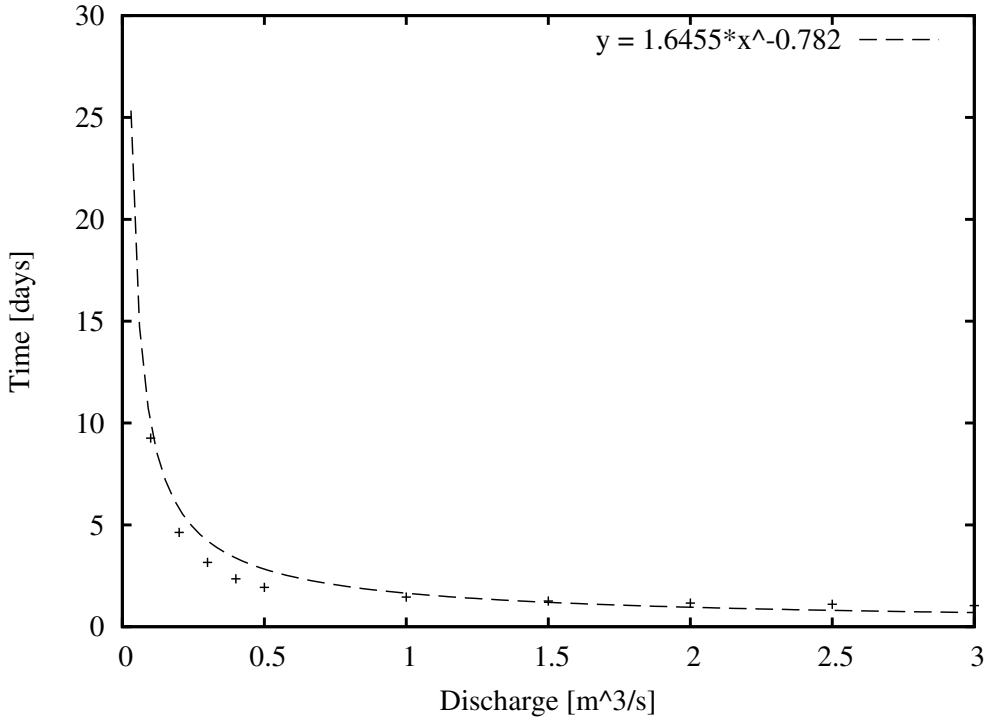

Figure E.64: Discharge-Time relationship between chainage 83500-84000m.

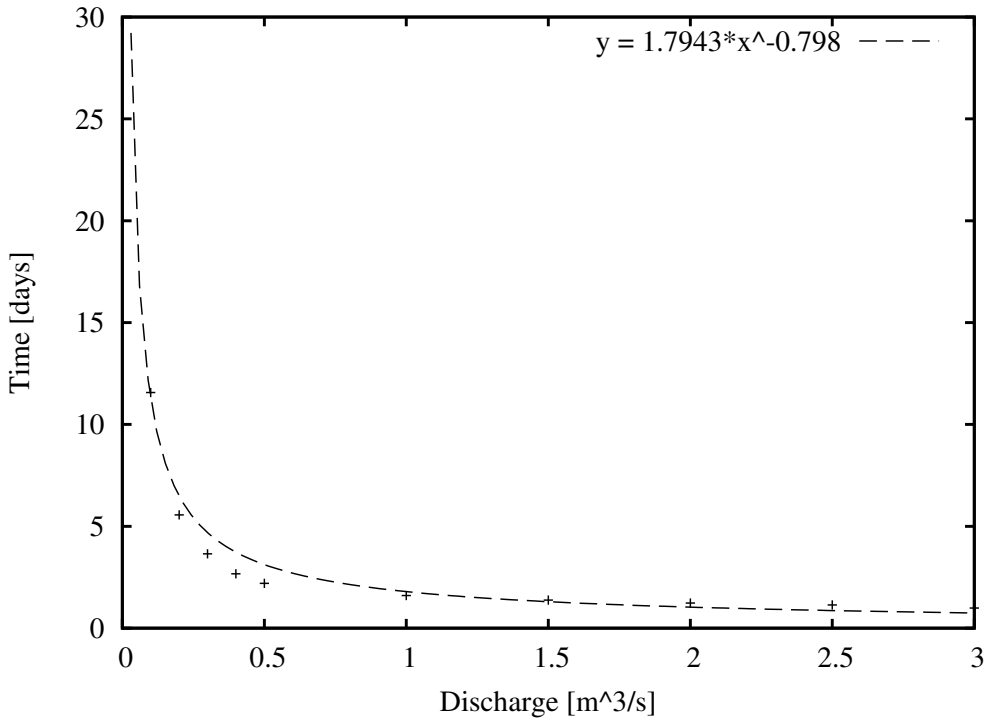

Figure E.65: Discharge-Time relationship between chainage 84000-84500m.

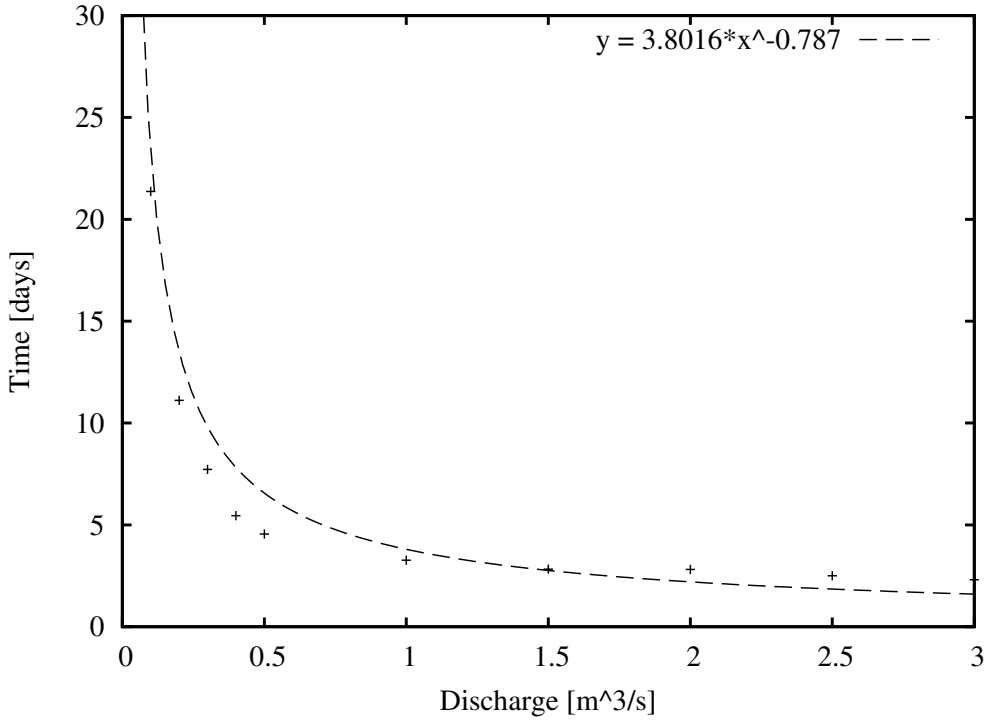

Figure E.66: Discharge-Time relationship between chainage 84500-85500.

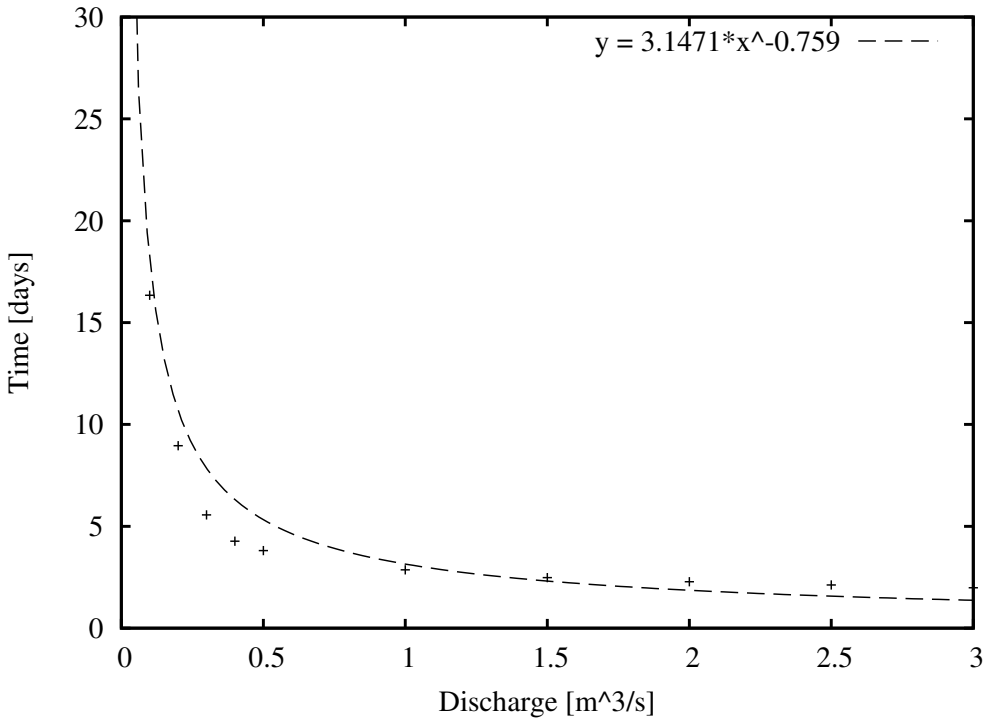

Figure E.67: Discharge-Time relationship between chainage 85500-86500m.

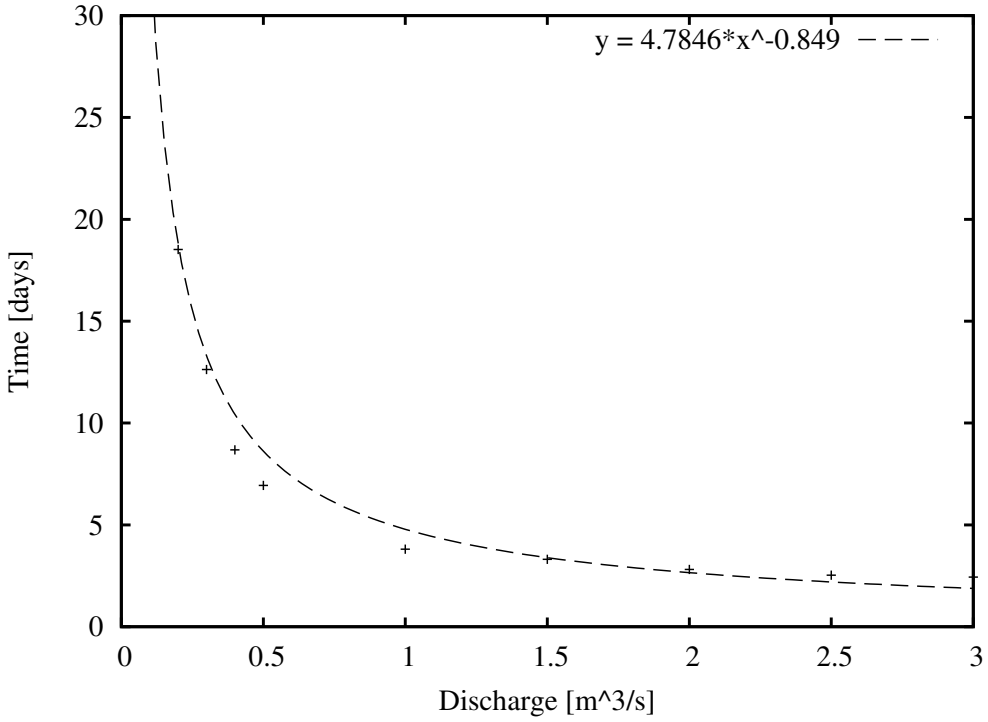

Figure E.68: Discharge-Time relationship between chainage 86500-87500m.

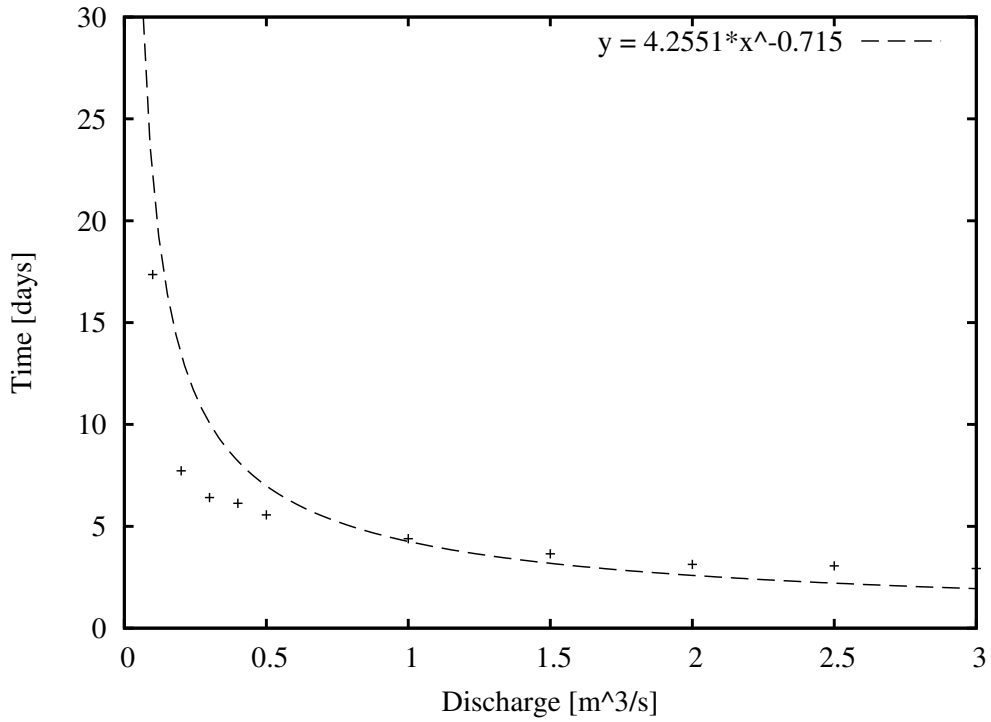

Figure E.69: Discharge-Time relationship between chainage 87500-89000m.

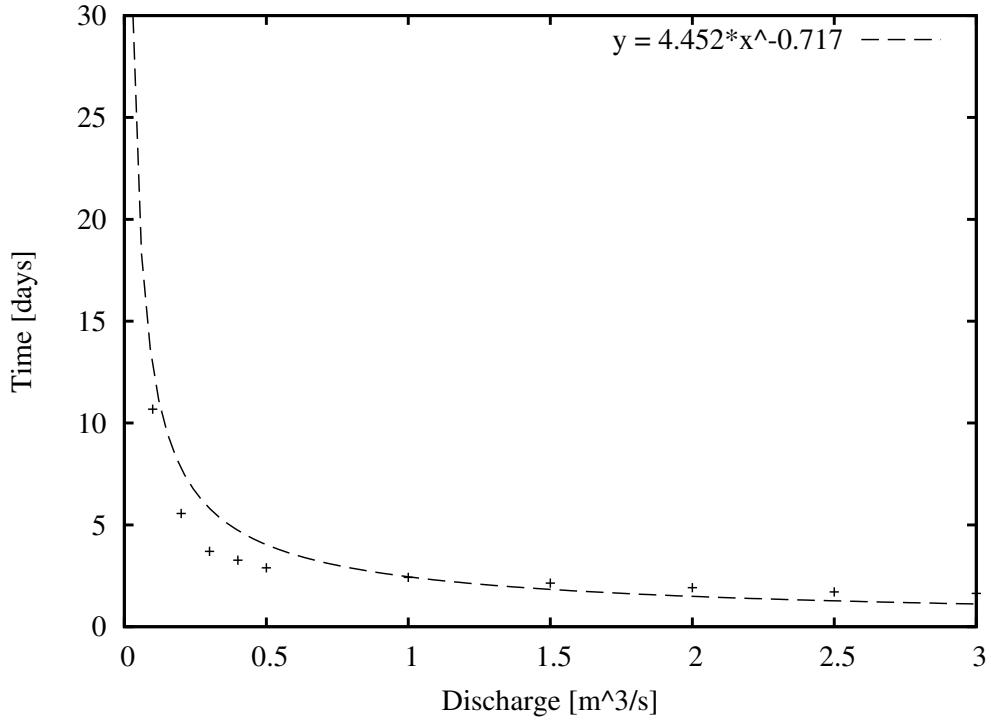

Figure E.70: Discharge-Time relationship between chainage 89000-90000m.

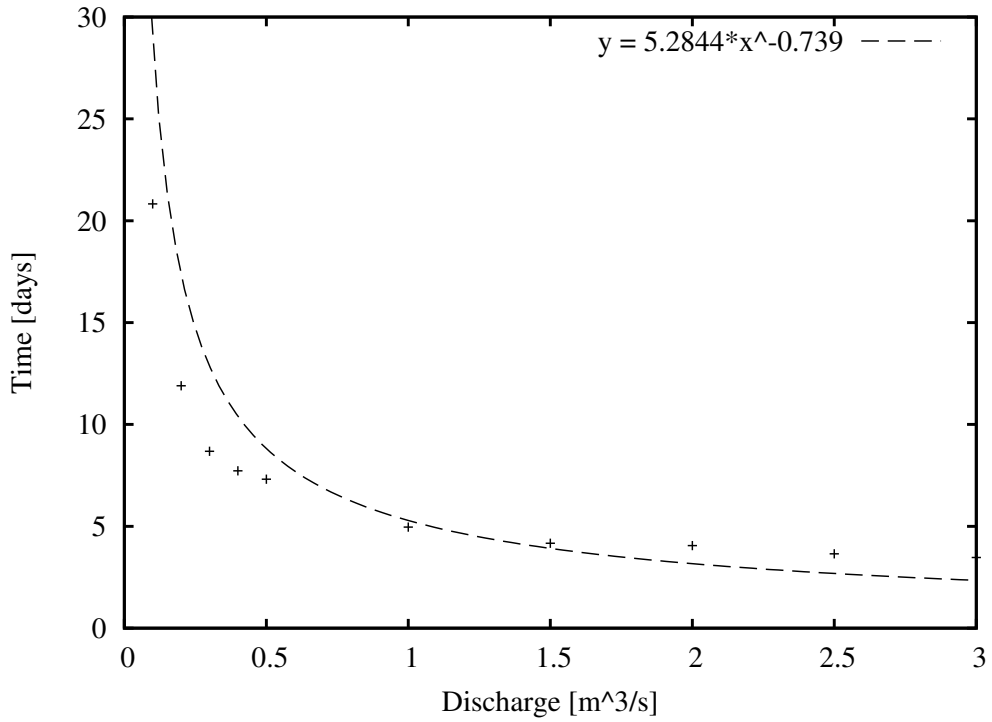

Figure E.71: Discharge-Time relationship between chainage 90000-91500m.

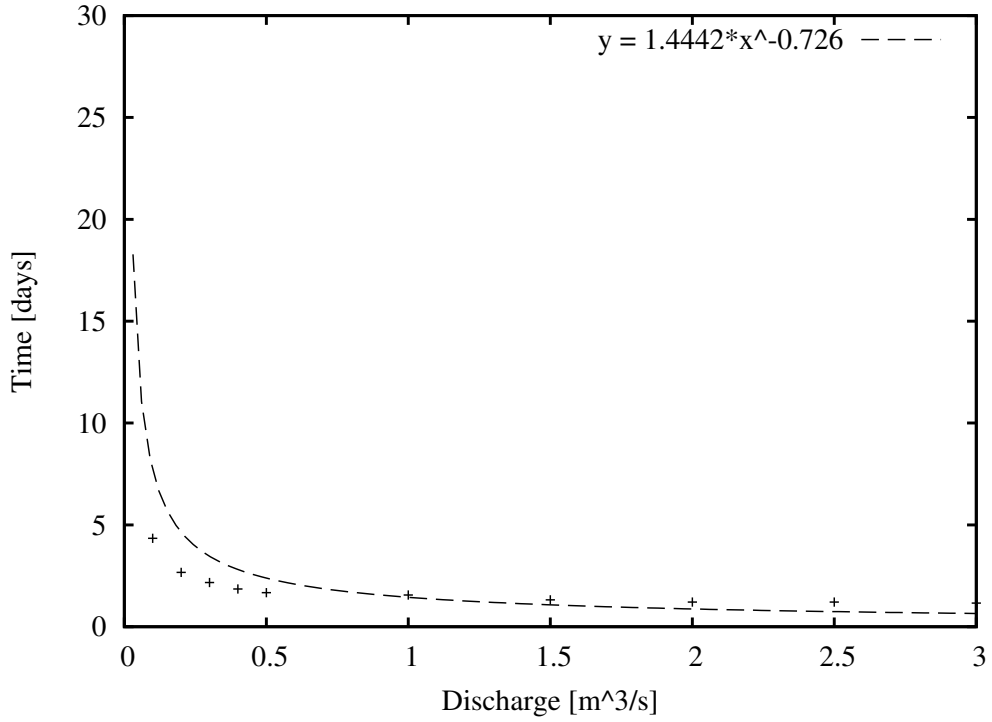

Figure E.72: Discharge-Time relationship between chainage 91500-92000m.

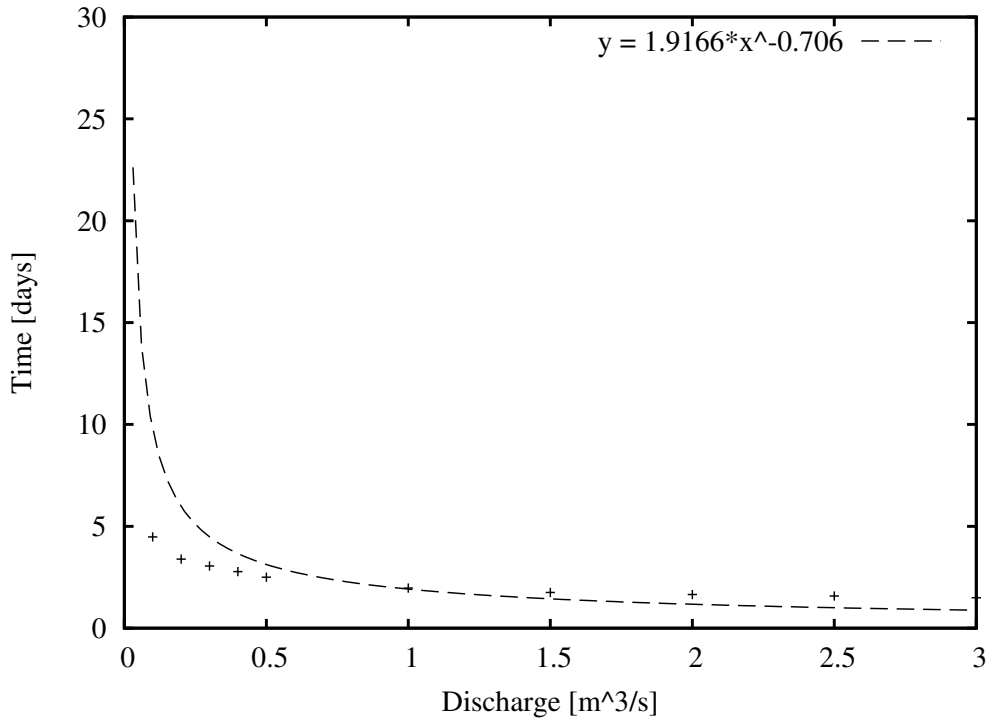

Figure E.73: Discharge-Time relationship between chainage 92000-93000m.

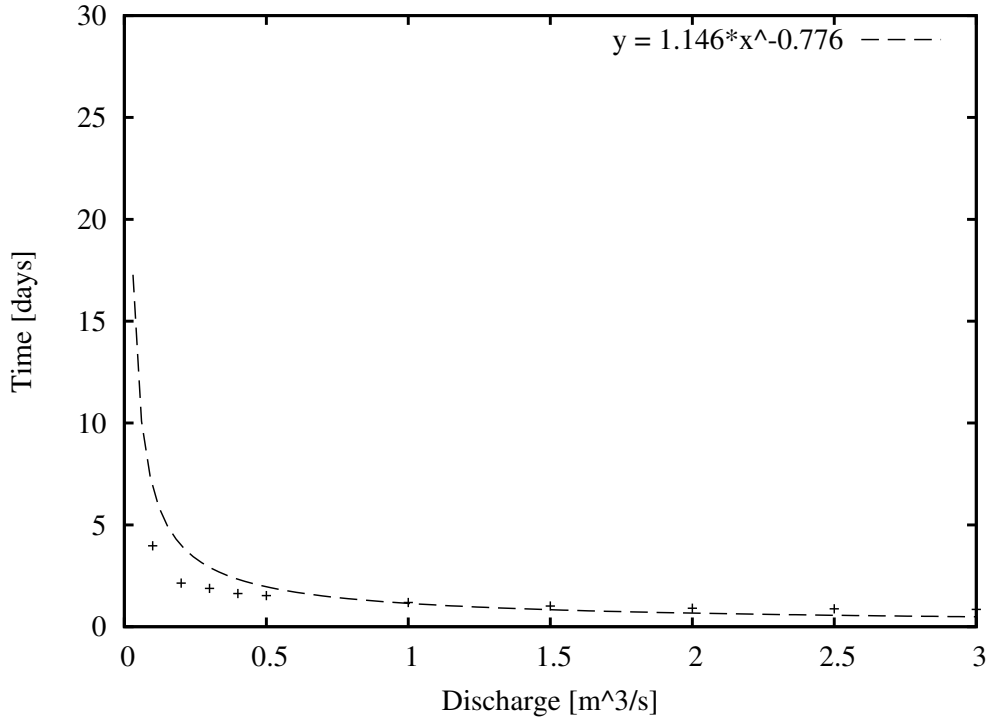

Figure E.74: Discharge-Time relationship between chainage 93000-93500m.

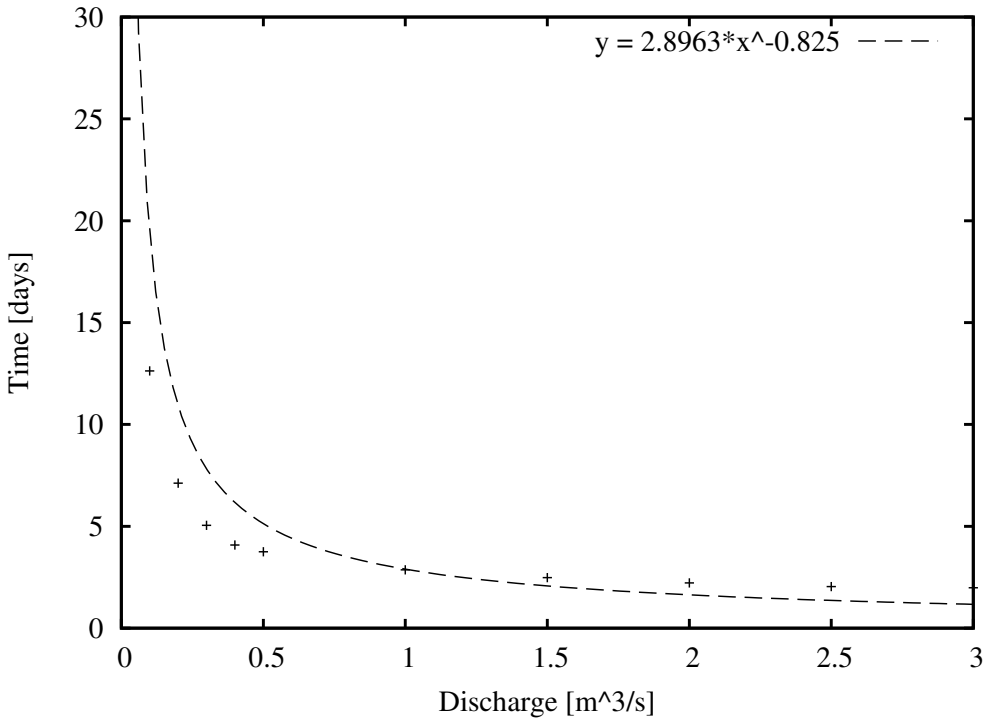

Figure E.75: Discharge-Time relationship between chainage 93500-94500m.

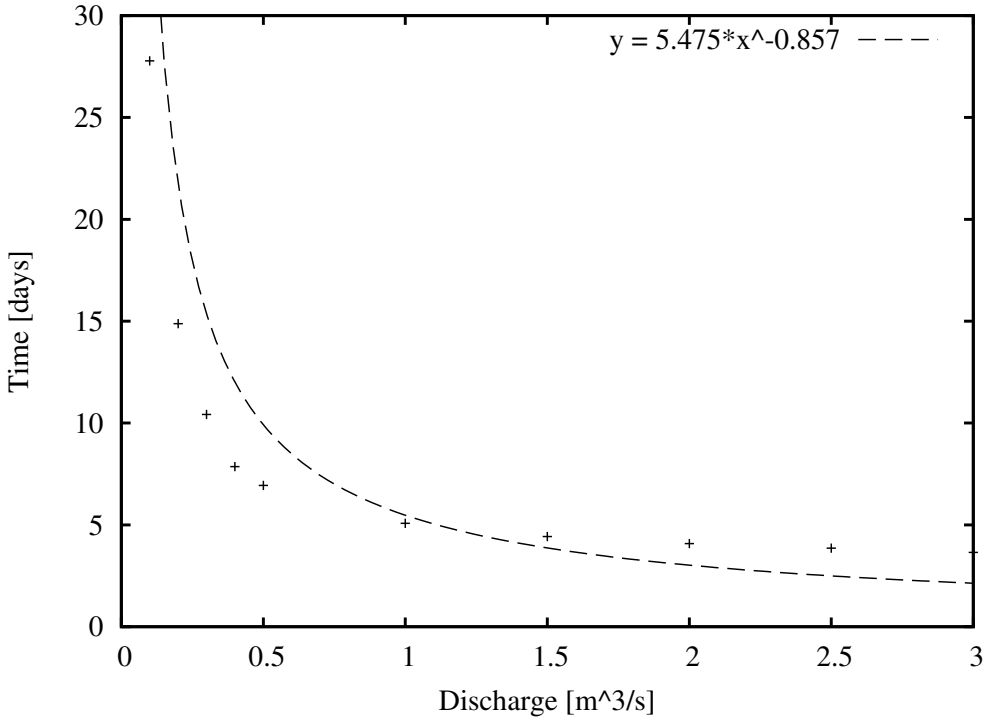

Figure E.76: Discharge-Time relationship between chainage 94500-96000m.

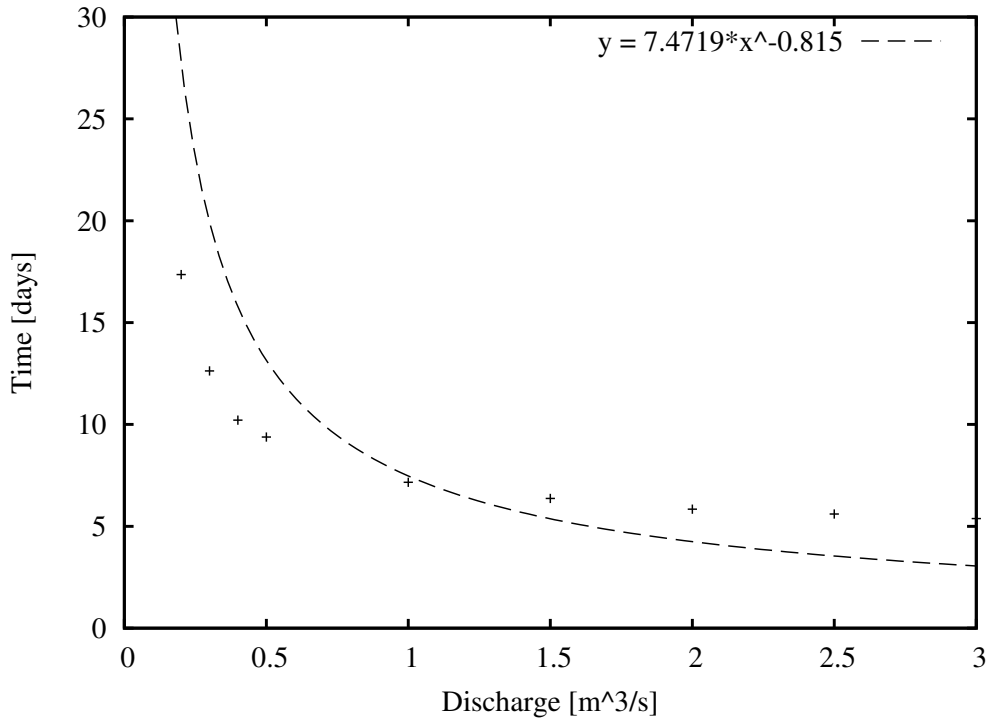

Figure E.77: Discharge-Time relationship between chainage 96000-98500m.

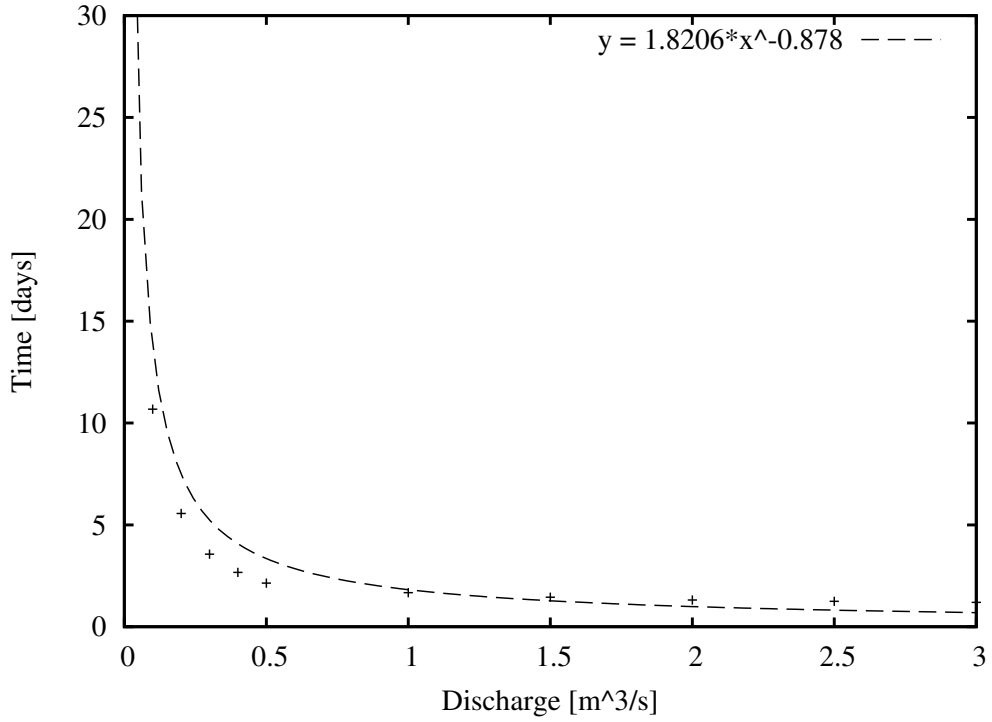

Figure E.78: Discharge-Time relationship between chainage 98500-99000m.

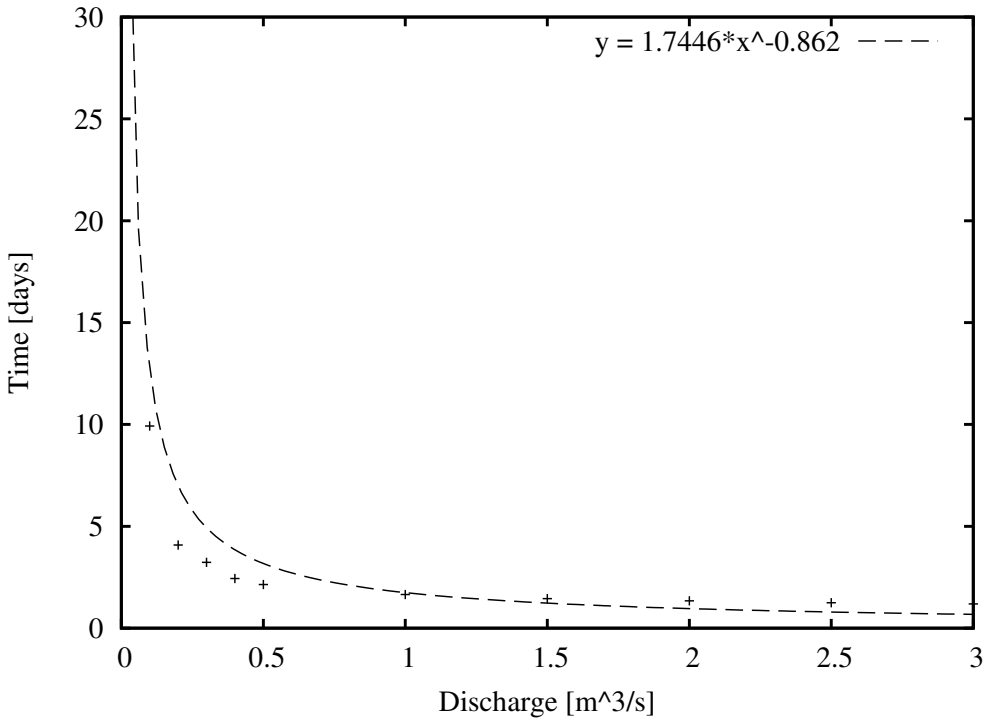

Figure E.79: Discharge-Time relationship between chainage 99000-99500m.

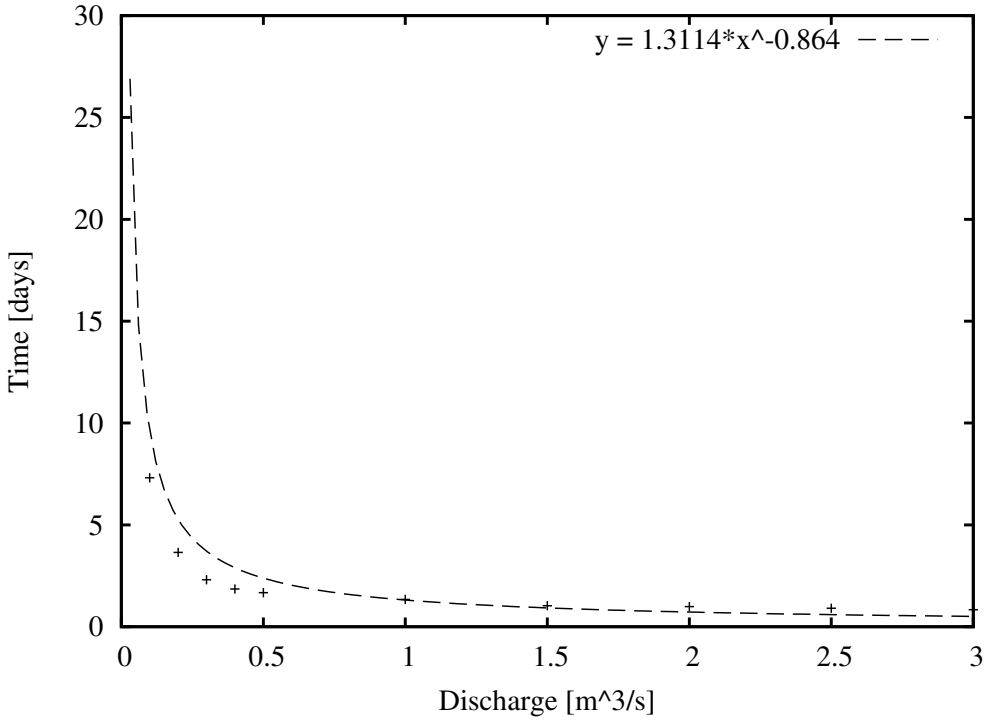

Figure E.80: Discharge-Time relationship between chainage 99500-100000m.

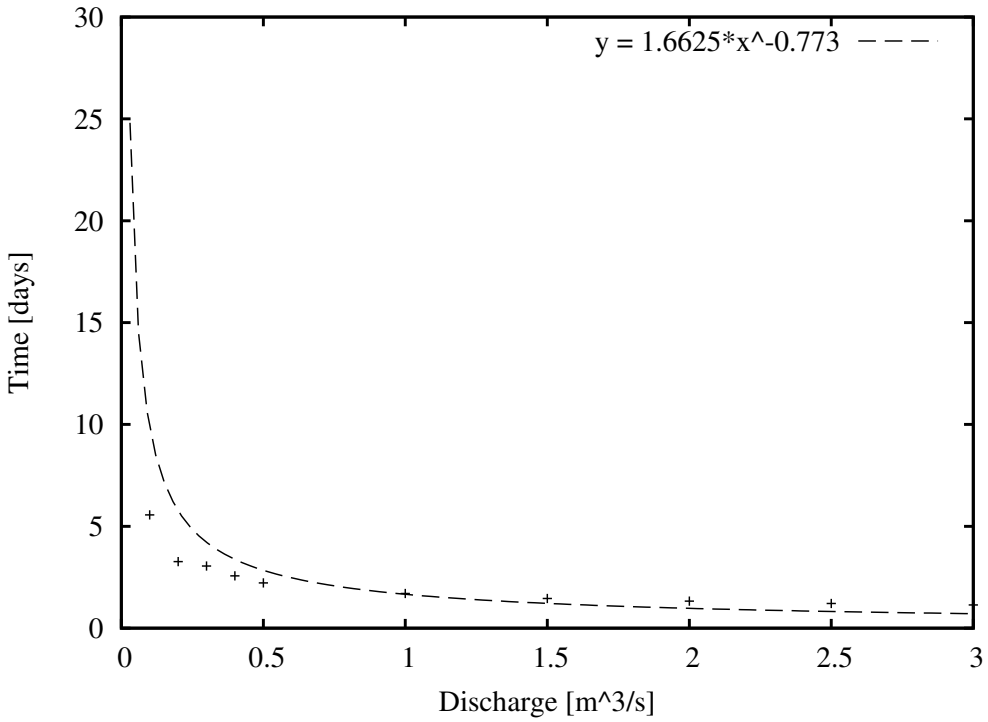

Figure E.81: Discharge-Time relationship between chainage 100000-101000m.

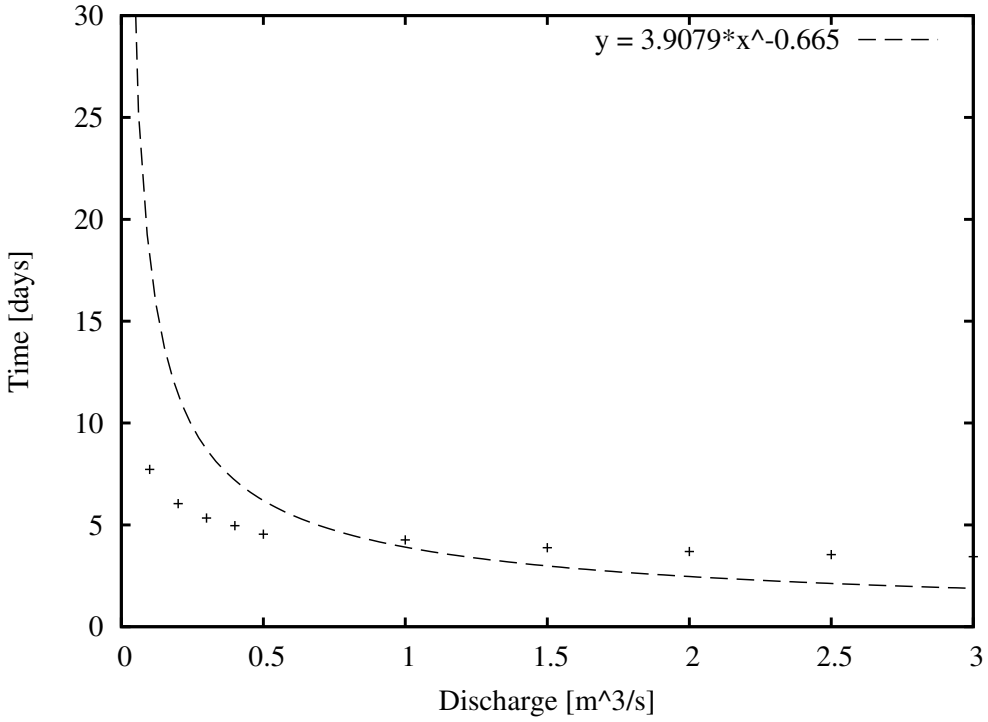

Figure E.82: Discharge-Time relationship between chainage 101000-103500m.

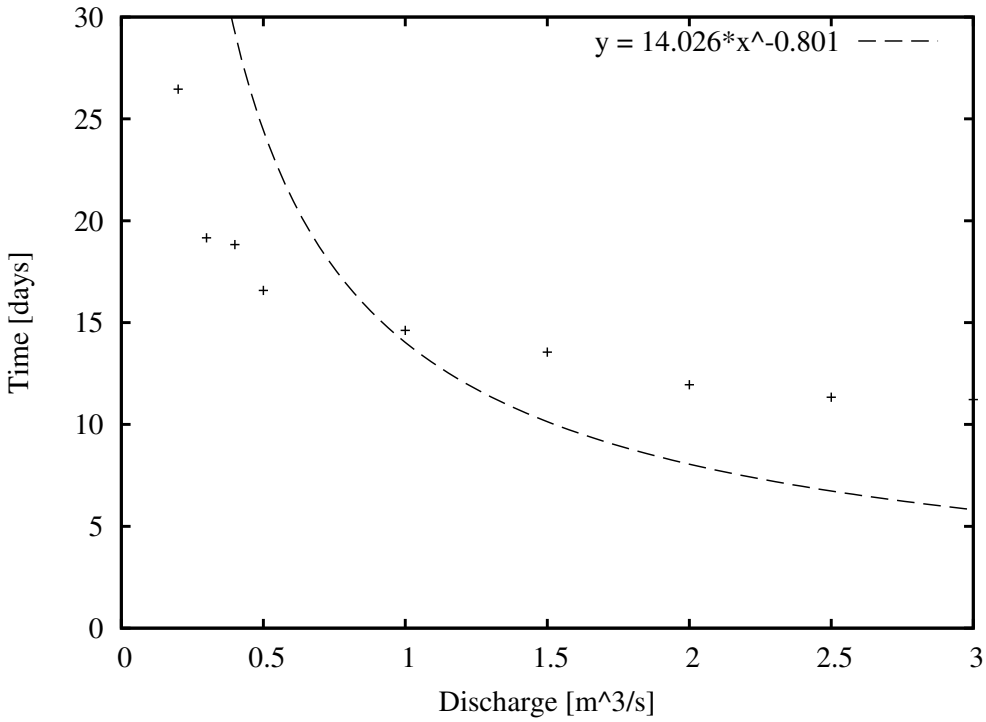

Figure E.83: Discharge-Time relationship between chainage 103500-107500m.

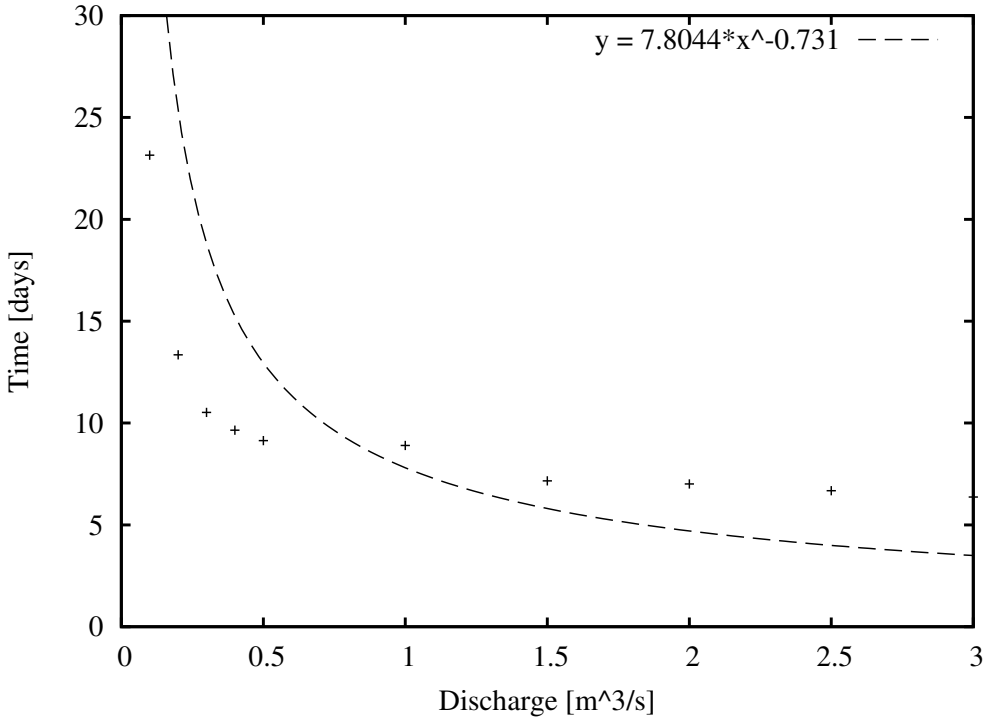

Figure E.84: Discharge-Time relationship between chainage 107500-110000m.

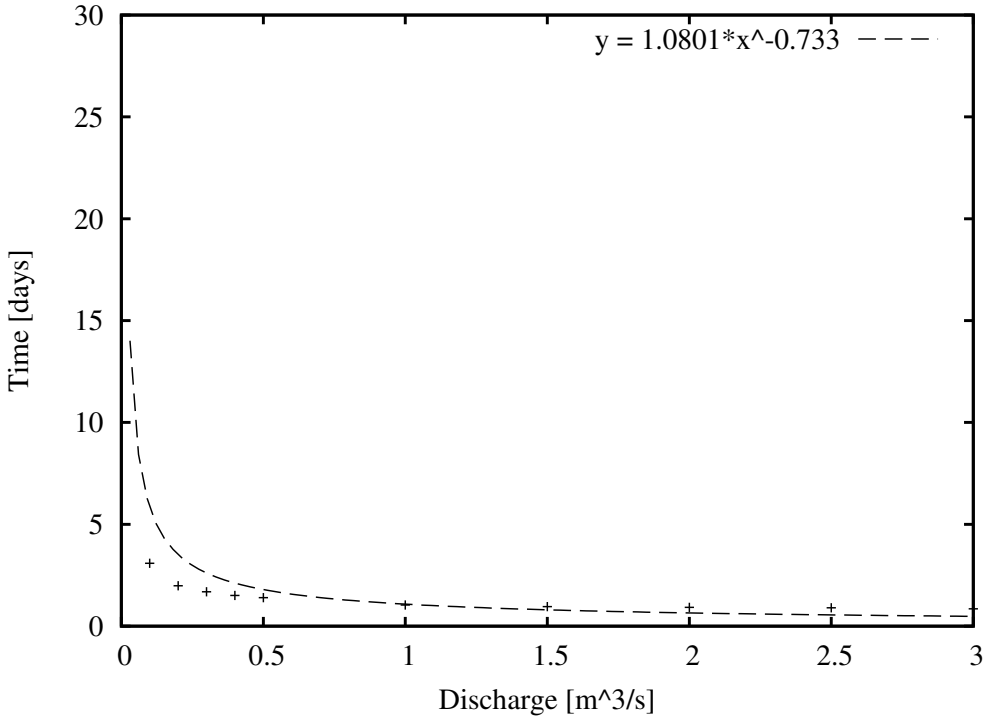

Figure E.85: Discharge-Time relationship between chainage 110000-110500m.

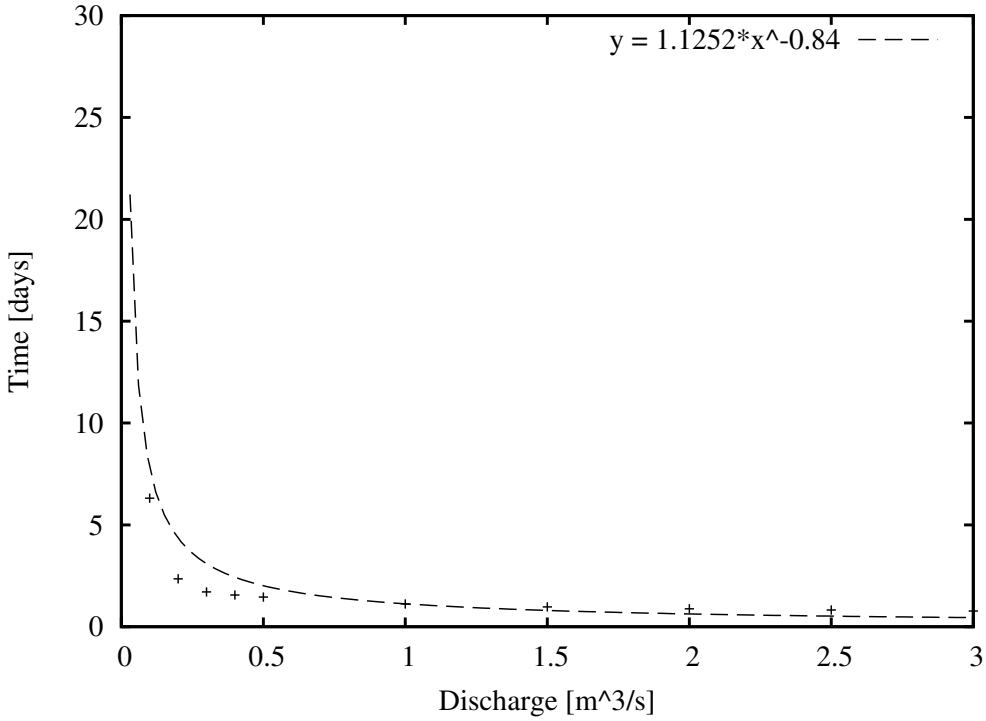

Figure E.86: Discharge-Time relationship between chainage 110500-111000m.

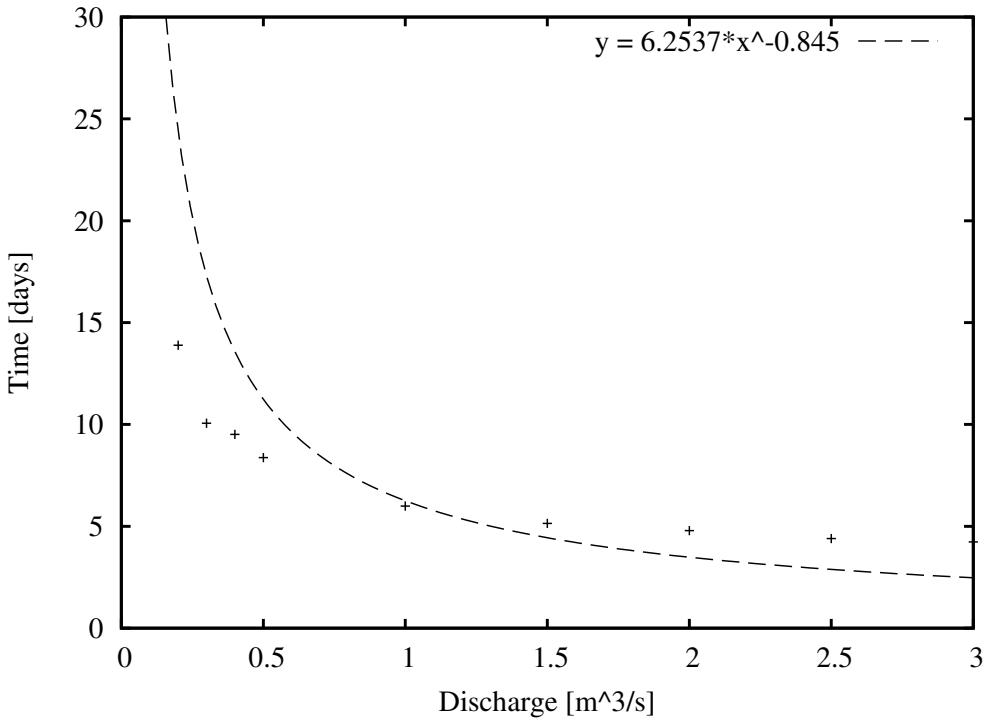

Figure E.87: Discharge-Time relationship between chainage 111000-113500m.

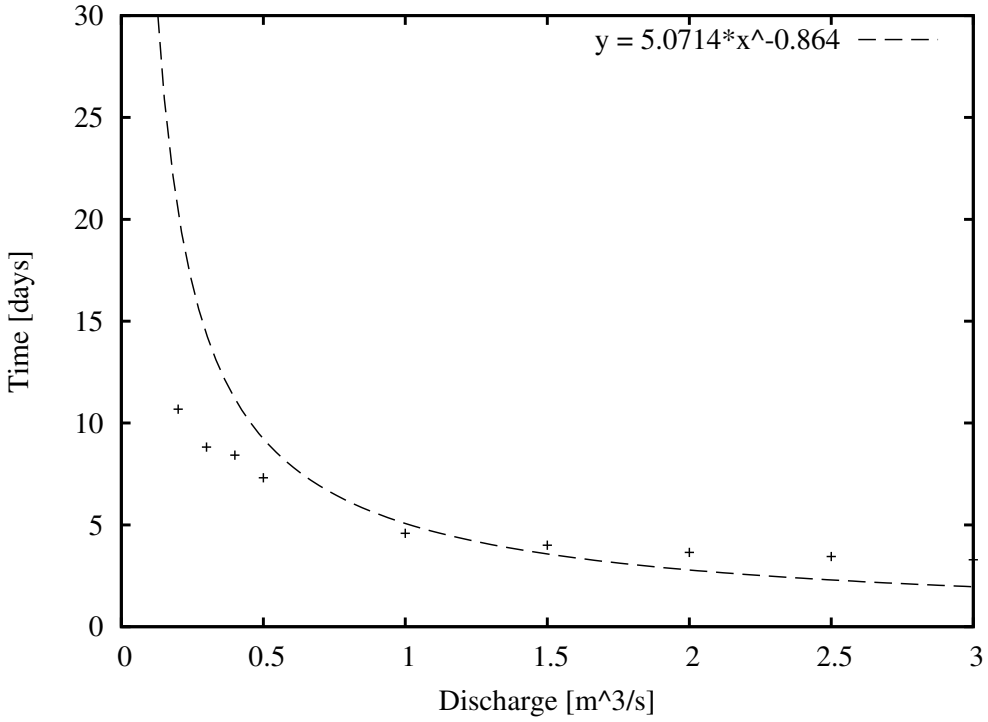

Figure E.88: Discharge-Time relationship between chainage 113500-115500m.

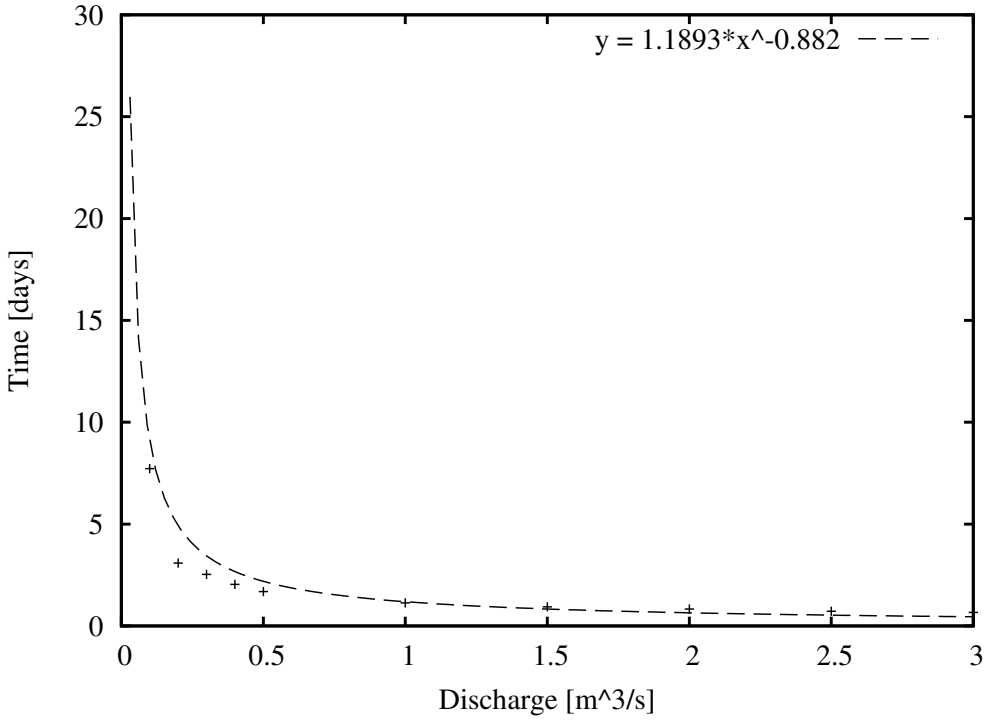

Figure E.89: Discharge-Time relationship between chainage 115500-116000m.